

Canagliflozin impairs T cell effector function via metabolic suppression in autoimmunity

Benjamin James Jenkins

Submitted to Swansea University in fulfilment of the requirements for the Degree of Doctor of Philosophy



Swansea University
Prifysgol Abertawe

Medical School
Ysgol Feddygaeth

2023

Summary

Autoimmune diseases are characterised by augmented T cell function, ultimately leading to chronic inflammation and tissue damage. Altered T cell function is supported by metabolic dysregulation in the setting of autoimmunity, therefore targeting immunometabolism by repurposing clinically approved metabolic modulators, such as those used to treat type 2 diabetes (T2D), is an attractive prospect. Canagliflozin – a member of the newest class of T2D drugs, sodium glucose co-transporter 2 (SGLT2) inhibitors – has known off-target effects including inhibition of mitochondrial glutamate dehydrogenase (GDH) and complex I of the electron transport chain. Importantly, these properties are not shared with other SGLT2 inhibitors, particularly dapagliflozin which has very limited off-target effects. The effects of canagliflozin on human T cell function are unknown.

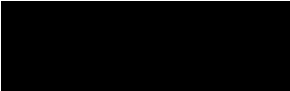
This study revealed that canagliflozin, but not dapagliflozin, compromised the proliferation and effector function of human T cells. The inhibitory effect of canagliflozin was underpinned by reduced T cell activation. Proteomic analysis revealed that canagliflozin mediates changes on a global scale, inhibiting various aspects of T cell fitness including metabolism, mitochondrial function and protein translation. Specifically, MYC inhibition emerged as a predicted upstream regulator of the canagliflozin-induced changes in protein expression. Compromised cellular metabolism was confirmed in canagliflozin-treated CD4⁺ T cells, whereby oxidative phosphorylation and glycolysis were markedly impaired following inhibition of GDH and complex I. Mechanistically, canagliflozin inhibits early T cell receptor signalling, which subsequently impacted the downstream activity of signalling proteins including ERK, mTOR and MYC.

Importantly, canagliflozin treatment of T cells derived from patients with autoimmune disorders – rheumatoid arthritis and systemic lupus erythematosus – significantly impaired their effector function. Again, these changes were underpinned by perturbed cellular metabolism and diminished activation. Together, this work provides a foundation for the repurposing of canagliflozin as a treatment for autoimmune disease.

Declaration and Statements


Declaration

This work has not previously been accepted in substance for any degree and is not being concurrently submitted in candidature for any degree.

Signed  (Candidate)
Date..... 21 / 03 / 2023

Statement 1

This work is the result of my own independent study/investigation, except where otherwise stated. Other sources are acknowledged by footnotes giving explicit references. A bibliography is appended.

Signed..  (Candidate)
Date..... 21 / 03 / 2023

Statement 2

I hereby give my consent for my work, if relevant and accepted, to be available for photocopying and for inter-library loan, and for the title and summary to be made available to outside organisations.

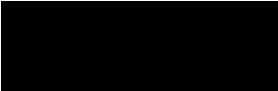
Signed  (Candidate)
Date..... 21 / 03 / 2023

Table of Contents

Summary	i
Declaration and Statements	ii
Table of Contents	iii
Table of Figures	x
List of Tables	xvii
Acknowledgements	xix
Abbreviations	xx
Conferences	xxiii
Chapter One	1
1 Introduction	2
1.1 General overview	2
1.2 T cells	3
1.2.1 T cell receptor	3
1.2.2 T cell development	4
1.2.3 T cell subset populations	6
1.2.4 T cell activation	10
1.2.5 T cell signalling	14
1.3 T cell metabolism	16
1.3.1 Substrate transportation	17
1.3.2 Glycolysis	18
1.3.3 Fates of pyruvate	21
1.3.4 Tricarboxylic acid cycle	22
1.3.5 Oxidative phosphorylation	24
1.3.6 Metabolic rewiring upon T cell activation	25
1.3.7 Metabolic regulation of T cell lineage	32
1.4 T cell-mediated autoimmune disease	39
1.4.1 Rheumatoid arthritis	40

1.4.2	Systemic lupus erythematosus	46
1.5	The role of T cell metabolism in autoimmune disease	49
1.5.1	T cell metabolism in rheumatoid arthritis	50
1.5.2	T cell metabolism in systemic lupus erythematosus	55
1.6	Repurposing type 2 diabetes drugs in autoimmunity	60
1.6.1	Thiazolidinediones	62
1.6.2	Metformin	63
1.7	Sodium glucose co-transporter 2 inhibitors	66
1.7.1	Off-target effects of SGLT2 inhibitors	67
1.7.2	Repurposing SGLT2 inhibitors in inflammatory diseases	70
1.8	Aims and objectives	73
Chapter Two		74
2	Experimental procedures	75
2.1	Human blood collection	75
2.2	Primary cell tissue culture	75
2.3	Peripheral blood mononuclear cell isolation	75
2.4	Human T cell isolation	76
2.4.1	Pan CD4+ T cell isolation	77
2.4.2	Naïve CD4+ T cell isolation	78
2.4.3	CD4+ T effector cell isolation	78
2.4.4	CD8+ T cell isolation	79
2.5	Cell counting	79
2.6	Cell culture	79
2.7	Flow cytometry	80
2.7.1	Purity monitoring	80
2.7.2	T cell activation	83
2.7.3	Blastogenesis and proliferation	83

2.7.4	Intracellular flow cytometry	84
2.7.5	Compensation	84
2.7.6	Quality control	85
2.7.7	Data analysis	85
2.8	Enzyme-linked immunosorbent assay	86
2.9	Metabolic analysis	87
2.10	Immunoblotting	90
2.10.1	Sample preparation	90
2.10.2	Protein estimation	90
2.10.3	Gel production	91
2.10.4	Sodium dodecyl sulphate-polyacrylamide gel electrophoresis	92
2.10.5	Semi-dry membrane transfer	92
2.10.6	Immunoblotting	92
2.10.7	Densitometry	93
2.11	Statistical analysis	93
Chapter Three		94
3	Canagliflozin modulates activated T cell function	95
3.1	Introduction	95
3.1.1	Rationale	97
3.1.2	Hypothesis	97
3.2	Experimental procedures	98
3.2.1	Human blood collection	98
3.2.2	T cell isolation	98
3.2.3	Cell culture	98
3.2.4	Flow cytometry	98
3.2.5	Enzyme-linked immunosorbent assay	98
3.2.6	Statistical analysis	99

3.3	Results	99
3.3.1	Canagliflozin impairs activated T cell activation and function	99
3.3.2	Canagliflozin retains its inhibitory effects on T cell function in physiological media conditions	103
3.3.3	Canagliflozin modestly inhibits already-activated T cell function	113
3.4	Discussion	118
3.5	Conclusions	120
Chapter Four		122
4	Canagliflozin mediates global changes to T cell function at the transcript and protein level	123
4.1	Introduction	123
4.1.1	Rationale	126
4.1.2	Hypothesis	126
4.2	Experimental procedures	127
4.2.1	Human blood collection	127
4.2.2	T cell isolation	127
4.2.3	Cell culture	127
4.2.4	Flow cytometry	127
4.2.5	Immunoblotting	127
4.2.6	RNA isolation	127
4.2.7	Nanostring analysis	128
4.2.8	Proteomic analysis	130
4.2.9	Statistical analysis	132
4.3	Results	133
4.3.1	Global changes in T cell gene expression upon canagliflozin treatment	133
4.3.2	Canagliflozin remodels the T cell proteome	143
4.3.3	Canagliflozin suppresses MYC signalling	151

4.4	Discussion	158
4.5	Conclusions	163
Chapter Five		165
5	Canagliflozin suppresses T cell receptor signalling to impair metabolic reprogramming	166
5.1	Introduction	166
5.1.1	Rationale	168
5.1.2	Hypothesis	168
5.2	Experimental procedures	169
5.2.1	Human blood collection	169
5.2.2	T cell isolation	169
5.2.3	Cell culture	169
5.2.4	Flow cytometry	169
5.2.5	Enzyme-linked immunosorbent assay	170
5.2.6	Metabolic assay	170
5.2.7	Immunoblotting	171
5.2.8	Extracellular glucose assay	171
5.2.9	Extracellular lactate assay	171
5.2.10	Stable isotope tracer analysis	171
5.2.11	Statistical analysis	173
5.3	Results	173
5.3.1	T cell mitochondrial dysfunction is characteristic of canagliflozin treatment	173
5.3.2	Canagliflozin drives T cell metabolism towards quiescence through its off-target effects	182
5.3.3	Canagliflozin impairs TCA cycle metabolism via GDH inhibition	187
5.3.4	T cells undergo metabolic reprogramming to adapt to canagliflozin treatment	195

5.3.5	Canagliflozin-driven T cell dysregulation is not solely driven by inhibition of complex I and glutamate dehydrogenase	200
5.3.6	Canagliflozin impairs T cell receptor signalling	203
5.4	Discussion	209
5.5	Conclusions	215
Chapter Six		217
6	Canagliflozin inhibits T cell function in systemic lupus erythematosus and rheumatoid arthritis	218
6.1	Introduction	218
6.1.1	Rationale	221
6.1.2	Hypothesis	221
6.2	Experimental procedures	221
6.2.1	Human blood collection	221
6.2.2	Autoimmune patient cohort samples	221
6.2.3	T cell isolation	224
6.2.4	Cell culture	224
6.2.5	Flow cytometry	224
6.2.6	Enzyme-linked immunosorbent assay	228
6.2.7	Metabolic analysis	228
6.2.8	Extracellular glucose assay	228
6.2.9	Statistical analysis	228
6.3	Results	229
6.3.1	Canagliflozin impairs T effector cell activation, function and proliferation	229
6.3.2	Canagliflozin alters the distribution of Th subsets within the T effector cell population	236
6.3.3	Canagliflozin inhibits CD8+ T cell function	242
6.3.4	Canagliflozin inhibits CD4+ T cell function in systemic lupus erythematosus and rheumatoid arthritis	246

6.3.5	Canagliflozin inhibits the function of human T cells isolated from arthritogenic synovial fluid	259
6.4	Discussion	264
6.5	Conclusions	268
Chapter Seven		270
7	General Discussion	271
7.1	Overview	271
7.2	Canagliflozin modulates activated T cell function	273
7.3	Canagliflozin mediates global changes to T cell function at the transcript and protein level	274
7.4	Canagliflozin promotes mitochondrial dysfunction to impair T cell metabolic reprogramming	275
7.5	Canagliflozin inhibits T cell function in systemic lupus erythematosus and rheumatoid arthritis	277
7.6	Further work and limitations	278
7.7	The future for canagliflozin	280
Chapter Eight		282
8	Appendices	283
8.1	Fructose reprogrammes glutamine-dependent oxidative metabolism to support LPS-induced inflammation	283
8.2	A role for metabolism in determining neonatal immune function	296
8.3	Does Altered Cellular Metabolism Underpin the Normal Changes to the Maternal Immune System during Pregnancy?	309
8.4	Immunometabolic adaptation and immune plasticity in pregnancy and the bi-directional effects of obesity	332
Chapter Nine		347
9	Bibliography	348

Table of Figures

Figure 1.1	Components of the T cell receptor	4
Figure 1.2	Overview of T cell development	5
Figure 1.3	Overview of the polarising conditions associated with each major T helper subset	7
Figure 1.4	Stimulatory and inhibitory conditions regulating T cell activation	11
Figure 1.5	Overview of T cell memory	13
Figure 1.6	T cell receptor signalling cascade	15
Figure 1.7	Summary of the substrate transporters used by T cells	18
Figure 1.8	The glycolysis pathway	21
Figure 1.9	The fates of pyruvate	22
Figure 1.10	The tricarboxylic acid cycle	23
Figure 1.11	The electron transport chain	25
Figure 1.12	T cell metabolism upon activation	27
Figure 1.13	T cell metabolism during memory formation	31
Figure 1.14	T cell metabolism in differentiation	39
Figure 1.15	An example of T cell pathogenesis in autoimmune disease	45
Figure 1.16	Summary of T cell metabolism in autoimmune disease	60
Figure 1.17	The impact of canagliflozin on cellular function	68
Figure 2.1	Summary of density gradient centrifugation	76
Figure 2.2	Principle of magnetic separation	77
Figure 2.3	Example of the gating strategy used to monitor CD4+ T cell purity	81
Figure 2.4	Example of the gating strategy used to monitor naïve and effector T cell purity	82
Figure 2.5	Example of the gating strategy used to monitor CD8+ T cell purity	82
Figure 2.6	Example of the spectral overlap between fluorophores	85
Figure 2.7	Summary of enzyme-linked immunosorbent assay	87
Figure 2.8	Respiratory inhibitors and activators within the electron transport chain	88

Figure 2.9	Calculation of metabolic parameters	89
Figure 3.1	Experimental procedure employed to assess the impact of canagliflozin and dapagliflozin on naïve T cells activated in RPMI	100
Figure 3.2	Canagliflozin, but not dapagliflozin, impairs IL-2 production in a dose-dependent manner	101
Figure 3.3	Canagliflozin impairs T cell activation	102
Figure 3.4	SGLT2 inhibitors limit activated T cell blastogenesis	102
Figure 3.5	Activated T cell viability is not compromised by canagliflozin and dapagliflozin	103
Figure 3.6	Experimental procedure employed to assess the impact of canagliflozin and dapagliflozin on naïve T cells activated in HPLM	104
Figure 3.7	Canagliflozin impairs IL-2 production by T cells activated in HPLM	104
Figure 3.8	T cell activation in HPLM is blunted by canagliflozin	105
Figure 3.9	Canagliflozin constrains activated T cell blastogenesis	106
Figure 3.10	Canagliflozin and dapagliflozin do not compromise the viability of CD4+ T cells activated in HPLM	107
Figure 3.11	SGLT2 inhibitors do not affect the phenotype of unstimulated naïve T cells	108
Figure 3.12	Experimental procedure employed to assess the long-term impact of canagliflozin and dapagliflozin on naïve T cells activated in HPLM	109
Figure 3.13	Canagliflozin impairs long-term IL-2 production by CD4+ T cells activated in HPLM	109
Figure 3.14	Long-term activated T cell blastogenesis is not significantly affected by SGLT2 inhibitors	110
Figure 3.15	Canagliflozin impairs T cell proliferation in HPLM	111
Figure 3.16	Experimental procedure employed to assess rescue of impaired effector function by IL-2 in activated T cells treated with canagliflozin	112
Figure 3.17	IL-2 does not reverse the inhibitory effect of canagliflozin on activated T cells	113
Figure 3.18	Blastogenesis is diminished by canagliflozin in already-activated T cells	114
Figure 3.19	Canagliflozin is effective when introduced prior to T cell activation	115

Figure 3.20	Canagliflozin has a limited effect on effector function in T cells pre-activated longer-term	116
Figure 3.21	Higher concentrations of canagliflozin are required to limit T cell proliferation and function in already-activated T cells	117
Figure 4.1	Nanostring nCounter® analysis experimental procedure	129
Figure 4.2	Canagliflozin, but not dapagliflozin, alters global gene expression in T cells	133
Figure 4.3	Autoimmunity-associated genes are differentially expressed in T cells treated with canagliflozin	134
Figure 4.4	Differentially downregulated genes in canagliflozin-treated T cells	135
Figure 4.5	Selected differentially upregulated genes in canagliflozin-treated T cells	135
Figure 4.6	Autoimmunity-associated pathways are upregulated at the gene transcript level in T cells treated with canagliflozin	136
Figure 4.7	Immunometabolism-associated genes are upregulated by canagliflozin	138
Figure 4.8	Canagliflozin alters the expression of metabolism-associated genes in T cells	139
Figure 4.9	Cell cycle genes are downregulated by canagliflozin	140
Figure 4.10	Differential expression of metabolism-associated pathways in canagliflozin-treated T cells	141
Figure 4.11	Canagliflozin downregulates the MYC pathway, but does not alter MYC expression at the transcript level	143
Figure 4.12	Canagliflozin-treated T cells fail to increase cell protein mass upon activation	144
Figure 4.13	Canagliflozin remodels the T cell proteome	145
Figure 4.14	Canagliflozin alters the distribution of subcellular compartments	146
Figure 4.15	MYC is downregulated by canagliflozin	147
Figure 4.16	Canonical pathways differentially regulated in T cells upon canagliflozin treatment	148
Figure 4.17	Canagliflozin inhibits cell cycle protein expression and function	149

Figure 4.18	Predicted upstream regulators of canagliflozin-induced changes in protein expression	151
Figure 4.19	MYC expression is reduced in canagliflozin-treated T cells	152
Figure 4.20	MYC-associated metabolic proteins are downregulated by canagliflozin	152
Figure 4.21	Canagliflozin reduces ribosomal protein expression	153
Figure 4.22	Protein translation machinery is downregulated by canagliflozin	155
Figure 4.23	Canagliflozin does not upregulate the levels of translational repressors	156
Figure 4.24	Canagliflozin impairs the upregulation of amino acid transporters upon T cell activation	157
Figure 5.1	Mitochondrial complexes are upregulated within T cells in response to canagliflozin	174
Figure 5.2	Increased expression of mitochondrial complexes in CD4+ T cells upon canagliflozin treatment	175
Figure 5.3	Canagliflozin increases mitochondrial biogenesis in activated T cells	176
Figure 5.4	Canagliflozin promotes mitochondrial reactive oxygen species production	177
Figure 5.5	Proteins associated with the response to reactive oxygen species are upregulated within T cells in response to canagliflozin	178
Figure 5.6	Glutathione and N-acetyl-cysteine partially rescue T cell function after canagliflozin treatment	179
Figure 5.7	Canagliflozin downregulates the expression of downstream mTOR targets	181
Figure 5.8	Canagliflozin impairs glycolysis in activated T cells	182
Figure 5.9	Canagliflozin limits the capacity for oxidative respiration in activated T cells	184
Figure 5.10	OCR/ECAR ratio of activated T cells treated with SGLT2 inhibitors	185
Figure 5.11	Canagliflozin limits the bioenergetic scope of activated T cells	186
Figure 5.12	Glucose uptake is modestly impaired by canagliflozin	187
Figure 5.13	Reduced abundance of TCA cycle intermediates in canagliflozin-treated T cells	188

Figure 5.14	Canagliflozin impairs lactate release by activated T cells	189
Figure 5.15	Stable isotope tracing of ¹³ C-glutamine in activated T cells	190
Figure 5.16	Canagliflozin impairs glutamine incorporation into the TCA cycle in activated T cells	191
Figure 5.17	Reduced incorporation of glutamine into amino acids pools in activated T cells treated with canagliflozin	192
Figure 5.18	Canagliflozin restricts the incorporation of glutamine-derived 13-carbon into metabolic intermediates in activated T cells	193
Figure 5.19	Glutamine uptake by activated T cells is constrained by canagliflozin	194
Figure 5.20	α-ketoglutarate does not rescue T cell function following canagliflozin treatment	195
Figure 5.21	Stable isotope tracing of ¹³ C-glucose in activated T cells	196
Figure 5.22	Canagliflozin limits the incorporation of ¹³ C-glucose into lactate	197
Figure 5.23	Canagliflozin-treated T cells adapt to glutamate dehydrogenase inhibition by becoming reliant on glucose-derived TCA cycle intermediates	198
Figure 5.24	Increased glucose incorporation into amino acids pools in activated T cells treated with canagliflozin	199
Figure 5.25	Canagliflozin promotes the incorporation of glucose-derived 13-carbon into metabolic intermediates in activated T cells	200
Figure 5.26	Canagliflozin is a superior inhibitor of T cell function compared to other mitochondrial complex I inhibitors	201
Figure 5.27	Canagliflozin is a superior inhibitor of T cell function versus combined inhibition of mitochondrial complex I and glutamate dehydrogenase	203
Figure 5.28	Canagliflozin impairs TCR signalling during early T cell activation	204
Figure 5.29	ERK signalling following early T cell activation is impaired following canagliflozin treatment	204
Figure 5.30	Canagliflozin impairs early T cell activation	205
Figure 5.31	TCR-independent activation rescues cytokine production by canagliflozin-treated T cells	206
Figure 5.32	Canagliflozin impairs MYC expression in a similar manner to mTOR inhibition and ERK inhibition	207

Figure 5.33	Canagliflozin phenocopies mTOR inhibition and ERK inhibition during early T cell activation	207
Figure 5.34	Canagliflozin impairs T cell function in a similar manner to mTOR inhibition and ERK inhibition	209
Figure 6.1	Gating strategy to identify Th subsets based on chemokine receptor expression	226
Figure 6.2	Gating strategy to identify synovial fluid CD4+ and CD8+ T cells	227
Figure 6.3	Experimental procedure employed to assess the impact of canagliflozin on T effector cells in HPLM	230
Figure 6.4	Canagliflozin suppresses cytokine production by T effector cells	231
Figure 6.5	T effector cell activation is impaired by canagliflozin	232
Figure 6.6	Canagliflozin restricts T effector cell blastogenesis	232
Figure 6.7	Canagliflozin reduces T effector cell proliferation	233
Figure 6.8	Canagliflozin does not compromise T effector cell viability	234
Figure 6.9	Nutrient transporter expression is reduced on T effector cell surface by canagliflozin	235
Figure 6.10	Canagliflozin-treated T effector cells do not become anergic	236
Figure 6.11	Th subset profile of canagliflozin-treated T effector cells	237
Figure 6.12	Changes within the T effector cell compartment upon canagliflozin treatment	238
Figure 6.13	Canagliflozin disrupts the balance between Th subsets	239
Figure 6.14	Canagliflozin alters chemokine receptor expression on T effector cells	240
Figure 6.15	Canagliflozin reduces the expression of lineage-associated transcription factors	241
Figure 6.16	Canagliflozin limits the expression of factors associated with regulatory T cell differentiation	242
Figure 6.17	Experimental procedure employed to assess the impact of canagliflozin on CD8+ T cells	243
Figure 6.18	CD8+ T cell activation is impaired by canagliflozin	243
Figure 6.19	Canagliflozin constrains CD8+ T cell blastogenesis	244

Figure 6.20	Canagliflozin impairs CD8+ T cell effector function	245
Figure 6.21	CD8+ T cell viability is not compromised by canagliflozin	245
Figure 6.22	Experimental procedure employed to assess the impact of canagliflozin on patient-derived CD4+ T cells	246
Figure 6.23	Donor variability in bioenergetic analysis of SLE patient-derived CD4+ T cells	247
Figure 6.24	Donor variability in bioenergetic analysis of RA patient-derived CD4+ T cells	248
Figure 6.25	Canagliflozin impairs CD4+ T cell glycolysis in SLE and RA	249
Figure 6.26	Canagliflozin limits the respiratory capacity of CD4+ T cells in SLE and RA	251
Figure 6.27	OCR/ECAR ratio of SLE and RA patient-derived CD4+ T cells treated with canagliflozin	252
Figure 6.28	Canagliflozin limits the bioenergetic scope of CD4+ T cells in SLE and RA	253
Figure 6.29	Canagliflozin-treated CD4+ T cells retain metabolic flexibility in SLE and RA	254
Figure 6.30	Canagliflozin promotes mitochondrial reactive oxygen species production in RA patient-derived CD4+ T cells	255
Figure 6.31	CD4+ T cell activation is impaired by canagliflozin in SLE and RA	256
Figure 6.32	Canagliflozin restricts CD4+ T cell blastogenesis in RA	257
Figure 6.33	CD4+ T cell viability is not markedly compromised by canagliflozin in SLE and RA	258
Figure 6.34	Canagliflozin impairs effector function in SLE and RA	259
Figure 6.35	Experimental procedure employed to assess the impact of canagliflozin on patient-derived synovial fluid mononuclear cells	260
Figure 6.36	Canagliflozin impairs the activation of synovial fluid T cells	261
Figure 6.37	Canagliflozin restricts synovial fluid T cell blastogenesis	262
Figure 6.38	Synovial fluid T cell viability is not compromised by canagliflozin	263
Figure 6.39	Canagliflozin inhibits proinflammatory cytokine production by synovial fluid mononuclear cells	264

List of Tables

Table 1.1	Characteristics of CD4+ T helper subsets	9
Table 2.1	Antibodies used for purity monitoring	81
Table 2.2	Antibodies used for activation marker analysis	83
Table 2.3	Definitions of proliferation-associated parameters	84
Table 2.4	Calculation of mitochondrial respiratory parameters	89
Table 2.5	Calculation of glycolytic parameters	89
Table 2.6	Pre-optimised recipe for 10% resolving gel	91
Table 2.7	Pre-optimised recipe for stacking gel	91
Table 3.1	Increased concentrations of canagliflozin are required to inhibit already-activated T cells	117
Table 4.1	Differential regulation of autoimmunity-associated pathways by canagliflozin, based on changes in gene expression	137
Table 4.2	Differential expression of cell cycle-associated genes by canagliflozin	140
Table 4.3	Differential regulation of metabolic pathways by canagliflozin, based on changes in gene expression	142
Table 4.4	Changes in eIF4A1:PDCD4 ratio following canagliflozin treatment	157
Table 5.1	Mitochondrial ROS levels are elevated during early T cell activation by canagliflozin	176
Table 5.2	<i>p</i> -values of ¹³ C ₅ -glutamine-derived mass isotopologues for vehicle versus canagliflozin	190
Table 5.3	<i>p</i> -values of ¹³ C ₆ -glucose-derived mass isotopologues for vehicle versus canagliflozin	197
Table 5.4	Canagliflozin is a superior inhibitor of T cell function versus other complex I inhibitors	201
Table 5.5	Canagliflozin is a superior inhibitor of T cell function versus complex I inhibition and GDH inhibition	202
Table 5.6	Early T cell activation is compromised following canagliflozin treatment	205
Table 6.1	Systemic lupus erythematosus patient demographics	222

Table 6.2	Rheumatoid arthritis patient demographics	223
Table 6.3	Antibodies used for nutrient transporter analysis	224
Table 6.4	Antibodies used for T helper cell subset analysis	225
Table 6.5	Panel to identify T helper cell subsets based on chemokine receptor expression	225
Table 6.6	Antibodies used for synovial fluid mononuclear cell analysis	226
Table 6.7	Antibodies used for intracellular transcription factor analysis	227

Acknowledgements

Firstly, I would like to thank Professor Cathy Thornton and Dr. Nick Jones for the opportunity to complete my PhD under their supervision. This project hasn't come without its challenges, especially amidst the COVID-19 pandemic, and I'll always be grateful of their guidance and advice throughout. I'd also like to give thanks to Dr. James Cronin and Dr. Gareth Jones of Bristol University, who have also volunteered their support throughout this project. I can't believe how quickly the past few years have gone, but I've really enjoyed it (when the experiments have worked!) and I'm gutted that it's coming to an end.

Thank you to all of the donors that have volunteered their blood over the years and to nurses that have bled them, as this work would not be possible without their contribution. A special thanks also to Tom, Em, Cynthia, Alethea and Fernando for volunteering their valuable time when nurses haven't been available, I'm really grateful in your help keeping the project ticking along.

It's been great to be able share this experience with some great friends, particularly Oliver Richards, Dr. April Rees and Meg Chambers, who have kept me sane right from the start of this PhD, and more recently Dr. Fernando Ponce Garcia, who's been so helpful in the final stretch of this project. I didn't think I'd meet someone as obsessed with rugby as I am, but I've met my match with Ol, and I think we've slowly made each other worse over the years! I'm looking forward to working alongside most of you over the next few years (and hopefully beyond), I'm sure there's plenty of chatting left to be done as well! Although she's defected from the 2nd floor lab, I'd also like to mention Kathryn Munn, who's also been with me since we did our MSci projects with Cathy, now instead with our (not regular enough) coffee breaks when she comes down from the 4th floor. Thank you to anyone who's helped me in any way over the last few years, particularly to those on the 2nd floor that helped me when I first started in the lab.

Finally, I would like to say a massive thank you to my family – Mam, Dad, Yas, Mamgu and Dadcu. I wouldn't have been able to finish this PhD without your support through the highs and lows. I'm really grateful for all of the sacrifices that you've made for me to be in a position to write this. I'm not sure how much sense it will make when you read it – I'm not sure if it even makes sense to me anymore after all the writing and proofreading – but I hope that you're proud of it.

Abbreviations

α -KG	alpha-ketoglutarate
2-DG	2-deoxyglucose
ACC	acetyl-CoA carboxylase
ACLY	ATP citrate lyase
ADP	adenosine diphosphate
AMP	adenosine monophosphate
AMPK	AMP-activated protein kinase
ANOVA	analysis of variance
APC	antigen presenting cell / allophycocyanin
APS	ammonium persulphate
ATP	adenosine triphosphate
BSA	bovine serum albumin
cana	canagliflozin
CD	cluster of differentiation
CFSE	carboxyfluorescein succinimidyl ester
CPT1a	carnitine palmitoyltransferase 1a
CTL	cytotoxic T lymphocyte
dapa	dapagliflozin
DM α KG	dimethyl α -ketoglutarate
DNA	deoxyribonucleic acid
ECAR	extracellular acidification rate
ELISA	enzyme-linked immunosorbent assay
ERK	extracellular signal-related kinase
ETC	electron transport chain
FBS	fetal bovine serum
FCCP	carbonyl cyanide-p-trifluoromethoxyphenylhydrazine
FDR	false discovery rate

FITC	fluorescein isothiocyanate
FSC	forward scatter
GAPDH	glyceraldehyde 3-phosphate dehydrogenase
GC-MS	gas chromatography-mass spectrometry
GDH	glutamate dehydrogenase
GLUT	glucose transporter
HBSS	Hank's buffered salt solution
HK	hexokinase
HPLM	human plasma-like medium
HRP	horseradish peroxidase
IFN	interferon
IL	interleukin
IRF	interferon regulatory factor
KO	knock out
LAT	large neutral amino acid transporter
LC-MS	liquid chromatography-mass spectrometry
MFI	median fluorescence intensity
MHC	major histocompatibility complex
MS	multiple sclerosis
mTOR	mechanistic target of rapamycin
OCR	oxygen consumption rate
OXPPOS	oxidative phosphorylation
PAGE	polyacrylamide gel electrophoresis
PBS	phosphate buffered saline
PBMC	peripheral blood mononuclear cell
PD-1	programmed cell death protein 1
PE	phycoerythrin
PMN	polymorphonuclear cell

PPP	pentose phosphate pathway
QC	quality control
RA	rheumatoid arthritis
RNA	ribonucleic acid
ROS	reactive oxygen species
RPMI	Roswell Park Memorial Institute
RT	room temperature
SDS	sodium dodecyl sulphate
SEM	standard error of the mean
SFMC	synovial fluid mononuclear cell
SGLT2	sodium glucose co-transporter 2
SLC	solute carrier protein
SLE	systemic lupus erythematosus
SSC	side scatter
T2D	type 2 diabetes mellitus
TBS	tris buffered saline
TCA	tricarboxylic acid
Tcm	central memory T cell
TCR	T cell receptor
Tem	effector memory T cell
TGF	transforming growth factor
Th	T helper cell
TMRE	tetramethylrhodamine, ethyl ester
TNF	tumour necrosis factor
Tnv	naïve T cell
Treg	regulatory T cell

Conferences

1. Jenkins B.J., Jones N., Thornton C.A. Immunological adaptation of NK cells during pregnancy. UK Natural Killer Cells Workshop, 10th January 2020. Oral presentation.
2. Jenkins B.J., Jones N., Thornton C.A. Immunological adaptation of NK cells during pregnancy. Swansea University Medical School Postgraduate Research Conference (Online), 28th – 29th June 2021. Oral presentation.
3. Jenkins B.J., Jones N., Thornton C.A. Immunological adaptation of NK cells during pregnancy. BSI Congress, 28th November – 1st December 2021. Poster presentation.
4. Jenkins B.J., Thornton C.A., Jones N. Canagliflozin impairs T-cell effector function via metabolic suppression in autoimmunity. Swansea University FHMLS Postgraduate Research Conference, 11th – 13th July 2022. Oral presentation.
5. Jenkins B.J., Blagih, J., Hanlon, M.H., Jury, E.C., Veale, D.J., Vousden, K.H., Fearon, U., Sinclair, L.V., Jones, G.W., Vincent. E.E., Jones, N. Canagliflozin impairs T-cell effector function via metabolic suppression in autoimmunity. BSI Congress, 5th December – 8th December 2022. Poster presentation.

Chapter One

Introduction

1 Introduction

1.1 General overview

The human immune system comprises three layers of defence: anatomical barriers, innate immunity and adaptive immunity. Together, these diverse yet integrated mechanisms contribute to the maintenance of systemic equilibrium within the host – protecting against various pathogens such as bacteria, viruses and parasites. A central tenet of successful immune function is the ability to distinguish between self and non-self to maintain host tolerance. Leukocytes are arguably one of the fundamental components of the human immune system, straddling both innate and adaptive immunity. Circulating leukocytes, alongside those found in the lymphatic system, migrate to possible areas of infection where they begin to mount an immune response. Amongst this population of cells are T cells – lymphocytes within the adaptive immune system with specialised roles in the recruitment of other immune cell populations and the clearance of pathogens. The importance of T cell function will be explored comprehensively throughout this thesis.

An appropriate immune response is underpinned by the ability to meet the energetic demands required for this process. Consequently, leukocytes have evolved to integrate a multitude of metabolic pathways to ultimately generate adenosine triphosphate (ATP), the primary cellular energy currency (O'Neill et al., 2016). For example, whilst T cells predominantly metabolise glucose to fuel their effector function, other substrates such as glutamine and fatty acids are also critical in maintaining their cellular processes (Buck et al., 2015). Given the extreme bioenergetic demands of immune cell activation, metabolic reprogramming occurs under these conditions to generate the biosynthetic precursors necessary for cell growth and proliferation (Buck et al., 2015). Upon activation, T cells markedly increase their glucose metabolism, primarily through the upregulation of glycolysis, in a similar manner to cancer cells in a phenomenon typically known as the 'Warburg effect' (Macintyre & Rathmell, 2013).

Autoimmunity is one of several complications that arise from the breakdown of immune system function. Conditions such as rheumatoid arthritis (RA) and systemic lupus erythematosus (SLE) are characterised by the failure to properly recognise self-antigens, leading to chronic inflammation within host tissues (Ospelt, 2017; Tsokos, 2011). Given the

central role that aberrant T cell function plays in such conditions, this has subsequently led to their designation as T cell-mediated autoimmune diseases. Recent advances have revealed that there is a metabolic foundation to the proinflammatory T cell function that precipitates chronic inflammation in autoimmunity (B. Wu et al., 2020). As such, ongoing investigations have focused on identifying metabolic modulators that could alleviate autoimmune disease (Angiari et al., 2020), especially given the debilitating side effects associated with current medications (Li et al., 2017). Since the clinical translation of using novel drugs is challenging, given the toxicity of inhibiting cellular metabolism at a systemic level, other studies have considered repurposing already-approved drugs with established safety profiles in the setting of autoimmunity. For example, type 2 diabetes (T2D) drugs predominantly target cellular metabolism – a property which has been exploited to manipulate T cell metabolism in models of autoimmune disease (Kang et al., 2013; Yin et al., 2015). Consequently, the T2D drug metformin has shown therapeutic benefit in clinical trials of autoimmunity (Gharib et al., 2021; Sun, Geng, et al., 2020), further underlining the potential of repurposing similar drugs in this disease setting.

1.2 T cells

T cells are specialised lymphocytes that develop within the thymus that play an important role in the adaptive immune response. They are distinct from other immune cell types in their expression of the T cell receptor (TCR) on their cell surface, which is randomly rearranged in order to recognise a wide variety of antigen targets and generate an immune response. T cells can be classified into several different subsets based upon their unique effector function – the two major subtypes being CD4⁺ T helper (Th) cells and CD8⁺ cytotoxic T cells. For example, CD4⁺ T cells produce cytokines to recruit other immune cell populations to the site of inflammation, whilst CD8⁺ T cells are directly involved in the clearance of virally-infected cells through the release of cytotoxic mediators.

1.2.1 T cell receptor

Most T cells express a TCR heterodimer consisting of an α and β polypeptide (Figure 1.1A). Both contain several random elements to provide wide variety for antigen recognition (Davis & Bjorkman, 1988). Only around 5% of T cells express a TCR containing γ and δ polypeptides (Figure 1.1B), making them rare in secondary lymphoid organs, but are

more readily found in the periphery in tissues such as the skin, lung and gut (Ribot et al., 2021). Interestingly, $\gamma\delta$ T cells perform functions characteristic of both the innate and adaptive immune system, including: antigen-sensing independent of MHC class I/II; killing of infected cells and microbes similar to NK cells; and acting as professional antigen-presenting cells (Gustafsson et al., 2020). Since $\gamma\delta$ T cell responses are not restricted to MHC or tumour-associated neoantigens, this has made them an interesting prospect in cancer immunotherapy research (Sebestyen et al., 2020; Silva-Santos et al., 2019).

CD3 proteins also comprise the TCR complex, arranged as CD3 $\gamma\epsilon$ and CD3 $\delta\epsilon$ heterodimers and a CD3 $\zeta\zeta$ homodimer. The association of CD3 proteins with the TCR are required for its cell-surface localisation (Shah et al., 2021). Further information surrounding the downstream signalling pathways engaged following TCR-dependent activation will be detailed during later sections (see Chapter 1.2.4 and 1.2.5).

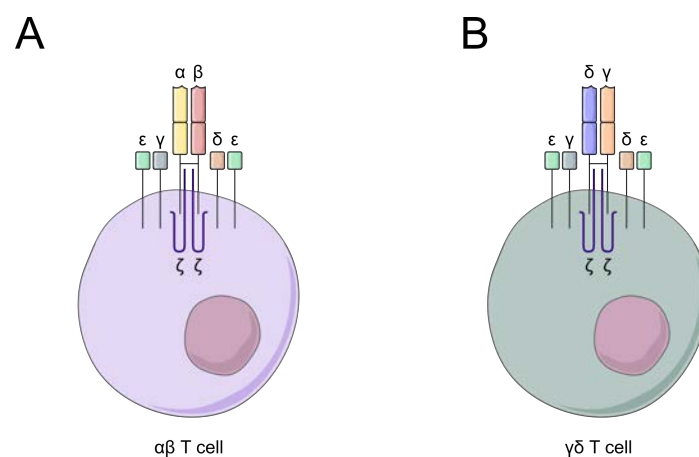


Figure 1.1 – Components of the T cell receptor

(A-B) The T cell receptor complex consisting of either (A) TCR α and TCR β chains or (B) TCR γ and TCR δ chains, alongside signalling molecules CD3 ϵ , CD3 γ , CD3 δ and CD3 ζ .

1.2.2 T cell development

T cells originate in the bone marrow as haematopoietic stem cells before differentiation towards a common lymphoid progenitor. They later migrate to the thymus where they progress to an immature stage of T cell development and are known as thymocytes. Here, these cells are committed to the T cell lineage and undergo a series of divisions, TCR rearrangements and positive- and negative-selection resulting in mature, functional T cells (Figure 1.2).

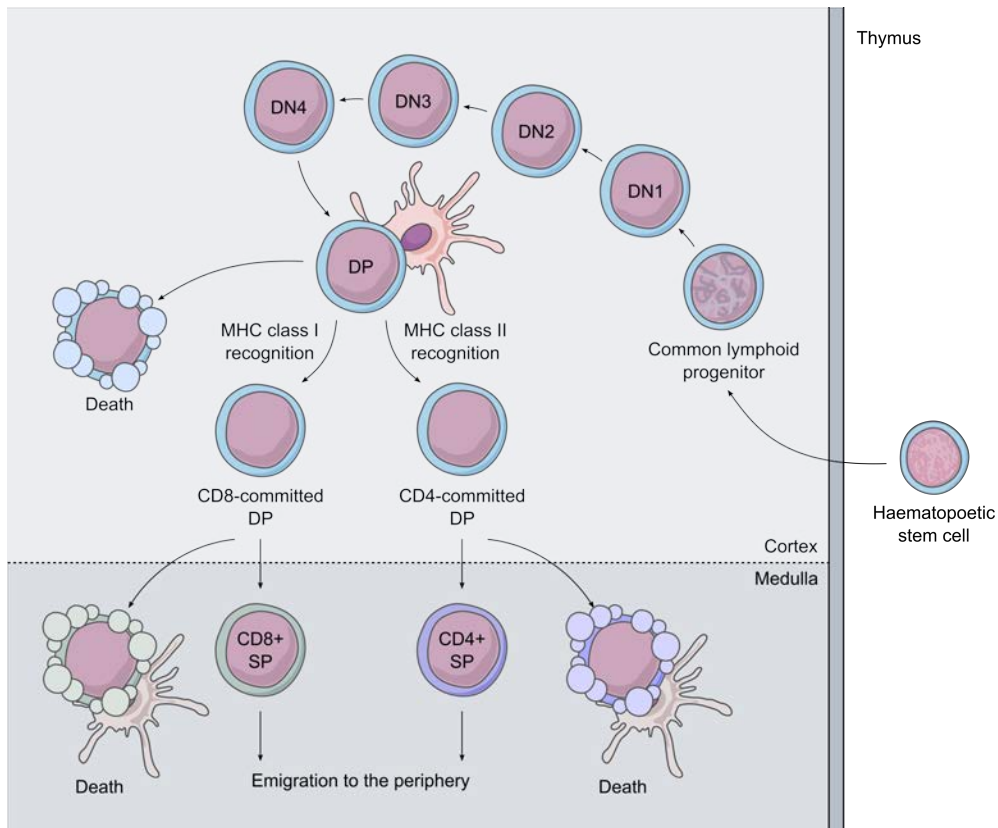


Figure 1.2 – Overview of T cell development

Haematopoietic stem cells originating in the bone marrow migrate to the thymus and become developing thymocytes. Double negative (DN) thymocytes undergo several rounds of TCR rearrangement and division to generate a functional TCR. Upregulation of CD4 and CD8 gives rise to double positive (DP) thymocytes. Appropriate interaction with self-antigens expressed on MHC classes I and II is required for effective maturation. Double positive thymocytes that react with MHC class I successfully become CD8⁺ T cells, whilst those that react with MHC class II successfully become CD4⁺ T cells. Too weak an interaction (positive selection) and too strong an interaction (negative selection) results in premature apoptosis. Survival of these processes results in naïve T cells that are ready to migrate to the periphery. Adapted from (Germain, 2002).

Initially, common lymphoid progenitors arrive in the thymus, becoming double negative thymocytes, whereby they lack the expression of a functional TCR, CD4 and CD8. Thymocytes can only mature to an active T cell if it survives the process of developing a functional TCR (Germain, 2002). This double negative phase of T cell development can be subdivided into four distinct stages based on the surface expression of CD25 and CD44: DN1, CD25⁻CD44⁺; DN2, CD25⁺CD44⁺; DN3, CD25⁺CD44⁻; DN4, CD25⁻CD44⁻ (Godfrey et al., 1993). Double negative thymocytes can develop into $\alpha\beta$ -T cells or $\gamma\delta$ -T cells, depending on

the TCR complex present (see Chapter 1.2.1). Cells progressing through the $\alpha\beta$ pathway undergo several rounds of TCR rearrangement during the double negative phase in an attempt to generate a functional TCR. Initially, the TCR- β locus is rearranged following upregulation of recombination activating genes (RAG)-1 and -2 (Mombaerts et al., 1992; Shinkai et al., 1993). DN3 thymocytes later express an invariant α -chain called the pre-TCR α which pairs with the TCR β -chain to prevent any further rearrangement (Germain, 2002). Following successful β -selection, late-DN3 to DN4 thymocytes undergo several rounds of proliferation prior to recombination of the TCR- α locus and subsequent formation of the mature TCR. At this stage, thymocytes also begin to express both co-receptor proteins – initially CD8, followed by CD4 – and are termed double positive (Robey & Fowlkes, 1994). Double positive thymocytes migrate deeper into the thymic cortex where they interact with cortical epithelial cells that highly express self-antigens on both MHC class I and II (von Boehmer et al., 1989). Their survival requires an appropriate response following ligation of the TCR – thymocytes must react well following interaction with MHC ligands, therefore inadequate signalling in response to self-antigens results in apoptosis (positive selection) (Germain, 2002). However, too robust of a reaction to MHC ligands also consigns developing thymocytes to apoptosis, which is tested again deeper within the thymus by medullary epithelial cells or dendritic cells (negative selection) (Germain, 2002). Double positive thymocytes that form a suitable interaction between TCR and MHC class I become CD8+ T cells, whereas those that form a suitable interaction between TCR and MHC class II become CD4+ T cells. Most thymocytes fail to successfully endure positive selection, nevertheless those that successfully undergo this development process migrate to the periphery.

1.2.3 T cell subset populations

Whilst CD4+ and CD8+ T cells are selected within the thymus (see Chapter 1.2.2), T cells undergo further differentiation in the periphery to specialised cells with different functions. CD4+ T helper (Th) cells play an important role in the adaptive immune response through the secretion of cytokines and subsequent recruitment and activation of other immune cell types – including macrophages, B cells and CD8+ T cells – whilst also being particularly important in the maturation of B cells into either plasma cells or memory B cells. CD4+ T cells can be subdivided into distinct subsets based on the effector cytokines they produce (Table 1.1; Figure 1.3).

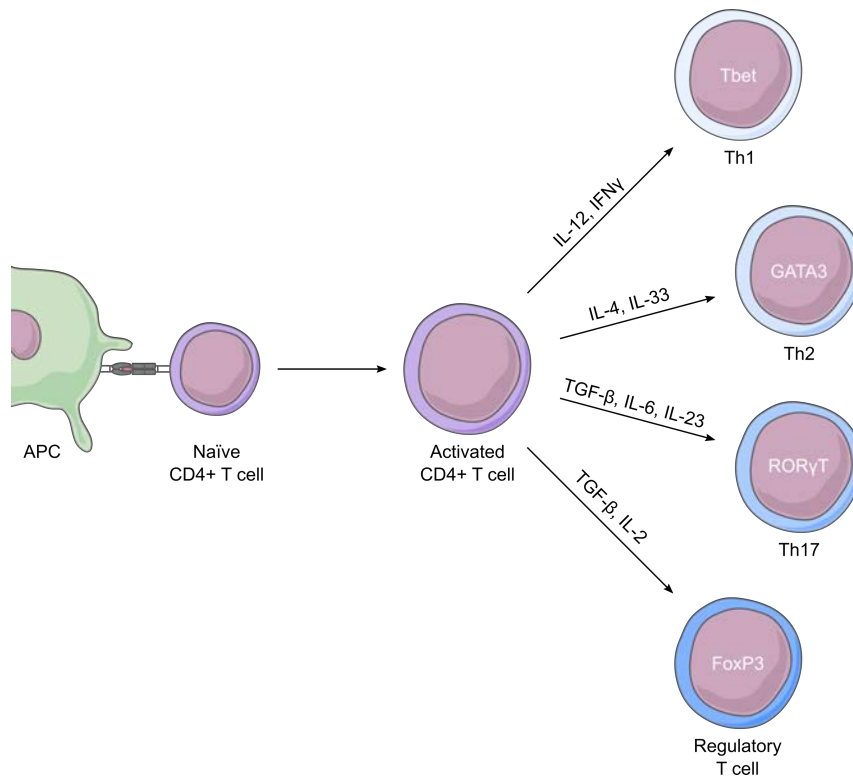


Figure 1.3 – Overview of the polarising conditions associated with each major T helper subset

The four predominant T helper cell subsets: Th1, Th2, Th17 and regulatory T (Treg) cells. The cytokines present during T cell activation influence the differentiation of T cells. Development towards a specific lineage requires the expression of signature transcription factor: Tbet (Th1), GATA3 (Th2), ROR γ T (Th17) or FoxP3 (Treg). Adapted from (Zhu & Paul, 2008).

Th1 cells play an important role in mediating the immune response against intracellular pathogens (Mosmann & Coffman, 1989; Zhu & Paul, 2008). CD4⁺ T cells become committed towards this lineage following activation of the transcription factor Tbet, which is favoured by several factors including IFN γ , IL-2 and IL-12, driving intracellular signalling through STAT1, -5 and -4, respectively (Raphael et al., 2015). Particularly important, expression of the IL-12 receptor complex is induced by robust TCR activation and is thereafter maintained by IL-2 and IFN γ stimulation, promoting further expression of IFN γ (Afkarian et al., 2002; Szabo et al., 1997). Characteristically, Th1 cells are potent producers of IFN γ and IL-2, however, they have also more recently been associated with the production of lymphotoxin α (LT α), tumour necrosis factor (TNF) and granulocyte-macrophage colony-stimulating factor (GM-CSF) (Raphael et al., 2015; Zhu & Paul, 2008). IFN γ production is important in the activation of macrophages and enhancing their phagocytic capacity

(Schroder et al., 2004; Suzuki et al., 1988), whilst the production of IL-2 is important for the induction of memory in both CD4+ and CD8+ T cells (Darrach et al., 2007; Williams et al., 2006). Given their well-described proinflammatory function, Th1 cells have been closely associated with the induction of autoimmune disease (see Chapter 1.4). For example, LT α has been identified as a biomarker of disease severity in multiple sclerosis (MS) patients (Selmaj et al., 1991), whilst LT α -deficient mice are resistant to experimental autoimmune encephalomyelitis (EAE; a murine model of MS) (Suen et al., 1997).

Conversely, Th2 cells are involved in the clearance of extracellular parasites and contribute to allergy and atopic disease (Zhu & Paul, 2008). Differentiation towards the Th2 phenotype occurs in response to weak TCR activation in the presence of IL-2 and IL-4, culminating in subsequent GATA3 and STAT6 signalling (DuPage & Bluestone, 2016). Expression of the IL-4 receptor is increased during Th2 differentiation, whilst IL-2 receptor expression is greater versus their Th1 counterparts (Zhu & Paul, 2008). Th2 cells are most associated with the production of IL-4, IL-5 and IL-13, but also known to produce IL-9, IL-10 and IL-25 (Raphael et al., 2015). Crucially, IL-4 mediates antibody class switching in B cells – favouring IgE – which leads to the secretion of histamines and serotonin in the allergy response (Kopf et al., 1993). An additional role has been described for IL-4 in supporting the function of M2 macrophages involved in tissue repair following helminth infection (Chen et al., 2012). Moreover, IL-13 plays a similar role through the clearance of parasitic infection and promoting airway hypersensitivity (Urban et al., 1998), meanwhile IL-5 plays a critical role in the maturation and recruitment of eosinophils (Coffman et al., 1989).

Th17 cells facilitate and shape immune responses to extracellular pathogens such as bacteria and fungi (Zhu & Paul, 2008). IL-23 was initially identified as the primary driver towards the Th17 lineage, however, shortly afterwards IL-6 and TGF- β were also implicated in this process, stabilising the expression of key transcription factor retinoic acid receptor-related orphan receptor γ T (ROR γ T) (Ivanov et al., 2006; Langrish et al., 2005; Veldhoen et al., 2006). As their name suggests, this T cell subset produces proteins of the IL-17 family, whilst also producing IL-21 and IL-22, but are known primarily as a major source of both IL-17A and IL-17F (Zhu & Paul, 2008). The IL-17 receptor signalling pathway is engaged following ligation with either IL-17A or IL-17F, with the former displaying a greater binding affinity, suggesting that both cytokines facilitate similar effector functions (Hymowitz et al., 2001). Indeed, IL-17 family members are involved in the activation of other immune cell types including

neutrophils and macrophages (Fossiez et al., 1998; Jovanovic et al., 1998). However, given the proinflammatory nature of Th17 cells, there is a wealth of evidence demonstrating their involvement in autoimmune disease pathogenesis (see Chapter 1.4).

Regulatory T cells (Treg) are required for the maintenance of immunological self-tolerance (Sakaguchi, 2004). As such, their expansion and function are important in settings such as autoimmune disease, where their immunoregulatory properties alleviate disease severity (Costantino et al., 2008). Expression of the signature transcription factor FoxP3 is essential for the development of both Treg cells derived directly from the thymus (tTreg) or Treg cells induced (iTreg) by the presence of IL-2 and transforming growth factor- β (TGF- β) (Chen et al., 2003; Sakaguchi, 2004). Immunosuppressive Treg cell function is primarily supported by their production of anti-inflammatory mediators such as IL-10 and TGF- β (Sakaguchi, 2004).

Table 1.1 - Characteristics of CD4+ T helper subsets

Subset	Transcription Factor	Effector cytokine(s)	Function
Th1	Tbet	IFN γ	Immunity against intracellular pathogens such as virus, microbes Autoimmunity and inflammation
Th2	GATA3	IL-4, IL-5, IL-13	Immunity against extracellular pathogens (parasites such as helminths) Allergy / asthma / IgE
Th9	PU-1	IL-9	Allergy Autoimmunity
Th17	ROR γ T	IL-17A, IL-17F, IL-22	Immunity against extracellular pathogens Autoimmunity and inflammation
Th22	AHR	IL-22	Infection Tissue regeneration and wound healing
Tfh	Bcl-6	IL-21	Antibody production
Treg	Foxp3	IL-10, IL-35, TGF- β	Immunosuppression Tolerance

adapted from (Jiang & Dong, 2013)

Other peripheral T helper subsets have more recently been identified. Previously characterised as Th2 cells, IL-9-producing T cells have now become a distinct Th9 subset, where they are primarily involved in allergic responses (Tan & Gery, 2012). Furthermore, recently identified Th22 cells predominantly produce IL-22 to maintain epidermal immunity (Duhon et al., 2009), but are also closely related to Th17 cells and therefore implicated in several autoimmune diseases (Tian et al., 2013). Finally, follicular T helper (Tfh) cells promote B cell activation and antibody production to trigger germinal centre formation (Jiang & Dong, 2013).

1.2.4 T cell activation

T cells can be further classified in terms of their activation status. Successful T cell activation is initiated through the simultaneous engagement of the TCR (signal 1) and co-stimulatory molecules (signal 2) at the immunological synapse (Figure 1.4). Ultimately, this results in cytokine-mediated T cell differentiation and expansion (signal 3; see Chapter 1.2.3).

MHC-bound antigen peptides are presented to the TCR by professional antigen-presenting cells (APCs), which also express co-stimulatory ligands that bind to CD28. Conversely, co-inhibitory ligands expressed on the surface of APCs engage their respective receptors on T cells to regulate the consequent immune response. Together, this interaction between T cell and APC determines which signalling pathways are activated downstream to shape the resulting effector functions (see Chapter 1.2.5).

Initially naïve T cells (T_{nv}) are maintained in the periphery via TCR engagement with self-peptide MHC molecules and exposure to IL-7 (Sprent & Surh, 2011). Eventually, extrathymic T_{nv} cells migrate to secondary lymphoid organs, where they encounter various professional APCs, most notably dendritic cells (DCs) (Miller et al., 2004). Here, antigen peptides are presented to CD4⁺ T cells via MHC class II, thereby forming an immunological synapse (Miller et al., 2004). Further co-stimulatory ligands are presented on the surface of mature DCs, whereupon CD80 and CD86 probably represent the most important co-stimulatory pathway (Hubo et al., 2013). Typically, CD80 and CD86 bind CD28, inducing a strong activation signal within T cells (Lenschow et al., 1996), however, the co-inhibitory receptor CTLA-4 is upregulated during T cell activation, competing with CD28 for interaction with CD80 and CD86 (Greene et al., 1996). Given that CTLA-4 binds both ligands with higher

affinity than CD28, this allows the regulation of T cell activation and aims to prevent hyperactivation (Hubo et al., 2013).

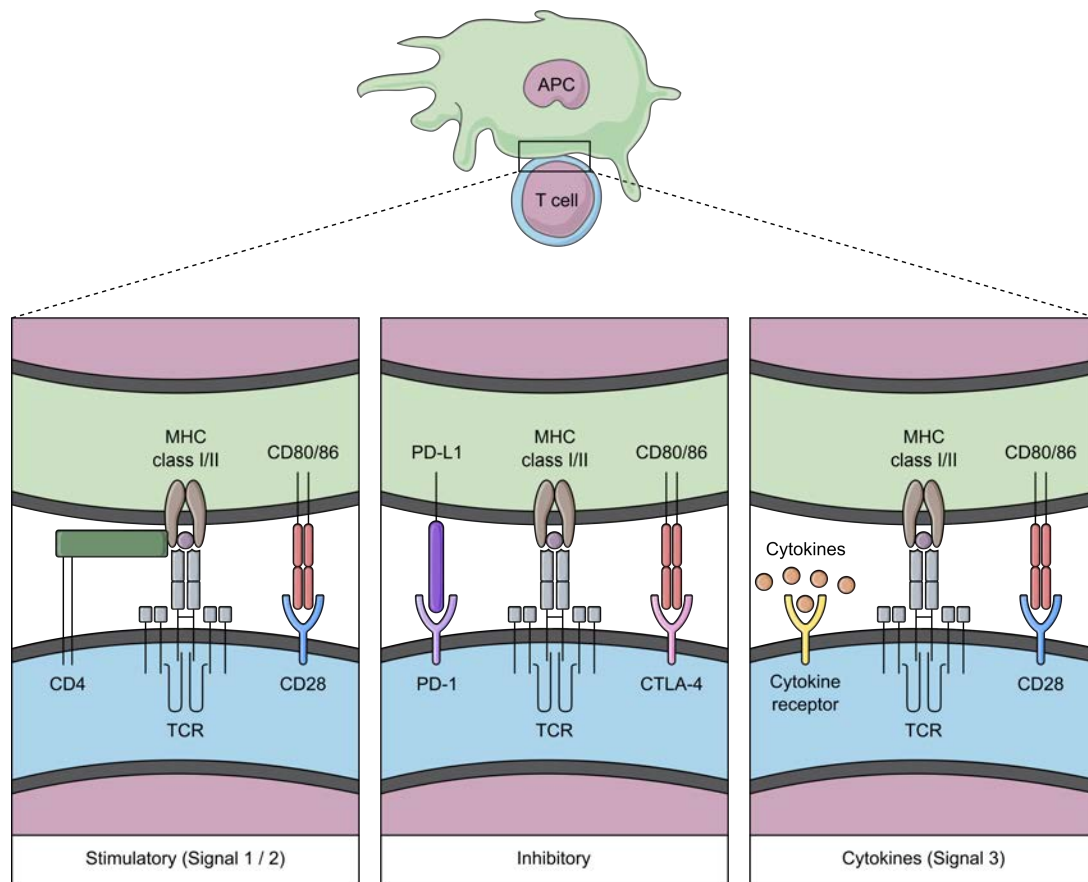


Figure 1.4 – Stimulatory and inhibitory conditions regulating T cell activation

Overview of the stimulatory and inhibitory molecules involved in T cell activation. Interaction between the T cell receptor (TCR) and the antigen peptide presented on MHC class I/II initiates activation (signal 1). This is further induced by the co-receptor CD4 (or CD8) and interaction between CD28 and co-stimulatory molecules CD80/CD86 (signal 2). In contrast, T cell activation is modulated by the interaction between inhibitory receptors PD-1 and CTLA-4 with PD-L1 and CD80/86, respectively. The cytokine milieu present during activation determines differentiation towards distinct lineages (signal 3).

Co-stimulation is particularly important in T cell activation, as TCR engagement alone culminates in anergy (Smith-Garvin et al., 2009). The importance of CD28 co-stimulation is well-documented, previously shown to promote T cell proliferation, rewire cellular metabolism, and induce cytokine production (Acuto & Michel, 2003). Phosphoinositide 3-kinase (PI3K) is a major downstream target of CD28, where it is involved in the Akt-mediated

nuclear localisation of NFAT and subsequent transcription of IL-2 (Burr et al., 2001; Okkenhaug et al., 2001). The resulting IL-2 produced further enhances T cell activation – especially T_H cell activation – through binding to its associated receptor in an auto- or paracrine manner (Boyman & Sprent, 2012; Or et al., 1992). Alternatively, CD28 can also promote IL-2 production by inducing arginine methylation on VAV1 (Blanchet et al., 2005). Functionally related to CD28, the eponymous inducible co-stimulator (ICOS) becomes inducibly expressed on the surface of activated T cells and interacts with its cognate ligand (Hutloff et al., 1999; Yoshinaga et al., 1999). Although ICOS does not induce IL-2 gene transcription like CD28, several functions are shared between both molecules including the regulation of T cell proliferation and survival (Coyle et al., 2000; Harada et al., 2003). Members of the tumour necrosis factor receptor family are also involved in co-stimulation, amplifying T cell activation through similar mechanisms as CD28 and ICOS, albeit through alternate downstream signalling pathways (Watts, 2005). Given that a large number of the same genes are regulated by the aforementioned co-stimulatory receptors, the likely reason for such is a consequence of the timing of their expression. For example, CD28 is critical for early T cell activation, whereas ICOS, OX40 and 4-1BB are important in sustaining the immune response, with the latter two also pivotal in the generation of memory (Smith-Garvin et al., 2009).

Necessary regulatory mechanisms are required to limit T cell activation to maintain self-tolerance and prevent the development of autoimmunity. Co-inhibitory molecules oppose the function of co-stimulatory molecules, which include cytotoxic T lymphocyte protein 4 (CTLA-4) and programmed cell death protein 1 (PD-1), whereby their cell surface expression peaks 24-48 h post-activation (Smith-Garvin et al., 2009). CTLA-4 competes with CD28 for interaction with co-stimulatory ligands CD80 and CD86 (Greene et al., 1996). However, it is unclear how CTLA-4 dampens T cell function, with initial evidence suggesting the recruitment of phosphatases to the TCR complex that subsequently limit downstream signalling pathways (Lee et al., 1998). Alternatively, it has been proposed that CTLA-4 is able to facilitate the endocytosis of CD80 and CD86 from the surface of APCs, preventing any further stimulation through CD28 (Qureshi et al., 2011). On the other hand, PD-1 has specialised ligands, PD-L1 and PD-L2, with the former expressed on several immune and non-immune cell types, whereas the latter is reserved for expression on professional APCs (Zhong et al., 2007). PD-1 functions by inhibiting PI3K – whose activation is induced by co-stimulation – leading to suppressed cytokine production, the loss of cell survival and the induction of

apoptosis (Keir et al., 2008). Together, these mechanisms demonstrate the delicate interplay that occurs in successful regulation of the induction, maintenance and modulation of T cell activation following engagement of the TCR and ligation of co-receptors.

Upon recognition of the unique MHC class II peptide and simultaneous co-stimulation that is necessary to surpass the signalling threshold required for successful T cell activation, naïve T cells undergo rapid proliferation and cytokine production to become effector memory T cells that serve to eliminate the recognised pathogen (Figure 1.5). Following successful clearance of the immunological threat, these effector memory T cells either succumb to apoptosis, or transition into long-lived central memory T cells that can rapidly expand and perform effector functions following re-encounter with the cognate antigen (Figure 1.5). Individual subsets within the memory T cell compartment can be identified based upon their heterogenous expression of cell surface markers such as CD45RO, CCR7, CD28 and CD95 (Mahnke, Brodie, et al., 2013). Naïve T cells are characterised as CD45RO⁻CCR7⁺CD28⁺CD95⁻ T cells that also express high levels of the homing receptor CD62L to promote their localisation to the lymph nodes (Mahnke, Brodie, et al., 2013). Upon transition into effector memory T cells, CD62L becomes downregulated to allow migration into other regions within the periphery, whilst CD45RO and CD95 become upregulated prior to the loss of both CD28 and CCR7 (Mahnke, Brodie, et al., 2013). Central memory T cells exhibit a phenotype between that of effector memory and naïve subsets – CD45RO⁺CCR7⁺CD28⁺CD95⁺ T cells that also express CD62L for their containment within the lymph nodes and related secondary lymphoid organs (Mahnke, Brodie, et al., 2013). This highly dynamic process allows the conversion of T cells between hyperproliferative and functionally active states in order to support a successful immune response to both inexperienced and previously-experienced cognate antigens.

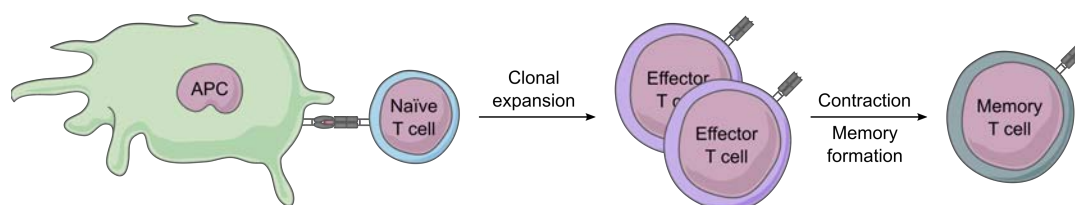


Figure 1.5 – Overview of T cell memory

Upon recognition of their cognate antigen, naïve T cells undergo rapid clonal expansion to become highly-functional effector T cells. Following clearance of the encountered pathogen, effector T cells either become long-lived memory T cells or succumb to apoptosis.

1.2.5 T cell signalling

Ligation between the TCR and peptide-MHC complexes, presented to T cells by professional APCs, initiates downstream signal transduction pathways to generate an immune response (Figure 1.6). This interaction results in the recruitment of CD4 or CD8 co-receptors to the TCR complex, following binding to either MHC class II or I, respectively (Parnes et al., 1989). The SRC family protein tyrosine kinase Lck binds to the intracellular regions of either co-receptor, where it begins to phosphorylate the ITAM motifs within the intracellular CD3 domains of the TCR to enable the anchoring and activation of the protein tyrosine kinase ZAP70 (Barber et al., 1989; Chan et al., 1992; Samelson et al., 1986). Here, ZAP70 phosphorylates its major downstream target, transmembrane adaptor linker for activation of T cells (LAT), to allow aggregation and docking of further signalling molecules such as phospholipase C γ (PLC γ), IL-2-inducible tyrosine kinase (ITK) and VAV1 (Horejsi et al., 2004; Paz et al., 2001). Importantly, the LAT signalosome formed propagates signal transduction in three major pathways: nuclear factor of activated T cells (NFAT), nuclear factor- κ B (NF- κ B) and mitogen-activated protein kinase/extracellular signal-regulated kinase (MAPK/ERK). PLC γ is central to this process, whereby it hydrolyses phosphatidylinositol-4,5-bisphosphate (PI-4,5-P₂) at the plasma membrane to activate the secondary messengers diacylglycerol (DAG) and inositol triphosphate (IP₃), which in turn activate several signalling mediators (Horejsi et al., 2004).

Once mobilised, IP₃ localises to the endoplasmic reticulum (ER) where it binds to its receptor to activate calcium channels on the ER membrane and induces the influx of calcium into the cytoplasm (Putney, 1987). Subsequently, low levels of calcium within the ER causes the clustering of stromal interaction molecules (STIM1) on the ER membrane, leading to the activation of calcium release-activated channels (CRAC) on the plasma membrane (Srikanth & Gwack, 2013). The resulting influx of calcium from the extracellular space into the cytosol aggregates and binds calmodulin and activates calcineurin, ultimately activating NFAT and facilitating its nuclear translocation.

DAG is involved in the induction of multiple signalling pathways. One of these downstream targets is protein kinase C (PKC). Particularly important in T cells, DAG activates PKC θ , which phosphorylates CARMA1 to allow it to function as a scaffold protein (Wang et al., 2004). This allows the subsequent binding of BCL-10 and K63-ubiquitinated TRAF6 to the cytosolic domain, facilitating further recruitment of NF- κ B signalling molecules such as TAK1

and IKK- β (Gaide et al., 2002; Sun et al., 2004). Phosphorylation events between TAK1, IKK- β and I κ B eventually consign I κ B to proteasomal degradation, leading to the nuclear translocation of RelA and p50 and their binding to the NF- κ B response element (Hinz & Scheidereit, 2014). Together with NFAT signalling, activation of NF- κ B allows the complete transcription of IL-2 (Shaw et al., 1988; Verweij et al., 1991).

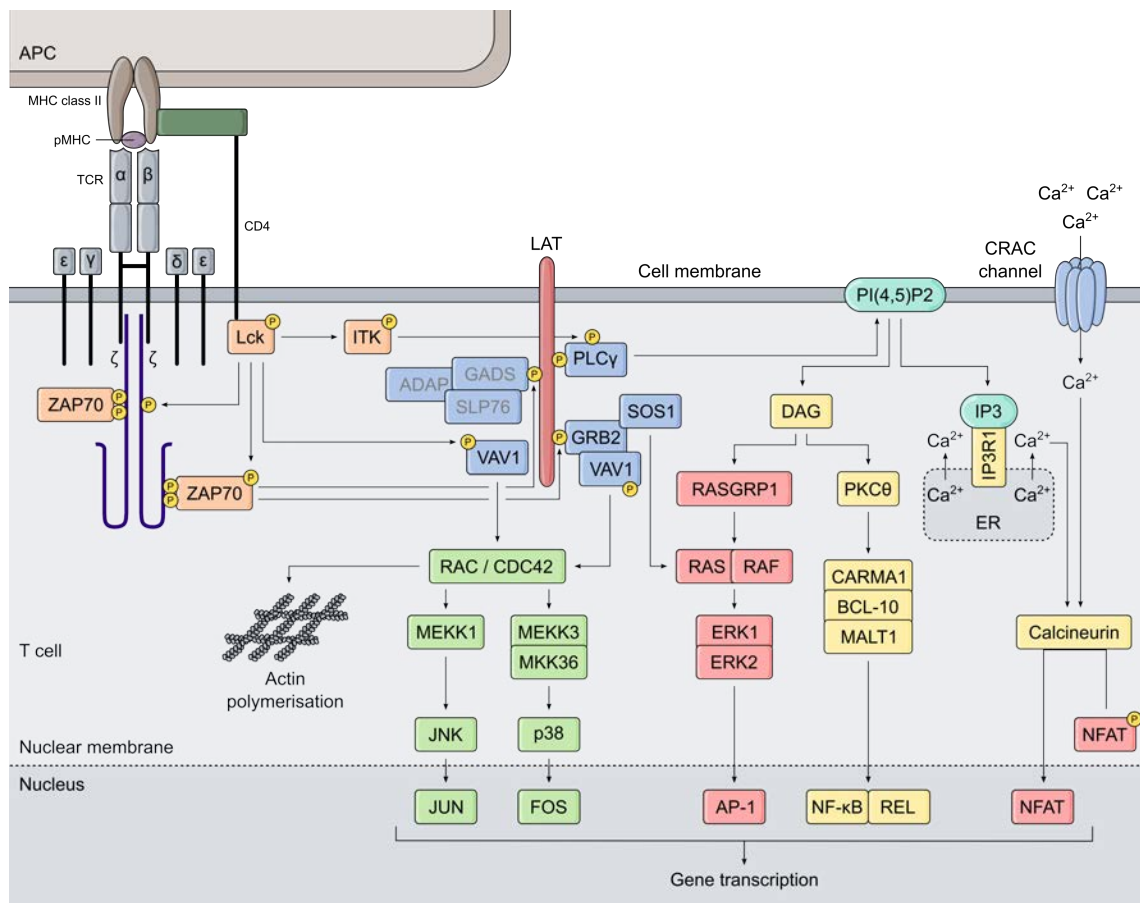


Figure 1.6 – T cell receptor signalling cascade

Overview of the T cell signalling cascade. Upon engagement of the T cell receptor (TCR), Lck and ZAP70 are recruited and phosphorylated to establish the LAT signalosome. Here, several effector molecules are recruited to engage three major downstream signalling pathways: the NFAT, MAP kinase and NF- κ B signalling pathways. Adapted from (Gaud et al., 2018).

Simultaneously, DAG also engages the MAPK/ERK pathway, initially binding to the C1-domain of RasGRP1 (Carrasco & Merida, 2004). There is a corresponding signalling cascade through Ras/Raf and ERK, culminating in the activation of activator protein 1 (AP-1) within the nucleus (D'Ambrosio et al., 1994; Roose et al., 2005). Ras/Raf signalling is also amplified by

interaction with SOS1, which is involved earlier in the TCR signalling pathway when it is recruited by the LAT signalosome (Zhang et al., 1998). Alternate constituents of the MAPK/ERK pathway are also engaged by TCR signalling. For example, VAV1 – also recruited following LAT phosphorylation – is a GTP exchange factor capable of activating RAC, as well as possibly CDC42 (Gaud et al., 2018). Phosphorylation of these Rho family GTPases plays an important two-pronged role, inducing actin polymerisation, in addition to the downstream activation of the transcription factors JUN and FOS. Collectively, the activity of the aforementioned transcription factors results in, but is not limited to, T cell proliferation, migration and effector function.

1.3 T cell metabolism

The influence of cellular metabolism on leukocyte phenotype and function is a burgeoning area of immunology. Termed ‘immunometabolism’, this provides a framework for understanding the dynamic adaptations in leukocytes upon activation and engaging effector functions. Critically, metabolic adaptations are induced to meet the energetic demands of the immune response, which is achieved through the production of ATP, the energy-providing molecule of the cell (O'Neill et al., 2016). ATP can be derived through the metabolism of numerous substrates – including glucose, amino acids and lipids – through a number of integrated cellular pathways. The breakdown of ATP to ADP and inorganic phosphate is an exothermic reaction, whereby the hydrolysis of the phosphoanhydride bond releases the energy required for cellular function. However, cellular metabolism is not only required for the production of ATP, but is also essential in the generation of biosynthetic intermediates needed in various cellular processes (O'Neill et al., 2016).

T cells primarily metabolise glucose for their energy production, wherein ATP is typically derived from either glycolysis only, or complete glucose metabolism through glycolysis, the link reaction, the TCA cycle and oxidative phosphorylation (OXPHOS) (Buck et al., 2015). The ATP generated through these pathways is used to drive cellular functions such as proliferation and cytokine production, particularly following activation through the TCR (see Chapter 1.3.6). However, T cells are not restricted to glucose metabolism, where they can utilise alternative substrates such as amino acids and lipids to fuel these metabolic processes (Buck et al., 2015). Importantly, there are several unique metabolic programmes

that underpin distinct aspects of T cell fate and function, which will be outlined throughout the coming sections.

1.3.1 Substrate transportation

Metabolites are taken up by T cells through a range of transporters spanning the plasma membrane (Figure 1.7). Glucose uptake is regulated by solute carrier protein family 2A (SLC2A), more commonly referred to as glucose transporters (GLUT). Murine CD4⁺ T cells express GLUT1, -3, -6 and -8 (Macintyre et al., 2014). Of these GLUT family members, GLUT1 and GLUT3 are the most abundant on T cells, with relatively low expression of the other two transporters, comparatively (Macintyre et al., 2014). Inhibition of GLUT1 reduced the proliferation and cytokine production of activated T cells, underlining the importance of glucose uptake in T cell effector function (Macintyre et al., 2014). Upon activation, the upregulation of GLUT1 is an mTORC1-dependent process (Howden et al., 2019), with MYC inhibition having little effect on the activation-induced expression of GLUT1, exceeding normal expression in some cases (Marchingo et al., 2020). Additionally, activated T cells also express the transporters necessary for lactate export – SLC16A1, SLC16A3 and SLC16A6 (Howden et al., 2019; Pucino et al., 2017).

Amino acid uptake is controlled by a series of different transporters. Most importantly, large neutral amino acids are taken up by SLC7A5, through the 'leucine-preferring' system L transporter (Sinclair et al., 2013). Failure to take up amino acids through this transporter prevents the metabolic reprogramming necessary upon T cell activation, ultimately impairing T cell function (Sinclair et al., 2013). Sustained amino acid uptake via SLC7A5 is essential for the expression of the key metabolic modulators mTORC1 and MYC (Sinclair et al., 2013). Single-cell assays have been developed to monitor uptake through SLC7A5, where it has been found that kynurenine, the immunomodulatory tryptophan metabolite, can enter T cells via this transporter (Sinclair et al., 2018). Likewise, SLC1A5 is another critical amino acid transporter expressed by T cells (Nakaya et al., 2014). Also known as ASCT2, this transporter facilitates rapid glutamine uptake following T cell activation (Nakaya et al., 2014). In the absence of glutamine uptake, T cells fail to upregulate mTORC1 upon activation and cannot properly differentiate towards typical effector lineages (Nakaya et al., 2014). Proteomic analyses have revealed that numerous other amino acid transporters

are expressed on activated T cells to facilitate the substrate uptake needed for biosynthesis (Howden et al., 2019; Marchingo et al., 2020).

In contrast, fatty acid transportation is not restricted to solute carrier proteins. Instead, fatty acid uptake is controlled at the plasma membrane by multiple methods including fatty acid transport proteins, fatty acid binding proteins and the transporter CD36 (Glatz et al., 2010). Some studies have demonstrated that fatty acids might readily diffuse across the plasma membrane in T cells (Rossetti et al., 1997; Szamel et al., 1989). Passive diffusion appears to be possible by both short-chained fatty acids (SCFAs) and long-chained fatty acids (LCFAs), although some transporter proteins might also be involved in these processes (Park et al., 2015; Rossetti et al., 1997; Szamel et al., 1989).

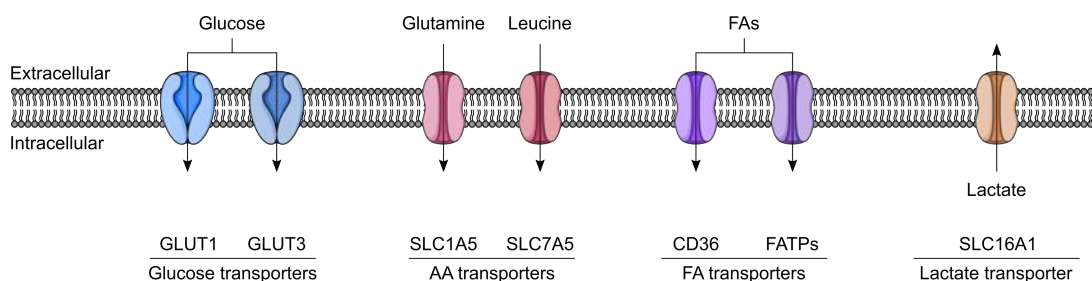


Figure 1.7 – Summary of the substrate transporters used by T cells

Overview of the main substrate transporter proteins utilised by T cells. Glucose is primarily taken up from the extracellular space via GLUT1 and GLUT3 – particularly following T cell activation. SLC1A5 and SLC7A5 are primarily responsible for the uptake of the amino acids glutamine and leucine, respectively. Fatty acids (FAs) can be taken up via transporter proteins including CD36 and FA transporter proteins (FATPs), whilst there is some evidence to suggest that they can readily diffuse across the plasma membrane. SLC16A1 is essential for the export of the glycolytic product, lactate, to maintain increased flux through this pathway.

1.3.2 Glycolysis

Glycolysis is a metabolic pathway that involves the breakdown of a six-carbon monosaccharide – usually glucose, although not limited to – through a series of tightly-regulated enzyme-catalysed reactions, resulting in the net generation of two molecules of pyruvate, two molecules of NADH + H⁺ and two molecules of ATP (Figure 1.8). These reactions occur in the cytoplasm and are generally regarded as inefficient due to the low number of ATP molecules produced per glucose molecule. Although four ATP molecules are produced

during glycolysis, two molecules of ATP are expended throughout this series of enzymatic reactions, hence only a net gain of two ATP molecules.

The first reaction in the glycolytic pathway is the phosphorylation of glucose, which is catalysed by hexokinase and serves to retain glucose within the cell. However, this is an energy-intensive process, requiring the expenditure of one ATP molecule. Subsequently, glucose 6-phosphate, the phosphorylated product, is converted into fructose 6-phosphate in a reaction catalysed by phosphoglucose isomerase. Alternatively, glucose 6-phosphate can act as a substrate for the pentose phosphate pathway (PPP), wherein pentoses, nucleotide precursors and NADPH are generated. In the following glycolytic reaction, fructose 6-phosphate is further phosphorylated by phosphofructokinase (PFK) to form fructose 1,6-bisphosphate. This is the second and final energy-dependent reaction, in which one ATP molecule is required. The phosphorylation of fructose 6-phosphate to fructose 1,6-bisphosphate is irreversible and signifies the commitment of the initial glucose substrate towards glycolysis. Destabilisation of the hexose ring in the previous reaction allows the enzyme aldolase to catalyse the conversion of fructose 1,6-bisphosphate into two three-carbon molecules: glyceraldehyde 3-phosphate and dihydroxyacetone phosphate. Triosephosphate isomerase rapidly converts dihydroxyacetone phosphate into a second molecule of glyceraldehyde 3-phosphate, therefore all succeeding reactions and their products are duplicated. Glyceraldehyde 3-phosphate is oxidised and phosphorylated by glyceraldehyde phosphate dehydrogenase (GAPDH), which yields one molecule of 1,3-bisphosphoglycerate and one molecule of NADH + H⁺ per reaction (i.e., two per glucose molecule). The next step involves the transfer of a phosphate group from 1,3-bisphosphoglycerate to an ADP molecule, catalysed by phosphoglycerate kinase to yield 3-phosphoglycerate and a molecule of ATP per reaction. Phosphoglycerate mutase then isomerises 3-phosphoglycerate into 2-phosphoglycerate. The enzyme enolase next catalyses the conversion of 2-phosphoglycerate to phosphoenolpyruvate, releasing water as a by-product. Finally, a phosphate group is transferred from phosphoenolpyruvate to an ADP molecule in a reaction catalysed by pyruvate kinase, resulting in the formation of one molecule of pyruvate and one molecule of ATP. Together, the enzymatic breakdown of glucose to pyruvate via the glycolytic pathway results in the net gain of two ATP molecules and two NADH + H⁺ molecules.

Quiescent T cells engage low levels of glycolysis in both mice and humans (Cao et al., 2014; Jones et al., 2017). Whilst CD8+ T_H1 cells exhibit elevated levels of glycolysis versus their CD4+ counterparts in murine models (Cao et al., 2014), this appears to be reversed in humans whereby basal rates of glycolysis are higher in CD4+ T cells (Jones et al., 2017). However, it is more important to consider the importance of glycolysis upon T cell activation, where their metabolism is rewired to substantially drive flux through this pathway (see Chapter 1.3.6). Although glycolysis is reasoned to be an ineffective energy-generating process – given the disparity in ATP produced versus other metabolic pathways such as OXPHOS – it plays an important role in T cell activation due to its ability to more quickly utilise glucose (Macintyre & Rathmell, 2013). This enables T cells to rapidly produce ATP to support energy-demanding processes such as cytokine production upon their activation.

Additionally, there are a number of horizontal metabolic pathways associated with glycolysis, including the pentose phosphate pathway (PPP), glycogen synthesis pathway, glucosamine pathway and serine synthesis pathway. Here, glycolytic intermediates can branch off from glycolysis and can instead be used as the intermediates of these other metabolic pathways. For example, glucose-6-phosphate can initiate the PPP in the oxidative phase, whilst fructose-6-phosphate and glyceraldehyde-3-phosphate can enter at various points during the subsequent non-oxidative phase. Ultimately, the PPP serves to generate NADPH and pentose sugars, in addition to forming the precursors for nucleotide synthesis such as ribose-5-phosphate. Glucose 6-phosphate can also feed into glycogenesis, wherein it is initially converted into glucose 1-phosphate by phosphoglucomutase before subsequent conversions to UDP-glucose and finally glycogen. When required, glycogen is mobilised through the reverse of these reactions, termed glycogenolysis, where the glucose that is generated can re-enter metabolic pathways such as glycolysis. Meanwhile, fructose 6-phosphate and 3-phosphoglycerate make up the precursors of the glucosamine and serine synthesis pathways, respectively.

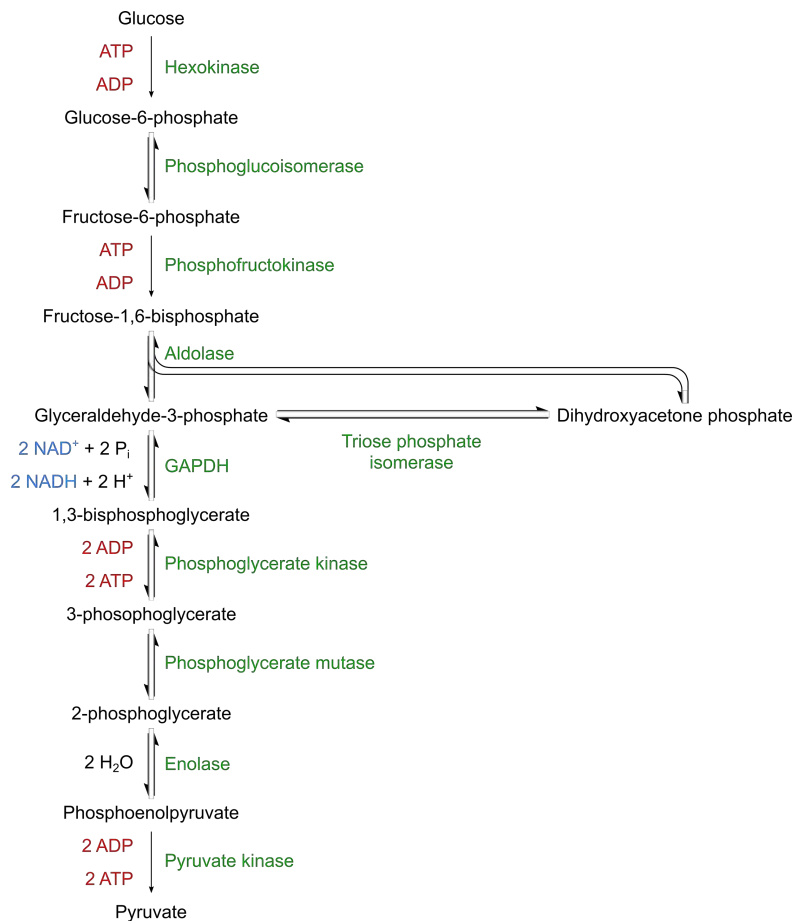


Figure 1.8 – The glycolysis pathway

One molecule of glucose is converted to two molecules of pyruvate through a number of reactions occurring outside the mitochondria. In addition to the formation of pyruvate, there is a net production of two molecules of ATP, 2 NADH and 2 H⁺. GAPDH, glyceraldehyde 3-phosphate dehydrogenase.

1.3.3 Fates of pyruvate

The conversion of pyruvate to acetyl-CoA is known as the link reaction (Figure 1.9). This multi-step reaction occurs within the mitochondria and is catalysed by the pyruvate dehydrogenase complex, which is composed of enzymes referred to as E1 (pyruvate dehydrogenase), E2 and E3. Together, components of the pyruvate dehydrogenase complex catalyse the decarboxylation of pyruvate, generation of NADH + H⁺ and the transfer of coenzyme A to form acetyl-CoA. Importantly, pyruvate dehydrogenase is allosterically regulated by pyruvate dehydrogenase kinase – a kinase that is activated by ATP, NADH and acetyl-CoA, but inhibited by ADP, NAD⁺ and pyruvate.

Alternatively, under certain conditions – for example, hypoxia or following T cell activation – pyruvate is instead converted to lactate by lactate dehydrogenase (Figure 1.9). Importantly, this reaction facilitates the regeneration of NAD^+ for use in further rounds of glycolysis – it is a cofactor in the reaction catalysed by GAPDH. Following T cell stimulation, the production of lactate increases up to 40-fold of basal rates (Kominsky et al., 2010) in a process known as the Warburg effect or ‘aerobic glycolysis’. Moreover, activated T cells maintain their elevated levels of glycolysis through efficient export of the lactate through SLC16A1, -3 and -6 (Howden et al., 2019; Marchingo et al., 2020). Aside from its primary role as a substrate for subsequent cellular metabolism, acetyl-CoA can be utilised for other functions including fatty acid synthesis and histone/protein acetylation. Additional roles for lactate include posttranslational modification in the form of lactylation, which has recently been associated with metabolic reprogramming (Liu et al., 2022), as well as recently being described as a carbon source to fuel CD8+ T cell metabolism (Kaymak et al., 2022).

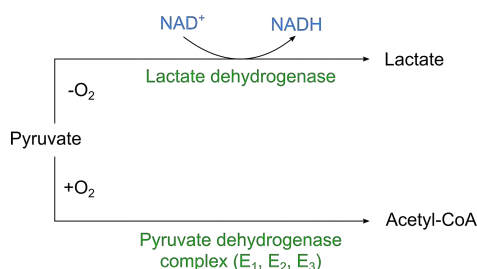


Figure 1.9 – The fates of pyruvate

In the presence of oxygen, pyruvate is typically converted to acetyl-CoA in a 3-step reaction catalysed by the pyruvate dehydrogenase complex within the mitochondria. Alternatively, in the absence of oxygen, pyruvate is converted to lactate by lactate dehydrogenase to regenerate NADH. However, upon T cell activation, the generation of lactate is preferred for rapid ATP generation, even in oxygen replete conditions in a process known as ‘aerobic glycolysis’.

1.3.4 Tricarboxylic acid cycle

The tricarboxylic acid (TCA) cycle is a series of enzymatic reactions that occur within the mitochondria that involves the initial conversion of acetyl-CoA and oxaloacetate into citrate (Figure 1.10). A complete round of the TCA cycle results in the generation of reducing equivalents that fuel downstream OXPHOS: three molecules of $\text{NADH} + \text{H}^+$ and one molecule of FADH_2 . By-products such as CO_2 and GTP are also formed during this set of reactions. Given

that one molecule of glucose generates two molecules of pyruvate, two complete cycles are realised per glucose molecule.

Acetyl-CoA becomes committed to the TCA cycle through the irreversible conversion of acetyl-CoA, oxaloacetate and H₂O to citrate and CoA-SH, which is catalysed by citrate synthase. Citrate is next isomerised to isocitrate in a coupled dehydration and hydration reaction catalysed by aconitase. Isocitrate dehydrogenase catalyses the next set of coupled reactions, in which isocitrate is initially oxidised, yielding oxalosuccinate and one molecule of NADH + H⁺, before oxalosuccinate is then decarboxylated to generate α-ketoglutarate and one molecule of CO₂. These reactions are followed by a further oxidative decarboxylation reaction, whereby α-ketoglutarate dehydrogenase catalyses conversion of α-ketoglutarate, NAD⁺ and CoA-SH to succinyl-CoA, NADH + H⁺ and CO₂. Next, succinyl-CoA is converted to succinate in a reaction catalysed by succinyl-CoA synthetase, also yielding one molecule of GTP by substrate-level phosphorylation. The next step of the TCA cycle is the oxidation of succinate in a reaction catalysed by succinate dehydrogenase, yielding fumarate and one molecule of FADH₂. There is subsequent hydration of fumarate to malate, catalysed by fumarase, before malate dehydrogenase catalyses the regeneration of oxaloacetate to fuel the next round of the TCA cycle.

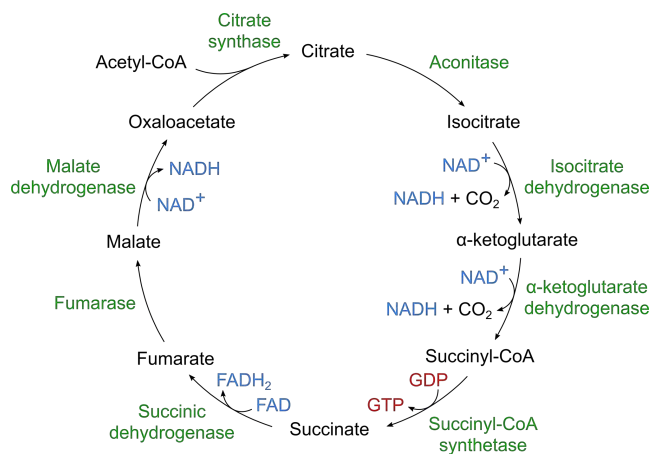


Figure 1.10 – The tricarboxylic acid cycle

The reactions of the tricarboxylic acid (TCA) cycle occur within the mitochondria. Acetyl-CoA and oxaloacetate are converted to citrate which initiates the cycle. Therefore, two cycles occur per glucose molecule metabolised via this pathway. The reactions of the TCA cycle result in the reduction of cofactors (three NADH and one FADH₂) and the formation of GTP and carbon dioxide.

During quiescence, murine and human T cells exhibit relatively low metabolic rates through the TCA cycle (Cao et al., 2014; Jones et al., 2017). Glucose is typically incorporated into the TCA cycle (Jones et al., 2019), however, under glucose-limiting conditions T cells compensate for this loss through the anaplerosis of other metabolites such as glutamine (Blagih et al., 2015). Alternatively, T cells can also engage the TCA cycle with acetyl-CoA derived from the fatty acid oxidation pathway (O'Sullivan et al., 2014). Alternate fuel usage becomes particularly important upon T cell activation, whereby glucose becomes re-routed towards aerobic glycolysis and oxidative metabolism is sustained by glutaminolysis and the anaplerosis of metabolic substrates (see Chapter 1.3.6).

1.3.5 Oxidative phosphorylation

Oxidative phosphorylation (OXPHOS) is the second main cellular energy-producing pathway. Alongside the link reaction and the TCA cycle, OXPHOS occurs within the mitochondria, generating greater than 30 molecules of ATP per glucose molecule (Figure 1.11). The reducing equivalents produced during glycolysis ($\text{NADH} + \text{H}^+$) and the TCA cycle ($\text{NADH} + \text{H}^+$ and FADH_2) produce the protons and electrons necessary to drive a series of redox reactions at the inner mitochondrial membrane. Here, the electrons are transferred along a group of proteins known as the electron transport chain, made up of the following complexes: NADH-ubiquinone oxidoreductase (complex I), succinate dehydrogenase (complex II), coenzyme Q : cytochrome c oxidoreductase (complex III), and cytochrome c oxidase (complex IV). The subsequent reduction of oxygen by complex IV makes it the terminal electron acceptor. Importantly, the transfer of electrons between these mitochondrial complexes facilitates proton pumping across the mitochondrial membrane into the intermembrane space by complexes I, III and IV. This establishes a proton gradient, whereby a greater number of protons are present in the intermembrane space versus the mitochondrial matrix. Consequently, protons are transported via this electrochemical gradient through ATP synthase (complex V), a protein consisting of two significant regions, F_0 and F_1 . Protons transported through the F_0 region generates the proton-motive force to rotate elements of the F_1 region, resulting in the energy required to catalyse the conversion of ADP and P_i into ATP.

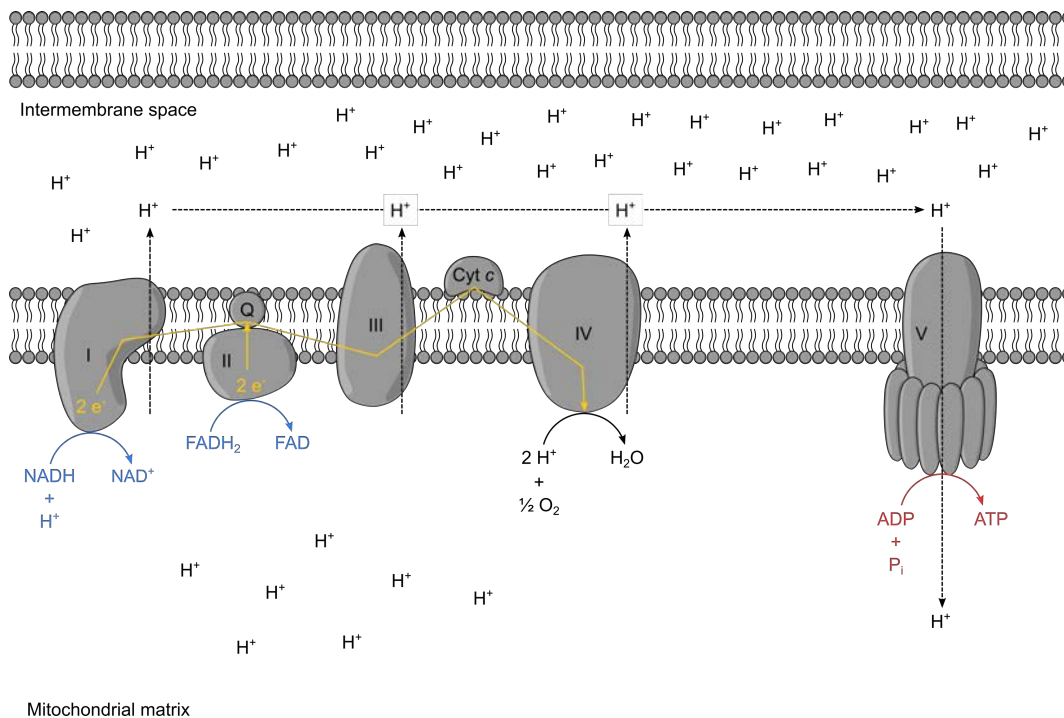


Figure 1.11 – The electron transport chain

The electron transport chain is located on the inner mitochondrial membrane and is the site of oxidative phosphorylation. Electrons are transferred from reduced cofactors to their respective complexes, before transfer through the complexes of the electron transport chain in a series of redox reactions to finally reduce oxygen. Through electron transfer, protons are pumped across the inner mitochondrial membrane by complexes I, II and IV to create a greater concentration of protons within the intermembrane space. Protons return to the mitochondrial matrix down the electrochemical gradient through ATP synthase, resulting in the generation of ATP from ADP + Pi. *Complex I, NADH:ubiquinone oxidoreductase; complex II, succinate dehydrogenase; complex III, coenzyme Q:cytochrome c oxidoreductase; complex IV, cytochrome c oxidase; complex V, ATP synthase; Cyt c, cytochrome c; Q, coenzyme Q.*

1.3.6 Metabolic rewiring upon T cell activation

T cells undergo extensive metabolic rewiring upon their activation to support the biosynthetic pathways necessary for effector function (Figure 1.12). Early studies demonstrated that engagement of the TCR, alongside CD28 co-stimulation, increased glucose uptake to sustain elevated levels of glycolysis (Frauwirth et al., 2002). Augmented glucose metabolism was underpinned by activation of the AKT and upregulation of the glucose transporter GLUT1 – both processes regulated by the inhibitory ligand CTLA-4 (Frauwirth et al., 2002). Likewise, high levels of glutamine metabolism are also required for successful T cell

activation (Carr et al., 2010). Upon activation, T cells selectively increase glutamine uptake and downstream anaplerotic metabolism in an ERK-dependent manner to perpetuate proliferation and cytokine production (Carr et al., 2010). Further studies have demonstrated that activation-induced metabolic reprogramming also includes – in addition to elevated glycolysis and glutaminolysis – reduced levels of fatty acid β -oxidation, reduced levels of pyruvate oxidation via the TCA cycle and increased flux through the PPP (Wang et al., 2011). Interestingly, these metabolic changes were supported by MYC-dependent upregulation of the enzymes involved in glycolysis and glutaminolysis (Wang et al., 2011). Inhibition of AKT and ERK – the aforementioned kinases implicated in T cell metabolic reprogramming (Carr et al., 2010; Frauwirth et al., 2002) – limited the expression of MYC, which might suggest that these pathways regulate activated T cell metabolism, at least partially, through their regulation of MYC expression (Wang et al., 2011). The absence of MYC in activated T cells results in blunted T cell growth and proliferation (Wang et al., 2011). These findings have recently been complemented by quantitative proteomic analyses, wherein MYC was demonstrated to control cell growth by selectively remodelling the T cell proteome upon activation (Marchingo et al., 2020). The importance of MYC in maintaining augmented glycolysis and glutaminolysis was also further explored, confirmed to control the rate-limiting steps of each pathway, lactate transporter expression and glutamate dehydrogenase expression, respectively (Marchingo et al., 2020). Moreover, MYC enhanced amino acid transporter expression in activated T cells to establish a positive feedback loop to maintain its own expression and drive further metabolic reprogramming (Marchingo et al., 2020).

Other metabolic modulators have also been implicated in T cell activation. Glucose uptake and glycolysis are regulated by mammalian target of rapamycin complex 1 (mTORC1) in activated CD8⁺ T cells (Finlay et al., 2012). Changes in glucose metabolism were mediated by the interaction of mTORC1 with hypoxia-inducible factor 1 α (HIF-1 α) in an AKT- and PI3K-independent manner, which promoted glycolytic enzyme expression to sustain the elevated glycolytic rates necessary for downstream migration and function (Finlay et al., 2012). mTORC1 expression and activation, like MYC, requires sustained uptake of the amino acid leucine (Sinclair et al., 2013). Under glucose limiting conditions, there is a metabolic checkpoint controlled by AMP-activated protein kinase (AMPK) which ensures that T cells adapt to meet the metabolic demands of activation (Blagih et al., 2015). This enables switching to alternative fuels such as glutamine to power mitochondrial metabolism and

maintain T cell fitness (Blagih et al., 2015). Interestingly, there are slight differences in the metabolic programmes of CD4+ and CD8+ T cells. Whilst both subsets enhanced their glycolytic metabolism following activation, CD4+ retain a more oxidative phenotype versus CD8+ T cells, displaying an increased respiratory capacity and associated with increased mitochondrial content (Cao et al., 2014). However, the enhanced glycolytic metabolism of CD8+ T cells allowed an increased capacity for ensuing cell growth and proliferation (Cao et al., 2014).

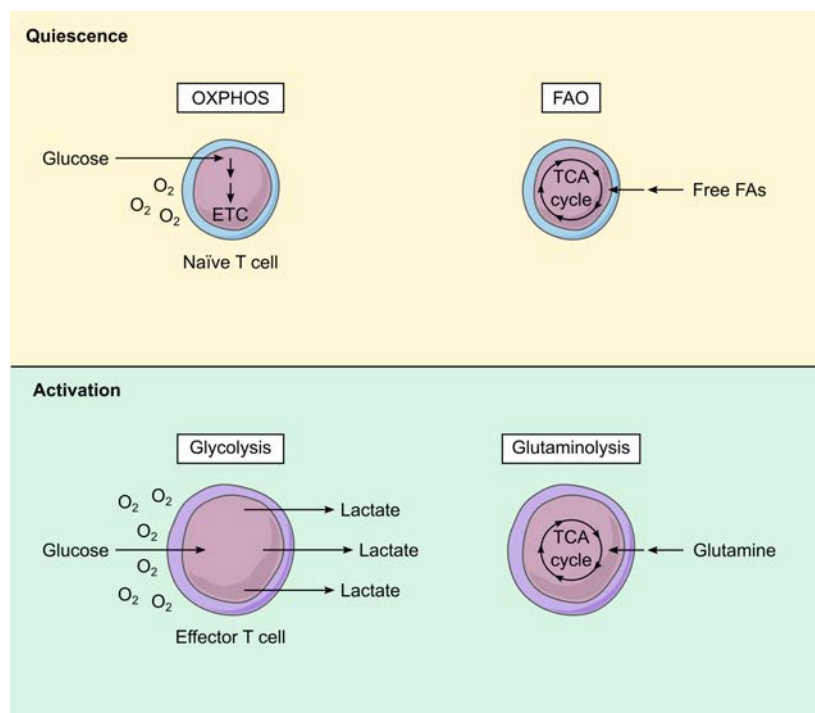


Figure 1.12 – T cell metabolism upon activation

Overview of the metabolic programmes underpinning T cell activation. During quiescence, T cells typically maintain their function through oxidative metabolism, whereby OXPHOS is primarily fuelled by glucose metabolism, but also supplemented by the oxidation of fatty acids. Upon activation, a 'glycolytic switch' is engaged – glucose is primarily used to fuel glycolysis even in oxygen replete conditions. Moreover, the amino acid glutamine enters the TCA cycle to fuel OXPHOS. These changes occur to meet the increased energetic demands of T cell effector function.

ETC, electron transport chain; FAO, fatty acid oxidation; TCA, tricarboxylic acid.

Importantly, enhanced glucose metabolism also fuels human T cell activation. Consistent with murine studies, activation thorough TCR ligation promotes rapid glucose uptake to power enhanced glycolytic flux (Macintyre et al., 2014). Whilst oxidative glucose metabolism is also promoted following T cell activation, levels of glycolysis supersede OXPHOS to preferentially utilise aerobic glycolysis (Macintyre et al., 2014). Once more, metabolic programming is paramount to T cell fate and fitness, driving cell growth and proliferation (Macintyre et al., 2014). Similar observations were also made in CD8⁺ T cells, whereby the activation-induced 'glycolytic switch' was required for optimal IFN γ production (Gubser et al., 2013). In both human CD4⁺ and CD8⁺ T cell subsets, increased glycolysis is driven by marked upregulation of the glycolytic enzymes hexokinase II, PFK and GAPDH, alongside an increase in the expression of GLUT1 (Jones et al., 2017). Moreover, increased expression of lactate dehydrogenase following activation supports the switch to aerobic glycolysis (Jones et al., 2017). Whilst both subsets are reliant on glucose metabolism for optimal activation and cytokine production, CD8⁺ T cells appear to be more reliant on mitochondrial metabolism to carry out these processes than their CD4⁺ counterparts (Jones et al., 2017). This early metabolic switch in human T cells is orchestrated by a combination of AKT and STAT5, which are essential in upregulating glycolysis and glutaminolysis, respectively (Jones et al., 2019). The activation of mTORC1 is intertwined in both of these signalling pathways (Jones et al., 2017; Jones et al., 2019), highlighting the importance of all three pathways in the metabolic reprogramming of human T cells. Importantly, perturbed glutamine metabolism culminated in a loss of IL-2 production by human T cells (Jones et al., 2019). Previous work has demonstrated that under glutamine-limiting conditions, activated human T cells displayed a regulatory phenotype, characterised by elevated FoxP3 expression, but also readily produced proinflammatory cytokines including IL-17 and IFN γ (Metzler et al., 2016). Together, these data elucidate the metabolic reprogramming that occurs in murine and human T cells upon their activation, which is characterised by a switch to elevated rates of glycolysis, further supported by enhanced glutamine metabolism.

Regulatory mechanisms are required to limit T cell activation and maintain immunological tolerance (see Chapter 1.2.4). Early work revealed that there might be a metabolic underpinning to this dampening of the activation response, demonstrating that CTLA-4 inhibited the activation-induced upregulation of glucose metabolism in T cells (Frauwirth et al., 2002). Specifically, CTLA-4 prevents the glycolytic reprogramming needed

upon T cell activation, whereby glycolytic enzyme expression remained similar to that of unstimulated human T cells (Patsoukis et al., 2015). In a similar vein, PD-1 also inhibits activation-induced glucose metabolism (Patsoukis et al., 2015). Human CD4+ T cells activated in the presence of PD-1 fail to upregulate their glucose or glutamine metabolism, instead pivoting towards a metabolic programme characterised by enhanced fatty acid oxidation (Patsoukis et al., 2015). Consequently, PD-1 signalling in CD4+ T cells unlocks an enhanced respiratory capacity versus activated T cells, mediated by inhibition of the AKT and ERK pathways downstream of the TCR signalling cascade (Patsoukis et al., 2015). Thus, metabolic programmes are in place within T cells to regulate their activation and prevent the development of autoimmunity.

The progression of naïve T cells towards effector T cells, and ultimately, central memory T cells is further supported by underlying changes in metabolism. Numerous investigations have outlined the importance of fatty acid metabolism, amongst other metabolic changes, in this process. Initially, it was demonstrated that murine CD8+ T cells displaying defective fatty acid oxidation failed to generate long-lived memory populations after immunisation (Pearce et al., 2009). These changes were driven by aberrant AMPK activation, which could be restored by metformin to re-establish fatty acid oxidation and memory cell formation (Pearce et al., 2009). Moreover, CD8+ memory T cells have an increased capacity for mitochondrial respiration, facilitated by an IL-15-induced increase in mitochondrial biogenesis (van der Windt et al., 2012). Importantly, this spare respiratory capacity in memory T cells is dependent on fatty acid oxidation, further supported by upregulation of the rate-limiting enzyme carnitine palmitoyl transferase (CPT1a) (van der Windt et al., 2012). Additionally, glycolytic inhibition enhances memory formation (Sukumar et al., 2013). Interestingly, memory T cells do not acquire considerable levels of extracellular fatty acids to fuel these processes, instead using extracellular glucose to generate the substrates necessary to sustain elevated rates of fatty acid oxidation and OXPHOS (O'Sullivan et al., 2014). Indeed, enhanced lipolysis is characteristic of T cell memory, supporting their development and survival (O'Sullivan et al., 2014). Changes in mitochondrial dynamics also play an important role in mediating the metabolic adaptations necessary for memory formation (Buck et al., 2016). For example, memory T cells have mitochondria that are characterised by fused networks – maintained by OPA1 – that arranges the electron transport chain complexes in a configuration biased towards enhanced fatty acid oxidation and OXPHOS

(Buck et al., 2016). In contrast to these findings, a recent study demonstrated that T cell memory generation did not require CPT1a, instead suggesting that etomoxir – a drug that inhibits CPT1a activity – perturbs memory formation through ‘off-target’ effects on metabolism (Raud et al., 2018). Whilst low doses of etomoxir inhibit CPT1a activity in murine and human T cells, higher doses ($> 100 \mu\text{M}$) disturbed the TCA cycle and subsequent OXPHOS independent of fatty acid oxidation (Raud et al., 2018). Together, there is a wealth of data supporting the importance of fatty acid oxidation in T cell memory formation, however, experiments involving etomoxir must be interpreted with caution given the recently described ‘off-target’ effects on other areas of metabolism.

The rapid recall ability of memory T cells is underpinned by another metabolic programme. Upon activation, the resulting secondary effector T cells generate increased levels of ATP versus their primary effector counterparts (van der Windt et al., 2013). Here, memory T cells sustained rates of glycolysis and OXPHOS at greater levels than naïve T cells, supported by their increased mitochondrial mass (van der Windt et al., 2013). Moreover, these metabolic adaptations allow the secondary effector T cells generated to proliferate more rapidly and produce more cytokines than primary effector T cells (van der Windt et al., 2013). Further evidence has highlighted the importance of a rapid glycolytic switch following memory T cell stimulation to support the production of IFN γ (Gubser et al., 2013). Signalling via the AKT pathway promoted elevated levels of glycolytic flux, which was driven by greater GAPDH activity versus naïve T cells activated under comparable conditions (Gubser et al., 2013). Enhanced GAPDH activity has since been associated with post-translational modification of the enzyme in memory T cells (Balmer et al., 2016). Increased acetate concentrations contribute to optimal memory function through expansion of acetyl-CoA pools, whilst also promoting the acetylation of GAPDH, culminating in enhanced glycolytic metabolism and effector function (Balmer et al., 2016). Most recently, it has also been shown that memory T cells activate glycogen phosphorylase B upon TCR signalling, mobilising glycogen stores as an alternative carbon source for glycolysis during rapid recall function (Longo et al., 2022). Thus, whilst oxidative metabolism supports the survival of long-lived memory T cells, their rapid effector function following recall is fuelled by a shift towards predominantly glycolytic metabolism (Figure 1.13).

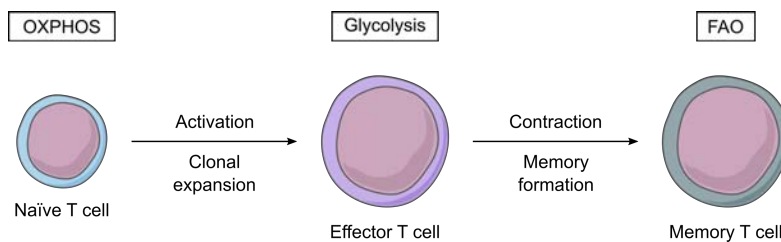


Figure 1.13 – T cell metabolism during memory formation

Naïve T cells typically exhibit a quiescent phenotype, which is primarily driven by oxidative glucose metabolism. Upon activation and downstream effector T cell formation, metabolism is reprogrammed to meet the energetic demands of effector function. Following clearance of the immunological threat, effector T cells are either committed to apoptosis (not shown) or progress to become memory T cells. The survival of long-lived memory T cells is underpinned by a return to oxidative metabolism using fatty acids as their fuel.

It is now understood that the asymmetric cell division T cells undergo following activation is governed by disparate metabolic programmes. During the process of mitotic division, the daughter cell positioned closest to the APC, also known as the ‘proximal’ daughter cell, is most likely to inherit an effector phenotype, whereas the ‘distal’ daughter cell progresses towards memory (Verbist et al., 2016). Interestingly, this is mediated by an uneven distribution of the metabolic modulator MYC, wherein the proximal daughter T cell receives greater levels of the protein (Verbist et al., 2016). MYC expression is sustained in proximal daughter cells by elevated amino acid transporter expression, increased uptake of amino acids through these channels, and subsequent increased mTORC1 activity (Verbist et al., 2016). Moreover, the partitioning of mTORC1 activity leads to elevated levels of glycolysis within the proximal daughter cell to drive their effector function (Pollizzi et al., 2016). In contrast, the distal daughter cells exhibit increased rates of fatty acid metabolism, concomitant with the expression of several anti-apoptotic proteins to support the long-term survival of these memory cells (Pollizzi et al., 2016). Together, these metabolic changes induce the differences in effector function and differentiation between the two populations.

Whilst T cell metabolism is well-tuned for their numerous states and functions, external factors can also cause metabolic alterations. For example, transforming growth factor (TGF)- β derived from the tumour microenvironment was able to suppress T cell metabolism, preventing the generation of ATP required to meet the demands of effector function (Dimeloe et al., 2019). More recently, the TCA cycle metabolite, succinate, which

accumulates within the tumour microenvironment, has been demonstrated to impair flux through the TCA cycle (Gudgeon et al., 2022). Inhibition of the enzyme succinyl-CoA synthetase prevents the progression of metabolites through the TCA cycle, thus inhibiting oxidative glucose metabolism, culminating in defective cytokine production and degranulation in human CD4⁺ and CD8⁺ T cells (Gudgeon et al., 2022). Following these advances in understanding the integration of T cell metabolism in downstream effector function, efforts are being made to improve our knowledge of how T cell metabolism underpins other facets of T cell biology.

1.3.7 Metabolic regulation of T cell lineage

Given that metabolism underpins T cell function – particularly following activation – its influence on differentiation towards different lineages has been explored (Figure 1.14). Early experiments determined that glutamine availability influenced expression of Th1-associated cytokines, whilst the production of Th2-associated cytokines did not depend on optimal glutamine levels (Chang et al., 1999). This concept was developed further, wherein the metabolic regulator mTOR was required for differentiation towards effector lineages, including Th1, Th2 and Th17 cell subsets (Delgoffe et al., 2009). These changes were associated with a failure to express the necessary transcription factors, arising from impaired STAT activation in mTOR-deficient cells (Delgoffe et al., 2009). Interestingly, CD4⁺ T cells lacking mTOR instead differentiated into Treg cells, displaying hypersensitivity towards TGF- β , a key Treg cell inducer (Delgoffe et al., 2009). This mechanism was further elucidated, whereby mTORC1 activation is required for differentiation into Th1 and Th17 subsets, whilst mTORC2 activation is necessary for differentiation into the Th2 subset (Delgoffe et al., 2011). Together, these findings developed a framework linking metabolic signalling pathways and T cell differentiation.

Subsequent studies have built upon this model, dissecting the relationship between metabolism and differentiation into distinct T cell subsets. These analyses, mostly performed using murine models, have unearthed intriguing metabolic checkpoints that regulate diverging pathways in commitment towards opposing T cell subsets (e.g., Th1 versus Th2, Th17 versus Tregs). Focussing firstly on Th1 and Th2 cell differentiation, both subsets are dependent on high glycolytic activity, but are also inhibited by increasing levels of lipid oxidation (Michalek et al., 2011). Both subsets also express high levels of GLUT1, which is

necessary to maintain elevated rates of glycolysis to support their survival and effector function (Macintyre et al., 2014). Interestingly, in human T cells, stimulation of the complement receptor CD46 has been associated with enhanced expression of GLUT1 and increased glycolysis, both of which were necessary for successful Th1 cell function (Kolev et al., 2015). Another link was also established between the complement system and increased amino acid transporter expression – subsequent upregulation of an amino acid-sensing Rag-mTOR complex, ultimately fuelling OXPHOS as well as glycolysis (Kolev et al., 2015). Additionally, aerobic glycolysis has been demonstrated to promote Th1 cell differentiation via an epigenetic mechanism, whereby lactate dehydrogenase A maintains high concentrations of acetyl-CoA, which enhances histone acetylation and transcription of signature cytokine IFN γ (Peng et al., 2016). Most recently, there is further evidence to suggest the importance of OXPHOS, however, distinct nodes of this process are associated with different Th1 cell functions (Bailis et al., 2019). For example, the activity of complex II is required for effector function such as the production of IFN γ , yet this also suppresses proliferation via an epigenetic mechanism, thus the balance of this network acts to determine cell state (Bailis et al., 2019). In an interesting clinical study, dietary carbohydrates shaped the Th1 / Th2 balance towards a Th1-associated phenotype, represented by increased IL-2 production and concomitant reductions in IL-4 production (Caris et al., 2014). Collectively, these data outline that there are shared and subset-specific metabolic uses of glucose, established to optimise lineage functions.

Peroxisome proliferator-activated receptor (PPAR) γ – the master regulator of lipid metabolism – connects lipid metabolism to Th1 / Th2 balance and effector function. Murine memory Th2 cells upregulate several metabolic enzymes and transporters involved in lipid metabolism following activation (Angela et al., 2016). PPAR γ mediates this upregulation of lipid-associated pathways, which are required for further metabolic reprogramming in Th2 cells – such as increasing the glycolytic output of these cells – to further support activation and proliferation (Angela et al., 2016). Genomic analyses have also revealed that pathways associated with lipid metabolism are enriched in Th2 cells, possibly due to the increased number of PPAR γ binding sites present at these loci compared to other subsets (Tibbitt et al., 2019). In addition, there were similar dependencies on both glucose metabolism and lipid metabolism in Th2 cells isolated from an *in vivo* model of airway inflammation, thus metabolism underpins pathogenic functions such as eosinophil recruitment (Tibbitt et al.,

2019). Additionally, PPAR γ has been found to be a driver of Th2 function in other disease settings such as asthma and nematode infection (T. Chen et al., 2017). Further genomic analyses have determined that signature Th2 markers – e.g., IL-5, IL-13 and GATA3 – are also included amongst target genes for PPAR γ binding (Henriksson et al., 2019). Despite these findings outlining that PPAR γ promotes Th2 responses, its contribution to IL-4 production is unclear, as there is evidence to suggest that PPAR γ increases, decreases or has no significant effect on IL-4 expression (T. Chen et al., 2017; Nobs et al., 2017; Park et al., 2014). Together, these data demonstrate that PPAR γ – through its action of cellular metabolism and downstream effector function – drives Th2-mediated responses in health and disease.

Another clear metabolic checkpoint between Th1 / Th2 cell fate emerges in their utilisation of glutamine. Early work using a murine model of asthma determined that glutamine inhibited Th2-mediated responses – including eosinophilia and mucus formation – by limiting the activation of the enzyme cytosolic phospholipase A₂ (Ko et al., 2008). Indeed, deletion of the glutamine transporter ASCT2 enhanced the generation of Th2 cells, with concomitant increases in the expression of the signature transcription factor GATA3 and effector cytokine IL-4 (Nakaya et al., 2014). Contrastingly, Th1 responses were highly dependent on glutamine, whereby ASCT2-deficient cells displayed reduced Tbet expression and markedly reduced IFN γ expression (Nakaya et al., 2014). Thus, these data present a paradigm in which Th1 versus Th2 responses are sensitive to glutamine uptake and metabolism. Supplementation of glutamine-deprived Th1 cells with the membrane permeable analogue of the glutamine-derived metabolite α -ketoglutarate is sufficient to rescue Tbet expression and IFN γ production, alongside a concomitant increase in mTOR activity (Klysz et al., 2015), which provides further evidence that it is the anaplerotic metabolism of glutamine that drives differentiation in the direction of the Th1 lineage. However, it is important to consider that dimethyl- α -ketoglutarate has distinct effects on metabolism (Parker et al., 2021), so these analyses should be interpreted with caution. Interestingly, the changes resulting from altered glutamine availability are realised physiologically, as dietary glutamine tips the Th1 / Th2 balance in favour of the former in human clinical studies, evidenced by increased IL-2 production and reduced IL-4 production (Caris et al., 2014). Other amino acids have also been implicated in Th1 versus Th2 differentiation, albeit to a lesser extent than glutamine. Initially investigated in the setting of pregnancy, reduced levels of the tryptophan-catabolising enzyme IDO (indoleamine 2,3-

dioxygenase) were correlated with increased ratios of Th1 / Th2 cells, ultimately resulting in murine pregnancy failure (Clark et al., 2005). The absence of IDO within the lung has since been associated with impaired Th2-mediated responses in the inflamed airway, whereby the production of IL-4, IL-5 and IL-13 were all reduced (Xu et al., 2008). Furthermore, IDO deficiencies appeared to have a less marked impact on Th1 responses (Xu et al., 2008), therefore tryptophan metabolism appears to differentially modulate differentiation and function in both subsets. Together, these data highlight numerous metabolic mechanisms – involving various aspects of glucose, lipid and amino acid metabolism – that are involved in maintaining the balance of Th1 / Th2 cells in health and disease.

A similar dichotomy is observed between Th17 / Treg cell fate and function. Early murine work demonstrated distinct metabolic programmes were utilised by Teff cells compared to Treg cells to support their separate functions. Th1, Th2 and Th17 cells all exhibited high levels of glycolytic activity, whereas Treg cells engaged minimal glycolysis, instead opting for increased lipid oxidation (Michalek et al., 2011). Consequently, inducing GLUT1 expression selectively expanded Teff cell populations, whilst AMPK activation promoted the expansion of Treg cells, demonstrating that manipulation of these metabolic pathways is sufficient to alter T cell lineage (Michalek et al., 2011). Increased glycolytic function is driven by increased expression of HIF-1 α in CD4⁺ T cells, whereby Treg cells expressed the lowest levels (Shi et al., 2011). In particular, Th17 cells expressed markedly increased levels of HIF-1 α , suggesting that it is especially important in polarisation towards the Th17 lineage (Shi et al., 2011). Indeed, inhibition of HIF-1 α prevented the necessary upregulation of the glycolytic machinery, resulting in blunted Th17 development whilst promoting Treg cell generation (Shi et al., 2011). Thus, elevated levels of glycolysis, driven by the increased activity of HIF-1 α and its upstream activator mTOR, illustrates an important metabolic checkpoint in the differentiation of Th17 and Treg cells. In settings such as inflammatory disease, GLUT1 deficiencies can suppress the expansion of Teff cells *in vivo*, skewing differentiation towards Treg cells (Macintyre et al., 2014). This improved disease outcomes (Macintyre et al., 2014), highlighting the therapeutic potential of manipulating differentiation programmes through their underpinning metabolic profiles. Importantly, similar mechanisms have been demonstrated in human T cells, whereby Th17-polarising conditions were associated with upregulation of glycolysis, whilst inhibition of this process through either glucose deprivation or mTOR inhibition reduced the number of Th17 cells

(Cluxton et al., 2019). Although human Treg cells also display increased levels of glycolysis, they do not depend on glycolysis, instead more reliant on increased levels of OXPHOS and lipid oxidation (Cluxton et al., 2019). However, another investigation in human Treg cells stressed that optimal expression of functional regulatory molecules requires glycolytic metabolism (Tanimine et al., 2019). More recently, murine models have highlighted the importance of OXPHOS in differentiation towards the Th17 lineage. Under Th17-polarising conditions, extensive metabolic reprogramming drives increased levels of OXPHOS to fuel murine T cell metabolism (Shin et al., 2020). In the absence of mitochondrial metabolism, there is a loss of pathogenic effector function following inhibition of the expression of Th17 signature genes (Shin et al., 2020). Moreover, OXPHOS-inhibited CD4⁺ T cells preferentially express the transcription factor FoxP3 to become suppressive Treg cells (Shin et al., 2020). Mechanistically, STIM1 downstream of the TCR signalling cascade is responsible for the upregulation of OXPHOS in Th17 cells, whereby deletion of STIM1 results in attenuated OXPHOS and the development of non-pathogenic Th17 cells (Kaufmann et al., 2019). Most recently, these mechanisms have been investigated in the context of cancer. Interestingly, lymphoma tumour burden skewed CD4⁺ T cell function towards a regulatory phenotype, preceded by downregulation of glucose uptake and mitochondrial metabolism (Hesterberg et al., 2022). This demonstrates how poorly immunogenic cancers manipulate underlying T cell metabolism to their advantage to suppress immune function. Together, these data establish glucose metabolism – involving both glycolysis and OXPHOS – as an important metabolic checkpoint in the regulation of Th17 and Treg cell differentiation.

Fatty acid metabolism has also been demonstrated to play a critical role in controlling differentiation between Th17 and Treg cells. Initially, the dependence of Th17 cell fate on fatty acid synthesis was demonstrated in both murine and human CD4⁺ T cells (Berod et al., 2014). Inhibition of acetyl-CoA carboxylase 1 (ACC1) – a key enzyme in the regulation of fatty acid metabolism – interfered with Th17 cell development, impairing the expression of signature transcription markers and effector molecules (Berod et al., 2014). Interestingly, inhibition of ACC1 also perturbed cellular glycolysis, impairing flux through the glycolytic-lipogenic pathway (Berod et al., 2014), again highlighting the importance of glycolysis in deciding Th17 / Treg fate. Meanwhile, Treg cells are not dependent on fatty acid synthesis, expanding even under conditions favouring Th17 polarisation when this pathway was inhibited (Berod et al., 2014). Changes in T cell fatty acid metabolism are regulated by AMPK,

which is highly active in Treg cells. Pharmacological activation of AMPK using the AMP analogue AICAR strongly enhanced Treg cell induction, whilst concomitantly inhibiting Th17 cell polarisation (Gualdoni et al., 2016). This AMPK-dependent mechanism enhanced both mitochondrial respiration and lipid oxidation (Gualdoni et al., 2016), in keeping with some of the previous findings discussed. Critically, similar mechanisms have also been observed in human CD4⁺ T cells, wherein inhibition of fatty acid synthesis diminished the Th17 cell population (Cluxton et al., 2019). On the other hand, Treg cells were not reliant on fatty acid synthesis and thrived under conditions promoting fatty acid oxidation (Cluxton et al., 2019). Other aspects of fatty metabolism have also been explored. For example, murine CD4⁺ T cells treated with SCFAs such as sodium butyrate were skewed towards a regulatory phenotype versus Th17 cells, mechanistically associated with inhibition of haem oxygenase 1 and IL-6 receptor-related processes (X. Q. Chen et al., 2017). Cholesterol metabolism has also been implicated in deciding Treg / Th17 fate, whereby liver kinase B1 (LKB1) supported Treg function through AMPK-independent activation of the mevalonate pathway (Timilshina et al., 2019). Interestingly, LKB1 supports several other metabolic pathways in Treg cells, including OXPHOS and lipid oxidation, which are critical to their fitness and survival (He et al., 2017; Yang et al., 2017). Most recently, investigation of fatty metabolism in T cell differentiation has focussed primarily on Treg cells. To this end, fatty acid binding protein 5 (FABP5) has been implicated in the maintenance of mitochondrial integrity, OXPHOS and lipid metabolism – all of which supported Treg cell function (Field et al., 2020). Furthermore, the fatty acid translocase CD36 modulates the mitochondrial fitness of Treg cells to support their immunosuppressive function (Wang et al., 2020). Both mechanisms have been demonstrated to orchestrate the function and survival of intratumoural Treg cells (Field et al., 2020; Wang et al., 2020). Collectively, murine models demonstrate the importance of differential carbohydrate and lipid metabolism in deciding Th17 versus Treg cell development. Importantly, the overarching findings of these studies have also been replicated in human CD4⁺ T cells.

Amino acid metabolism has also been implicated in controlling Th17 / Treg cell fate. Multiple murine studies have centred around the importance of glutamine in CD4⁺ T cell differentiation, since it is critical during T cell activation. Early studies determined that the availability of amino acids was a key determinant of T cell differentiation, where increased extracellular amino acid concentrations were associated with increased mTOR activity

(Cobbold et al., 2009). To this end, amino acid starvation limited mTOR activity, which promoted Treg cell differentiation (Cobbold et al., 2009). Subsequently, glutamine uptake – and the downstream activation of mTOR – was demonstrated to be essential for differentiation towards the Th17 lineage (Nakaya et al., 2014). A later study observed that glutamine-deprived CD4⁺ T cells adopt a regulatory phenotype, even under conditions that would normally induce proinflammatory function (Klysz et al., 2015). Furthermore, these data indicated that decreased levels of intracellular α -ketoglutarate, caused by limited glutamine availability, skewed the balance of differentiation towards Treg cells (Klysz et al., 2015). However, a similar study using human T cells determined that supplementation with α -ketoglutarate did not rescue the development of inflammatory FoxP3^{lo} T cell subsets following glutamine deprivation (Metzler et al., 2016), suggesting that glutamine might influence T cell differentiation through alternative mechanisms outside of its entry into the TCA cycle. Indeed, the accumulation of α -ketoglutarate within murine T cells can influence epigenetic modifications related to Th17 / Treg cell balance (Xu et al., 2017). The expression of FoxP3 is inhibited by hypermethylation within its demethylated region; this process is facilitated by 2-hydroxyglutarate, derived from GOT1-mediated transamination of α -ketoglutarate (Xu et al., 2017). Additionally, recent work in CD8⁺ T cells has demonstrated that GOT1 promotes glycolytic metabolism through regulation of HIF1 α (Xu et al., 2023), which could also explain the role of GOT1 in controlling Th17 / Treg cell fate. Interestingly, glutamine could also affect T cell differentiation independent of glutaminolysis. Whilst deficiency in glutaminase, an enzyme critical in glutamine anaplerosis, reduced differentiation towards the Th17 lineage, this had no effect on the Treg cell population (Johnson et al., 2018). Together, these data demonstrate that glutamine – through processes dependent and independent of glutaminolysis – also modulates the balance of Th17 / Treg cells. Accordingly, Th17 cell versus Treg cell responses are controlled by multiple aspects of cellular metabolism, highlighting the importance of immunometabolism in the context of inflammatory disease.

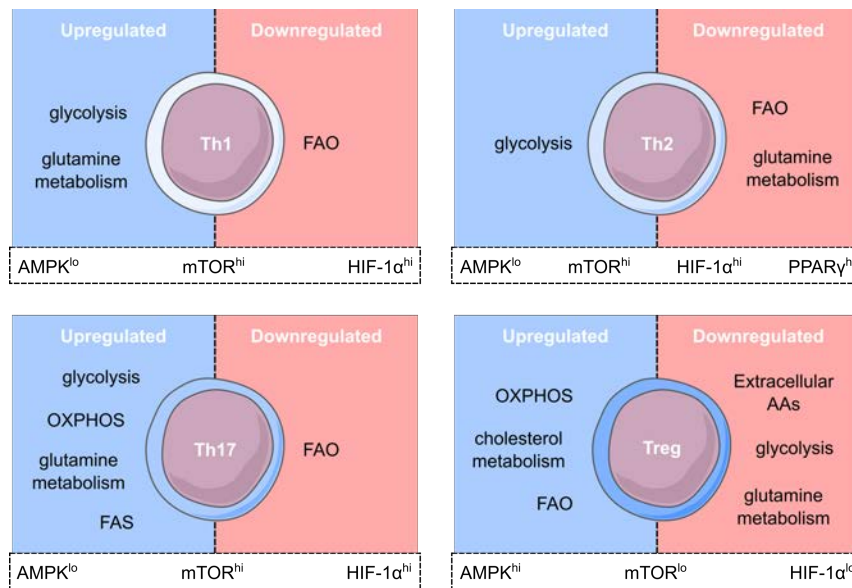


Figure 1.14 – T cell metabolism in differentiation

Overview of the distinct metabolic programmes engaged by T helper subsets. The function of effector T cells (i.e., Th1, Th2 and Th17) is primarily driven by increased levels of glycolysis, whilst not as dependent on oxidative metabolism. Contrastingly, regulatory T (Treg) cell function is highly dependent on OXPHOS and fatty acid oxidation.

1.4 T cell-mediated autoimmune disease

T cell-mediated autoimmune diseases are characterised as chronic inflammatory conditions, in which the T cell compartment is responsible for hyperinflammation, which ultimately leads to local tissue damage. Examples of such diseases (non-exhaustive list) include rheumatoid arthritis (RA), systemic lupus erythematosus (SLE) and multiple sclerosis (MS). Collectively, autoimmune disease affects around 4-5% of the population (Vyse & Todd, 1996), where incidence is greater in females compared to males – for example, RA (three-fold) (Alamanos & Drosos, 2005), SLE (nine-fold) (Danchenko et al., 2006) and MS (two-fold) (Pugliatti et al., 2006). Unfortunately, relapse to current treatments is commonplace. Given the earlier outlined functional differences between individual T helper cell subsets (see Chapter 1.2.3), it is important to understand their distinct contributions towards autoimmune disease pathogenesis. Understanding which aspects of T cell function can be targeted would be beneficial in the development of new therapeutic strategies.

1.4.1 Rheumatoid arthritis

Rheumatoid arthritis (RA) is a chronic condition characterised by peripheral inflammation, predominantly localised within the joint. Pain and deformity arise following bone erosion mediated by fibroblast-like synoviocytes that rapidly proliferate within the synovium (Ospelt, 2017). However, the inflammatory environment synonymous with disease pathogenesis is primarily established by the various immune cell populations – including T cells, B cells and macrophages – that infiltrate the synovial fluid. Attempts to suppress the activation of T cells within the inflamed synovium have previously shown therapeutic benefit (Kremer et al., 2003), which outlines the contribution of the T cell compartment towards RA pathogenesis. Indeed, memory CD4⁺ T cell populations, including effector and central memory phenotypes, are abundant in the synovial fluid of RA patients (Thomas et al., 1992). Furthermore, the inflammatory milieu within the RA joint encourages clonal CD4⁺ T cell expansion during early disease (Klarenbeek et al., 2012). Genetic studies have further underlined the pathogenic role of T cells in RA. Polymorphisms affecting the interaction between the human leukocyte antigen (HLA) and T cell receptor – especially within the *HLA-DRB1* allele – confer the strongest risk (Viatte et al., 2015). Several of these *HLA-DRB1* alleles have been associated with the formation of anti-citrullinated protein antibodies (ACPAs) critical in RA pathogenesis (Chemin et al., 2016; Gerstner et al., 2016). Outside of HLA-associated alleles, other genes that increase susceptibility towards RA are involved in T cell activation and function (Hu et al., 2014).

IFN γ -producing CD4⁺ T cells are enriched within the human synovium during RA, whilst IL-4 production by the CD4⁺ T cell compartment is minimal (Dolhain et al., 1996; Miltenburg et al., 1992). This is further supported by the presence of IL-12, IL-18 and IFN γ – cytokines typically associated with differentiation towards the Th1 lineage – in the RA synovium (Gracie et al., 1999; Morita et al., 1998). As such, skewing the Th1 / Th2 dichotomy in the direction of a Th2 phenotype – either through inhibition of Th1 cell differentiation and function, or promoting Th2 differentiation – is expected to be favourable in RA (Schulze-Koops & Kalden, 2001). For example, it has been proposed that the efficacy of disease-modifying antirheumatic drugs (DMARDs) stems from the immunomodulatory effect that they have on T cell function. Sulfasalazine downregulated IL-12 production by mouse macrophages, subsequently reducing their ability to induce IFN γ -producing CD4⁺ T cells, whilst increasing their ability to induce IL-4 production by CD4⁺ T cells (Kang et al., 1999). Similarly,

methotrexate treatment of patient-derived PBMCs *in vitro* suppressed the production of IFN γ and IL-2 and concomitantly induced the production of IL-4 and IL-10 (Constantin et al., 1998). Further studies have demonstrated that ciclosporin and bucillamine primarily inhibit the function of Th1 cells, with no effect observed on Th2 cell function (Kim et al., 2000; Morinobu et al., 2000). Despite our understanding of the CD4 $^{+}$ T cell populations that are typically localised to the inflamed joint in human RA, our insight into their antigen-specificity is limited. Citrulline-specific T cells are more abundant in the peripheral blood of RA patients versus healthy controls (James et al., 2014). Interestingly, a greater proportion of these autoreactive T cells exhibited a Th1 memory phenotype (James et al., 2014), further highlighting the influence of Th1 cell in the pathogenesis of RA. Indeed, the presence of ACPAs in established RA are associated with worsened disease severity, whilst their presence prior to clinical diagnosis has significant predictive value (Avouac et al., 2006). Surprisingly, the proinflammatory cytokine response profile of synovial CD4 $^{+}$ T cells appears to be increased in ACPA $^{-}$ RA patients compared to their counterparts in ACPA $^{+}$ patients (Floudas et al., 2021).

Naturally, the increased activity of Th1 cells within the synovial fluid impacts the function of other immune cell populations. For example, Th1 effector cytokines are typical drivers of macrophage activation, which induces the production of proinflammatory cytokines such as IL-6 and TNF α (Maruotti et al., 2007). In the context of RA, IFN-activated macrophages are associated with TNF α production, playing a central role in the induction of chronic inflammation within the synovium (Weyand & Goronzy, 2021; Zhang et al., 2019). Despite the clear link between IFN γ production by Th1 cells and disease pathogenesis, attempts to target this in RA have proven unsuccessful. A clinical trial assessing the use of fontolizumab, a monoclonal antibody treatment directly targeting IFN γ , in the setting of RA was discontinued as it did not meet the clinical endpoint (National Library of Medicine [NLM], NCT00281294). Efforts in murine models have also been unsuccessful, whereby IFN γ receptor knockout exacerbated disease severity in collagen-induced arthritis (Vermeire et al., 1997). Interestingly, further work using this model indicated that IFN γ was necessary in regulating proinflammatory Th17 cell function (Lee et al., 2013).

At first, IL-17 was detected within RA patient-derived synovial tissues and synovial fluid (Chabaud et al., 1998; Ziolkowska et al., 2000). As understanding of the Th17 subset advanced, these IL-17-producing CD4 $^{+}$ T cells were detected in high frequency within the human synovium during RA (Pene et al., 2008). Indeed, the cytokine milieu within the

circulation of RA patients is favourable for differentiation towards the Th17 lineage, with increased levels of key polarising cytokines IL-1 β and IL-6 compared to healthy individuals (Cascao et al., 2010).

Previously, IL-17 has been demonstrated to enhance the production of the proinflammatory IL-6, alongside its related cytokine leukaemia inhibitory factor, by RA patient-derived synoviocytes (Chabaud et al., 1998). Furthermore, the synergistic effect that IL-17 has with other proinflammatory cytokines, particularly IL-1 β , appears to shape the proinflammatory cytokine profile of the inflamed synovium (Chabaud et al., 1998). When directly assessing the influence of Th17 cells, those that infiltrate the synovium during RA maintain an arsenal of cytokines that includes well-known influencers of disease pathogenesis, TNF α and lymphotoxin- β , in addition to classic Th17 cytokines IL-17 and IL-22 (Pene et al., 2008). Their expression of the chemokine receptor CCR6, with concomitant production of its ligand CCL20, further underlined the tissue-infiltrating ability of rheumatic Th17 cells (Pene et al., 2008). The presence of IL-17+/TNF α +CCR6+ CD4+ T cells can be detected in the peripheral blood of RA patients during early disease, where they are able to maintain their phenotype even in the absence of Th17-associated polarising cytokines (van Hamburg et al., 2011). Moreover, Th17 cells closely synergise with synovial fibroblasts, establishing a proinflammatory cytokine-based feedback loop that promotes the tissue-destructive function of the latter (van Hamburg et al., 2011). Additionally, the production of IL-17 and TNF α by Th17 cells likely plays an important contribution towards the recruitment of neutrophils to the site of inflammation (Griffin et al., 2012).

However, it is important to consider that Th17 responses are dependent on the cytokines present within that microenvironment. For example, anti-TNF treatment induces the production of IL-10 by patient-derived CD4+ T cells – including IL-10 expression by Th17 cells (Evans et al., 2014). Attempts to directly inhibit Th17 cell function for therapeutic benefit have been limited in RA. Nevertheless, existing treatments such as ciclosporin A appear to indirectly inhibit pathogenic Th17 cell function, preventing their production of IL-17 (Ziolkowska et al., 2000).

Other subsets within the CD4+ T cell compartment also contribute towards RA pathogenesis. Early work demonstrated that synovial T cells are involved in B cell activation (Thomas et al., 1992). Moreover, germinal centres have been described in the synovium of some RA patients (Kim et al., 1999; Schroder et al., 1996). Importantly, most RA patients

possess ACPAs and are seropositive for rheumatoid factor (RF). Together, these findings suggest a role for follicular helper T (Tfh) cells in RA. Recently, studies have identified increased frequencies of circulating Tfh cells in RA patients, correlated with disease severity and serum anti-cyclic citrullinated protein levels (Ma et al., 2012; Wang et al., 2013). Surprisingly, relatively few Tfh cells are found within RA synovium, where peripheral T helper (Tph) cells instead primarily interact with B cells (Chu et al., 2014; Rao et al., 2017). Interestingly, in contrast to Tfh cells, Tph cells are able to produce effector cytokines such as IFN γ , which suggests they are able to influence multiple aspects of RA pathogenesis (Rao et al., 2017). Although Tph cells are the predominant population within the synovium of patients with RA compared to Tfh cells, the latter subset is still present within the tissue and display a polyfunctional phenotype (Floudas et al., 2022). However, the importance of this CD4 $^{+}$ T cell population requires further investigation. Collectively, these findings outline the contribution of T cells – both directly, and indirectly through the activation of other immune cell populations – towards the inflammatory environment of the synovium that is characteristic of the pathogenesis of RA.

Alternatively, the function of Treg cells would contribute towards alleviating inflammation within the synovium during RA. CD4 $^{+}$ T cells expressing classical Treg cell markers are readily identified in patient-derived synovial fluid and synovial tissues (Cao et al., 2003). Early *in vitro* experiments determined that synovial Treg cells isolated from RA patients were functional, maintaining their ability to suppress the proliferation of T cells originating from either peripheral blood or synovium (Cao et al., 2003). Further studies demonstrated that in fact patient-derived Treg cells had increased suppressive capacity, however, this was counterbalanced by increased resistance to this function by T cells isolated from inflamed synovial fluid (Basdeo et al., 2015; van Amelsfort et al., 2004). Specifically, it appears that a population of CD4 $^{+}$ T cells expressing CD161 are more resistant to Treg-mediated suppression, as depletion of this subset restores the regulatory capability of synovial Treg cells (Basdeo et al., 2015). In contrast, other studies have established that the inflammatory cytokine profile of the rheumatic joint is detrimental to Treg cell function, whereby proinflammatory cytokines such as IL-6 and TNF α markedly reduced suppression of other T cell populations (Herrath et al., 2011). Additionally, further characterisation of Treg cells isolated from the synovium identified a CD39-expressing population that is enriched in RA (Herrath et al., 2014). Interestingly, CD39 $^{+}$ Treg cells displayed greater suppressive function

than their counterparts lacking the expression of CD39 – readily suppressing the production of proinflammatory cytokines such as IFN γ and TNF α (Herrath et al., 2014). However, CD39+ Treg cells were unable to influence the production of IL-17A (Herrath et al., 2014). Whilst Treg cell frequency is increased in the synovial fluid of patients with RA versus their peripheral blood, there is almost an absence of naïve Treg cells within inflamed tissue (Floudas et al., 2022), which could be detrimental to regulatory responses given that FoxP3 expression is not stable in memory Treg cells (Hoffmann et al., 2006). Although the origin of Treg cells found within the synovium is currently unclear, this could be supported by TGF- β – critical for the induction of Treg differentiation – which is abundant in RA synovial fluid (Fava et al., 1989).

Consequently, treatment strategies that promote or restore the function of synovial Treg cells are likely to alleviate inflammation within the rheumatic joint. For example, RA patients responding to anti-TNF α therapy displayed an expansion of the Treg cell population (Ehrenstein et al., 2004). Similarly, IL-6 receptor blockade treatment resulted in ameliorated disease severity, associated with an increase in the Treg cell population, with a concomitant reduction in the Th17 cell population also observed (Samson et al., 2012). Recently, clinical trials have explored the use of low-dose IL-2 treatment – which aims to drive Treg cell differentiation. Promisingly, low-dose IL-2 selectively expanded the Treg cell population across several autoimmune diseases, including but not limited to RA, improving patient outcomes (Rosenzweig et al., 2019).

Most recently, polyfunctional T cells have been identified within the synovium of patients with RA, whilst also being present in individuals at risk of RA (IAR), showing that dysregulation of T cell function towards polyfunctionality precedes clinical onset of the disease (Floudas et al., 2022). Initially, CD161⁺/CD4⁺ Th cells were identified in RA synovial fluid, displaying increased expression of cytokines such as TNF α , GM-CSF and IL-17 (Basdeo et al., 2015). Importantly, these polyfunctional CD4⁺ T cells are enriched within the synovium of patients with RA compared to the peripheral blood of both RA patients and healthy controls (Basdeo et al., 2015). Functionally, CD161⁺ Th cells typically produce at least three or more cytokines, making them more capable of inducing proinflammatory synovial fibroblast function, and are also more resistant to Treg-mediated suppression (Basdeo et al., 2015). Whilst a small population of polyfunctional T cells with heightened cytokine production were present in the synovium of healthy controls, this included high expression levels of IL-4 and GM-CSF, which were poorly expressed by both patient groups (Floudas et al., 2022). This

demonstrates that it is the proinflammatory polyfunctionality of T cells in IAR and RA, rather than just polyfunctionality in general, that supports RA pathogenesis (Floudas et al., 2022). This is further supported by the observed correlation between the frequency of CD4+/CD8+ double-positive T cells within the synovial fluid and disease severity (Floudas et al., 2022). Together, these data demonstrate that aberrant T cell effector function and an imbalance in typical subset frequencies underpins the chronic inflammation within the synovium during RA (Figure 1.15).

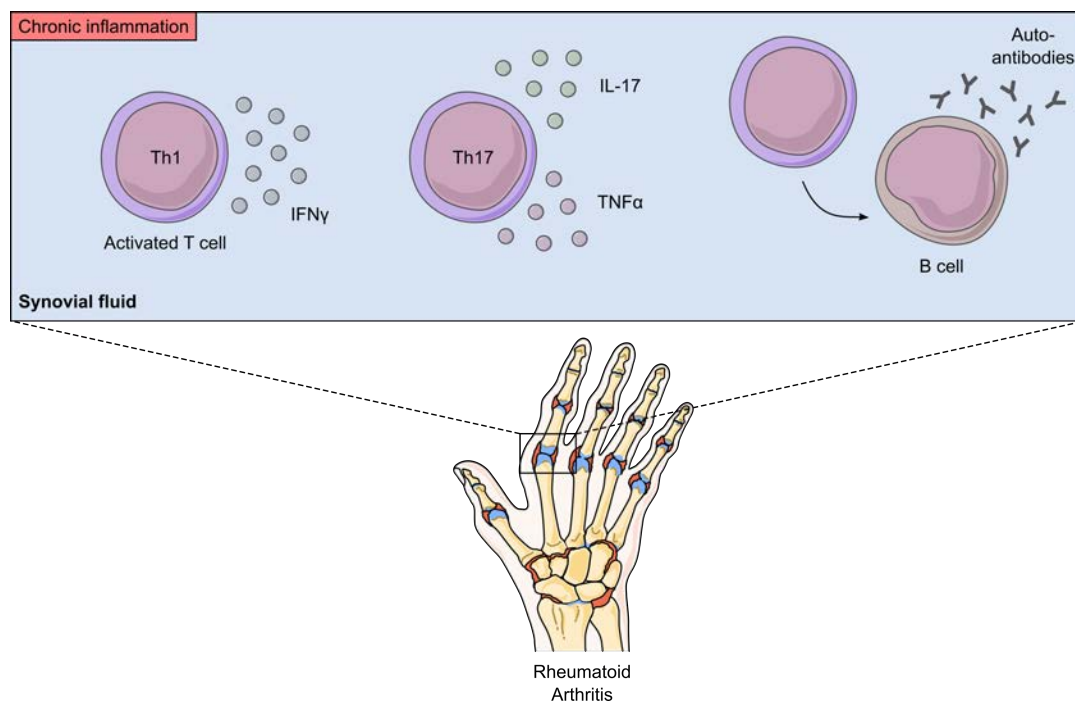


Figure 1.15 – An example of T cell pathogenesis in autoimmune disease

Overview of how T cell function contributes to pathogenesis in the T cell-mediated autoimmune disease, rheumatoid arthritis (RA). Hyperactivated T cells predominate the inflamed synovium, typically exhibiting Th1 and Th17 phenotypes. Their production of proinflammatory cytokines such as IFN γ , IL-17 and TNF α drives the activation of other immune cells to ultimately damage the surrounding tissues. Moreover, T cells can also recruit B cells to the inflamed synovium, which can lead to further production of autoantibodies. Similar mechanisms underpin disease pathogenesis in other T cell-mediated autoimmune diseases.

1.4.2 Systemic lupus erythematosus

Although initially thought to primarily damage skin tissue, systemic lupus erythematosus (SLE) is an autoimmune condition affecting numerous organs and tissues through aberrant immune cell activity (Tsokos, 2011). Given the heterogeneity between SLE cases, this presents a challenge in both the diagnosis and clinical management of the condition. However, it is widely accepted that aberrant T cell function plays a major contribution in the pathogenesis of SLE. Characteristically, T cells isolated from SLE patients display aberrant TCR signalling patterns. It is understood that expression of TCR ζ is either absent or significantly reduced on patient-derived T cells, which increases intracellular tyrosine phosphorylation and Ca²⁺ influx (Liou et al., 1998). These findings have been subsequently linked to altered lipid raft formation, which facilitates the heightened activation of T cells in SLE (Krishnan et al., 2004). Indeed, the expression of the tyrosine-protein kinase Syk – previously shown to associate with lipid rafts – is increased in the T cells of SLE patients (Krishnan et al., 2008). Here, Syk takes the place of ZAP70 within the TCR signalling cascade, where it is enzymatically 100-fold more potent than the latter (Krishnan et al., 2008). Consequently, measures to either silence Syk, or restore TCR ζ expression, have been shown to normalise SLE T cell function (Krishnan et al., 2008; Nambiar et al., 2003). The described changes to the TCR signalling pathway primes T cells to enhanced activation towards disease autoantibodies.

There is an accumulation of memory CD4⁺ T cells in SLE patients, ascribed to the protective effects of increased PI3K activity against cell death (Suarez-Fueyo et al., 2011). Additionally, Th17 cells are enriched amongst the CD4⁺ T cell compartment of SLE patients, with concomitant downregulation of Th1 and Treg subsets (Talaat et al., 2015). Numerous studies have demonstrated the increased presence of circulating IL-17 in SLE patients, with accompanying increases in IL-6 and IL-23 further emphasising the involvement of Th17-driven inflammation in disease pathogenesis (Vincent et al., 2013; Wong et al., 2000; Wong et al., 2008). Indeed, the number of circulating Th17 cells are significantly increased in SLE versus healthy controls (Wong et al., 2008). Mechanistically, CD4⁺ T cells from SLE patients express TLR2 through an FC γ RIIIa / pSyk-mediated co-stimulation pathway (Chauhan et al., 2016). Activation through TLR2 *in vitro* enhances the secretion of IL-6, IL-17 and TNF α by patient-derived CD4⁺ T cells (Liu et al., 2015). TLR2-mediated changes in CD4⁺ T cell function are facilitated via either epigenetic mechanisms involving increased histone acetylation and

reduced DNA methylation at IL-17 promoter regions, or activation of the NF- κ B pathway (Liu et al., 2015; O'Gorman et al., 2015). Additionally, another controller of the IL-17 promoter, protein phosphatase 2A, is upregulated in SLE and through its epigenetic modulatory function could regulate the activation of another promoter of Th17 cell differentiation, rho-associated proteins kinase (Isgro et al., 2013; Sunahori et al., 2013). In contrast, deletion of TLR7 can induce a lupus-like condition in mice, characterised by increases in the frequency of CD4⁺ T_H17 cells and T_H1 cells in an MyD88-dependent manner (G. J. Brown et al., 2022).

Despite the considerable involvement of Th17 cells in SLE pathogenesis, therapies targeting the IL-17 axis have been scarce. Manipulation of important Th17-associated pathways *in vitro* in CD4⁺ T cells isolated from SLE patients – more specifically, silencing of calcium/calmodulin-dependent kinase IV (CAMK4) – inhibited Th17 cell differentiation (Koga et al., 2014). Murine models have demonstrated that activation of CAMK4 increases expression of CCR6, a chemokine receptor important in the homing of CD4⁺ T cells to the kidney (Koga et al., 2016). In humans, CCR6 expression is correlated with the extent of tissue damage observed in SLE (Koga et al., 2016), which suggests that therapeutically targeting this pathway could be beneficial. Furthermore, the use of the anti-IL-17 monoclonal antibody, secukinumab, alleviated disease severity in SLE (Satoh et al., 2018), however it must be considered that these data only included a single case patient. These data propose that therapies inhibiting Th17-driven immune responses warrant further investigation in the context of SLE.

As with many other autoimmune diseases, the production of autoantibodies is implicated in SLE pathogenesis, where anti-dsDNA antibodies confer the greatest susceptibility to severe disease (Tsokos, 2011). Subsequently, numerous studies have shown increased circulating frequencies of CD4⁺ T cells exhibiting a T_H17 cell-like phenotype in SLE patients (Choi et al., 2015; Wang et al., 2014). This CXCR5⁺ / CD4⁺ T cell population have demonstrated CD40L-mediated interaction with B cells *in vitro*, which is required for downstream autoantibody production (Xu et al., 2015). Interestingly, PD-1 expression correlated with disease severity, indicating the influence that T_H17-like cells possess in active SLE (Choi et al., 2015). The aberrant T_H17 cell response is driven via an OX40-dependent mechanism, whereby patient-derived myeloid APCs express high surface levels of OX40L in active disease, which when recognised by CD4⁺ T cells induces the generation of the T_H17 phenotype (Jacquemin et al., 2015). Moreover, the cytokine milieu observed in SLE – namely

decreased levels of IL-2, in combination with increased levels of both IL-6 and IL-21 (Ohl & Tenbrock, 2011) – is generally favourable for the generation of Tfh cells.

Changes in CD4⁺ Treg cell responses – which play an important immunosuppressive role – are not yet fully understood in SLE. There are conflicting reports about whether the number of circulating Treg cells is reduced (Lyssuk et al., 2007), increased (Lin et al., 2007) or remains unchanged (Alvarado-Sanchez et al., 2006) in SLE. This conflict likely stems from inconsistency in the markers used to identify the Treg cell population in such studies (Ohl & Tenbrock, 2015). Functionally, there is a breakdown in the ability to suppress effector T cell activity, where several studies have reported that the immunosuppressive capability of Treg cells is impaired in patients with active SLE. Primarily, these analyses identified an inability to suppress effector T cell proliferation by patient-derived CD4⁺/CD25⁺ Treg cells (Alvarado-Sanchez et al., 2006; Bonelli et al., 2008; Valencia et al., 2007). Interestingly, defective Treg cell function was only observed in active SLE (Alvarado-Sanchez et al., 2006; Valencia et al., 2007). However, there is other evidence to suggest that Treg cell function remains intact in SLE patients (Miyara et al., 2005). Instead, it has been demonstrated that whilst normal suppressive Treg cell function is maintained, patient-derived effector T cells become more resistant to suppression, leading to defects in the Treg-effector cell interaction in SLE (Vargas-Rojas et al., 2008). As such, the extent of Treg cell-mediated regulation observed has been inversely correlated to disease in SLE patients (Venigalla et al., 2008). Nonetheless therapies that improve Treg cell function would be favourable in SLE. Initially, low-dose IL-2 treatment was shown to be effective in a patient with a long history of SLE (Humrich et al., 2015). Furthermore, a more recent clinical trial involving 6 SLE patients also found low-dose IL-2 treatment beneficial, further outlining the potential of this treatment strategy (Rosenzweig et al., 2019). *In vitro* analyses determined that low-dose IL-2 treatment rescued the phenotype and function of patient-derived Treg cells (von Spee-Mayer et al., 2016). Furthermore, low-dose IL-2 treatment has also been associated with modulation of inflammation-driving effector T cells such as Th17 and Tfh cell subsets (He et al., 2016). Together, these data demonstrate the importance of restoring Treg cell function in SLE – whether through rescuing defective Treg function or boosting function against resistant effector cells. These work have also highlighted the significance of reinstating a normal Treg / Th17 cell balance.

mTOR activity plays a significant role in T cell lineage determination in SLE (Kato & Perl, 2014). In patient-derived T cells, mTOR activation is increased, which then induces expression of IL-17-producing T cells, whilst concomitantly reducing the frequency of Treg cells (Kato & Perl, 2014). Treatment with the mTOR inhibitor, rapamycin, impaired the differentiation of Th17 cells and expanded the Treg cell population *in vitro* (Banica et al., 2016; Kato & Perl, 2014), underlining the therapeutic potential of regulating mTOR activity in SLE. Indeed, SLE patients treated with N-acetylcysteine (NAC) – an antioxidant that indirectly inhibits mTOR – displayed improved disease outcome across the 3-month trial period, underpinned by Treg cell expansion resulting from inhibited mTOR activity (Lai et al., 2012). Moreover, inhibiting mTOR directly using sirolimus improved disease outcomes in SLE in a more recent clinical trial, with underlying increases in the Treg cell population and a concomitant reduction in IL-17 production (Lai et al., 2018).

Another mechanism by which the balance of Th17 / Treg cells is skewed is through CAMK4 activity. Initially, it was demonstrated that CAMK4 activation is increased in T cell isolated from SLE patients, where it was responsible for the downregulation Treg cell number and function (Koga et al., 2012). Using murine models, CAMK4 activity has since been implicated in inducing IL-17-producing CD4⁺ T cells (Koga et al., 2016), which strongly suggests that CAMK4 plays a central role in controlling divergence between Th17 and Treg cell phenotypes in SLE. Collectively, these data demonstrate that SLE is a Th17-driven autoimmune condition, supported by the increased activity of autoantibody-associated Tfh cells, with a concomitant dampening of Treg cell suppressive function.

1.5 The role of T cell metabolism in autoimmune disease

Metabolites have long been associated with modulating the immune response. In particular, inflammatory sites such as the synovium in RA are characterised by an accumulation of lactate. In healthy individuals, physiological lactate levels are maintained around 2 mM in sera and tissues, however, this can rise to around 10 mM within the inflammatory synovium of RA patients (Haas et al., 2015; Pucino et al., 2017). Initial work on murine T cells demonstrated that lactate uptake through SLC5A12 markedly inhibited chemotaxis in CD4⁺ T cells (Haas et al., 2015). These CD4⁺ T cells displayed defects in glycolysis, whereby reduced hexokinase I expression was concomitant with lower ECAR, which prevented the necessary response to chemokine ligation and resulted in impaired

migration (Haas et al., 2015). Additionally, lactate also modulated CD4⁺ T cell effector function, promoting the induction of a Th17 signature characterised by upregulation of *IL-17* and *RORG* (Haas et al., 2015). Consistent with these data, human CD4⁺ T cells express the lactate transporter SLC5A12 upon activation, whilst lactate within the synovial fluid can further augment levels on the surface of patient-derived T cells (Pucino et al., 2019). Again, glycolysis was also impaired, meanwhile OXPHOS was unaffected with increased incorporation of lactate into TCA cycle intermediates such as acetyl-CoA and citrate (Pucino et al., 2019). Furthermore, lactate-treated CD4⁺ T cells upregulated their expression of IL-17, with the Th17 phenotype supported by the expression of ROR γ T, the lineage-associated transcription factor, and reduced expression of FOXO1, a transcription factor that limits Th17 differentiation (Pucino et al., 2019). Lactate induced IL-17 expression via a two-pronged approach, wherein dimerisation and translocation of PKM2 to the nucleus and enhanced fatty acid synthesis increased STAT3 phosphorylation, therefore inducing the transcription of IL-17 (Pucino et al., 2019). Moreover, amelioration of disease severity following SLC5A12 blockade demonstrates that the lactate-mediated reprogramming of glycolysis and fatty acid synthesis inhibits the migration of CD4⁺ T cells from the synovium and retains them within the inflamed tissue to contribute to disease pathogenesis (Haas et al., 2015; Pucino et al., 2019). Together these data support that lactate is an important metabolic signalling molecule, particularly in disease states of inflammation such as autoimmune disease. Given that serum lactate levels are increased in patients of other autoimmune diseases including MS (Arnorini et al., 2014), the impact of lactate on CD4⁺ T cell function likely plays an important in the pathogenesis of further autoimmune diseases. The following sections outline disease-specific changes to T cell metabolism that ultimately underpin their pathogenesis (Figure 1.16).

1.5.1 T cell metabolism in rheumatoid arthritis

RA CD4⁺ T cells display defective glucose metabolism, whereby glucose consumption and lactate production are reduced, resulting in diminished ATP production and indicating impaired glycolysis (Yang et al., 2013). Consequently, T cells from RA patients are more susceptible to apoptosis, which was in line with the reduced proliferation and elevated apoptosis observed in glucose-deprived healthy T cells, where these changes are not associated with any changes in T cell differentiation or anergy (Yang et al., 2013). Despite the expression of most glycolytic enzymes remaining similar to control levels upon activation,

patient-derived T cells failed to sufficiently upregulate the key rate-limiting enzyme 6-phosphofructo-2-kinase/fructose-2,6-bisphosphate (PFKFB3) (Yang et al., 2013). T cells with PFKFB3 KO exhibited similar defects in glycolysis to RA T cells, whilst PFKFB3-deficient T cells were more susceptible to apoptosis (Yang et al., 2013). Indeed, restoring PFKFB3 expression in RA T cells rescues the observed phenotype to protect against apoptosis (Yang et al., 2013). The importance of maintaining glycolytic flux has been further demonstrated in murine models of RA, whereby replenishing the product of PFKFB3, fructose-1,6-bisphosphate, attenuated disease severity through the generation of extracellular adenosine, which subsequently activated its anti-inflammatory receptor A2aR (Veras et al., 2015).

Alternatively, glucose-6-phosphate dehydrogenase (G6PD) is upregulated in T cells isolated from RA patients, which shunts glucose into the PPP (Yang et al., 2016). Subsequently, PPP products including NADPH and glutathione accumulate within patient-derived T cells, resulting in defective reactive oxygen species (ROS) upregulation in response to TCR stimulation (Yang et al., 2016). Upregulation of G6PD coincides with downregulation of PFKFB3, where the resulting increased ratio of G6PD:PFKFB3 is correlated with increased disease severity, thus suggesting a relevant pathological role for altered glucose utilisation in RA T cells (Yang et al., 2016). Given the importance of the PPP in macromolecule synthesis, elevated flux through this pathway has a profound effect on proliferation, whereby RA patient-derived T cells are hyperproliferative compared to healthy controls and more rapidly differentiate into a memory phenotype (Yang et al., 2016). Pharmacological and genetic inhibition of G6PD normalises flux through the PPP – restoring NADPH, glutathione and ROS to normal levels – and rectified the unrestrained proliferation observed in RA T cells (Yang et al., 2016). These changes are underpinned by a delicate interplay between the DNA repair kinase ataxia telangiectasia mutated (ATM) and ROS. Previous work detailed that ATM deficiency disrupted DNA damage repair in RA T cells, increasing their susceptibility to apoptosis (Shao et al., 2009). Decreased ROS levels prevent sufficient dimerisation and phosphorylation of ATM upon T cell activation, causing patient-derived T cells to prematurely exit the G2/M checkpoint and undergo unrestricted proliferation (Yang et al., 2016). Furthermore, insufficient ATM activation facilitated by ROS deficiency promotes the hyperinvasiveness and proinflammatory effector functions characteristic of RA T cells, concomitantly polarising these cells towards Th1 and Th17 lineages (Yang et al., 2016). Insufficient ATM activity intensified arthritis development *in vivo*, wherein the synovium was

enriched with proinflammatory cytokines such as IL-1 β , IL-6 and TNF α , alongside increased expression of RANKL to support the bone-damaging function of osteoclasts (Yang et al., 2016). Offsetting the reductive stress induced by augmented PPP activity corrected Th1-biased differentiation in RA patient-derived T cells and reversed their arthritogenic phenotype (Yang et al., 2016). Therefore, redirecting glucose from glycolysis towards the PPP reconditions CD4⁺ T cells from their conventional energy-intensive phenotype to a more anabolic, hyperproliferative phenotype capable of heightened proinflammatory function in RA.

Further work has suggested that shunting glucose towards the PPP might augment NADPH-dependent fatty acid synthesis. Increased migration and invasion by RA T cells is facilitated by upregulation of the locomotion machinery including motility and membrane extension proteins – specifically, TSK5 was necessary for synovium infiltration and its expression is associated with disease score in RA (Shen et al., 2017). Interestingly, the expression of TSK5 and other motility-associated genes was under metabolic control, in which reduced glycolysis and increased fatty acid synthesis were necessary for upregulating locomotion function (Shen et al., 2017). Indeed, the accumulation of lipid droplets within RA T cells supports the development of augmented NADPH-dependent fatty acid synthesis in response to increased PPP activity (Shen et al., 2017). Lipid droplet formation was underpinned by the upregulation of several lipogenic and droplet-forming genes, most importantly *FASN*, whose expression was dependent on reduced glycolytic activity (Shen et al., 2017). Together, these data emphasise that impaired glycolytic flux and the redirection of glucose into the PPP fuels augmented lipid metabolism to divert energy use towards biosynthetic processes. Accordingly, these metabolic defects underpin the arthritogenic phenotype of T cells, facilitating increased proliferative capacity, enhanced migration and invasion, and heightened proinflammatory effector functions. These data might also further implicate DNA repair enzymes in the control of T cell metabolism in RA. DNA-PKcs is upregulated in patient-derived T cells (Shao et al., 2010), and in other cell types it has previously been demonstrated to suppress mitochondrial activity (Park et al., 2017) and induce lipogenesis (Y. H. Wang et al., 2015; Wong et al., 2009).

Defects in RA T cell lipid metabolism have since been linked to impaired AMPK activation. N-myristoyltransferases (NMT) catalyse the addition of the fatty acid myristate to the N-terminal glycine of proteins to allow their subcellular trafficking. Myristoylation is required for AMPK function. Despite containing greater intracellular concentrations of free

fatty acids, myristoylated proteins are less abundant within RA patient-derived T cells due to a translational defect that reduces the expression of NMT1 (Wen et al., 2019). Increasing ratios of ADP/ATP and AMP/ATP should activate the energy sensor AMPK in RA T cells, however, its phosphorylation is reduced compared to healthy controls (Wen et al., 2019). Failure to myristoylate AMPK prevents its subcellular localisation to the lysosome surface which subsequently prohibits its phosphorylation, allowing unrestricted mTORC1 activity within patient-derived T cells (Wen et al., 2019). Consequently, this increases the frequency and proinflammatory functions of Th1 and Th17 cells, which is readily reversible through either the overexpression of NMT1 or downstream activation of AMPK (Wen et al., 2019). Collectively, these data indicate that aberrant T cell metabolism is reprogrammed via the AMPK/mTOR axis in RA, which is itself regulated by metabolic changes.

In addition to the rewiring of glycolysis and perturbed lipid metabolism, metabolic defects have also been described in the mitochondria of RA patient-derived T cells. Despite containing similar levels of mitochondrial mass to healthy controls, OXPHOS was reduced at both basal and maximal levels, associated with uncoupling from ATP production (Li et al., 2019). In agreement with previous work, glycolysis was also found to be reduced in patient-derived T cells, and together with suppressed OXPHOS resulted in diminished ATP production (Li et al., 2019). Interestingly, these changes in mitochondrial metabolism were linked to the DNA repair enzyme MRE11A. Premature senescence is a characteristic of CD4⁺ T cells isolated from RA patients, and it has recently been proposed that the mechanism for telomeric erosion is mediated by impaired MRE11A activity (Li et al., 2016). Interestingly, current investigation demonstrates that MRE11A is involved in regulating T cell mitochondrial function, where MRE11A^{low} T cells displayed a similar metabolic profile to RA T cells, with profound reductions in OXPHOS and ATP production (Li et al., 2019). Moreover, suppression of mitochondrial MRE11A activity culminates in mitochondrial DNA leakage into the cytoplasm, triggering caspase-1-mediated T cell lysis, culminating in inflammation within the synovial fluid (Li et al., 2019). These data highlight the extended role of MRE11A in mitochondrial function and suggests that its deficiency in RA underpins aberrant T cell metabolism and promotes pyroptotic cell death.

Subsequent analyses established that defects in mitochondrial metabolism were caused by an underlying abnormality within the TCA cycle. Downregulation of the GDP-forming β subunit of the enzyme succinate-CoA ligase (SUCLG2) reversed the TCA cycle

towards reductive carboxylation, resulting in the loss of succinate and accumulation of α -ketoglutarate, citrate and acetyl-CoA (B. W. Wu et al., 2020). Overexpression of SUCLG2 reversed the arthritogenic phenotype of RA T cells and suppressed synovial inflammation *in vivo*, thus defects in mitochondrial metabolism can facilitate the proinflammatory effector function of patient-derived T cells (B. W. Wu et al., 2020). Additionally, acetyl-CoA overabundance and active citrate transport induced tubulin hyperacetylation, a process typically associated with microtubule organisation, which enhanced T cell motility and maintained their tissue invasiveness (B. W. Wu et al., 2020). Critically, this process requires cellular elongation for the formation of uropods, alongside the perinuclear clustering of mitochondria – both of which were dependent on SUCLG2 deficiency and excess acetyl-CoA (B. W. Wu et al., 2020). Alongside these changes, mitochondrial metabolism has also been connected to the fitness of the ER in RA T cells. Here, reduced mitochondrial membrane potential was associated with increased ER biomass, facilitated by increased abundance of membrane phospholipid phosphatidylcholine (Wu et al., 2021). Expansion occurred in response to ER stress signals, whereby the expression of ER stress-related genes was upregulated following impaired OXPHOS and could be reversed by transplanting healthy mitochondria into RA T cells (Wu et al., 2021). Given the involvement of mitochondrial metabolites in inter-organelle communication, the amino acid aspartate was identified as both a regulator of ER biomass and as an anti-inflammatory mediator in synovitis, however, patient-derived T cells are deficient in aspartate and its precursor oxaloacetate (Wu et al., 2021). Consequently, RA patient T cells fail to regenerate NAD⁺ in the cytoplasm via the malate-aspartate shuttle, which limits the NAD⁺-dependent ribosylation of the ER stress regulator BiP and thus places mitochondrial fitness upstream of ER function (Wu et al., 2021). The functional consequence of these changes in RA is that T cells become enriched in rough ER that are highly capable of producing large amounts of TNF α , which is then secreted to induce destructive tissue inflammation (Wu et al., 2021). Collectively, these data demonstrate that impaired mitochondrial metabolism and function facilitates the arthritogenic phenotype of RA T cells that culminates in chronic synovial inflammation.

Following their identification within the synovial fluid of patients with RA, the metabolism of polyfunctional T cells has most recently been explored. Interestingly, CD4⁺/CD8⁺ double-positive polyfunctional T cells appear to more dependent on OXPHOS versus their CD4⁺ single-positive counterparts, suggesting that the former subset has a

memory-like phenotype (Floudas et al., 2022). Despite this difference, inhibition of OXPHOS by oligomycin reduced the production of IFN γ , IL-2, IL-17 and TNF α in both polyfunctional subsets, whilst inhibition of glycolysis using 2-DG appeared to have a modest effect on cytokine production (Floudas et al., 2022). Interestingly, OXPHOS is significantly enriched in the polyfunctional T cells of ACPA⁺ RA patients versus those from ACPA⁻ patients, whilst glycolysis is more modestly enriched (Floudas et al., 2021), which might suggest that there is a metabolic underpinning to the differences in T cell function based on patient ACPA status. Together, this wealth of data demonstrates that dysregulated T cell metabolism underpins the pathogenesis of RA.

1.5.2 T cell metabolism in systemic lupus erythematosus

Distinct from the changes observed in RA, early data suggested that pathogenic lymphocytes meet their ATP demand using OXPHOS in SLE. Although glycolysis levels were comparable to healthy controls, splenocytes from lupus-prone mice increased glucose oxidation through the TCA cycle (Wahl et al., 2010). Furthermore, chronically activated T cells – which is a phenotype typically associated with SLE – depend on oxidative metabolism, suggesting that chronic antigen stimulation provides the foundation for the metabolic changes observed in SLE (Wahl et al., 2010). Subsequent bioenergetic analyses revealed that CD4⁺ T cells from both SLE patients and lupus-prone mice demonstrate enhanced metabolism, whereby levels of OXPHOS and glycolysis are elevated (Yin et al., 2015). In a murine model of SLE, T cells displayed an increased spare respiratory capacity, which is indicative of an increased energy store to drive effector function, whilst elevated glycolysis levels were confirmed through increased extracellular lactate production (Yin et al., 2015). Despite exhibiting increased flux through OXPHOS and glycolysis, cellular ATP production was indistinguishable from healthy controls (Yin et al., 2015), which might suggest that enhanced metabolism by SLE CD4⁺ T cells is coupled to increased ATP consumption. Changes in CD4⁺ T cell metabolism were attributable to changes in the metabolic profiles of CD4⁺ T cell subsets. T_{eff} cells are more abundant in SLE and could be the origin of enhanced metabolism, given that they display increased rates of glycolysis and OXPHOS compared to their T_{nv} counterparts, however, it is important to note that T_{nv} cells from lupus-prone mice displayed increased levels of glycolysis and OXPHOS versus their equivalent healthy controls (Yin et al., 2015). Increased mTORC1 activity was required to support elevated rates of glycolysis and

OXPHOS, whilst the altered expression of several metabolic enzymes suggest that SLE CD4+ T cells fuel their enhanced mitochondrial metabolism using glucose, fatty acids and amino acids (Yin et al., 2015). Similar observations were made at the transcript level in human CD4+ T cells, where OXPHOS, mTORC1 and MYC pathways were upregulated in SLE patient samples (Perry et al., 2020). Metabolomic approaches have also identified that the PPP appears to be upregulated in SLE-patient derived T cells – similar to that observed in RA – however, the mechanisms underlying this change are not known (Perl et al., 2015).

The aforementioned metabolic changes underpin CD4+ T cell dysfunction in SLE, wherein the metabolic modulators 2-DG and metformin can normalise effector functions both *in vitro* and *in vivo* through inhibition of glycolysis and OXPHOS, respectively. Interestingly, metformin and other inhibitors of the electron transport chain reduced IFN γ production by CD4+ T cells following short-term activation, whereas 2-DG inhibited IFN γ production following longer-term activation, which suggests differential regulation of IFN γ production by OXPHOS in the activation phase and glycolysis in the proliferative phase (Yin et al., 2015). Metformin also rescued CD4+ T cell IL-2 production, which is defective in SLE (Yin et al., 2015). Consequently, combined treatment with 2-DG and metformin was able to reverse disease in lupus-prone mice, governed by the normalisation of CD4+ T cell expansion, activation and differentiation *in vivo* (Yin et al., 2015). These effects have been further demonstrated in other murine models of SLE, wherein enhanced CD4+ T cell metabolism is reversed by metformin and 2-DG treatment to improve disease pathology (Yin et al., 2015; Yin et al., 2016). Importantly, general metabolic inhibition is not sufficient to reverse the CD4+ T cell disease phenotype in SLE. Here, dichloroacetate (DCA) was used to promote pyruvate oxidation at the expense of its conversion to lactate, yet OXPHOS and glycolysis were unchanged versus the vehicle control (Yin et al., 2016). Consequently SLE-derived T cells treated with DCA retained their phenotype with regards to their activation, differentiation and effector function, thus disease severity could not be alleviated *in vivo* (Yin et al., 2016). Although DCA treatment inhibited IL-17 production by CD4+ T cells from lupus-prone mice, IFN γ production was in contrast increased, which would further explain its ineffectiveness in reversing the SLE disease phenotype (Yin et al., 2016). Together, these data demonstrate that CD4+ T cells from SLE patients and lupus-prone mice exhibit a high demand for glucose metabolism through glycolysis and OXPHOS to drive their pathogenic effector function.

The influence of microbiota on host immune activity is a burgeoning area of autoimmune research, where there is evidence to suggest that it plays an important role in SLE (Azzouz et al., 2019). Most recently, this has led to an investigation into the impact of microbial metabolites on T cell function. Tryptophan is differentially catabolised in lupus-prone mice, primarily via the influence of the microbiota, given that the expression of tryptophan catabolic enzymes was indistinguishable to healthy controls (J. Brown et al., 2022; Choi et al., 2020). CD4+ T cell metabolism was modified directly by tryptophan, whereby several tryptophan catabolites were increased, whilst there was also a pronounced increase in metabolites associated with glycolysis, the PPP and the TCA cycle – all underpinned by the activation of mTOR (J. Brown et al., 2022). These data indicate that altered tryptophan metabolism underpins the observed increase in glycolytic and mitochondrial metabolism in SLE CD4+ T cells. Tryptophan-induced changes in metabolism have profound consequences on CD4+ T cell effector function, exhibiting hyperproliferative and hyperactive properties similar to the phenotype observed in SLE (Choi et al., 2020). Together, these data indicate that tryptophan metabolism possibly underpins changes in CD4+ T cell metabolism in SLE, highlighting the growing contribution of microbiota toward autoimmune disease pathogenesis.

Given that autoreactive CD4+ Tfh cells are central figures in SLE pathogenesis (see Chapter 1.4.2), changes in their underlying metabolism were central to more recent investigation. In lupus-prone mice there was expansion of CD4+ Tfh cells with increased mTORC1 activity that preceded disease onset (Choi et al., 2018). Previously, the combination of metformin and 2-DG was demonstrated to reduce typical measures of Tfh cell activity *in vivo*, including Tfh cell frequency, anti-dsDNA IgG production and germinal centre B cell frequency (Yin et al., 2015; Yin et al., 2016). However, treatment with 2-DG alone is sufficient to induce these changes in several murine models of SLE, also decreasing mTORC1 activity and proliferation, which suggests that pathogenic Tfh cells are more dependent on glycolysis (Choi et al., 2018). Interestingly, glycolytic inhibition selectively targets autoreactive Tfh cells, therefore their metabolic demands appear to be different to those of virus-specific Tfh cells, which makes metabolic manipulation an attractive avenue for the treatment of SLE (Choi et al., 2018). This can be partly explained by differences in solute carrier expression, whereby glycolysis-associated transporters such as *SLC2A6* and *SLC37A2* are upregulated in autoreactive Tfh cells, whilst other Tfh cell types display increased expression of glutamine-

associated transporters such as *SLC1A5* and *SLC7A5* (Choi et al., 2018). Collectively, these data demonstrate that the metabolic rewiring of CD4+ T cells in SLE is not the same across all subsets, which also differs from the conventional metabolic pathways utilised, presenting an interesting opportunity for targeting metabolism in the treatment of the disease.

Given their pathogenic function, the metabolism of Th17 cells has also been investigated in the setting of SLE. The transcription factor inducible cAMP early repressor/cAMP response element modulator (ICER/CREM) has been shown to promote differentiation towards the Th17 lineage through its binding to the *IL17a* promoter (Yoshida et al., 2016). Additionally, it has also been demonstrated that Th17 cells are more dependent on glycolysis than other subsets (Gerriets et al., 2015). In fact, ICER/CREM promotes glycolysis within Th17 cells through inhibition of pyruvate dehydrogenase phosphatase catalytic subunit 2 (PDP2) (Kono et al., 2018). Phosphorylation of pyruvate dehydrogenase (PDH) controls its activity, therefore is critical in regulating the balance between lactate production and oxidative phosphorylation. PDP2 promotes PDH activity, thus ICER/CREM-mediated inhibition of PDP2 reduces PDH activity, allowing the enhanced glycolysis that is required for successful Th17 functions (Kono et al., 2018). Interestingly, CD4+ T cells from SLE patients have displayed increased amounts of ICER and reduced amounts of PDP2 compared to healthy controls (Yoshida et al., 2016). Thus, overexpression of PDP2 in lupus-prone mice *ex vivo* and patient-derived CD4+ T cells diminished the Th17 compartment (Kono et al., 2018). This presents another favourable avenue for targeting metabolism for therapeutic benefit in SLE.

Changes in mitochondrial metabolism are just some of the changes in mitochondrial health that occur in SLE CD4+ T cells. Mitochondrial hyperpolarisation, measured by elevated mitochondrial transmembrane potential and increased ROS levels, has long been implicated in SLE pathogenesis (Gergely et al., 2002), and has been associated with increased mitochondrial biogenesis in SLE T cells (Nagy et al., 2004). Together with enhanced mitochondrial metabolism, this indicates that SLE T cells are in a state of persistent mitochondrial activation. Indeed, this is supported by diminished levels of the antioxidant glutathione, which in turn leads to oxidative stress within these cells (Doherty et al., 2014; Gergely et al., 2002), however, the upstream signals regulating these processes are currently not understood. Nevertheless, the downstream ramifications of mitochondrial stress have been investigated. Excessive mTORC1 activity has already been discussed in enhancing T cell metabolism, however, it is also implicated in dysregulated TCR signalling. The endocytic

recycling machinery is regulated by mTORC1, accordingly in SLE T cells with heightened mTORC1 activity this alters the cell surface expression of TCR ζ (Fernandez et al., 2009). Consequently, this is functionally replaced by the Fc ϵ R type I γ -chain (Fc ϵ R1 γ) which is associated with increased Ca²⁺ fluxing to induce the pathogenic phenotype in SLE (Enyedy et al., 2001; Nambiar et al., 2003). Moreover, increased mTORC1 activation has also been associated with promoting T cell IL-4 and IL-17 production at the expense of the Treg population in SLE (Kato & Perl, 2014). This demonstrates that mTORC1 hyperactivation and the induction of oxidative stress is central to the pathogenic CD4⁺ T cell phenotype in SLE. Naturally, the glutathione precursor N-acetylcysteine (NAC) has been shown to alleviate disease severity in lupus-prone mice and human clinical trials (Lai et al., 2012; Suwannaroj et al., 2001). Furthermore, treatment using the mTORC1 inhibitor rapamycin has also had a beneficial effect in SLE patient cohorts, normalising the Ca²⁺ of patient-derived CD4⁺ T cells (Fernandez et al., 2006), and improving disease outcome at clinical trial (Lai et al., 2018).

A minor role has been described for lipid metabolism in SLE CD4⁺ T cells. Glycosphingolipids and cholesterol form specialised membrane structures that are important in TCR signalling (He et al., 2005). Alterations in lipid raft composition makes patient-derived T cells more sensitive to TCR stimulation, reducing the threshold required to induce Ca²⁺ fluxing (Krishnan et al., 2004). Indeed, T cells isolated from patients with SLE displayed increased expression of the lipid raft-associated ganglioside GM1, which affected the regulation of the TCR signalling molecule Lck (Jury et al., 2004). Moreover, targeting alterations in lipid raft composition using atorvastatin is able to rescue the SLE-associated abnormalities in T cell signalling, normalising patient-derived T cell effector function (Jury et al., 2006). More recently, CD4⁺ T cells isolated from SLE patients have been demonstrated to have markedly altered glycosphingolipid profiles compared to healthy controls, with a general increase in the abundance of most glycosphingolipid species (McDonald et al., 2014). This was associated with increased expression of liver X receptor β (LXR) – a nuclear receptor involved in lipid trafficking and immune responses – which resulted in the accumulation and trafficking of glycosphingolipids, which is reminiscent of glycolipid storage disease (McDonald et al., 2014). Restoring glycosphingolipid homeostasis through inhibiting its biosynthesis normalised CD4⁺ T cell signalling and rescued effector function, suggesting that targeting lipid metabolism in SLE has therapeutic benefit (McDonald et al., 2014). Additional roles have since been described for LXR, such as its ability to directly regulate glycosphingolipid metabolism,

which can cause reduced lipid stability within the plasma membrane at the immunological synapse, causing aberrant activation of TCR signalling molecules (Waddington et al., 2021). Interestingly, reduced plasma membrane lipid order appears to be required for optimal Treg cell function, suggesting its importance in the distinct functional programmes observed between subsets (Waddington et al., 2021).

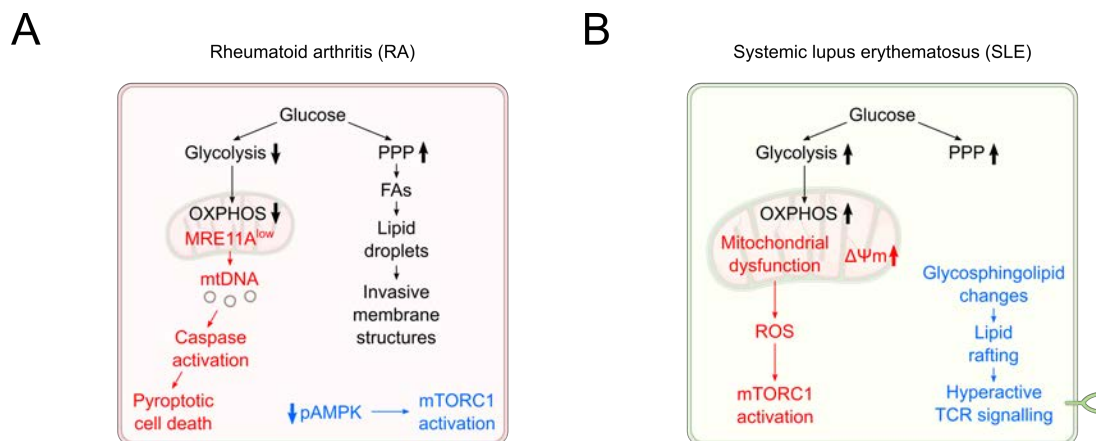


Figure 1.16 – Summary of T cell metabolism in autoimmune disease

Overview of the metabolic pathways that underpin aberrant T cell function in (A) rheumatoid arthritis and (B) systemic lupus erythematosus. Crucially, heterogenous metabolic programmes underpin T cell-mediated autoimmune disease, despite T cells playing a similar role in disease pathogenesis. For example, the function of RA patient T cells are driven by a marked reduction in glucose metabolism, whilst those from SLE patients display augmented glucose metabolism. However, some aspects of metabolism are shared between autoimmune conditions, such as the activation of mTORC1.

1.6 Repurposing type 2 diabetes drugs in autoimmunity

Traditional treatments for autoimmune disease have long been accompanied by crippling side effects. For instance, non-selective steroidal anti-inflammatory drugs (NSAIDs) that inhibit COX-1 and COX-2 can cause significant gastrointestinal problems such as ulceration, bleeding and perforation (Fujita et al., 2013). Regrettably, gastrointestinal complications are symptomatic of numerous anti-inflammatory medications, including glucocorticoids (Ethgen et al., 2013) and disease-modifying anti-rheumatic drugs (DMARDs) such as sulfasalazine (Skosey, 1988). Whilst the use of selective COX-2 inhibitors overcome these gastrointestinal issues (Dajani & Islam, 2008), both NSAID types are associated with

severe cardiovascular complications (Hermann & Ruschitzka, 2006; Ray et al., 2002). Furthermore, the renal toxicity of NSAIDs (Murray & Brater, 1993), in addition to ciclosporin (Gabriel et al., 2001), is concerning. Whilst targeted therapeutics against TNF α are the latest class of medication that have been effective in treating autoimmune disease, there are still challenges concerning their safety (Li et al., 2017), in addition to their limited efficacy in some patient subgroups (Roda et al., 2016).

Given the debilitating side effects associated with current treatments, investigation into alternative therapeutics is warranted. Multiple pre-clinical trials have demonstrated therapeutic benefit from targeting T cell metabolism. For example, tetramerisation of the glycolytic enzyme pyruvate kinase (PKM2 isoform) within murine T cells ameliorated EAE (Angiari et al., 2020). Upon T cell activation, PKM2 translocates into the nucleus, activating metabolic modulators including mTORC1, MYC and HIF1 α to engage the elevated levels of glycolysis necessary for a proinflammatory response (Angiari et al., 2020). Treatment of T cells with the small molecule TEPP-46 prevented the translocation of PKM2, subsequently limiting Th1 and Th17 cell development – a process that is highly dependent on glycolytic activity (Angiari et al., 2020). Encouragingly, there were similar observations made when human T cells were treated with TEPP-46 *in vitro* (Angiari et al., 2020), however, it is important to consider the potential toxicity of using such high doses of this molecule. Inhibiting glucose metabolism through alternative mechanisms have also been effective. Targeting mitochondrial metabolism using the ATP synthase inhibitor oligomycin reduced disease severity in a murine model of MS through its ability to inhibit Th17 cell pathogenicity (Shin et al., 2020). Th17 cells rapidly engage OXPHOS during development, therefore inhibition of this pathway suppressed their signature gene expression, where they instead displayed a regulatory phenotype epitomised by FoxP3 expression (Shin et al., 2020). Furthermore, targeting glucose metabolism with 2-DG and mitochondrial metabolism with metformin improved immune tolerance in a murine model of SLE by inhibiting the expansion of Tfh cells and their associated germinal centre B cells (Wilson et al., 2021). Patients with SLE often develop serious kidney damage that can require transplantation, which is often susceptible to autoimmunity and allogenic rejection, increasing the subsequent risk of graft failure (Contreras et al., 2010). This combination of metformin and 2-DG, in addition to standard therapy, can also improve graft survival compared to using the standard therapy alone, further outlining the possible clinical benefits (Wilson et al., 2021). Interestingly, glutamine

metabolism has also been manipulated for therapeutic gain in pre-clinical studies of autoimmunity. Here, deletion of glutaminase – a central enzyme in glutamine anaplerosis – reduced inflammation in a model of graft-versus-host disease (Johnson et al., 2018). Glutaminase deficiency was characterised by impaired Th17 cell function and modest inhibition of Th1 cell function (Johnson et al., 2018). Despite these encouraging results, the translation of these studies into a clinical setting is difficult given the challenge of inhibiting metabolism at a whole-body level. Indeed, recent clinical trials concerning the use of IACS-010759, a small molecule complex I inhibitor, in the treatment of acute myeloid leukaemia were terminated due to the limited target inhibition observed at safely tolerated doses (Yap et al., 2023). Moreover, the development of novel drugs is a costly process – both in terms of time and finances. Consequently, repurposing existing FDA-approved drugs (also known as drug repositioning), which have established safety profiles in humans, is an attractive prospect – particularly in the search for alternative therapies in autoimmune disease. Given that T2D drugs often target cellular metabolism, several different classes of these drugs have shown promise in autoimmune disease by targeting T cell metabolism.

1.6.1 Thiazolidinediones

Originally, thiazolidinediones (TZDs) – including rosiglitazone, pioglitazone and the later withdrawn troglitazone – were investigated in autoimmune disease. Initially, troglitazone and rosiglitazone were shown to improve patient outcomes in psoriasis and ulcerative colitis, respectively (Ellis et al., 2000; Lewis et al., 2001). Troglitazone has been demonstrated to dampen human T cell activation and proliferation, possibly through promoting the association of PPAR γ with NFAT (Yang et al., 2000). Thus, T cell-mediated autoimmune diseases were next studied, whereby pioglitazone improved disease outcome in EAE, partly through its ability to impair T cell activation and function (Feinstein et al., 2002). This effect was reproducible in human T cells from both healthy and MS individuals – pioglitazone treatment impaired T cell proliferation and inhibited production of proinflammatory cytokines IFN γ and TNF α *in vitro*, whilst oral treatment maintained an anti-proliferative effect on T cells in one MS patient (Schmidt et al., 2004). Subsequently, this translated into a notable improvement in weight gain, muscle strength and prevention of brain atrophy when trialled in an MS patient (Pershad Singh et al., 2004). Further clinical trials indicated that pioglitazone was well-tolerated in MS patients, and that there were noticeable

improvements in lesion burden and the prevention of new lesions, thus warranting further investigation (Kaiser et al., 2009; Shukla et al., 2010). Interestingly, there was no evidence demonstrating that rosiglitazone would be beneficial in the treatment of MS (Miller et al., 2005). Together, this suggests that there is no overarching class effect for TZDs in the treatment of autoimmune disease, but rather individual members this group of drugs have unique properties that establish their efficacy.

Pioglitazone has also showed promise in murine experimental autoimmune uveitis, reducing the production of numerous inflammatory markers such as IFN γ and IL-6, with a simultaneous increase in T_H1 and Treg cells within the lymph nodes (Okunuki et al., 2013). Disease outcome was not only improved in whole-phase treatment, but also effector phase treatment, which suggests that pioglitazone might be effective in autoimmune uveitis even after the onset of disease (Okunuki et al., 2013). Similar observations were made in patients with a combination of metabolic syndrome and MS, wherein IL-6 and TNF α production by PBMCs was reduced, whilst there was an increase in the frequency of Treg cells (Negrotto et al., 2016). Concomitant with the pioglitazone-induced expansion of Treg cells, T_H1 cell proliferation was inhibited, and this was supported by the increased secretion of the anti-inflammatory cytokine IL-10 (Negrotto et al., 2016). These data also revealed an interesting role for adipokine levels in TZD treatment of autoimmune disease. Leptin has previously been associated with proinflammatory conditions, whilst adiponectin is linked to anti-inflammatory contexts (Versini et al., 2014). Here, pioglitazone treatment induced a dichotomous effect on circulating adipokine levels, reducing leptin whilst increasing adiponectin, describing an additional metabolic underpinning for its efficacy in autoimmunity (Negrotto et al., 2016). Most recently, rosiglitazone improved atopic dermatitis outcome in obese mice, again highlighting the potency of TZDs particularly in the presence of metabolic affliction (Bapat et al., 2022). However, unlike previous reports assessing pioglitazone, rosiglitazone was able to reduce Th17 cell-mediated inflammation (Bapat et al., 2022). Th2 cells were also re-established within the T cell compartment as seen with lean controls, restoring the efficacy of anti-IL-4 and anti-IL-13 antibody treatment (Bapat et al., 2022).

1.6.2 Metformin

The biguanide metformin has arguably been the most extensively studied T2D drug in the setting of autoimmune disease. Currently the preferred first-line medication for T2D,

metformin was approved for use in the disease in 1995, and there is growing interest in its ability to modulate cellular metabolism as an activator of AMPK and inhibitor of complex I of the electron transport chain. Numerous studies have since attempted to exploit the activity of metformin for benefit in autoimmunity.

Early murine models demonstrated that metformin, through its activation of AMPK, improved disease outcomes in EAE when introduced both before and after disease onset (Nath et al., 2009). Metformin reduced the infiltration of lymphocytes into the central nervous system (CNS), where there was also a subsequent reduction in proinflammatory cytokines – indeed, metformin directly inhibited the production of an array of proinflammatory mediators by macrophages and T cells (Nath et al., 2009). Notably, metformin also diminished Th1 and Th17 cell populations, downregulating their distinctive transcription factors, Tbet and ROR γ T, respectively (Nath et al., 2009). Similar observations were made when metformin was used alone and in combination with lovastatin, a member of the statin family of cholesterol lowering agents (Nath et al., 2009). Alterations within the metformin-treated T cell compartment also extended to Th2 cells and possibly other regulatory phenotypes (Paintlia et al., 2013). Later work confirmed that metformin treatment expanded Treg populations within EAE mice (Sun et al., 2016). However, the more salient point gleaned from these data was that the neuroprotective and anti-inflammatory effects of metformin in murine models of MS are mediated by inhibition of mTOR/HIF1 α signalling – key metabolic regulators that are downstream targets of AMPK (Sun et al., 2016).

Modulation of the AMPK/mTOR axis by metformin has been confirmed in other murine models of autoimmune disease, where this mechanism remains central to the inhibition of Th17-mediated inflammation. In collagen antibody-induced arthritis, metformin prevented cartilage destruction, reduced circulating proinflammatory cytokine levels, and restricted Th17 differentiation by inhibiting STAT3 phosphorylation via the AMPK/mTOR pathway (Kang et al., 2013). The same observations were made in collagen-induced arthritis, an arthritis model with slower onset of the disease (Son et al., 2014). This study built upon previous work by showing that metformin treatment resulted in a concomitant expansion of Treg cells upon Th17 inhibition, whilst inhibition of osteoclast proliferation and function ceased bone damage, again through changes to the STAT3/AMPK/mTOR nexus (Son et al., 2014). These findings have been further confirmed in mouse models of inflammatory bowel disease, SLE and graft-versus-host disease (Lee et al., 2015; Lee et al., 2017; Park et al., 2016).

Given that dysregulated T cell metabolism underpins autoimmune disease (see Chapter 1.5), it is unsurprising that metformin harnesses some of its efficacy in autoimmunity by manipulating T cell metabolism. In murine SLE-derived T cells with heightened metabolic activity, metformin counteracted this metabolic defect by limiting the rate of OXPHOS to reverse disease phenotypes, particularly during early T cell activation where effector function was more reliant on oxidative metabolism (Yin et al., 2015). Surprisingly, in terms of glycolysis, high-dose metformin increased flux through this pathway, which rendered it ineffective in restoring normal function in already-activated T cells that are highly dependent on glycolysis (Yin et al., 2015). Consequently, this led to use of 2-DG in combination with metformin to offer greater efficacy against SLE by inhibiting both major glucose metabolism pathways to restrict pathological effector function (Yin et al., 2015). These data were reproducible in other murine models of SLE, as well as other types of autoimmune disease such as autoimmune lymphoproliferative syndrome, whereby metformin and 2-DG combined to reduce the rates of glycolysis and OXPHOS to limit T cell activation and function (Yin et al., 2016). Importantly, it was also determined that cessation of treatment resulted in relapse to a disease phenotype, demonstrating that constant exposure of T cells to metformin and 2-DG is required to maintain a protective effect against autoimmunity (Yin et al., 2016). In contrast to previous work, monotherapy with either metformin or 2-DG appeared to have a beneficial effect in some models of lupus (Yin et al., 2016), highlighting the significance of appraising disease-by-disease differences in susceptibility to metformin treatment.

Despite the promising anti-inflammatory effects of metformin demonstrated in murine models of autoimmune disease, human studies remain scarce. T cells isolated from SLE patients displayed similarly increased metabolic output, which fuels increased IFN γ production that is reversible by metformin *in vitro* (Yin et al., 2015). Despite the promise shown by metformin in both murine and human studies of autoimmune disease, the mechanism by which it exerts its anti-inflammatory effect on T cells remains uncertain. It is unclear whether metformin is taken up by T cells at physiological doses, as the primary transporter SLC22A1 is not expressed by most T cell subsets, where it is only scarcely expressed by Treg cells (Uhlen et al., 2019)(Human Protein Atlas, proteomics.org).

A proof-of-concept trial exploring the use of metformin as an add-on to traditional prednisone concluded that this reduced disease flares compared to the placebo group (H. T.

Wang et al., 2015). A second clinical trial also observed a decrease in the frequency of flares when metformin was used alongside prednisone, however, this study was underpowered to draw any definite conclusions (Sun, Wang, et al., 2020). Post-hoc analyses combining the finding from both trials observed a significant reduction in flares in response to metformin treatment, with individuals that are in early disease (duration < 5 years) or serologically quiescent showing increased sensitivity to treatment (Sun, Geng, et al., 2020). Importantly, metformin was well-tolerated throughout these clinical trials (Sun, Geng, et al., 2020), underlining the advantage of an established safety profile when repurposing drugs. Most recently, metformin has also been shown to alleviate disease severity in RA, whereby inflammation was reduced after 6 months of treatment, whilst quality of life was improved as early as 3 months following metformin treatment (Gharib et al., 2021).

A study assessing the use of metformin in patients with MS and metabolic syndrome offered some insight into the underlying mechanisms supporting its efficacy in human autoimmune diseases. Firstly, metformin was effective in reducing disease activity in MS, reducing the number of active lesions within the brain 6 months post-treatment (Negrotto et al., 2016). Interestingly, metformin treatment was associated with increased AMPK expression in patient-derived PBMCs, with cytokine production and transcription factor expression patterns suggesting reduced frequencies of disease-associated Th1 and Th17 cells, with a concomitant increase in the Treg cell population (Negrotto et al., 2016). These findings are similar to the changes observed in murine models. Furthermore, enhanced activity of this expanded Treg cell population in metformin-treated MS patients inhibited effector T cell proliferation, again drawing parallels with earlier murine studies (Negrotto et al., 2016). Together, these data highlight the potential that T2D drugs exhibit in the setting of autoimmunity through targeting T cell metabolism and emphasises the importance of repurposing drugs with established safety profiles to circumvent the toxicity that directly targeting metabolism can impose on whole body function.

1.7 Sodium glucose co-transporter 2 inhibitors

Sodium glucose co-transporter 2 (SGLT2) inhibitors are the most recently approved class of T2D drugs, with clinical examples including canagliflozin, dapagliflozin, empagliflozin and ertugliflozin. First approved in 2013 as a monotherapy, SGLT2 inhibitors (also known as gliflozins) target SGLT2, which facilitates glucose reabsorption within the nephron. By

inhibiting this process, glycaemic control is improved through increased clearance of glucose in urine, thus regulating blood glucose levels (Mosley et al., 2015).

1.7.1 Off-target effects of SGLT2 inhibitors

Interestingly, some SGLT2 inhibitors have off-target action that affects cellular metabolism and mitochondrial dynamics. Of particular interest, canagliflozin has been shown to inhibit complex I of the electron transport chain (Villani et al., 2016) and mitochondrial glutamate dehydrogenase (GDH), an enzyme that is essential in glutamine anaplerosis (Secker et al., 2018) (Figure 1.17). Initially, canagliflozin was demonstrated to induce AMPK activation in HEK-293 cells, underpinned by mitochondrial inhibition causing increased cellular AMP levels (Hawley et al., 2016). Changes in acetyl-CoA carboxylase phosphorylation, a downstream target of AMPK, likely altered cellular lipid metabolism, whilst glucose uptake was also impaired via an SGLT2-independent mechanism (Hawley et al., 2016). Further analysis using murine cells determined that mitochondrial inhibition in canagliflozin-treated cells was specific to complex I of the electron transport chain (Hawley et al., 2016). In human cell lines, inhibition of complex I by canagliflozin supported the reduced proliferation and clonogenic survival of several different prostate and lung cancer cell lines (Villani et al., 2016). Although canagliflozin treatment was also associated with AMPK activation in these cells, this was not required to mediate its anti-proliferative properties (Villani et al., 2016). Importantly, these changes were also not caused by the on-target effects of canagliflozin, as glucose uptake through SGLT2 was not essential (Villani et al., 2016). Complex I inhibition by canagliflozin has also been confirmed in renal proximal tubule epithelial cells, reprogramming cellular metabolism through suppression of OXPHOS and increasing dependence on glycolytic metabolism (Secker et al., 2018). Conversely, canagliflozin limited glycolytic flux in human umbilical-vein epithelial cells (HUVECs), which might suggest that canagliflozin modulates glycolysis in a cell-dependent manner (Zugner et al., 2022). Mitochondrial dysfunction within canagliflozin-treated cells was associated with increased superoxide formation (Secker et al., 2018). Additionally, mitochondrial GDH was also inhibited by canagliflozin, which prevented the entry of glutamine into the TCA cycle and drastically altered the cellular amino acid profile (Secker et al., 2018). This inhibition of GDH, but not complex I, was demonstrated to be the primary cause of reduced cell viability (Secker et al., 2018). These findings have been verified in breast cancer cell lines, whereby canagliflozin mediated its anti-proliferative effect

primarily through the inhibition of glutamine metabolism (Papadopoli et al., 2021). In HUVECS, reduced proliferation was sustained through the inhibition of DNA synthesis and cell cycle arrest at G0/G1 phase through the loss of cyclin A and retinoblastoma protein phosphorylation (Behnammanesh et al., 2019). This blockade of proliferation occurred in the absence of cell death, revealing canagliflozin mediated cytostatic rather than cytotoxic properties in these cells, again highlighting its differential effects on different cell types (Behnammanesh et al., 2019). Further functions inhibited by the off-target effects of canagliflozin included proinflammatory cytokine and chemokine responses, whereby IL-6 and MCP-1 secretion by IL-1 β -stimulated HUVECs was reduced (Mancini et al., 2018). Crucially, inhibition of complex I and mitochondrial GDH is a property unique to canagliflozin – dapagliflozin, empagliflozin and ertugliflozin exhibited either no effect or modest effects on the parameters measured across various cell types. More importantly, the aforementioned off-target effects occurred at physiologically relevant doses of canagliflozin, which is typically in the region of 10 μ M in the circulation of patients with T2D that are prescribed the drug (Devineni et al., 2013).

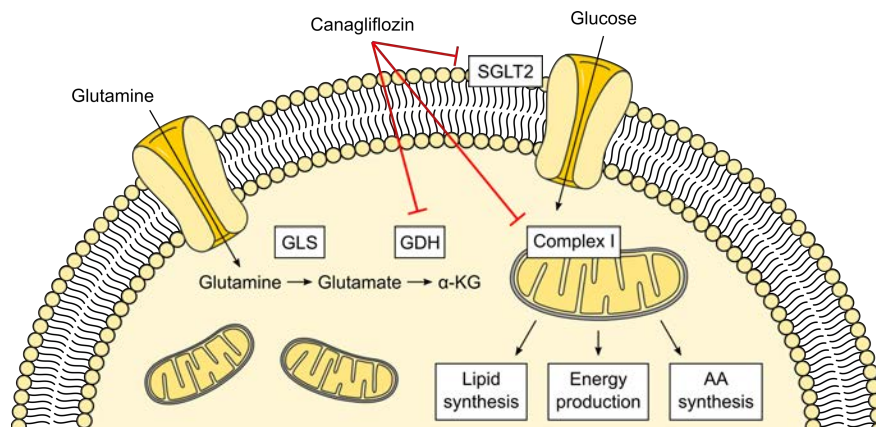


Figure 1.17 – The impact of canagliflozin on cellular function

Overview of the on- and off-target effects that canagliflozin has on cellular function. Primarily, canagliflozin inhibits glucose uptake via sodium glucose co-transporter 2 (SGLT2). Canagliflozin also has off-target effects including inhibition of glutamate dehydrogenase (GDH) and complex I of the electron transport chain.

Alternatively, empagliflozin regulates mitochondrial function by distinct mechanisms compared to canagliflozin. In murine cardiac microvascular endothelial cells, empagliflozin diminished diabetes-induced mitochondrial fragmentation through re-establishing the homeostasis of mitochondrial fusion and fission proteins (Zhou et al., 2018). Here, empagliflozin increased the expression of mitofusin-1 and -2, whilst simultaneously reducing the expression of fission-associated proteins Fis-1 and mitochondrial fission factor (Zhou et al., 2018). Empagliflozin-induced activation of AMPK also retained the critical fission regulator, dynamin-related protein-1, within in the cytosol and together the changes in mitochondrial dynamics protected against cell senescence and improved vascular cell migration (Zhou et al., 2018). Similar observations were made in the myocardium of diabetic rats, whereby empagliflozin treatment was associated with fewer, but larger, mitochondria (Mizuno et al., 2018). Further to the changes to mitochondrial fission, Bnip-3 – which acts as a mitochondrial receptor for autophagosomes to eliminate mitochondria – is upregulated at both transcript and protein levels, suggesting that empagliflozin also promotes the clearance of small mitochondria via mitophagy (Mizuno et al., 2018). Beyond these findings, increased intermitochondrial joints within empagliflozin-treated myocardium post-cardiac arrest suggested the presence of more highly active mitochondria (Tan et al., 2021). Indeed, mitochondrial complex I activity was elevated and ATP production increased in these empagliflozin-treated cells (Tan et al., 2021). A concomitant reduction in serum lactate levels might suggest reduced glycolytic output, therefore empagliflozin could prime cells towards oxidative metabolism (Tan et al., 2021). Recent studies have since confirmed improved mitochondrial membrane potential and mitochondrial complex I and II activity in cardiac tissue following empagliflozin treatment (Wang et al., 2022; Zou et al., 2022). This has revealed that empagliflozin exhibits anti-oxidative properties, whereby the prevention of oxidative stress limited the activation of the DNA-PKcs pathway involved in Fis-1 phosphorylation (Zou et al., 2022). Although it has not been directly confirmed whether the off-target effects of empagliflozin involved in shaping mitochondrial dynamics are SGLT2-independent, the limited expression of the transporter within the assessed tissues might suggest that this is the case (Chen et al., 2010; Vrhovac et al., 2015).

Currently, there is limited evidence outlining the off-target effects of dapagliflozin. Investigation into cardiomyocytes in rat metabolic syndrome revealed a cardioprotective role for dapagliflozin (Durak et al., 2018). Metabolic syndrome exacerbated mitochondrial

depolarisation within cardiomyocytes, which was accompanied by an altered ratio of the mitochondrial fusion proteins mitofusin-1 and -2, as well as increased expression of the mitochondrial fission protein Fis-1 (Durak et al., 2018). These data highlight the potential for dapagliflozin to shape mitochondrial dynamics and influence mitochondrial function. To this end, there is growing evidence that SGLT2 inhibitors can influence cellular metabolism through their off-target effects – each with unique metabolic targets and downstream changes in cell function.

1.7.2 Repurposing SGLT2 inhibitors in inflammatory diseases

Consequently, some studies have flagged the potential of SGLT2 inhibitors as treatments for inflammatory disease. Promisingly, canagliflozin has displayed beneficial effects in chronic kidney disease at clinical trial (Perkovic et al., 2019). Here, the relative risk of kidney failure was approximately 30% lower in the group treated with canagliflozin, benefitting patients at several stages throughout the course of disease (Perkovic et al., 2019). Interestingly, patients treated with canagliflozin also had a lower risk of cardiovascular complications, including cardiovascular death, myocardial infarction and stroke, in addition to reduced hospitalisation for heart failure (Perkovic et al., 2019). The effect of canagliflozin in heart failure was further explored in another clinical trial, where it was shown that canagliflozin improved patient outcomes regardless of ejection fraction or diabetes status (Spertus et al., 2022). Importantly, both chronic kidney disease and heart failure have underlying inflammatory elements. In heart failure, numerous immune cell populations become activated, whilst patients with reduced ejection fraction can also have increased levels of proinflammatory cytokines within the circulation (Adamo et al., 2020). Similarly, patients with chronic kidney disease also have heightened circulating levels of proinflammatory cytokines, resulting from reduced cytokine clearance (Akchurin & Kaskel, 2015). Together, these studies highlighted the potential to repurpose canagliflozin in the setting of inflammatory disease. Interestingly, it has also been shown that canagliflozin extends the lifespan of male, but not female, mice (Miller et al., 2020). Despite this sexual dimorphism, canagliflozin regulated blood glucose levels and improved glucose tolerance in both sexes (Miller et al., 2020). However, canagliflozin was also only able to reduce fat mass in female mice, demonstrating that there are also differential effects in weight loss (Miller et al., 2020).

Unsurprisingly, there have been several other studies examining the use of SGLT2 inhibitors in other inflammatory conditions. For example, canagliflozin displayed anti-inflammatory properties in mouse and human monocyte/macrophage cell lines (Xu et al., 2018). Here, IL-6 and TNF α production was reduced, albeit using concentrations of the drug towards the upper limit of physiological relevance (Xu et al., 2018). Canagliflozin impaired glycolysis within these immune cell lines, possibly through the inhibition of PFK, and promoted autophagy in an AMPK-dependent manner, both of which were required to limit inflammation (Xu et al., 2018). Despite no class-specific effect being demonstrated by treatment with either dapagliflozin or empagliflozin, it is unclear whether direct inhibition of SGLT2 contributed to the anti-inflammatory action of canagliflozin (Xu et al., 2018). Interpretation of non-human data must be approached with caution, as analyses using primary human macrophages demonstrated that dapagliflozin can in fact elicit anti-inflammatory properties (Abdollahi et al., 2022). Treatment with dapagliflozin limited proinflammatory cytokine production by inhibiting the NF- κ B signalling pathway, reversing LPS-induced polarisation towards an M1 phenotype (Abdollahi et al., 2022). Dapagliflozin was able to mediate similar changes under both normal glucose and high glucose conditions, suggesting that it acts on macrophages via an SGLT2-independent mechanism (Abdollahi et al., 2022). Recently, in the setting of murine experimental autoimmune myocarditis, canagliflozin could alleviate cardiac tissue inflammation by inhibiting the NLRP3 inflammasome through inactivation of the NF- κ B pathway (Long et al., 2022). The NLRP3 inflammasome has previously been associated with Th17 cell differentiation in other autoimmune diseases (Zhao et al., 2018). Indeed, Th1 and Th17 cells are critical mediators of myocarditis (Yuan et al., 2010; Zhu et al., 2021), and there was a correlation – but not a definitive, causative link – between NLRP3 activation and Th17-associated function (Long et al., 2022). Thus, canagliflozin can influence murine CD4⁺ T cell differentiation, particularly suppressing Th1 and Th17 cell populations (Long et al., 2022). Alas, the underpinning mechanism mediating these changes has not been elucidated.

The off-target effects of empagliflozin on human T cell function have recently been explored. Immune thrombocytopenia is an autoimmune disease characterised by increased Th1 and Th17 populations and an accompanying reduction in Tregs (Ma et al., 2008; Yu et al., 2008). The T cell subset landscape in the disease is shaped by their metabolic reprogramming, namely a shift towards glycolytic metabolism, which could be reversed by empagliflozin

treatment (Qin et al., 2022). Thought to mediate its effect through mTOR inhibition, empagliflozin inhibited glycolysis and increased OXPHOS levels to restore the balance of Th1, Th17 and Treg cells back to that observed in healthy individuals (Qin et al., 2022). Thus, there is precedent to further investigate SGLT2 inhibitors in autoimmune disease.

Currently, the effect that canagliflozin has on human T cell function is not known. SGLT2 (also known as SLC5A2) is not expressed by T cells (Uhlen et al., 2019)(Human Protein Atlas, *proteinatlas.org*), therefore it is unlikely that canagliflozin would modulate T cell fate by its canonical inhibition of glucose uptake. However, given that T cell metabolic reprogramming underpins autoimmune disease (see Chapter 1.5), the aforementioned off-target changes on mitochondrial complex I and GDH pose an interesting avenue to investigate.

1.8 Aims and objectives

T cell-mediated autoimmunity is responsible for a range of conditions including rheumatoid arthritis (RA) and systemic lupus erythematosus (SLE). Aberrant T cell metabolism underpins many of these autoimmune conditions, most of which have no cure. Type 2 diabetes (T2D) drugs have previously shown therapeutic benefit in the setting of autoimmunity through their action on T cell metabolism. Sodium glucose co-transporter 2 inhibitors are the most recently approved class of T2D, in which canagliflozin also has off-target effects that inhibit mitochondrial metabolism. These off-target effects have made canagliflozin an attractive therapy in other inflammatory settings including chronic kidney disease and cardiovascular disease, however, the impact that canagliflozin has on the immune system is unknown. The aim of this thesis is to determine whether canagliflozin could alleviate disease severity in T cell-mediated autoimmune diseases by addressing four main objectives:

1. To establish whether canagliflozin, through its off-target effects on mitochondrial complex I and glutamate dehydrogenase, compromises CD4⁺ T cell activation to impair effector function.
2. To investigate the global impact that canagliflozin has on CD4⁺ T cell function, based upon changes at the transcript and protein level.
3. To determine the underlying mechanisms that facilitate canagliflozin-mediated changes in T cell function. This includes the impact of canagliflozin on mitochondrial complex I and glutamate dehydrogenase, as well as its general effect on glycolysis and oxidative phosphorylation.
4. To verify whether canagliflozin maintains its inhibitory effect on T cell function in effector T cells and in autoimmune patient cohorts (RA and SLE) *ex vivo*.

Chapter Two

Experimental Procedures

2 Experimental procedures

2.1 Human blood collection

Ethical approval was obtained from Wales Research Ethics Committee 6 for the collection of peripheral blood from healthy volunteers (13/WA/0190). Blood from healthy, non-fasted donors was collected between 8.30am and 10.00am at the Clinical Research Facility. From each donor a maximum of 120 ml of blood was collected into heparinised Vacuettes™ (Greiner Bio-One, Austria).

2.2 Primary cell tissue culture

All primary cell tissue culture, including cell isolation and cell culture, was carried out under sterile conditions in a Scanlaf class II Mars hood.

2.3 Peripheral blood mononuclear cell isolation

Peripheral blood mononuclear cells (PBMCs) consist of peripheral blood cells containing a single-lobed nucleus. This includes lymphocytes such as T cells, B cells and NK cells, as well as monocytes. PBMCs were isolated by carefully layering 10 ml of whole blood onto 10 ml of Lymphoprep™ (density 1.077 g/ml; STEMCELL Technologies, Canada), before density gradient centrifugation at 805 x *g* for 20 min, no brake. Centrifugation results in four distinct layers: plasma, a layer of PBMCs, Lymphoprep™ and polymorphonuclear cells (PMNs) with red blood cells (Figure 2.1). Plasma was carefully discarded using a sterile 3 ml Pasteur pipette before PBMCs were collected. Cells were washed twice using RPMI medium 1640 (1X) + Glutamax™ (Gibco, USA) and centrifugation at 515 x *g*. The PBMC pellet was resuspended in RPMI medium 1640 (1X) + Glutamax™ before the number of PBMCs was determined by using the Countess® automated cell counter (Invitrogen, USA; see Chapter 2.5).

A

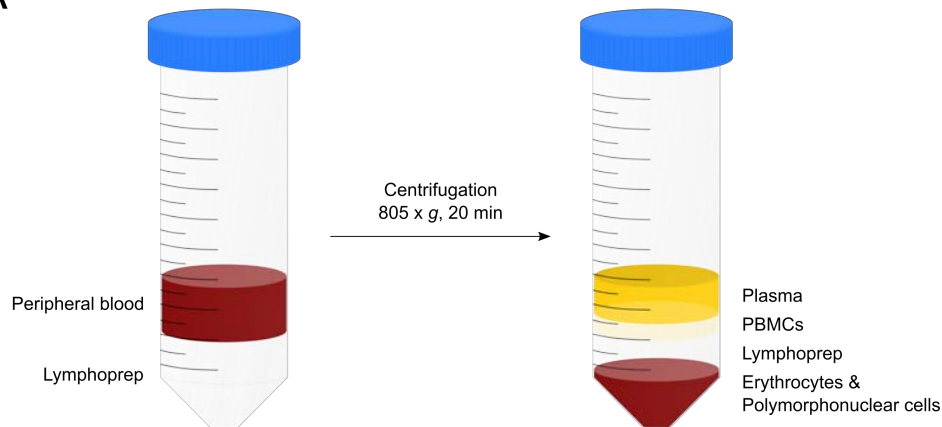


Figure 2.1 – Summary of density gradient centrifugation

10 ml whole blood is carefully layered onto 10 ml of Lymphoprep™. Density gradient centrifugation at 805 x *g* for 20 min results in 4 distinct layers: plasma, peripheral blood mononuclear cells, Lymphoprep™ and the erythrocyte and polymorphonuclear layer. *PBMCs, peripheral blood mononuclear cells.*

2.4 Human T cell isolation

Human T cell populations were isolated using magnetic microbeads on the autoMACS® Pro cell separator as per the manufacturer's instructions (Miltenyi, Germany). Centrifugation of the relevant cell-containing fraction at 300 x *g* for 10 min post-separation allows resuspension of the cell pellet in the appropriate medium for downstream analysis. The number of T cells isolated was determined using the Countess® automated cell counter (see Chapter 2.5).

Differential expression of cell surface markers between immune cell subsets, in addition to the ability to label these markers with nano-sized superparamagnetic beads, forms the basis of automated magnetic separation (Figure 2.2). Microbead-labelled cells are retained within the magnetic column so that non-labelled cells are eluted separately, generating pure populations of the desired cell type. The fraction used for downstream analysis is dependent on whether the isolation protocol used labels the cell type of interest (positive selection) or all cells other than the cell type of interest (negative selection). Negative selection is the preferred method, as unlabelled cells are less likely to be inadvertently activated by the separation process.

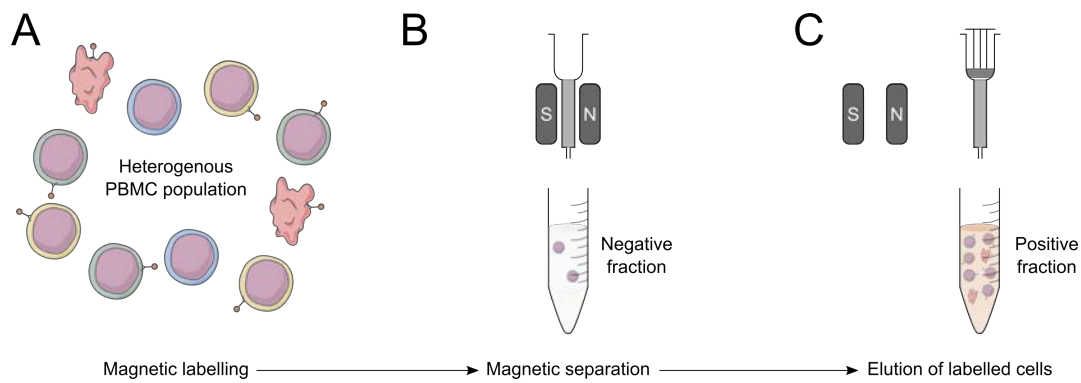


Figure 2.2 – Principle of magnetic separation

(A) The “depletes” running programme involves the labelling of non-target cells to obtain a pure target cell population. (B) Labelled non-target cells are magnetically retained in the column during separation, whilst the target cells are collected in the flow-through in the negative fraction. (C) Following the elution of non-labelled cells, removal of the column from the magnets allows the elution of labelled cells in the positive fraction.

2.4.1 Pan CD4+ T cell isolation

Pan CD4+ T cells were negatively-selected using a CD4+ T cell isolation kit as per the manufacturer's guidelines (Miltenyi, Germany). Following centrifugation at 300 x *g* for 10 min, cells were resuspended in 40 µl of MACS buffer (2% fetal bovine serum (FBS; Merck, Germany) in phosphate buffered saline (PBS; Gibco, USA)) per 10⁷ cells and 10 µl of antibody cocktail (Miltenyi, Germany) per 10⁷ cells and incubated at 4°C for 5 min. This antibody cocktail contains antibodies against the following markers: CD8, CD14, CD15, CD16, CD19, CD36, CD56, CD123, TCR γ/δ and CD235a. A further addition of 30 µl MACS buffer per 10⁷ cells and 20 µl CD4+ T cell-specific microbeads per 10⁷ cells (Miltenyi, Germany) was made and incubated at 4°C for 10 min. The cell-microbead solution was transferred to a 15 ml falcon before running through the autoMACS® on the “Depletes” running programme. Following conclusion of the separation, the CD4+ T cell-containing negative fraction was run through a second “Depletes” separation programme to improve the purity of the CD4+ T cell fraction. Following conclusion of the second separation, the CD4+ T cell-containing negative fraction was collected for further analysis and positive fractions discarded.

2.4.2 Naïve CD4+ T cell isolation

Naïve T cells (T_{nv}) were negatively-selected using a CD4+ naïve T cell isolation kit as per the manufacturer's guidelines (Miltenyi, Germany). Following centrifugation at 300 x *g* for 10 min, cells were resuspended in 40 µl of MACS buffer per 10⁷ cells and 10 µl of antibody cocktail (Miltenyi, Germany) per 10⁷ cells and incubated at 4°C for 5 min. This antibody cocktail contains antibodies against the following markers: CD8, CD14, CD15, CD16, CD19, CD25, CD34, CD36, CD45RO, CD56, CD123, HLA-DR, TCR γ/δ, and CD235a. A further addition of 30 µl MACS buffer per 10⁷ cells and 20 µl T_{nv} cell-specific microbeads per 10⁷ cells (Miltenyi, Germany) was made and incubated at 4°C for 10 min. The cell-microbead solution was transferred to a 15 ml falcon before running through the autoMACS® on the "Depletes" running programme. Following conclusion of the separation, the T_{nv} cell-containing negative fraction was run through a second "Depletes" separation programme to improve the purity of the T_{nv} cell fraction. Following conclusion of the second separation, the T_{nv} cell-containing negative fraction was collected for further analysis and positive fractions discarded.

2.4.3 CD4+ T effector cell isolation

T effector cells (T_{eff}) were negatively-selected using a CD4+ T effector memory cell isolation kit as per the manufacturer's guidelines (Miltenyi, Germany). Following centrifugation at 300 x *g* for 10 min, cells were resuspended in 40 µl of MACS buffer per 10⁷ cells and 10 µl of antibody cocktail (Miltenyi, Germany) per 10⁷ cells and incubated at 4°C for 10 min. This antibody cocktail contains antibodies against the following markers: CD8, CD14, CD15, CD16, CD19, CD34, CD36, CD45RA, CD56, CD123, TCR γ/δ, and CD235a. Cells were then washed in MACS buffer and centrifugation at 300 x *g* for 10 min. The cell pellet was resuspended in 80 µl MACS buffer per 10⁷ cells and an addition of 20 µl T_{eff} cell-specific microbeads per 10⁷ cells (Miltenyi, Germany) was made and incubated at 4°C for 15 min. The cell-microbead solution was transferred to a 15 ml falcon before running through the autoMACS® on the "Deplete025" running programme. Following conclusion of the separation, the T_{eff} cell-containing negative fraction was collected for further analysis and the positive fraction discarded.

2.4.4 CD8+ T cell isolation

CD8+ T cells were negatively-selected using a CD8+ T cell isolation kit as per the manufacturer's guidelines (Miltenyi, Germany). Following centrifugation at 300 x *g* for 10 min, cells were resuspended in 40 µl of MACS buffer per 10⁷ cells and 10 µl of antibody cocktail (Miltenyi, Germany) per 10⁷ cells and incubated at 4°C for 5 min. This antibody cocktail contains antibodies against the following markers: CD4, CD15, CD16, CD19, CD34, CD36, CD56, CD123, TCR γ/δ, and CD235a. A further addition of 30 µl MACS buffer per 10⁷ cells and 20 µl CD4+ T cell-specific microbeads per 10⁷ cells (Miltenyi, Germany) was made and incubated at 4°C for 10 min. The cell-microbead solution was transferred to a 15 ml falcon before running through the autoMACS® on the “Depletes” running programme. Following conclusion of the separation, the CD8+ T cell-containing negative fraction was run through a second “Depletes” separation programme to improve the purity of the CD8+ T cell fraction. Following conclusion of the second separation, the CD8+ T cell-containing negative fraction was collected for further analysis and positive fractions discarded.

2.5 Cell counting

For cell counting, cells were diluted according to the cell number expected – usually based on the size of the pellet present. 10 µl of the diluted cell solution was mixed 1:1 with 10 µl of Trypan Blue (AlphaMetrix, Germany). 10 µl of the cell-Trypan blue solution was added to the counting slide to be inserted into the Countess® automated cell counter. The calculated cell number was adjusted to factor the dilution.

2.6 Cell culture

Isolated T cells were cultured in human plasma-like medium (HPLM; Gibco, USA), unless stated otherwise, and seeded at a density of 1x10⁶ cells per ml. Cell culture plates were coated overnight with 2 µg/ml anti-CD3 antibody (BioLegend, USA) prior to T cell activation. T cells were co-stimulated with 20 µg/ml anti-CD28 (BioLegend, USA). Unstimulated cells were cultured in uncoated wells and in the absence of anti-CD28. Cells were treated with 10 µM canagliflozin (Cambridge Bioscience, UK), 10 µM dapagliflozin (Combi-Blocks, USA) or dimethyl sulphoxide (DMSO) vehicle control (Merck, Germany). Plates were incubated at 37°C in 5% CO₂ for the desired amount of time. Following 3 h incubation, culture medium was supplemented with 10% dialysed FBS to prevent impaired T cell activation.

2.7 Flow cytometry

Flow cytometry allows the measurement of the properties of a population of cells. Cells are labelled with fluorochrome-conjugated antibodies against various markers of interest to stain them. Once labelled, the cell suspension runs through the flow cytometer and is hydrodynamically focused so that single cells pass through a series of lasers. The specific wavelengths of these lasers cause excitation of the attached fluorochromes which results in a signal that is converted to a computed measurement. These lasers are split through a number of channels, each of which is carefully selected during analysis to allow the maximal emission of light to be detected following fluorochrome excitation. This allows high-throughput, multi-parameter analysis of thousands of cells. The cytometer used was a Novocyte® flow cytometer (Agilent, USA), which makes use of a combination of 3 lasers (violet, 405 nm; blue, 488 nm; red, 640 nm) and 12 band-pass filters to allow detection of up to 14 fluorophores / parameters simultaneously. Assay specific uses of flow cytometry have been outlined in the experimental procedures section of their respective chapters.

2.7.1 Purity monitoring

The purity of isolated T cell populations was monitored using flow cytometry. At least 0.1×10^6 cells were stained with subset-specific antibodies for 30 min on ice in the dark. Cells were washed post-staining using FACS buffer (0.05% sodium azide (Sigma-Aldrich, UK), 0.2% bovine serum albumin (BSA; Sigma-Aldrich, UK) in PBS) and centrifugation at $515 \times g$ for 7 min at 4°C. Cells were resuspended in FACS buffer to analyse. Cell doublets were excluded from analysis based on forward scatter height versus forward scatter area. Pan CD4+ T cells were identified as CD3+/CD4+ lymphocytes (Figure 2.3). T_{nv} and T_{eff} cells were identified based on their differential expression of CD45RA, CD45RO and CD197, whereby T_{nv} cells are CD45RA+/CD45RO-/CD197+, whilst T_{eff} cells are CD45RA-/CD45RO+/CD197- (Figure 2.4). CD8+ T cells were identified as CD3+/CD8+ lymphocytes (Figure 2.5). The purity of isolated cells populations typically exceeded 90%.

Table 2.1 – Antibodies used for purity monitoring

Antibody	Fluorochrome	Clone	Isotype	Manufacturer
Anti-CD3	Brilliant Violet 570™	UCHT1	Mouse IgG1, κ	BioLegend, USA
Anti-CD4	AlexaFluor® 647	OKT4	Mouse IgG1, κ	BioLegend, USA
Anti-CD8	FITC	BW135/80	Mouse IgG2a, κ	Miltenyi, Germany
Anti-CD45RA	Brilliant Violet 605™	HI100	Mouse IgG2b, κ	BioLegend, USA
Anti-CD45RO	FITC	UCHL1	Mouse IgG2a, κ	BioLegend, USA
Anti-CD197	Pacific Blue™	G043H7	Mouse IgG2a, κ	BioLegend, USA

A

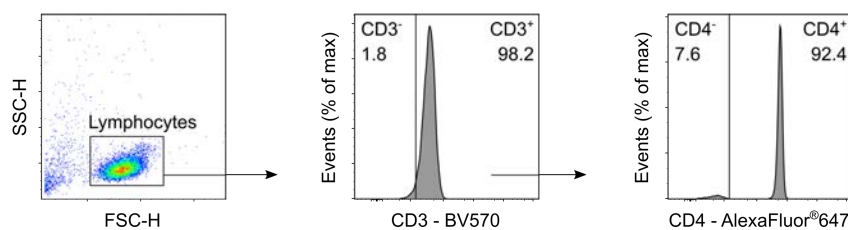
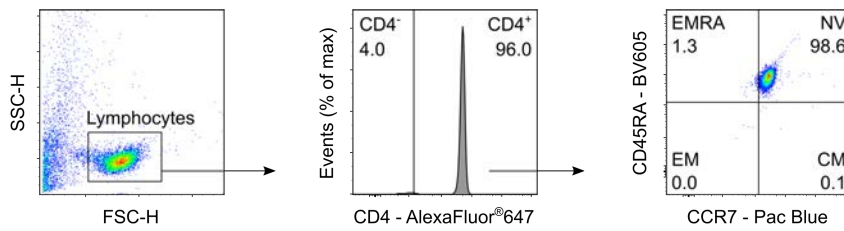


Figure 2.3 – Example of the gating strategy used to monitor CD4+ T cell purity

(A) Gating strategy used to monitor the purity of CD4+ T cells isolated using magnetic microbeads. Lymphocytes are initially gated based on forward-scatter height versus side-scatter height, excluding any debris present. CD4+ T cells were identified by their expression of CD3 and CD4. Percentages represent frequency of cells in parent population. Purity was typically > 90%.

A



B

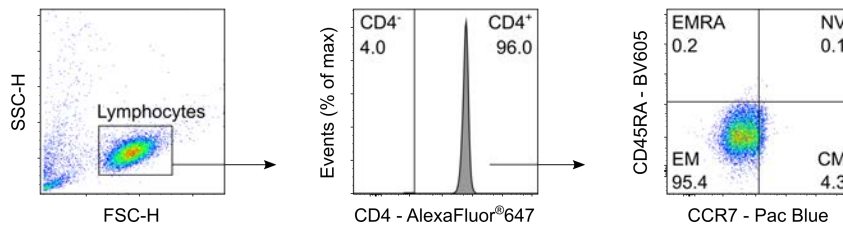


Figure 2.4 – Example of the gating strategy used to monitor naïve and effector CD4+ T cell purity
 (A-B) Gating strategy used to monitor the purity of naïve and effector CD4+ T cells isolated using magnetic microbeads. Lymphocytes are initially gated based on forward-scatter height versus side-scatter height, excluding any debris present. (A) Naïve CD4+ T cells were identified as CD4+/CCR7+/CD45RA+ lymphocytes. (B) Effector CD4+ T cells were identified as CD4+/CCR7-/CD45RA- lymphocytes. Percentages represent frequency of cells in parent population. Purity was typically > 90%.

A

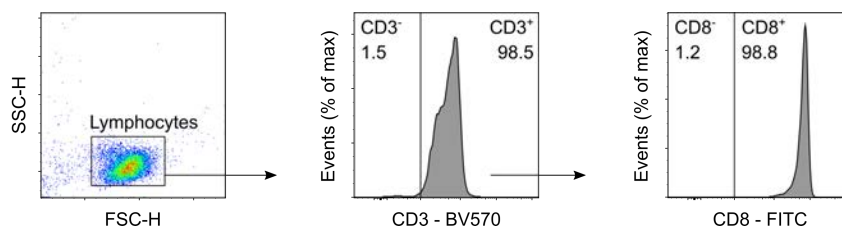


Figure 2.5 – Example of the gating strategy used to monitor CD8+ T cell purity
 (A) Gating strategy used to monitor the purity of CD8+ T cells isolated using magnetic microbeads. Lymphocytes are initially gated based on forward-scatter height versus side-scatter height, excluding any debris present. CD8+ T cells were identified by their expression of CD3 and CD8. Percentages represent frequency of cells in parent population. Purity was typically > 90%.

2.7.2 T cell activation

Expression of CD25, CD44 and CD69 was used to assess T cell activation. Following 24 h or 72 h activation (see Chapter 2.6), cells were resuspended and collected before centrifugation at 500 x *g* for 5 min. Cell-free supernatants were collected for ELISA analysis, whilst cells were resuspended in 100 µl FACS buffer. Dead cells were excluded using DRAQ7® (Biostatus, UK). Cell doublets were excluded as previously described. Cells were stained for 15 min at room temperature (RT) in the dark (Table 2.2). An unstained sample provided a negative control. Cells were washed in FACS buffer and centrifugation at 515 x *g* post-staining and resuspended in FACS buffer to analyse.

Table 2.2 – Antibodies used for activation marker analysis

Antibody	Fluorochrome	Clone	Isotype	Manufacturer
Anti-CD25	Brilliant Violet 605™	BC96	Mouse IgG1, κ	BioLegend, USA
Anti-CD44	Pacific Blue™	BJ18	Mouse IgG1, κ	BioLegend, USA
Anti-CD69	PE	FN50	Mouse IgG1, κ	BioLegend, USA
DRAQ7™	APC-Cy7	-	-	Biostatus, UK

2.7.3 Blastogenesis and proliferation

T cell size was determined by forward-scatter area and used as a measure of blastogenesis, whilst CellTrace™ CFSE (Invitrogen, USA) was used to assess T cell proliferation (Table 2.3). Cells were stained with 0.4 µM CellTrace™ CFSE for 5 min with gentle mixing. Following staining, cells were washed twice with PBS and centrifugation at 500 x *g* for 5 min. Cells were then resuspended in HPLM and cultured as previously described (see Chapter 2.6). Following 72 h activation, cells were resuspended and collected before centrifugation at 500 x *g* for 5 min. Cell-free supernatants were collected for ELISA analysis, whilst cells were resuspended in 100 µl FACS buffer. Dead cells and cell doublets were excluded as previously described. Cells were stained for 15 min at RT in the dark. An unstained sample provided a negative control. Cells were washed in FACS buffer and centrifugation at 515 x *g* post-staining and resuspended in FACS buffer to analyse.

Table 2.3 – Definitions of proliferation-associated parameters

Parameter	Definition
Division Index	Total number of divisions / the number of cells at start of culture
Proliferation Index	Total number of divisions / cells that went into division
Expansion Index	Total number of cells / cells at start of culture
Replication Index	Total number of divided cells / cells that went into division

2.7.4 Intracellular flow cytometry

Intracellular content was assessed using the Inside Stain Kit (Miltenyi, Germany) following the manufacturer's guidelines. Following surface staining, cells were fixed using Inside Fix (Miltenyi, Germany) for 20 min at RT in the dark. Cells were washed in FACS buffer and centrifugation at 515 x *g* post-fixation before permeabilisation using Inside Perm (Miltenyi, Germany). Cells were stained for intracellular markers for 10 min at RT in the dark, unless otherwise stated. Following intracellular staining, cells were washed in Inside Perm permeabilisation buffer and centrifugation at 515 x *g* and resuspended in FACS buffer to analyse.

2.7.5 Compensation

Any samples with more than one fluorophore present require compensation to account for any potential spectral overlap (Figure 2.6). For the majority of compensation, UltraComp eBeads™ compensation beads (Invitrogen, UK) or anti-REA MACS Comp Beads (Miltenyi, Germany) were stained with a single fluorophore in each separate tube. Compensation for DRAQ7® was carried out by staining cells with the dye, ensuring that distinct live and dead populations were present. Compensation for other fluorescence-based dyes was carried out by staining cells with the desired dye and ensuring that distinct positive and negative populations were present. In all cases, positively- and negatively-stained populations were gated on FlowJo version 10.6.1 or later to set-up a compensation matrix that could be applied when analysing samples with multiple fluorophores. The compensation matrix specifies the percentage of spectral overlap between the different fluorophores present.

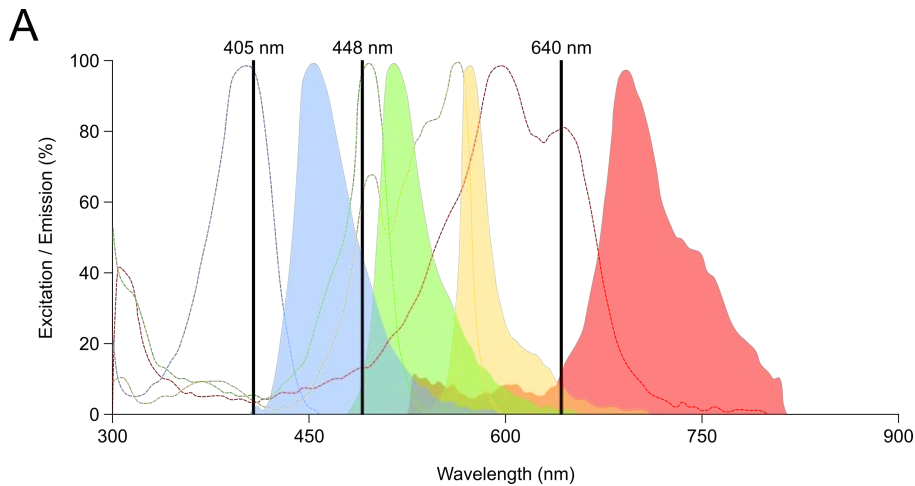


Figure 2.6 – Example of the spectral overlap between fluorochromes

Spectral overlap results in non-specific fluorescence from other fluorochromes contributing towards the signal of other fluorochromes of interest – potentially causing either false-positives, or fluorescence values greater than the true value. Here is an example of spectral overlap between the fluorochromes Pacific Blue, FITC, PE and APC. For example, without compensation, the APC fluorescence reading would be the fluorescence of APC, as well a part of the fluorescence of PE. Compensation involves adjusting the measured fluorescence values to account for this overlap, giving a truer fluorescence value for each fluorochrome.

2.7.6 Quality control

Daily quality control tests were undertaken to monitor Novocyte[®] performance and ensure optimal instrument conditions during sample analysis. Novocyte[®] QC particles were resuspended in 1X NovoRinse[®] solution (both Agilent, USA) as per the manufacturer's instructions.

2.7.7 Data analysis

Unless stated, all data generated by the Novocyte[®] flow cytometer was analysed using FlowJo version 10.6.1 or later (Treestar, USA). Proliferation modelling through the FlowJo Proliferation Platform was used to calculate proliferation-associated parameters (Table 2.3).

2.8 Enzyme-linked immunosorbent assay

An ELISA allows the quantification of protein present in the supernatant from the overnight cell cultures (Figure 2.6). The absorbance measured can be substituted into the equation of the standard curve to convert the value into a concentration.

ELISAs were performed as per the manufacturers' guidelines to measure the concentration of various cytokines (all R&D systems, USA). 96-well half-area plates were coated with capture antibody appropriately diluted to a working concentration in PBS. This was incubated at 4°C at least overnight prior to the assay. After discarding the capture antibody, plates were then blocked for at least an hour with block buffer (1% BSA in PBS) to prevent the binding of any non-specific proteins. The plate was washed 3 times by adding 200 µl per well of washing buffer (0.05% Tween-20 (Merck, Germany) in PBS) prior to the addition of the cell-free culture supernatants and the protein standard of interest. Both the standards and samples were diluted to an appropriate concentration in the appropriate reagent diluent and incubated for 2 h at RT with gentle mixing on a plate shaker. The plate was washed 4 times before the detection antibody was added. The detection antibody was diluted to a working concentration in reagent diluent before incubation for 2 h at RT with gentle mixing on a plate shaker. The plate was washed 4 times before addition of streptavidin horseradish peroxidase (HRP). Streptavidin-HRP was diluted to a working concentration in reagent diluent and incubated at RT for exactly 20 min with gentle mixing on a plate shaker. The plate was washed a final 6 times before adding the enzyme substrate. Addition of a 1:1 solution of tetramethylbenzidine and hydrogen peroxide (both BD biosciences, UK) causes a colour change reaction to occur. The plate was incubated at RT in the dark to allow the colour to develop. An initial blue colour developed and the reaction was stopped when the desired hue is reached by adding 50 µl of 1 M sulphuric acid per well. This changes the colour to a yellow hue. Plates were then read at 450 nm using a POLARstar Omega plate reader spectrophotometer (BMG LABTECH, Germany).

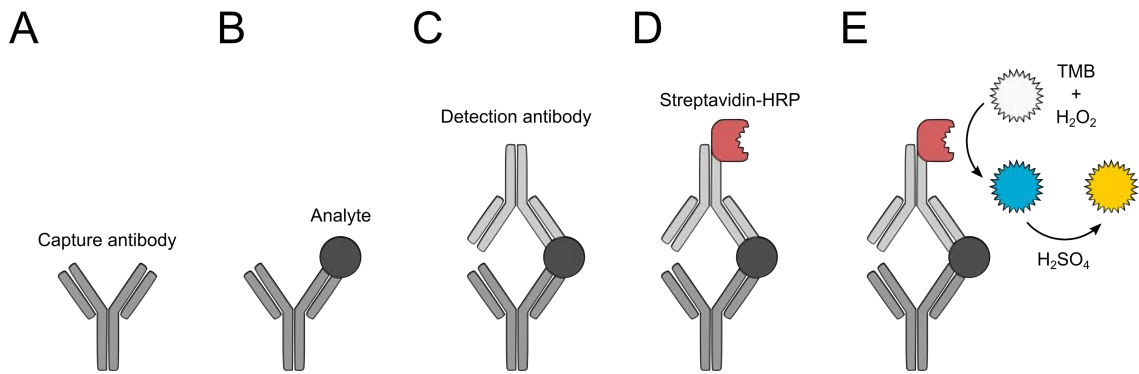


Figure 2.7 – Summary of enzyme-linked immunosorbent assay

(A) Plate is coated overnight with a capture antibody that detects an epitope of the antigen being analysed. (B) Sample is added and the specific antigen binds to the capture antibody. (C) Detection antibody is added to bind specifically to a different epitope on the antigen of interest. (D) Streptavidin-HRP conjugated enzyme binds to the detection antibody. (E) Addition of a 1:1 solution of TMB and hydrogen peroxide induces a colour change catalysed by streptavidin-HRP. The intensity of the colour change is representative of the amount of antigen present. Sulphuric acid stops the reaction so that the absorbance can be measured.

2.9 Metabolic analysis

Following 24 h activation, T cells were resuspended before centrifugation at $500 \times g$ for 5 min. Cell-free supernatants were collected for ELISA analysis. Cells were resuspended in phenol red-free RPMI medium supplemented with glucose (10 mM), pyruvate (1 mM) and glutamine (2 mM; all Agilent, USA) before seeding at 0.2×10^6 cells per Cell-Tak coated well (Corning, USA). OCR and ECAR were measured following a series of previously optimized injections. Injections for both the mitochondrial stress assay and glycolysis assay include oligomycin (1 μ M), FCCP (1 μ M), antimycin A and rotenone (both 1 μ M) and monensin (20 μ M; all Merck, Germany) to inhibit distinct proteins of the electron transport chain (Figure 2.8). Metabolic analyses were performed using the Seahorse XFe96 analyser (Agilent, USA).

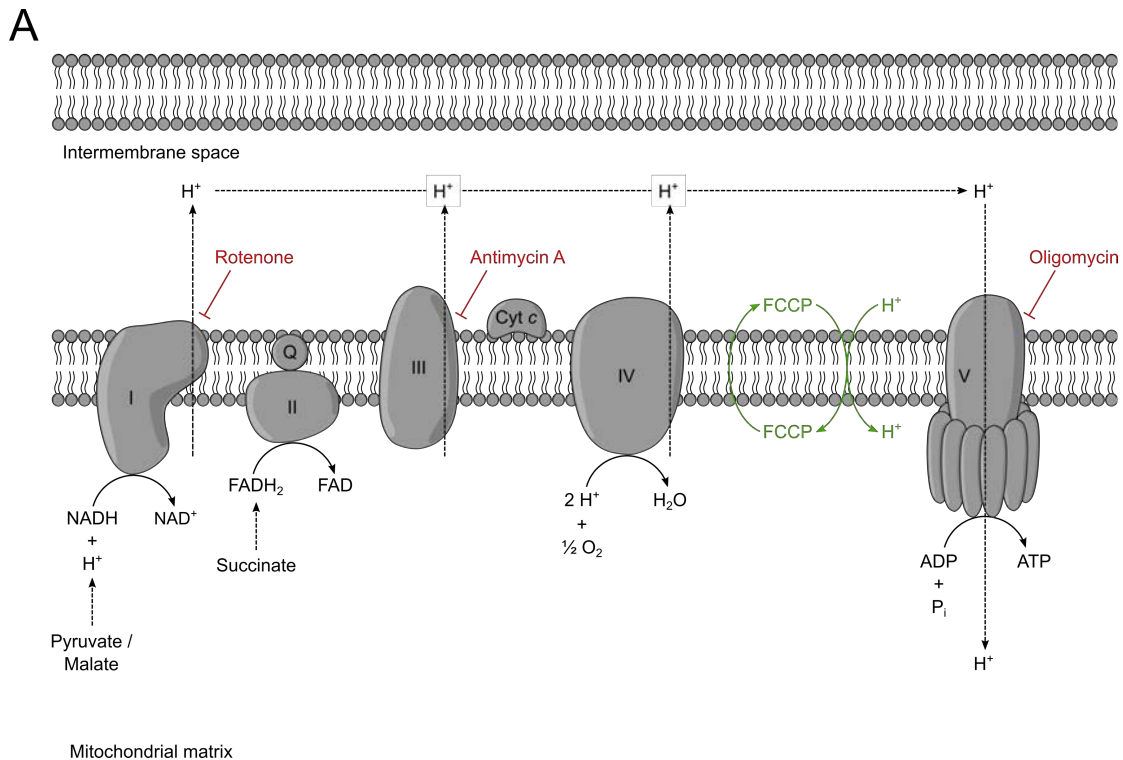


Figure 2.8 – Respiratory inhibitors and activators within the electron transport chain

(A) Both glycolysis and the oxidation of pyruvate via the TCA cycle promotes reduction of NAD⁺ to NADH. NADH donates its electrons to complex I, which are then transferred from complex I to coenzyme Q, complex III and finally complex IV. The oxidation of succinate to fumarate promotes the reduction of FAD to FADH₂. FADH₂ donates its electrons to complex II, which are then transferred from complex II to complex III and complex IV. The activity of each complex can be specifically inhibited using inhibitors such as rotenone, antimycin A and oligomycin. FCCP can uncouple the proton gradient across the inner mitochondrial membrane, allowing the electron transport chain to function at its maximal rate. *Complex I, NADH:ubiquinone oxidoreductase; complex II, succinate dehydrogenase; complex III, coenzyme Q : cytochrome c oxidoreductase; complex IV, cytochrome c oxidase; complex V, ATP synthase; Cyt c, cytochrome c; Q, coenzyme Q.*

Metabolic parameters were calculated as per the following definitions (Table 2.4 and 2.5; Figure 2.9). Joules of ATP produced, as well as associated parameters, were calculated as previously described (Mookerjee et al., 2017).

Table 2.4 – Calculation of mitochondrial respiratory parameters

Parameter	Calculation*
Basal respiration	Initial three measurements – non-mitochondrial respiration
ATP-linked respiration	Initial three measurements – three measurements after oligo
Maximal respiratory capacity	Three measurements after FCCP – non-mitochondrial respiration
Spare respiratory capacity	Maximal respiratory capacity – basal respiration
Non-mitochondrial respiration	Final three measurements
Proton leak	Three measurements after oligo – non-mitochondrial respiration

*each triplicate measurement averaged

Table 2.5 – Calculation of glycolytic parameters

Parameter	Calculation*
Basal glycolysis	Initial three measurements
Maximal glycolysis	Final three measurements

*each triplicate measurement averaged

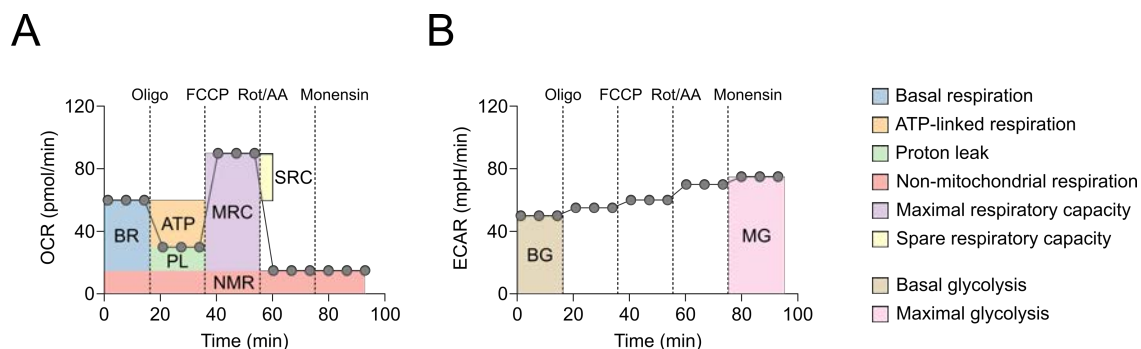


Figure 2.9 – Calculation of metabolic parameters

(A-B) Visualisation of the how metabolic parameters of (A) mitochondrial respiration and (B) glycolysis are calculated using data collected from the Seahorse XFe96 analyser.

2.10 Immunoblotting

Immunoblotting allows analysis of protein expression – normalised protein levels can be compared between groups. It is used to detect the presence, absence, or relative abundance of specific proteins from a cell lysate. Densitometry allows semi-quantitative analysis of protein bands.

2.10.1 Sample preparation

The processing of samples for immunoblotting was carried out on ice to avoid the degradation of protein. Cells were centrifuged at 500 x *g* for 5 min so that the cells could be collected and supernatant discarded/collected. Cells were resuspended in ice-cold PhosphoSafe™ extraction reagent (Merck, Germany) at 1x10⁶ cells per 100 µl. The cell suspension was kept on ice for a further 5 min before being stored at -20°C for downstream use. Prior to use for protein estimation and immunoblotting, cell lysates were thawed on ice and centrifuged at 10,000 x *g* for 10 min at 4°C in a pre-cooled centrifuge.

2.10.2 Protein estimation

The protein standard curve and samples to be analysed are diluted to their appropriate concentrations in ddH₂O. Protein standards and samples were added at 5 µl per well to a 96-well full-area microplate. DC assay reagent S was mixed 1:50 with DC assay reagent A (both BioRad, USA) and 25 µl added to each well. 200 µl of DC assay reagent B (BioRad, USA) was added to each well to cause a colour change reaction. The plate was incubated at RT in the dark with gentle agitation for 15 min to allow a black/grey colour to develop. Following incubation, the absorbance at 450 nm was read using a POLARstar Omega plate reader spectrophotometer.

A linear-regression fit was used in order to convert the absorbance values measured into a concentration value using the standard curve produced. The concentration of protein to be loaded was normalised either to the cell lysate sample with the lowest protein concentration, or to a pre-determined protein concentration. A maximum of 45 µl of the lowest protein concentration was loaded, with the volumes of other cell lysates adjusted accordingly.

2.10.3 Gel production

Glass plates were washed with water and 70% ethanol and dried before use. These plates were clamped together and placed in a stand with the bottom of both plates aligned flush to the sponge floor. Gels consisted of two distinct regions: a stacking region from the top of the gel to around the bottom of the wells, with a resolving region as the remainder. Typically, a 10% resolving gel was used for electrophoresis following the pre-optimised recipe (Table 2.6). Reagents were added in the order listed, with ammonium persulphate (APS) and tetraethylmethylenediamine (TEMED) added shortly before use to avoid premature gel polymerisation. The resolving gel solution was added between the two clamped gels up to the well-forming comb using a plastic Pasteur pipette, with a small volume of 70% ethanol added to flatten the top of the gel and remove any bubbles. Once the resolving gel was set, all ethanol was discarded, before an excess of stacking gel solution is added (Table 2.7). Reagents were again added in the order listed avoid the premature gel polymerisation. The gel was either used immediately or stored overnight at 2-8°C for use the following day.

Table 2.6 – Pre-optimised recipe for 10% resolving gel

Reagent	Volume (µl)	Manufacturer
ddH ₂ O	2500	-
30% Acrylamide	3000	BioRad, USA
Resolving gel buffer, pH 8.8	1875	BioRad, USA
Sodium Dodecyl Sulphate	75	BioRad, USA
10% Ammonium Persulfate	37.5	Sigma-Aldrich, UK
Tetraethylmethylenediamine	7.5	BioRad, USA

Table 2.7 – Pre-optimised recipe for stacking gel

Reagent	Volume (µl)	Manufacturer
ddH ₂ O	1500	-
30% Acrylamide	325	BioRad, USA
Stacking gel buffer, pH 6.8	625	BioRad, USA
Sodium Dodecyl Sulphate	25	BioRad, USA
10% Ammonium Persulfate	12.5	Sigma Aldrich, UK
Tetraethylmethylenediamine	2.5	BioRad, USA

2.10.4 Sodium dodecyl sulphate-polyacrylamide gel electrophoresis

Normalised protein lysates were added to 5 µl of 5X loading buffer (10% w/v SDS, 10 mM β-mercaptoethanol, 20% v/v glycerol, 0.2M Tris-HCl (pH 6.8) and 0.05% w/v bromophenolblue) before heating at 95°C for 5 min. Samples were applied carefully to individual wells of the SDS-polyacrylamide gel. Precision Plus Protein™ dual colour standard ladders (BioRad, USA) were also added to flank each set of samples. Gel electrophoresis was carried out using a mini-PROTEAN tetra cell (BioRad, USA). Gels were submerged in running buffer (10% TGS (25 mM Tris, 192 mM glycine, 0.1% SDS, pH 8.3); BioRad, USA) before running at 120 V for approximately 90 min. Voltage was applied using a PowerPac™ basic power supply (BioRad, USA).

2.10.5 Semi-dry membrane transfer

Shortly before completion of the gel electrophoresis, a polyvinylidene difluoride (PVDF) membrane (Merck, Germany) was soaked in methanol for 20 s before being transferred into cold transfer buffer (20% methanol, 10% TG buffer (25 mM Tris, 192 mM glycine, pH 8.3; BioRad, USA)). Blot absorbent filter paper (BioRad, USA) was soaked in cold transfer buffer for 10 min. The gel was carefully placed onto the PVDF membrane and sandwiched by pre-soaked filter paper. The Trans-Blot® Turbo™ transfer system (BioRad, USA) was used to transfer the proteins from the gel onto the membrane.

Following transfer, the membrane was immersed in block buffer (5% BSA, 0.1% Tween-20 in TBS (BioRad, USA)) for 1 h at RT with gentle mixing on a rocker to prevent any non-specific protein binding.

2.10.6 Immunoblotting

Membranes were incubated with primary antibodies overnight at 4°C with gentle mixing on a rocker. Following incubation, membranes were washed three times with wash buffer (0.1% Tween-20 in TBS). HRP-conjugated detection bodies were used at a 1:1000 dilution with wash buffer, unless otherwise stated. The appropriate anti-mouse and anti-rabbit detection bodies (7076S and 7074S, respectively; both Cell Signaling Technology, USA) were incubated with the membrane for 1 h at RT with gentle mixing on a rocker. Membranes were washed a further 3 times in wash buffer before imaging.

Protein levels were visualised by enhanced chemiluminescence using the ChemiDoc™ XRS+ imaging system (BioRad, USA). Membranes were incubated for up to 2 min with Amersham™ ECL Select™ Western Blotting detection reagent (GE Healthcare, USA) before imaging. Non-saturated images were saved for analysis.

Membranes to be re-analysed were immersed in Restore™ PLUS Western Blot stripping buffer (ThermoFisher Scientific, USA) for 10 min to remove any bound antibodies. Membranes were washed 3 times in wash buffer, before blocking for 1 h at RT with block buffer. Following blocking, membranes were incubated with the desired primary antibody and the protocol continued as normal.

2.10.7 Densitometry

Semi-quantification of proteins was achieved using densitometry. Non-saturated images were imported to ImageJ image processing software (FIJI) and rectangles drawn around the bands of interest to ensure they were selected. Straight lines were drawn to remove any background signal, before the area of the histogram was calculated. This value was then normalised to the equivalent β -actin band.

2.11 Statistical analysis

Unless otherwise stated, statistical analysis was carried out using GraphPad Prism version 8 or later. Data are expressed as the mean \pm standard error of the mean (SEM). The normality of the data was initially tested using the Shapiro-Wilk test to determine the appropriate method of analysis. For data comparing two sample groups, normally distributed data were analysed using a parametric t test, whilst a non-parametric t test was used to analyse data not normally distributed. One-way analysis of variance (ANOVA) followed by the post-hoc Dunnett test was used to analyse three or more group means of a single variable to the vehicle control group. Significant values were taken as $p \leq 0.05$ and denoted as follows: * $p \leq 0.05$, ** $p \leq 0.01$, *** $p \leq 0.001$ and **** $p \leq 0.0001$.

Chapter Three

Canagliflozin modulates activated T cell function

3 Canagliflozin modulates activated T cell function

3.1 Introduction

T cell-mediated autoimmunity is responsible for a range of conditions including rheumatoid arthritis (RA) and systemic lupus erythematosus (SLE). Upon antigen encounter, T cells engage robust anabolic metabolism to enhance the generation of biosynthetic intermediates required to support an immune response. Aberrant T cell metabolism underpins several autoimmune conditions (see Chapter 1.5) – most of which currently have no cure. Moreover, many of the current treatment strategies employed cause debilitating side effects (Li et al., 2017), therefore there is a desperate need to develop alternative medicines. However, the development of new drugs is often a costly, laborious process with a high risk of failure, therefore alternative strategies are required to overcome this burden. Consequently, repurposing existing FDA-approved drugs that are oftentimes used in other disease settings provides an attractive, efficient approach for the development of novel therapeutic agents. Particularly advantageous in the model of drug repositioning is that candidate treatments have well-developed safety profiles in humans. Several pre-clinical studies have demonstrated therapeutic benefit from targeting T cell metabolism in autoimmunity: glutaminase suppression (Johnson et al., 2018), tetramerisation of the glycolytic enzyme pyruvate kinase (Angiari et al., 2020), inhibition of OXPHOS using oligomycin (Shin et al., 2020) and the use of 2-deoxyglucose to limit glucose metabolism (Wilson et al., 2021). Although promising, the clinical translation of these studies remains a challenge due to the toxicity of systemically impairing metabolism. Indeed, clinical trials involving the use of IACS-010759, a highly-selective small molecule inhibitor of complex I of the electron transport chain, for the treatment of cancer have recently been discontinued following concerns around its toxicity (Yap et al., 2023). Unfortunately, tolerated levels of IACS-010759 were only able to modestly inhibit its target, which subsequently limited its antitumour activity (Yap et al., 2023).

Despite these challenges, targeting metabolic processes using repurposed type 2 diabetes (T2D) drugs has been promising in several inflammatory conditions. Initially, thiazolidinediones were the subject of these investigations, where rosiglitazone and troglitazone were shown to have a beneficial effect in psoriasis and ulcerative colitis,

respectively (Ellis et al., 2000; Lewis et al., 2001). Following these findings, another member from the thiazolidinedione class of drugs, pioglitazone, improved patient outcomes in multiple sclerosis (MS) (Kaiser et al., 2009; Pershadsingh et al., 2004; Shukla et al., 2010). Subsequent *ex vivo* studies outlined that the impact that pioglitazone has on pathogenic proliferative and proinflammatory properties of MS patient-derived T cells contributes to therapeutic success in autoimmunity (Schmidt et al., 2004). The biguanide, metformin, has been more extensively researched in the setting of inflammation. As the predominant treatment for T2D, there is growing interest in the ability of metformin to modulate metabolism through activation of AMP-activated protein kinase (AMPK) and inhibition of complex I of the electron transport chain. In humans, the use of metformin alongside traditional treatments has alleviated disease severity in patients with SLE and RA (Gharib et al., 2021; Sun, Geng, et al., 2020). Metformin has been demonstrated to mediate this anti-inflammatory effect on human SLE T cells through the reversal of the aberrant metabolic output characteristic of this condition (Yin et al., 2015). These findings are founded upon numerous murine models that establish that metformin modulates the AMPK/mTOR axis to suppress T cell function in autoimmune disease (Kang et al., 2013; Lee et al., 2015; Son et al., 2014; Sun et al., 2016). Together, these findings highlight the potential of repositioning T2D drugs that modulate metabolism in settings such as autoimmunity, where aberrant T cell function can be targeted through metabolic suppression.

Sodium glucose co-transporter 2 (SGLT2) inhibitors are the most recently approved T2D medication, examples of which include canagliflozin, dapagliflozin and empagliflozin. Interestingly, extensive roles beyond glycaemic control have been described for SGLT2 inhibitors, particularly in the case of canagliflozin which can also inhibit key metabolic proteins complex I (Villani et al., 2016) and glutamate dehydrogenase (Secker et al., 2018). Additional benefits include the protective clinical outcomes that canagliflozin elicits in chronic kidney disease (Perkovic et al., 2019) and cardiovascular disease (Spertus et al., 2022). Recently, the use of canagliflozin has been explored in other inflammatory conditions, wherein inhibition of immune cell metabolism restricted their release of proinflammatory cytokines (Xu et al., 2018). Glycolysis was impaired in monocyte / macrophage cell lines treated with canagliflozin – inhibiting the expression of the rate-limiting enzyme, phosphofructokinase – which significantly inhibited their production of IL-6 and TNF α (Xu et al., 2018). However, interpretation of these findings requires caution as supraphysiological

concentrations of canagliflozin were required to elicit such anti-inflammatory properties, in addition to the suboptimal use of a cell line model for these analyses. Promisingly, recent work has demonstrated that canagliflozin can influence T cell differentiation. In the setting of experimental autoimmune myocarditis, canagliflozin treatment impaired differentiation towards Th1 and Th17 lineages, which translated into fewer Th17 cells infiltrating the inflamed tissue (Long et al., 2022). However, the impact of canagliflozin on human T cell function has yet to be elucidated. Given the previous success of repurposed T2D drugs in autoimmunity, alongside the promising initial studies on the anti-inflammatory function of canagliflozin, we believe that this warrants further investigation.

3.1.1 Rationale

Human CD4⁺ T_H17 cells were chosen as the primary study material, as this immune cell subset is highly plastic and is able to repopulate the site of inflammation in autoimmune disease. The preliminary aims of this project were: (i) to investigate the impact of canagliflozin and dapagliflozin on T cell activation and function, in particular whether the hypothesised inhibitory effects are specific to the off-target effects of canagliflozin; (ii) investigate whether the same inhibitory effects on T cell function are observed under more physiologically relevant conditions (i.e., culture medium that more closely resembles human plasma); and (iii) determine whether canagliflozin remains effective in inhibiting the effector function of already-activated T cells.

3.1.2 Hypothesis

- (i) Canagliflozin, but not dapagliflozin, impairs activated T cell function
- (ii) Activated T cell function remains impaired by canagliflozin under more physiologically accurate conditions
- (iii) Canagliflozin has a modest effect on already-activated T cells

3.2 Experimental procedures

3.2.1 Human blood collection

Ethical approval was obtained from Wales Research Ethics Committee 6 for the collection of peripheral blood from healthy volunteers (13/WA/0190). Blood from healthy donors was processed as previously described (see Chapter 2.1).

3.2.2 T cell isolation

Peripheral blood mononuclear cells (PBMCs) were isolated as previously described (see Chapter 2.3). The PBMC pellet was resuspended in the appropriate downstream media for analysis and the number of PBMCs was determined by using the Countess[®] automated cell counter (see Chapter 2.5). Pan CD4⁺ T cells and CD4⁺ T_H1 cells were isolated using automated magnetic separation as previously described (see Chapter 2.4).

3.2.3 Cell culture

Isolated T cells were activated and cultured in human plasma-like medium (HPLM) as previously described (see Chapter 2.6), unless otherwise stated. Initial cell culture experiments were performed in RPMI medium 1640 (1X) + Glutamax[™] (Gibco, USA). Cell-free supernatants were stored for further analysis, whilst cells were collected for downstream analysis.

3.2.4 Flow cytometry

T cell activation, blastogenesis and proliferation were assessed as previously described (see Chapter 2.7). Purity of isolated T cells was monitored as previously described (see Chapter 2.7.1) and was typically > 90%.

3.2.5 Enzyme-linked immunosorbent assay

ELISAs were performed as per the manufacturer's guidelines to measure the concentration of the following cytokines in cell-free supernatants: IL-2 (DY202) and IFN γ (DY285B; both R&D systems, USA).

3.2.6 Statistical analysis

Unless otherwise stated, statistical analysis was carried out using GraphPad Prism version 8 or later. Data are expressed as the mean \pm standard error of the mean (SEM). The normality of the data was initially tested using the Shapiro-Wilk test to determine the appropriate method of analysis. For data comparing two sample groups, normally distributed data were analysed using a parametric T test, whereas a non-parametric T test was used to analyse data not normally distributed. One-way analysis of variance (ANOVA) followed by the post-hoc Dunnett's test was used to analyse three or more group means of a single variable compared to the vehicle control. A one-sample T test was used to analyse data normalised to the vehicle control group. Significant values were taken as $p \leq 0.05$ and denoted as follows: * $p \leq 0.05$, ** $p \leq 0.01$, *** $p \leq 0.001$ and **** $p \leq 0.0001$.

3.3 Results

3.3.1 Canagliflozin impairs activated T cell activation and function

Here, we investigated the efficacy of two different FDA-approved SGLT2 inhibitors: canagliflozin, which has known off-target effects on GDH and mitochondrial complex I, and dapagliflozin, which has fewer known off-target effects (see Chapter 1.7.1). Tnv cells were activated in the presence or absence of physiologically relevant doses of canagliflozin and dapagliflozin and their downstream function assessed (Figure 3.1).

A

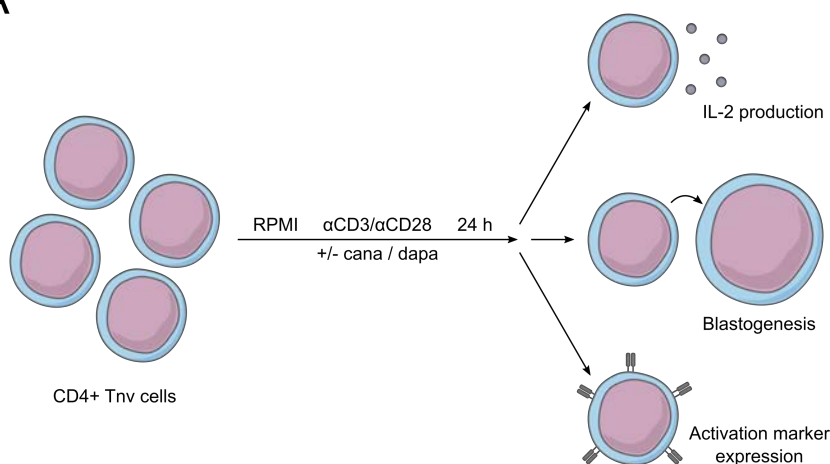


Figure 3.1 – Experimental procedure employed to assess the impact of canagliflozin and dapagliflozin on naïve T cells activated in RPMI

(A) Schematic overview outlining the experimental design in RPMI – anti-CD3 (2 µg/ml) and anti-CD28 (20 µg/ml) activated CD4+ Tnv cells in the presence and absence of canagliflozin or dapagliflozin (both 10 µM).

Pharmacokinetic studies have previously determined that circulating levels of canagliflozin reach a concentration of 10.5 µM in T2D patients administered a 300 mg dose of the drug (Devineni et al., 2013). Despite circulating levels of dapagliflozin peaking at around 0.5 µM in T2D patients prescribed a typical dose of the drug (Kasichayanula et al., 2014), a supraphysiological concentration of 10 µM was used for comparison with canagliflozin, our drug of interest. Where appropriate, data were normalised to the vehicle control group in order to account for variability between donors.

Canagliflozin reduced IL-2 production by activated T cells in a dose-dependent manner (0.01 µM: $p = 0.8512$; 0.1 µM: $p = 0.4984$; 1 µM: $p = 0.2034$; 10 µM: $p = 0.0065$), with a particularly striking effect at a concentration of 10 µM (Figure 3.2A). In contrast, dapagliflozin had no significant effect on IL-2 production (0.01 µM: $p = 0.8926$; 0.1 µM: $p = 0.7357$; 1 µM: $p = 0.6969$; 10 µM: $p = 0.3355$; Figure 3.2B).

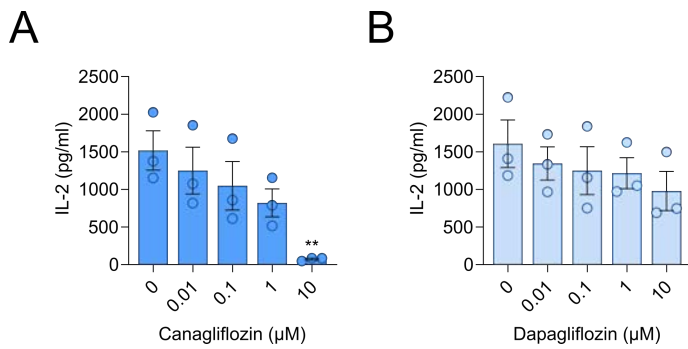


Figure 3.2 – Canagliflozin, but not dapagliflozin, impairs IL-2 production in a dose-dependent manner

(A-B) IL-2 secretion by anti-CD3 (2 μg/ml) and anti-CD28 (20 μg/ml) activated CD4+ T cells in the presence and absence of (A) canagliflozin and (B) dapagliflozin, determined by ELISA of cell-free supernatants. Data are representative of three independent experiments. Statistical analysis was performed using a one-way ANOVA followed by Dunnett’s multiple comparisons test. Data expressed as mean ± SEM; ** $p \leq 0.01$.

Moreover, canagliflozin inhibited T cell activation, with reduced expression of the classical T cell activation markers CD25 ($p = 0.0014$), CD44 ($p = 0.0006$) and CD69 ($p < 0.0001$; Figure 3.3). Dapagliflozin also limited T cell activation, with reduced expression of both CD44 ($p = 0.0499$) and CD69 ($p = 0.0374$) – although to a much lesser extent than observed with canagliflozin – whilst there was no significant change in CD25 expression ($p = 0.1584$; Figure 3.3).

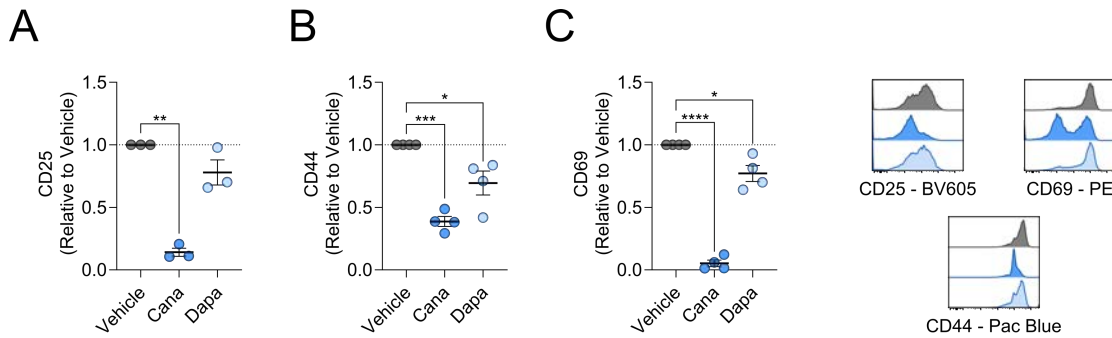


Figure 3.3 – Canagliflozin impairs T cell activation

(A-C) Relative surface expression of activation markers (A) CD25, (B) CD44 and (C) CD69 on anti-CD3 (2 µg/ml) and anti-CD28 (20 µg/ml) activated CD4+ T cells in the presence and absence of canagliflozin or dapagliflozin (both 10 µM), determined by flow cytometry. Representative overlaid histogram plots. Data are representative of three (A) or four (B-C) independent experiments. All relative data are normalised to the vehicle control group. Statistical analysis was performed using a one-sample T test. Data expressed as mean ± SEM; * $p \leq 0.05$, ** $p \leq 0.01$, *** $p \leq 0.001$, **** $p < 0.0001$.

We next assessed T cell blastogenesis, and whilst both SGLT2 inhibitors significantly reduced cell size (canagliflozin: $p = 0.0286$; dapagliflozin: $p = 0.0376$), canagliflozin again appeared to have a greater effect (Figure 3.4).

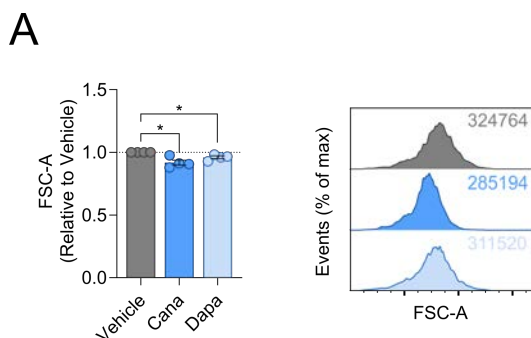


Figure 3.4 – SGLT2 inhibitors limit activated T cell blastogenesis

(A) Relative cell size of anti-CD3 (2 µg/ml) and anti-CD28 (20 µg/ml) activated CD4+ T cells in the presence and absence of canagliflozin and dapagliflozin (both 10 µM), determined by flow cytometry using forward-scatter area. Representative overlaid histogram plots, numbers indicate forward-scatter area. Data are representative four independent experiments. All relative data are normalised to the vehicle control group. Statistical analysis was performed using a one-sample T test. Data expressed as mean ± SEM; * $p \leq 0.05$.

Importantly, the observed changes in T cell activation and function were not due to compromised viability (canagliflozin: $p = 0.9808$; dapagliflozin: $p = 0.2531$; Figure 3.5).

A

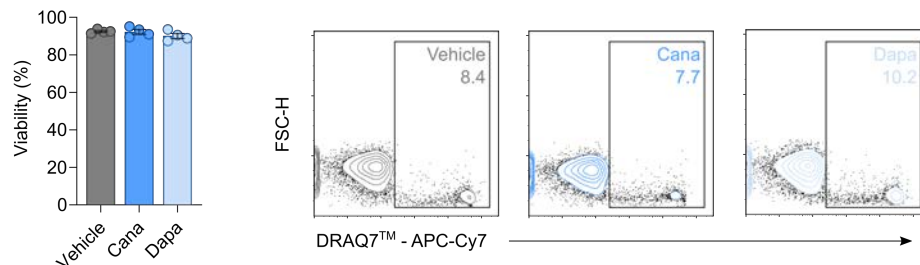


Figure 3.5 – Activated T cell viability is not compromised by canagliflozin and dapagliflozin

(A) Cell viability of anti-CD3 (2 $\mu\text{g}/\text{ml}$) and anti-CD28 (20 $\mu\text{g}/\text{ml}$) activated CD4+ T cells in the presence and absence of canagliflozin and dapagliflozin (both 10 μM), determined by flow cytometry using DRAQ7™. Representative contour plots, numbers indicate frequency of dead cells. Data are representative of four independent experiments. Statistical analysis was performed using a one-way ANOVA followed by Dunnett's multiple comparisons test. Data expressed as mean \pm SEM.

3.3.2 Canagliflozin retains its inhibitory effects on T cell function in physiological media conditions

With the recent advancement towards media containing more physiological nutrient levels, we wanted to ascertain whether canagliflozin remains effective in this environment. Human plasma-like medium (HPLM) more closely resembles human plasma compared to more traditional media such as RPMI, wherein RPMI contains elevated concentrations of several amino acids and altogether lacking numerous important lipid mediators (Cantor et al., 2017). These differences been previously shown to have a noteworthy effect on T cell activation (Leney-Greene et al., 2020). Tnv cells were activated as previously described and treated with physiological concentrations of canagliflozin or dapagliflozin (Figure 3.6).

A

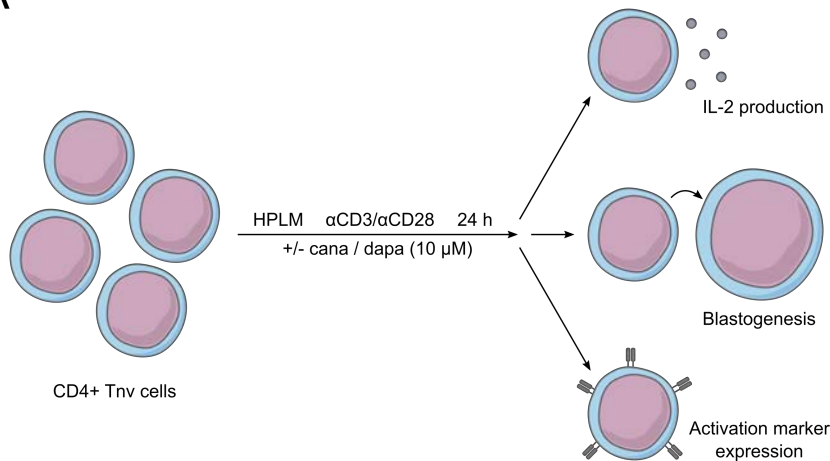


Figure 3.6 – Experimental procedure employed to assess the impact of canagliflozin and dapagliflozin on naïve T cells activated in HPLM

(A) Schematic overview outlining the experimental design in HPLM – anti-CD3 (2 µg/ml) and anti-CD28 (20 µg/ml) activated CD4+ Tnv cells in the presence and absence of canagliflozin or dapagliflozin (both 10 µM).

Here, when using HPLM, activated T cell function following canagliflozin treatment was consistent with our previous experiments, whereby canagliflozin reduced IL-2 production ($p = 0.0016$) and dapagliflozin had no observed effect ($p = 0.1098$; Figure 3.7).

A

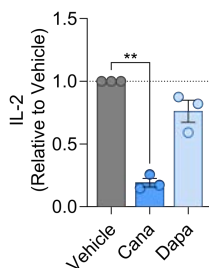


Figure 3.7 – Canagliflozin impairs IL-2 production by T cells activated in HPLM

(A) Relative IL-2 secretion by anti-CD3 (2 µg/ml) and anti-CD28 (20 µg/ml) activated CD4+ T cells in the presence and absence of canagliflozin and dapagliflozin (both 10 µM), determined by ELISA of cell-free supernatants. Data are representative of three independent experiments. All relative data are normalised to the vehicle control group. Statistical analysis was performed using a one-sample T test. Data expressed as mean ± SEM; ** $p \leq 0.01$.

In further agreement, activation marker expression was significantly reduced by canagliflozin, with substantial downregulation of CD25 ($p = 0.0005$), CD44 ($p = 0.0016$) and CD69 ($p = 0.0109$; Figure 3.8A-C). Although dapagliflozin also significantly reduced the expression of CD44 ($p = 0.0426$), this change was far less pronounced compared to canagliflozin, whilst the expression of CD25 ($p = 0.8248$) and CD69 ($p = 0.0754$) was not altered (Figure 3.8A-C). Moreover, canagliflozin-treated activated T cells displayed increased retention of CD62L on their cell surface ($p = 0.0808$) – which is typically shed following TCR engagement – again, indicative of dampened activation in these cells (Figure 3.8D).

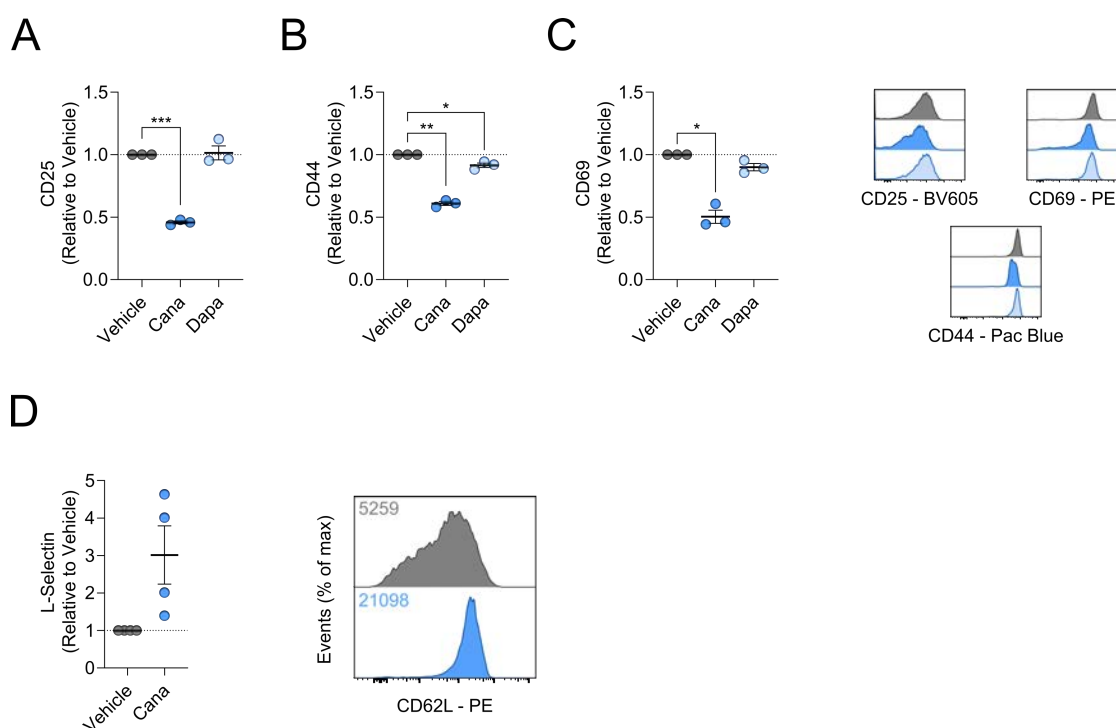


Figure 3.8 – T cell activation in HPLM is blunted by canagliflozin

(A-C) Relative surface expression of activation markers (A) CD25, (B) CD44 and (C) CD69 on anti-CD3 (2 $\mu\text{g/ml}$) and anti-CD28 (20 $\mu\text{g/ml}$) activated CD4⁺ T cells in the presence and absence of canagliflozin or dapagliflozin (both 10 μM), determined by flow cytometry. (D) Relative surface expression of activation marker CD62L as in (A-C). Representative overlaid histogram plots, numbers indicate median fluorescence intensity. Data are representative of three (A-C) or four (D) independent experiments. All relative data are normalised to the vehicle control group. Statistical analysis was performed using a one-sample T test. Data expressed as mean \pm SEM; * $p \leq 0.05$, ** $p \leq 0.01$, *** $p \leq 0.001$.

Finally, activated T cell blastogenesis was assessed and was more profoundly suppressed by canagliflozin ($p = 0.0064$) than previously observed in RPMI (Figure 3.9). Interestingly, in contrast with our previous findings, dapagliflozin did not constrain activated T cell blastogenesis in HPLM ($p = 0.2133$; Figure 3.9).

A

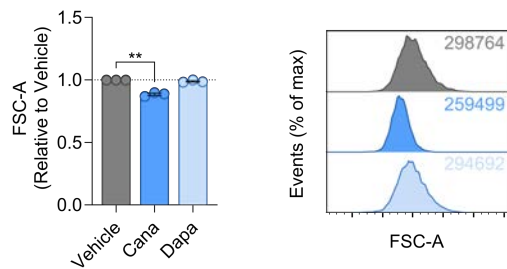


Figure 3.9 – Canagliflozin constrains activated T cell blastogenesis

(A) Relative cell size of anti-CD3 (2 $\mu\text{g}/\text{ml}$) and anti-CD28 (20 $\mu\text{g}/\text{ml}$) activated CD4+ T cells in the presence and absence of canagliflozin and dapagliflozin (both 10 μM), determined by flow cytometry using forward-scatter area. Representative overlaid histogram plots, numbers indicate forward-scatter area. Data are representative of three independent experiments. All relative data are normalised to the vehicle control group. Statistical analysis was performed using a one-sample T test. Data expressed as mean \pm SEM; ** $p \leq 0.01$.

It is again important to note that these changes are not the product of compromised cell viability (canagliflozin: $p = 0.4634$; dapagliflozin: $p = 0.9810$; Figure 3.10).

A

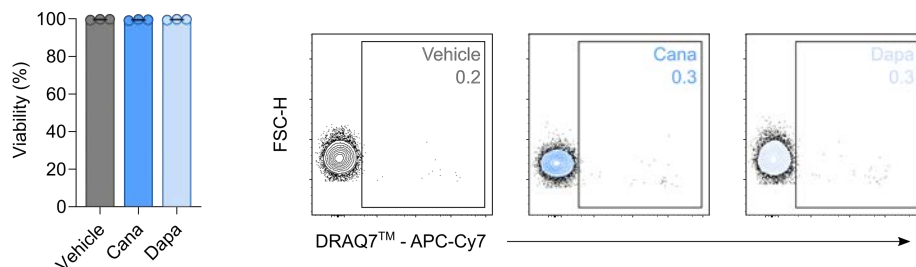


Figure 3.10 – Canagliflozin and dapagliflozin do not compromise the viability of CD4+ T cells activated in HPLM

(A) Cell viability of anti-CD3 (2 $\mu\text{g}/\text{ml}$) and anti-CD28 (20 $\mu\text{g}/\text{ml}$) activated CD4+ T cells in the presence and absence of canagliflozin and dapagliflozin (both 10 μM), determined by flow cytometry using DRAQ7™. Representative contour plots, numbers indicate frequency of dead cells. Data are representative of three independent experiments. Statistical analysis was performed using a one-way ANOVA followed by Dunnett's multiple comparisons test. Data expressed as mean \pm SEM.

Furthermore, we also confirmed that canagliflozin does not alter the phenotype of unstimulated Tnv cells, with no changes in basal activation marker expression (CD25: $p = 0.9970$; CD44: $p = 0.1179$; CD69: $p = 0.9901$), blastogenesis ($p = 0.2677$) or viability ($p = 0.4606$; Figure 3.11). Unstimulated Tnv cells expressed low levels of CD25, CD44 and CD69 (Figure 3.11A-C). Taken together, these data demonstrate that canagliflozin, but not dapagliflozin, impairs activated T cell function in physiological media conditions.

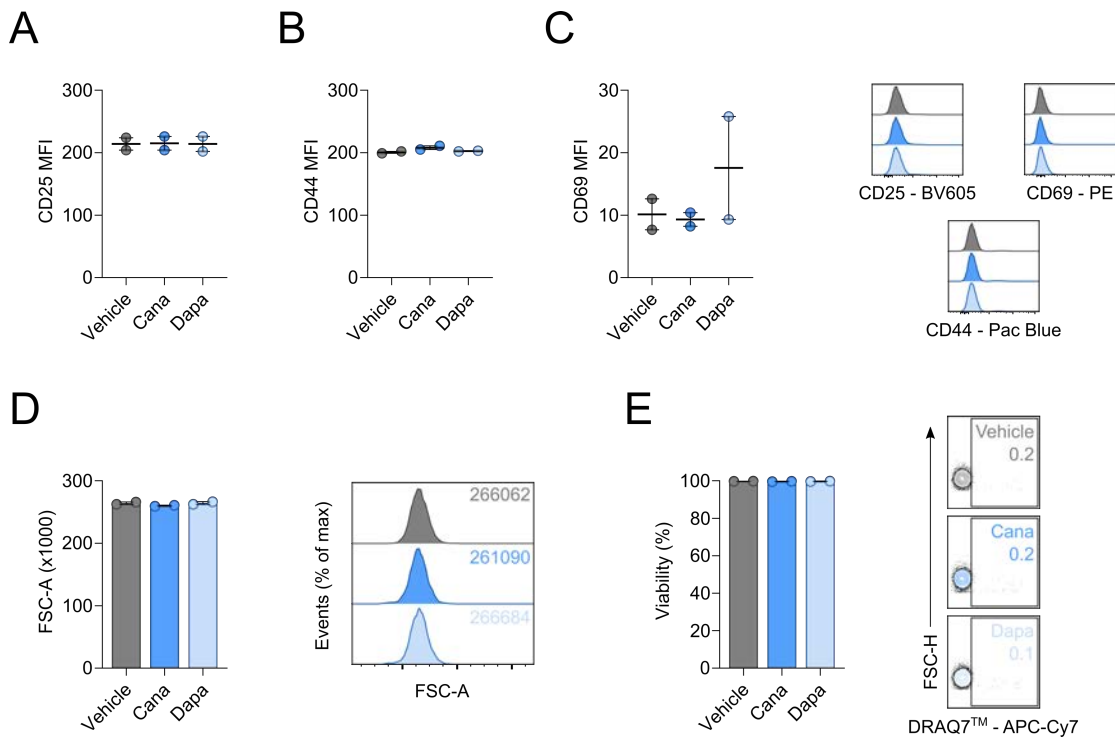


Figure 3.11 – SGLT2 inhibitors do not affect the phenotype of unstimulated naïve T cells

(A-C) Relative surface expression of activation markers (A) CD25, (B) CD44 and (C) CD69 on unstimulated CD4⁺ T_{nv} cells in the presence and absence of canagliflozin or dapagliflozin (both 10 μ M), determined by flow cytometry. (D) Relative cell size determined by flow cytometry using forward-scatter area. Representative overlaid histogram plots, numbers indicate forward-scatter area. (E) Cell viability determined by flow cytometry using DRAQ7[™]. Representative contour plots, numbers indicate frequency of dead cells. Data are representative of two independent experiments. Statistical analysis was performed using a one-way ANOVA followed by Dunnett's multiple comparisons test. Data expressed as mean \pm SEM.

We next considered the effect of SGLT2 inhibitors on long-term T cell activation. Cells were activated in the presence and absence of canagliflozin or dapagliflozin for 72 h and downstream effector function analysed (Figure 3.12).

A

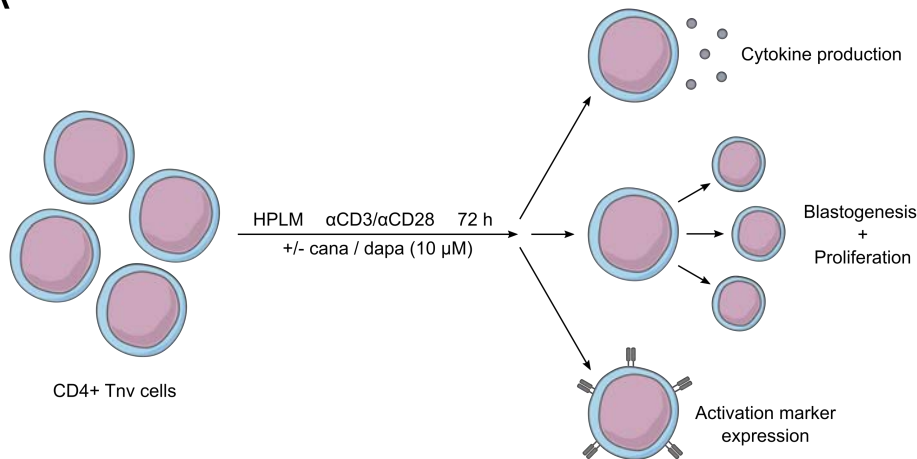
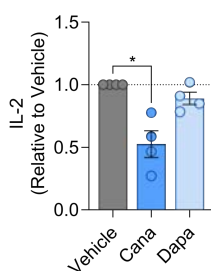


Figure 3.12 – Experimental procedure employed to assess the long-term impact of canagliflozin and dapagliflozin on naïve T cells activated in HPLM

(A) Schematic overview outlining the long-term experimental design in HPLM – anti-CD3 (2 µg/ml) and anti-CD28 (20 µg/ml) activated CD4+ Tnv cells in the presence and absence of canagliflozin or dapagliflozin (both 10 µM).

Here, we confirmed that only canagliflozin impairs long-term IL-2 production ($p = 0.0207$), with no significant change observed with dapagliflozin ($p = 0.1159$; Figure 3.13A). However, neither canagliflozin ($p = 0.1384$) or dapagliflozin ($p = 0.6922$) altered IFN γ production at 72 h (Figure 3.13B).

A



B

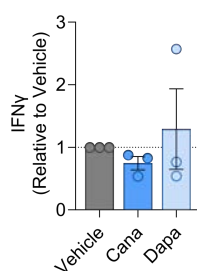


Figure 3.13 – Canagliflozin impairs long-term IL-2 production by CD4+ T cells activated in HPLM

(A-B) Relative secretion of (A) IL-2 and (B) IFN γ by anti-CD3 (2 µg/ml) and anti-CD28 (20 µg/ml) activated CD4+ T cells in the presence and absence of canagliflozin and dapagliflozin (both 10 µM), determined by ELISA of cell-free supernatants. Data are representative of four (A) or three (B) independent experiments. All relative data are normalised to the vehicle control group. Statistical analysis was performed using a one-sample T test. Data expressed as mean \pm SEM; * $p \leq 0.05$.

Additionally, neither SGLT2 inhibitor exerted any effect on activated T cell blastogenesis at this later time point (canagliflozin: $p = 0.3984$; dapagliflozin: $p = 0.6990$; Figure 3.14).

A

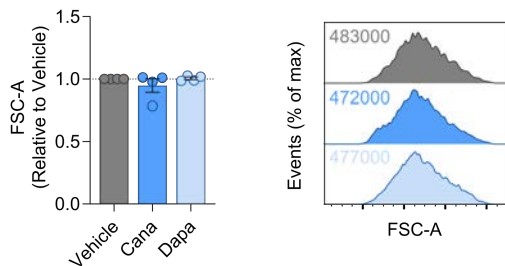


Figure 3.14 – Long-term activated T cell blastogenesis is not significantly affected by SGLT2 inhibitors

(A) Relative cell size of anti-CD3 (2 $\mu\text{g/ml}$) and anti-CD28 (20 $\mu\text{g/ml}$) activated CD4+ T cells in the presence and absence of canagliflozin and dapagliflozin (both 10 μM), determined by flow cytometry using forward-scatter area. Representative overlaid histogram plots, numbers indicate forward-scatter area. Data are representative of four independent experiments. All relative data are normalised to the vehicle control group. Statistical analysis was performed using a one-sample T test. Data expressed as mean \pm SEM.

For a more specific appraisal of long-term T cell function, we next assessed the impact of canagliflozin and dapagliflozin on proliferation by flow cytometry. Despite no observable changes in blastogenesis, canagliflozin was able to constrain proliferation, with fewer cells dividing compared to the vehicle control ($p = 0.0607$; Figure 3.15A). As expected, this feature was specific to canagliflozin, with no discernible change in proliferative capacity observed with dapagliflozin treatment ($p = 0.2526$; Figure 3.15A). In agreement with this, the calculated division index – a measure of the total number of divisions versus the number of cells at the start of culture – was also reduced in canagliflozin T cells (canagliflozin: $p = 0.0340$; Figure 3.15B). Additionally, canagliflozin also mediated a reduction in the expansion index of activated T cells (canagliflozin: $p = 0.0237$; Figure 3.15C). Both the proliferation index and replication index – parameters that only include cells that went into division – were unchanged by canagliflozin treatment (proliferation: $p = 0.3801$; replication: $p = 0.3417$), which suggests that the cells that can divide efficiently under these conditions proliferate in

a similar manner to untreated cells (Figure 3.15D-E). There were no changes to any of these proliferation-associated parameters in activated T cells treated with dapagliflozin (division: $p = 0.5192$; expansion: $p = 0.8356$; proliferation: $p = 0.4058$; replication: $p = 0.3120$; Figure 3.15B-E). Collectively, these results demonstrate that canagliflozin, but not dapagliflozin, mollifies short-term and long-term Tnv cell activation and function in physiological HPLM.

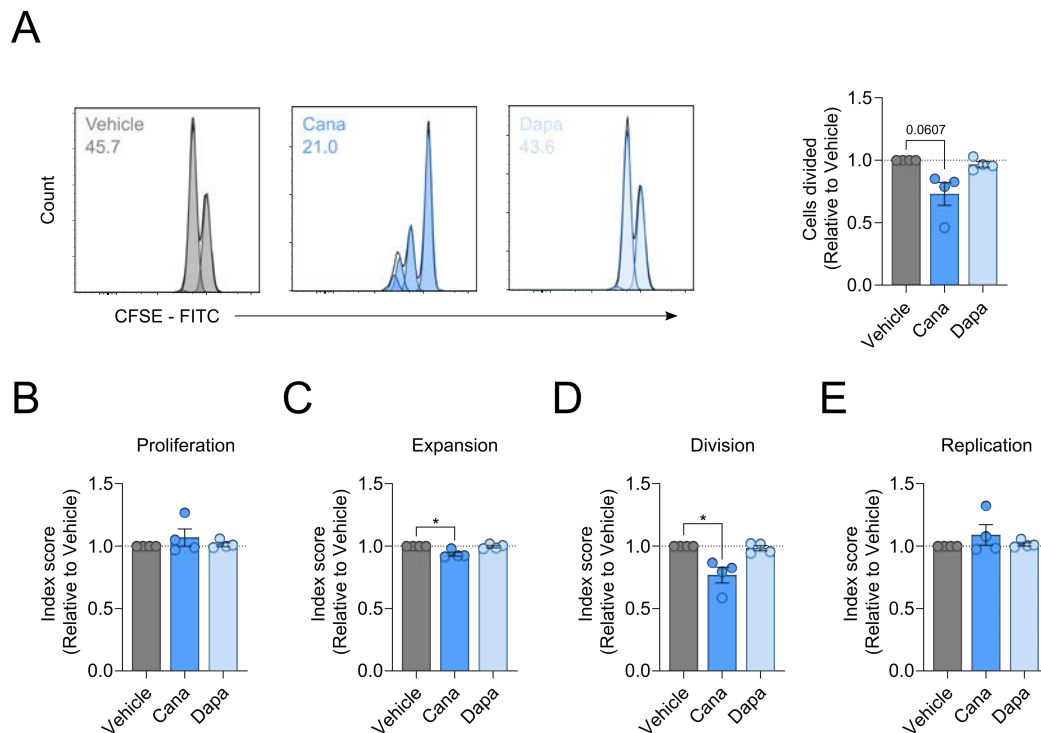


Figure 3.15 – Canagliflozin impairs T cell proliferation in HPLM

(A) Relative percentage of anti-CD3 (2 $\mu\text{g/ml}$) and anti-CD28 (20 $\mu\text{g/ml}$) activated CD4⁺ T cells divided in the presence and absence of canagliflozin and dapagliflozin (both 10 μM), determined by flow cytometry using CellTrace™ CFSE. Representative overlaid histogram plots, numbers indicate percentage of cells divided. (B-E) Calculated proliferation parameters including (B) proliferation, (C) expansion, (D) division and (E) replication. Data are representative of four independent experiments. All relative data are normalised to the vehicle control group. Statistical analysis was performed using a one-sample T test. Data expressed as mean \pm SEM; * $p \leq 0.05$.

Given the considerable loss of IL-2 production by T cells in response to canagliflozin treatment, we sought to assess whether supplementation with exogenous IL-2 would rescue their altered phenotype, thus we activated Tnv cells in the presence and absence of canagliflozin, with or without IL-2 (Figure 3.16).

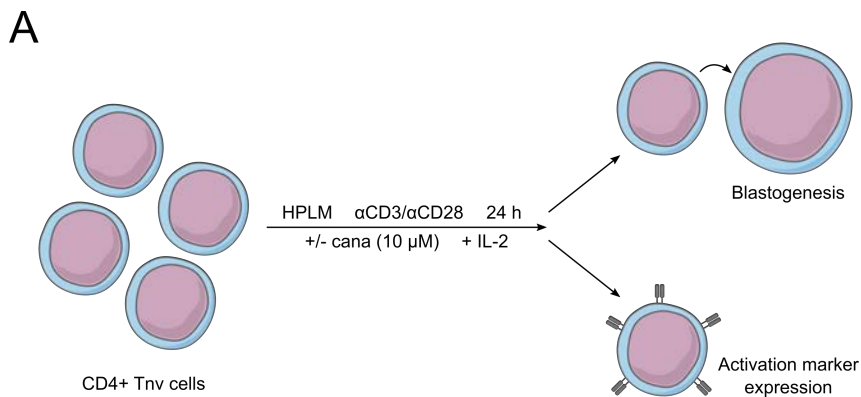


Figure 3.16 – Experimental procedure employed to assess rescue of impaired effector function by IL-2 in activated T cells treated with canagliflozin

(A) Schematic overview outlining the experimental design in HPLM – anti-CD3 (2 μg/ml) and anti-CD28 (20 μg/ml) activated CD4+ Tnv cells in the presence and absence of canagliflozin (10 μM), with or without IL-2 (10 ng/ml).

Here, the addition of IL-2 was unable to reverse the inhibitory effects of canagliflozin, as CD69 expression remained lower ($p = 0.0602$), CD62L was retained on the cell surface ($p = 0.0272$) and blastogenesis was diminished ($p = 0.0166$; Figure 3.17). This might suggest that the IL-2 receptor signalling pathway is not central to the immunomodulatory effects mediated by canagliflozin in Tnv cells. However, given that we observe a marked reduction in the expression of CD25, a component of the IL-2 receptor, it is unclear whether supplying excess IL-2 would have the same effect in these cells, therefore are unable to fully elucidate the role of IL-2 signalling in canagliflozin-treated T cells.

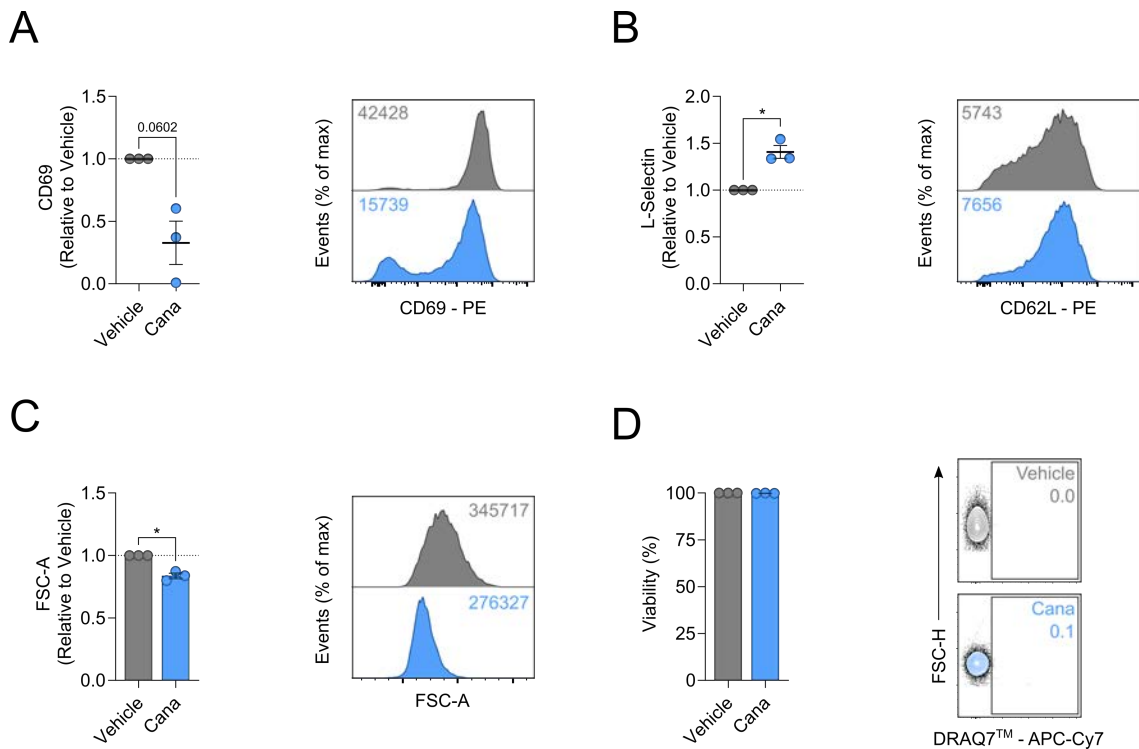


Figure 3.17 – IL-2 does not reverse the inhibitory effect of canagliflozin on activated T cells

(A-B) Relative surface expression of activation markers (A) CD69 and (B) CD62L on anti-CD3 (2 µg/ml) and anti-CD28 (20 µg/ml) activated CD4⁺ T cells in the presence and absence of canagliflozin (10 µM), supplemented with IL-2 (10 ng/ml), determined by flow cytometry. (C) Relative cell size, determined by flow cytometry using forward-scatter area. Representative overlaid histogram plots, numbers indicate either median fluorescence intensity or forward-scatter area. (D) Cell viability determined by flow cytometry using DRAQ7[™]. Representative contour plots, numbers indicate frequency of dead cells. Data are representative of three independent experiments. All relative data are normalised to the vehicle control group. Statistical analysis was performed using a one-way ANOVA followed by Dunnett's multiple comparisons test. For normalised data, statistical analysis was performed using a one-sample T test. Data expressed as mean ± SEM; * $p \leq 0.05$.

3.3.3 Canagliflozin modestly inhibits already-activated T cell function

To investigate whether canagliflozin can exert its inhibitory effect on already activated T cells, several distinct methods were employed. Dapagliflozin was dropped from these analyses, given the lack of an inhibitory effect previously observed. Initially, Tnv cell were pre-activated for 24 h before introducing canagliflozin to the final 24 h of culture (Figure 3.18A).

Whilst CD69 expression was unaltered ($p = 0.5920$), canagliflozin was able to reduce blastogenesis in already-activated T cells ($p = 0.0348$; Figure 3.18B-E).

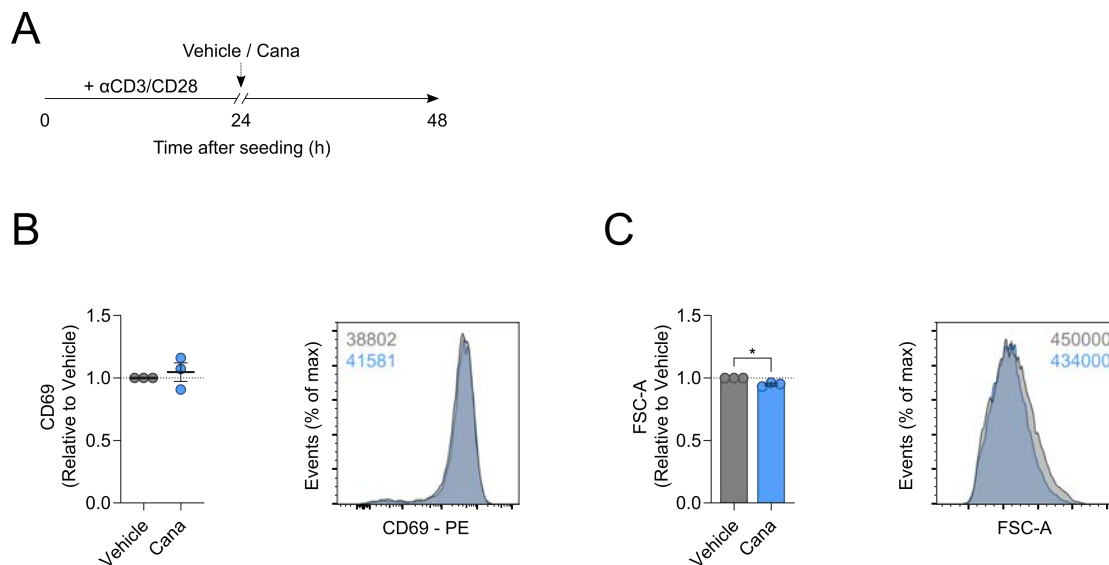


Figure 3.18 – Blastogenesis is diminished by canagliflozin in already-activated T cells

(A) Schematic overview outlining the experimental design of late drug challenge in HPLM – anti-CD3 (2 μ g/ml) and anti-CD28 (20 μ g/ml) pre-activated CD4+ T cells in the presence and absence of canagliflozin (10 μ M). (B) Relative surface expression of activation marker CD69, determined by flow cytometry. (C) Relative cell size, determined by flow cytometry using forward-scatter area. Representative overlaid histogram plots, numbers indicate either median fluorescence intensity or forward-scatter area. Data are representative of three independent experiments. All relative data are normalised to the vehicle control group. Statistical analysis was performed using a one-sample T test. Data expressed as mean \pm SEM; * $p \leq 0.05$.

To confirm that canagliflozin remains effective when introduced at the start of a 48 h culture, activation was measured through CD69 and CD62L expression, where CD69 was reduced and CD62L retained by canagliflozin treatment (Figure 3.19).

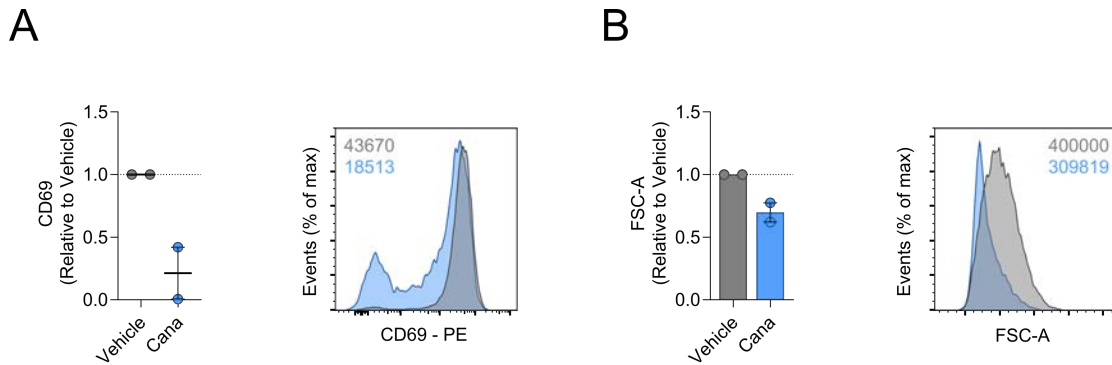


Figure 3.19 – Canagliflozin is effective when introduced prior to T cell activation

(A) Relative surface expression of activation marker CD69 on anti-CD3 (2 µg/ml) and anti-CD28 (20 µg/ml) activated CD4+ T cells in the presence and absence of canagliflozin (10 µM), determined by flow cytometry. (B) Relative cell size, determined by flow cytometry using forward-scatter area. Representative overlaid histogram plots, numbers indicate either median fluorescence intensity or forward-scatter area. Data are representative of two independent experiments. All relative data are normalised to the vehicle control group. Data expressed as mean ± SEM.

To better understand whether longer-term activation causes T cells to become more resistant to the inhibitory effects of canagliflozin, Tnv cells were pre-activated for 48 h before introducing canagliflozin to the final 48 h of culture (Figure 3.20A). Here, there were no longer any observed changes in CD69 expression ($p = 0.1131$) or blastogenesis ($p = 0.4859$; Figure 3.20B-C). Curiously, when these longer-term cultures were supplemented with IL-2, canagliflozin was able to elicit a significant reduction in CD69 expression ($p = 0.0046$), albeit to a lesser extent than when it is added at the beginning of culture (Figure 3.20D). However, blastogenesis remained unchanged when IL-2 was added ($p = 0.8055$; Figure 3.20E).

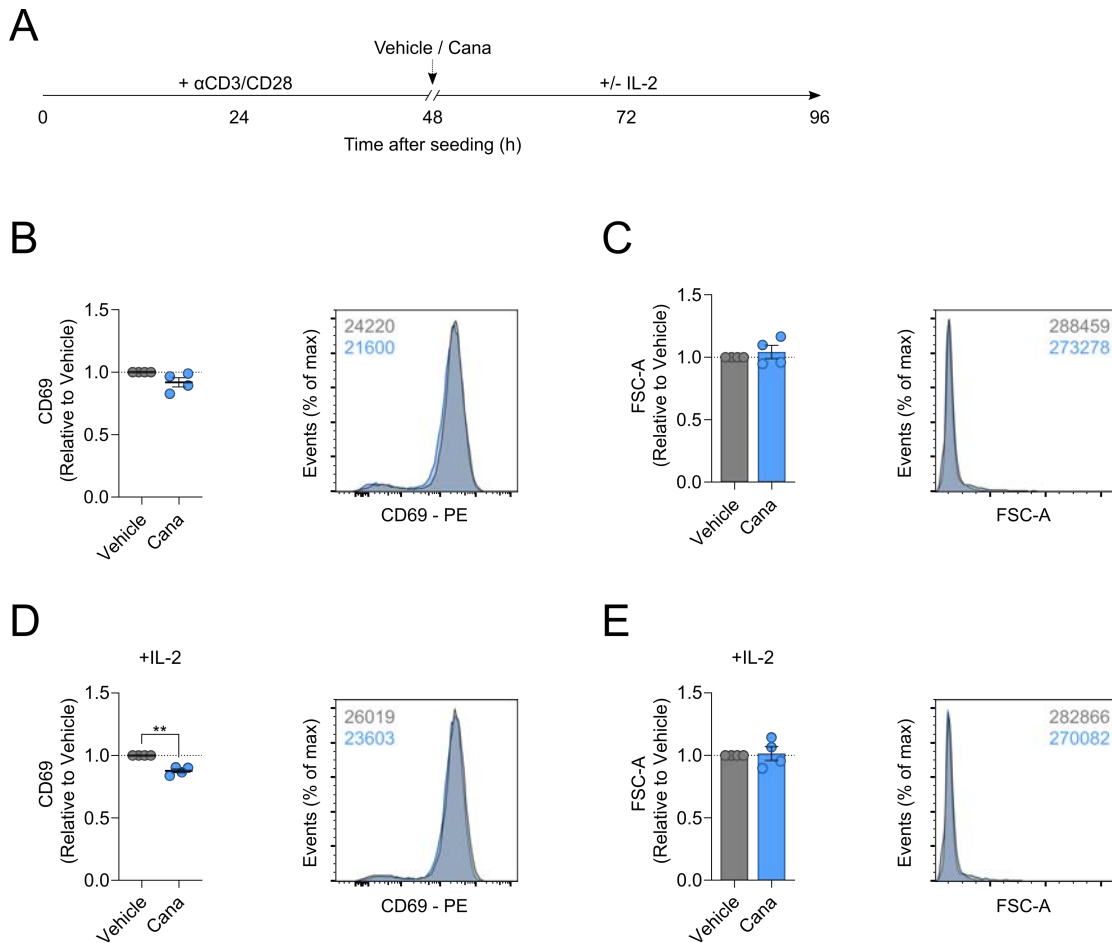


Figure 3.20 – Canagliflozin has a limited effect on effector function in T cells pre-activated longer-term

(A) Schematic overview outlining the experimental design of late drug challenge in HPLM – anti-CD3 (2 µg/ml) and anti-CD28 (20 µg/ml) pre-activated CD4+ T cells in the presence and absence of canagliflozin (10 µM), with or without IL-2 (10 ng/ml). (B) Relative surface expression of activation marker CD69, determined by flow cytometry. (C) Relative cell size, determined by flow cytometry using forward-scatter area. (D) Relative surface expression of activation marker CD69 when supplemented with IL-2, determined by flow cytometry. (E) Relative cell size when supplemented with IL-2, determined by flow cytometry using forward-scatter area. Representative overlaid histogram plots, numbers indicate either median fluorescence intensity or forward-scatter area. Data are representative of four independent experiments. All relative data are normalised to the vehicle control group. Data expressed as mean ± SEM; ** $p \leq 0.01$.

Finally, to determine whether prolonged exposure to canagliflozin can inhibit the function of already-activated T cells, pan CD4+ T cells were pre-activated for 24 h before introducing various concentrations of canagliflozin for the final 72 h of culture, again

supplemented with IL-2 (Figure 3.21A). Canagliflozin suppressed CD4+ T cell counts and IFN γ production, but required higher concentrations were required to achieve this (Table 3.1; Figure 3.21B-C). Together, these data show that canagliflozin significantly impairs T cell activation and function under physiological conditions, particularly prior to TCR co-stimulation.

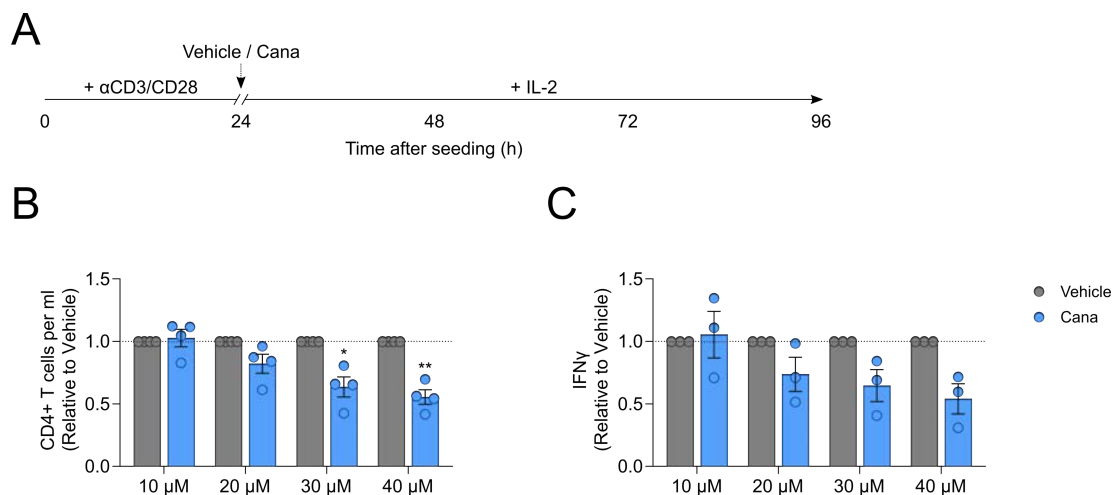


Figure 3.21 – Higher concentrations of canagliflozin are required to limit T cell proliferation and function in already-activated T cells

(A) Schematic overview outlining the experimental design of late drug challenge in HPLM – anti-CD3 (2 $\mu\text{g}/\text{ml}$) and anti-CD28 (20 $\mu\text{g}/\text{ml}$) pre-activated CD4+ T cells in the presence and absence of canagliflozin (10 μM), supplemented with IL-2 (10 ng/ml). (B) Relative T cell proliferation, determined by cell number per volume. (C) Relative secretion of IFN γ , determined by ELISA of cell-free supernatants. Data are representative of four (A) or three (B) independent experiments. All relative data are normalised to the vehicle control group. Statistical analysis was performed using a one-sample T test. Data expressed as mean \pm SEM; * $p \leq 0.05$, ** $p \leq 0.01$.

Table 3.1 – Increased concentrations of canagliflozin are required to inhibit already-activated T cells

Concentration (μM)	p -value compared to vehicle control group	
	Cell count	IFN γ production
10	0.7011	0.7914
20	0.0958	0.1928
30	0.0189	0.1085
40	0.0043	0.0619

3.4 Discussion

Co-stimulation through the TCR and CD28 is required for rapid activation of T cells to initiate effector functions such as cytokine production. However, T cell-mediated autoimmune diseases are characterised by aberrant T cell activation leading to chronic inflammation, where relapse to current treatments is common. Here, for the first time we show that canagliflozin impairs human T cell effector function, likely through its off-target effects inhibiting mitochondrial complex I and GDH. Dapagliflozin does not display any notable off-target effects (see Chapter 1.7.1), therefore the observed difference in efficacy between both treatment conditions would suggest that canagliflozin impacts T cell function through its off-target effects, rather than general SGLT2 inhibition using this class of drug. However, further work investigating the function of both mitochondrial complex I and GDH in T cells treated with canagliflozin is required to draw any definite conclusions. Canagliflozin impaired IL-2 production following TCR engagement and CD28 co-stimulation in a dose-dependent manner, underpinned by defective T cell activation. In contrast, dapagliflozin did not significantly impact IL-2 production at any dose, and T cell activation was inhibited to a lesser extent compared to canagliflozin. However, both canagliflozin and dapagliflozin constrained T cell blastogenesis following activation. Importantly, these changes occurred in the absence of cell death. As this study aims to determine the suitability of repurposing canagliflozin for therapeutic use in T cell-mediated autoimmune disease, known physiological concentrations were used to ensure that our findings were clinically relevant. Inhibition of T cell function by canagliflozin was observed at a concentration of 10 μ M, which is achieved in the plasma of patients taking canagliflozin (Devineni et al., 2013). Given the importance of T cell metabolism in establishing successful effector function (see Chapter 1.3.6), these data support the hypothesis that canagliflozin inhibits T cell function through its off-target effects on mitochondrial complex I and GDH.

Having established that canagliflozin impairs T cell function, further investigation was undertaken to confirm that this is also accurate under more physiologically relevant conditions. Recently, there has been a push in the field of immunometabolism towards using media containing more physiological nutrient levels in order to enhance any downstream translation of *in vitro* work. Therefore, where appropriate, we cultured T cells in HPLM for the remainder of our experiments, as the nutrient composition more closely resembles adult human plasma than traditional media. In fact, previous work has shown that there are marked

differences in human T cell activation when cultured in RPMI compared to HPLM (Lenev-Greene et al., 2020). Similar observations were made as in the initial experiments carried out in RPMI, whereby canagliflozin impaired T cell activation and IL-2 production, whilst dapagliflozin had only a modest effect on activation. An additional retention of CD62L on the cell surface of canagliflozin-treated T cells further demonstrated impaired activation. Furthermore, canagliflozin displayed more pronounced inhibition of T cell blastogenesis than dapagliflozin. Again, these changes were not caused by changes in T cell viability. Following long-term activation, T cells undergo expansion to enhance the number present at the site of action (see Chapter 1.2.4). When cultured with canagliflozin, fewer T cells divided following TCR engagement resulting in reduced expansion, whereas proliferation was unaffected by treatment with dapagliflozin. Moreover, IL-2 production remained suppressed by canagliflozin at this later time point, whilst neither canagliflozin or dapagliflozin affected IFN γ production. This shows that canagliflozin retains its inhibitory effect on activated T cell function under more physiologically relevant media conditions and remains effective following extended T cell activation. Given that autoimmune disease pathogenesis is alleviated through regulation of hyperactive immune cells at the site of inflammation, it is important that the inhibitory effects of canagliflozin are targeted and did not impact the function of unstimulated T cells.

IL-2 plays an important role in T cell activation, where it acts as a growth factor promoting proliferation and enhancing the generation of effector and memory T cells (see Chapter 1.2.4). Given the considerable loss of IL-2 production observed in the presence of canagliflozin, we determined whether the addition of exogenous IL-2 would rescue the observed phenotype. However, T cell activation remained suppressed following supplementation with IL-2, therefore canagliflozin must induce a more global inhibition of T cell function.

Since T cell-mediated autoimmune disease is characterised by the accumulation of hyperactivated T cells at the site of inflammation, it was important to consider the impact of canagliflozin on already-activated T cells. Various strategies were employed to investigate the efficacy of late drug challenge, however, canagliflozin was unable to exert a consistent effect under these treatment conditions with modest effects to T cell activation and blastogenesis only occasionally observed. Higher doses of canagliflozin were required to achieve consistent inhibition of effector function in already-activated T cells – proliferation was inhibited at a

concentration of around 30 μM , whereas inhibition of IFN γ production was reached at a concentration of 40 μM . Given that a consistent effect is only observed at supraphysiological concentrations – around 3-4 times greater than the plasma concentration typically observed in patients taking canagliflozin – it is unclear whether canagliflozin is able to modulate the function of already-activated T cells as effectively. Further work is required to determine the length of activation at which T cells become resistant to the effects of canagliflozin, and whether sustained exposure (i.e., 72+ h) to canagliflozin can overcome these challenges.

3.5 Conclusions

Canagliflozin is currently used as a treatment for T2D, whereby it inhibits glucose reabsorption in the kidney through inhibition of SGLT2. However, it has also been established that it has off-target effects that inhibit mitochondrial complex I of the electron transport chain and GDH. Here, canagliflozin has been shown to have an inhibitory effect on T cell function, where IL-2 production was reduced in a dose-dependent manner, underpinned by reduced activation. Importantly, this loss of T cell function did not result from compromised viability. These findings were observed in both traditional culture media and more physiologically-relevant media. Extended cell culture experiments revealed that long-term T cell functions, such as proliferation and cytokine production, were also impaired by canagliflozin. Despite the considerable loss of IL-2 following canagliflozin treatment, supplementation with exogenous IL-2 was not able to reverse the observed phenotype in T cells.

Dapagliflozin, a member of the same class of T2D drugs, inhibits SGLT2 in the same manner as canagliflozin, but demonstrates no notable off-target effects. Here, dapagliflozin did not display the same inhibitory properties on T cell function, only modestly reducing their activation. This would suggest that canagliflozin modulates T cell function independent of SGLT2 inhibition, instead through its off-target effects on mitochondrial complex I and GDH. This is the first time that the impact of canagliflozin on T cell effector function has been described in humans.

Given that pathogenic T cells are hyperactivated at the site of inflammation in autoimmune disease, it was important to consider the effect of canagliflozin on already-activated T cells. Higher doses of canagliflozin – beyond physiological concentrations

recorded in the plasma of patients prescribed canagliflozin – were required to inhibit proliferation and IFN γ production in already-activated T cells. Since canagliflozin induces global T cell suppression, further work was undertaken to establish the changes in gene expression that occur, and how these changes translate into changes at the protein level.

Chapter Four

**Canagliflozin mediates global changes
to T cell function at the transcript and
protein level**

4 Canagliflozin mediates global changes to T cell function at the transcript and protein level

4.1 Introduction

Analysing gene expression by measuring the RNA content of hundreds to thousands of genes simultaneously has become a valuable technique in uncovering novel cell-to-cell changes with high resolution. For example, recent single-cell transcriptomic methods have revealed the dynamic changes in gene expression that occur following T cell activation. Changes included an enrichment of genes involved in cell cycle progression and, rather interestingly, downregulation of the electron transport chain complexes (Cano-Gamez et al., 2020). Importantly, these changes at the gene level were supported by similar proteomic changes (Cano-Gamez et al., 2020). Additionally, the influence of various differentiation-associated cytokine milieus on the T cell transcriptome was assessed. Cytokine-induced changes predominantly emerged days following stimulation, highlighting that differentiation programmes are only established following early changes in response to T cell activation (Cano-Gamez et al., 2020). Furthermore, whilst the gene expression patterns induced by cytokine stimulation shape the effector functions for subset-specific responsibilities, alternate cell states are induced depending on T cell activation status (i.e., naïve versus memory) (Cano-Gamez et al., 2020). Progression from naïve to memory phenotypes is accompanied by marked upregulation of cytokine- and chemokine-associated genes, providing evidence that memory T cells are primed to initiate rapid responses following activation (Cano-Gamez et al., 2020).

Transcriptomic analyses have more recently been utilised in the context of T cell metabolism. For instance, metabolic heterogeneity has been interlinked to the pathogenic potential of Th17 cells in autoimmune disease (Wagner et al., 2021). To this end, gene expression patterns in pathogenic Th17 cells revealed upregulation of glycolysis and aspects of OXPHOS compared to their non-pathogenic counterparts – both changes realised in subsequent bioenergetic analyses (Wagner et al., 2021). Alternatively, non-pathogenic Th17 cells were dependent on augmented lipid oxidation, which was also previously predicted in the genomic dataset (Wagner et al., 2021). Additionally, this analysis identified a novel role for the polyamine pathway in the control of Th17 function, whereby polyamine catabolism

was most significantly associated with pathogenicity (Wagner et al., 2021). Functional analyses confirmed that polyamines indeed accumulate within pathogenic Th17 cells, whilst inhibition of polyamine-dependent processes was sufficient to impair their effector function and alleviate disease severity in an experimental autoimmune encephalomyelitis model (Wagner et al., 2021). Single-cell transcriptomics have also been used to investigate the rewiring of CD8+ T cell metabolism in response to activation. Subsets were delineated by activation status from naïve through to late stages, which allowed the mapping of temporal changes in cellular metabolism, demonstrating previously known shifts towards aerobic glycolysis and glutamine metabolism following activation (Fernandez-Garcia et al., 2022). Amongst these changes, asparagine synthetase emerged as a novel regulator of T cell differentiation, whereby its expression peaks upon effector formation before diminishing upon progression to memory (Fernandez-Garcia et al., 2022). Functional assays that overexpressed asparagine synthetase confirmed that this enzyme favours differentiation towards an effector phenotype, which could be harnessed in disease setting to enhance the anti-tumour response (Fernandez-Garcia et al., 2022). Together, these studies showcase that single-cell transcriptomic methods can be employed to assess global changes in cellular pathways, leading to novel discoveries that can be manipulated for therapeutic benefit. Furthermore, it is crucial that the findings of such studies are supported through either proteomic analyses or functional assays.

Nanostring nCounter® analyses have yet to be utilised to resolve T cell metabolism. However, there are some examples of this technology being used to analyse T cells in the setting of autoimmune disease. Most recently, naïve CD8+ T cells (T_{nv}) isolated from rheumatoid arthritis (RA) patients clustered more closely to activated T cell subsets (i.e., effector populations) than T_{nv} cells from healthy controls, based on their expression of near 400 transcripts (Cammarata et al., 2019). Interestingly, patient-derived CD8+ T_{nv} cells expressed a number of proinflammatory effector molecules such as granzyme B and tumour necrosis factor- α , whereas these transcripts were not detected in CD8+ T_{nv} cells isolated from healthy individuals (Cammarata et al., 2019). Therefore, Nanostring nCounter® analysis is a genomics platform that allows interrogation of the cellular transcriptome using limited samples volumes – an alternative to more popular single-cell RNA sequencing techniques.

Direct proteomic approaches have also been used to further our understanding of global changes in T cell function. Particularly interesting are the studies that have investigated

the importance of various metabolic signalling proteins to the global T cell proteome, and how this is intertwined with such processes as T cell activation and differentiation. Both murine T cell subsets – CD4+ and CD8+ T cells – greatly increase their protein content following their activation via the T cell receptor (TCR), which becomes even further heightened upon their transition towards an effector population (Howden et al., 2019). However, this does not translate to a large-scale upregulation of existing proteins; instead, there is a dynamic reshaping of the proteome tailored to their functional requirements (Howden et al., 2019). For example, activated T cells upregulate their expression of both amino acid transporters and protein translation machinery to meet the demands of elevated protein synthesis and successful T cell activation (Howden et al., 2019). Importantly, this study also highlights the significance of the metabolic regulator mTOR in T cell differentiation, controlling several checkpoints including cellular metabolism, solute transporter expression and protein translation (Howden et al., 2019). A similar involvement has also been described for MYC, another key metabolic protein, using the same proteomic methods. MYC-deficient T cells failed to generate the protein content necessary for successful T cell activation, displaying similar protein levels to naïve T cells (Marchingo et al., 2020). Interestingly, amongst these changes were a group of proteins that remained strongly upregulated even in the absence of MYC, including the classical T cell activation markers CD44 and CD69 (Marchingo et al., 2020). However, MYC was again critical in the selective upregulation of amino acid transporters, translational machinery and cellular metabolic pathways – all essential to T cell activation (Marchingo et al., 2020). Moreover, elevated amino acid transporter expression is required for sustained MYC activation, in turn driving further MYC-dependent processes to sustain activation and differentiation (Marchingo et al., 2020). Recently, the role of extracellular signal-regulated kinases (ERK) – a key subset of signalling molecules downstream of TCR signalling – has been explored in the context of T cell activation using a proteomic-based means. Although ERK is actively involved in the remodelling of the CD8+ T cell proteome following engagement of the TCR, it is surprising that much of the proteome can be restructured in the absence of ERK activation (Damasio et al., 2021). However, amongst the several ERK-dependent protein changes are the upregulation of crucial proteins involved in activation, as well as effector molecules such as granzyme B (Damasio et al., 2021). Unlike inhibition of mTOR and MYC, proteomic changes associated with cellular metabolism were only modestly affected by ERK inhibition (Damasio et al., 2021). Together,

these data highlight that the integration of various signalling pathways involved in T cell metabolism and transcriptional reprogramming is essential in promoting T cell activation and differentiation. Moreover, these studies also underline the value in using 'omics'-based approaches to elucidate the impact of various signalling pathways on global T cell function. Given that we anticipate that canagliflozin will considerably modulate T cell metabolism, whilst also impacting other possible areas of T cell fitness currently unknown to us, genomic and proteomic based approaches would be beneficial in revealing some of the mechanisms wherein canagliflozin inhibits T cell function.

4.1.1 Rationale

Human CD4⁺ T_H1 cells were chosen as the study material. The reasons were: (i) to investigate global changes in T cell gene expression following treatment with canagliflozin or dapagliflozin; (ii) investigate how canagliflozin-induced changes in gene expression translate to changes at the protein level; and (iii) better understand the underpinning changes to T cell metabolism upon canagliflozin treatment through interrogation of both 'omics' datasets.

4.1.2 Hypothesis

- (i) Global changes in T cell gene expression are induced by canagliflozin, but not dapagliflozin
- (ii) Canagliflozin remodels the T cell proteome
- (iii) The expression of metabolism-associated proteins is drastically altered by canagliflozin

4.2 Experimental procedures

4.2.1 Human blood collection

Ethical approval was obtained from Wales Research Ethics Committee 6 for the collection of peripheral blood from healthy volunteers (13/WA/0190). Blood from healthy donors was processed as previously described (see Chapter 2.1).

4.2.2 T cell isolation

Peripheral blood mononuclear cells (PBMCs) were isolated as previously described (see Chapter 2.3). The PBMC pellet was resuspended in the appropriate downstream media for analysis and the number of PBMCs was determined by using the Countess[®] automated cell counter (see Chapter 2.5). CD4⁺ T_H1 cells were isolated using automated magnetic separation as previously described (see Chapter 2.4).

4.2.3 Cell culture

Isolated T cells were activated and cultured in human plasma-like medium (HPLM) as previously described (see Chapter 2.6). Cell-free supernatants were stored for further analysis, whilst cells were collected for downstream analysis.

4.2.4 Flow cytometry

Purity of isolated T cells was monitored as previously described (see Chapter 2.7.1) and was typically > 90%.

4.2.5 Immunoblotting

Immunoblotting was performed as previously described (see Chapter 2.10). Membranes were probed with antibodies specific to c-MYC (Cell Signalling, USA) and used at a 1:1000 dilution.

4.2.6 RNA isolation

RNA isolation was performed using an RNeasy[®] Mini Kit as per the manufacturers' guidelines (all Qiagen, Germany – unless otherwise stated). Cells were lysed in a 1:1 solution of RLT buffer and 70% high-grade ethanol (Fisher Bioreagents, USA) and mixed well with a needled syringe. Lysed cells were then transferred to an RNeasy[®] Mini spin column placed in

a 2 ml collection tube and centrifuged at 8000 x *g* for 15 s. The spin column was then washed once with RW1 buffer, followed by two wash steps using RPE buffer, with subsequent centrifugation at 8000 x *g* for 15 – 120 s following the addition of each reagent. The resulting flow-through was discarded each time. Following washing, the spin column was placed in a new collection tube and 30 µl of RNase-free water was added directly to the spin column membrane in order to elute the RNA following centrifugation at 8000 x *g* for 1 min. The collected eluate was re-placed on the spin column membrane and centrifuged again to further increase the final concentration of the collected RNA.

Purity was assessed using a NanoDrop™ spectrophotometer by measuring the ratio of absorbance at 260 nm versus 280 nm or 230 nm. Measured A260/A280 and A260/A230 ratios were typically ~2.0. Any RNA samples with A260/230 ratio below 2.0 were precipitated using 0.3 M sodium acetate solution (ThermoFisher, USA) and isopropanol. RNA was diluted to 300 µl in RNase-free water before addition of sodium acetate. An equal volume of isopropanol was then added to the RNA solution, which was incubated overnight at -20°C. RNA was recovered by centrifugation at 14000 x *g* for 10 min at 4°C and the resulting pellet was washed twice in 70% ethanol. The final pellet was dried at RT before dissolving in RNase-free water. Subsequent measured A260/A230 ratios were typically improved to ≥ 2.0.

Once purity was established, RNA was stored at -80°C until required for downstream analysis. Freeze-thaw cycles were avoided in order to prevent RNA degradation.

4.2.7 Nanostring analysis

The nCounter® platform allows multiplex analysis of up to 800 RNA, DNA or protein targets (Figure 4.1). Sample RNA is hybridised with target-specific capture and reporter probes in order to create a library of unique target-probe complexes. Each target is labelled with a specific molecular barcode, which can then be detected and counted using an automated fluorescence microscope. Detection and scanning were performed by the nCounter® SPRINT Profiler analysis system (Nanostring, USA).

RNA samples stored at -80°C were thawed on ice prior to hybridisation reactions. Reporter probes were diluted in 70 µl of hybridisation buffer and gently mixed to create a master mix. To set up the hybridisation reactions, 5 µl of each sample was added to 8 µl of master mix. Hybridisation reactions were then completed by adding 2 µl of Capture ProbeSet and incubation at 65°C for 20 h. Probe set-target RNA hybridisation solution is then further

diluted to a final volume of 35 μ l. 33 μ l of the diluted hybridisation solution is loaded onto a SPRINT microfluidic cartridge, with an air bubble also inserted to the stop point. The SPRINT microfluidic cartridge is then loaded onto the nCounter SPRINT Profiler (Nanostring, USA) to initiate analysis.

Raw data appraisal, quality control and normalisation were all performed using the nSolver™ analysis software. Quality control included an imaging QC of > 75% FOV registration, binding density QC within a range of 0.1 - 2.25, positive control linearity QC with $R^2 \geq 0.95$, and a positive control limit of detection QC set as 0.5 fM positive control above 2 standard deviations above the negative controls. Normalisation was performed using negative controls, positive controls and housekeeping genes selected by the nSolver™ normalisation module and normalised data was used as input for further analysis.

For differential expression analysis, a log₂ fold-change of > 1 or < -1 and an adjusted *p*-value ≤ 0.05 determined differentially expressed genes. *p*-values were adjusted using the Benjamini-Yekutieli method to control the false discovery rate (FDR). Pathway scores were calculated as the first principal component of the pathway genes' normalised expression.

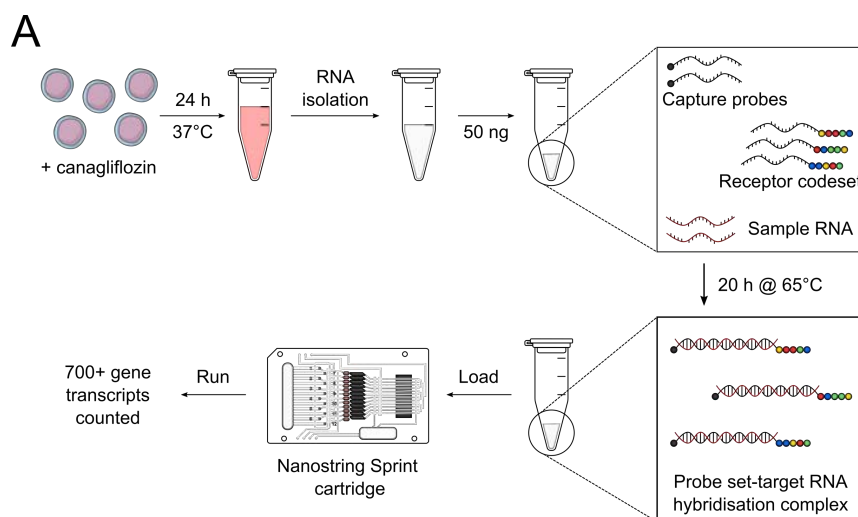


Figure 4.1 – Nanostring nCounter® analysis experimental procedure

(A) Schematic overview of the experimental procedure for Nanostring nCounter® analysis. RNA isolation simplified (see Chapter 4.2.6).

4.2.8 Proteomic analysis

Sample Processing: 2×10^6 isolated Tnv cell were pelleted and washed in Hank's Balanced Salt Solution (Gibco, USA) before storing at -80°C for proteomic analysis. Samples were resuspended to 200 μl with S-Trap lysis buffer (10% SDS, 100mM Triethylammonium bicarbonate) and sonicated for 15 min (30 s on, 30 s off, 100% Amplitude, 70% Pulse). After centrifugation the supernatant was transferred to fresh tubes and the proteins quantified using the Micro BCA Protein Assay (ThermoFisher, USA). 150 μg of protein was processed using S-Trap mini columns (Protifi, USA). The samples were digested overnight with 3.75 μg of trypsin (Pierce Trypsin Protease MS-Grade; ThermoFisher, USA) with a second digest with the same amount of trypsin for 6 h the following day. Peptides were extracted and dried under vacuum. The peptides were then resuspended to 50 μl with 1% Formic Acid and quantified using the Pierce Quantitative Fluorometric Peptide Assay (both ThermoFisher, USA).

Mass Spectrometry: Peptides equivalent of 1.5 μg were injected onto a nanoscale C18 reverse-phase chromatography system (UltiMate 3000 RSLCnano) and electrosprayed into an Orbitrap Exploris 480 Mass Spectrometer (both ThermoFisher, USA). For liquid chromatography the following buffers were used: buffer A (0.1% formic acid in Milli-Q water (v/v)) and buffer B (80% acetonitrile and 0.1% formic acid in Milli-Q water (v/v)). Samples were loaded at 10 $\mu\text{L}/\text{min}$ onto a trap column (100 $\mu\text{m} \times 2 \text{ cm}$, PepMap nanoViper C18 column, 5 μm , 100 \AA , ThermoFisher, USA) equilibrated in 0.1% trifluoroacetic acid (TFA). The trap column was washed for 3 min at the same flow rate with 0.1% TFA then switched in-line with a resolving C18 column (75 $\mu\text{m} \times 50 \text{ cm}$, PepMap RSLC C18 column, 2 μm , 100 \AA ; Thermo Scientific, USA). Peptides were eluted from the column at a constant flow rate of 300 nl/min with a linear gradient from 3% buffer B to 6% buffer B in 5 min, then from 6% buffer B to 35% buffer B in 115 min, and finally from 35% buffer B to 80% buffer B within 7 min. The column was then washed with 80% buffer B for 4 min. Two blanks were run between each sample to reduce carry-over. The column was kept at a constant temperature of 50°C .

Data was acquired using an easy spray source operated in positive mode with spray voltage at 2.60 kV, and the ion transfer tube temperature at 250°C . The MS was operated in DIA mode. A scan cycle comprised a full MS scan (m/z range from 350-1650), with RF lens at 40%, AGC target set to custom, normalised AGC target at 300%, maximum injection time mode set to custom, maximum injection time at 20 ms, microscan set to 1 and source

fragmentation disabled. MS survey scan was followed by MS/MS DIA scan events using the following parameters: multiplex ions set to false, collision energy mode set to stepped, collision energy type set to normalized, HCD collision energies set to 25.5, 27 and 30%, orbitrap resolution 30000, first mass 200, RF lens 40%, AGC target set to custom, normalized AGC target 3000%, microscan set to 1 and maximum injection time 55 ms. Data for both MS scan and MS/MS DIA scan events were acquired in profile mode.

Raw Data Analysis: Analysis of the DIA data was carried out using Spectronaut (version 15.4.210913.50606, Biognosys, AG). The directDIA workflow, using the default settings (BGS Factory Settings) with the following modifications was used: decoy generation set to mutated; Protein LFQ Method was set to QUANT 2.0 (SN Standard) and Data Filtering to Qvalue; Cross Run Normalization was selected with global normalization on the median; Precursor Qvalue Cutoff and Protein Qvalue Cutoff (Experimental) set to 0.01. For the Pulsar search, the settings were: maximum of 2 missed trypsin cleavages; PSM, Protein and Peptide FDR levels set to 0.01; cysteine carbamidomethylation set as fixed modification and acetyl (N-term), deamidation (asparagine, glutamine), dioxidation (methionine, tryptophan), glutamine to pyro-Glu and oxidation of methionine set as variable modifications. The database used was the *H.sapiens* proteome downloaded from uniprot.org on 2021-05-11 (77, 027 entries). Samples were grouped according to the condition (vehicle or canagliflozin) to allow a comparison to be made between the control and treated samples. Sample processing and mass spectrometry was performed by the FingerPrints Proteomics Facility at the University of Dundee.

Further analysis: Protein copy numbers were calculated as previously described (Wisniewski et al., 2014). Here, the MS signal of histones is proportional to the DNA within the sample, which can then be used as a measure of the number of cells present. This “proteomic ruler” method transforms the MS signals generated to an absolute scale, whereby the protein copy numbers per cell can be estimated. Additionally, protein concentration was also determined to account for any differences in total cellular protein content.

The Database for Annotation, Visualisation and Integrated Discovery (DAVID, USA) was used to perform protein set enrichment analysis (PSEA; also known as overrepresentation analysis), whereby proteins were assessed against the following databases: Gene Ontology (Molecular Function, Biological Function, Cellular Components) and Biological Pathways (KEGG Database, Reactome Database). This considers expression

differences across pre-defined groups of proteins related to a biological context to identify enriched functional-related gene groups. Mitochondrial complex proteins were identified using the following Gene Ontology Cellular Component terms: mitochondrial respiratory chain complex I (GO:0005747); mitochondrial respiratory chain complex II, succinate dehydrogenase complex (ubiquinone) (GO:0005749); mitochondrial respiratory chain complex III (GO:0005750); mitochondrial respiratory chain complex IV (GO:0005751); mitochondrial proton-transporting ATP synthase complex (GO:0005753).

Ingenuity Pathway Analysis (IPA; Qiagen, Germany) was used to predict which pathways could be altered based on the changes in protein expression observed in the dataset. Each pathway is given a *p*-value based on how enriched that pathway is compared to a background list of proteins.

IPA Upstream Regulator analysis (Qiagen, Germany) was used to predict the upstream regulators (i.e., transcription factors, microRNAs, kinases, small molecule inhibitors, etc.) that could explain the observed gene expression changes in the dataset. The calculated activation z-score infers the activation state of that upstream regulator. Positive z-scores represent activation, whereas negative z-scores represent inhibition. In the case of small molecules (drugs and compounds) and microRNAs, the terms “activated” and “inhibited” are better described as increased activity or decreased activity, respectively.

4.2.9 Statistical analysis

Unless otherwise stated, statistical analysis was carried out using GraphPad Prism version 8 or later. Data are expressed as the mean \pm standard error of the mean (SEM). The normality of the data was initially tested using the Shapiro-Wilk test to determine the appropriate method of analysis. For data comparing two sample groups, normally distributed data were analysed using a parametric T test, whereas a non-parametric T test was used to analyse data not normally distributed. One-way analysis of variance (ANOVA) followed by the post-hoc Dunnett’s test was used to analyse three or more group means of a single variable compared to the vehicle control. A one-sample T test was used to analyse data normalised to the vehicle control group. Significant values were taken as $p \leq 0.05$ and denoted as follows: * $p \leq 0.05$, ** $p \leq 0.01$, *** $p \leq 0.001$ and **** $p \leq 0.0001$.

4.3 Results

4.3.1 Global changes in T cell gene expression upon canagliflozin treatment

To better understand the impact of canagliflozin treatment on T cell phenotype and function, we examined changes to their global gene transcription. A two-pronged approach was employed, whereby function and metabolism was broadly assessed using gene expression panels associated with autoimmunity and metabolism, respectively. We initially focused on changes to T cell function following activation in the presence and absence of either canagliflozin or dapagliflozin. A total of 784 genes were investigated using the Nanostring nCounter® Autoimmune Profiling Panel, where the majority exceeded the background limit of detection. Canagliflozin induced greater changes in gene expression than dapagliflozin when both drugs were compared to the vehicle control (Figure 4.2).

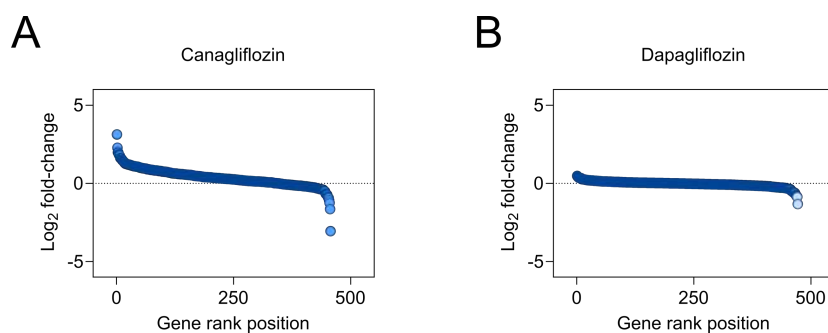


Figure 4.2 – Canagliflozin, but not dapagliflozin, alters global gene expression in T cells

(A-B) Changes in gene expression in anti-CD3 (2 µg/ml) and anti-CD28 (20 µg/ml) activated CD4+ T cells in the presence and absence of (A) canagliflozin or (B) dapagliflozin (both 10 µM), determined using Nanostring nCounter® Autoimmune Profiling Panel. Changes in gene expression measured as log₂ fold-change compared to the vehicle control and ranked in descending order. Data are representative of six (A) or four (B) independent experiments.

In fact, our differential expression analysis revealed that there were no significant changes in gene expression in cells treated with dapagliflozin (\log_2 fold-change ≤ -1 or ≥ 1 , Benjamini-Yekutieli adjusted $p \leq 0.05$; Figure 4.3). Meanwhile, 42 distinct genes were differentially expressed upon canagliflozin treatment, of which 3 were downregulated, whilst the other 39 were upregulated (Figure 4.3). Several other genes demonstrated a log₂ fold-change in expression of less than -1 or greater than 1 but failed to meet a level of significance

post-FDR correction. Naturally, there were also genes that expressed an adj. p -value ≤ 0.05 , but were accompanied by a \log_2 fold-change in expression between -1 and 1.

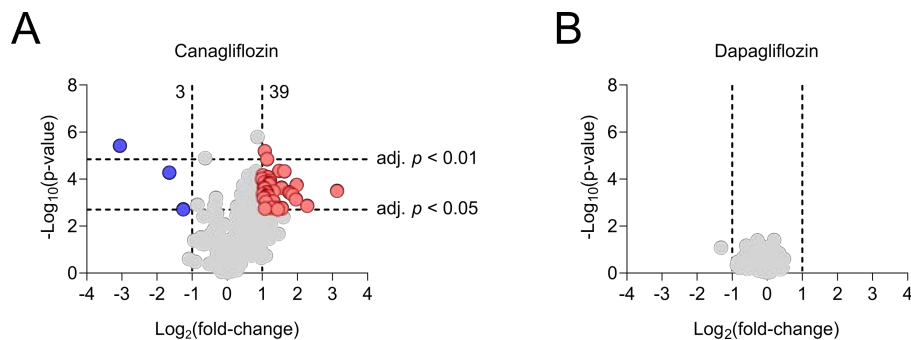


Figure 4.3 – Autoimmunity-associated genes are differentially expressed in T cells treated with canagliflozin

(A-B) Differential expression analysis of genes in anti-CD3 (2 $\mu\text{g/ml}$) and anti-CD28 (20 $\mu\text{g/ml}$) activated CD4⁺ T cells treated with (A) canagliflozin or (B) dapagliflozin (both 10 μM), determined using Nanostring nCounter[®] Autoimmune Profiling Panel. Blue and red data points represent downregulated and upregulated genes compared to the vehicle control group, respectively. Genes with a \log_2 fold-change ≤ -1 or ≥ 1 and a Benjamini-Yekutieli adjusted p -value ≤ 0.05 were considered differentially expressed. Data are representative of six (A) or four (B) independent experiments.

Consistent with our previous data showing reduced IL-2 production upon canagliflozin treatment (see Chapter 3.3), there was a significant reduction in *IL2* at the gene transcript level ($p = 0.0495$; Figure 4.4A). Interestingly, *CSF2* and *CCL20* were also downregulated by canagliflozin (*CSF2*: $p = 0.0059$; *CCL20*: $p = 0.0156$) and are typically associated with a Th17 signature (Ramesh et al., 2014) (Figure 4.4B-C).

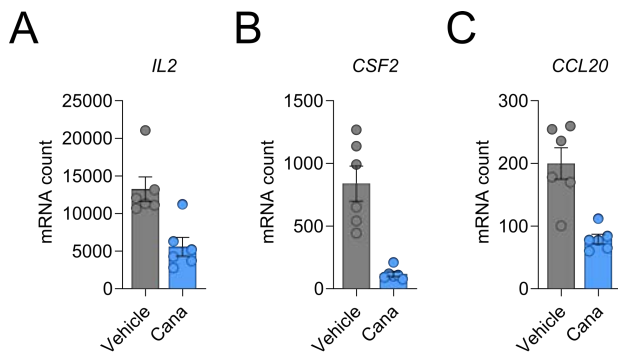


Figure 4.4 – Differentially downregulated genes in canagliflozin-treated T cells

(A-C) Normalised mRNA counts for (A) *IL-2*, (B) *CSF2* and (C) *CCL20* in anti-CD3 (2 µg/ml) and anti-CD28 (20 µg/ml) activated CD4⁺ T cells treated with canagliflozin (10 µM). Data are representative of six independent experiments. Statistical analysis was performed using a non-parametric T test and adjusted for the false discovery rate using the Benjamini-Yekutieli method. Data expressed as mean ± SEM.

Furthermore, upregulation of *SELL* (CD62L) by canagliflozin ($p = 0.0253$) was also consistent with our previous findings at the protein level (see Chapter 3.3.2; Figure 4.5A). Several interferon regulatory factors (IRFs) were also amongst the observed upregulated proteins, including IRF2 ($p = 0.0165$), IRF4 ($p = 0.0156$) and IRF9 ($p = 0.0066$; Figure 4.5B-D).

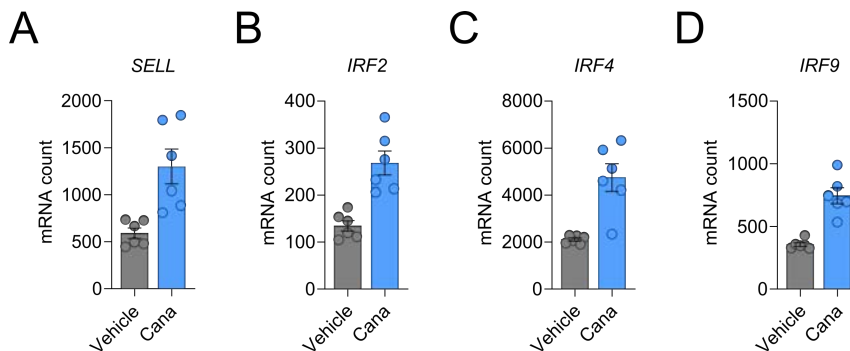


Figure 4.5 – Selected differentially upregulated genes in canagliflozin-treated T cells

(A-D) Normalised mRNA counts for (A) *SELL*, (B) *IRF2*, (C) *IRF4* and (D) *IRF9* in anti-CD3 (2 µg/ml) and anti-CD28 (20 µg/ml) activated CD4⁺ T cells treated with canagliflozin (10 µM). Data are representative of six independent experiments. Statistical analysis was performed using a non-parametric T test and adjusted for the false discovery rate using the Benjamini-Yekutieli method. Data expressed as mean ± SEM.

To try and understand these changes in a wider biological context, a pathway score was calculated for several autoimmune-related pathways based on changes in expression within pre-defined gene sets. The directionality of these scores determined whether a pathway is upregulated or downregulated by canagliflozin compared to the vehicle control group. Surprisingly, canagliflozin induced a predicted increase in activity in all pathways analysed – with the exception of *cytotoxicity* and *MHC class II antigen presentation* (Figure 4.6; Table 4.1).

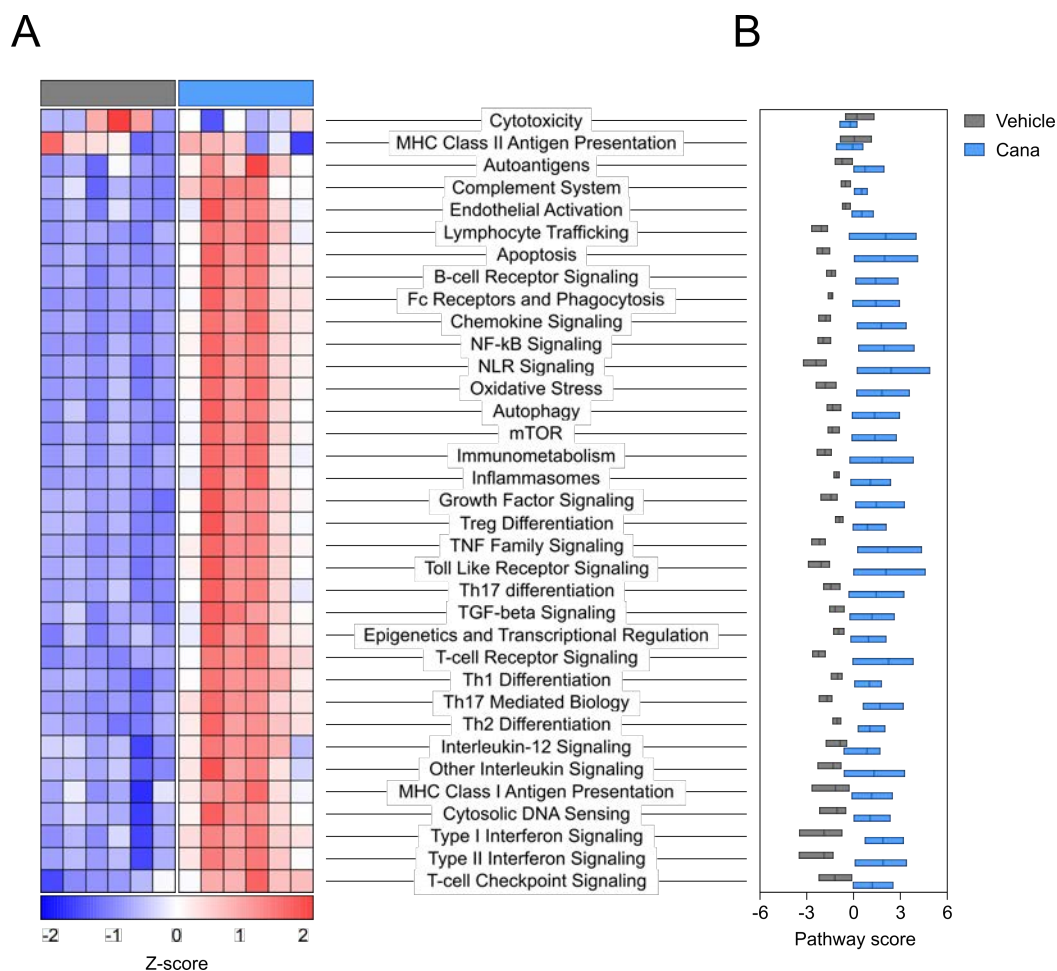


Figure 4.6 – Autoimmunity-associated pathways are upregulated at the gene transcript level in T cells treated with canagliflozin

(A) Heatmap of autoimmune pathway scores in anti-CD3 (2 $\mu\text{g/ml}$) and anti-CD28 (20 $\mu\text{g/ml}$) activated CD4⁺ T cells in the presence and absence of canagliflozin (10 μM). Pathway scores expressed as z-scores. Data are representative of six independent experiments. Data expressed as mean \pm minimum and maximum.

Table 4.1 – Differential regulation of autoimmunity-associated pathways by canagliflozin, based on changes in gene expression

Pathway	↑/↓	Adj. <i>p</i> -value	Rank	FDR sig
Th17 Mediated Biology	↑	< 0.0001	1	Y
Th2 Differentiation	↑	< 0.0001	2	Y
T-cell Receptor Signaling	↑	< 0.0001	3	Y
Th1 Differentiation	↑	0.0001	4	Y
Type I Interferon Signaling	↑	0.0001	5	Y
Chemokine Signaling	↑	0.0001	6	Y
TNF Family Signaling	↑	0.0001	7	Y
NF-κB Signaling	↑	0.0001	8	Y
B-cell Receptor Signaling	↑	0.0002	9	Y
Fc Receptors and Phagocytosis	↑	0.0002	10	Y
Type II Interferon Signaling	↑	0.0002	11	Y
NLR Signaling	↑	0.0002	12	Y
Oxidative Stress	↑	0.0003	13	Y
Apoptosis	↑	0.0003	14	Y
T-cell Checkpoint Signaling	↑	0.0003	15	Y
Lymphocyte Trafficking	↑	0.0003	16	Y
Toll Like Receptor Signaling	↑	0.0003	17	Y
Growth Factor Signaling	↑	0.0004	18	Y
Complement System	↑	0.0004	19	Y
mTOR	↑	0.0004	20	Y
Autophagy	↑	0.0006	21	Y
Epigenetics and Transcriptional Regulation	↑	0.0007	22	Y
TGF-beta Signaling	↑	0.0008	23	Y
Treg Differentiation	↑	0.0009	24	Y
Th17 differentiation	↑	0.0009	25	Y
Cytosolic DNA Sensing	↑	0.0010	26	Y
Immunometabolism	↑	0.0010	27	Y
Inflammasomes	↑	0.0011	28	Y
Autoantigens	↑	0.0017	29	Y
MHC Class I Antigen Presentation	↑	0.0019	30	Y
Endothelial Activation	↑	0.0019	31	Y
Other Interleukin Signaling	↑	0.0021	32	Y
Interleukin-12 Signaling	↑	0.0023	33	Y
Cytotoxicity	-	0.2499	34	N
MHC Class II Antigen Presentation	-	0.8101	35	N

Given canagliflozin targets metabolism through mitochondrial complex I and GDH inhibition, it was particularly surprising to see that the defined *immunometabolism* pathway was upregulated by canagliflozin (Figure 4.7).

A

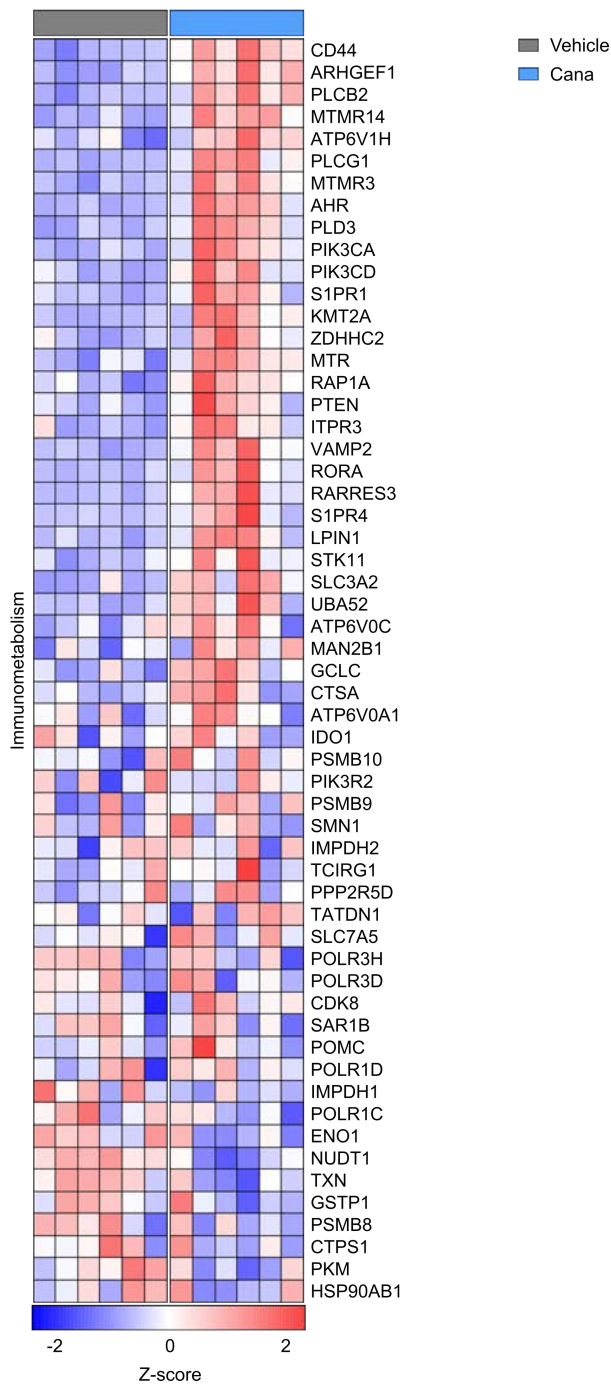


Figure 4.7 – Immunometabolism-associated genes are upregulated by canagliflozin

(A) Heatmap of immunometabolism-associated gene expression in anti-CD3 (2 µg/ml) and anti-CD28 (20 µg/ml) activated CD4+ T cells in the presence and absence of canagliflozin (10 µM). Gene expression expressed as z-scores. Data are representative of six independent experiments.

Consequently, we next assessed global changes in T cell metabolism using the Nanostring nCounter® Metabolic Pathways Panel. Given the limited change in gene expression previously observed when T cells were treated with dapagliflozin, our analysis of metabolism-associated genes focused on canagliflozin only. 748 metabolism-associated genes were profiled, of which the majority were above the limit of detection. Differential expression analysis identified 14 upregulated genes and 24 downregulated genes in activated T cells treated with canagliflozin (Figure 4.8).

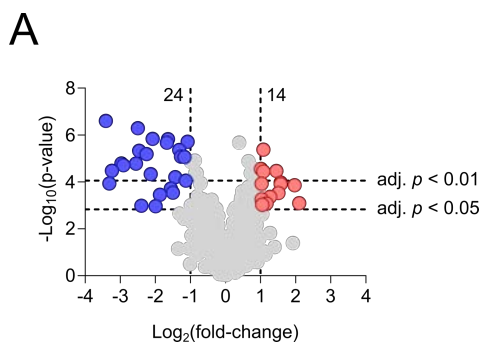


Figure 4.8 – Canagliflozin alters the expression of metabolism-associated genes in T cells

(A) Differential expression analysis of genes in anti-CD3 (2 µg/ml) and anti-CD28 (20 µg/ml) activated CD4⁺ T cells treated with canagliflozin (10 µM), determined using Nanostring nCounter® Metabolic Pathways Panel. Blue and red data points represent downregulated and upregulated genes compared to the vehicle control group, respectively. Genes with a log₂ fold-change ≤ -1 or ≥ 1 and a Benjamini-Yekutieli adjusted *p*-value ≤ 0.05 were considered differentially expressed. Data are representative of six independent experiments.

Notably, 17 of the 24 genes that were downregulated following canagliflozin treatment were associated with the cell cycle, including *MYBL2* (*p* = 0.0009), *CDCA5* (*p* = 0.0009) and *CCNA2* (*p* = 0.0031; Figure 4.9; Table 4.2). *SMAD3* was the only cell cycle-associated gene upregulated by canagliflozin (*p* = 0.0210; Figure 4.9; Table 4.2). These data are in agreement with the reduced proliferation we have previously observed (see Chapter 3.3.2).

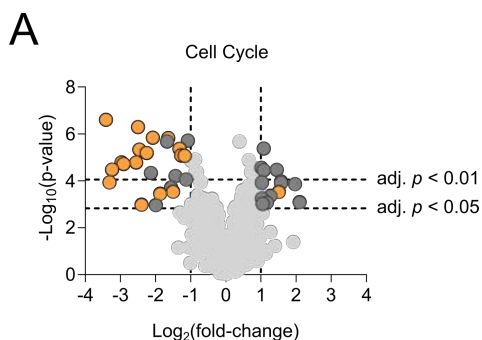


Figure 4.9 – Cell cycle genes are downregulated by canagliflozin

(A) Differential expression analysis of genes in anti-CD3 (2 $\mu\text{g}/\text{ml}$) and anti-CD28 (20 $\mu\text{g}/\text{ml}$) activated CD4+ T cells treated with canagliflozin (10 μM), determined using Nanostring nCounter[®] Metabolic Pathways Panel. Orange data points represent differentially expressed cell cycle genes, grey data points represent other differentially expressed genes compared to the vehicle control group. Genes with a log₂ fold-change ≤ -1 or ≥ 1 and a Benjamini-Yekutieli adjusted p -value ≤ 0.05 were considered differentially expressed. Data are representative of six independent experiments.

Table 4.2 – Differential expression of cell cycle-associated genes by canagliflozin

Gene	↑/↓	Log ₂ (fold-change)	Adj. p -value
MYBL2	↓	-3.41	0.0009
CDCA5	↓	-2.50	0.0009
RAD51	↓	-2.08	0.0010
BUB1B	↓	-1.64	0.0010
BRCA2	↓	-1.32	0.0016
CLSPN	↓	-2.46	0.0016
TYMS	↓	-2.25	0.0020
BUB1	↓	-1.27	0.0022
CDC20	↓	-1.17	0.0022
CCNA2	↓	-2.97	0.0031
TK1	↓	-2.55	0.0031
EXO1	↓	-2.91	0.0035
NCAPH	↓	-3.24	0.0050
TPX2	↓	-3.31	0.0106
BRCA1	↓	-1.50	0.0210
SMAD3	↑	1.51	0.0210
RRM2	↓	-1.87	0.0243
GTSE1	↓	-2.40	0.0414

Once again, the contribution of gene sets to specific metabolic pathways were evaluated using the calculated pathway scores. A total of 34 pathways were analysed, whereby 30 were differentially regulated by canagliflozin (Figure 4.10; Table 4.3). There were several interesting pathways amongst those upregulated by canagliflozin, including *mitochondrial respiration*, *mTOR*, *amino acid transporters* and *glutamine metabolism* (Figure 4.10; Table 4.3). As expected, *cell cycle* was one of the top downregulated pathways, alongside *DNA damage repair*, *glycolysis*, *Myc* and *nucleotide synthesis* (Figure 4.10; Table 4.3).

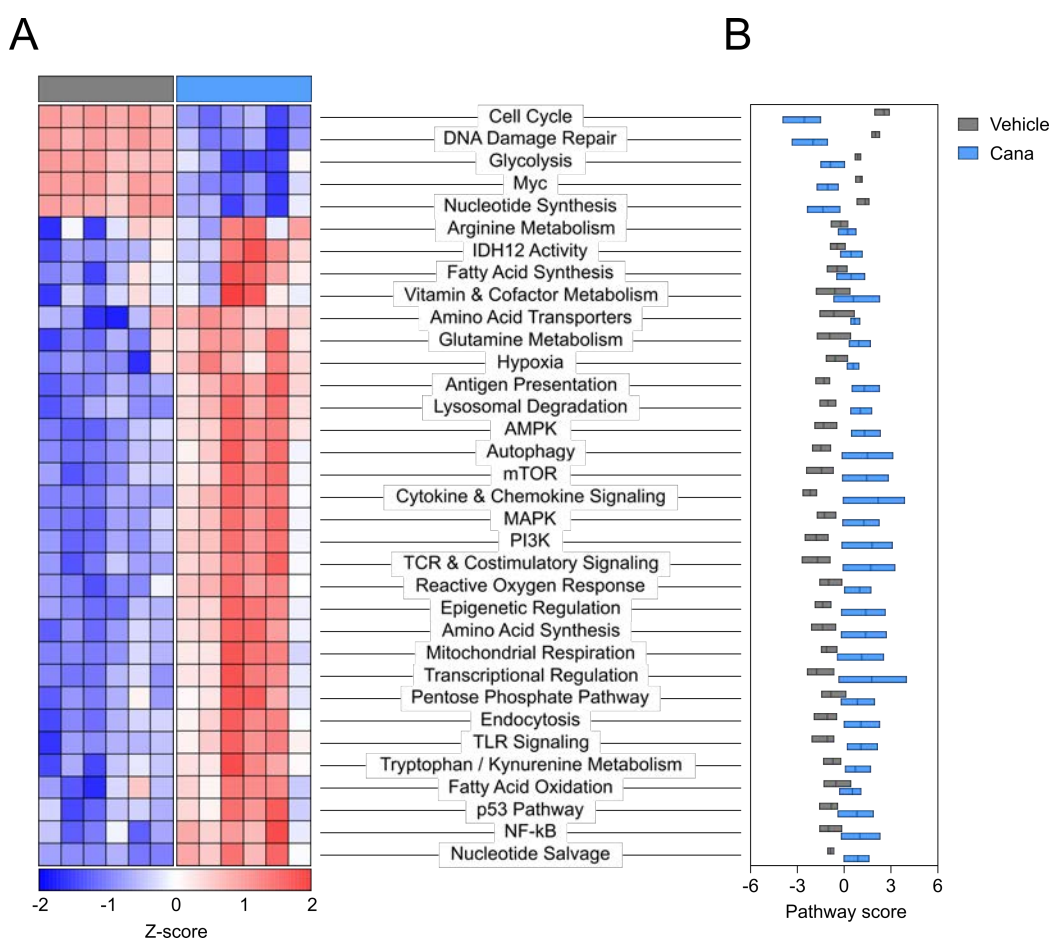


Figure 4.10 – Differential expression of metabolism-associated pathways in canagliflozin-treated T cells

(A) Heatmap of metabolic pathway scores in anti-CD3 (2 μ g/ml) and anti-CD28 (20 μ g/ml) activated CD4⁺ T cells in the presence and absence of canagliflozin (10 μ M). Pathway scores expressed as z-scores. Data are representative of six independent experiments. Data expressed as mean \pm minimum and maximum.

Table 4.3 – Differential regulation of metabolic pathways by canagliflozin, based on changes in gene expression

Pathway	↑/↓	Adj. p-value	Rank	FDR sig
Cell Cycle	↓	< 0.0001	1	Y
DNA Damage Repair	↓	< 0.0001	2	Y
Myc	↓	< 0.0001	3	Y
Antigen Presentation	↑	< 0.0001	4	Y
Nucleotide Synthesis	↓	< 0.0001	5	Y
Lysosomal Degradation	↑	< 0.0001	6	Y
Nucleotide Salvage	↑	< 0.0001	7	Y
Cytokine & Chemokine Signalling	↑	0.0001	8	Y
PI3K	↑	0.0001	9	Y
AMPK	↑	0.0001	10	Y
Reactive Oxygen Response	↑	0.0001	11	Y
TCR & Costimulatory Signalling	↑	0.0001	12	Y
MAPK	↑	0.0002	13	Y
Glycolysis	↓	0.0002	14	Y
Epigenetic Regulation	↑	0.0002	15	Y
TLR Signalling	↑	0.0004	16	Y
Amino Acid Synthesis	↑	0.0005	17	Y
Autophagy	↑	0.0005	18	Y
Hypoxia	↑	0.0006	19	Y
Glutamine Metabolism	↑	0.0006	20	Y
NF-kB	↑	0.0007	21	Y
mTOR	↑	0.0007	22	Y
Transcriptional Regulation	↑	0.0008	23	Y
Endocytosis	↑	0.0009	24	Y
Mitochondrial Respiration	↑	0.0015	25	Y
Tryptophan/Kynurenine Metabolism	↑	0.0016	26	Y
p53 Pathway	↑	0.0033	27	Y
Amino Acid Transporters	↑	0.0034	28	Y
Pentose Phosphate Pathway	↑	0.0037	29	Y
IDH12 Activity	↑	0.0106	30	Y
Fatty Acid Oxidation	-	0.0128	31	N
Fatty Acid Synthesis	-	0.0320	32	N
Vitamin & Cofactor Metabolism	-	0.0782	33	N
Arginine Metabolism	-	0.1420	34	N

Interestingly, despite most genes within the *Myc* pathway being downregulated, canagliflozin did not alter *MYC* expression at the gene transcript level ($p > 0.9999$; Figure 4.11).

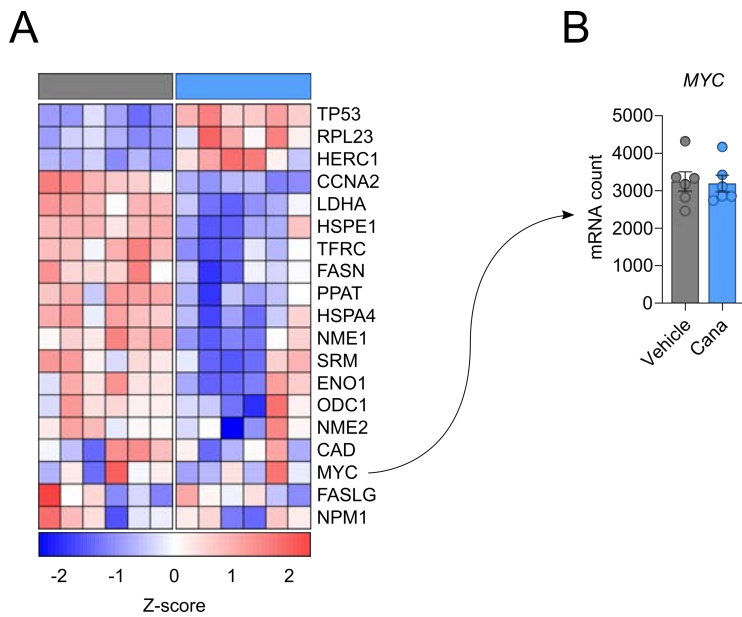


Figure 4.11 – Canagliflozin downregulates the MYC pathway, but does not alter MYC expression at the transcript level

(A) Heatmap of MYC-associated gene expression in anti-CD3 (2 $\mu\text{g}/\text{ml}$) and anti-CD28 (20 $\mu\text{g}/\text{ml}$) activated CD4⁺ T cells in the presence and absence of canagliflozin (10 μM). Gene expression expressed as z-scores. (B) Normalised mRNA counts for MYC. Data are representative of six independent experiments. Statistical analysis was performed using a non-parametric T test and adjusted for the false discovery rate using the Benjamini-Yekutieli method. Data expressed as mean \pm SEM.

4.3.2 Canagliflozin remodels the T cell proteome

To understand how the impact that canagliflozin has on the global gene expression translates to the protein level, we utilised label-free LC-MS to unveil changes to the activated T cell proteome. In line with our earlier data showing a reduction in cell size (see Chapter 3.3), activated T cells treated with canagliflozin contained significantly less protein compared to the vehicle control group ($p = 0.0009$; Figure 4.12).

A

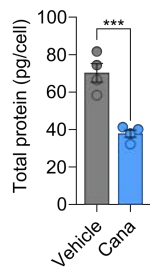


Figure 4.12 – Canagliflozin-treated T cells fail to increase cell protein mass upon activation

(A) Total protein content, measured as pg protein per cell in anti-CD3 (2 $\mu\text{g}/\text{ml}$) and anti-CD28 (20 $\mu\text{g}/\text{ml}$) activated CD4⁺ T cells in the presence and absence of canagliflozin (10 μM). Data are representative of four independent experiments. Statistical analysis was performed using a non-parametric T test. Data expressed as mean \pm SEM; *** $p \leq 0.001$.

A total of 5655 proteins were detected and we used the “proteomic ruler” method to estimate protein copy number based on the histone MS signal (Wisniewski et al., 2014). Differential expression analysis revealed that at the copy number level, 4421 proteins were downregulated in response to canagliflozin, whilst one protein was upregulated – the cell cycle inhibitor CDKN1B (Figure 4.13A). However, given the marked reduction in total protein content upon canagliflozin treatment, we took into consideration changes in protein concentration to instead assess changes in the composition of the T cell proteome. Here, the concentration of 481 proteins was reduced, whereas the concentration of 203 proteins was increased in response to canagliflozin treatment (Figure 4.13B). These data revealed that some downregulated proteins decrease in scale with the overall decrease in protein mass that occurs following canagliflozin treatment, resulting in no change to their concentration, whereas some proteins were decreased beyond scaling to cause a reduction in their concentration.

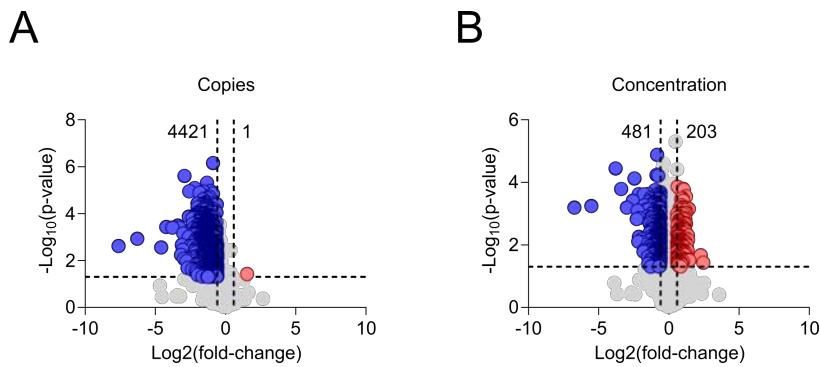


Figure 4.13 – Canagliflozin remodels the T cell proteome

(A-B) Differential expression analysis based on (A) protein copy number and (B) protein concentration in anti-CD3 (2 $\mu\text{g}/\text{ml}$) and anti-CD28 (20 $\mu\text{g}/\text{ml}$) activated CD4+ T cells treated with canagliflozin (10 μM), determined by label-free mass spectrometry. Blue and red data points represent downregulated and upregulated genes, respectively. Proteins with a \log_2 fold-change ≤ -0.585 or ≥ 0.585 and a Benjamini-Hochberg adjusted p -value ≤ 0.05 were considered differentially expressed. Data are representative of four independent experiments.

To gain a broad understanding of which proteins were enriched and depleted in our proteomics dataset, we compared the contribution of core subcellular compartments to the total protein mass. Here, there was an overall decrease in protein mass dedicated to core subcellular components in T cells treated with canagliflozin (Figure 4.14A). Individually, there was a reduction in the mass of proteins associated with glycolysis ($p = 0.0498$), mitochondria ($p = 0.0324$), nuclear envelope ($p = 0.0308$) and ribosomes ($p = 0.0033$; Figure 4.14B-E).

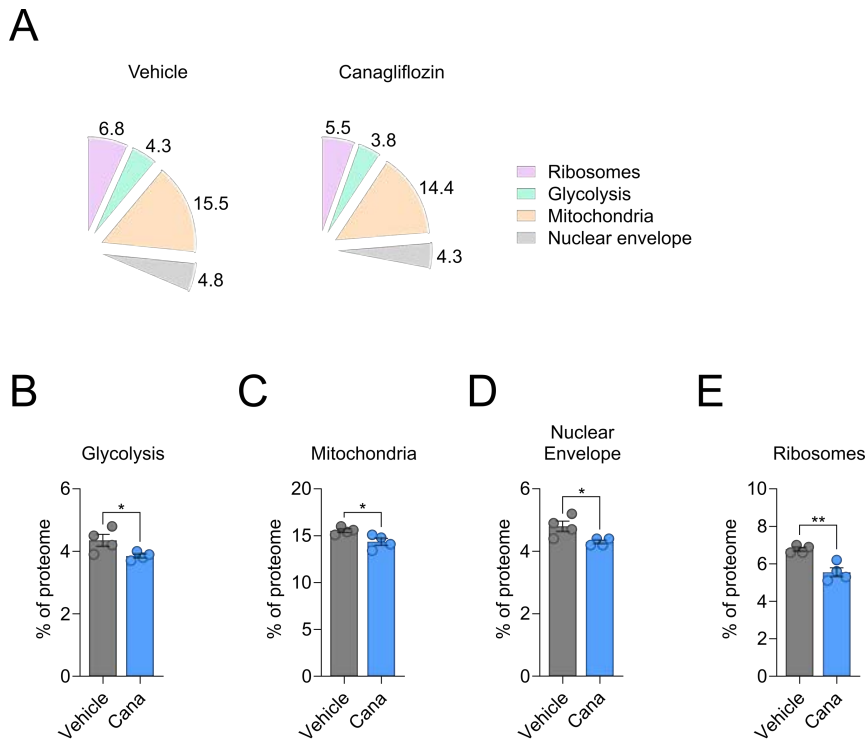


Figure 4.14 – Canagliflozin alters the distribution of subcellular compartments

(A) Contribution of protein mass towards core subcellular compartments in anti-CD3 (2 $\mu\text{g}/\text{ml}$) and anti-CD28 (20 $\mu\text{g}/\text{ml}$) activated CD4⁺ T cells treated with canagliflozin (10 μM), determined by label-free mass spectrometry. Contribution measured as percentage of total protein mass. (B-E) Percent protein mass dedicated to (B) glycolysis, (C) mitochondria, (D) nuclear envelope and (E) ribosomes as in (A). Data are representative of four independent experiments. Statistical analysis was performed using an unpaired T test. Data expressed as mean \pm SEM; * $p \leq 0.05$, ** $p \leq 0.01$.

An interesting example of scaling versus depletion is the metabolic regulator MYC. The number of MYC protein copies per T cell is reduced $\sim 63\%$ upon canagliflozin treatment ($p = 0.0037$; Figure 4.15). This reduction in MYC goes beyond the scaling effect, resulting in a $\sim 33\%$ decrease in MYC concentration ($p = 0.0104$; Figure 4.15). Together, these data show that canagliflozin triggers specific changes to the activated T cell proteome.

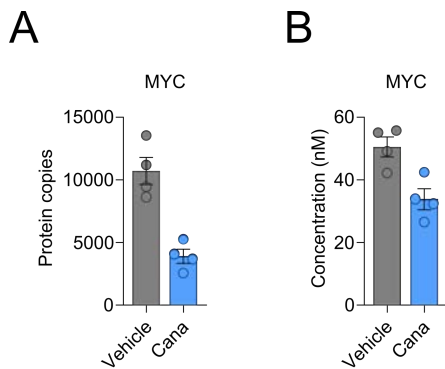


Figure 4.15 – MYC is downregulated by canagliflozin

(A-B) Expression of MYC based on (A) protein copy number and (B) protein concentration in anti-CD3 (2 $\mu\text{g}/\text{ml}$) and anti-CD28 (20 $\mu\text{g}/\text{ml}$) activated CD4⁺ T cells treated with canagliflozin (10 μM), determined by label-free mass spectrometry. Data are representative of four independent experiments. Statistical analysis was performed using a non-parametric T test. Data expressed as mean \pm SEM.

To better understand the biological relevance of canagliflozin-induced changes in protein expression, ingenuity pathway analysis (IPA) was employed to consider the contribution of individual proteins towards various canonical cellular pathways and determine which became enriched or depleted following canagliflozin treatment. Here, *cell cycle control of chromosomal replication* was revealed as the most significantly downregulated pathway ($p < 0.0001$; Figure 4.16A), supporting the observed effects on T cell proliferation (see Chapter 3.3.2).

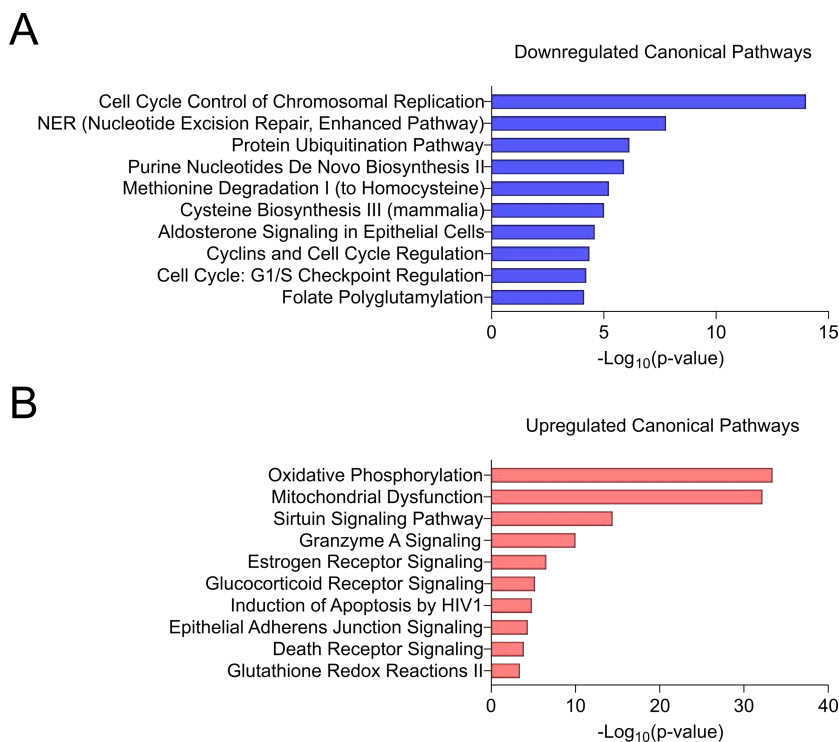
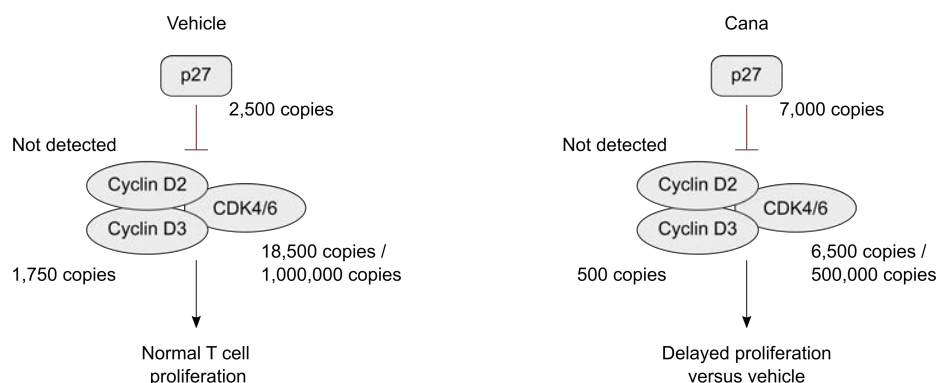


Figure 4.16 – Canonical pathways differentially regulated in T cells upon canagliflozin treatment

(A-B) Ingenuity pathway analysis of canonical pathways based on (A) downregulated and (B) upregulated proteins in anti-CD3 (2 $\mu\text{g}/\text{ml}$) and anti-CD28 (20 $\mu\text{g}/\text{ml}$) activated CD4⁺ T cells treated with canagliflozin (10 μM), determined by label-free mass spectrometry. Top 10 enriched pathways compared to the vehicle control are shown. Data are representative of four independent experiments.

Further downregulated pathways were associated with cell cycle maintenance, including *cyclins and cell cycle regulation* ($p < 0.0001$) and *cell cycle: G1/S checkpoint regulation* ($p < 0.0001$) within the top 10 (Figure 4.16A). Indeed, this is consistent with the pronounced downregulation of cell cycle regulation observed at the transcript level (see Chapter 4.3.1). Further interrogation of the proteomics dataset revealed that canagliflozin reduced the expression of cell cycle checkpoint proteins – including cyclin D3, and its associated kinases CDK4 and CDK6 – with a concomitant increase in an inhibitor of this process, p27 (CDKN1B; Figure 4.17). These findings suggest a mechanism by which cell cycle progression and proliferation are delayed in canagliflozin-treated T cells.

A



B

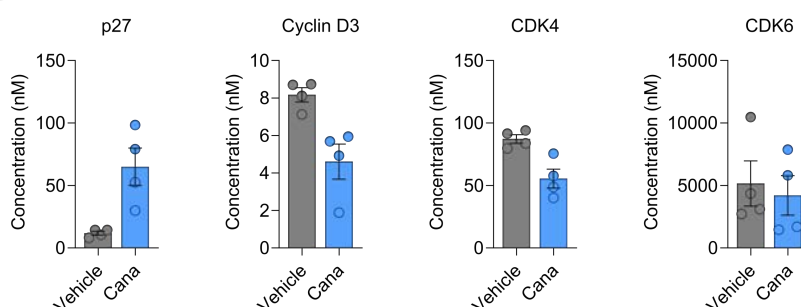


Figure 4.17 – Canagliflozin inhibits cell cycle protein expression and function

(A) Stoichiometric models for cell cycle entry and progression in anti-CD3 (2 $\mu\text{g}/\text{ml}$) and anti-CD28 (20 $\mu\text{g}/\text{ml}$) activated CD4+ T cells treated with canagliflozin (10 μM), determined by label-free mass spectrometry. Proteins copy numbers are presented for p27 (CDKN1B), cyclin D2 (CCND2), cyclin D3 (CCND3), cyclin-dependent kinase 4 (CDK4) and cyclin-dependent kinase 6 (CDK6). (B) Expression of cell cycle proteins as in (A). Data are representative of four independent experiments. Statistical analysis was performed using a non-parametric T test. Data expressed as mean \pm SEM.

Pathways associated with metabolism were also amongst the most downregulated, including *purine nucleotides de novo biosynthesis* ($p < 0.0001$), *methionine degradation to homocysteine* ($p < 0.0001$), *cysteine biosynthesis* ($p < 0.0001$) and *folate polyglutamylation* ($p < 0.0001$; Figure 4.16A).

Given the known effects of canagliflozin on mitochondrial proteins – particularly complex I and GDH – it was not surprising that *oxidative phosphorylation* ($p < 0.0001$) and *mitochondrial dysfunction* ($p < 0.0001$) emerged as the two predominant pathways upregulated in T cells following canagliflozin treatment (Figure 4.16B). Concomitant with *mitochondrial dysfunction*, other top upregulated pathways included *sirtuin signalling*

pathway ($p < 0.0001$) and *glutathione redox reactions* ($p < 0.0001$; Figure 4.16B). Upregulation of proteins-associated with *glutathione redox reactions* is particularly interesting given the relationship between mitochondrial complex I and reactive oxygen species (ROS).

Subsequent ingenuity upstream regulator analysis allowed us to identify potential transcription factors, microRNAs, kinases and small molecule inhibitors that are associated with the observed changes in the T cell proteome following canagliflozin treatment. The activation z-score calculated predicts the activation state of each predicted upstream regulator (i.e., activated or inhibited). Concurrent with our Nanostring data, reduced expression of 84 distinct targets predicted that MYC might be an upstream regulator which is repressed following canagliflozin treatment (Figure 4.18A). Beyond the top 20 most downregulated upstream regulators, it was also important to note that it was predicted that the activity of mTOR – closely associated with MYC signalling – was also downregulated by canagliflozin. Interestingly, the drug torin-1 and the protein RICTOR, classically central regulators of the mTOR axis, were also predicted to be suppressed based on the expression pattern of upregulated proteins in canagliflozin-treated T cells (Figure 4.18B).

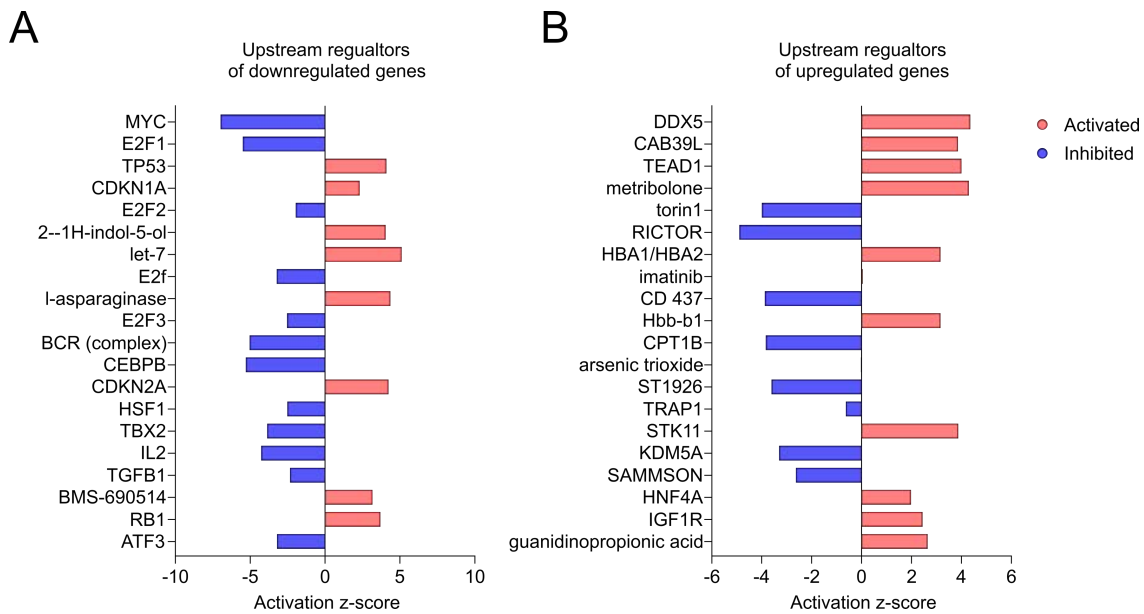


Figure 4.18 – Predicted upstream regulators of canagliflozin-induced changes in protein expression

(A-B) Predicted upstream regulators of protein expression based on (A) downregulated and (B) upregulated proteins in anti-CD3 (2 µg/ml) and anti-CD28 (20 µg/ml) activated CD4+ T cells treated with canagliflozin (10 µM), determined by label-free mass spectrometry. Top 20 predicted upstream regulators compared to the vehicle control are shown. The z-score predicts the likely activation states of upstream regulators; a positive z-score suggests activation whilst a negative z-score suggest inhibition. Data are representative four independent experiments.

4.3.3 Canagliflozin suppresses MYC signalling

Given the agreement between transcriptional and proteomic analysis on changes in MYC-associated pathways upon canagliflozin treatment, we decided to explore this further by focusing on how MYC influences the observed changes in T cell function. Firstly, we confirmed that MYC expression is downregulated by canagliflozin via immunoblotting of activated T cells (Figure 4.19). MYC expression is suppressed as early as 4 h following treatment with canagliflozin ($p = 0.0113$), and remained reduced at 24 h ($p = 0.0026$; Figure 4.19).

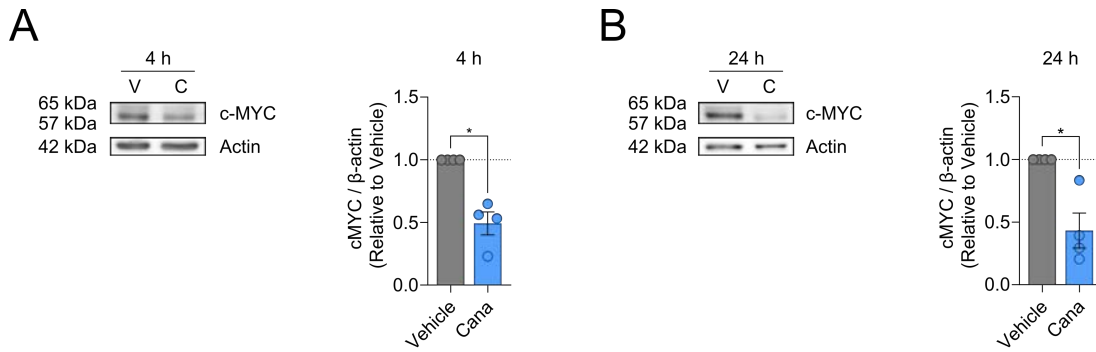


Figure 4.19 – MYC expression is reduced in canagliflozin-treated T cells

(A-B) Representative immunoblots of MYC in anti-CD3 (2 $\mu\text{g}/\text{ml}$) and anti-CD28 (20 $\mu\text{g}/\text{ml}$) activated CD4⁺ T cells treated with canagliflozin (10 μM) for (A) 4 h or (B) 24 h. Data are representative of four independent experiments. Statistical analysis was performed using a one-sample T test. Data expressed as mean \pm SEM; * $p \leq 0.05$.

Subsequently, we further interrogated the proteomics dataset and observed that several MYC-associated metabolic targets were significantly inhibited, including SLC2A1 (GLUT1; $p = 0.0082$), hexokinase 2 (HK2; $p = 0.0104$), dihydrofolate reductase (DHFR; $p = 0.0006$), ATP citrate lyase (ACLY; $p = 0.0027$) and fatty acid synthase (FASN; $p = 0.0014$; Figure 4.20).

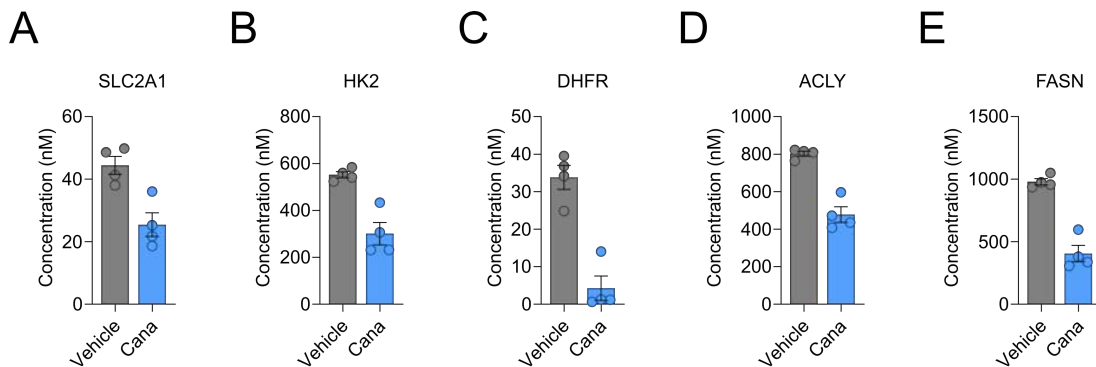


Figure 4.20 – MYC-associated metabolic proteins are downregulated by canagliflozin

(A-E) Expression of MYC targets (A) SLC2A1, (B) HK2, (C) DHFR, (D) ACLY and (E) FASN in anti-CD3 (2 $\mu\text{g}/\text{ml}$) and anti-CD28 (20 $\mu\text{g}/\text{ml}$) activated CD4⁺ T cells treated with canagliflozin (10 μM), determined by label-free mass spectrometry. Data are representative of four independent experiments. Statistical analysis was performed using a non-parametric T test. Data expressed as mean \pm SEM.

Previous data have demonstrated that the loss of MYC expression within activated T cells results in a failure to adequately increase cell mass (Marchingo et al., 2020), which is similar to what we observe with canagliflozin treatment, hence we sought to uncover whether this is caused by defective translation by analysing changes in the translation machinery within our proteomics dataset. A reduction in the ribosomal compartment was identified in the dataset (Figure 4.14E), owing to a reduction in most ribosomal proteins detected (Figure 4.21).

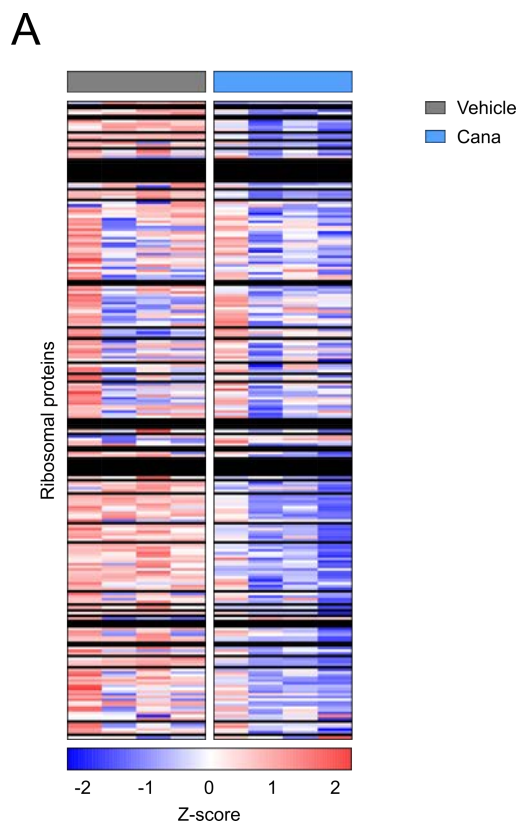


Figure 4.21 – Canagliflozin reduces ribosomal protein expression

(A) Expression of ribosomal proteins in anti-CD3 (2 $\mu\text{g}/\text{ml}$) and anti-CD28 (20 $\mu\text{g}/\text{ml}$) activated CD4+ T cells treated with canagliflozin (10 μM), determined by label-free mass spectrometry. Protein expression expressed as z-scores. Black indicates proteins not detected. Data are representative of four independent experiments.

Eukaryotic initiation factor 4F (eIF4F) complexes are required for the translation of 5'-capped mRNA and typically consist of the following proteins: eIF4A1, eIF4E, eIF4G1 and PABPC1 (Figure 4.22A). In our proteomics dataset, there was a significant reduction in all EIF4F complex members upon canagliflozin treatment (eIF4A1: $p = 0.0104$; eIF4E: $p = 0.0314$; eIF4G1: $p = 0.0043$; PABPC1: $p = 0.0008$; Figure 4.22B). Furthermore, there was also a reduction in the eukaryotic initiation factor 2 (EIF2) complexes responsible for controlling the transfer of tRNA to ribosomes and tRNA synthases (EIF2S1: $p = 0.0285$; EIF2S2: $p = 0.0072$; EIF2S3: $p = 0.0046$; Figure 4.22C). Together, these data show that less of the protein mass in activated T cells is dedicated to mRNA translation.

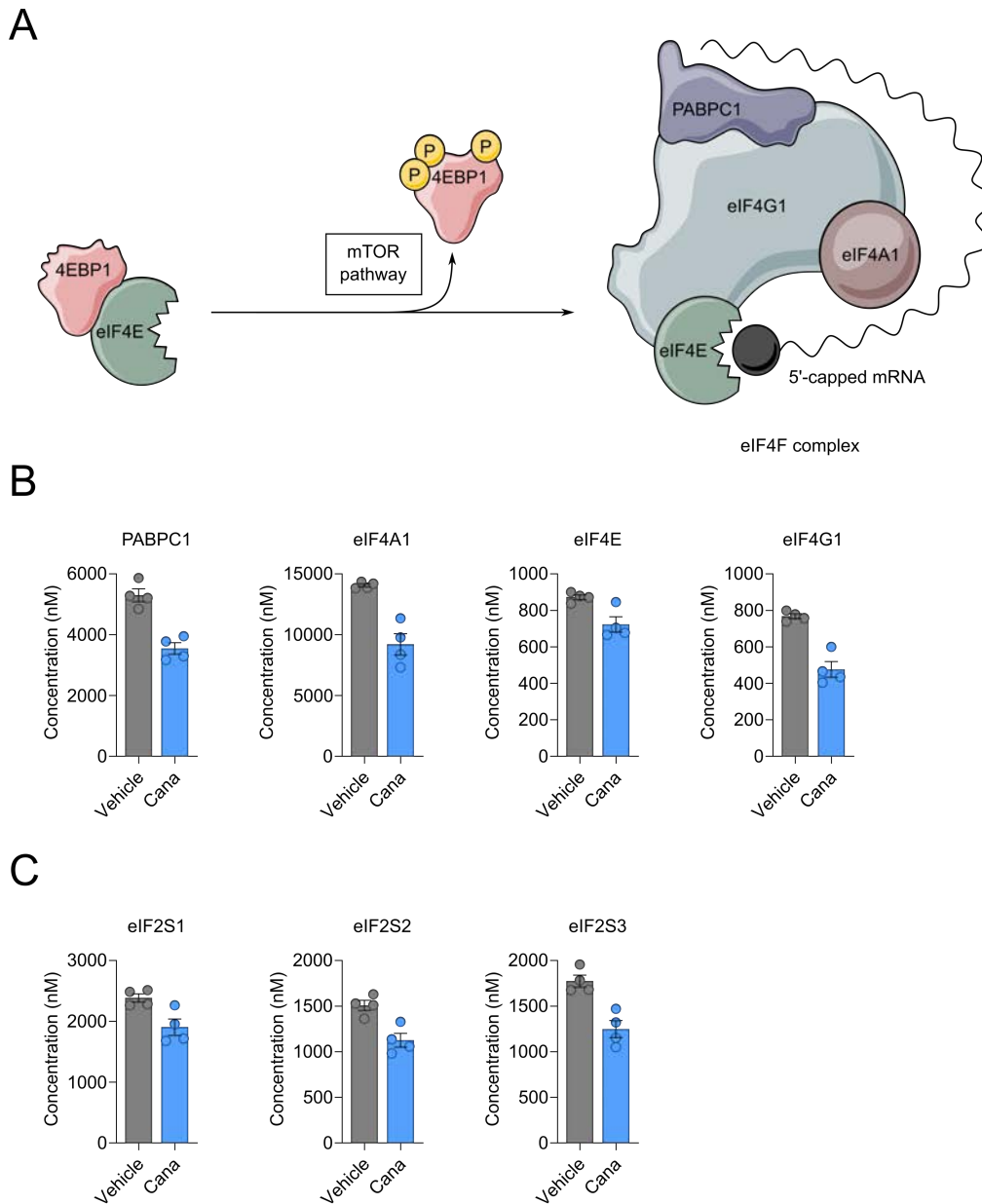


Figure 4.22 – Protein translation machinery is downregulated by canagliflozin

(A) Schematic overview of the machinery involved in mRNA translation. (B) Expression of eIF4F complex members eIF4A1, eIF4E, eIF4G1 and PABPC1 in anti-CD3 (2 $\mu\text{g/ml}$) and anti-CD28 (20 $\mu\text{g/ml}$) activated CD4⁺ T cells treated with canagliflozin (10 μM), determined by label-free mass spectrometry. (C) Expression of EIF2S proteins as in (B). Data are representative of four independent experiments. Statistical analysis was performed using a non-parametric T test. Data expressed as mean \pm SEM.

However, for a more complete understanding of translation dynamics within T cells, it is important to consider any changes to translational repressors following canagliflozin treatment. Although the eIF4F complex inhibitors, eIF4E-binding proteins 1 and 2 (4E-BP1 and 4E-BP2), could not be detected within our proteomics dataset, the translational repressor programmed cell death 4 (PDCD4) was abundant. Here, there was no observable difference in PDCD4 levels between canagliflozin-treated T cells and the vehicle control group ($p = 0.5645$; Figure 4.23A). As each PDCD4 protein simultaneously inhibits up to two eIF4A1 proteins, we measured the ratio between the two proteins to see if there were any differences when T cells were treated with canagliflozin (Figure 4.23B). Despite a reduction in eIF4A1:PDCD4 ratio by canagliflozin ($p = 0.0243$), PDCD4 was still outnumbered ~15-fold in the vehicle control group and ~10-fold in the canagliflozin-treated group, therefore PDCD4 was fully saturated under both treatment conditions (Table 4.4; Figure 4.23C). Collectively, these data suggest that mRNA translation is reduced by canagliflozin, through downregulation of the translation machinery rather than translation repression mechanisms.

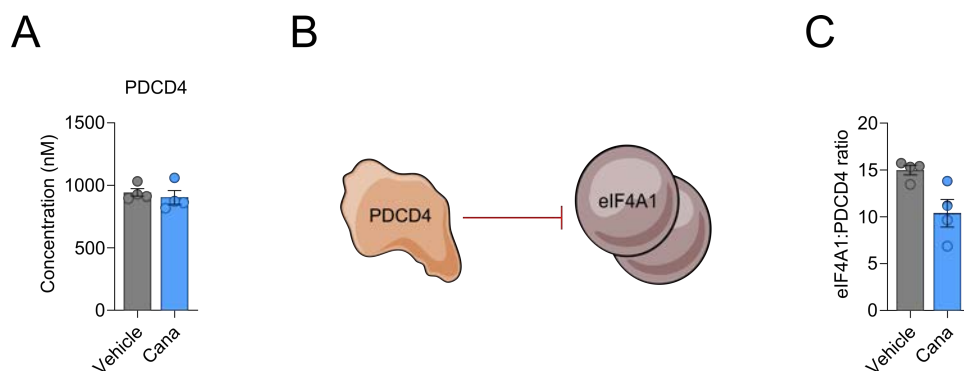


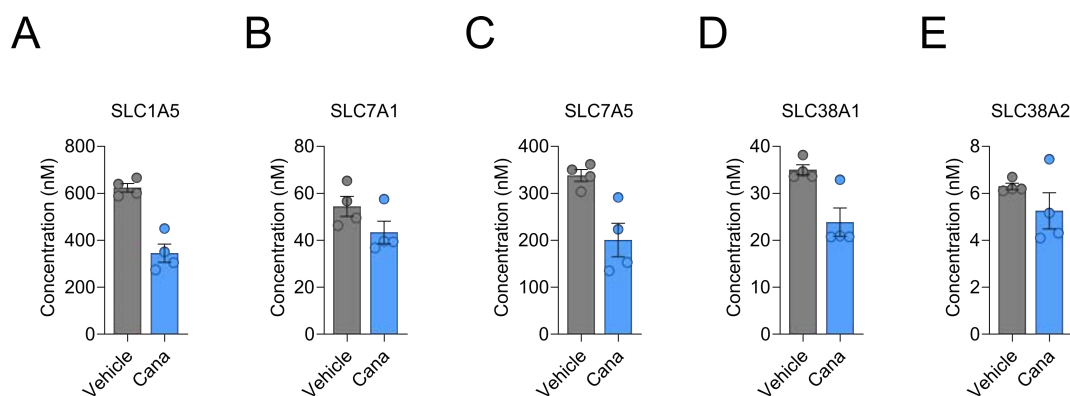
Figure 4.23 – Canagliflozin does not upregulate the levels of translational repressors

(A) Expression of translational repressor PDCD4 in anti-CD3 (2 $\mu\text{g/ml}$) and anti-CD28 (20 $\mu\text{g/ml}$) activated CD4⁺ T cells treated with canagliflozin (10 μM), determined by label-free mass spectrometry. (B) Schematic overview of PDCD4 inhibition of eIF4A1. (C) Ratio of eIF4A1:PDCD4 as in (A). Data are representative of four independent experiments. Statistical analysis was performed using a non-parametric T test. Data expressed as mean \pm SEM.

Table 4.4 – Changes in eIF4A1:PDCD4 ratio following canagliflozin treatment

	eIF4A1 copies	PDCD4 copies	eIF4A1:PDCD4
Vehicle	2979558 ± 211430	200772 ± 20391	~15:1
Canagliflozin	1064426 ± 148902	102298 ± 1442	~10:1

Another fundamental requirement for increased cell mass is amino acid availability, thus T cells increase their expression of several amino acid transporters upon activation (Hosios et al., 2016; Marchingo et al., 2020). To this end, we further interrogated our proteomics dataset to establish whether any changes in solute carrier expression occur in canagliflozin-treated T cells. There was a striking reduction in several MYC-associated amino acid transporters, including SLC1A5 ($p = 0.0023$), SLC7A5 ($p = 0.0249$) and SLC38A1 ($p = 0.0281$; Figure 4.24). Moreover, SLC7A1 and SLC38A2 were also reduced by canagliflozin, but these changes were not as pronounced (SLC7A1: $p = 0.1336$; SLC38A2: $p = 0.2684$; Figure 4.24).

**Figure 4.24 – Canagliflozin impairs the upregulation of amino acid transporters upon T cell activation**

(A-E) Expression of amino acid transporters (A) SLC1A5, (B) SLC7A1, (C) SLC7A5, (D) SLC38A1, (E) SLC38A2 in anti-CD3 (2 $\mu\text{g/ml}$) and anti-CD28 (20 $\mu\text{g/ml}$) activated CD4⁺ T cells treated with canagliflozin (10 μM), determined by label-free mass spectrometry. Data are representative of four independent experiments. Statistical analysis was performed using a non-parametric T test. Data expressed as mean \pm SEM.

Together, these data suggest that canagliflozin-treated T cells fail to accurately remodel the proteome upon activation, primarily through defects in protein translation. It is likely that this is driven by a marked reduction in MYC, which has been previously highlighted to have a fundamental role in upregulation of the translation machinery and facilitating sufficient amino acid uptake.

4.4 Discussion

Having established that canagliflozin inhibits T cell effector function, an exhaustive analysis of global changes to T cell function was undertaken at both the gene transcript and protein level. Nanostring nCounter[®] analysis is a relatively new technique allowing multiplex analysis of up to 800 RNA targets. Here, we used the nCounter[®] Autoimmune Profiling Panel and Metabolic Pathways Panel to gain insight into the global functions that canagliflozin affects in T cells, alongside the underlying changes in metabolism that mediate these functional changes. Initially, most of the 784 target genes identified using the Autoimmune Profiling Panel were above the background limit of detection. Differential expression analysis revealed that canagliflozin significantly altered the expression of 42 autoimmunity-associated genes – 3 downregulated, 39 upregulated. Targets with a log₂ fold-change ≤ -1 or ≥ 1 and Benjamini-Yekutieli adjusted $p \leq 0.05$ were considered differentially expressed. Therefore, differentially expressed gene transcripts were either twice as abundant, or half as abundant, compared to the vehicle control group. Given the volume of gene transcripts analysed, it was important to account for the false discovery rate of such large-scale analyses, using the more stringent Benjamini-Yekutieli adjustment as recommended by Nanostring. In agreement with our previous work (see Chapter 3.3) – where IL-2 production was significantly reduced – canagliflozin reduced the number of *IL2* transcripts compared to the vehicle control. Interestingly, both other downregulated genes, *CSF2* and *CCL20*, have previously been associated with a Th17 signature (Ramesh et al., 2014). Since Th17 cells play a critical role in autoimmune disease pathogenesis (see Chapter 1.4), it is favourable that canagliflozin alters Th17-associated functions. Furthermore, canagliflozin also upregulated several interferon regulatory proteins (IRFs) – *IRF2*, *IRF4* and *IRF9* – which are involved in regulating T cell differentiation into various Th subsets. Therefore, further work should investigate the impact of canagliflozin on the distribution of Th subsets within CD4⁺ T cells. In regards to the other

autoimmunity-associated genes upregulated by canagliflozin, there were no standouts in terms of their biological relevance. However, upregulation of *SELL* was consistent with the retention of the encoded protein CD62L on the surface of canagliflozin-treated T cells demonstrated previously (see Chapter 3.3.2). In order to analyse the observed changes in gene transcript levels in a wider biological context, their contribution towards defined cellular pathways was calculated as a score – the directionality of the pathway score predicting whether that particular pathway was up- or downregulated. All autoimmunity-associated pathways were predicted to be upregulated by canagliflozin, even *immunometabolism*, which is surprising given the off-target effect that canagliflozin has on mitochondrial complex I and GDH. Crucially, dapagliflozin had no effect on global T cell function, whereby no genes were differentially expressed compared to the vehicle control group. Thus, canagliflozin alters global T cell function independent of SGLT2 inhibition.

Metabolic changes were investigated further using the Nanostring nCounter® Metabolic Pathways Panel. Dapagliflozin was dropped from these analyses given that it did not induce any changes in gene transcript levels previously. Here, a total of 748 genes were identified, with most above the background limit of detection. Differential expression analysis revealed that canagliflozin significantly altered the expression of 38 metabolism-associated genes in T cells – 14 upregulated and 24 downregulated. Genes were considered differentially expressed using the same criteria as previously. Interestingly, ~70% of the genes downregulated by canagliflozin were associated with *cell cycle*. This is again in agreement with our previous work, whereby T cell proliferation was impaired in the presence of canagliflozin (see Chapter 3.3.2). Furthermore, this collection of *cell cycle* genes included *CCNA2* encoding cyclin A2, where previous work in human-umbilical-vein endothelial cells demonstrated that the observed anti-proliferative effect of canagliflozin was mediated by strong inhibition of cyclin A (Behnammanesh et al., 2019). Although the mechanism by which canagliflozin suppresses cyclin A is not clear, previous studies have demonstrated that glutamine metabolism and anaplerosis within the TCA cycle is critical for cyclin A expression and subsequent endothelial cell proliferation (Huang et al., 2017; Kim et al., 2017), which intertwines with the known canagliflozin-mediated inhibition of GDH. The above changes in gene expression were also used to calculate pathway scores for several metabolism-associated pathways. Most of the pathways analysed were differentially regulated by canagliflozin, where 5 were downregulated and the rest upregulated. As expected, *cell cycle*

was the most significantly downregulated pathway, alongside related pathways *DNA damage repair* and *nucleotide synthesis*. Interestingly, *MYC* and *glycolysis* were also downregulated and warranted further investigation. Amongst the upregulated pathways were *mitochondrial respiration*, *mTOR*, *amino acid transporters* and *glutamine metabolism*, which was surprising given some of the known pathways that canagliflozin inhibits. These findings proposed the idea that perhaps the observed changes in gene transcripts might instead demonstrate a compensatory mechanism for the canagliflozin-induced loss of these functions. Moreover, it was also important to consider whether the observed changes in gene transcripts translated into similar changes at the protein level.

To address this issue, we employed label-free LC-MS to unveil changes to the activated T cell proteome following canagliflozin treatment. The “proteomic ruler” method was performed as previously described (Wisniewski et al., 2014), to estimate protein copy number based on the histone MS signal. T cells treated with canagliflozin contained markedly less protein, and as a result differential expression analysis revealed that 4421 proteins were downregulated in terms of their protein copy number, with only single protein (CDKN1B) upregulated. For our proteomics analysis, targets were considered differentially expressed with \log_2 fold-change ≤ -0.585 or ≥ 0.585 and Benjamini-Hochberg adjusted $p \leq 0.05$. These cut-offs were recommended by the FingerPrints Proteomics Facility at the University of Dundee, who routinely perform analysis of large proteomic datasets. Given the profound reduction in protein content upon canagliflozin treatment, it was unsurprising to see a reduction in copy number for the vast majority of proteins, thus this differential expression data was of little value. Instead, to account for the change total protein content, differential expression analysis was performed based on the concentration of our target proteins. This allowed us to elucidate which proteins comprise a greater proportion of the proteome compared to the vehicle control (i.e., are upregulated); and which proteins comprise a smaller proportion of the proteome compared to the vehicle control (i.e., are downregulated). Here, differential expression analysis revealed that canagliflozin reduced the concentration of 481 proteins, whilst increasing the concentration of 203 proteins. This demonstrates that the copy number of most proteins originally described is decreased proportional to the decrease in total T cell protein. The changes in protein expression detected culminated in fewer proteins dedicated to core subcellular compartments such as glycolysis, mitochondria, nuclear envelope and ribosomes. Given our interest in *MYC* from our Nanostring data

(see Chapter 4.3.1), this demonstrates an interesting example of scaling versus depletion. Canagliflozin reduced MYC copy number ~2.7-fold compared to the vehicle control, which goes beyond the scaling of the overall reduction in T cell protein content, resulting in ~1.5-fold reduction in the concentration of MYC. The observed difference between expression measured at the transcript level versus the protein level is a salient point. For example, despite an observed decrease in the *Myc* pathway in our dataset, there was no change in *MYC* at the transcript level in our Nanostring data. Decreased MYC signalling was also predicted by our proteomics dataset – consistent with data at the transcript level – however, our proteomics dataset also revealed a striking reduction in MYC expression at the protein level. Moreover, reduced MYC expression was also observed by immunoblotting. Therefore, this emphasises the need to confirm whether changes observed at the gene transcript level translate into similar changes at the protein level.

To gain better understanding of how changes to the T cell proteome relate to biological changes in metabolism and function, IPA analysis was used to realise the contribution of individual proteins towards various canonical pathways. Here, *cell cycle control of chromosomal replication* emerged as the most downregulated pathway in response to canagliflozin treatment, which supports both our gene expression data and earlier observed effect on T cell proliferation. This was further supported by the appearance of other cell-cycle associated pathways, including *cyclins and cell cycle regulation* and *cell cycle: G1/S checkpoint regulation*, amongst the top 10 most downregulated pathways. Several metabolism-associated pathways were also markedly downregulated, including *purine nucleotides de novo biosynthesis*, *methionine degradation to homocysteine*, *cysteine biosynthesis* and *folate polyglutamylation*. In contrast, *mitochondrial dysfunction* and *oxidative phosphorylation* were the two pathways predominantly upregulated by canagliflozin. The upregulation of *mitochondrial dysfunction* was unsurprising given the profound effect canagliflozin has on mitochondrial complex I and GDH. The increase in *oxidative phosphorylation* was supported by our earlier Nanostring analysis, whereby *mitochondrial respiration* was increased, however, this finding is more surprising given that complex I inhibition would have an adverse effect on this pathway. Thus, further work should be undertaken to determine the impact of canagliflozin on T cell metabolism, to better understand the actual change in functional output. Finally, concomitant with *mitochondrial dysfunction*, canagliflozin also upregulated *sirtuin signalling pathway* and *glutathione redox*

reactions – the latter particularly interesting given the relationship between mitochondrial complex I inhibition and ROS production (Li et al., 2003). Further IPA analysis allowed us to predict which transcription factors, microRNAs, kinases and small molecule inhibitors might induce the observed changes at the protein level in T cells treated with canagliflozin. The activation z-score calculated predicts the activation state of each predicted upstream regulator (i.e., activated or inhibited), and in agreement with our Nanostring data which predicted downregulation of the MYC pathway, downregulation of 84 distinct MYC target proteins predicted that upstream MYC activity is inhibited. Additionally, canagliflozin also downregulated several mTOR target proteins, which predicted that its activity is also inhibited. Together, MYC and mTOR regulate many metabolic pathways, therefore, this provides further evidence that changes in T cell metabolism following canagliflozin treatment warrant further investigation.

To conclude the work in this chapter, we decided to concentrate on changes in MYC, given the agreement between both our transcriptional and proteomics data on changes in MYC-associated pathways. We first confirmed by immunoblotting that MYC was in fact downregulated in T cells by canagliflozin. Further interrogation of our proteomics dataset revealed that several metabolism-associated MYC targets were downregulated, including SLC2A1 (GLUT1), hexokinase 2 (HK2), dihydrofolate reductase (DHFR), ATP citrate lyase (ACLY) and fatty acid synthase (FASN). Previous proteomic analysis has demonstrated that MYC is required for the increase in T cell mass upon activation (Marchingo et al., 2020). This is similar to our observed reduction in T cell mass following canagliflozin treatment, suggesting that MYC might be a key mediator of this change. Indeed, MYC is critical for elevated protein translation upon T cell activation (Marchingo et al., 2020), therefore, we investigated whether canagliflozin impaired expression of the translation machinery. The expression of most ribosomes, eIF4F complex proteins and EIF2S proteins were all downregulated by canagliflozin, which would severely limit the translation of proteins and explains the observed reduction in T cell protein mass. Given the importance of amino acid availability for protein translation, T cells upregulate several amino acid transporters upon activation via a MYC-driven process (Hosios et al., 2016; Marchingo et al., 2020). Several amino acids transporters were downregulated on canagliflozin-treated T cells, providing further evidence that the protein translation machinery is defective, leading to a profound reduction in cellular protein levels. Amino acid uptake via SLC7A5 has previously been demonstrated to be critical for the

sustained expression of both MYC and mTOR (Sinclair et al., 2013). Additionally, in NK cells it has been demonstrated that the expression of the amino acid transporter SLC7A5, as well as glutamine uptake through this transporter, is critical for the expression of MYC (Loftus et al., 2018). Since SLC7A5 expression was reduced by canagliflozin, this could cause a feedback loop, contributing to reduced MYC levels within these T cells. Evaluation of glutamine uptake by canagliflozin-treated cells would further provide valuable insight into this hypothesis.

4.5 Conclusions

After demonstrating that canagliflozin inhibits T cell function and activation, information-rich techniques were utilised to assess the global changes that occur in these cells. Nanostring nCounter® analysis showed that canagliflozin, but not dapagliflozin, induced global changes in autoimmunity-associated genes. Differentially expressed genes included *IL2*, which was downregulated in agreement with our previous findings, whilst upregulation of *SELL* was consistent with the retention of CD62L previously observed. Together, canagliflozin-induced changes in gene transcript levels resulted in predicted upregulation of several autoimmunity-associated pathways in T cells.

Changes in gene transcription were also assessed in the setting of metabolism. Several genes were differentially expressed in canagliflozin-treated T cells compared to the vehicle control group, with marked downregulation of many associated with the cell cycle. Indeed, *cell cycle* was the most downregulated pathway upon canagliflozin treatment, alongside additional downregulation of *MYC* and *glycolysis*. However, most other metabolism-associated pathways were upregulated by canagliflozin, similar to our previous observations within the Nanostring dataset.

It was important to confirm the above findings at the protein level. To this end, proteomic analysis by label-free LC-MS was used to analyse canagliflozin-induced changes in the T cell proteome. Canagliflozin strikingly reduced total cellular protein content, resulting in downregulation of most proteins based on their copy number. However, we took this reduction in protein content per cell into consideration by assessing changes in individual proteins based on their concentration. Differential expression analysis revealed that 481 proteins were downregulated in response to canagliflozin treatment, whilst 203 genes were upregulated. To put these changes into a wider biological context, IPA analysis was employed

to determine which canonical pathways were altered upon canagliflozin. Several pathways associated with cell cycle and metabolism comprised the top 10 downregulated pathways, whereas *mitochondrial dysfunction* and *oxidative phosphorylation* were the two predominantly upregulated pathways. Furthermore, the observed protein expression patterns observed following canagliflozin treatment predicted that both upstream MYC and mTOR activity was inhibited.

Further interrogation of the proteomics dataset, with a focus on MYC in particular, demonstrated several metabolism-associated MYC targets were downregulated by canagliflozin. Moreover, canagliflozin also downregulated several components of the protein translation machinery, as well as numerous amino acid transporters – with downregulation of both MYC-associated processes likely contributing to reduced cellular protein content. Further work was undertaken to determine the extent of mitochondrial dysfunction in canagliflozin-treated T cells, and whether this affects energy-producing metabolic pathways.

Chapter Five

Canagliflozin suppresses T cell receptor signalling to impair metabolic reprogramming

5 Canagliflozin suppresses T cell receptor signalling to impair metabolic reprogramming

5.1 Introduction

Metabolic reprogramming is essential upon T cell activation. Fatty acid oxidation and pyruvate oxidation via the TCA cycle is replaced by increased flux through aerobic glycolysis, glutaminolysis and the pentose phosphate pathway (Wang et al., 2011). This metabolic switch is regulated by the transcription factor MYC, which drives the metabolic gene changes that are necessary for activation-induced T cell growth and proliferation (Wang et al., 2011). Specifically, MYC is rapidly induced following T cell activation and is responsible for the observed increases in glycolysis and glutaminolysis by upregulating the expression of several enzymes involved in each respective pathway (Wang et al., 2011). MYC protein has a very short half-life, hence the increased uptake of amino acids is required to maintain its expression in activated T cells (Sinclair et al., 2013). Deletion of the amino acid transporter SLC7A5 resulted in an inability to sustain MYC expression, preventing the expression of the metabolic enzymes and transporters required to support elevated glutamine and glucose metabolism (Sinclair et al., 2013). Recently, proteomic analysis has revealed how MYC-dependent changes remodel the T cell proteome following activation (Marchingo et al., 2020). As previously described, T cell mass is markedly reduced when activated in the absence of MYC signalling, which is primarily driven by the selective downregulation of several of the most highly abundant proteins (Marchingo et al., 2020). There remains a subset of around 400 proteins that are strongly induced upon T cell activation independent of MYC expression, including the classical activation markers CD44 and CD69 (Marchingo et al., 2020). Surprisingly, upon activation MYC-deficient T cells increased the expression of glucose transporters (GLUT1 and GLUT3) and several glycolytic enzymes, although to a slightly lesser extent than control T cells (Marchingo et al., 2020). However, MYC expression has a marked impact on lactate transporter expression (SLC16A1) (Marchingo et al., 2020), which would impair the export of intracellular lactate and thereby limit glycolytic flux through this feedback mechanism when MYC is absent. Concurrent with previous findings, elevated glutamine metabolism is supported by MYC-dependent upregulation of several, but not all, enzymes involved in glutaminolysis and pyrimidine and purine biosynthesis pathways (Marchingo et

al., 2020). Moreover, MYC induces the expression of several amino acid transporters to meet the demands of heightened translation for proteome remodelling following activation, whilst additionally maintaining its own continued expression to sustain further changes in protein expression (Marchingo et al., 2020). These findings highlight the importance of MYC-dependent metabolic reprogramming in supporting successful T cell activation.

Earlier studies demonstrated the importance of other signalling proteins in the metabolic reprogramming that occurs during T cell activation. Initially, AKT-dependent upregulation of glucose uptake and glycolysis was established in activated T cells (Frauwirth et al., 2002). Co-stimulation via CD28 was essential for activation-induced metabolic changes, as engagement of the same receptor by the inhibitory protein CTLA-4 impaired AKT expression and limited glucose metabolism following activation (Frauwirth et al., 2002). Subsequent studies directly linked T cell receptor (TCR) signalling to downstream changes in metabolic programming. Enhanced glutamine metabolism upon activation is regulated by the activity of ERK – a member of the MAPK signal transduction family downstream of TCR ligation (Carr et al., 2010). ERK signalling is required for optimal glutamine uptake, in addition to promoting the activity of enzymes involved in anaplerotic glutamine metabolism including glutaminase, glutamate dehydrogenase (GDH), glutamic-oxaloacetic transaminase (GOT) and glutamic-pyruvic transaminase (GPT) (Carr et al., 2010). In addition to AKT and ERK signalling, a similar role has been described for mTOR in the metabolic reprogramming of activated T cells. Here, mTOR activity was required to support elevated glucose uptake and glycolysis upon activation, mediating these changes through the upregulation of HIF1 α expression (Finlay et al., 2012). Critically, the mTOR/HIF1 α pathway functioned independent of PI3K and AKT to upregulate glycolytic enzyme expression and ultimately linked metabolic changes to effector function (Finlay et al., 2012). Interestingly, inhibition of either AKT, ERK or mTOR is sufficient to significantly limit the induction of MYC and HIF1 α during T cell activation, subsequently perturbing downstream glycolytic activity (Wang et al., 2011). These findings might suggest that AKT-, ERK- and mTOR-mediated signalling controls metabolic reprogramming in activated T cells, at least to some extent, through their regulation of MYC and HIF1 α expression. Furthermore, proteomic analysis has revealed that MYC is the predominant regulator of the metabolic proteome following T cell activation (Damasio et al., 2021). Although there were overlaps identified in the proteins regulated by ERK, mTOR and MYC signalling, there were also a large number of unique targets for each pathway, wherein

to this end MYC controlled the expression of over half the activated T cell proteome, versus 30% and 10% of the proteome for mTOR and ERK, respectively (Damasio et al., 2021). Collectively, these data demonstrate that MYC plays a critical role in T cell activation, facilitating the metabolic reprogramming and proteomic remodelling necessary for successful effector function. Furthermore, MYC appears to be a central node in numerous other metabolic programmes, integrating signals from AKT, ERK and mTOR downstream of the TCR signalling cascade.

5.1.1 Rationale

Human CD4⁺ T_H1 and pan CD4⁺ T cells were chosen as the study material. The aims of this section of work were: (i) to investigate whether canagliflozin exhibits the same off-target effects on mitochondrial complex I and GDH in human T cells; (ii) investigate whether canagliflozin, through its dual inhibition of mitochondrial complex I and GDH, is a more potent inhibitor of T cell function than known inhibitors of complex I such as rotenone and metformin; and (iii) determine whether impaired effector function is underpinned by canagliflozin-mediated changes in T cell metabolism, particularly through its off-target effects.

5.1.2 Hypothesis

- (i) Canagliflozin impairs T cell function via its off-target effects on both mitochondrial complex I and GDH.
- (ii) Canagliflozin is superior inhibitor of T cell function compared to other complex I inhibitors due to the additional off-target effects.
- (iii) Mitochondrial dysfunction within canagliflozin-treated T cells rewires metabolic programmes.

5.2 Experimental procedures

5.2.1 Human blood collection

Ethical approval was obtained from Wales Research Ethics Committee 6 for the collection of peripheral blood from healthy volunteers (13/WA/0190). Blood from healthy donors was processed as previously described (see Chapter 2.1).

5.2.2 T cell isolation

Peripheral blood mononuclear cells (PBMCs) were isolated as previously described (see Chapter 2.3). The PBMC pellet was resuspended in the appropriate downstream media for analysis and the number of PBMCs was determined by using the Countess[®] automated cell counter (see Chapter 2.5). Pan CD4⁺ T cells and CD4⁺ T_H1 cells were isolated using automated magnetic separation as previously described (see Chapter 2.4).

5.2.3 Cell culture

Isolated T cells were activated and cultured in human plasma-like medium (HPLM) as previously described (see Chapter 2.6), unless otherwise stated. Cell-free supernatants were stored for further analysis, whilst cells were collected for downstream analysis.

For partial rescue in anti-CD3 and anti-CD28 activated CD4⁺ T cells treated with canagliflozin, cells were cultured as previously described (see Chapter 2.6) with either L-glutathione (GSH, 5 mM) or N-acetyl-L-cysteine (NAC, 10 mM) to buffer intracellular ROS; or dimethyl 2-oxoglutarate (DM α KG, 0.3 mM; all Merck, Germany) to bypass GDH inhibition.

To assess the specificity of the inhibitory effects of canagliflozin, anti-CD3 and anti-CD28 activated CD4⁺ T cells were cultured as previously described (see Chapter 2.6) with other complex I inhibitors: rotenone (1 μ M; Merck, Germany) or metformin (10 mM; MedChemExpress, USA). For combined inhibition of complex I and GDH, anti-CD3 and anti-CD28 activated CD4⁺ T cells were cultured as previously described (see Chapter 2.6) in the presence and absence of the complex I inhibitor piericidin A (500 nM; Enzo Life Sciences, USA) and GDH inhibitor R162 (10 μ M; Merck, Germany).

To determine whether ERK and mTOR inhibition phenocopies anti-CD3 and anti-CD28 activated T cells treated with canagliflozin, cells were cultured as previously described (see Chapter 2.6) in the presence and absence of PD-98,059 (25 μ M; Merck, Germany) and rapamycin (100 nM; Merck, Germany), respectively.

5.2.4 Flow cytometry

T cell activation and blastogenesis was assessed as previously described (see Chapter 2.7). Intracellular analysis of phospho-ERK (ERK-1/2^{Thr202/Tyr204}; PE, 6B8B69, Mouse IgG2a κ ; BioLegend, USA) was performed as previously described (see Chapter 2.7.4). Purity of isolated T cells was monitored as previously described (see Chapter 2.7.1) and was typically > 90%.

MitoTracker™ Green FM (100 nM; ThermoFisher, USA) was used to assess mitochondrial content. MitoSOX™ Red (5 μ M; ThermoFisher, USA) was used to assess mitochondrial ROS. Tetramethylrhodamine ethyl ester (TMRE; 50 nM; Abcam, USA) was used to assess mitochondrial membrane potential. For all mitochondrial staining, cells were incubated with the respective dye for 20 min at 37°C. Cells were washed in FACS buffer and centrifugation at 515 x *g* post-staining and resuspended in FACS buffer to analyse.

Protein translation was assessed using anti-Puromycin (AlexaFluor® 488, rat IgG, 12D10; Merck, Germany). Puromycin (10 μ M; Merck, Germany) was added 15 min prior to the end of either 4 h and 24 h T cell activation. Cells were washed in ice-cold PBS before intracellular staining was performed using Inside Stain Kit (Miltenyi, Germany), whereby cells were fixed for 20 min at RT in Inside Fix before 15 min permeabilisation using Inside Perm (both Miltenyi, Germany). Cells were stained at 4°C for 1 h in Inside Perm permeabilisation buffer before a final wash. Cells were resuspended in FACS buffer to analyse.

5.2.5 Enzyme-linked immunosorbent assay

ELISAs were performed as per the manufacturer's guidelines to measure the concentration of the following cytokines in cell-free supernatants: IL-2 (DY202) and IFN γ (DY285B; all R&D systems, USA).

5.2.6 Metabolic analysis

Following 24 h activation in RPMI 1640 (1X) + Glutamax™, cells were resuspended and collected before centrifugation at 500 x *g* for 5 min. Cell-free supernatants were collected for ELISA analysis. Cells were resuspended in phenol red-free RPMI medium supplemented with glucose (10 mM), pyruvate (1 mM) and glutamine (2 mM; all Agilent, USA) before seeding at 2.0x10⁵ cells per Cell-Tak coated well. OCR and ECAR were measured following a series of previously optimized injections. Injections for both the mitochondrial stress assay and

glycolysis assay include oligomycin (1 μ M), FCCP (1 μ M), antimycin A and rotenone (both 1 μ M) and monensin (20 μ M). Metabolic parameters were calculated as previously described (see Chapter 2.9).

5.2.7 Immunoblotting

Immunoblotting was performed as previously described (see Chapter 2.10). Membranes were probed with antibodies specific to: phospho-S6 ribosomal protein (2211), S6 ribosomal protein (2217), phospho-AMPKa (2535), AMPKa (2532), phospho-acetyl-CoA carboxylase (3661) and 4EBP1 (9644). Mitochondrial complexes were assessed using the Total OXPHOS Human WB antibody cocktail (Abcam, USA). All antibodies were purchased from Cell Signaling, USA and used at a 1:1000 dilution, unless otherwise stated.

5.2.8 Extracellular glucose assay

Extracellular glucose levels in cell-free supernatants were assessed using Glucose Assay Kit I (Eton Biosciences, USA) as per the manufacturer's instructions. The glucose standard curve and samples were diluted to a working concentration using dH₂O. Glucose Assay Solution was added to each well and incubated for 15 min at 37°C in a CO₂-free incubator. The reaction was stopped by adding acetic acid (0.5 M; Merck, Germany). Plates were then read at 490 nm using a plate reader spectrophotometer.

5.2.9 Extracellular lactate assay

Extracellular lactate levels in cell-free supernatants were assessed using L-Lactate Assay Kit I (Eton Biosciences, USA) as per the manufacturer's instructions. The lactate standard curve and samples were diluted to a working concentration using dH₂O. L-Lactate Assay Solution was added to each well and incubated for 15 min at 37°C in a CO₂-free incubator. The reaction was stopped by adding acetic acid (0.5 M; Merck, Germany). Plates were then read at 490 nm using a plate reader spectrophotometer.

5.2.10 Stable isotope tracer analysis

CD4⁺ T_{nv} cells were cultured with either 11 mM universally-labelled ¹³C₆-glucose (Cambridge Isotopes, USA) in glucose-free RPMI 1640 (1X) medium (Gibco, USA) or 2 mM universally-labelled ¹³C₅-glutamine (Cambridge Isotopes, USA) in glutamine-free RPMI 1640

(1X) medium (Gibco, USA) and activated as previously described (see Chapter 2.6). Following 8 h activation, samples were prepared for stable isotope tracer analysis (SITA) by liquid chromatography-mass spectrometry (LC-MS). Cells were washed twice in 1 ml ice-cold saline and then lysed in 800 µl ice-cold 80% methanol. Cell extracts were then dried down at 4°C using a speed-vacuum concentrator.

Metabolite extraction and analysis was performed in the Vousden Lab by Dr Julianna Blagih at The Francis Crick Institute, London. Metabolite analysis was performed by LC-MS using a Q-EXACTIVE Plus (Orbitrap) mass spectrometer coupled with a Vanquish UHPLC system (both ThermoFisher, USA). The chromatographic separation was performed on a SeQuant® Zic®pHILIC (Merck Millipore) column (5 µm particle size, polymeric, 150 x 4.6 mm). The injection volume was 5 µL, the oven temperature was maintained at 25°C, and the autosampler tray temperature was maintained at 4°C. Chromatographic separation was achieved using a gradient program at a constant flow rate of 300 µl/min over a total run time of 25 min. The elution gradient was programmed as decreasing percentage of B from 80 % to 5 % for 17 minutes, holding at 5 % of B for 3 minutes and finally re-equilibrating the column at 80 % of B for 4 minutes. Solvent A was 20 mM ammonium carbonate solution in water supplemented by 4 ml/L of a solution of ammonium hydroxide at 35% in water, and solvent B was acetonitrile. MS was performed with positive/negative polarity switching using a Q-EXACTIVE Plus Orbitrap with a HESI II probe. MS parameters were as follows: spray voltage 3.5 and 3.2 kV for positive and negative modes, respectively; probe temperature 320°C; sheath and auxiliary gases were 30 and 5 arbitrary units, respectively; and full scan range: 70–1050 m/z with settings of AGC target and resolution as balanced and high (3×10^6 and 70000), respectively.

Data were recorded using Xcalibur 4.2.47 software (ThermoFisher, USA). Mass calibration was performed for both ESI polarities before analysis using the standard Calmix solution (ThermoFisher, USA). To enhance calibration stability, lock-mass correction was also applied to each analytical run using ubiquitous low-mass contaminants. Parallel reaction monitoring acquisition parameters were the following: resolution 17500; collision energies were set individually in HCD (high-energy collisional dissociation) mode. Metabolites were identified and quantified by accurate mass and retention time and by comparison to the retention times, mass spectra and responses of known amounts of authentic standards, using TraceFinder 4.1 EFS software (ThermoFisher, USA).

5.2.11 Statistical analysis

Unless otherwise stated, statistical analysis was carried out using GraphPad Prism version 8. Data are expressed as the mean \pm standard error of the mean (SEM). The normality of the data was initially tested using the Shapiro-Wilk test to determine the appropriate method of analysis. For data comparing two sample groups, normally distributed data were analysed using a parametric T test, whereas a non-parametric T test was used to analyse data not normally distributed. One-way analysis of variance (ANOVA) followed by the post-hoc Dunnett's test was used to analyse three or more group means of a single variable compared to the vehicle control. A one-sample T test was used to analyse data normalised to the vehicle control group. Significant values were taken as $p \leq 0.05$ and denoted as follows: * $p \leq 0.05$, ** $p \leq 0.01$, *** $p \leq 0.001$ and **** $p \leq 0.0001$.

5.3 Results

5.3.1 T cell mitochondrial dysfunction is characteristic of canagliflozin treatment

To improve our understanding of the relationship between canagliflozin and mitochondrial biology, we performed an exhaustive analysis of the changes to mitochondrial proteins within our proteomics dataset. Here, canagliflozin upregulated several electron transport chain complex-associated proteins, where only complex II associated proteins remained largely unaffected (Figure 5.1). Interestingly, complex I was associated with the greatest number of changes, with a total of 18 associated proteins upregulated, potentially suggesting that upregulation of these proteins is a compensatory mechanism to overcome its inhibition by canagliflozin (Figure 5.1).

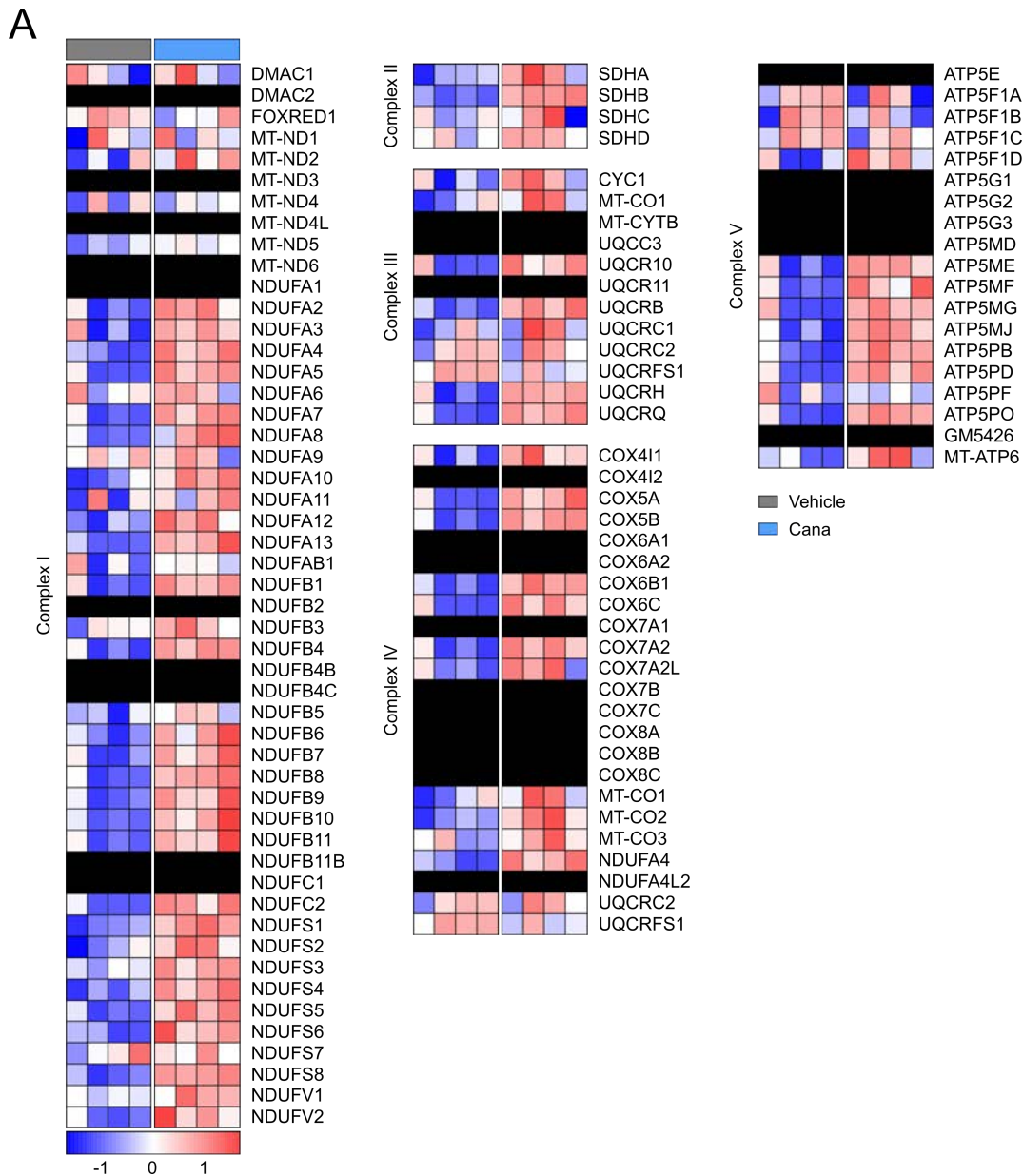


Figure 5.1 – Mitochondrial complexes are upregulated within T cells in response to canagliflozin

(A) Heatmap of mitochondrial complex protein expression in anti-CD3 (2 $\mu\text{g}/\text{ml}$) and anti-CD28 (20 $\mu\text{g}/\text{ml}$) activated CD4⁺ T cells in the presence and absence of canagliflozin (10 μM). Proteins identified based on Gene Ontology Cellular Component terms; values expressed as protein-specific z-scores. Data are representative of four independent experiments.

In support of these data, immunoblotting analysis of activated CD4⁺ T cells showed that the expression of all five mitochondrial electron transport chain complexes was increased following treatment with canagliflozin (Figure 5.2).

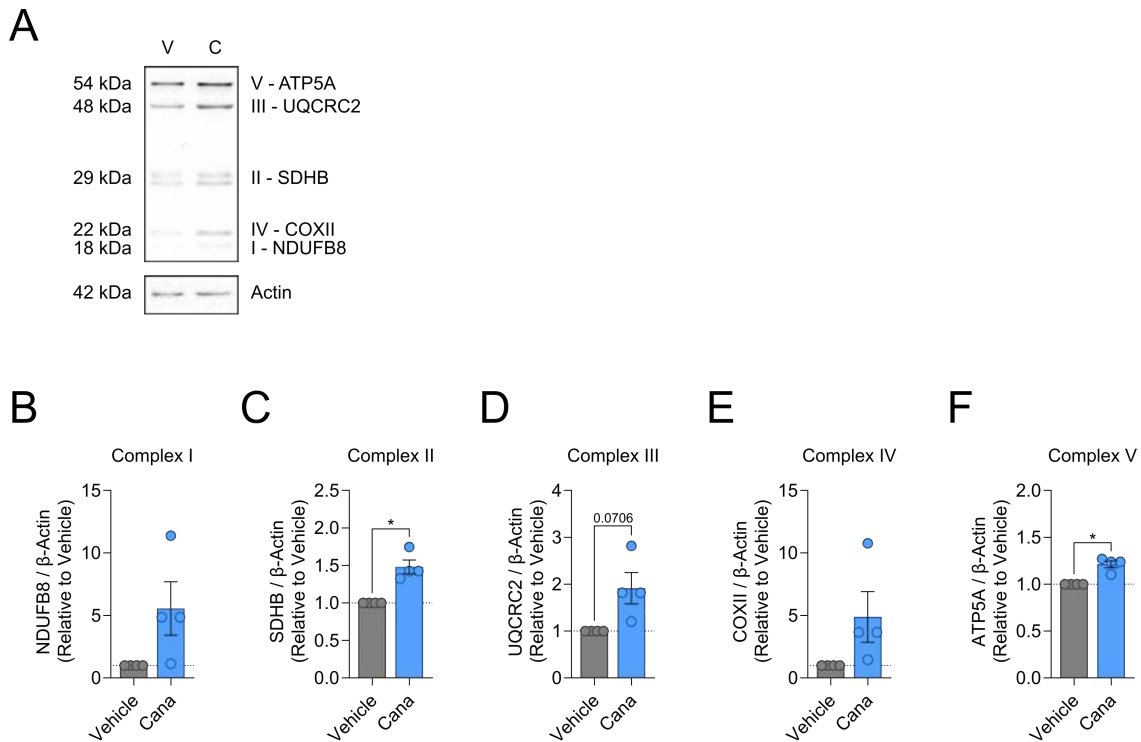


Figure 5.2 – Increased expression of mitochondrial complexes in CD4+ T cells upon canagliflozin treatment

(A) Representative immunoblots of mitochondrial complexes in anti-CD3 (2 μ g/ml) and anti-CD28 (20 μ g/ml) activated CD4+ T cells in the presence and absence of canagliflozin (10 μ M). (B) Densitometry analysis of immunoblots in (A). Data are representative of four independent experiments. Statistical analysis was performed using a one-sample T test. Data expressed as mean \pm SEM; * $p \leq 0.05$.

Using the mitochondrial probe MitoTracker™ Green and membrane potential indicator TMRE, we next aimed to establish whether the observed increase in electron transport chain proteins translated into a tangible increase in mitochondrial mass and function. Indeed, CD4+ T cells displayed increased mitochondrial mass when treated with canagliflozin ($p = 0.0213$; Figure 5.3A). Although mitochondrial membrane potential was modestly elevated in canagliflozin-treated cells, this did not reach significance ($p = 0.2476$; Figure 5.3B). The mitochondrial uncoupler FCCP – known to depolarise membrane potential – was used as a control for the assay, where it caused a marked reduction in mitochondrial membrane potential as expected ($p = 0.0001$; Figure 5.3B).

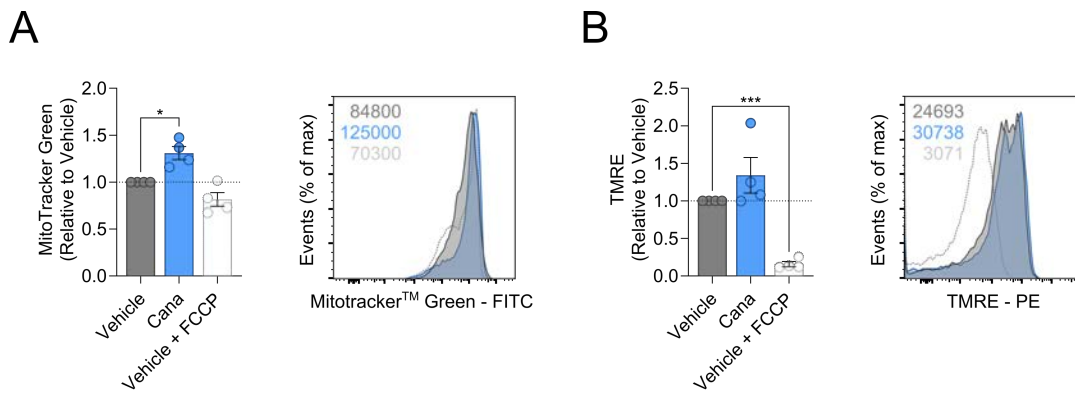


Figure 5.3 – Canagliflozin increases mitochondrial biogenesis in activated T cells

(A) Relative mitochondrial biogenesis in anti-CD3 (2 µg/ml) and anti-CD28 (20 µg/ml) activated CD4+ T cells in the presence and absence of canagliflozin (10 µM) or FCCP (1 µM), determined by flow cytometry using MitoTracker™ Green. (B) Relative mitochondrial membrane potential, determined by flow cytometry using TMRE. Representative overlaid histogram plots, numbers indicate median fluorescence intensity. Data are representative of four independent experiments. Statistical analysis was performed using a one-sample T test. Data expressed as mean ± SEM; * $p \leq 0.05$, *** $p \leq 0.001$.

Given that increased mitochondrial biogenesis and complex I inhibition have previously been associated with increased mitochondrial ROS (mitoROS) production (Dugan et al., 2013; Li et al., 2003), we next analysed early mitoROS production by CD4+ T cells treated with canagliflozin. Here, there was an increase in mitoROS production as early as 15 min post-activation in canagliflozin-treated T cells, where mitoROS levels remained elevated at all further time points measured compared to the vehicle control (Table 5.1; Figure 5.4).

Table 5.1 – Mitochondrial ROS levels are elevated during early T cell activation by canagliflozin

Time (min)	15	30	60	120	240
<i>p</i> -value	0.0643	0.0064	0.0009	0.0022	0.0003

A

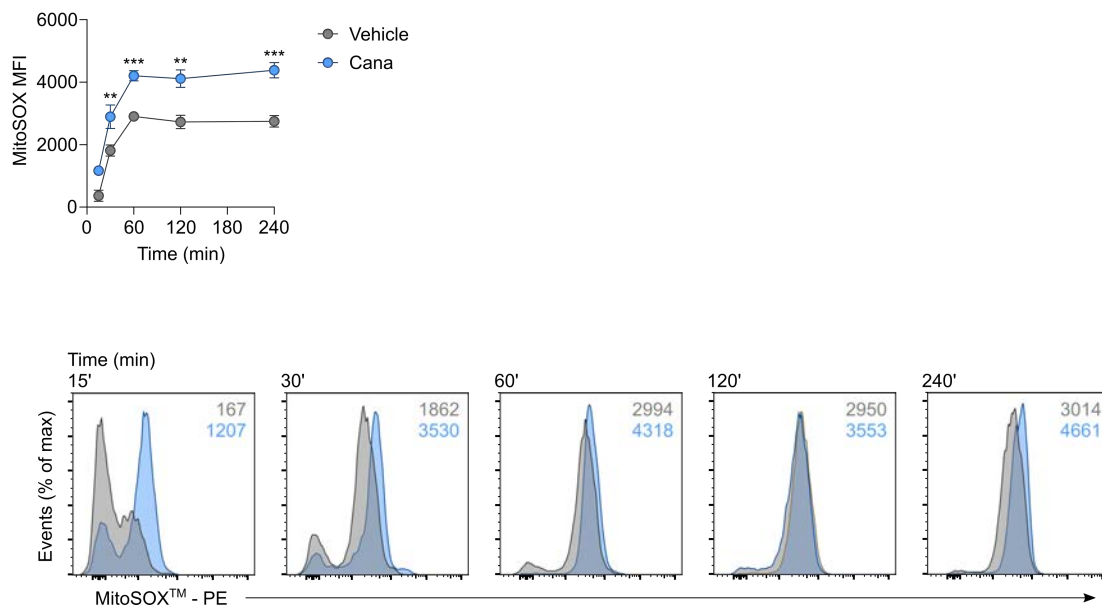


Figure 5.4 – Canagliflozin promotes mitochondrial reactive oxygen species production

(A) Mitochondrial ROS in anti-CD3 (2 $\mu\text{g}/\text{ml}$) and anti-CD28 (20 $\mu\text{g}/\text{ml}$) activated CD4⁺ T cells in the presence and absence of canagliflozin (10 μM), determined by flow cytometry using MitoSOX[™] Red superoxide indicator. Representative overlaid histogram plots, numbers indicate median fluorescence intensity. Data are representative of four independent experiments. Statistical analysis was performed using a two-way ANOVA followed by Šidák's multiple comparisons test. Data expressed as mean \pm SEM; ** $p \leq 0.01$, *** $p \leq 0.001$.

Aberrant mitoROS production was further supported by the increased expression of several proteins involved in the response to ROS (Figure 5.5). Interestingly, it was the mitochondrial isoforms of these antioxidant proteins that were upregulated, further suggesting that augmented ROS production in response to canagliflozin treatment was localised to the mitochondria (Figure 5.5).

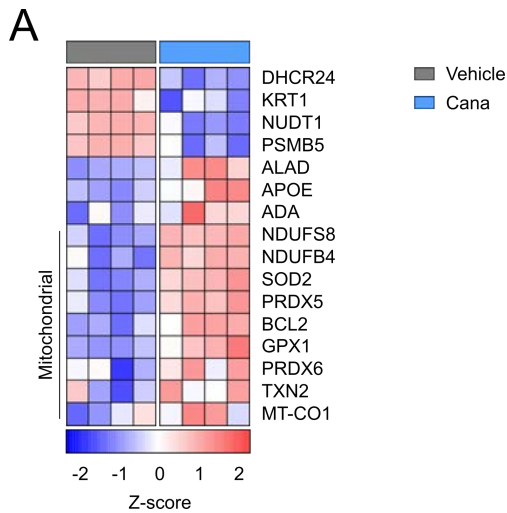


Figure 5.5 – Proteins associated with the response to reactive oxygen species are upregulated within T cells in response to canagliflozin

(A) Heatmap of reactive oxygen response protein expression in anti-CD3 (2 $\mu\text{g}/\text{ml}$) and anti-CD28 (20 $\mu\text{g}/\text{ml}$) activated CD4⁺ T cells in the presence and absence of canagliflozin (10 μM). Proteins identified based on Gene Ontology Cellular Component terms; values expressed as protein-specific z-scores. Data are representative of four independent experiments.

To determine the significance of elevated mitoROS levels towards loss of T cell function, we cultured CD4⁺ T cells in the presence and absence of canagliflozin as previously described, supplementing these cultures with endogenous antioxidants glutathione (GSH) and N-acetyl-cysteine (NAC). Both GSH and NAC were able to partially rescue the activation and size of canagliflozin-treated T cells (Figure 5.6A-B). Furthermore, increased expression of downstream mTORC1 target CD98 upon supplementation with antioxidants suggests that GSH and NAC might also partially rescue mTOR activity (Figure 5.6C). However, T cell effector function remained impaired as neither GSH nor NAC could rescue the production of IFN γ by T cells treated with canagliflozin (Figure 5.6D).

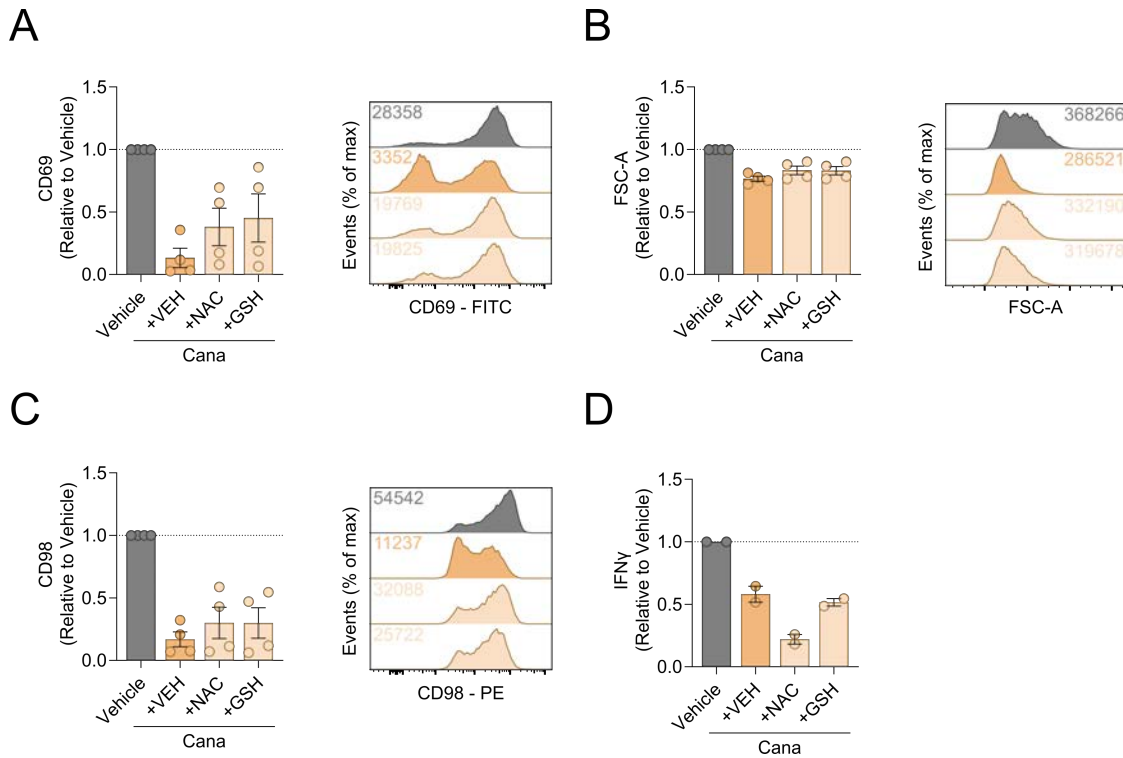
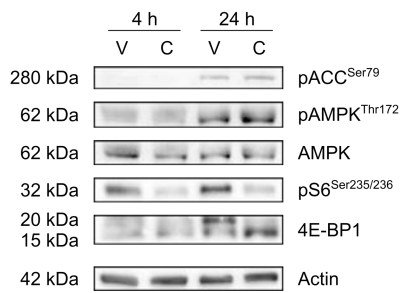
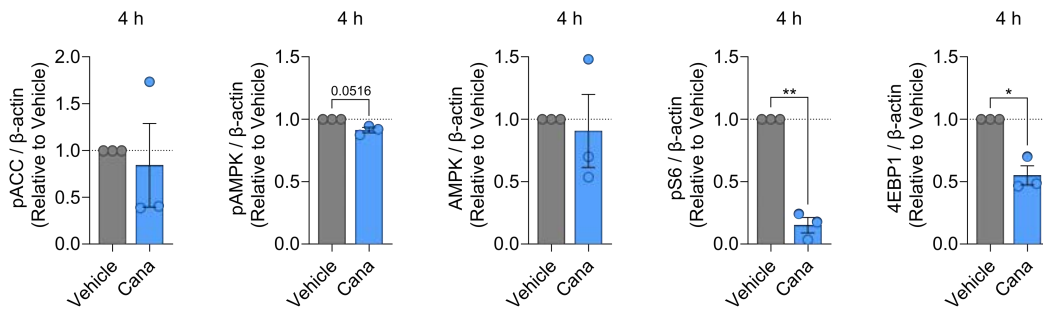
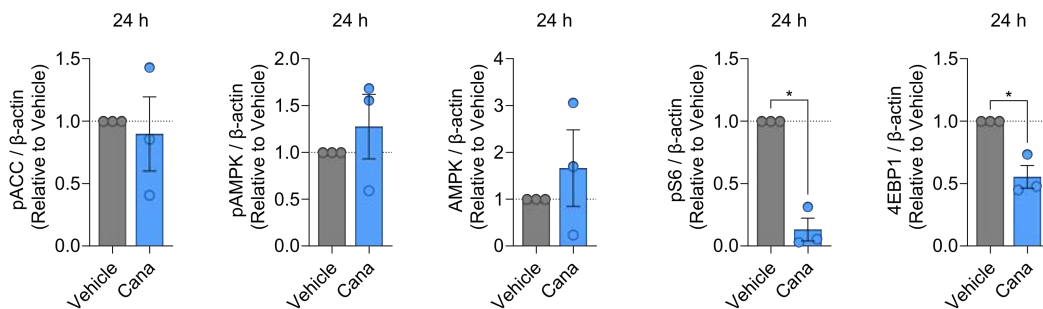


Figure 5.6 – Glutathione and N-acetyl-cysteine partially rescue T cell function after canagliflozin treatment

(A) Relative expression of activation marker CD69 in anti-CD3 (2 $\mu\text{g}/\text{ml}$) and anti-CD28 (20 $\mu\text{g}/\text{ml}$) activated CD4⁺ T cells treated with or without canagliflozin (10 μM), with or without glutathione (5 mM) or N-acetyl-cysteine (10 mM), determined by flow cytometry. (B) Blastogenesis, determined by flow cytometry using forward-scatter area. (C) Relative expression of downstream mTOR target CD98, determined by flow cytometry. Representative overlaid histogram plots, numbers indicate median fluorescence intensity or forward-scatter area. (D) Relative secretion of IFN γ , determined by ELISA of cell-free supernatants. Data are representative of four (A-C) or two (D) independent experiments. Data expressed as mean \pm SEM.

Whilst ROS are critical in early T cell activation and signal transduction, excessive ROS levels have been shown to disrupt the mTOR-Myc axis, compromising T cell function (Mak et al., 2017). Given that we previously confirmed perturbed MYC activity in T cells treated with canagliflozin using various protein-based approaches (see Chapter 4), we investigated the effect that this might have on mTOR activation. Here, several signalling targets downstream of mTOR were repressed by canagliflozin (Figure 5.7). Phosphorylated S6 – phosphorylated by p70S6K downstream of mTORC1 – was downregulated by canagliflozin at both 4 h and 24 h post-activation (Figure 5.7). Additionally, phosphorylated 4E-BP1, a direct target of mTOR, was also reduced in T cells upon canagliflozin treatment (Figure 5.7). However, total- and phosphorylated-AMPK were unchanged by canagliflozin, as well as its target pACC, suggesting that mTOR is not differentially regulated by AMPK (Figure 5.7). Collectively, these data show that T cell mitochondrial function is severely hampered by canagliflozin, associated with impaired activity of critical metabolic proteins including MYC and mTOR.

A**B****C****Figure 5.7 – Canagliflozin downregulates the expression of downstream mTOR targets**

(A) Representative immunoblots of phosphorylated-ACC, phosphorylated- and total-AMPK, phosphorylated-S6 and 4E-BP1 in anti-CD3 (2 μ g/ml) and anti-CD28 (20 μ g/ml) activated CD4+ T cells in the presence and absence of canagliflozin (10 μ M). (B-C) Densitometry analysis of immunoblots in (A) at (B) 4 h and (C) 24 h post-activation. Data are representative of three independent experiments. Statistical analysis was performed using a one-sample T test. Data expressed as mean \pm SEM; * $p \leq 0.05$, ** $p \leq 0.01$.

5.3.2 Canagliflozin drives T cell metabolism towards quiescence through its off-target effects

Given the mitochondrial dysfunction displayed in canagliflozin-treated T cells, we next investigated whether canagliflozin – through its off-target effects – alters T cell metabolism and underpins the functional changes previously observed. Thus, a bioenergetic profile was generated for activated T cells, treated in the presence and absence of canagliflozin or dapagliflozin, using a mitochondrial stress assay. Dapagliflozin was re-introduced for these experiments to ensure any observed changes in T cell metabolism occurred independent of SGLT2 inhibition. Interestingly, canagliflozin perturbed glycolysis in activated T cells, with significant reductions in the rates of both basal ($p < 0.0001$) and maximal glycolysis ($p < 0.0001$; Figure 5.8A-C). As a result, there was a significant reduction in ATP produced from glycolysis at both basal ($p < 0.0001$) and maximal rates through this pathway ($p < 0.0001$; Figure 5.8D). Dapagliflozin-treated T cells displayed no decline in the rates of either basal glycolysis ($p = 0.3553$) or maximal glycolysis ($p = 0.3121$; Figure 5.8A-C) or their ability to produce ATP from this pathway (basal: $p = 0.3682$; maximal: $p = 0.3078$; Figure 5.8D).

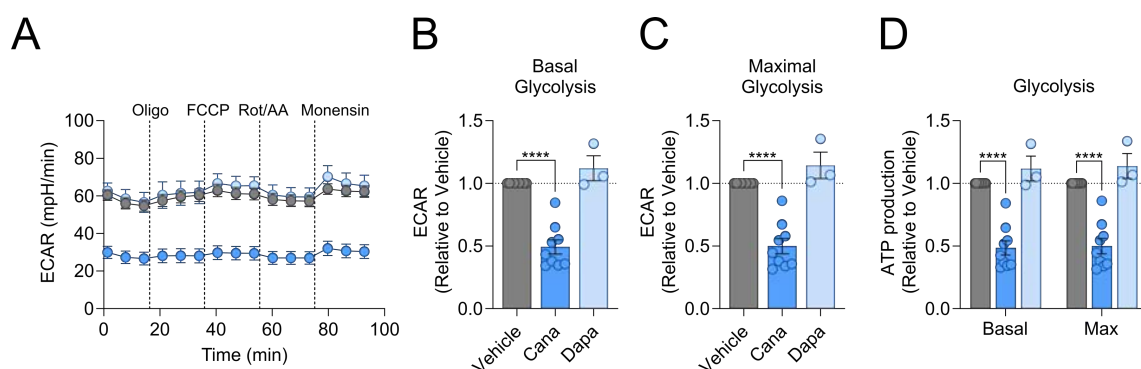


Figure 5.8 – Canagliflozin impairs glycolysis in activated T cells

(A) Seahorse trace of the extracellular acidification rate (ECAR) in anti-CD3 (2 $\mu\text{g/ml}$) and anti-CD28 (20 $\mu\text{g/ml}$) activated CD4⁺ T cells in the presence and absence of canagliflozin and dapagliflozin (both 10 μM). ECAR measured using oligomycin, FCCP, antimycin A/rotenone (all 1 μM) and monensin (20 μM). (B-C) Glycolytic parameters including (B) basal glycolysis and (C) maximal glycolysis. (D) Joules of ATP produced from glycolysis at basal and maximal levels. Data are representative of nine-three independent experiments. Statistical analysis was performed using a one-sample T test. Data expressed as mean \pm SEM; **** $p < 0.0001$.

Comparatively, the impact of canagliflozin on OXPHOS in activated T cells was not as pronounced as that on glycolysis, but was striking nonetheless (Figure 5.9). Here, there were reductions in basal respiration ($p = 0.0050$) and ATP-linked respiration ($p = 0.0201$), in addition to more marked reductions in the maximal respiratory capacity ($p < 0.0001$) and spare respiratory capacity of these cells ($p < 0.0001$; Figure 5.9A-E). Consequently, ATP production from OXPHOS was reduced at its basal rate ($p = 0.0178$), whilst even fewer joules of ATP were produced relative to the vehicle control group when functioning at its maximal rate ($p < 0.0001$; Figure 5.9F). Again, dapagliflozin did not alter any of the OXPHOS-associated parameters: basal respiration ($p = 0.1238$), ATP-linked respiration ($p = 0.1238$), maximal respiratory capacity ($p = 0.2157$), spare respiratory capacity ($p = 0.2395$; Figure 5.9A-E); or ATP produced from OXPHOS at its basal ($p = 0.1241$) or maximal rate ($p = 0.2155$; Figure 5.9F).

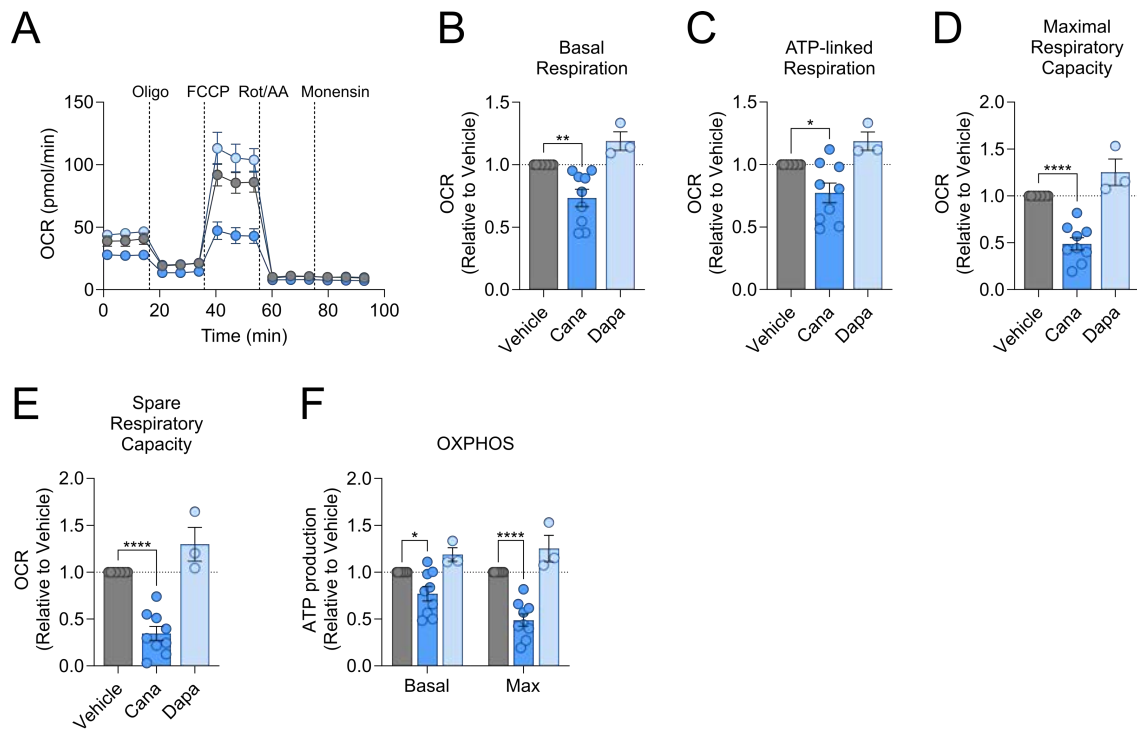


Figure 5.9 – Canagliflozin limits the capacity for oxidative respiration in activated T cells

(A) Seahorse trace of oxygen consumption rate (OCR) in anti-CD3 (2 $\mu\text{g}/\text{ml}$) and anti-CD28 (20 $\mu\text{g}/\text{ml}$) activated CD4⁺ T cells in the presence and absence of canagliflozin and dapagliflozin (both 10 μM). OCR measured using oligomycin, FCCP, antimycin A/rotenone (all 1 μM) and monensin (20 μM). (B-E) Respiratory parameters including (B) basal respiration, (C) ATP-linked respiration, (D) maximal respiratory capacity and (E) spare respiratory capacity. (F) Joules of ATP produced from OXPHOS at basal and maximal levels. Data are representative of nine-three independent experiments. Statistical analysis was performed using a one-sample T test. Data expressed as mean \pm SEM; * $p \leq 0.05$, ** $p \leq 0.01$, **** $p < 0.0001$.

Taken together, activated T cells treated with dapagliflozin displayed a metabolic profile similar to that of the vehicle control group ($p = 0.7759$), whilst canagliflozin-treated T cells tended to demonstrate a more oxidative phenotype ($p = 0.0487$; Figure 5.10). However, the metabolic phenotype displayed by canagliflozin-treated cells is most likely to be a feature of the greater inhibition of glycolysis observed compared to OXPHOS.

A

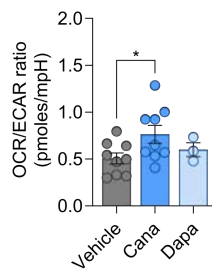


Figure 5.10 – OCR/ECAR ratio of activated T cells treated with SGLT2 inhibitors

(A) OCR/ECAR ratio of anti-CD3 (2 $\mu\text{g}/\text{ml}$) and anti-CD28 (20 $\mu\text{g}/\text{ml}$) activated CD4+ T cells in the presence and absence of canagliflozin and dapagliflozin (both 10 μM). OCR and ECAR measured with oligomycin, FCCP, antimycin A/rotenone (all 1 μM) and monensin (20 μM); OCR/ECAR ratio calculated using basal respiration and basal glycolysis. Data are representative of nine-three independent experiments. Statistical analysis was performed using a one-way ANOVA followed by Dunnett's multiple comparisons test. Data expressed as mean \pm SEM; * $p \leq 0.05$.

To better understand the combined effect of the changes to both glycolysis and OXPHOS, the bioenergetic scope – this is the product of ATP produced from both pathways – was calculated in activated T cells. Unsurprisingly, the bioenergetic scope was unchanged by dapagliflozin (basal: $p = 0.2432$; maximal: $p = 0.2689$) but was diminished in T cells treated with canagliflozin at both basal and maximal rates (basal: $p < 0.0001$; maximal: $p < 0.0001$; Figure 5.11A-B). Finally, the metabolic plasticity of activated T cells to respond to changes in ATP demand and source of their ATP supply – measured as their supply flexibility index – was not changed by either canagliflozin or dapagliflozin (canagliflozin: $p = 0.2066$; dapagliflozin: $p = 0.4307$; Figure 5.11C).

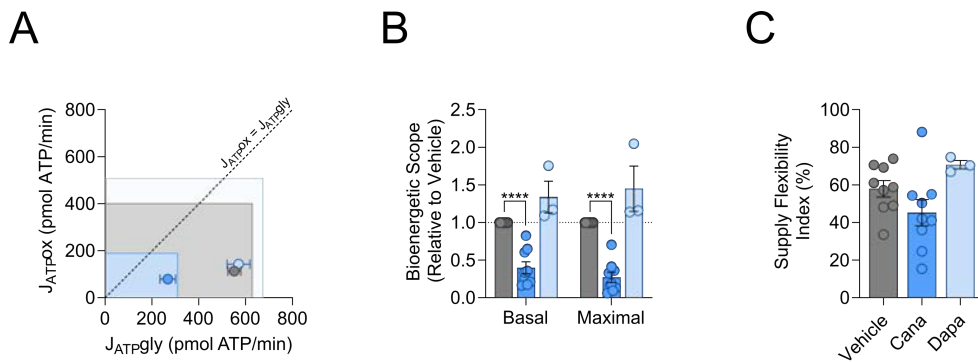


Figure 5.11 – Canagliflozin limits the bioenergetic scope of activated T cells

(A) Bioenergetic map representing joules of ATP produced from glycolysis and OXPHOS in anti-CD3 (2 $\mu\text{g}/\text{ml}$) and anti-CD28 (20 $\mu\text{g}/\text{ml}$) activated CD4⁺ T cells in the presence and absence of canagliflozin and dapagliflozin (both 10 μM). OCR and ECAR measured using oligomycin, FCCP, antimycin A/rotenone (all 1 μM) and monensin (20 μM). Symbols represent ATP produced under basal metabolic conditions; rectangles represent ATP produced under maximal metabolic conditions. (B) Bioenergetic scope at basal and maximal levels. (C) Supply flexibility index. Data are representative of nine-three independent experiments. Statistical analysis was performed using a one-sample T test (B) or a one-way ANOVA followed by Dunnett’s multiple comparisons test (C). Data expressed as mean \pm SEM; **** $p < 0.0001$.

Crucially, supernatants collected from T cells activated in the presence of canagliflozin tend to contain increased concentrations of glucose ($p = 0.1121$), which might suggest reduced glucose uptake compared to the vehicle control (Figure 5.12). Together, these data show that canagliflozin – through its off-target effects on GDH and mitochondrial complex I, rather than SGLT2 inhibition – perturbs T cell metabolism which underlies their impaired activation and function.

A

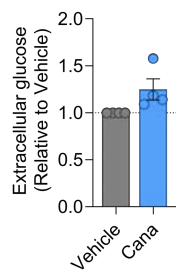


Figure 5.12 – Glucose uptake is modestly impaired by canagliflozin

(A) Relative extracellular glucose concentrations in cell-free supernatants from anti-CD3 (2 µg/ml) and anti-CD28 (20 µg/ml) activated CD4+ T cells in the presence and absence of canagliflozin (10 µM). Data are representative of four independent experiments. All relative data are normalised to the vehicle control group. Statistical analysis was performed using a one-sample T test. Data expressed as mean ± SEM.

5.3.3 Canagliflozin impairs TCA cycle metabolism via GDH inhibition

Given the profound effect canagliflozin exhibited on T cell metabolism, we sought to investigate this further using liquid chromatography-mass spectrometry (LC-MS). Metabolites were extracted from activated T cells to determine their abundance following canagliflozin treatment. Notably, canagliflozin-treated cells contained reduced levels of the following TCA cycle intermediates: citrate ($p = 0.0186$), α -ketoglutarate (α -KG: $p = 0.0170$), fumarate ($p = 0.0227$), malate ($p = 0.0479$; Figure 5.13A). Although proline levels were also reduced by canagliflozin ($p = 0.0023$), there were no significant changes in other amino acids such as glutamate ($p = 0.1054$) or aspartate ($p = 0.1952$; Figure 5.13B), or the glycolysis product lactate ($p = 0.2000$; Figure 5.13C).

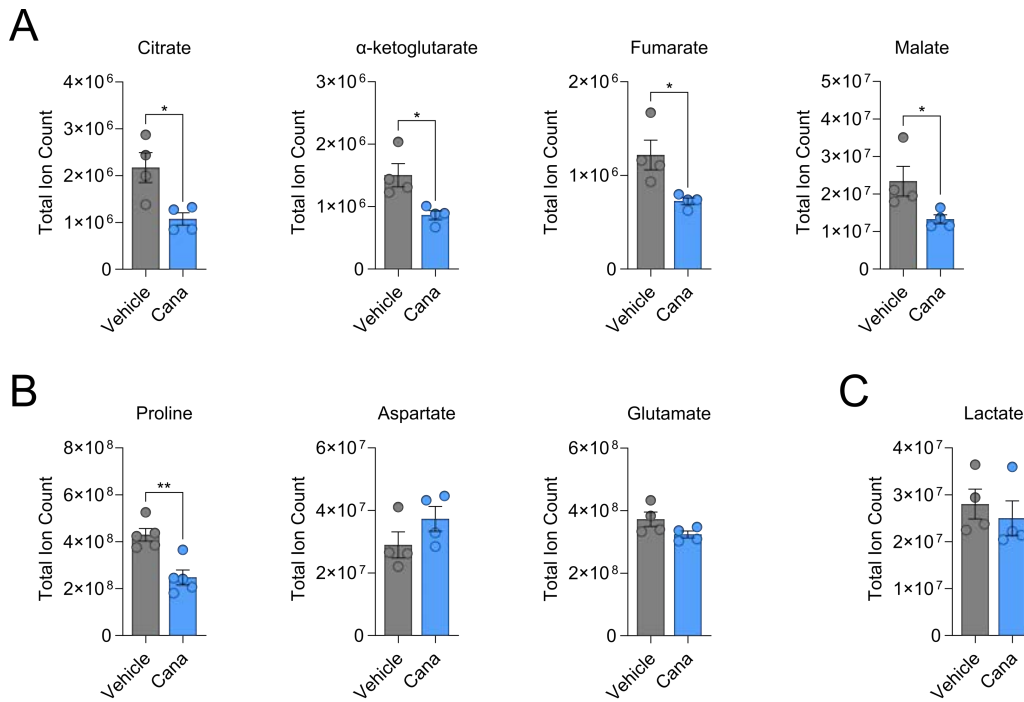


Figure 5.13 – Reduced abundance of TCA cycle intermediates in canagliflozin-treated T cells

(A-C) Total ion counts of (A) TCA cycle metabolites: citrate, α-ketoglutarate, fumarate and malate; (B) amino acids: proline, glutamate and aspartate; and (C) lactate following extraction from anti-CD3 (2 μg/ml) and anti-CD28 (20 μg/ml) activated CD4⁺ T cells treated with or without canagliflozin (10 μM). Data are representative of four independent experiments. Statistical analysis was performed using an unpaired T test. Data expressed as mean ± SEM; * $p \leq 0.05$, ** $p \leq 0.01$.

However, we did observe a significant reduction in released lactate in cell-free supernatants from Tnv cells cultured in the presence of canagliflozin in both RPMI ($p = 0.0003$) and HPLM ($p < 0.0001$; Figure 5.14).

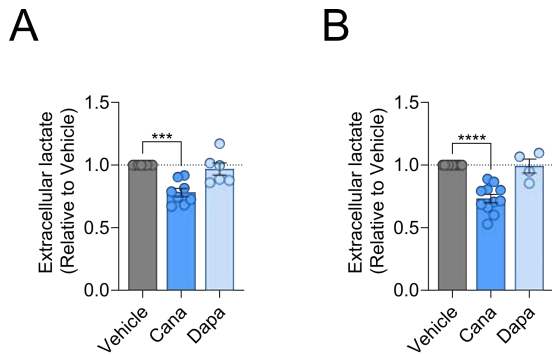


Figure 5.14 – Canagliflozin impairs lactate release by activated T cells

(A-B) Relative extracellular lactate concentrations in cell-free supernatants from anti-CD3 (2 µg/ml) and anti-CD28 (20 µg/ml) activated CD4+ T cells in the presence and absence of canagliflozin (10 µM), cultured in either (A) RPMI or (B) HPLM. Data are representative of eight-six (A) or eleven-four (B) independent experiments. All relative data are normalised to the vehicle control group. Statistical analysis was performed using a one-sample T test. Data expressed as mean ± SEM. *** $p \leq 0.001$, **** $p < 0.0001$.

To determine whether canagliflozin inhibits mitochondrial GDH in activated T cells, we employed a stable isotope tracing method, whereby uniformly labelled $^{13}\text{C}_5$ -glutamine was used to measure the incorporation of glutamine-derived carbon into the TCA cycle via GDH (Figure 5.15).

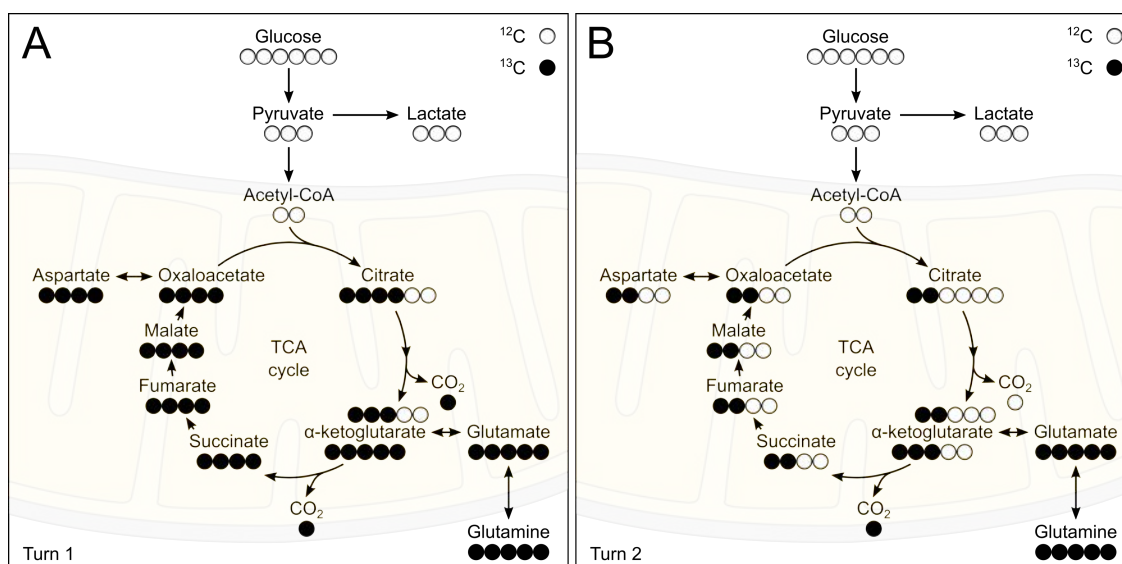


Figure 5.15 – Stable isotope tracing of ^{13}C -glutamine in activated T cells

(A) Schematic overview outlining stable isotope tracing of uniformly labelled ^{13}C -glutamine into the TCA cycle following (A) one and (B) two cycles. Tracing assessed in anti-CD3 (2 $\mu\text{g}/\text{ml}$) and anti-CD28 (20 $\mu\text{g}/\text{ml}$) activated CD4+ T cells treated with or without canagliflozin (10 μM).

Here, canagliflozin limited the incorporation of 13-carbon from glutamine into α -ketoglutarate – the point at which glutamine enters the TCA cycle (Figure 5.16A). Reduced abundance of the $m + 5$ mass isotopologue of α -KG, in addition to increased abundance of the unlabelled $m + 0$ mass isotopologue, is indicative of impaired glutaminolysis in canagliflozin-treated T cells (Table 5.2; Figure 5.16A). Indeed, this trend is also observed in other TCA cycle metabolites such as citrate, fumarate and malate (Table 5.2; Figure 5.16B-D).

Table 5.2 – p -values of $^{13}\text{C}_5$ -glutamine-derived mass isotopologues for vehicle versus canagliflozin

Metabolite	m + 0	m + 1	m + 2	m + 3	m + 4	m + 5	m + 6
Citrate	< 0.0001	0.8678	> 0.9999	0.8653	0.3276	0.6917	> 0.9999
α -KG	< 0.0001	0.9801	0.9999	0.9998	0.9989	< 0.0001	-
Fumarate	0.0019	0.7564	> 0.9999	0.8942	0.0008	-	-
Malate	0.0156	0.2585	0.8295	0.9048	< 0.0001	-	-
Glutamate	0.0004	0.1922	0.8839	0.9862	> 0.9999	< 0.0001	-
Aspartate	0.1120	0.1313	0.8855	0.9057	0.0002	-	-

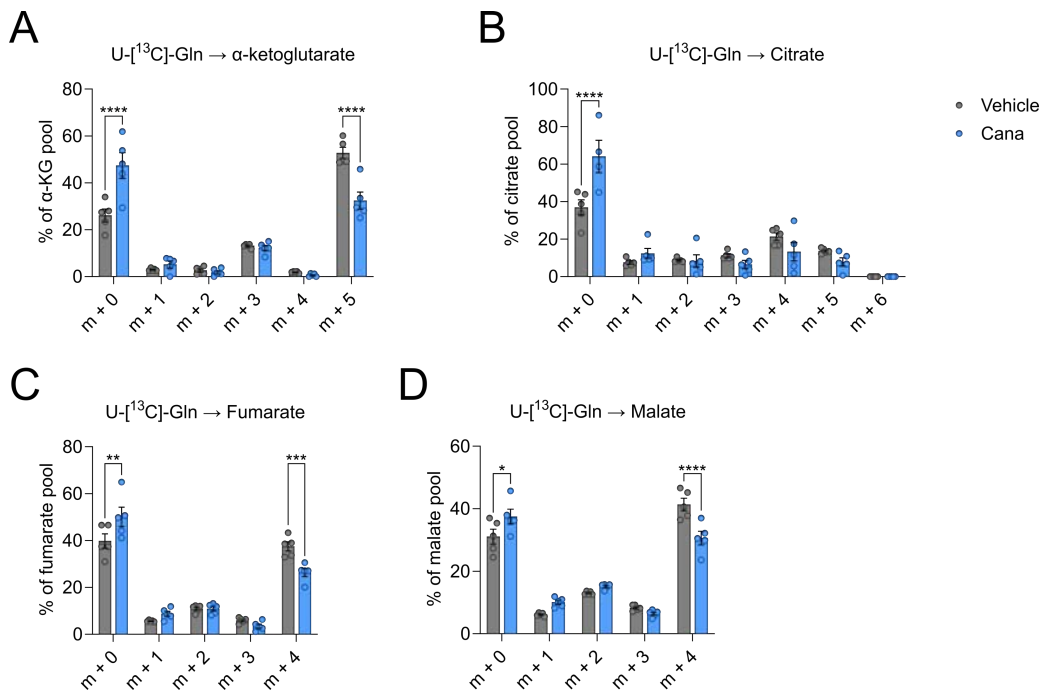


Figure 5.16 – Canagliflozin impairs glutamine incorporation into the TCA cycle in activated T cells (A-D) Mass isotopologue distribution, represented as a percentage of pool, of TCA cycle metabolites: (A) α-ketoglutarate, (B) citrate, (C) fumarate and (D) malate in anti-CD3 (2 μg/ml) and anti-CD28 (20 μg/ml) activated CD4+ T cells treated with or without canagliflozin (10 μM). Numbers on the x-axis represent the number of 13-carbons incorporated. Data are representative of five independent experiments. Statistical analysis was performed using a two-way ANOVA followed by Šidák's multiple comparisons test. Data expressed as mean ± SEM; * $p \leq 0.05$, ** $p \leq 0.01$, *** $p \leq 0.001$, **** $p < 0.0001$.

Furthermore, there is also reduced incorporation of ¹³C-glutamine into the amino acids glutamate and aspartate (Table 5.2; Figure 5.17).

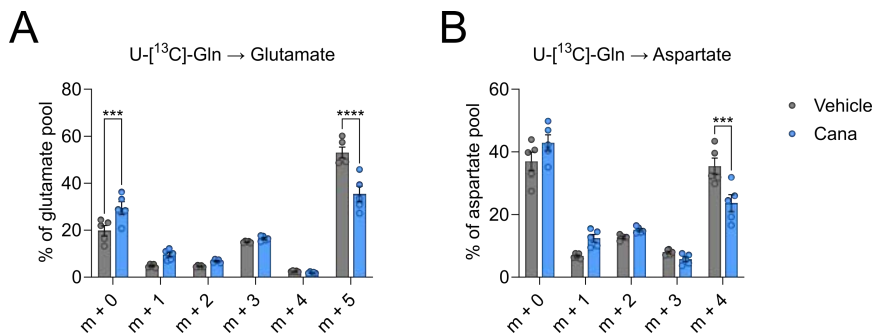


Figure 5.17 – Reduced incorporation of glutamine into amino acids pools in activated T cells treated with canagliflozin

(A) Mass isotopologue distribution, represented as a percentage of pool, of amino acids: (A) glutamate and (B) aspartate in anti-CD3 (2 µg/ml) and anti-CD28 (20 µg/ml) activated CD4+ T cells treated with or without canagliflozin (10 µM). Numbers on the x-axis represent the number of ¹³-carbons incorporated. Data are representative of five independent experiments. Statistical analysis was performed using a two-way ANOVA followed by Šidák's multiple comparisons test. Data expressed as mean ± SEM; *** $p \leq 0.001$, **** $p < 0.0001$.

When analysing the incorporation of ¹³-carbon into metabolite pools irrespective of mass isotopologue distribution, significantly less glutamine-derived carbon was incorporated into T cell metabolites upon canagliflozin treatment ($p = 0.0363$; Figure 5.18A). Focussing on the TCA cycle intermediates, there was only significantly reduced incorporation of ¹³C-glutamine into citrate ($p = 0.0010$) and α -KG ($p < 0.0001$), despite a general decrease being observed across the other metabolites measured (fumarate: $p = 0.2780$; malate: $p = 0.7857$; glutamate: $p = 0.3543$; aspartate: $p = 0.1715$; Figure 5.18B).

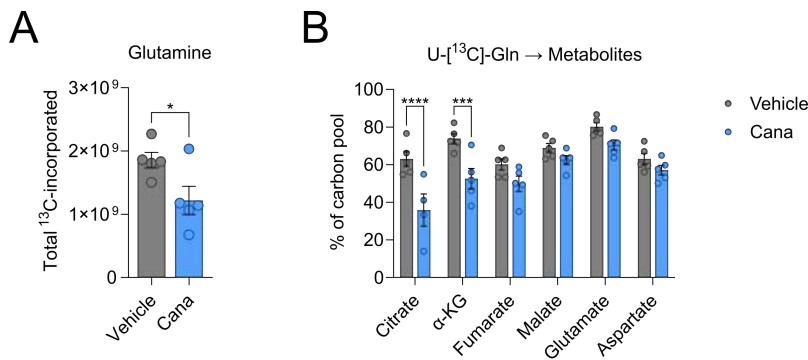


Figure 5.18 – Canagliflozin restricts the incorporation of glutamine-derived 13-carbon into metabolic intermediates in activated T cells

(A) Total incorporation of ¹³C-glutamine into metabolites of anti-CD3 (2 μg/ml) and anti-CD28 (20 μg/ml) activated CD4+ T cells treated with or without canagliflozin (10 μM). (B) Abundance of ¹³C-glutamine derived metabolites: citrate, α-ketoglutarate, fumarate, malate, glutamate and aspartate, represented as a percentage of the total carbon pool. Data are representative of five independent experiments. Statistical analysis was performed using an unpaired T test (A) or a two-way ANOVA followed by Šidák's multiple comparisons test (B). Data expressed as mean ± SEM; * $p \leq 0.05$, *** $p \leq 0.001$, **** $p < 0.0001$.

To better understand if there were any defects in glutamine uptake in T cells upon canagliflozin treatment, the abundance of ¹³C-glutamine was compared with the vehicle control. Here, there was significantly less ¹³C-glutamine present in canagliflozin-treated T cells ($p = 0.0174$), suggesting that its uptake could be impaired (Figure 5.19A). Furthermore, a concomitant decrease in the abundance of α-ketoglutarate ($p = 0.0238$) and unchanged glutamate levels ($p = 0.4006$) suggests that 13-carbon accumulates in glutamate pools, which could be indicative of blocked entry of glutamine into the TCA cycle (Figure 5.19B-C).

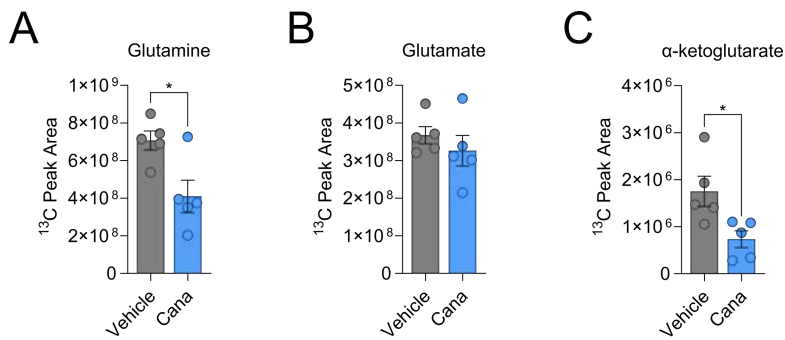


Figure 5.19 – Glutamine uptake by activated T cells is constrained by canagliflozin

(A-C) Total 13-carbon ion counts of (A) glutamine, (B) glutamate and (C) α -ketoglutarate following extraction from anti-CD3 (2 $\mu\text{g}/\text{ml}$) and anti-CD28 (20 $\mu\text{g}/\text{ml}$) activated CD4+ T cells treated with or without canagliflozin (10 μM). Data are representative of five independent experiments. Statistical analysis was performed using an unpaired T test. Data expressed as mean \pm SEM; * $p \leq 0.05$.

In an attempt to bypass GDH inhibition, canagliflozin-treated T cells were supplemented with a cell membrane permeable form of α -ketoglutarate, dimethyl- α -ketoglutarate. However, there was not an observed rescue of CD69 expression by α -ketoglutarate supplementation, whilst there were also no changes in T cell blastogenesis or CD98 expression (Figure 5.20A-C). Moreover, the addition of α -ketoglutarate did not rescue effector function, whereby IFN γ production and IL-2 production were unchanged (Figure 5.20D-E). Together, these data demonstrate that canagliflozin impairs glutamine incorporation into the TCA cycle and associated amino acids, which is indicative of canagliflozin-mediated GDH inhibition.

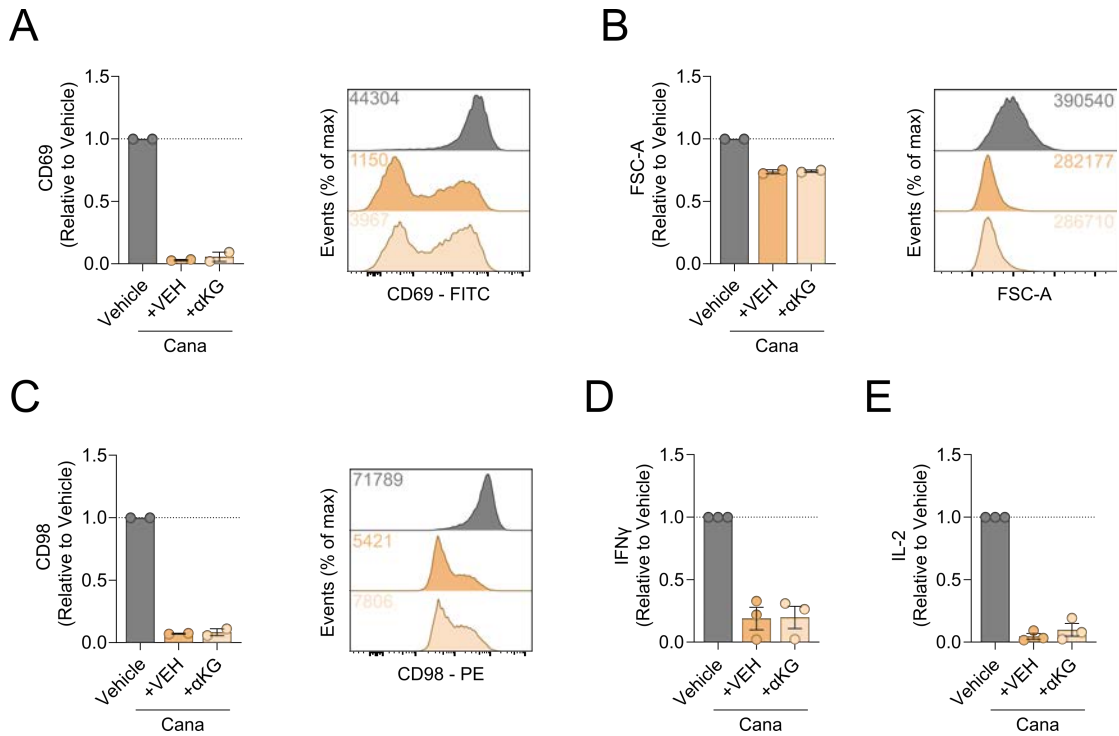


Figure 5.20 – α -ketoglutarate does not rescue T cell function following canagliflozin treatment

(A) Relative expression of activation marker CD69 in anti-CD3 (2 μ g/ml) and anti-CD28 (20 μ g/ml) activated CD4⁺ T cells treated with or without canagliflozin (10 μ M), with or without dimethyl- α -ketoglutarate (0.3 mM), determined by flow cytometry. (B) Blastogenesis, determined by flow cytometry using forward-scatter area. (C) Relative expression of downstream mTOR target CD98, determined by flow cytometry. Representative overlaid histogram plots, numbers indicate median fluorescence intensity or forward-scatter area. (D-E) Relative secretion of (D) IFN γ and (E) IL-2, determined by ELISA of cell-free supernatants. Data are representative of two (A-C) or three (D-E) independent experiments. Data expressed as mean \pm SEM.

5.3.4 T cells undergo metabolic reprogramming to adapt to canagliflozin treatment

Given metabolic perturbation is associated with plasticity in human T cells (Jones et al., 2019), we sought to determine whether altered glutamine metabolism elicited by canagliflozin impacts glucose metabolism. Thus, T cells were activated as before in the presence of $^{13}\text{C}_6$ -glucose and downstream metabolite pools monitored (Figure 5.21).

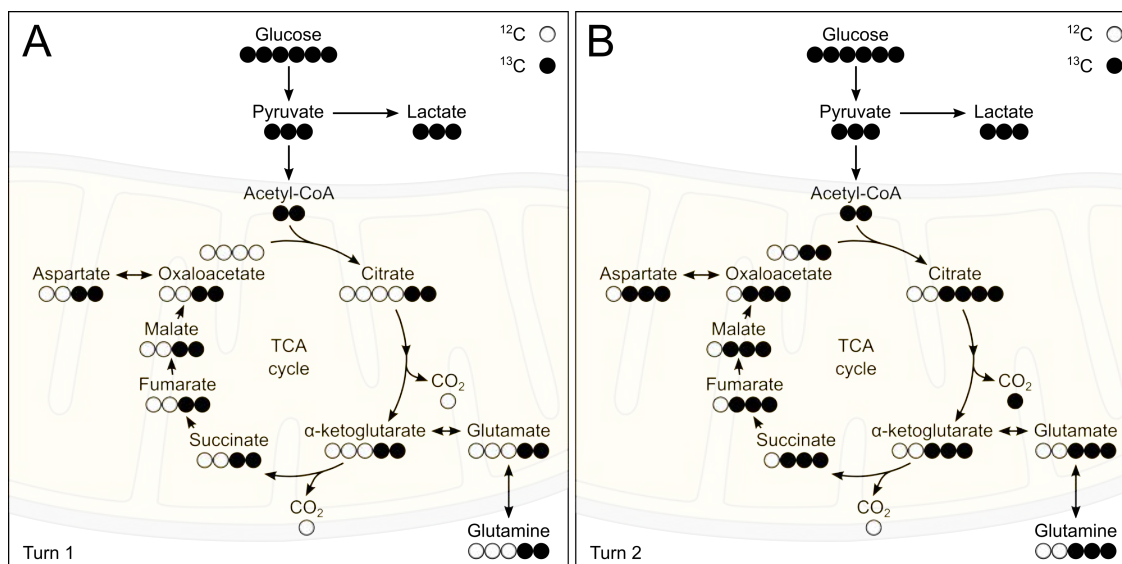


Figure 5.21 – Stable isotope tracing of ^{13}C -glucose in activated T cells

(A) Schematic overview outlining stable isotope tracing of uniformly labelled ^{13}C -glucose into the TCA cycle following (A) one and (B) two cycles. Tracing assessed in anti-CD3 (2 $\mu\text{g}/\text{ml}$) and anti-CD28 (20 $\mu\text{g}/\text{ml}$) activated CD4⁺ T cells treated with or without canagliflozin (10 μM).

Canagliflozin impaired glucose-derived lactate production, as evidenced by reduced levels of the $m + 3$ mass isotopologue of lactate ($p < 0.0001$) and a concomitant increase in the unlabelled $m + 0$ mass isotopologue ($p < 0.0001$; Figure 5.22A). Indeed, canagliflozin reduced the total abundance of heavy-labelled lactate ($p = 0.0286$; Figure 5.22B), which is consistent with our previous experiments highlighting reduced glycolysis in canagliflozin-treated T cells (see Chapter 5.3.2).

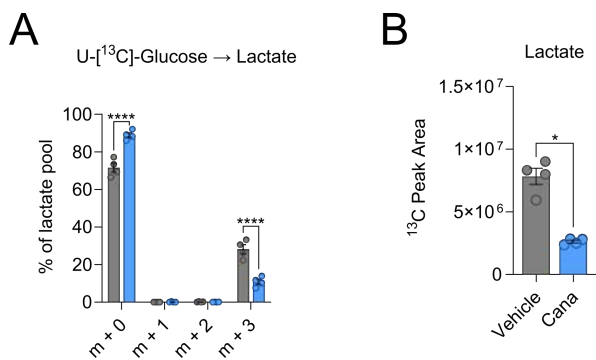


Figure 5.22 – Canagliflozin limits the incorporation of ¹³C-glucose into lactate

(A) Mass isotopologue distribution, represented as a percentage of pool, of lactate in anti-CD3 (2 µg/ml) and anti-CD28 (20 µg/ml) activated CD4+ T cells treated with or without canagliflozin (10 µM). Numbers on the x-axis represent the number of 13-carbons incorporated. Data are representative of four independent experiments. Statistical analysis was performed using a two-way ANOVA followed by Šidák's multiple comparisons test (A) or a non-parametric Mann-Whitney test (B). Data expressed as mean ± SEM; * $p \leq 0.05$. **** $p < 0.0001$.

Interestingly, T cells treated with canagliflozin increased the incorporation of ¹³C-glucose into the TCA cycle compared to the vehicle control, whereby there was an increase in the abundance of heavy-labelled mass isotopologues, and a reduction in the abundance of unlabelled metabolites (Table 5.3; Figure 5.23).

Table 5.3 – p -values of ¹³C₆-glucose-derived mass isotopologues for vehicle versus canagliflozin

Metabolite	m + 0	m + 1	m + 2	m + 3	m + 4	m + 5	m + 6
Citrate	0.6381	0.9826	0.9939	> 0.9999	> 0.9999	> 0.9999	> 0.9999
α-KG	0.0019	0.9951	0.1236	0.9030	0.9318	> 0.9999	-
Fumarate	0.0090	0.9394	0.9394	> 0.9999	0.3553	-	-
Malate	< 0.0001	0.6252	0.0044	0.2279	0.9542	-	-
Glutamate	< 0.0001	0.9998	< 0.0001	0.1024	0.1367	0.9721	-
Aspartate	< 0.0001	0.5048	0.0003	0.0253	0.8814	-	-

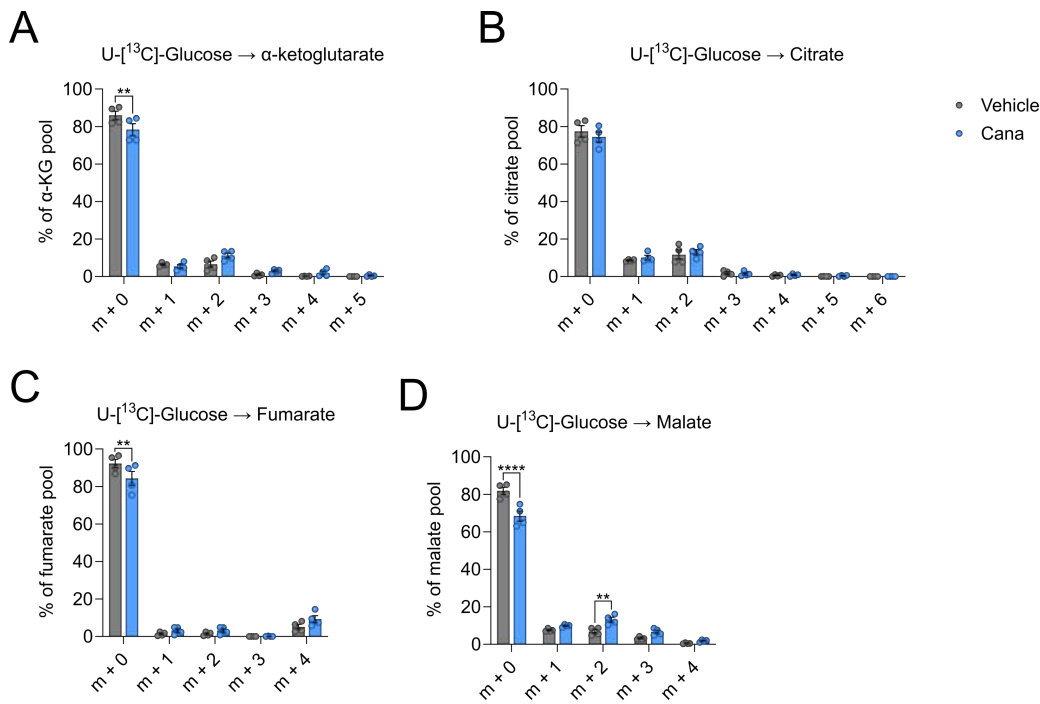


Figure 5.23 – Canagliflozin-treated T cells adapt to glutamate dehydrogenase inhibition by becoming reliant on glucose-derived TCA cycle intermediates

(A-D) Mass isotopologue distribution, represented as a percentage of pool, of TCA cycle metabolites: (A) α-ketoglutarate, (B) citrate, (C) fumarate and (D) malate in anti-CD3 (2 μg/ml) and anti-CD28 (20 μg/ml) activated CD4⁺ T cells treated with or without canagliflozin (10 μM). Numbers on the x-axis represent the number of ¹³-carbons incorporated. Data are representative of four independent experiments. Statistical analysis was performed using a two-way ANOVA followed by Šidák's multiple comparisons test. Data expressed as mean ± SEM; ** $p \leq 0.01$, **** $p < 0.0001$.

Moreover, there was a striking increase in the incorporation of ¹³C-glucose into glutamate and aspartate amino acid metabolite pools (Table 5.3; Figure 5.24).

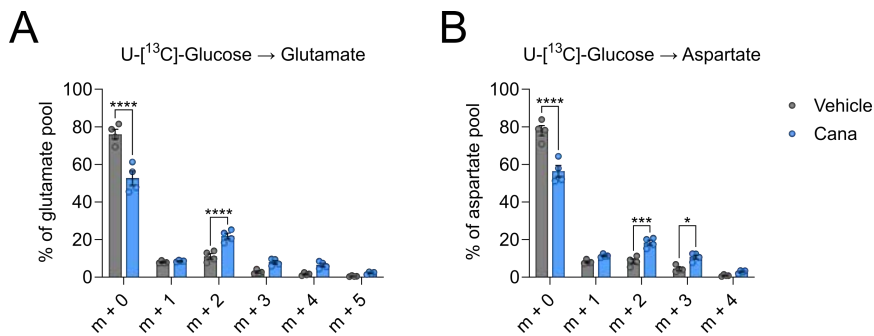


Figure 5.24 – Increased glucose incorporation into amino acids pools in activated T cells treated with canagliflozin

(A) Mass isotopologue distribution, represented as a percentage of pool, of amino acids: (A) glutamate and (B) aspartate in anti-CD3 (2 µg/ml) and anti-CD28 (20 µg/ml) activated CD4+ T cells treated with or without canagliflozin (10 µM). Numbers on the x-axis represent the number of 13-carbons incorporated. Data are representative of four independent experiments. Statistical analysis was performed using a two-way ANOVA followed by Šidák's multiple comparisons test. Data expressed as mean ± SEM; * $p \leq 0.05$, *** $p \leq 0.001$, **** $p < 0.0001$.

Surprisingly, when non-zero mass isotopologue distributions were merged, there was a reduction in the incorporation of glucose-derived carbon into T cell metabolites upon canagliflozin treatment ($p = 0.0687$; Figure 5.25A). However, in terms of TCA cycle metabolites, there was a general increase in ¹³C-glucose incorporation, yet this was only significant for malate, glutamate and aspartate (citrate: $p = 0.9767$; α-KG: $p = 0.3362$; fumarate: $p = 0.3014$; malate: $p = 0.0121$; glutamate: $p < 0.0001$; aspartate: $p = 0.0001$; Figure 5.25B). Collectively, these data suggest that GDH inhibition by canagliflozin rewires activated T cell metabolism, promoting the utilisation of glucose within the TCA cycle, and for the production of associated amino acids.

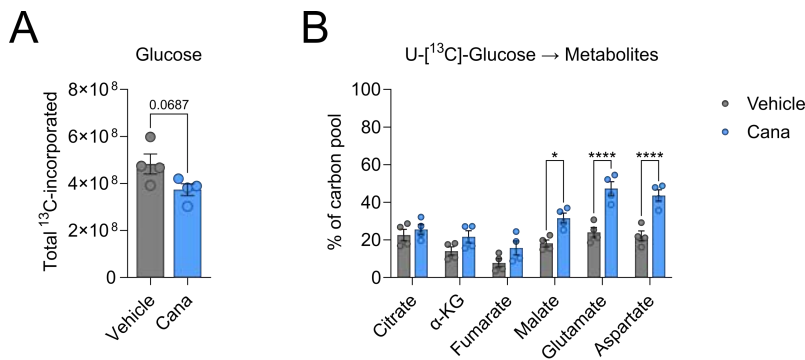


Figure 5.25 – Canagliflozin promotes the incorporation of glucose-derived 13-carbon into metabolic intermediates in activated T cells

(A) Total incorporation of ¹³C-glucose into metabolites of anti-CD3 (2 μg/ml) and anti-CD28 (20 μg/ml) activated CD4+ T cells treated with or without canagliflozin (10 μM). (B) Abundance of ¹³C-glucose derived metabolites: citrate, α-ketoglutarate, fumarate, malate, glutamate and aspartate, represented as a percentage of the total carbon pool. Data are representative of four independent experiments. Statistical analysis was performed using a two-way ANOVA followed by Šidák's multiple comparisons test. Data expressed as mean ± SEM; * $p \leq 0.05$, **** $p < 0.0001$.

5.3.5 Canagliflozin-driven T cell dysregulation is not solely driven by inhibition of complex I and glutamate dehydrogenase

To determine whether the impact that canagliflozin has on T cell function can be explained by inhibition of mitochondrial complex I, we compared canagliflozin to known inhibitors of complex I. Accordingly, CD4+ T cells were activated in the presence of canagliflozin, rotenone or metformin. Importantly, given that the primary metformin transporter (SLC22A1) is not readily expressed by T cells (Uhlen et al., 2019)(Human Protein Atlas, *proteinatlas.org*), high-dose metformin was used to bypass any transporter specific uptake. Canagliflozin was the superior inhibitor of T cell function, significantly reducing IFN γ production by activated CD4+ T cells (Table 5.4; Figure 5.26A). This was underpinned by a more pronounced reduction in CD69 expression and cell size by canagliflozin in comparison to rotenone and metformin (Table 5.4; Figure 5.26B-C).

Table 5.4 – Canagliflozin is a superior inhibitor of T cell function versus other complex I inhibitors

Comparison	<i>p</i> -value compared to vehicle control		
	Canagliflozin	Rotenone	Metformin
IFN γ	0.0073	0.0747	0.3099
CD69	0.0104	0.0205	0.0144
FSC-A	0.0090	0.0349	0.0538

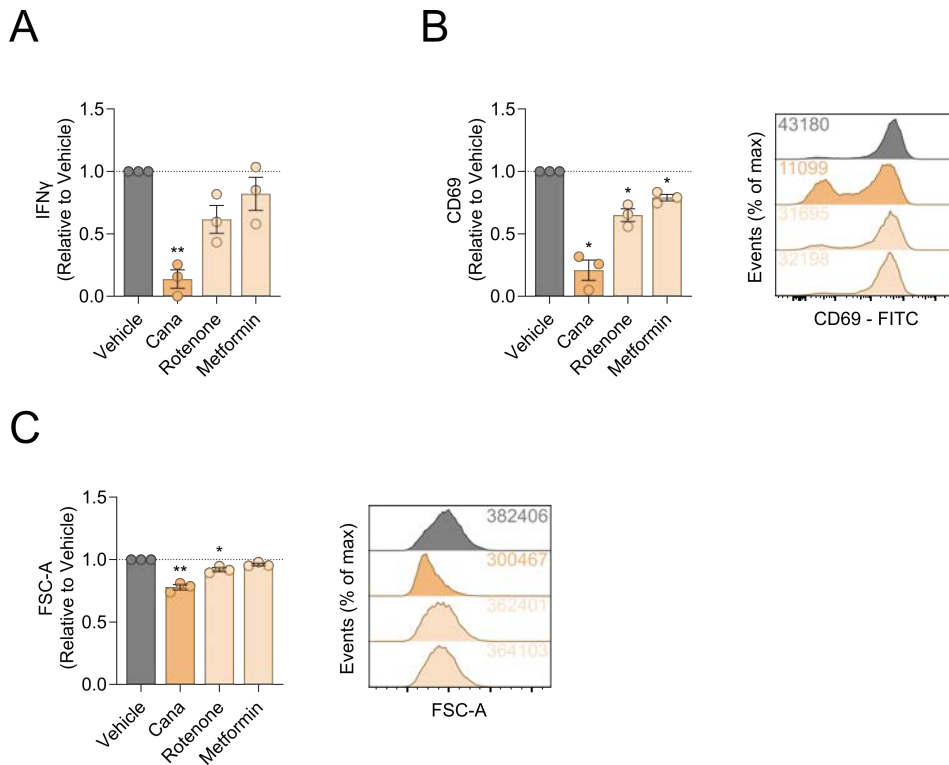


Figure 5.26 – Canagliflozin is a superior inhibitor of T cell function compared to other mitochondrial complex I inhibitors

(A) Relative secretion of IFN γ by anti-CD3 (2 μ g/ml) and anti-CD28 (20 μ g/ml) activated CD4+ T cells in the presence and absence of canagliflozin (10 μ M), rotenone (1 μ M) or metformin (10 mM), determined by ELISA of cell-free supernatants. (B) Relative expression of activation marker CD69, determined by flow cytometry. (C) Blastogenesis, determined by flow cytometry using forward-scatter area. Representative overlaid histogram plots, numbers indicate median fluorescence intensity or forward-scatter area. Data are representative of three independent experiments. Statistical analysis was performed using a one-sample T test. Data expressed as mean \pm SEM; * $p \leq 0.05$, ** $p \leq 0.01$.

Given these findings, we next investigated whether combined inhibition of complex I and GDH underpins the phenotype observed following canagliflozin treatment. To this end, CD4+ T cells were activated in the presence and absence of either canagliflozin, piericidin A (a more potent inhibitor of complex I), R162 (an inhibitor of GDH) or a combination of piericidin A and R162. Here, canagliflozin remained the superior inhibitor of T cell function when compared to GDH inhibition alone, complex I inhibition alone, as well as combined inhibition (Table 5.5; Figure 5.27A). Again, this was underpinned by impaired activation and blastogenesis (Table 5.5; Figure 5.27B-C). Collectively, these data suggest that the inhibition of mitochondrial complex I and GDH are not the sole drivers of canagliflozin-driven T cell dysregulation.

Table 5.5 – Canagliflozin is a superior inhibitor of T cell function versus complex I inhibition and GDH inhibition

Comparison	<i>p</i> -value compared to vehicle control			
	Canagliflozin	R162	Piericidin A	Combination
IFN γ	0.0002	0.6289	0.6239	0.0232
CD69	0.0007	0.2867	0.0080	0.0007
FSC-A	0.0005	0.2326	0.0244	0.0069

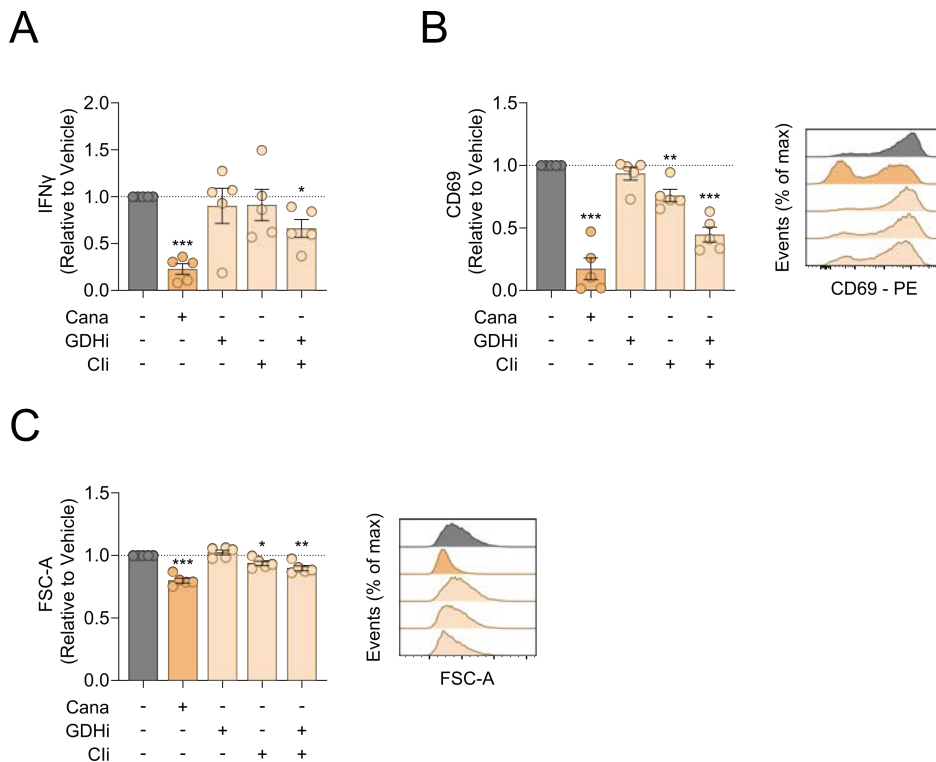


Figure 5.27 – Canagliflozin is a superior inhibitor of T cell function versus combined inhibition of mitochondrial complex I and glutamate dehydrogenase

(A) Relative expression of activation marker CD69 in anti-CD3 (2 $\mu\text{g/ml}$) and anti-CD28 (20 $\mu\text{g/ml}$) activated CD4 $^+$ T cells treated with or without canagliflozin (10 μM), R162 (10 μM), piericidin A (500 nM), determined by flow cytometry. (B) Blastogenesis, determined by flow cytometry using forward-scatter area. Representative overlaid histogram plots. (C) Relative secretion of IFN γ , determined by ELISA of cell-free supernatants. Data are representative of five independent experiments. Data expressed as mean \pm SEM; * $p \leq 0.05$, ** $p \leq 0.01$, **** $p < 0.0001$.

5.3.6 Canagliflozin impairs T cell receptor signalling

We have previously demonstrated that canagliflozin impacts the function of mTOR and MYC – key regulators of T cell metabolism. Given that both signalling proteins are sensitive to the TCR signalling cascade, we sought to investigate the significance of canagliflozin treatment on downstream signalling events following engagement of the TCR. Here, we analysed early signalling events – namely the phosphorylation of PLC γ , ZAP70 and LAT. Canagliflozin inhibited the phosphorylation of all three TCR signalling proteins at all early time points assessed (Figure 5.28).

A

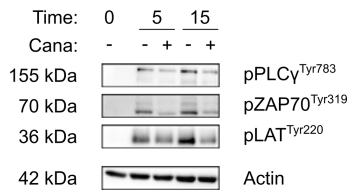
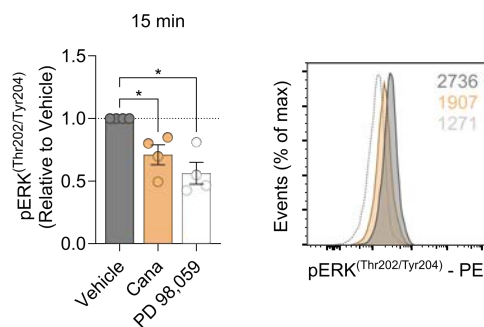


Figure 5.28 – Canagliflozin impairs TCR signalling during early T cell activation

(A) Representative immunoblots of TCR signalling proteins in anti-CD3 (2 µg/ml) and anti-CD28 (20 µg/ml) activated CD4⁺ T cells in the presence and absence of canagliflozin (10 µM). Data are representative of four independent experiments.

We next examined whether the observed loss of early signalling events compromised the phosphorylation of ERK – a critical mediator of T cell activation. Here, 15- and 30-min post-TCR ligation, levels of pERK were significantly reduced upon canagliflozin treatment (15 min: $p = 0.0346$; 30 min: $p = 0.0025$; Figure 5.29). The magnitude of pERK downregulation was comparable to inhibition of MAPK activation directly upstream of ERK by PD-98,059 (15 min: $p = 0.0150$; 30 min: $p = 0.0243$; Figure 5.29).

A



B

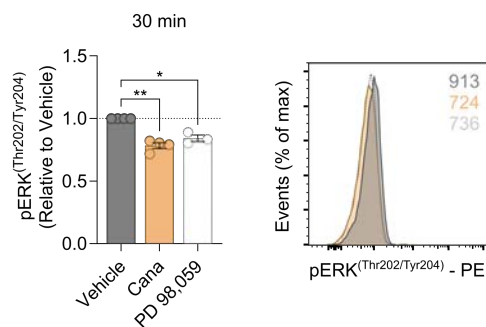


Figure 5.29 – ERK signalling following early T cell activation is impaired following canagliflozin treatment

(A-B) Relative expression of phosphorylated-ERK^{Thr202/Tyr204} in anti-CD3 (2 µg/ml) and anti-CD28 (20 µg/ml) activated CD4⁺ T cells in the presence and absence of canagliflozin (10 µM), determined by flow cytometry (A) 15 min and (B) 30 min post-activation. MAP kinase inhibitor PD-98,059 (25 µM) used as a positive control. Representative overlaid histogram plots, numbers indicate median fluorescence intensity. Data are representative of four independent experiments. Statistical analysis was performed using a one-sample T test. Data expressed as mean ± SEM; * $p \leq 0.05$, ** $p \leq 0.01$.

To determine the downstream effect on T cell activation, we monitored CD69 expression through a course of several early time points. In line with blunted ERK phosphorylation, T cell activation was blunted by canagliflozin as early as 120 min post-treatment (Table 5.6; Figure 5.30).

Table 5.6 – Early T cell activation is compromised following canagliflozin treatment

Time (min)	15	30	60	120
<i>p</i> -value	> 0.9999	> 0.9999	0.3245	0.0096

A

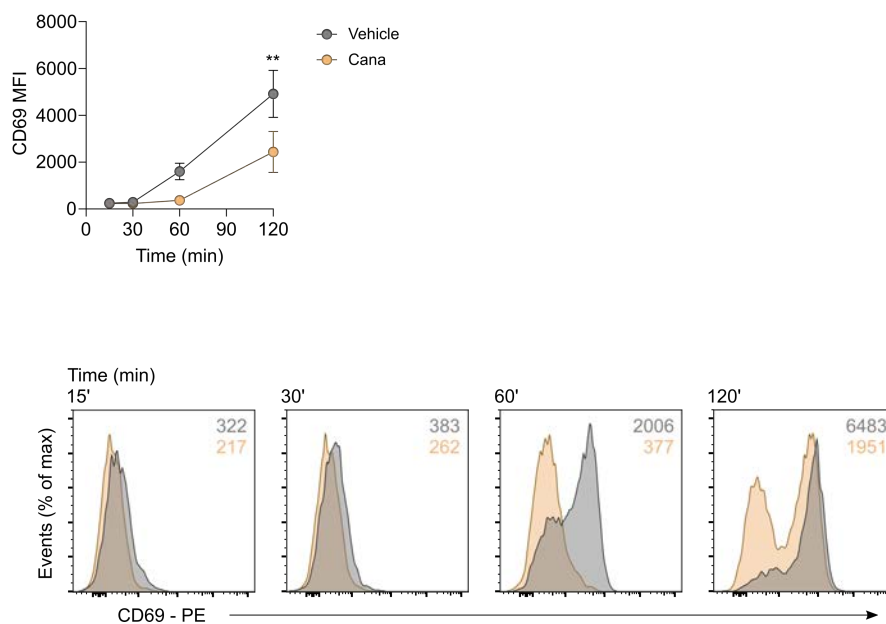


Figure 5.30 – Canagliflozin impairs early T cell activation

(A) Expression of activation marker CD69 in anti-CD3 (2 µg/ml) and anti-CD28 (20 µg/ml) activated CD4⁺ T cells in the presence and absence of canagliflozin (10 µM), determined by flow cytometry. Representative overlaid histogram plots, numbers indicate median fluorescence intensity. Data are representative of three independent experiments. Statistical analysis was performed using a two-way ANOVA followed by Šidák's multiple comparisons test. Data expressed as mean ± SEM; ** *p* ≤ 0.01.

Given the pronounced impact of canagliflozin on early TCR signalling events, we considered the effect that impaired signalling downstream of the TCR might have on effector function. Consequently, we activated T cells with PMA and ionomycin to bypass TCR-dependent activation and engage several of the intracellular pathways further downstream in the signalling cascade. Interestingly, T cells activated with PMA and ionomycin in the presence and absence of canagliflozin displayed no defect IFN γ production – neither in terms of the amount of IFN γ produced ($p = 0.0525$) and the frequency of cells producing IFN γ ($p = 0.1696$), when compared to the vehicle control group (Figure 5.31).

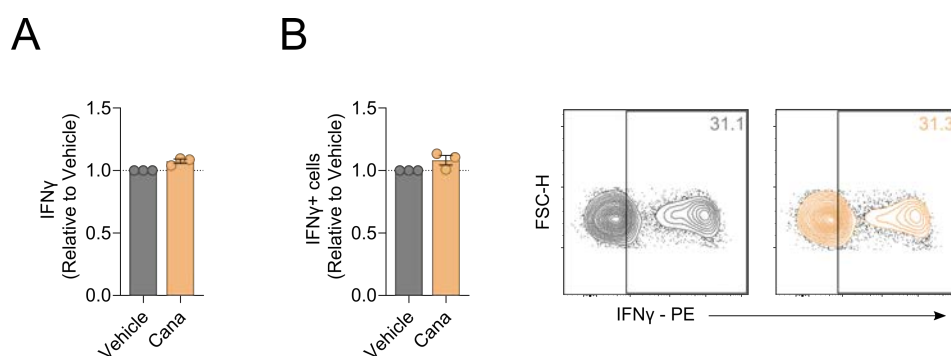


Figure 5.31 – TCR-independent activation rescues cytokine production by canagliflozin-treated T cells

(A) Relative production of IFN γ in 4 h PMA (10 ng/ml) and ionomycin (500 ng/ml) activated CD4+ T cells treated with or without canagliflozin (10 μ M), determined by flow cytometry. (B) Relative frequency of IFN γ -producing CD4+ T cells, as determined by flow cytometry. Representative contour plots, numbers indicate frequency. Statistical analysis was performed using a one-sample T test. Data are representative of three independent experiments. Data expressed as mean \pm SEM.

Since canagliflozin dysregulates intracellular signalling mediated by critical nodes including ERK and mTOR, we hypothesised that canagliflozin treatment would phenocopy targeted inhibition of either ERK and mTOR. To this end, T cells were activated in the presence and absence of canagliflozin, rapamycin (mTOR inhibitor) and PD-98,059 (MAPK inhibitor) before assessing effector function. Here – as early as 4 h post-activation – canagliflozin reduced MYC expression to a similar extent as both mTOR inhibition and ERK inhibition (Figure 5.32).

A

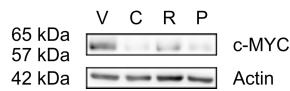
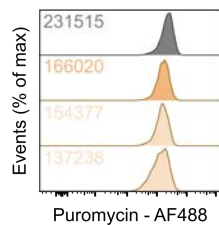
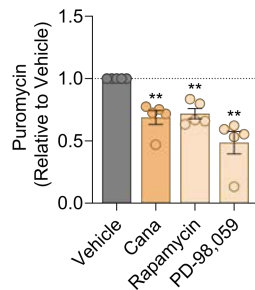


Figure 5.32 – Canagliflozin impairs MYC expression in a similar manner to mTOR inhibition and ERK inhibition

(A) Representative immunoblots of MYC in anti-CD3 (2 $\mu\text{g}/\text{ml}$) and anti-CD28 (20 $\mu\text{g}/\text{ml}$) activated CD4⁺ T cells treated with and without canagliflozin (10 μM), rapamycin (R; 500 nM) or PD-98,059 (P; 25 μM). Data are representative of four independent experiments.

Additionally, global protein translation – as measured by puromycin incorporation – was similarly inhibited by canagliflozin, rapamycin and PD-98,059 at this early time point (canagliflozin: $p = 0.0049$; rapamycin: $p = 0.0023$; PD-98,059: $p = 0.0046$; Figure 5.33A). However, T cell blastogenesis was only modestly affected following 4 h treatment with canagliflozin, rapamycin or PD-98,059 (canagliflozin: $p = 0.0198$; rapamycin: $p = 0.0293$; PD-98,059: $p = 0.0162$; Figure 5.33B).

A



B

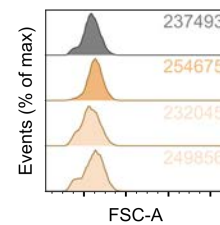
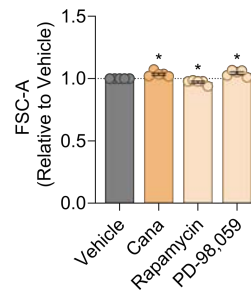


Figure 5.33 – Canagliflozin phenocopies mTOR inhibition and ERK inhibition during early T cell activation

(A) Relative puromycin incorporation in 4 h anti-CD3 (2 $\mu\text{g}/\text{ml}$) and anti-CD28 (20 $\mu\text{g}/\text{ml}$) activated CD4⁺ T cells treated with or without canagliflozin (10 μM), rapamycin (500 nM) or PD-98,059 (25 μM), determined by flow cytometry. Puromycin (10 μM) was introduced for the final 15 min of culture. (B) Blastogenesis, determined by flow cytometry using forward-scatter area. Representative overlaid histogram plots, numbers indicate median fluorescence intensity or forward-scatter area. Data are representative of five independent experiments. Statistical analysis was performed using a one-sample T test. Data expressed as mean \pm SEM.

When measuring the same functions 24 h post-activation, canagliflozin continued to phenocopy both the inhibition of mTOR and the inhibition of ERK, with similar reductions in protein translation (canagliflozin: $p = 0.0131$; rapamycin: $p = 0.0004$; PD-98,059: $p = 0.0132$; Figure 5.34A) and blastogenesis (canagliflozin: $p = 0.0001$; rapamycin: $p < 0.0001$; PD-98,059: $p = 0.0034$; Figure 5.34B). Furthermore, effector function was similarly impaired by all three conditions, whereby canagliflozin, rapamycin and PD-98,059 significantly limited IFN γ production (all $p < 0.0001$; Figure 5.34C). Together, these data demonstrate that mechanistically, canagliflozin impairs TCR signalling, which subsequently suppresses signalling through downstream metabolic nodes. Moreover, our data support that the observed reduction in MYC expression is mediated by the upstream inhibition of mTOR and ERK signalling via this mechanism.

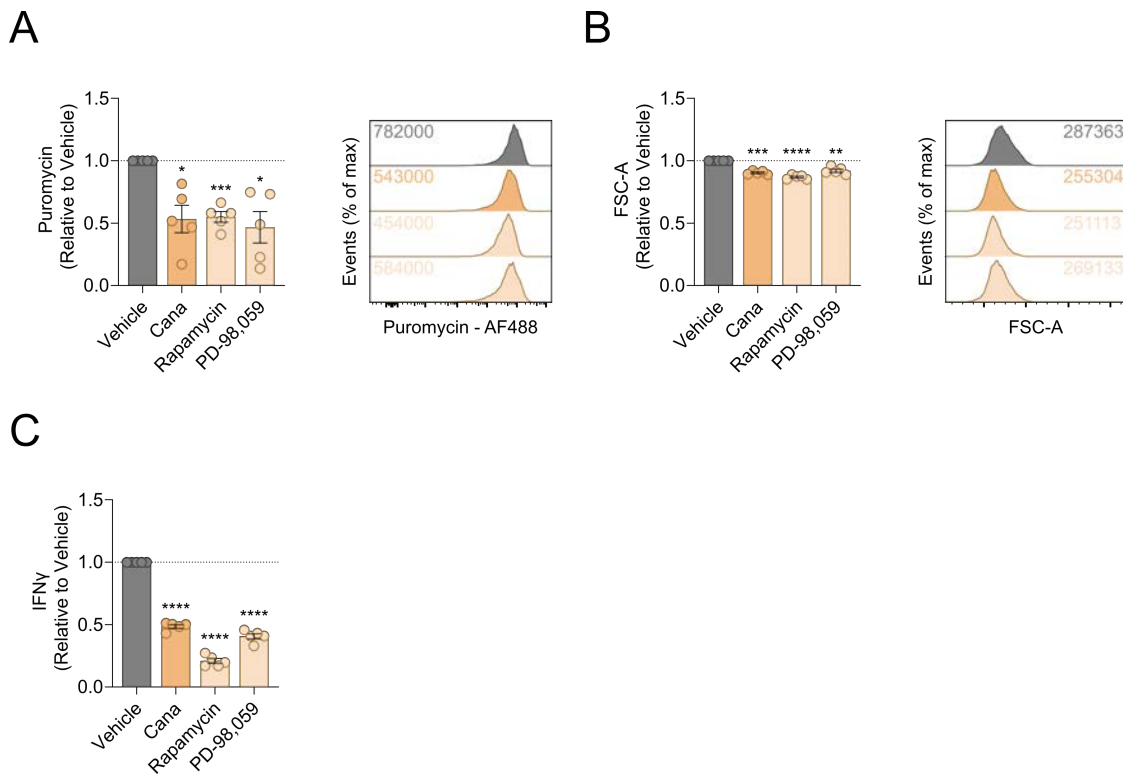


Figure 5.34 – Canagliflozin impairs T cell function in a similar manner to mTOR inhibition and ERK inhibition

(A) Relative puromycin incorporation in 24 h anti-CD3 (2 μ g/ml) and anti-CD28 (20 μ g/ml) activated CD4⁺ T cells treated with or without canagliflozin (10 μ M), rapamycin (500 nM) or PD-98,059 (25 μ M), determined by flow cytometry. Puromycin (10 μ M) was introduced for the final 15 min of culture. (B) Blastogenesis, determined by flow cytometry using forward-scatter area. Representative overlaid histogram plots, numbers indicate median fluorescence intensity or forward-scatter area. (C) Relative secretion of IFN γ , determined by ELISA of cell-free supernatants. Data are representative of five independent experiments. Statistical analysis was performed using a one-sample T test. Data expressed as mean \pm SEM.

5.4 Discussion

Elucidating the underlying mechanisms that mediate the inhibitory effects of canagliflozin is required for our understanding of how global T cell function is impaired. Initially, mitochondrial function was scrutinised, given the known off-target effects that canagliflozin imposes on mitochondrial proteins complex I and GDH. Interrogation of our proteomics dataset revealed upregulation of several electron transport chain complex-associated proteins following canagliflozin treatment. Interestingly, mitochondrial complex I

– the electron transport chain complex specifically inhibited by canagliflozin – was associated with the most changes with 18 associated proteins upregulated. In support of these data, our immunoblotting analysis further confirmed upregulation of all mitochondrial complex proteins, whilst a previous study in hepatocellular carcinoma cells has also described increased expression of several mitochondrial complex proteins (Nakano et al., 2020). This might suggest that in response to canagliflozin-induced inhibition of complex I, T cells upregulate mitochondrial complex proteins to compensate the loss of electron transport chain function. Indeed, our earlier ingenuity pathway analysis on our proteomic dataset revealed that *oxidative phosphorylation* was one of the predominant upregulated pathways. Collectively, this led to increased mitochondrial biogenesis within T cells treated with canagliflozin, with no significant effect on mitochondrial membrane potential. An alternative hypothesis could be that canagliflozin-treated T cells double their mitochondrial content in preparation for cell division but later fail to divide.

In other cell types, both inhibition of mitochondrial complex I (Li et al., 2003) and increased mitochondrial biogenesis (Dugan et al., 2013) have been associated with increased production of ROS. Canagliflozin rapidly induced the production of mitoROS, with elevated levels compared to the vehicle control as early as 15 min following treatment, remaining elevated at all further time points measured. The production of mitoROS was measured by flow cytometry using the mitochondrial superoxide indicator mitoSOX™ Red – which is a mitochondria-targeted hydroethidine dye. There are some limitations to consider when using this technique, whereby the fluorescence detected could be misleading due to the overlapping spectra of the non-specific oxidation product ethidium, and the superoxide-specific product 2-hydroxyethidium, that the probe can form (Murphy et al., 2022). As a result, it is difficult to differentiate between the contribution of non-specific and superoxide-specific oxidation to the fluorescence measured (Murphy et al., 2022). Furthermore, mitochondrial properties such as membrane potential and mass should also be considered (Murphy et al., 2022). Future experiments involving compounds that specifically heighten mitochondrial superoxide formation as per Murphy et al. (2022) could confirm downstream findings to support our conclusions. In agreement with the increased mitoROS observed following canagliflozin treatment, our proteomics dataset revealed that several antioxidant proteins involved in the response to ROS are upregulated. It was interesting to note that most of these proteins were either the mitochondrial isoform of the protein or were at least

associated with the mitochondria in some capacity, which supports the belief that enhanced ROS production within canagliflozin-treated T cells is localised to the mitochondria following complex I inhibition. In contrast to our findings, a previous study showed that canagliflozin inhibits ROS production in a human macrophage cell line (Xu et al., 2018). Therefore, further work is required to determine whether: (i) antioxidant proteins are upregulated to compensate the increase in mitoROS; or (ii) antioxidant proteins are upregulated by canagliflozin independent of ROS production, but not to sufficient levels to prevent the increase observed increase in mitoROS. Interestingly, recent work in human-umbilical-vein endothelial cells showed that NADPH pools were reduced by canagliflozin (Zugner et al., 2022). This could indicate that either canagliflozin affects the cells' ability to regulate ROS, or that NADPH levels are already depleted in response to increased ROS levels.

We attempted to rescue the observed phenotype using GSH and NAC to buffer mitoROS. Here, supplementing cell cultures with GSH and NAC partially rescued suppression of T cell activation and blastogenesis. Previously, GSH has been shown to support the activity of both mTOR and MYC in T cells by regulating intracellular ROS (Mak et al., 2017). In our rescue experiments, supplementation with GSH and NAC increased the expression of CD98 – a known downstream target of mTOR – which might suggest that buffering mitoROS might partially mitigate the canagliflozin-induced disruption of the mTOR/MYC axis. Despite partial rescue of T cell activation, GSH and NAC did not rescue effector function, therefore changes more critical than ROS accumulation must regulate the loss of T cell function upon canagliflozin treatment. Whilst ROS are required in early T cell activation and signal transduction, excessive levels can have deleterious effects on metabolic reprogramming through the mTOR/MYC axis, resulting in inflammation (Mak et al., 2017). Consequently, downstream metabolism was paralysed. Phosphorylation of S6 protein was downregulated – either via p90 ribosomal S6 kinase (RSK) as a direct result of ERK inhibition, or through downstream inhibition of mTOR activity – alongside phosphorylation of the mTORC1 target 4E-BP1. However, there appeared to be no change in AMPK activity.

Given the mitochondrial dysfunction observed in response to canagliflozin, elucidating the metabolic changes that occur within T cells is critical for our understanding of changes in effector function. Extracellular flux analysis is a technique that allows study of metabolic pathways within cells, where the oxygen consumption rate and extracellular acidification rate monitored can be used as measures of oxidative phosphorylation and glycolysis, respectively.

Here, canagliflozin limited both the basal and maximal rates of glycolysis, reducing the joules of ATP produced by this pathway. In terms of their oxidative metabolism, canagliflozin had a more modest impact, whereby the maximal respiratory capacity and spare respiratory capacity were most affected. Consequently, there was a modest reduction in the joules of ATP produced from this pathway at basal rates, becoming more pronounced when the pathway is at its maximal rate. Together, canagliflozin-treated T cells display an oxidative phenotype resembling metabolic quiescence. It is interesting that canagliflozin appears to have a more profound effect on glycolytic metabolism, given that it inhibits mitochondrial complex I directly involved in OXPHOS, which might emphasise the impact that the loss of MYC expression has on glycolysis. Indeed, upon T cell activation, MYC controls metabolic reprogramming by promoting a switch from oxidative metabolism towards glycolytic and glutaminolytic-based metabolism (Wang et al., 2011). Metabolic reprogramming following activation is essential to provide the energy necessary for appropriate effector function (see Chapter 1.3.6), therefore it is unsurprising that the reduced bioenergetic scope of canagliflozin-treated T cells, particularly at maximal rates of metabolism, underpins defective cytokine production and proliferation. In concert with these data, the upregulation of electron transporter chain complex protein in response to canagliflozin treatment could be interpreted in several ways: (i) it is a compensatory mechanism that occurs in response to reduced OXPHOS; (ii) it protects OXPHOS from as profound an inhibition as glycolysis; or (iii) it is indicative of reprogramming towards a more oxidative phenotype associated with metabolic quiescence. Crucially, to ensure changes in metabolism were independent of SGLT2 inhibition, dapagliflozin was also included in our metabolic analysis, where it had no obvious effect on any of the metabolic parameters measured, indicating that the off-target effects of canagliflozin orchestrate changes in OXPHOS and glycolysis.

Since metabolism is rewired in T cells following canagliflozin, it was important to understand how different metabolites are utilised for energy production. The abundance of several TCA cycle metabolites – citrate, α -ketoglutarate, fumarate and malate – were all reduced by canagliflozin. However, amino acid (glutamate and aspartate) and lactate levels appeared to be unchanged. Stable isotope tracer analysis was subsequently employed, whereby T cells were cultured with or without canagliflozin in medium containing metabolites labelled with carbon-13. The difference in mass is detected by mass spectrometry, especially when heavy-labelled carbons become incorporated into the metabolites of pathways such as

glycolysis and the TCA cycle, the distribution of carbon-12 and carbon-13 within each metabolite gives us information on the flux through these pathways. Glutamine is required for successful T cell activation and function (Carr et al., 2010). When used to fuel the TCA cycle, glutamine is converted to α -ketoglutarate via a process called glutaminolysis, which involves a series of reactions catalysed by glutaminase and GDH. Given that canagliflozin inhibits GDH – the final step before entry into the TCA cycle – it was important to assess glutamine utilisation by following the incorporation of glutamine-derived carbon-13 into the TCA cycle and beyond. As expected, canagliflozin impaired the incorporation of glutamine-derived carbons into α -ketoglutarate, indicating impaired entry of glutamine into the TCA cycle via glutaminolysis. Indeed, this was confirmed by reduced incorporation of glutamine-derived into other metabolites of the TCA cycle, including citrate, fumarate and malate. Additionally, fewer glutamine-derived carbons were incorporated into the amino acids, glutamate and aspartate. Together, canagliflozin reduced the incorporation of glutamine into T cell metabolite pools, particularly impairing glutamine anaplerosis within the TCA cycle. Our data also suggested that glutamine uptake might be impaired by canagliflozin, whereby there was a reduction in the total abundance of ^{13}C -glutamine within T cells. This is consistent with our proteomics dataset (see Chapter 4.3.3), wherein T cells failed to upregulate amino acid transporters upon activation, notably SLC1A5 which is associated with glutamine uptake. Additionally, a concomitant decrease in ^{13}C - α -ketoglutarate abundance, alongside an unchanged abundance of ^{13}C -glutamate, further supports that glutamine entry into the TCA cycle is blocked, where it accumulates as glutamate prior to the final step of glutaminolysis. Interestingly, supplementation with a membrane-permeable analogue of α -ketoglutarate failed to rescue any aspect of T cell function.

Changes in glucose metabolism are also necessary upon T cell activation (Frauwirth et al., 2002). Glucose mobilisation through metabolic pathways was again monitored through the incorporation of glucose-derived carbon-13 into glycolytic metabolites and the TCA cycle. Here, canagliflozin reduced the incorporation of glucose into lactate, which is in agreement with our extracellular flux analysis, whereby glycolysis is impaired. Interestingly, glucose incorporation into the TCA cycle and its associated amino acids was increased by canagliflozin, compensating for the reduced incorporation of glutamine-derived carbon. Increased aspartate pools were of particular interest, given that aspartate deficiency in T cells has recently been associated with increased TNF α production and subsequent tissue

inflammation in autoimmune disease (Wu et al., 2021). These data suggest that canagliflozin-treated T cells demonstrate plasticity in glucose metabolism, promoting glucose anaplerosis within the TCA cycle to compensate for GDH inhibition.

The importance of mitochondrial complex I inhibition for canagliflozin-induced inhibition of T cell function was determined by comparing the effects of canagliflozin to rotenone and metformin, known inhibitors of complex I. High-dose metformin was used to bypass transporter specific uptake, as T cells lack the transporter responsible for metformin uptake (SLC22A1) (Uhlen et al., 2019)(Human Protein Atlas, *proteinatlas.org*). Canagliflozin was superior to both rotenone and metformin in inhibiting T cell activation and function, which would suggest that the dual inhibition of both mitochondrial complex I and GDH mediates the inhibitory effects of canagliflozin. However, despite inhibiting T cell function to a greater extent than complex I inhibition alone, combined inhibition of complex I and GDH remained inferior to the inhibitory effects of canagliflozin. These data would suggest that the inhibitory effect of canagliflozin is mediated by additional factors beyond inhibition of mitochondrial complex I and GDH. In particular, impaired protein translation through impaired expression of the protein translational machinery is likely challenging to reverse, given the energy demand required for these processes. Indeed, these additional factors are likely related to disruption of the mTOR/MYC axis. Despite displaying inferior inhibition of T cell function, metformin has already demonstrated exciting results in pre-clinical and clinical settings of MS, SLE and RA (Gharib et al., 2021; Negrotto et al., 2016; Sun, Geng, et al., 2020). In human T cells, it appears that metformin mediates its anti-inflammatory effects by reprogramming the underlying metabolism (Yin et al., 2015). This is an exciting precedent in terms of repurposing canagliflozin in autoimmune disease, given that it has shown improved anti-inflammatory properties over metformin in our *in vitro* experiments. However, it is important that the inhibitory effects are targeted specifically to the hyperactivated T cells that contribute to chronic inflammation in disease pathogenesis.

As mTOR and MYC are upregulated in response to the downstream signals of TCR-mediated activation, we hypothesised that this cascade might be impaired by canagliflozin. Consequently, early signalling events were analysed in canagliflozin-treated T cells, where reduced phosphorylation of several key nodes – PLC γ , ZAP70 and LAT – was observed. Therefore, several components involved in early activation were monitored – CD69 expression was downregulated as early as 2 h following treatment, preceded by reduced

upstream ERK phosphorylation. This demonstrated that early TCR signalling is impaired by canagliflozin, which is further supported by the reduction in CD25 expression at 24 h (see Chapter 3.3). To confirm the importance of these findings, T cells were activated independent of TCR ligation using the DAG mimetic PMA and the calcium ionophore ionomycin, to determine whether bypass of the affected early signalling events rescued effector function. Excitingly, IFN γ production was not affected by canagliflozin in PMA/ionomycin-activated T cells, highlighting that inhibition of early signalling events downstream of the TCR significantly impacts on key intracellular metabolic nodes that are sensitive to this pathway. Given that we have previously outlined dysregulation of mTOR and ERK following canagliflozin treatment (see Chapters 4.3.3 and 5.3.6), we aimed to confirm these findings by using known inhibitors rapamycin and PD-98,059 (inhibits MAPK kinase directly upstream of ERK), respectively. Canagliflozin phenocopied inhibition of both nodes, with similar defects in MYC expression, protein translation and effector function observed in all three conditions. Collectively, these data suggest that mechanistically, canagliflozin impairs TCR signalling leading to suppressed signalling through metabolic nodes. Furthermore, our data indicate that MYC protein expression is downstream of ERK and mTOR signalling in human T cells.

5.5 Conclusions

The work in this chapter outlines the mitochondrial dysfunction induced by canagliflozin to support impaired T cell metabolism. Previous chapters have shown that canagliflozin inhibits T cell activation and function, mediated by global changes across the proteome. Here, the mechanisms underlying these changes were investigated, focusing on the inhibition of mitochondrial complex I and GDH. Canagliflozin increased mitochondrial biogenesis, and together with complex I inhibition this has previously been associated with ROS production. Indeed, canagliflozin rapidly promoted the accumulation of mitoROS. GSH and NAC were used to buffer mitoROS, and partially rescued T cell activation following canagliflozin treatment, yet their effector function remained impaired. Mitochondrial dysfunction also impaired the expression of metabolic targets downstream of mTOR.

Canagliflozin-induced changes in T cell activation and function are underpinned by perturbed metabolism. Glycolysis was limited by canagliflozin, reducing the ATP produced

from this pathway, whilst a reduced capacity for oxidative respiration resulted in limited ATP production from OXPHOS. Thus, canagliflozin retains T cells in a metabolically quiescent state. Given the metabolic reprogramming that occurs in T cells upon canagliflozin treatment, stable isotope tracer analysis was used to monitor changes in substrate utilisation. As expected, the incorporation of glutamine into the TCA cycle was impaired by canagliflozin-mediated inhibition of GDH, however, the plasticity of their glucose metabolism allowed these cells to promote glucose incorporation into the TCA cycle to try and compensate for the loss of glutamine-derived carbon. Supplementation of α -ketoglutarate had no effect on T cell activation and function.

Comparison of canagliflozin with other known mitochondrial complex I inhibitors – rotenone and metformin – demonstrated that canagliflozin was superior in inhibiting T cell activation and function. Additionally, combined inhibition of complex I and GDH failed to match the inhibitory function of canagliflozin. The mechanistic action of canagliflozin was revealed, whereby early TCR signalling events are impaired by canagliflozin. Phosphorylation of PLC γ , ZAP70 and LAT was limited through all early time points, subsequently limiting downstream phosphorylation of ERK, inhibiting early T cell activation. Bypass of TCR-mediated signalling was sufficient to rescue the effector function of canagliflozin. This pathway is important in canagliflozin-mediated inhibition of metabolic nodes. Indeed, canagliflozin treatment phenocopied mTOR inhibition and ERK inhibition in the context of MYC expression and several downstream effector functions. Further work was undertaken to determine whether canagliflozin maintains its inhibitory function in more biologically relevant scenarios. This included analysis the impact of canagliflozin on Teff cells – the primary mediators of inflammation in autoimmune disease – and T cells isolated from two autoimmune patient cohorts.

Chapter Six

Canagliflozin inhibits T cell function in systemic lupus erythematosus and rheumatoid arthritis

6 Canagliflozin inhibits T cell function in systemic lupus erythematosus and rheumatoid arthritis

6.1 Introduction

Many autoimmune diseases are characterised by dysregulated T cell function, including rheumatoid arthritis (RA) and systemic lupus erythematosus (SLE). Generally, pathogenic immune responses in these conditions are driven by the hyperactivated, proinflammatory function of CD4⁺ T cell populations, which subsequently promotes the activation of other immune cell types. Despite sharing this overarching pathway for autoimmunity, there are slight differences in the CD4⁺ T cells that contribute to chronic inflammation in each condition (see Chapter 1.4). For example, inflammation within the synovium of RA patients is primarily induced by the proinflammatory function of Th1 and Th17 cells. Initially, the abundance of IFN γ -producing CD4⁺ T cells within the synovial tissue of RA patients was thought to be the main driver of inflammation through the activation of immune cell populations including macrophages (Dolhain et al., 1996; Maruotti et al., 2007). Whilst the presence of IL-17 within the synovial fluid had already been established in early studies (Chabaud et al., 1998), only later was the proinflammatory function of synovium-infiltrating, IL-17-producing CD4⁺ T cells elucidated. Th17 cells are enriched within the inflamed synovium, where they: (i) produce well-known mediators of RA pathogenesis (TNF α , lymphotoxin- β) alongside their classic effector cytokines (IL-17, IL-22) (Pene et al., 2008); and (ii) promote the tissue-destructive function of synovial fibroblasts (van Hamburg et al., 2011). Meanwhile, SLE presents as a predominantly Th17-driven condition. Compared to healthy controls, the number of circulating Th17 cells is significantly increased in SLE patients (Wong et al., 2008). Patient-derived CD4⁺ T cells express higher surface levels of TLR2, wherein stimulation through this signalling pathway enhances the production Th17-associated cytokines such as IL-6, IL-17 and TNF α (Liu et al., 2015). However, autoantibodies play an important role in most autoimmune conditions, therefore it is unsurprising that the number and function of T follicular helper (Tfh)-like cells is augmented in both RA (Rao et al., 2017) and SLE (Wang et al., 2014). In addition, effector T cell populations from inflamed tissues exhibit increased resistance to Treg cell-mediated suppression than their counterparts in healthy controls (van Amelsfort et al., 2004; Vargas-Rojas et al., 2008). Although there are

similarities in the observed changes to CD4+ T cell function, there are distinct mechanisms by which they arise in each condition.

Recent work has unearthed some of the immunometabolic changes that underpin disease pathogenesis in T cell-mediated autoimmune diseases. However, the changes that occur are not common across this entire class of autoimmune disease, with instead disease-specific changes to T cell metabolism being revealed. For example, in rheumatoid arthritis (RA), glucose is diverted from glycolysis into the pentose phosphate pathway (PPP), which subsequently fuels augmented lipid metabolism to drive the hyperproliferative and proinflammatory phenotype of pathogenic T cells (Shen et al., 2017; Yang et al., 2016). Additionally, the reduced glycolytic capacity of arthritogenic T cells limits downstream oxidative phosphorylation (OXPHOS), where these cells are also associated with other perturbations in mitochondrial function (Li et al., 2019). It is likely that these metabolic changes are mediated by unrestricted mTOR activation in the absence of AMPK phosphorylation (Wen et al., 2019). Whilst T cells from SLE patients also exhibit excessive mTOR activation (Fernandez et al., 2009), their pathogenic function is driven by different metabolic programmes versus those described in RA. Alternatively, the function of pathogenic T cells is driven by elevated levels of glycolysis and OXPHOS in SLE, supported through increased mTORC1 activity and metabolic enzyme expression (Yin et al., 2015). Despite these distinct metabolic differences between the T cells isolated from patients with SLE and RA, there are some similarities across both diseases, where they share mutual upregulation of the PPP (Perry et al., 2020). In contrast, changes in T cell lipid metabolism dominated initial investigations in multiple sclerosis (MS) immunometabolism. Cholesterol metabolism was originally implicated, whereby the treatment of MS patient-derived T cells with the HMG-CoA reductase inhibitor simvastatin reduced their proinflammatory cytokine production (Zhang et al., 2011). Other areas of lipid metabolism have since been associated with MS pathogenesis, including *de novo* fatty acid synthesis-mediated control of Th17 and Treg cell fate (Berod et al., 2014).

Given the importance of T cell metabolism in autoimmune disease pathogenesis, several drugs that target metabolism have been explored as potential therapeutic options. Consequently, the use of type 2 diabetes (T2D) drugs – which often target aspects of cellular metabolism – to target pathogenic T cell metabolism has been encouraging in autoimmune disease (see Chapter 1.6). Most notable is metformin – an inhibitor of complex I and an

activator of AMPK. Early studies demonstrated that through its action on these targets, metformin was able to reduce the production of proinflammatory cytokines by T cells and macrophages, which ultimately attenuated disease severity in a murine model of experimental autoimmune encephalomyelitis (Nath et al., 2009). The inhibition of T cell-mediated responses was driven by a reduction in Th1 and Th17 cell populations, with a concomitant increase in the generation of IL-10 (Nath et al., 2009). Metabolic regulation is central to the anti-inflammatory properties of metformin, whereby modulation of the mTOR/AMPK axis restricted Th17 differentiation by inhibiting STAT3 phosphorylation, thereby reducing the proinflammatory cytokine levels (Kang et al., 2013). Further investigations have revealed that these metabolic changes facilitate simultaneous expansion of the Treg cell population (Son et al., 2014), which has been confirmed in numerous settings of inflammation including inflammatory bowel disease (Lee et al., 2015), SLE (Lee et al., 2017) and graft-versus-host-disease (Park et al., 2016). The wider effect that metformin has on cellular metabolism has been most comprehensively examined in the context of SLE. Metformin treatment alone was sufficient to inhibit OXPHOS, which normalised T cell function during early the early stages of activation when cells are more dependent on oxidative metabolism (Yin et al., 2015). However, metformin increased glycolytic function, therefore was unable to reverse the disease phenotype in already-activated T cells (Yin et al., 2015). Consequently, a combination of metformin and 2-deoxyglucose – an inhibitor of glycolysis and glucose uptake – was required to suppress cellular metabolism and proinflammatory function in pathogenic T cells (Yin et al., 2015). Human studies have been scarce, however, a study that explored metformin as a treatment for patients with MS and metabolic syndrome outlined some of the underlying effects on immune cell function. Here, metformin treatment increased AMPK activation in patient-derived PBMCs, which induced a cytokine and transcription factor profile indicative of increased regulatory function and reduced Th1 and Th17 cell function (Negrotto et al., 2016). Similar observations were made in a cohort of patients treated with pioglitazone – another class of T2D drug – wherein the production of proinflammatory cytokines such as IL-6 and TNF α was reduced, whilst accompanied by an expansion of the Treg cell population (Negrotto et al., 2016). Collectively, these findings present the anti-inflammatory effect of repurposed T2D drugs on T cell function in the setting of autoimmunity, largely underpinned by metabolic control. However, the potential

therapeutic benefit of SGLT2 inhibitors, the newest class of T2D drugs, has yet to be explored in T cell-mediated autoimmune disease.

6.1.1 Rationale

Human CD4⁺ Teff and pan CD4⁺ T cells were both chosen as the study material. The reasons were: (i) to investigate the impact of canagliflozin on Teff cells, that are typically found at the site of inflammation in autoimmune disease; (ii) investigate whether canagliflozin has the same effect on T cell effector function in CD4⁺ T cells isolated from autoimmune patient cohorts as observed in human volunteers; and (iii) determine if immunometabolic changes underpin any canagliflozin-mediated changes to autoimmune patient-derived CD4⁺ T cells. Elucidating whether canagliflozin can modulate the function of CD4⁺ T cells in the setting of autoimmunity is important in understanding its therapeutic potential.

6.1.2 Hypothesis

- (i) CD4⁺ Teff cell activation and function is impaired by canagliflozin
- (ii) Canagliflozin inhibits CD4⁺ T cell effector function in SLE and RA
- (iii) Reduced function of patient-derived CD4⁺ T cells following canagliflozin treatment is underpinned by metabolic reprogramming

6.2 Experimental procedures

6.2.1 Human blood collection

Ethical approval was obtained from Wales Research Ethics Committee 6 for the collection of peripheral blood from healthy volunteers (13/WA/0190). Blood from healthy donors was processed as previously described (see Chapter 2.1).

6.2.2 Autoimmune patient cohort samples

Cryopreserved PBMCs isolated from SLE patients were kindly gifted by Professor Elizabeth Jury from University College London (11/LO/0330; University College London). Cryopreserved PBMCs isolated from RA patients were kindly gifted by Professor Ursula Fearon from Trinity College Dublin (RS18-055; Trinity College Dublin). Cryopreserved synovial fluid

mononuclear cells (SFMCs) isolated from RA patients were kindly gifted by Professor Ursula Fearon and Professor Douglas Veale from Trinity College Dublin (RS18-055; Trinity College Dublin) and prepared by Dr Mary Canavan. Patient demographics are outlined in the tables below (Table 6.1; Table 6.2).

Table 6.1 – Systemic lupus erythematosus patient demographics

	Systemic Lupus Erythematosus (n = 8)
Age	
Mean (SD)	46.8 (± 11.0)
Median	49.0
Range	31.0 – 61.0
Gender n (%)	
Female	8 (100.0%)
Male	0 (0.0%)
Ethnicity	
White	3 (37.5%)
Black or African-American	2 (25.0%)
Asian	1 (12.5%)
Other	3 (37.5%)
Treatment	
Steroid	8 (100.0%)
Immunosuppressant	7 (87.5%)
NSAID	1 (12.5%)
Anti-malarial	2 (25.0%)
Blood thinner	1 (12.5%)
Other	6 (75.0%)

NSAID, non-steroidal anti-inflammatory drug

Table 6.2 – Rheumatoid arthritis patient demographics

	Rheumatoid Arthritis	
	PBMCs (n = 9)	SFMCs (n = 5)
Age		
Mean (SD)	53.0 (± 12.3)	58.8 (± 21.7)
Median	53.0	67.0
Range	36.0 – 70.0	23.0 – 78.0
Gender n (%)		
Female	4 (44.4%)	3 (60.0%)
Male	3 (33.3%)	2 (40.0%)
Not determined	2 (22.2%)	0 (0.0%)
Treatment		
No medication	0 (0.0%)	2 (40.0%)
bDMARD only	2 (22.2%)	1 (20.0%)
csDMARD only	2 (22.2%)	2 (40.0%)
bDMARD + csDMARD	1 (11.1%)	0 (0.0%)
bDMARD + TNF inhibitor	2 (22.2%)	0 (0.0%)
Not determined	2 (22.2%)	0 (0.0%)
Rheumatoid Factor		
Positive	6 (66.6%)	4 (80.0%)
Negative	2 (22.2%)	1 (20.0%)
Not determined	1 (11.1%)	0 (0.0%)
ACPA		
Positive	7 (77.7%)	4 (80.0%)
Negative	1 (11.1%)	1 (20.0%)
Not determined	1 (11.1%)	0 (0.0%)
DAS28		
Mean (SD)	4.1 (± 1.9)	4.0 (± 1.3)
Median	4.4	3.6
Range	1.5 – 7.6	2.6 – 5.7

ACPA, anti-citrullinated proteins antibodies; DAS28; disease activity score-28; DMARD; disease-modifying anti-rheumatic drug; PBMCs, peripheral blood mononuclear cells; SFMCs, synovial fluid mononuclear cells

6.2.3 T cell isolation

Peripheral blood mononuclear cells (PBMCs) were isolated as previously described (see Chapter 2.3). The PBMC pellet was resuspended in the appropriate downstream media for analysis and the number of PBMCs was determined by using the Countess® automated cell counter (see Chapter 2.5). Pan CD4+ T cells, CD4+ Teff cells and pan CD8+ T cells were isolated using automated magnetic separation as previously described (see Chapter 2.4).

6.2.4 Cell culture

Isolated T cells were activated and cultured in human plasma-like medium (HPLM) as previously described (see Chapter 2.6). Cell-free supernatants were stored for further analysis, whilst cells were collected for downstream analysis.

6.2.5 Flow cytometry

T cell activation, blastogenesis and proliferation were all assessed as previously described (see Chapter 2.7). Purity of isolated T cells was monitored as previously described (see Chapter 2.7.1) and was typically > 90%.

Expression of CD36, CD71 and CD98 was used to assess nutrient uptake capacity (Table 6.3). Following 24 h activation, cells were resuspended and collected before centrifugation at 500 x *g* for 5 min. Cell-free supernatants were collected for ELISA analysis, whilst cells were resuspended in 100 µl FACS buffer. Dead cells were excluded using DRAQ7®. Cell doublets were excluded based on forward-scatter height versus forward-scatter area. Cells were stained for 15 min at room temperature (RT) in the dark (Table 6.3). An unstained sample provided a negative control. Cells were washed in FACS buffer and centrifugation at 515 x *g* post-staining and resuspended in FACS buffer to analyse.

Table 6.3 – Antibodies used for nutrient transporter analysis

Antibody	Fluorochrome	Clone	Isotype	Manufacturer
Anti-CD36	PE	5-271	Mouse IgG2a, κ	BioLegend, USA
Anti-CD71	Brilliant Violet 650™	CY1G4	Mouse IgG2a, κ	BioLegend, USA
Anti-CD98	FITC	MEM-108	Mouse IgG1, κ	BioLegend, USA
DRAQ7™	APC-Cy7	-	-	Biostatus, UK

T helper (Th) subsets were identified by expression of the chemokine receptors CXCR3, CCR4, CCR6 and CCR10 (Table 6.4; Table 6.5; Figure 6.1) (Mahnke, Beddall, et al., 2013). Following 24 h activation, Teff cells were harvested and up to 0.1×10^6 cells resuspended in 100 μ l FACS buffer. Dead cells and cell doublets were excluded as previously described. Cells were stained for 15 min at RT in the dark. An unstained sample provided a negative control. Cells were washed in FACS buffer and centrifugation at 515 x *g* post-staining and resuspended in FACS buffer to analyse.

Table 6.4 – Antibodies used for T helper cell subset analysis

Antibody	Fluorochrome	Clone	Isotype	Manufacturer
Anti-CXCR3	FITC	REA232	Recombinant human IgG1	Miltenyi, Germany
Anti-CCR4	Brilliant Violet 605™	L291H4	Mouse IgG1, κ	BioLegend, USA
Anti-CCR6	PE-Vio®615	REA190	Recombinant human IgG1	Miltenyi, Germany
Anti-CCR10	APC	REA326	Recombinant human IgG1	Miltenyi, Germany
DRAQ7™	APC-Cy7	-	-	Biostatus, UK

Table 6.5 – Panel to identify T helper cell subsets based on chemokine receptor expression

Subset	CXCR3	CCR4	CCR6	CCR10
Th1	+	-	-	-
Th2	-	+	-	-
Th9	+/-	-	+	+/-
Th17	-	+	+	-
Th17.1	+	-	+	-
Th22	+/-	+	+	+

A

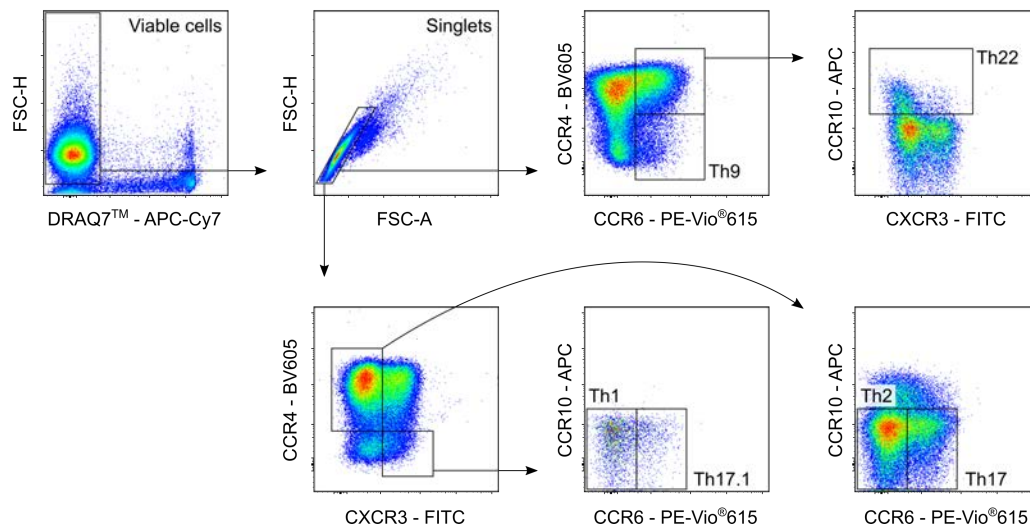


Figure 6.1 – Gating strategy to identify Th subsets based on chemokine receptor expression

(A) Gating strategy used to identify Th subsets within anti-CD3 (2 µg/ml) and anti-CD28 (20 µg/ml) activated CD4+ T effector cells based on their expression CXCR3, CCR4, CCR6 and CCR10.

Synovial fluid T cells were identified as CD3+ lymphocytes and were further divided into subsets based on their expression of CD4+ and CD8+ (Table 6.6; Figure 6.2). T cell activation and blastogenesis was assessed as previously described (see Chapter 2.7). Following 24 h activation, SFMCs were harvested and up to 0.5×10^6 cells resuspended in 100 µl FACS buffer. Dead cells and cell doublets were excluded as previously described. Cells were stained for 15 min at RT in the dark. An unstained sample provided a negative control. Cells were washed in FACS buffer and centrifugation at 515 x g post-staining and resuspended in FACS buffer to analyse.

Table 6.6 – Antibodies used for synovial fluid mononuclear cell analysis

Antibody	Fluorochrome	Clone	Isotype	Manufacturer
Anti-CD3	Brilliant Violet 570™	UCHT1	Mouse IgG1, κ	BioLegend, USA
Anti-CD4	Alexa Fluor® 647	OKT4	Mouse IgG2b, κ	BioLegend, USA
Anti-CD8	PE	HIT8a	Mouse IgG1, κ	BioLegend, USA
Anti-CD25	PE-Vio®615	REA570	Recombinant human IgG1	Miltenyi, Germany
Anti-CD44	Pacific Blue	BJ18	Mouse IgG1, κ	BioLegend, USA
Anti-CD69	FITC	FN50	Mouse IgG1, κ	BioLegend, USA

A

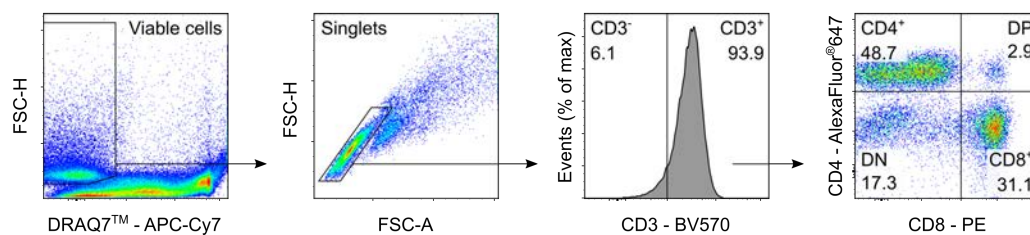


Figure 6.2 – Gating strategy to identify synovial fluid CD4+ and CD8+ T cells

(A) Gating strategy used to identify CD4+ and CD8+ T cells within anti-CD3 (2 µg/ml) and anti-CD28 (20 µg/ml) activated SFMC population.

Intracellular flow cytometry was used to assess the transcription factor content of activated T cells and performed as previously described (see Chapter 2.7.4). Following 24 h activation, Teff cells were harvested and up to 0.2×10^6 cells resuspended in 100 µl FACS buffer. Cell surface staining was performed as previously described prior to intracellular staining.

Expression of transcription factors associated with Th1, Th2 and Th17 cells was monitored by measuring intracellular Tbet, GATA3 and RORγT, respectively (Table 6.7). Regulatory T cell-associated transcription factor expression was monitored by measuring intracellular FoxP3 and CD25 and CD127 surface staining.

Table 6.7 – Antibodies used for intracellular transcription factor analysis

Antibody	Fluorochrome	Clone	Isotype	Manufacturer
Anti-CD25	PE	REA945	Recombinant human IgG1	Miltenyi, GER
Anti-CD127	APC-Vio®770	REA614	Recombinant human IgG1	Miltenyi, GER
Anti-FoxP3	Pacific Blue™	259D	Mouse IgG1, κ	BioLegend, USA
Anti-GATA3	PE	16E10A23	Mouse IgG2b, κ	BioLegend, USA
Anti-RORγT	Brilliant Violet 650™	Q21-559	Mouse IgG2b, κ	BD, USA
Anti-Tbet	Brilliant Violet 786™	O4-46	Mouse IgG1, κ	BD, USA

MitoSOX™ Red (5 µM; ThermoFisher, USA) was used to assess mitochondrial ROS. For mitochondrial staining, cells were incubated with the respective dye for 20 min at 37°C. Cells were washed in FACS buffer and centrifugation at 515 x g post-staining and resuspended in FACS buffer to analyse.

6.2.6 Enzyme-linked immunosorbent assay

ELISAs were performed as per the manufacturer's guidelines to measure the concentration of the following cytokines in cell-free supernatants: IL-2 (DY202), IL-4 (DY204), IL-10 (DY217B), IL-17 (DY317), IL-21 (DY8879), IFN γ (DY285B) and TNF α (DY210; all R&D systems, USA).

6.2.7 Metabolic analysis

Following 24 h activation in HPLM, cells were resuspended and collected before centrifugation at 500 x *g* for 5 min. Cell-free supernatants were collected for ELISA analysis. Cells were resuspended in phenol red-free RPMI supplemented with glucose (10 mM), pyruvate (1 mM) and glutamine (2 mM; all Agilent, USA) before seeding at 2.0x10⁵ cells per Cell-Tak coated well. OCR and ECAR were measured following a series of previously optimized injections. Injections for both the mitochondrial stress assay and glycolysis assay include oligomycin (1 μ M), FCCP (1 μ M), antimycin A and rotenone (both 1 μ M) and monensin (20 μ M). Metabolic parameters were calculated as previously described (see Chapter 2.9).

6.2.8 Extracellular glucose assay

Extracellular glucose levels in cell-free supernatants were assessed using Glucose Assay Kit I (Eton Biosciences, USA) as per the manufacturer's instructions. The glucose standard curve and samples were diluted to a working concentration using dH₂O. Glucose Assay Solution was added to each well and incubated for 15 min at 37°C in a CO₂-free incubator. The reaction was stopped by adding acetic acid (0.5 M; Merck, Germany). Plates were then read at 490 nm using a plate reader spectrophotometer.

6.2.9 Statistical analysis

Unless otherwise stated, statistical analysis was carried out using GraphPad Prism version 8. Data are expressed as the mean \pm standard error of the mean (SEM). The normality of the data was initially tested using the Shapiro-Wilk test to determine the appropriate method of analysis. For data comparing two sample groups, normally distributed data were analysed using a parametric T test, whereas a non-parametric T test was used to analyse data not normally distributed. One-way analysis of variance (ANOVA) followed by the post-hoc Dunnett's test was used to analyse three or more group means of a single variable compared

to the vehicle control. A one-sample T test was used to analyse data normalised to the vehicle control group. Significant values were taken as $p \leq 0.05$ and denoted as follows: * $p \leq 0.05$, ** $p \leq 0.01$, *** $p \leq 0.001$ and **** $p < 0.0001$.

6.3 Results

6.3.1 Canagliflozin impairs T effector cell activation, function and proliferation

Our data until this point has demonstrated that canagliflozin modulates activated Tnv cell function. Since the repertoire of cytokines secreted by Tnv cells is restricted, we next pursued the impact of canagliflozin on antigen-trained Teff cells. A similar approach to previous experiments was adopted, whereby Teff cells were activated in the presence and absence of canagliflozin in short-term (24 h) or long-term (72 h) culture (Figure 6.3). Once more, data were normalised to the vehicle control group, when appropriate, to account for any variability between donors.

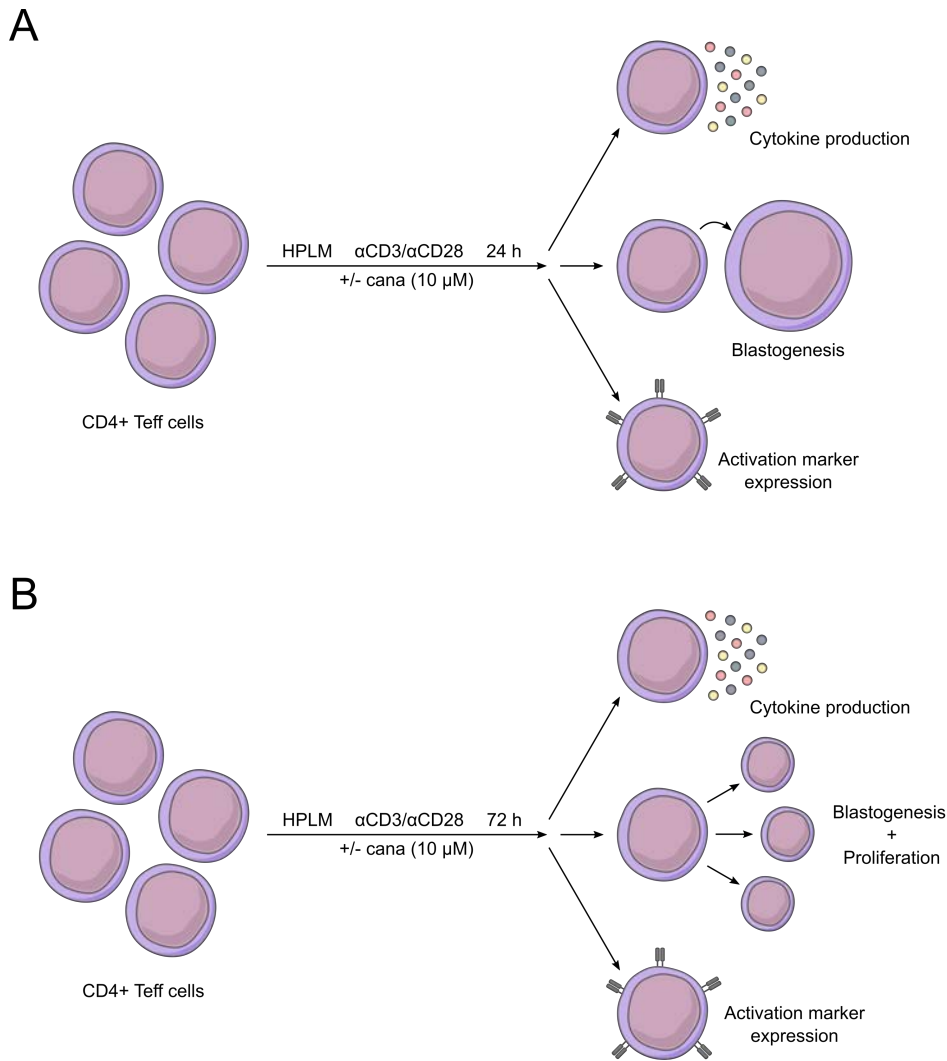


Figure 6.3 – Experimental procedure employed to assess the impact of canagliflozin on T effector cells in HPLM

(A) Schematic overview outlining the short-term experimental design in HPLM – anti-CD3 (2 μ g/ml) and anti-CD28 (20 μ g/ml) activated CD4+ T effector cells in the presence and absence of canagliflozin (10 μ M). (B) Schematic overview outlining the long-term experimental design in HPLM as in (A).

At 24 h, canagliflozin induced a marked decrease in the secretion of several cytokines, including: IFN γ ($p = 0.0005$), IL-2 ($p = 0.0045$), IL-4 ($p = 0.0164$), IL-10 ($p = 0.0092$), IL-17 ($p = 0.0004$) and IL-21 ($p = 0.0037$; Figure 6.4A). Most of these cytokines remained significantly repressed at 72 h, with the exception of IL-10 (IFN γ : $p = 0.0015$; IL-2: $p = 0.0094$; IL-4: $p = 0.0449$; IL-10: $p = 0.4766$; IL-17: $p = 0.0168$; IL-21: $p = 0.0006$; Figure 6.4B). However, the observed reductions were somewhat less pronounced at 72 h versus 24 h, particularly in the case of IFN γ (24 h: fold-change 0.253; 72 h: fold-change 0.501) and IL-17 (24 h: fold-change 0.322; 72 h: fold-change 0.720; Figure 6.4B).

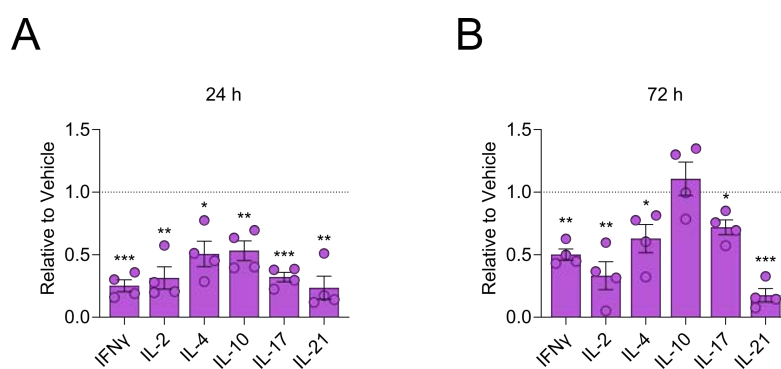


Figure 6.4 – Canagliflozin suppresses cytokine production by T effector cells

(A-B) Secretion of IFN γ , IL-2, IL-4, IL-10, IL-17 and IL-21 at (A) 24 h and (B) 72 h by anti-CD3 (2 μ g/ml) and anti-CD28 (20 μ g/ml) activated CD4 $^{+}$ T effector cells in the presence and absence of canagliflozin (10 μ M), determined by ELISA of cell-free supernatants. Data are representative of four independent experiments. Statistical analysis was performed using a one-sample T test. Data expressed as mean \pm SEM; * $p \leq 0.05$, ** $p \leq 0.01$, *** $p \leq 0.001$.

This was again underpinned by attenuated activation, where CD44 ($p = 0.0007$) and CD69 ($p = 0.0059$) expression was significantly reduced by canagliflozin, whilst CD25 expression trended towards decrease ($p = 0.0981$; Figure 6.5).

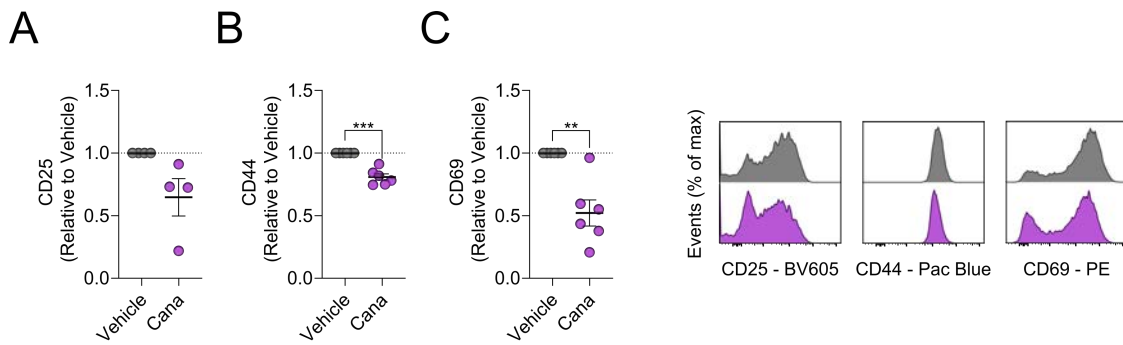


Figure 6.5 – T effector cell activation is impaired by canagliflozin

(A-C) Relative surface expression of activation markers (A) CD25, (B) CD44 and (C) CD69 on anti-CD3 (2 $\mu\text{g}/\text{ml}$) and anti-CD28 (20 $\mu\text{g}/\text{ml}$) activated CD4+ T effector cells in the presence and absence of canagliflozin (10 μM), determined by flow cytometry. Representative overlaid histogram plots. Data are representative of four (A) or six (B-C) independent experiments. All relative data are normalised to the vehicle control group. Statistical analysis was performed using a one-sample T test. Data expressed as mean \pm SEM; ** $p \leq 0.01$, *** $p \leq 0.001$.

Also consistent with previous work, blastogenesis was constricted ($p = 0.0006$) at 24 h in canagliflozin-treated Teff cells (Figure 6.6A).

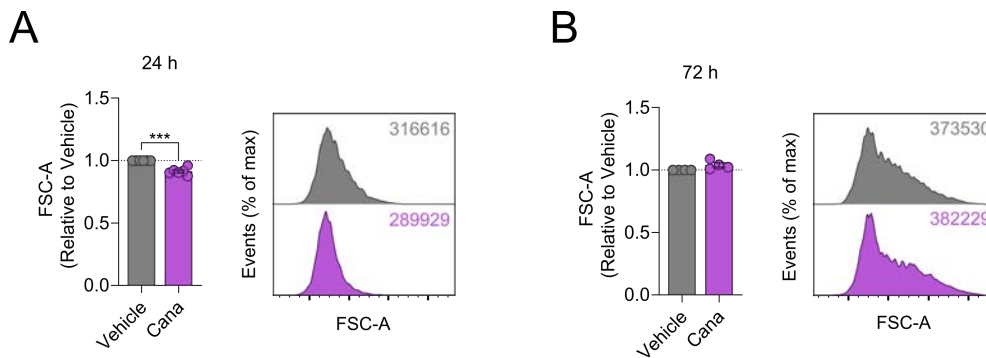


Figure 6.6 – Canagliflozin restricts T effector cell blastogenesis

(A-B) Relative cell size at (A) 24 h and (B) 72 h in anti-CD3 (2 $\mu\text{g}/\text{ml}$) and anti-CD28 (20 $\mu\text{g}/\text{ml}$) activated CD4+ Teff cells in the presence and absence of canagliflozin (10 μM), determined by flow cytometry using forward-scatter area. Representative overlaid histogram plots, numbers indicate forward scatter area. Data are representative of six (A) or four (B) independent experiments. All relative data are normalised to the vehicle control group. Statistical analysis was performed using a one-sample T test. Data expressed as mean \pm SEM; *** $p \leq 0.001$.

Regarding the longer-term impact of canagliflozin, Teff cell proliferation and blastogenesis was monitored at 72 h. Despite no reduction in blastogenesis at this time point ($p = 0.0985$; Figure 6.6B), Teff cell proliferation was modestly, yet significantly, suppressed by canagliflozin in terms of the number of cells divided ($p = 0.0306$; Figure 6.7A). However, there were no significant differences in any of the calculated proliferation parameters (Figure 6.7B-E).

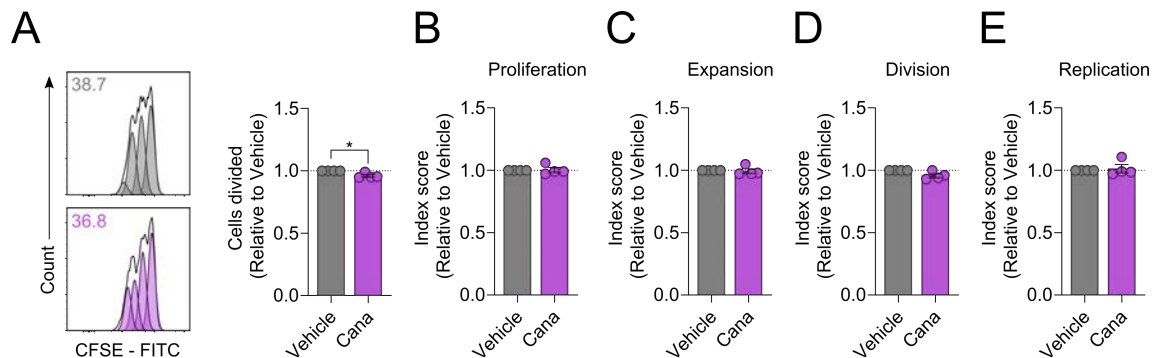


Figure 6.7 – Canagliflozin reduces T effector cell proliferation

(A) Relative frequency of anti-CD3 (2 $\mu\text{g/ml}$) and anti-CD28 (20 $\mu\text{g/ml}$) activated CD4⁺ T effector cells divided in the presence and absence of canagliflozin (10 μM), determined by flow cytometry using CellTrace™ CFSE. Representative overlaid histogram plots, numbers indicate percentage of cells divided. (B-E) Calculated proliferation parameters including (B) proliferation, (C) expansion, (D) division and (E) replication. Data are representative of four independent experiments. All relative data are normalised to the vehicle control group. Statistical analysis was performed using a one-sample T test. Data expressed as mean \pm SEM; * $p \leq 0.05$.

Crucially, the aforementioned changes in Teff cell function upon canagliflozin treatment were not attributable to reduced cell viability (24 h: $p = 0.2195$, 72 h: $p = 0.6608$; Figure 6.8).

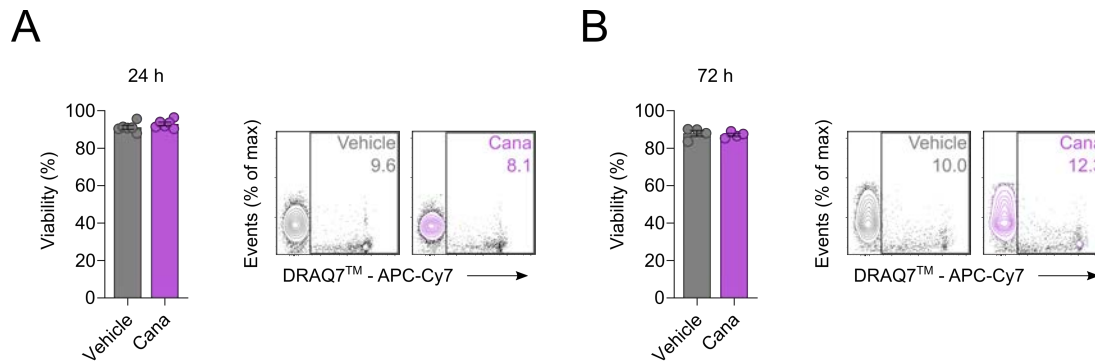


Figure 6.8 – Canagliflozin does not compromise T effector cell viability

(A-B) Cell viability at (A) 24 h and (B) 72 h of anti-CD3 (2 $\mu\text{g}/\text{ml}$) and anti-CD28 (20 $\mu\text{g}/\text{ml}$) activated CD4⁺ T effector cells in the presence and absence of canagliflozin (10 μM), determined by flow cytometry using DRAQ7™. Representative contour plots, numbers indicate frequency of viable cells. Data are representative of six (A) or four (B) independent experiments. Statistical analysis was performed using an unpaired T-test. Data expressed as mean \pm SEM.

We next explored the underlying processes that might govern canagliflozin-mediated changes in Teff cell function. Initially, we concentrated on metabolism, given the changes previously observed in Tnv cells (see Chapter 5.3). To gain a relatively quick insight, we measured the expression of several key nutrient transporters – including CD36 (fatty acid translocase), CD71 (transferrin receptor) and CD98 (large neutral amino acid transporter) – on the surface of 24 h activated Teff cells. All three transporters were significantly downregulated by canagliflozin (CD36: $p = 0.0454$; CD71: $p = 0.0014$; CD98: $p = 0.0128$; Figure 6.9A-C), which might suggest reduced nutrient uptake into Teff cells. Furthermore, extracellular glucose concentrations were elevated in cell-free supernatants collected from canagliflozin-treated Teff cells ($p = 0.0102$), which might also indicate reduced glucose uptake (Figure 6.9D).

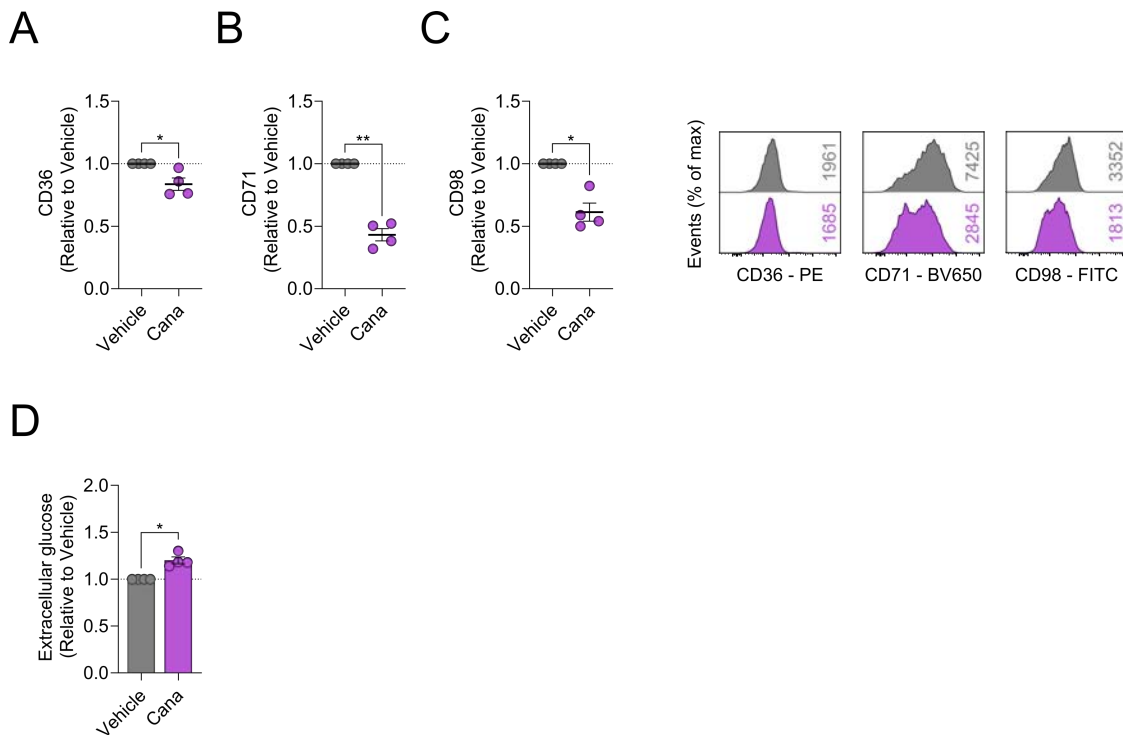


Figure 6.9 – Nutrient transporter expression is reduced on T effector cell surface by canagliflozin (A-C) Relative surface expression of nutrient transporters (A) CD36, (B) CD71 and (C) CD98 on anti-CD3 (2 µg/ml) and anti-CD28 (20 µg/ml) activated CD4+ T effector cells in the presence and absence of canagliflozin (10 µM), determined by flow cytometry. Representative overlaid histogram plots, numbers indicated median fluorescence intensity. (D) Extracellular glucose concentrations in cell-free supernatants. Data are representative of four independent experiments. All relative data are normalised to the vehicle control group. Statistical analysis was performed using a one-sample T test. Data expressed as mean ± SEM; * $p \leq 0.05$, ** $p \leq 0.01$.

As metabolic transporter expression, activation and effector function are all impaired by canagliflozin, we next investigated whether this might arise through Teff cell exhaustion. Classic T cell exhaustion markers – LAG3, PD-1 and TIM3 – were analysed by flow cytometry, however their expression was not increased by canagliflozin (Figure 6.10). In fact, exhaustion marker expression tended to decrease in the presence of canagliflozin, whereby PD-1 expression was significantly suppressed (LAG3: $p = 0.1666$; TIM3: $p = 0.1903$; PD-1: $p = 0.0123$; Figure 6.10). Together, these data demonstrate that canagliflozin modulates Teff cell activation and function independent of exhaustion, more likely through a compromised metabolic profile.

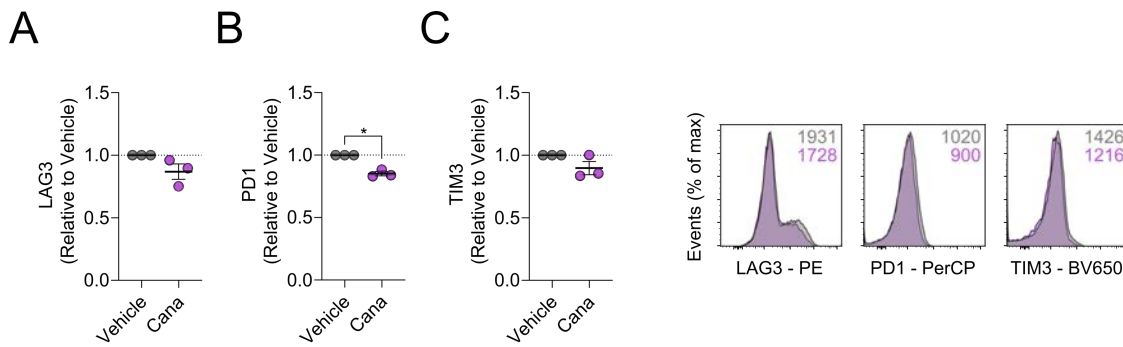


Figure 6.10 – Canagliflozin-treated T effector cells do not become anergic

(A-C) Relative surface expression of exhaustion markers (A) LAG3, (B) PD-1 and (C) TIM3 on anti-CD3 (2 $\mu\text{g}/\text{ml}$) and anti-CD28 (20 $\mu\text{g}/\text{ml}$) activated CD4⁺ Teff cells in the presence and absence of canagliflozin (10 μM), determined by flow cytometry. Representative overlaid histogram plots, numbers indicated median fluorescence intensity. Data are representative of three independent experiments. All relative data are normalised to the vehicle control group. Statistical analysis was performed using a one-sample T test. Data expressed as mean \pm SEM; * $p \leq 0.05$.

6.3.2 Canagliflozin alters the distribution of Th subsets within the T effector cell population

Given the observed changes in Teff cell cytokine production, we sought to investigate the effect that canagliflozin has on the distribution of Th cell subsets. Initially, the frequency of several Th cell subsets was determined based on their chemokine receptor expression patterns (see Chapter 6.2.5; Figure 6.1). Although canagliflozin did not drastically alter the Th subset profile of Teff cells, there were noticeable changes to individual subset compartments (Figure 6.11).

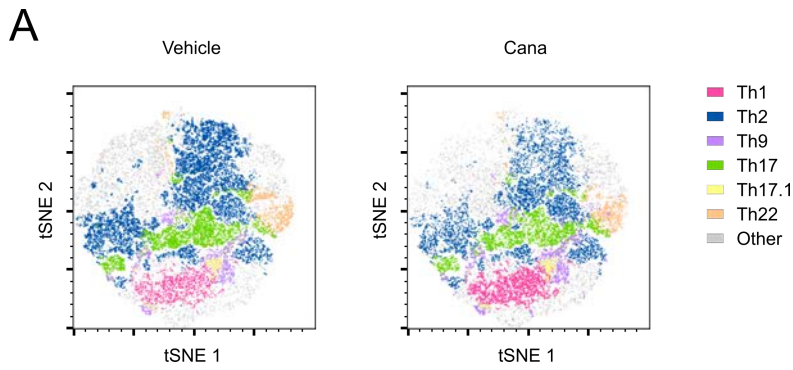


Figure 6.11 – Th subset profile of canagliflozin-treated T effector cells

(A) Representative global tSNE projection of Th subsets in anti-CD3 (2 µg/ml) and anti-CD28 (20 µg/ml) activated CD4+ T effector cells in the presence and absence of canagliflozin (10 µM), determined by flow cytometry based on chemokine receptor expression. Data are representative of five independent experiments.

When these changes were quantified, there was a significant, but unexpected, increase in the Th1 cell population ($p = 0.0098$), whilst there was a reduction in the frequency of both Th17 ($p = 0.0460$) and Th22 cells ($p = 0.0082$; Figure 6.12). Despite trending towards increase, the frequency of Th9 ($p = 0.0987$) and Th17.1 cells ($p = 0.2786$) were not significantly altered by canagliflozin treatment, and there was no pronounced change in the Th2 cell population ($p = 0.4285$; Figure 6.12).

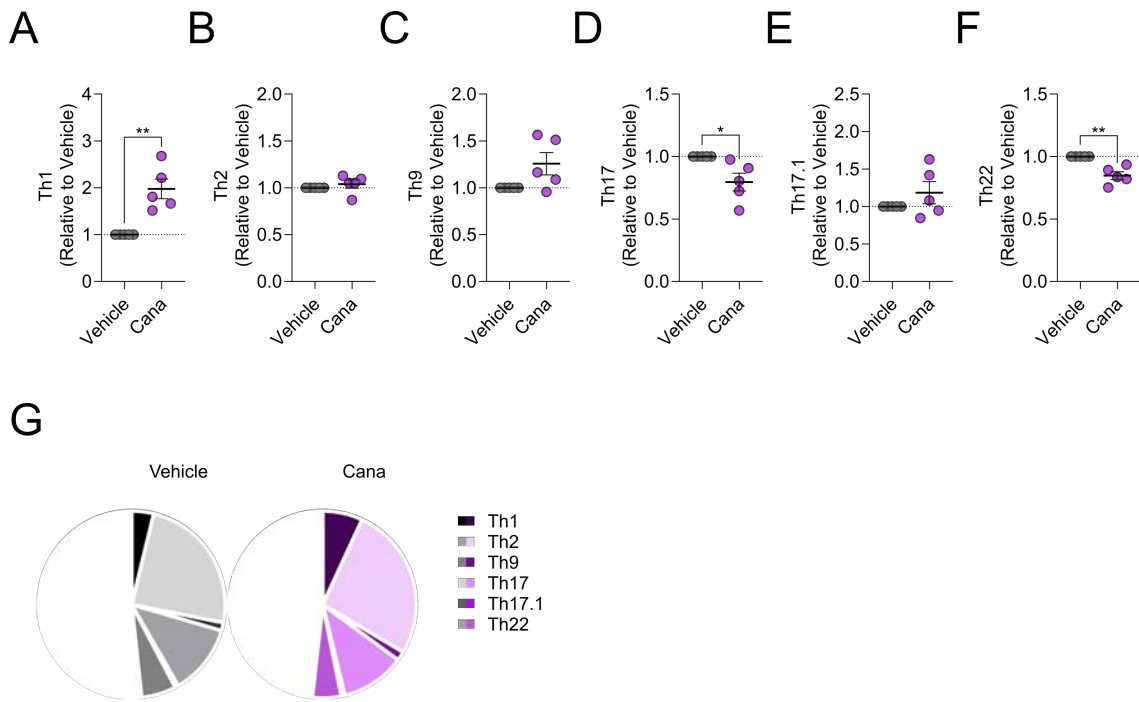


Figure 6.12 – Changes within the T effector cell compartment upon canagliflozin treatment

(A-F) Relative frequency of (A) Th1, (B) Th2, (C) Th9, (D) Th17, (E) Th17.1 and (F) Th22 cells within anti-CD3 (2 $\mu\text{g}/\text{ml}$) and anti-CD28 (20 $\mu\text{g}/\text{ml}$) activated CD4⁺ T effector cells in the presence and absence of canagliflozin (10 μM), determined by flow cytometry based on chemokine receptor expression. (G) Representative summary of Th subset distribution in canagliflozin-treated T effector cells and vehicle control. Data are representative of five independent experiments. All relative data are normalised to the vehicle control group. Statistical analysis was performed using a one-sample T test. Data are expressed as mean \pm SEM; * $p \leq 0.05$, ** $p \leq 0.01$.

Unsurprisingly, when assessing the canagliflozin-induced changes in ratio between various subsets, there was a significant increase in both the Th1 / Th2 ratio ($p = 0.0214$) and Th1 / Th17 ratio ($p = 0.0205$; Figure 6.13).

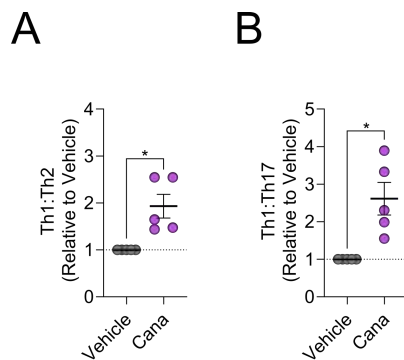


Figure 6.13 – Canagliflozin disrupts the balance between Th subsets

(A) Relative ratio of Th1 to Th2 cells and within anti-CD3 (2 $\mu\text{g/ml}$) and anti-CD28 (20 $\mu\text{g/ml}$) activated CD4+ T effector cells in the presence and absence of canagliflozin (10 μM), determined by flow cytometry. (B) Relative ratio of Th1 to Th17 cells as in (A). Data are representative of five independent experiments. All relative data are normalised to the vehicle control group. Statistical analysis was performed using a one-sample T test. Data are expressed as mean \pm SEM; * $p \leq 0.05$.

As it is unlikely that changes to the Th subset compartments are occurring in such short time frames, we next focussed on chemokine expression outside the context of Th subsets. Here there was an observed decrease in the expression of CCR4 ($p = 0.0006$) and CCR6 ($p = 0.0030$), however, CXCR3 ($p = 0.2164$) and CCR10 ($p = 0.1389$) remained unchanged by canagliflozin (Figure 6.14). The loss of CCR4 expression was particularly striking, especially in the northern hemisphere of the tSNE plot mainly comprised of Th2 cells (Figure 6.14B).

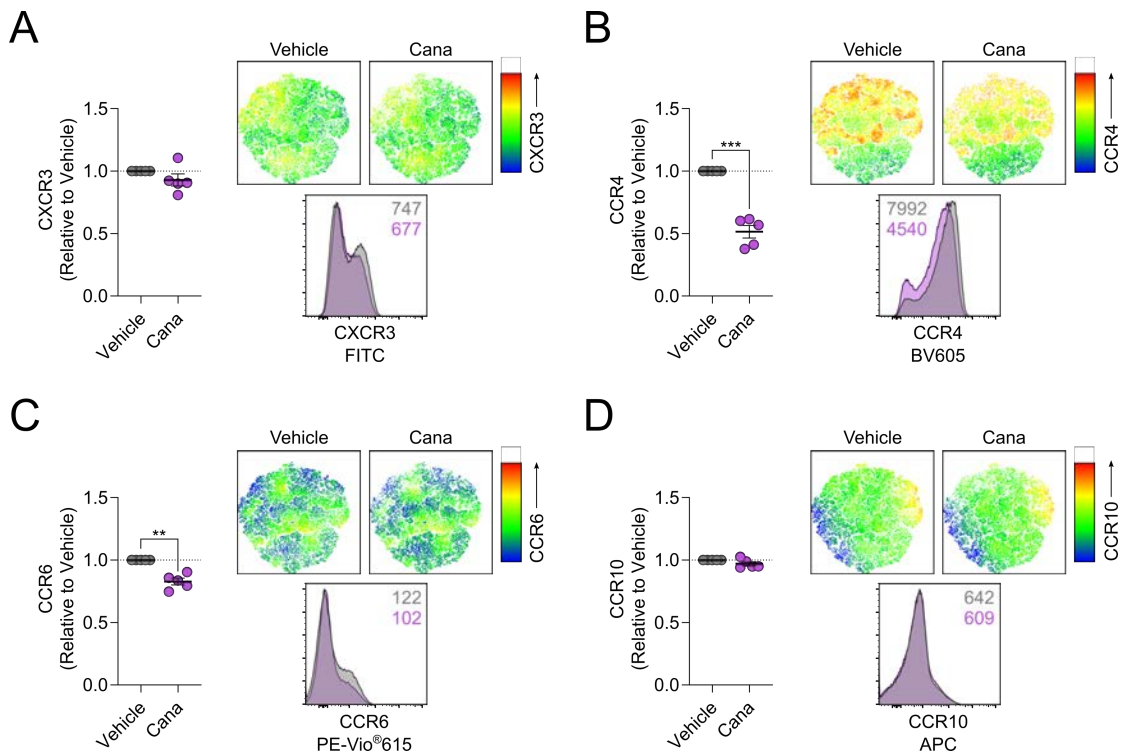


Figure 6.14 – Canagliflozin alters chemokine receptor expression on T effector cells

(A-D) Relative surface expression of chemokine receptors (A) CXCR3, (B) CCR4, (C) CCR6 and (D) CCR10 on anti-CD3 (2 $\mu\text{g}/\text{ml}$) and anti-CD28 (20 $\mu\text{g}/\text{ml}$) activated CD4⁺ T effector cells in the presence and absence of canagliflozin (10 μM), determined by flow cytometry. Representative tSNE plots, colour gradient indicates median fluorescence intensity: blue is associated with low expression; red is associated with high expression. Representative overlaid histogram plots, numbers indicated median fluorescence intensity. Data are representative of five independent experiments. All relative data are normalised to the vehicle control group. Statistical analysis was performed using a one-sample T test. Data are expressed as mean \pm SEM; ** $p \leq 0.01$, *** $p \leq 0.001$.

Next, we determined whether the changes in Th cell subset populations in response to canagliflozin are driven by their expression of key transcription factors. Despite the observed increase in the Th1 cell compartment based on Teff cell chemokine expression patterns, there was reduced expression of the Th1-associated transcription factor Tbet ($p = 0.0036$; Figure 6.15A). Intriguingly, there was also reduced expression of GATA3 in Teff cells treated with canagliflozin ($p = 0.0224$), although the Th2 cell population was unaffected based on their chemokine receptor expression (Figure 6.15B). Intracellular expression of ROR γ T – a key transcription factor in Th17 cells – was also reduced by canagliflozin ($p = 0.0164$; Figure 6.15C).

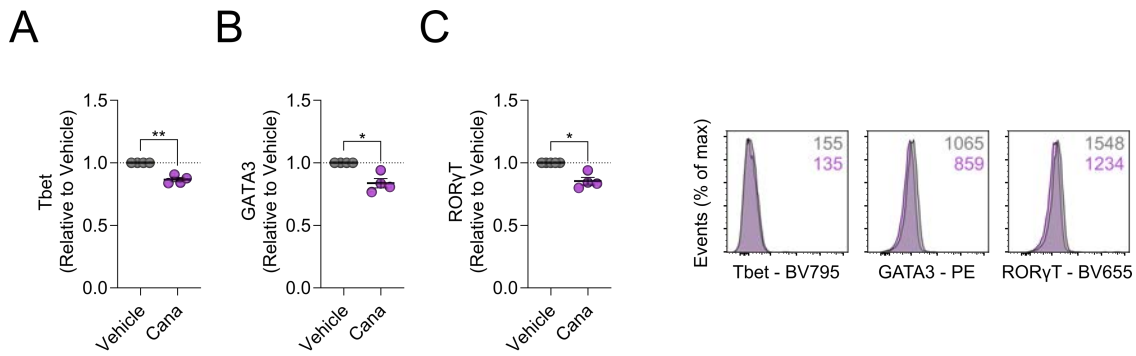


Figure 6.15 – Canagliflozin reduces the expression of lineage-associated transcription factors

(A-C) Relative intracellular expression of transcription factors (A) GATA3, (B) RORγT and (C) Tbet in anti-CD3 (2 μg/ml) and anti-CD28 (20 μg/ml) activated CD4⁺ T effector cells in the presence and absence of canagliflozin (10 μM), determined by flow cytometry. Representative overlaid histogram plots, numbers indicate median fluorescence intensity. Data are representative of four independent experiments. All relative data are normalised to the vehicle control group. Statistical analysis was performed using a one-sample T test. Data are expressed as mean ± SEM; * $p \leq 0.05$, ** $p \leq 0.01$.

Treg-associated markers were also monitored following canagliflozin treatment, whereby there was a significant reduction in cell-surface CD25 ($p = 0.0275$) in line with previous data, whilst cell-surface CD127 trended towards decrease ($p = 0.0859$; Figure 6.16A-B). Additionally, the intracellular expression of key transcription factor FoxP3 was also reduced ($p = 0.0670$) in canagliflozin-treated Teff cells (Figure 6.16). Together, these data demonstrate that the Th subset profile could potentially be altered by canagliflozin in Teff cells, however, it is unclear what mechanism ultimately drives changes to individual populations.

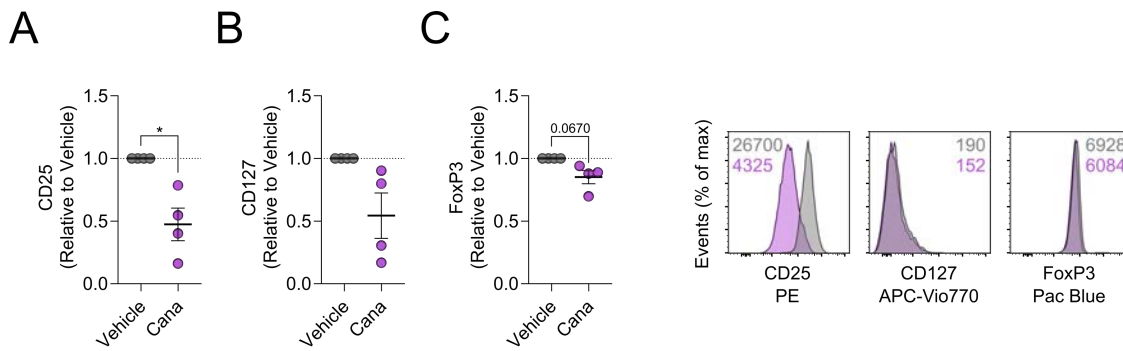


Figure 6.16 – Canagliflozin limits the expression of factors associated with regulatory T cell differentiation

(A-C) Relative expression of regulatory T cell-associated markers (A) CD25, (B) CD127 and (C) intracellular FoxP3 in anti-CD3 (2 $\mu\text{g}/\text{ml}$) and anti-CD28 (20 $\mu\text{g}/\text{ml}$) activated CD4⁺ T effector cells in the presence and absence of canagliflozin (10 μM), determined by flow cytometry. Representative overlaid histogram plots, numbers indicated median fluorescence intensity. Data are representative of four independent experiments. All relative data are normalised to the vehicle control group. Statistical analysis was performed using a one-sample T test. Data are expressed as mean \pm SEM; * $p \leq 0.05$.

6.3.3 Canagliflozin inhibits CD8⁺ T cell function

Given that canagliflozin has such a profound inhibitory effect on CD4⁺ T cell function, we sought to investigate whether this also applies to CD8⁺ T cells. The experimental procedure adopted was consistent with those employed to analyse CD4⁺ T cells, whereby CD8⁺ T cells were activated in the presence and absence of canagliflozin (Figure 6.17).

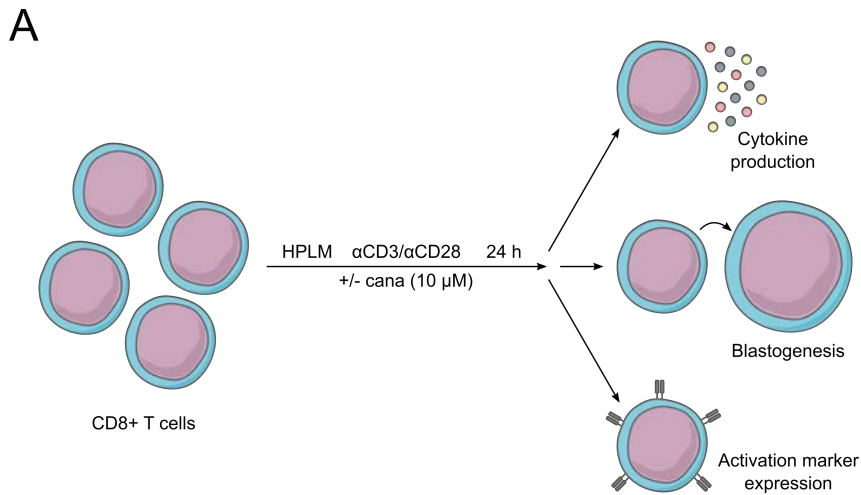


Figure 6.17 – Experimental procedure employed to assess the impact of canagliflozin on CD8+ T cells

(A) Schematic overview outlining the experimental design in HPLM – anti-CD3 (2 μ g/ml) and anti-CD28 (20 μ g/ml) activated CD8+ T cells in the presence and absence of canagliflozin (10 μ M).

In keeping with our previous findings in various CD4+ T cell subsets, canagliflozin impaired CD8+ T cell activation with a marked reduction in CD25 ($p = 0.0134$), CD44 ($p = 0.0047$) and CD69 expression ($p = 0.0003$; Figure 6.18).

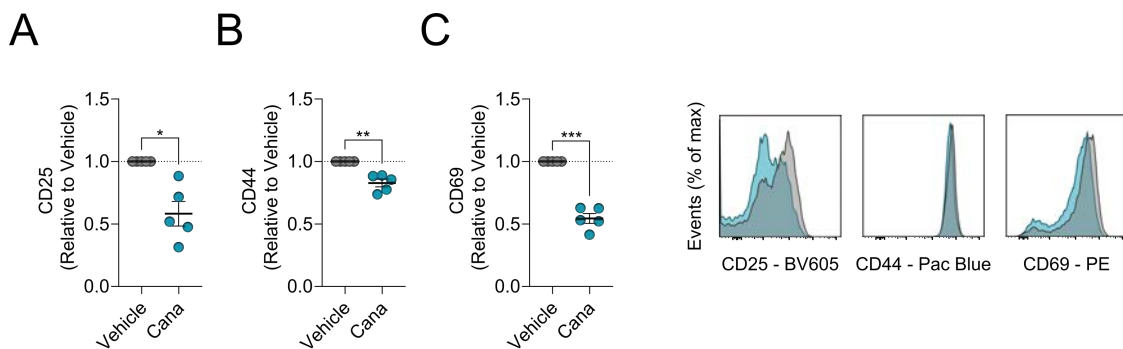


Figure 6.18 – CD8+ T cell activation is impaired by canagliflozin

(A-C) Relative surface expression of activation markers (A) CD25, (B) CD44 and (C) CD69 on anti-CD3 (2 μ g/ml) and anti-CD28 (20 μ g/ml) activated CD8+ T cells in the presence and absence of canagliflozin (10 μ M), determined by flow cytometry. Representative overlaid histogram plots. Data are representative of five independent experiments. All relative data are normalised to the vehicle control group. Statistical analysis was performed using a one-sample T test. Data expressed as mean \pm SEM; * $p \leq 0.05$, ** $p \leq 0.01$, *** $p \leq 0.001$.

Furthermore, blastogenesis was also significantly constrained following treatment with canagliflozin ($p = 0.0044$; Figure 6.19).

A

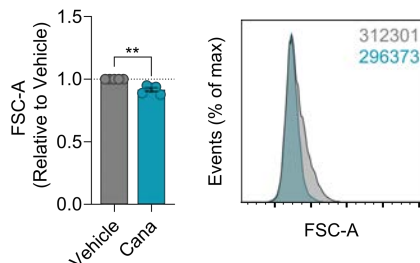


Figure 6.19 – Canagliflozin constrains CD8+ T cell blastogenesis

(A) Relative cell size in anti-CD3 (2 $\mu\text{g}/\text{ml}$) and anti-CD28 (20 $\mu\text{g}/\text{ml}$) activated CD8+ T cells in the presence and absence of canagliflozin (10 μM), determined by flow cytometry using forward-scatter area. Representative overlaid histogram plots, numbers indicate forward scatter area. Data are representative of five independent experiments. All relative data are normalised to the vehicle control group. Statistical analysis was performed using a one-sample T test. Data expressed as mean \pm SEM; ** $p \leq 0.01$.

Together, these changes culminated in diminished effector function, whereby the production of IL-2 ($p = 0.0040$), IFN γ ($p = 0.0012$) and granzyme B ($p = 0.0002$) were all markedly reduced in the presence of canagliflozin (Figure 6.20). Together, these changes in CD8+ T cell function are highly unsurprising, given the previously described impact that canagliflozin has on TCR signalling (see Chapter 5.3.6).

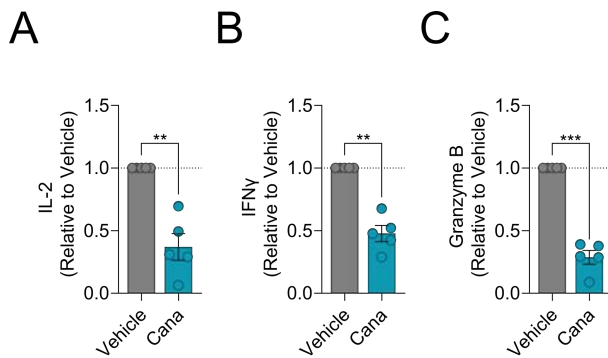


Figure 6.20 – Canagliflozin impairs CD8+ T cell effector function

(A-C) Secretion of (A) IL-2, (B) IFN γ and (C) granzyme B by anti-CD3 (2 $\mu\text{g/ml}$) and anti-CD28 (20 $\mu\text{g/ml}$) activated CD8+ T cells in the presence and absence of canagliflozin (10 μM), determined by ELISA of cell-free supernatants. Data are representative of five (A-B) or three (C) independent experiments. Statistical analysis was performed using a one-sample T test. Data expressed as mean \pm SEM; ** $p \leq 0.01$, *** $p \leq 0.001$.

Importantly, canagliflozin did not compromise CD8+ T cell viability ($p = 0.8238$; Figure 6.21). Together, these data show that canagliflozin exhibits an inhibitory effect on CD8+ T cells, similar to what has been more extensively analysed in several CD4+ T cell subsets.

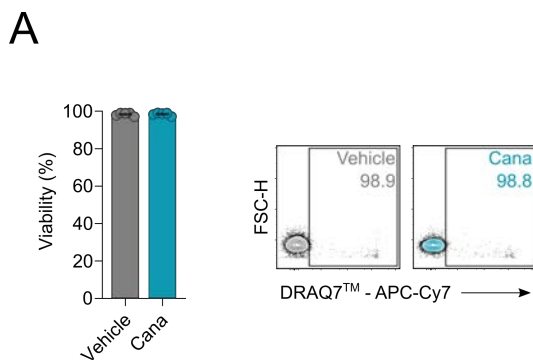


Figure 6.21 – CD8+ T cell viability is not compromised by canagliflozin

(A) Cell viability of anti-CD3 (2 $\mu\text{g/ml}$) and anti-CD28 (20 $\mu\text{g/ml}$) activated CD8+ T cells in the presence and absence of canagliflozin (10 μM), determined by flow cytometry using DRAQ7[™]. Representative contour plots, numbers indicate frequency of dead cells. Data are representative of five independent experiments. Statistical analysis was performed using an unpaired T-test. Data expressed as mean \pm SEM.

6.3.4 Canagliflozin inhibits CD4+ T cell function in systemic lupus erythematosus and rheumatoid arthritis

Ultimately, we wanted to determine whether canagliflozin can be repurposed in the setting of autoimmune disease. To better understand the actions of canagliflozin in this setting, CD4+ T cells isolated from two autoimmune patient cohorts – SLE and RA – were activated with anti-CD3 and anti-CD28 and treated with the drug to assess whether their function is altered as previously described for healthy donors (Figure 6.22). Dapagliflozin was discontinued for this analysis as cell numbers were limited from autoimmune patient samples and no substantial changes in function were previously recorded when CD4+ T cells were treated with the drug.

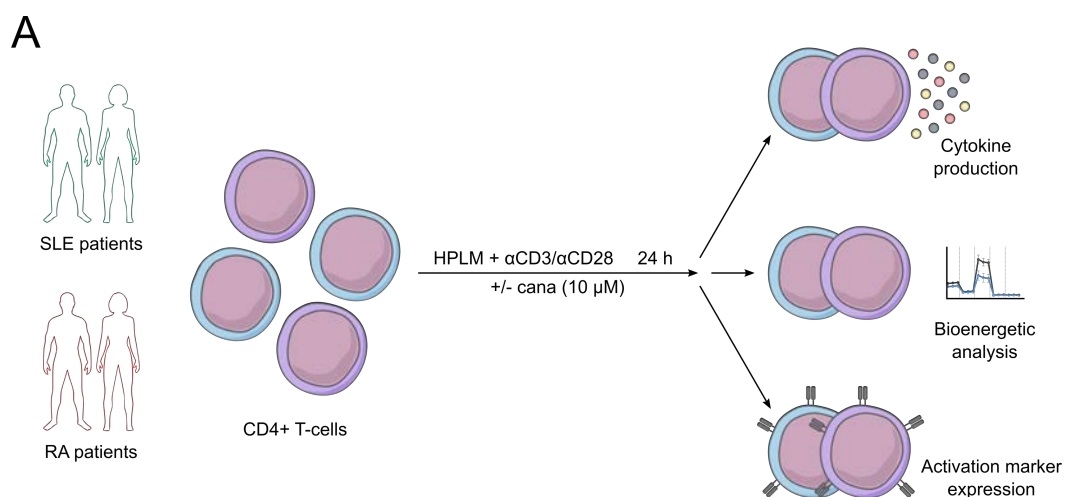
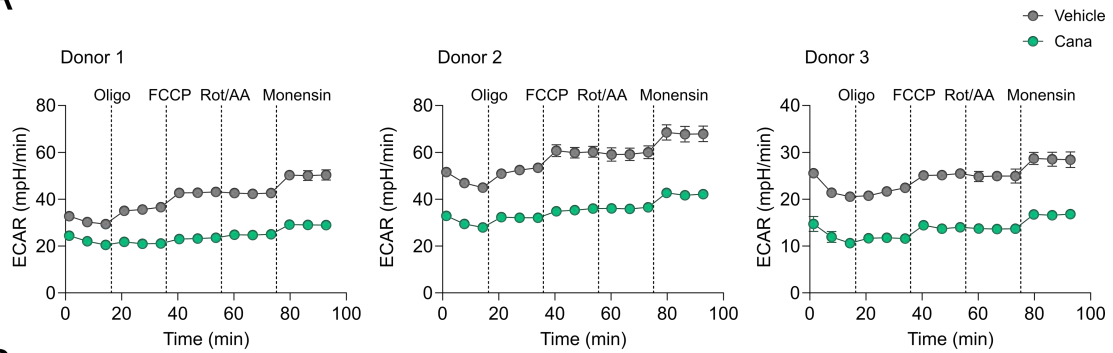


Figure 6.22 – Experimental procedure employed to assess the impact of canagliflozin on patient-derived CD4+ T cells

(A) Schematic overview outlining the experimental design in HPLM – anti-CD3 (2 μg/ml) and anti-CD28 (20 μg/ml) activated pan CD4+ T cells in the presence and absence of canagliflozin (10 μM).

Initially, we determined whether canagliflozin exercises its off-target effects and perturbs metabolism in T cells isolated from both autoimmune patient cohorts. A bioenergetic profile was generated for anti-CD3 and anti-CD28 activated CD4+ T cells that had been treated with either canagliflozin or DMSO vehicle control. Since there was variability between each patient sample (Figure 6.23 and 6.24), the metabolic parameters calculated were normalised to the control group to assess the relative change upon canagliflozin treatment.

A



B

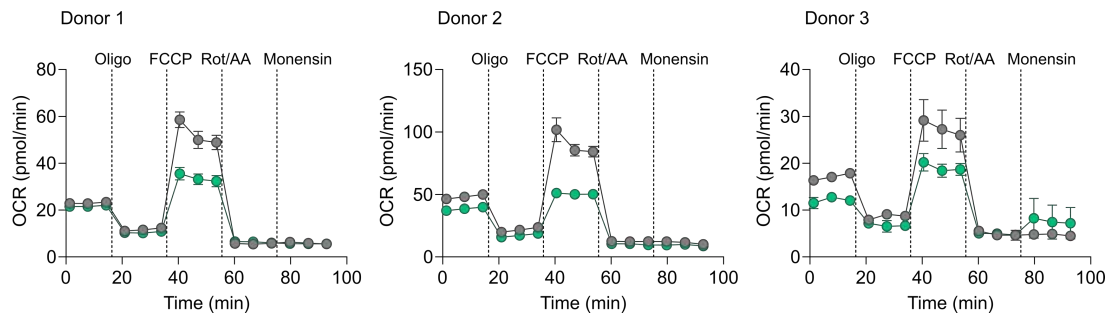


Figure 6.23 – Donor variability in bioenergetic analysis of SLE patient-derived CD4+ T cells

(A) Seahorse traces of glycolysis in anti-CD3 (2 $\mu\text{g/ml}$) and anti-CD28 (20 $\mu\text{g/ml}$) activated SLE patient-derived CD4+ T cells in the presence and absence of canagliflozin (10 μM), measured with oligomycin, FCCP, antimycin A/rotenone (all 1 μM) and monensin (20 μM). (B) Seahorse traces of OXPHOS as in (A). Data are representative of 2+ technical replicates. Data expressed as mean \pm SEM.

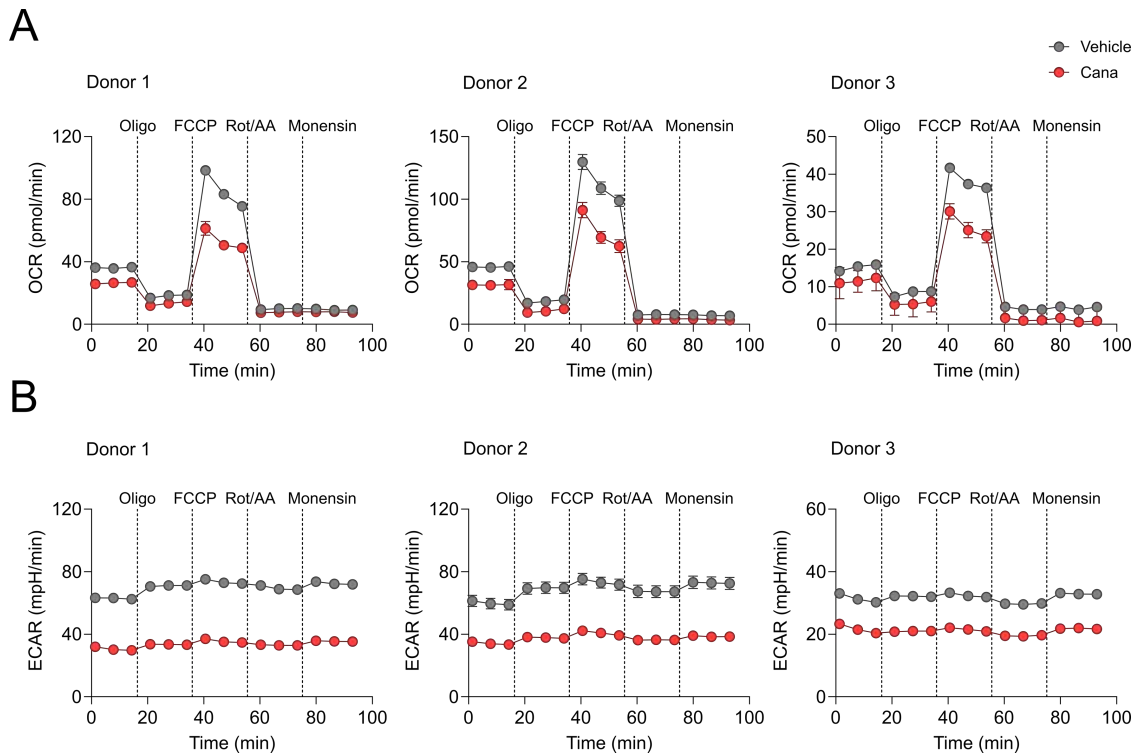


Figure 6.24 – Donor variability in bioenergetic analysis of RA patient-derived CD4+ T cells

(A) Seahorse traces of glycolysis in anti-CD3 (2 $\mu\text{g/ml}$) and anti-CD28 (20 $\mu\text{g/ml}$) activated RA patient-derived CD4+ T cells in the presence and absence of canagliflozin (10 μM), measured with oligomycin, FCCP, antimycin A/rotenone (all 1 μM) and monensin (20 μM). (B) Seahorse traces of OXPHOS as in (A). Data are representative of 2+ technical replicates. Data expressed as mean \pm SEM.

As previously observed in T cells derived from healthy donors, glycolysis was impaired by canagliflozin in CD4+ T cells isolated from both SLE and RA patients, as canagliflozin suppressed both basal glycolysis (SLE: $p = 0.0185$; RA: $p = 0.0192$) and maximal glycolysis (SLE: $p = 0.0017$; RA: $p = 0.0137$) in each patient group (Figure 6.25A-F). Consequently, there was a concomitant reduction in glycolysis-derived ATP levels at both basal (SLE: $p = 0.0172$; RA: $p = 0.0188$) and maximal (SLE: $p = 0.0011$; RA: $p = 0.0139$) rates of metabolism (Figure 6.25G-H).

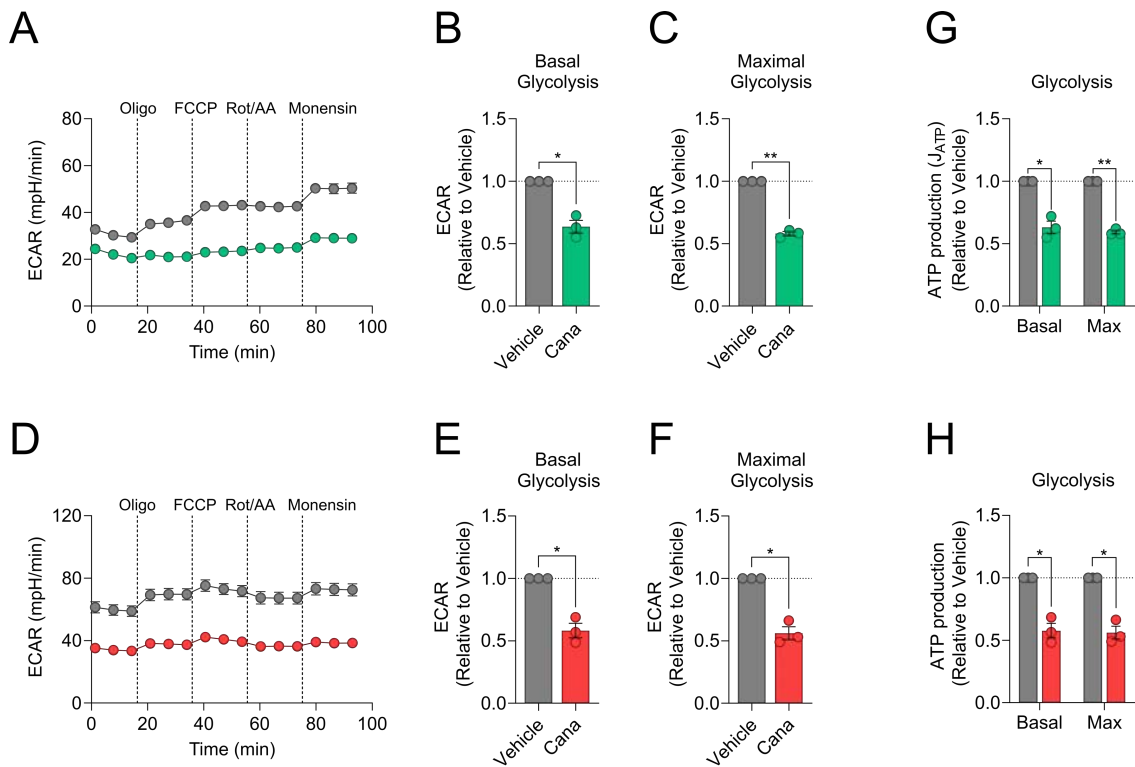


Figure 6.25 – Canagliflozin impairs CD4+ T cell glycolysis in SLE and RA

(A) Seahorse trace of glycolysis in anti-CD3 (2 $\mu\text{g/ml}$) and anti-CD28 (20 $\mu\text{g/ml}$) activated SLE patient-derived CD4+ T cells in the presence and absence of canagliflozin (10 μM), measured with oligomycin, FCCP, antimycin A/rotenone (all 1 μM) and monensin (20 μM). Trace representative of one patient sample only. (B-C) Glycolytic parameters including (B) basal glycolysis and (C) maximal glycolysis in SLE. (D) Seahorse trace of glycolysis as in (A) for RA patient-derived CD4+ T cells, representative of one patient sample only. (E-F) Glycolytic parameters including (E) basal glycolysis and (F) maximal glycolysis in RA. (G-H) Joules of ATP produced from glycolysis at basal and maximal levels in (G) SLE and (H) RA. Data are representative of three independent experiments. All relative data are normalised to the vehicle control group. Statistical analysis was performed using a one-sample T test. Data expressed as mean \pm SEM; * $p \leq 0.05$, ** $p \leq 0.01$.

Interestingly, compared to our previous findings in healthy individuals, there was only a modest reduction in OXPHOS in patient-derived T cells treated with canagliflozin (Figure 6.26). Here, basal respiration was not affected in either cohort (SLE: $p = 0.1021$; RA: $p = 0.1065$), whilst ATP-linked respiration was only repressed by canagliflozin in the RA patient cohort (SLE: $p = 0.2008$; RA: $p = 0.0406$). Similar to that observed in healthy donors, the capacity for oxidative respiration in treated CD4+ T cells was diminished in both SLE and RA, whereby their maximal respiratory capacity (SLE: $p = 0.0062$; RA: $p = 0.0111$) and spare respiratory capacity (SLE: $p = 0.0416$; RA: $p = 0.0053$) were significantly reduced (Figure 6.26A-J). Consequently, there was a reduction in the ATP produced from OXPHOS at basal rates of oxidative metabolism, which was significant in RA (SLE: $p = 0.1927$; RA: $p = 0.0444$), whilst even fewer joules of ATP were produced when OXPHOS was at its maximal rate (SLE: $p = 0.0062$; RA: $p = 0.0111$; Figure 6.26K-L).

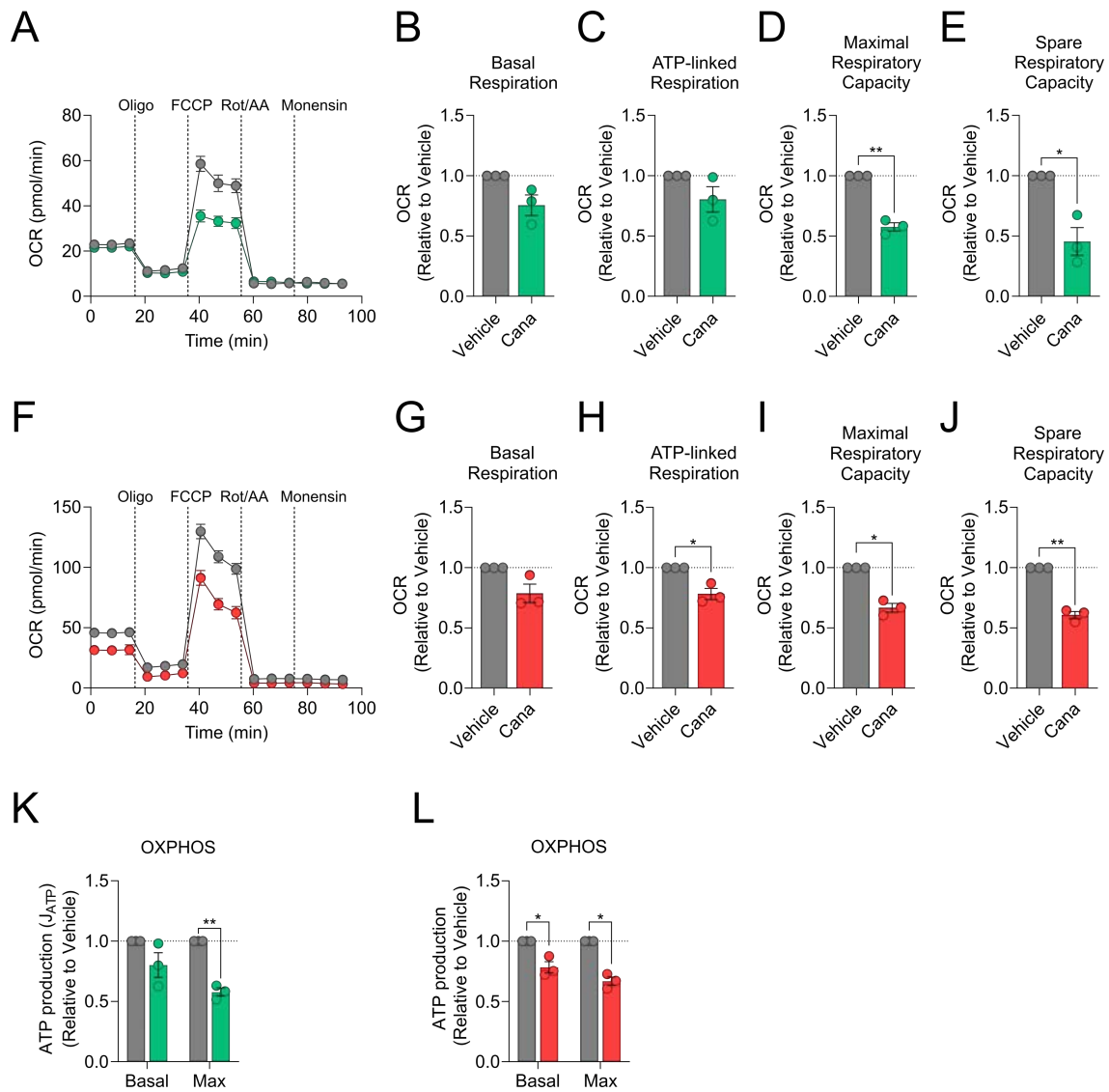


Figure 6.26 – Canagliflozin limits the respiratory capacity of CD4+ T cells in SLE and RA

(A) Seahorse trace of OXPHEROS in anti-CD3 (2 $\mu\text{g}/\text{ml}$) and anti-CD28 (20 $\mu\text{g}/\text{ml}$) activated SLE patient-derived CD4+ T cells in the presence and absence of canagliflozin (10 μM), measured with oligomycin, FCCP, antimycin A/rotenone (all 1 μM) and monensin (20 μM). Trace representative of one patient sample only. (B-E) Respiratory parameters including (B) basal respiration, (C) ATP-linked respiration, (D) maximal respiratory OCR capacity and (E) spare respiratory capacity in SLE. (F) Seahorse trace of OXPHEROS as in (A) for RA patient-derived CD4+ T cells. (G-J) Respiratory parameters including (G) basal respiration, (H) ATP-linked respiration, (I) maximal respiratory capacity and (J) spare respiratory capacity in RA. (K-L) Joules of ATP (J_{ATP}) produced from OXPHEROS at basal and maximal levels in (K) SLE and (L) RA. Data are representative of three independent experiments. All relative data are normalised to the vehicle control group. Statistical analysis was performed using a one-sample T test. Data expressed as mean \pm SEM; * $p \leq 0.05$, ** $p \leq 0.01$, *** $p \leq 0.001$.

Given the foregoing changes in CD4+ T cell metabolism, OCR/ECAR ratio tended to shift towards a more oxidative phenotype in canagliflozin-treated cells – largely owing to more profound inhibition of glycolysis by canagliflozin treatment (SLE: $p = 0.0770$; RA: $p = 0.0242$; Figure 6.27).

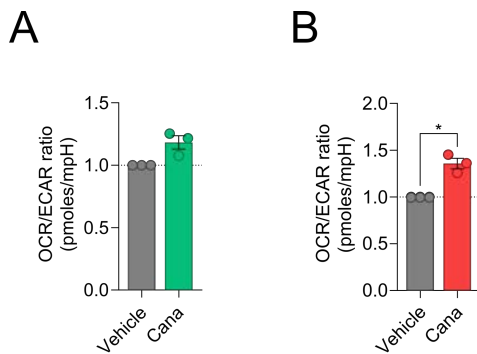


Figure 6.27 – OCR/ECAR ratio of SLE and RA patient-derived CD4+ T cells treated with canagliflozin (A-B) OCR/ECAR ratio calculated using basal respiration and basal glycolysis of anti-CD3 (2 μg/ml) and anti-CD28 (20 μg/ml) activated patient-derived CD4+ T cells in the presence and absence of canagliflozin (10 μM). CD4+ T cells derived from (A) SLE and (B) RA patients. Data are representative of three independent experiments. Statistical analysis was performed using a one-sample T test. Data expressed as mean ± SEM.

To further consider the global impact that canagliflozin exerts on T cells in autoimmune disease, changes in ATP production from glycolysis and OXPHOS were coupled to give the bioenergetic scope of CD4+ T cells – calculated as the product of ATP produced from glycolysis and ATP produced from OXPHOS. The bioenergetic scope of canagliflozin-treated cells declined at basal metabolic rates (SLE: $p = 0.0439$; RA: $p = 0.0183$) and became even more pronounced when metabolic flux was at its maximal rate (SLE: $p = 0.0004$; RA: $p = 0.0077$; Figure 6.28).

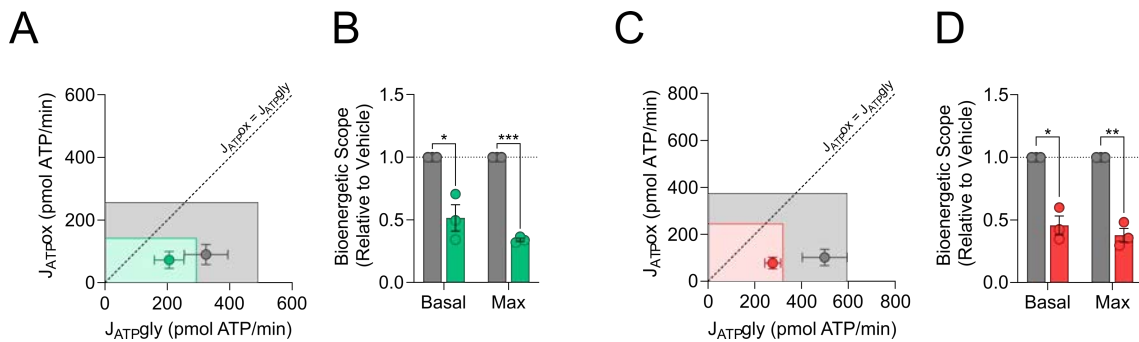


Figure 6.28 – Canagliflozin limits the bioenergetic scope of CD4+ T cells in SLE and RA

(A) Bioenergetic map representing joules of ATP (J_{ATP}) produced from glycolysis and OXPHOS in anti-CD3 (2 $\mu\text{g/ml}$) and anti-CD28 (20 $\mu\text{g/ml}$) activated SLE patient-derived CD4+ T cells in the presence and absence of canagliflozin (10 μM), measured with oligomycin, FCCP, antimycin A/rotenone (all 1 μM) and monensin (20 μM). Symbols represent J_{ATP} produced under basal metabolic conditions; rectangles represent J_{ATP} produced under maximal metabolic conditions. (B) Bioenergetic scope at basal and maximal levels in SLE. (C) Bioenergetic map representing J_{ATP} produced from glycolysis and OXPHOS as in (A) by RA patient-derived CD4+ T cells. (D) Bioenergetic scope at basal and maximal levels in RA. Data are representative of three independent experiments. Statistical analysis was performed using a one-sample T test. Data expressed as mean \pm SEM; * $p \leq 0.05$, ** $p \leq 0.01$, *** $p \leq 0.001$.

Despite the metabolic perturbation observed, the plasticity of these cells to respond to changes in ATP demand or the source of their ATP supply, as measured by their supply flexibility index, was not significantly altered by treatment with canagliflozin (SLE: $p = 0.4608$; RA: $p = 0.6884$; Figure 6.29). Together these data are in agreement with our previous experiments in healthy donors and demonstrates that canagliflozin maintains its ability to modulate T cell metabolism in the setting of SLE and RA.

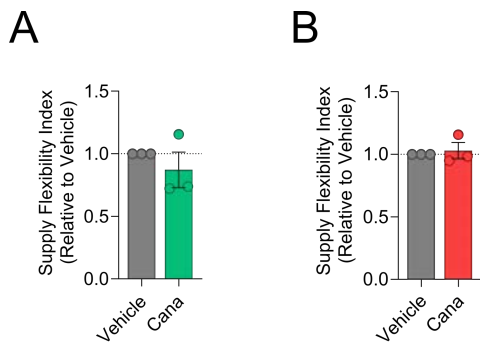


Figure 6.29 – Canagliflozin-treated CD4+ T cells retain metabolic flexibility in SLE and RA

(A-B) Supply flexibility index of anti-CD3 (2 $\mu\text{g}/\text{ml}$) and anti-CD28 (20 $\mu\text{g}/\text{ml}$) activated SLE patient-derived CD4+ T cells in the presence and absence of canagliflozin (10 μM), measured with oligomycin, FCCP, antimycin A/rotenone (all 1 μM) and monensin (20 μM). CD4+ T cell derived from (A) SLE or (B) RA patients. Data are representative of three independent experiments. Statistical analysis was performed using a one-sample T test. Data expressed as mean \pm SEM.

Previously, we described that canagliflozin enhances mitochondrial ROS through complex I inhibition, disrupting the mTOR/MYC axis and subsequently impairing T cell metabolism and function (see Chapter 5.3). Therefore, mitochondrial ROS production was measured in activated RA patient-derived T cells treated with canagliflozin to gain some insight into whether the same mechanisms underpin altered T cell metabolism and function in autoimmune disease. Consistent with our previous findings, mitochondrial ROS production was increased at 60 min in canagliflozin-treated T cells ($p = 0.0286$; Figure 6.30). This would suggest that canagliflozin induces mitochondrial dysfunction in autoimmune patient-derived T cells, similar to that observed in healthy individuals.

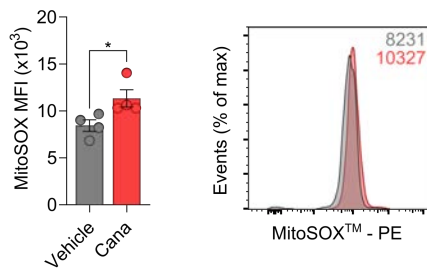
A

Figure 6.30 – Canagliflozin promotes mitochondrial reactive oxygen species production in RA patient-derived CD4+ T cells

(A) Mitochondrial ROS production in anti-CD3 (2 µg/ml) and anti-CD28 (20 µg/ml) activated RA patient-derived CD4+ T cells in the presence and absence of canagliflozin (10 µM), determined by flow cytometry using mitochondrial superoxide indicator MitoSOX™. Representative overlaid histogram plots, numbers indicate median fluorescence intensity. Data are representative of four independent experiments. Data expressed as mean ± SEM; * $p \leq 0.05$.

Next, we aimed to assess whether canagliflozin-induced alterations in T cell metabolism underlie the same changes in activation and function determined in healthy donors. Activation was measured in response to anti-CD3 and anti-CD28 co-stimulation by the surface expression of CD25, CD44 and CD69. Despite CD25 expression remaining unchanged on T cells derived from SLE patients in response to canagliflozin treatment ($p = 0.5696$), significant reductions were observed in the expression of the other activation markers – CD44 ($p = 0.0081$) and CD69 ($p = 0.0025$) – with the most pronounced reduction observed for the latter (Figure 6.31A-C). For RA patients, canagliflozin was detrimental to the expression of all three activation markers measured (CD25: $p = 0.0004$; CD44: $p = 0.0004$; CD69: $p < 0.0001$), with CD69 again the most affected (Figure 6.31D-F).

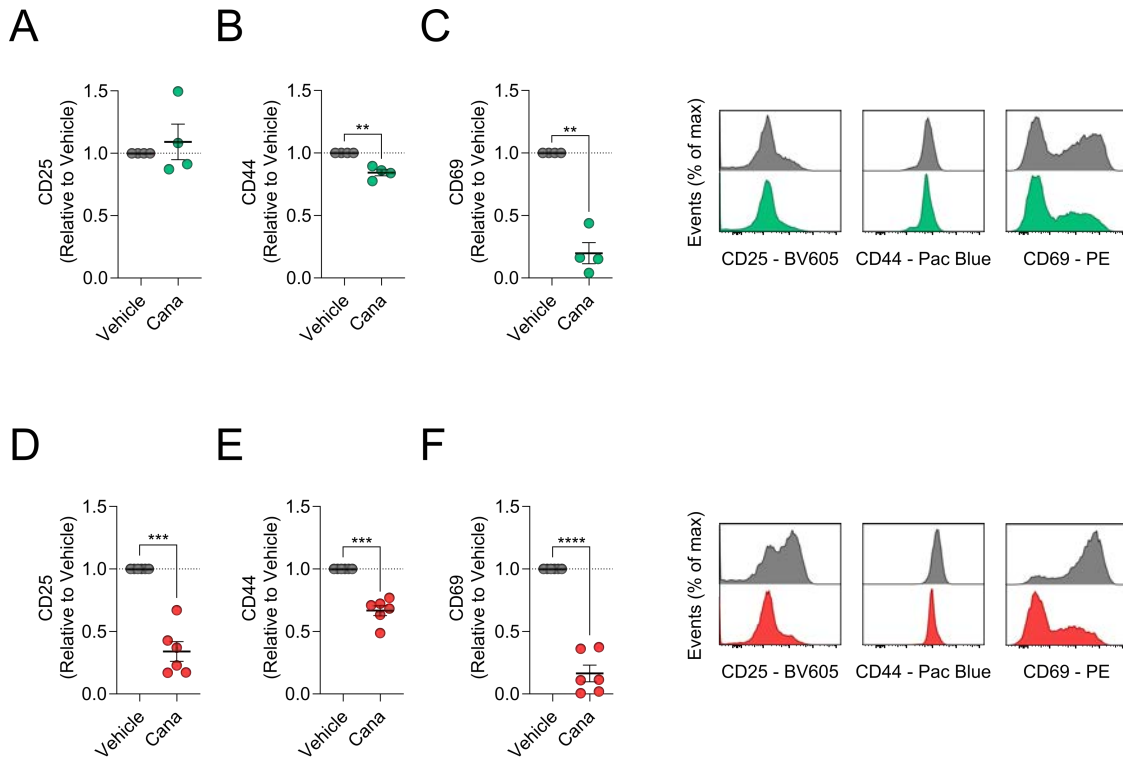


Figure 6.31 – CD4+ T cell activation is impaired by canagliflozin in SLE and RA

(A-C) Relative surface expression of activation markers (A) CD25, (B) CD44 and (C) CD69 on anti-CD3 (2 µg/ml) and anti-CD28 (20 µg/ml) activated SLE patient-derived CD4+ T cells in the presence and absence of canagliflozin (10 µM), determined by flow cytometry. (D-F) Relative surface expression of activation markers (D) CD25, (E) CD44 and (F) CD69 on RA patient-derived CD4+ T cells as in (A-C). Representative overlaid histogram plots. Data are representative of four (A-C) or six (D-F) independent experiments. All relative data are normalised to the vehicle control group. Statistical analysis was performed using a one-sample T test. Data expressed as mean ± SEM; ** $p \leq 0.01$, *** $p \leq 0.001$, **** $p < 0.0001$.

Contrary to our previous understanding in healthy donors, canagliflozin only exerted a modest impact on T cell blastogenesis in an autoimmune disease setting (SLE: $p = 0.0632$; RA: $p = 0.0408$; Figure 6.32).

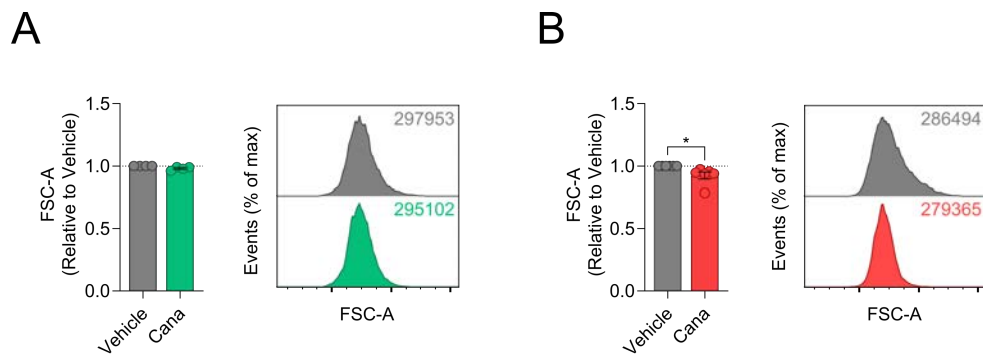


Figure 6.32 – Canagliflozin restricts CD4+ T cell blastogenesis in RA

(A) Relative cell size in anti-CD3 (2 $\mu\text{g}/\text{ml}$) and anti-CD28 (20 $\mu\text{g}/\text{ml}$) activated SLE patient-derived CD4+ T cells in the presence and absence of canagliflozin (10 μM), determined by flow cytometry using forward-scatter area. (B) Relative cell size in RA patient-derived CD4+ T cells as in (A). Representative overlaid histogram plots, numbers indicate forward scatter area. Data are representative of four (A) or six (B) independent experiments. All relative data are normalised to the vehicle control group. Statistical analysis was performed using a one-sample T test. Data expressed as mean \pm SEM; * $p \leq 0.05$.

Importantly, in spite of the aforementioned changes in metabolism and activation, CD4+ T cell viability was not majorly compromised in either patient cohort (Figure 6.33). Viability was unchanged in SLE patient-derived T cells following canagliflozin treatment ($p = 0.2532$), whilst there was only a modest reduction observed in T cells isolated from RA patients ($p = 0.0462$; Figure 6.33). Thus, canagliflozin impairs T cell activation in autoimmune disease, but does not adversely affect cell survival.

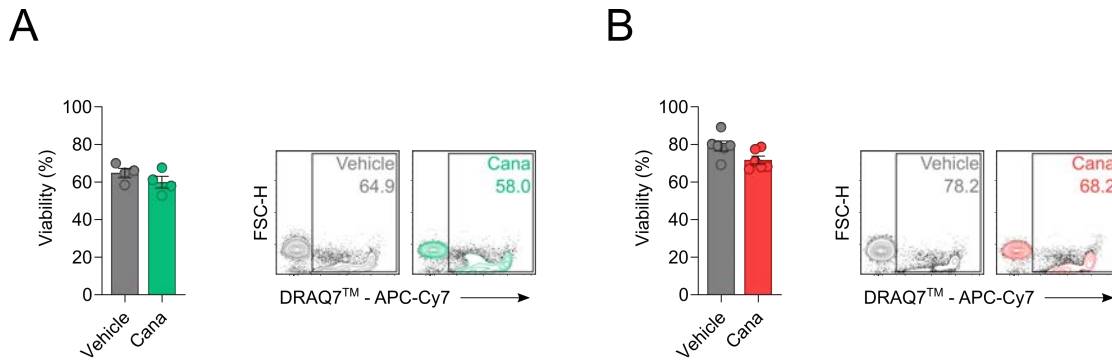


Figure 6.33 – CD4+ T cell viability is not markedly compromised by canagliflozin in SLE and RA

(A) Cell viability of anti-CD3 (2 $\mu\text{g}/\text{ml}$) and anti-CD28 (20 $\mu\text{g}/\text{ml}$) activated SLE patient-derived CD4+ T cells in the presence and absence of canagliflozin (10 μM), determined by flow cytometry using DRAQ7™. (B) Cell viability of RA patient-derived CD4+ T cells as in (A). Representative contour plots, numbers indicate frequency of dead cells. Data are representative of four (A) or six (B) independent experiments. Statistical analysis was performed using an unpaired T-test. Data expressed as mean \pm SEM.

Finally, to determine whether these changes to metabolism and activation culminate in blunted T cell function, proinflammatory cytokine secretion was measured by ELISA in anti-CD3 and anti-CD28 activated CD4+ T cells treated with canagliflozin. Here, there was a significant decrease in IFN γ secretion (SLE: $p = 0.0051$; RA: $p < 0.0001$) and IL-2 secretion (SLE: $p = 0.0026$; RA: $p < 0.0001$) by CD4+ T cells following canagliflozin treatment in both autoimmune patient cohorts (Figure 6.34A-D). Additionally, further reductions in both IL-17 secretion ($p < 0.0001$) and TNF α secretion ($p < 0.0001$) were observed in RA patients (Figure 6.34F-G). IL-17 could not be detected in the cell-free supernatants of CD4+ T cells isolated from SLE patients (Figure 6.34E). Collectively, these data support our previous experiments in healthy donors, whereby canagliflozin is a potent inhibitor of global T cell function.

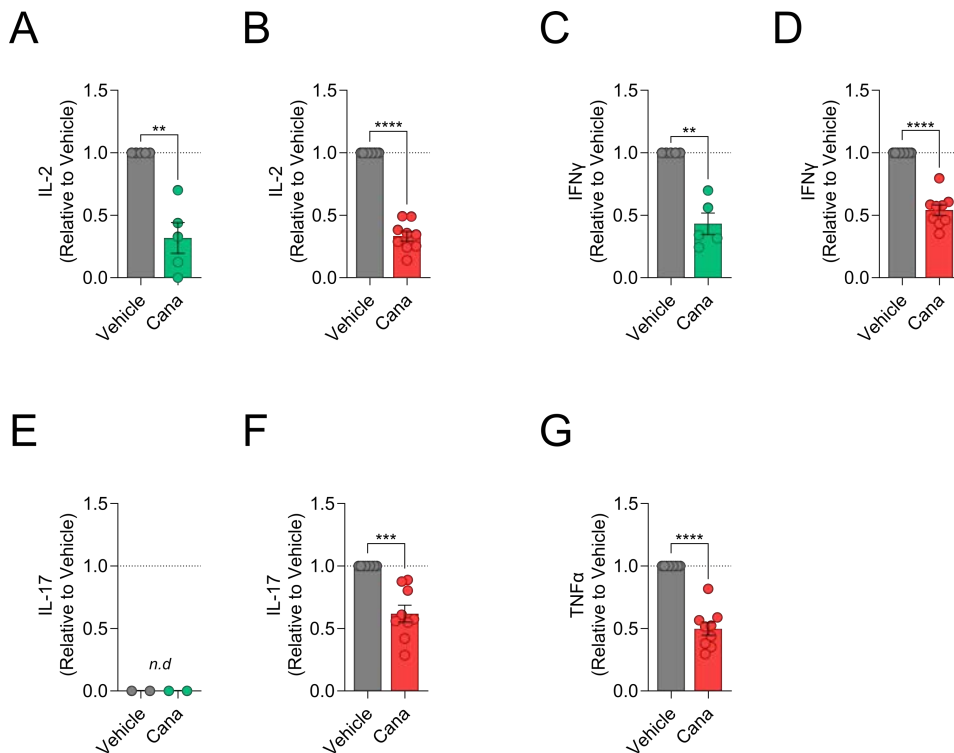


Figure 6.34 – Canagliflozin impairs effector function in SLE and RA

(A-G) Secretion of (A-B) IL-2, (C-D) IFN γ , (E-F) IL-17 and (G) TNF α by anti-CD3 (2 μ g/ml) and anti-CD28 (20 μ g/ml) activated patient-derived CD4+ T cells in the presence and absence of canagliflozin (10 μ M), determined by ELISA of cell-free supernatants. CD4+ T cells derived from SLE (A,C,E) and RA (B,D,F,G) patients. Data are representative of four (A,C), nine (B,D,F,G) or two (E) independent experiments. Statistical analysis was performed using a one-sample T test. Data expressed as mean \pm SEM; ** $p \leq 0.01$, *** $p \leq 0.001$, **** $p < 0.0001$.

6.3.5 Canagliflozin inhibits the function of human T cells isolated from arthritogenic synovial fluid

Lastly, we sought to assess whether canagliflozin remained effective in inhibiting T cell function in another human experimental model of autoimmune disease. Here, synovial fluid mononuclear cells (SFMCs) isolated from the knee of RA patients undergoing arthroscopic surgery were analysed for their activation marker expression and effector cytokine production following their activation in the presence and absence of canagliflozin (Figure 6.35).

A

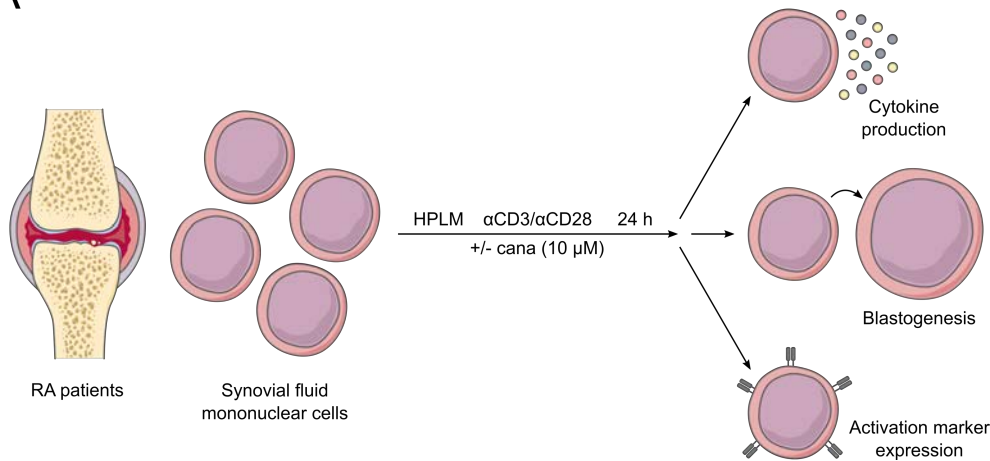


Figure 6.35 – Experimental procedure employed to assess the impact of canagliflozin on patient-derived synovial fluid mononuclear cells

(A) Schematic overview outlining the experimental design in HPLM – anti-CD3 (2 μg/ml) and anti-CD28 (20 μg/ml) activated synovial fluid mononuclear cells (SFMCs) in the presence and absence of canagliflozin (10 μM).

In agreement with our previous findings, canagliflozin largely impaired the activation of synovial fluid CD4⁺ T cells, with reduced expression of CD25 and CD44 in the majority of the patient cohort apart from one patient outlier (CD25: $p = 0.5398$; CD44: $p = 0.2080$; Figure 6.36A-B). However, the change in CD69 expression was less pronounced ($p = 0.9495$; Figure 6.36C). Furthermore, canagliflozin also impaired the activation of synovial fluid CD8⁺ T cells, whereby CD25 ($p = 0.0606$), CD44 ($p = 0.0706$) and CD69 ($p = 0.1267$) were all reduced, albeit to non-significant levels (Figure 6.36D-F).

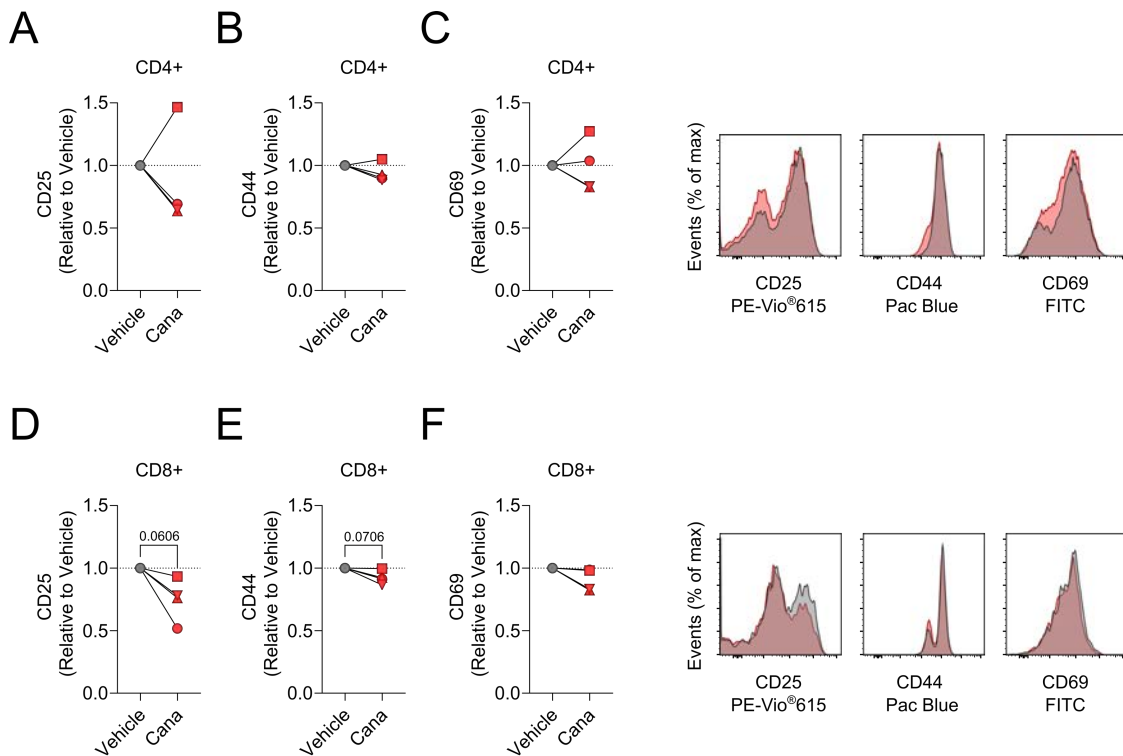


Figure 6.36 – Canagliflozin impairs the activation of synovial fluid T cells

(A-C) Relative surface expression of activation markers (A) CD25, (B) CD44 and (C) CD69 on anti-CD3 (2 $\mu\text{g/ml}$) and anti-CD28 (20 $\mu\text{g/ml}$) activated synovial fluid CD4+ T cells in the presence and absence of canagliflozin (10 μM), determined by flow cytometry. (D-F) Relative surface expression of activation markers (D) CD25, (E) CD44 and (F) CD69 on synovial fluid CD8+ T cells as in (A-C). Individual donors identified by symbol shape. Representative overlaid histogram plots. Data are representative of four independent experiments. All relative data are normalised to the vehicle control group. Statistical analysis was performed using a one-sample T test. Data expressed as mean with lines adjoining paired data points.

Additionally, reductions in CD4+ T cell blastogenesis were observed in three of the four patient samples ($p = 0.1926$) upon treatment with canagliflozin (Figure 6.37A). This change in blastogenesis was more pronounced in CD8+ T cells ($p = 0.0526$; Figure 6.37B).

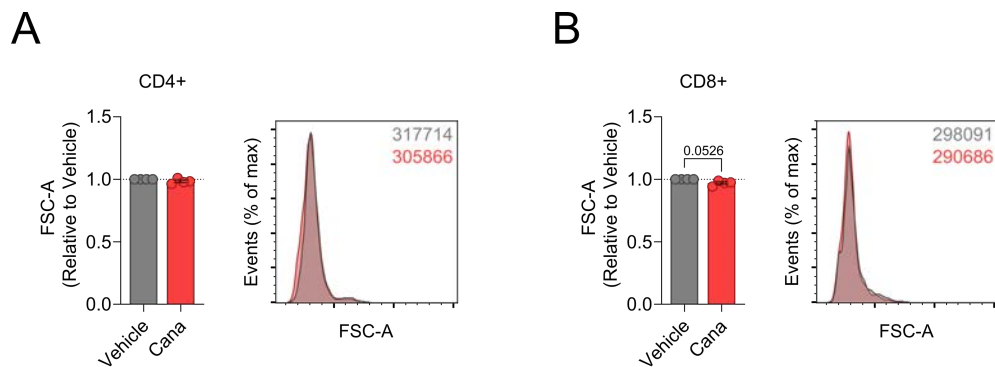


Figure 6.37 – Canagliflozin restricts synovial fluid T cell blastogenesis

(A) Relative cell size in anti-CD3 (2 $\mu\text{g}/\text{ml}$) and anti-CD28 (20 $\mu\text{g}/\text{ml}$) activated synovial fluid CD4+ T cells in the presence and absence of canagliflozin (10 μM), determined by flow cytometry using forward-scatter area. (B) Relative cell size in synovial fluid CD8+ T cells as in (A). Representative overlaid histogram plots, numbers indicate forward scatter area. Data are representative of four independent experiments. All relative data are normalised to the vehicle control group. Statistical analysis was performed using a one-sample T test. Data expressed as mean \pm SEM.

Importantly, canagliflozin-mediated changes in T cell activation and blastogenesis did not arise as a result of compromised viability (CD4: $p = 0.7222$; CD8: $p = 0.6761$; Figure 6.38). Together, these data demonstrate that canagliflozin retains its inhibitory effect on T cell activation in another setting of autoimmune disease.

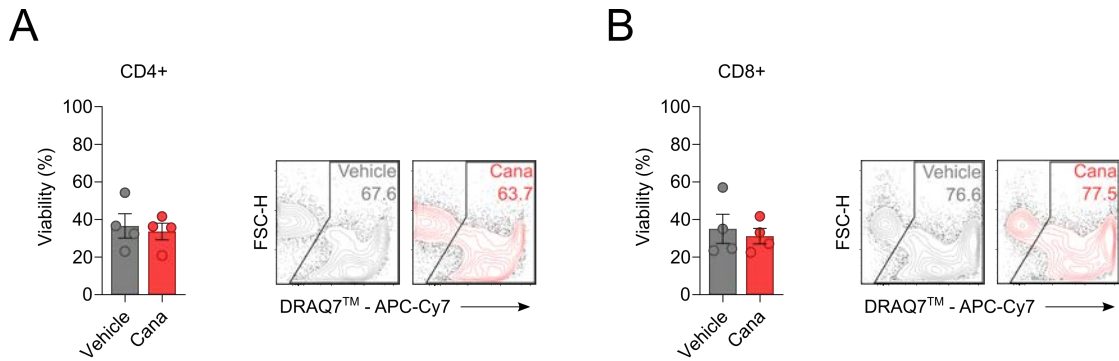


Figure 6.38 – Synovial fluid T cell viability is not compromised by canagliflozin

(A) Cell viability of anti-CD3 (2 $\mu\text{g}/\text{ml}$) and anti-CD28 (20 $\mu\text{g}/\text{ml}$) activated synovial fluid CD4+ T cells in the presence and absence of canagliflozin (10 μM), determined by flow cytometry using DRAQ7™. (B) Cell viability of synovial fluid CD8+ T cells as in (A). Representative contour plots, numbers indicate frequency of dead cells. Data are representative of four independent experiments. Statistical analysis was performed using an unpaired T-test. Data expressed as mean \pm SEM.

Naturally, we wanted to determine whether the impaired activation of synovial fluid T cells culminated in defective effector cytokine production – particularly those involved in the manifestation of chronic inflammation. Here, we observed a trend towards decrease in the expression of the proinflammatory cytokines IFN γ ($p = 0.0890$), IL-17 ($p = 0.0352$) and TNF α ($p = 0.2535$) by SFMCs following canagliflozin treatment (Figure 6.39). Collectively, this supports our previous findings in PBMCs isolated from healthy individuals and autoimmune patient cohorts such as SLE and RA. This demonstrates that canagliflozin has the ability to modulate T cell metabolism and downstream effector function in different human experimental models of autoimmune disease, therefore warranting further consideration as a therapy in this disease setting.

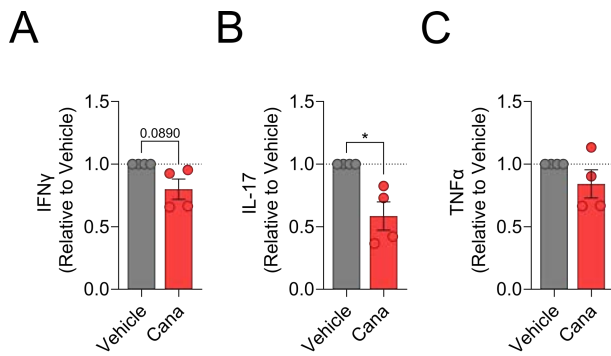


Figure 6.39 – Canagliflozin inhibits proinflammatory cytokine production by synovial fluid mononuclear cells

(A-C) Secretion of (A) IFN γ , (B) IL-17 and (C) TNF α by anti-CD3 (2 μ g/ml) and anti-CD28 (20 μ g/ml) activated SFMCs in the presence and absence of canagliflozin (10 μ M), determined by ELISA of cell-free supernatants. Data are representative of four independent experiments. Statistical analysis was performed using a one-sample T test. Data expressed as mean \pm SEM; * $p \leq 0.05$.

6.4 Discussion

The work in this chapter focuses on the significance of canagliflozin treatment in the setting of autoimmunity. Our initial experiments investigated the inhibitory effects of canagliflozin of antigen-trained Teff cells – the compartment that primarily comprises the hyperactivated T cells within the site of inflammation. Our focus then progressed onto the effects that canagliflozin had on CD4 $^{+}$ T cells isolated from two autoimmune patient cohorts.

Here, the inhibitory effect of canagliflozin on antigen-experienced Teff cells was shown for the first time. The secretion of several cytokines was markedly reduced by canagliflozin following both short-term and long-term activation. Interestingly, of the cytokines measured, the production of IL-10 was most resistant to canagliflozin treatment, with no significant change in its concentration observed following 72 h Teff cell activation. Typically, IL-10 is anti-inflammatory in nature and are produced by Treg cells. Increased proportions of Treg cells are associated with more favourable outcomes in autoimmune disease (see Chapter 1.4), therefore it is interesting that canagliflozin appears to specifically downregulate proinflammatory cytokine production. Furthermore, a pronounced reduction in both IFN γ and IL-17 is exciting given the importance of both cytokines in mediating disease pathogenesis (see Chapter 1.4). As previously described in activated T cells (see Chapter 3.3), reduced Teff cell activation following canagliflozin treatment underlies impaired effector

function, whilst long-term activation is associated with defects in both blastogenesis and proliferation. These data would suggest that canagliflozin exerts its inhibitory effects in a similar manner in all CD4+ T cell compartments, whereby there is accumulation of mitoROS and perturbation of metabolism through disruption of the mTOR/MYC axis following inhibition of mitochondrial complex I and GDH. Indeed, reduced expression of the nutrient transporters CD36, CD71 and CD98 upon canagliflozin treatment might cause reduced uptake of fatty acids, iron and amino acids, respectively, suggesting that changes in function are supported by metabolic rewiring. Moreover, reduced CD98 expression could be indicative of a reduction in MYC expression, whereas the reduction in both CD71 and CD98 could indicate a reduction in mTOR levels (Preston et al., 2015; Waickman & Powell, 2012). Decreased glucose uptake by Teff cells was estimated by increased extracellular glucose concentrations in the cell-free supernatants collected. It is currently difficult to predict glucose uptake using single-cell methods, given the recent issues highlighted when using the fluorescent glucose analogue 2-NBDG (D'Souza et al., 2022; Sinclair et al., 2020). However, it is unlikely that the change in glucose uptake is dependent on SGLT2 (SLC5A2), given that others have reported it is not expressed by T cells (Uhlen et al., 2019)(Human Protein Atlas, *proteinatlas.org*). Further work is required to fully elucidate the changes in Teff cell metabolism in response to canagliflozin treatment, using our earlier work in activated T cells with more sophisticated techniques as a blueprint (see Chapter 5.3). Surprisingly, despite the profound impact of canagliflozin on T cell function, reduced expression of the co-inhibitory receptors LAG3, PD-1 and TIM3 suggests that canagliflozin mediates its inhibitory effect independent of T cell exhaustion. However, the expression of these markers is not strongly impaired following canagliflozin treatment, therefore it is worth considering that the observed reduction could be in line with the reduction in cell size (see Chapter 4.3.3).

With regards to the distinct changes in cytokine production following canagliflozin treatment, further investigation was made into the composition of T helper subsets within the Teff cell compartment. Differential expression of four distinct chemokine receptors allowed the identification of several Th subsets by flow cytometry (Mahnke, Beddall, et al., 2013). Given the observed decrease in IFN γ production, an increase in the Th1 subset following canagliflozin treatment was unexpected. However, increased expression of IRF2 and IRF9 was observed in our Nanostring dataset, both of which promote Th1 responses (Lohoff & Mak, 2005), which could explain the increase in this subset. Typically, Th1 cells are

associated with poorer disease outcome in autoimmunity (see Chapter 1.4), but since IFN γ production is reduced by canagliflozin, this would suggest that even though there is an increase in the proportion of Th1 cells, these cells are dysfunctional and less able to contribute to disease pathogenesis. Promisingly, we also observed a reduction in the frequency of both Th17 and Th22 cell populations, further producers of the proinflammatory cytokines involved in autoimmune disease. There is a consequent increase in the ratio of Th1:Th17 cells, which has been recently associated with reduced disease severity in RA patients (Bazzazi et al., 2018). Changes in intracellular transcription factor expression (Tbet, GATA3 and ROR γ T) were inconsistent with the respective change in the associated Th subset, therefore it is unclear what drives canagliflozin-induced changes in the composition of Th subsets. Reduced expression of Treg associated markers would also suggest that canagliflozin is a general inhibitor of T cell function rather than a promoter of anti-inflammatory mediators. To better understand the underlying mechanisms driving altered differentiation to various Th subsets, future work should investigate the effect of canagliflozin in polarisation experiments. Culturing T cells alongside factors that push them towards a specific lineage should be carried out in the presence and absence of canagliflozin to determine whether: (i) it promotes/suppresses differentiation towards certain lineages; (ii) it pushes T cell towards an alternative lineage under these conditions; and (iii) successfully polarised T cells display any alternative function or complete loss of function.

Given the dramatic inhibitory effect observed thus far in CD4 $^{+}$ T cells in response to canagliflozin treatment, it was important to learn whether this is applicable to CD8 $^{+}$ T cells. Indeed, impaired effector function underpinned by limited T cell activation was observed in CD8 $^{+}$ T cells, which shows that canagliflozin does not elicit its effect on CD4 $^{+}$ T cells specifically. Further work is required to determine the full extent to which canagliflozin inhibits CD8 $^{+}$ T cell function, i.e., target cell killing, which could be of emerging importance in autoimmune disease (Deng et al., 2019), whilst potentially having merit in other disease settings such as cancer. Despite the need for further investigation, it would be unsurprising to see inhibition of additional effector functions, given the inhibitory effect that canagliflozin has on early TCR signalling events and the subsequent activity of any downstream signalling proteins.

Critically, our results are the first to demonstrate that canagliflozin can modulate immune cell function in the setting of autoimmunity. Here, canagliflozin retained its ability to

suppress CD4+ T cell function *ex vivo* in two human autoimmune patient cohorts – SLE and RA. Similar to our previous work analysing activated T cell metabolism (see Chapter 5.3), canagliflozin limited basal and maximal rates of glycolysis, resulting in less ATP being produced from this pathway. However, in contrast to our work in healthy individuals, canagliflozin had a more modest impact on oxidative respiration in patient-derived CD4+ T cells, with reductions in maximal respiratory capacity and spare respiratory capacity only within these cells. Again, this resulted in a reduced capacity for ATP production from OXPHOS. Taken together, this shows that canagliflozin retains T cells in a state of metabolic quiescence in the setting of autoimmunity. Importantly, perturbed metabolism in response to canagliflozin led to suppression of T cell activation and function, further advocating the repurposing of canagliflozin for use in autoimmune disease. Proinflammatory cytokines IFN γ , IL-2, IL-17 and TNF α were all reduced in response to canagliflozin.

In an attempt to strengthen our findings, we assessed the impact of canagliflozin in another human experimental model of autoimmunity, using RA SFMCs isolated during arthroscopic surgery. Promisingly, in keeping with our previous findings in healthy donors, canagliflozin impaired the activation of both CD4+ and CD8+ T cell compartments. Furthermore, these data were further supported by a trend towards decrease in the production of several proinflammatory cytokines including IFN γ , IL-17 and TNF α . Curiously, the patient outlier that did not respond to canagliflozin treatment (in terms of the activation markers expressed by synovial fluid T cells) had a diminished CD4+ T cell compartment compared to the other patients – 17.5% of CD3+ lymphocytes versus a mean of 51.9%. Together, these findings again show that canagliflozin is effective in inhibiting T cell function in an alternative setting of autoimmunity. Excitingly, this human experimental model used SFMCs that are present at the site of inflammation in disease setting, highlighting that canagliflozin treatment would be highly applicable to the hyperactivated T cell compartment that is characteristic of autoimmune disease. Additionally, the data gleaned from these experiments further supports our earlier work in which already-activated CD4+ T cells were treated with canagliflozin (see Chapter 3.3.3). SFMCs isolated from the inflamed synovium are also already activated, and in both settings, canagliflozin has only a modest effect in inhibiting T cell function. Despite these findings suggesting the potency of canagliflozin is reduced when T cells are already activated, it is also encouraging to see such similarities,

perhaps even strengthening the belief that canagliflozin does have an effect on already-activated T cell function, albeit in a distinct manner versus newly-activated T cells.

Despite these promising data, it is important to consider the limitations of the *ex vivo* nature of our study. Beyond the scope of this work, there is the possibility of further investigation proceeding directly to clinical trial, given canagliflozin is a clinically approved drug and the concentrations chosen in these analyses are known safe, physiological doses. Alternatively, it would be interesting to determine if there are patient data wherein T2D patients with concomitant autoimmune disorders have been prescribed canagliflozin. For example, autoimmune disease severity could be compared between individuals prescribed with metformin as a monotherapy versus those prescribed metformin and canagliflozin in combination (as canagliflozin is not yet given as a monotherapy). Further work could include an *in vivo* murine model of autoimmunity (e.g., experimental autoimmune encephalomyelitis), whereby canagliflozin is administered at a physiological concentration and disease severity monitored. It would also be important to isolate the CD4⁺ T cell compartment from these experiments – particularly from the site of inflammation – to confirm similar mechanisms of action are present within the mouse model, including impaired T cell metabolism and function. Furthermore, canagliflozin should be administered following the onset of disease to determine whether it is able to alleviate pathogenesis in ongoing disease. However, it is important to consider that human studies do not always translate well into a murine system and vice versa. These experiments should form the basis of the clinical development of canagliflozin as a treatment for autoimmune disease.

6.5 Conclusions

Our previous findings have shown that canagliflozin is a global inhibitor of T cell function, underpinned by metabolic perturbation via disruption of the mTOR/MYC axis. Considering T_H17 cells are an important contributor to chronic inflammation in autoimmune pathogenesis, the impact of canagliflozin on this CD4⁺ T cell compartment was determined. Here, canagliflozin impaired the secretion of several proinflammatory cytokines, underpinned by a reduction in T cell activation. Underlying T cell metabolism was also affected by canagliflozin, whereby glucose uptake was decreased and the expression of transporters responsible for fatty acid, amino acid and iron uptake were also reduced. However, the

aforementioned changes in effector function following canagliflozin treatment occurred independent of T cell exhaustion.

The Teff cell compartment is comprised of several Th subsets, each with a unique cytokine signature, therefore this was investigated further to determine whether the composition changes following canagliflozin treatment. An increase in the Th1 population alongside concomitant reductions in both Th17 and Th22 populations sets up a balance of subsets that is favourable in alleviating autoimmune disease severity. However, these changes were not driven by transcription factor expression, therefore it is unclear what mechanism facilitates changes in Th subset distribution upon canagliflozin treatment.

Crucially, canagliflozin maintained its inhibitory effect in two human *ex vivo* autoimmune patient cohorts. CD4⁺ T cells isolated from SLE and RA patients displayed perturbed metabolism following canagliflozin treatment, underpinning reduced activation and impaired effector function. Indeed, the production of the several proinflammatory cytokines including IFN γ , IL-2, IL-17 and TNF α were severely suppressed by canagliflozin. Additionally, canagliflozin inhibited T cell function in an alternative human experimental model of autoimmunity – SFMCs isolated from RA patients. Further work is required to establish the efficacy of canagliflozin *in vivo* in a murine model of autoimmunity. Together, these data provide the foundation for the clinical development of canagliflozin as a treatment for autoimmune disease.

Chapter Seven

General discussion

7 General discussion

7.1 Overview

Manipulating immune cell metabolism for therapeutic benefit is a burgeoning area of interest in an extensive range of diseases. The link between metabolism and inflammation has been established in T cells over the last two decades, whereby activated T cells adopt an anabolic metabolism highly dependent on glycolysis and the TCA cycle to fuel biosynthetic and energetic requirements (see Chapter 1.3.6). Aberrant T cell metabolism contributes to dysregulated function and the breakdown of self-tolerance in autoimmune diseases such as rheumatoid arthritis (RA), systemic lupus erythematosus (SLE) and multiple sclerosis (MS) (non-exhaustive list; see Chapter 1.5). For example, impaired mitochondrial metabolism in RA T cells precedes augmented TNF α production to induce tissue inflammation (Wu et al., 2021). Conversely, oxidative phosphorylation (OXPHOS) and glycolysis are elevated in T cells in SLE to facilitate heightened proinflammatory cytokine production (Yin et al., 2015). Given the relative ineffectiveness of current treatments in these conditions, investigation into novel therapies is warranted.

Initially, combined inhibition of glucose metabolism by 2-deoxyglucose (2-DG) and mitochondrial metabolism by metformin was able to reverse disease phenotype in murine models of SLE, restoring normal T cell metabolism and function (Yin et al., 2015). Recent studies have further demonstrated the therapeutic benefit of targeting T cell metabolism in autoimmunity, including tetramerization of the glycolytic enzyme pyruvate kinase (Angiari et al., 2020), inhibition of OXPHOS using oligomycin (Shin et al., 2020), use of the glycolytic inhibitor 2-DG alongside metformin (Wilson et al., 2021) and glutaminase suppression (Johnson et al., 2018). These studies highlight the exciting potential of targeting the metabolism of pathogenic T cells in autoimmunity for therapeutic gain. However, whilst promising, the clinical translation of these studies remains a challenge due to the toxic nature of impairing metabolism at a systemic level. One approach to circumvent these issues is repurposing drugs that target metabolism, such as those prescribed to patients with type 2 diabetes (T2D). Targeting metabolic processes using T2D drugs that have known safety profiles in humans has previously demonstrated therapeutic benefit in numerous inflammatory conditions in both pre-clinical and clinical settings (see Chapter 1.6). In this

thesis, we investigated repurposing canagliflozin – a member of the most recently approved class of T2D drugs, SGLT2 inhibitors – as a potential therapeutic agent in T cell-mediated autoimmunity. Gliflozins have extensive roles beyond improved glycaemic control. For instance, canagliflozin possesses unique off-target effects that include inhibition of metabolism-associated proteins such as complex I and glutamate dehydrogenase (GDH) (Secker et al., 2018; Villani et al., 2016). In addition to its on-target inhibition of SGLT2, this has enabled canagliflozin to elicit protective clinical outcomes in other inflammation-associated conditions such as chronic kidney disease and cardiovascular disease (Perkovic et al., 2019; Spertus et al., 2022). Given this encouraging precedent, canagliflozin as a treatment of autoimmunity is an attractive prospect. Published studies have not previously investigated the impact of canagliflozin on human T cell function. To date, canagliflozin has been demonstrated to inhibit murine T cell differentiation towards Th1 and Th17 lineages in a model of myocarditis (Long et al., 2022). However, it is important to consider that the percentage of cytokine-producing cells observed in these experiments was surprisingly low under every experimental condition (Long et al., 2022). Additionally, canagliflozin has also been shown to promote tumour infiltration by T cells, supporting the production of IFN γ by CD8+ T cells (Ding et al., 2023). Again, it is important to consider that these observations in the murine model might not necessarily translate into the human setting, whilst supraphysiological concentrations of canagliflozin were also required to elicit these effects (Ding et al., 2023). Moreover, this model involved the transfer of already-activated human PBMCs into canagliflozin-treated mice, which might not be the optimal setting in which to determine the effect that canagliflozin has on T cell function (Ding et al., 2023).

Whilst dysregulated metabolism has been reported in numerous autoimmune conditions (see Chapter 1.5), these changes are not universal and differ from disease to disease, therefore our aim is to use canagliflozin to target the typical immunometabolic profile of T cells for therapeutic benefit. Given its dual-pronged inhibition of mitochondrial metabolism, we hypothesised that canagliflozin would be a superior inhibitor of T cell function compared to other complex I inhibitors and thus improve its therapeutic value. Understanding the cellular changes that occur within human T cells following canagliflozin treatment is essential to provide the foundation for its clinical development as a treatment for autoimmune disease.

7.2 Canagliflozin modulates activated T cell function

A recent study demonstrated that targeting human CD4⁺ T cell metabolism using repurposed SGLT2 inhibitors is merited in autoimmune disease (Qin et al., 2022). Empagliflozin – a member of the same family of T2D drugs as canagliflozin – inhibited differentiation towards Th1 and Th17 lineages whilst increasing the Treg cell population *in vitro* in immune thrombocytopenia (an acquired autoimmune disease) (Qin et al., 2022). These changes were achieved through inhibition of the mTOR pathway to normalise CD4⁺ T cell metabolism to pre-disease levels (Qin et al., 2022). This is the only work to investigate on the impact of gliflozins on human T cell function in this setting to date.

For the first time we show that canagliflozin impairs human T cell function, whilst dapagliflozin does not display the same inhibitory properties. This difference would suggest that inhibition of T cell function occurs independent of SGLT2 inhibition, especially given that pharmacokinetic data shows that significantly lower doses of dapagliflozin are necessary to produce equivalent effects on renal glucose excretion (Devineni et al., 2013). Canagliflozin possesses unique off-target effects that inhibit mitochondrial complex I and glutamate dehydrogenase (GDH) (Secker et al., 2018; Villani et al., 2016), whilst dapagliflozin does not display any notable off-target effects. Canagliflozin, but not dapagliflozin, reduced IL-2 production in a dose-dependent manner, which was underpinned by impaired T cell activation. These findings were also confirmed under more physiologically relevant conditions, whereby traditional RPMI was replaced with human plasma-like media (HPLM) to more closely replicate physiological nutrient levels. Following longer-term activation, canagliflozin also impaired proliferation and maintained its inhibitory effect on IL-2 production. Despite the considerable loss of IL-2 upon canagliflozin treatment, supplementation with exogenous IL-2 was unable to rescue the observed phenotype. However, this could also be attributable to the significant loss of the IL-2 receptor (CD25) that was also observed.

Accumulation of hyperactivated T cells at the site of inflammation are a hallmark of autoimmunity (Thomas et al., 1992), therefore it was important to determine the effect that canagliflozin has on already-activated T cells. To this end, doses of canagliflozin beyond physiological relevance were required to inhibit the effector functions of T cells already co-stimulated through TCR and CD28. However, although canagliflozin does not impact the function of already-activated T cells, it could be argued that it might instead prevent the

repopulation of T cells at the site of inflammation, thus improving disease pathogenesis in an alternative manner. Collectively, these data provide evidence that canagliflozin is able to inhibit human T cell function.

7.3 Canagliflozin mediates global changes to T cell function at the transcript and protein level

The popularity of large-scale “omics” approaches is ever increasing. These techniques are valuable tools in that they allow rapid analysis of global changes in cellular function. It is important to distinguish between changes at the transcript and protein level to determine if targets are transcriptionally or translationally inhibited and whether changes in gene expression result in a tangible change in protein content. Here, we analysed global changes in T cell function following canagliflozin treatment using a combination of Nanostring nCounter® analysis and label-free liquid chromatography-mass spectrometry, allowing simultaneous interrogation of the genome and proteome, respectively.

Initially, analysis of autoimmunity-associated genes showed that canagliflozin induced global changes in gene expression. Crucially, dapagliflozin did not alter the expression of any of genes assessed on the panel. In agreement with our earlier experiments, *IL2* expression was downregulated in line with a decrease in IL-2 production, whilst the upregulation of *SELL* was consistent with the cell-surface preservation of CD62L. Adding to our previous knowledge, *CSF2* and *CCL20* were downregulated in activated T cells treated with canagliflozin – markers that are typically associated with a Th17 phenotype (Ramesh et al., 2014). Given the critical role that Th17 cells play in autoimmune disease pathogenesis (see Chapter 1.4), evidence of targeted inhibition of this subset by canagliflozin would be of great therapeutic benefit. Furthermore, upregulation of several interferon regulatory proteins (IRFs) involved in regulating T cell differentiation further suggests a role for canagliflozin in altering the composition of the T cell compartment and warrants further investigation. In terms of metabolic gene expression, canagliflozin again altered global gene expression. Here, the majority of the differentially expressed genes identified were associated with *cell cycle*, correlating nicely with our observed changes in T cell proliferation. Aggregation of these changes into a wider biological context revealed changes in several metabolism-associated pathways, amongst which the downregulation of *MYC* and *glycolysis* were particularly interesting. Interestingly, *MYC* itself was not affected at the transcript level.

It was imperative that we assessed the T cell proteome following canagliflozin treatment to determine whether the observed changes at the transcript level translate to similar changes in protein expression. This approach also allowed the interrogation of an extensive panel of targets – almost ten-fold that of our gene expression analysis – allowing a more complete investigation into the global changes in cellular function that canagliflozin facilitates. This exact proteomic approach previously established that MYC knockdown in murine T cells is detrimental to their proteomic remodelling in response to activation (Marchingo et al., 2020). In this thesis, there was a pronounced reduction in total protein content per cell upon canagliflozin treatment, therefore the use of the “proteomic ruler” method to estimate protein copy number, and subsequently cellular protein concentration, was vital in our understanding of how canagliflozin remodels the T cell proteome. Core subcellular compartments such as mitochondria, glycolysis and nuclear envelope were supported by fewer proteins in canagliflozin-treated T cells, underlining the inhibitory effect of canagliflozin. Highlighting the importance of examining the translational significance of changes in gene expression, MYC was downregulated at the protein level and ingenuity pathway analysis revealed that its inhibition was the most likely explanation for the observed array of proteins downregulated. Consistent with this prediction, canagliflozin treatment shared several of the same hallmarks as MYC knockdown in T cells (Marchingo et al., 2020). Indeed, several metabolism-associated MYC targets were downregulated, impaired expression of the translational machinery underpinned a failure to increase cell mass upon activation, whilst defective expression of several MYC-associated amino acid transporters likely compromised the amino acid uptake necessary to support normal protein expression, including the expression of MYC itself. These data provided valuable insight into the molecular changes that occur in response to canagliflozin treatment, informing our following experiments to better our understanding of its effect on T cell fate and function.

7.4 Canagliflozin promotes mitochondrial dysfunction to impair T cell metabolic reprogramming

Studying the inhibitory effects of canagliflozin on T cell function mechanistically is essential for a comprehensive understanding of drug interaction. Given that the evidence presented shows that canagliflozin, but not dapagliflozin, suppresses crucial T cell functions, this highlights the importance of appraising individual member of this drug class based on

their specific off-target effects on metabolism. Since canagliflozin inhibits mitochondrial complex I and GDH, elucidating how this affected T cell function was of great importance. Further interrogation of the proteomics dataset revealed upregulation of electron transport chain complex proteins – also confirmed later by immunoblotting. These data were in line with previous studies showing the upregulation of mitochondrial complex proteins in hepatocellular carcinoma cells treated with canagliflozin (Nakano et al., 2020). Perhaps this reveals a compensatory mechanism wherein T cells attempt to circumvent the inhibition of complex I and the subsequent reduction in OXPHOS. An additional increase in overall mitochondrial biogenesis identified the potential involvement of mitochondrial ROS (mitoROS) (Dugan et al., 2013; Li et al., 2003). Indeed, mitoROS were increased as early as 15 minutes post-canagliflozin treatment, unveiling a rapid mechanism by which this occurs, whilst 24 h later there was an observed increase several antioxidant proteins. ROS are critical during early TCR signalling, however, excessive levels have been shown to have a detrimental effect on metabolic reprogramming through MYC and mTOR (Mak et al., 2017).

The analysis of T cell metabolism provides insight into the processes that fuel the energetic demands of an immune response. In settings such as autoimmunity, perturbed metabolism often drives aberrant T cell function (see Chapter 1.5). Canagliflozin inhibited both glycolysis and OXPHOS in healthy T cells, reducing their ATP production from these pathways. This metabolically quiescent state would prevent the programmes necessary for T cell-mediated inflammation (see Chapter 1.3.6). Stable isotope tracer analysis using universally-labelled carbon-13 substrates allows the determination of whether glucose and glutamine are being diverted towards different pathways in canagliflozin-treated T cells. These approaches confirmed inhibition of GDH by canagliflozin, also revealing that T cells attempt to rewire their glucose metabolism to promote glucose incorporation into the TCA cycle to compensate for the loss of glutamine-derived carbon. Upon activation, human T cells adopt an anabolic metabolism highly dependent on glycolysis and glutamine anaplerosis to fuel their biosynthetic and energetic requirements (Wang et al., 2011). Targeting both pathways using canagliflozin provides an outstanding platform from which to inhibit T cell effector function.

Importantly, this dual-pronged approach employed by canagliflozin translated into superior suppression of T cell function versus other known inhibitors of complex I. Promisingly, metformin has already shown promise in the setting of autoimmunity, in

addition to other inflammatory conditions, through its action on T cell metabolism and function (Bharath et al., 2020) (also see Chapter 1.6.2), further emphasising the immense potential canagliflozin harnesses. Moreover, canagliflozin maintained its superior inhibitory effect on effector function over combined inhibition of complex I and GDH, which suggested that other mechanisms underpin dysregulated metabolism and function in canagliflozin-treated T cells. Indeed, mechanistically canagliflozin rapidly impairs early TCR signalling events, reducing the phosphorylation of critical signalling proteins ZAP70, LAT and PLC γ as early as five minutes following activation. Consequently, this impairs downstream phospho-ERK signalling and inhibits early T cell activation. Crucially, canagliflozin-treated T cells stimulated by PMA and ionomycin – which bypasses TCR-dependent activation but engages the downstream pathways in this signalling cascade – demonstrated no defects in effector function. Furthermore, canagliflozin treatment phenocopied inhibition of critical metabolic nodes mTOR and ERK, further demonstrating the consequences of debilitated TCR-mediated signalling in canagliflozin-treated T cells. Together, these findings establish the metabolic underpinnings that support the inhibitory effects that canagliflozin exerts on T cell effector function.

7.5 Canagliflozin inhibits T cell function in systemic lupus erythematosus and rheumatoid arthritis

T cell-mediated autoimmune diseases have been well characterised to involve hyperactivated T cells at the site of chronic inflammation (see Chapter 1.4). This primarily comprises of antigen-experienced Teff cells that secrete proinflammatory cytokines and recruit other immune cell types to ultimately cause damage to the surrounding tissue. This thesis has provided evidence that, in addition to activated T_H17 cell populations, canagliflozin has an inhibitory effect on Teff cell function. The secretion of several proinflammatory cytokines was dampened by canagliflozin, again underpinned by impaired T cell activation. Interestingly, IL-10 production appeared to be less affected by canagliflozin treatment, pointing towards selective inhibition of T cell functions. Despite not fully analysing the metabolism of canagliflozin-treated Teff cells using Seahorse extracellular flux analysis, reductions in the expression of several types of nutrient transporters, in addition to a likely reduction in glucose uptake, suggested that their metabolism is perturbed by canagliflozin in a similar manner as described in the previous section. Given that the Teff cell compartment

comprises several Th subsets, each with unique phenotypes, this area of research warranted further investigation. Despite some evidence showing that the balance of Th subsets we observed following canagliflozin treatment appears favourable – i.e., increased Th1 cell populations and reduced Th17 cell populations (Bazzazi et al., 2018) – it is questionable whether 24 h is long enough to begin to see any changes in T cell differentiation. Moreover, most of our subset analysis was based on the differential expression of various chemokine receptors (Mahnke, Beddall, et al., 2013), whereas the focus should perhaps be shifted towards the nuclear expression of signature transcription factors. It would be interesting to see the correlation between the observed changes in proinflammatory cytokine release with the function of their respective, associated signature Th subset.

Critically, canagliflozin retained its ability to suppress T cell function *ex vivo* in two human autoimmune patient cohorts. In both SLE and RA patient-derived CD4⁺ T cells, canagliflozin diminished proinflammatory cytokine production, underpinned by the same perturbations in activation and metabolism observed in healthy individuals. These experiments were also carried out in HPLM, which further advocates the repositioning of canagliflozin to treat autoimmunity. To consolidate these findings, another human experimental model was employed to analyse T cell function amongst a SFMC population isolated from RA patients, whereby canagliflozin modestly inhibited T cell activation and proinflammatory cytokine production. Critically, SFMCs localised in the inflamed tissue of RA patients are likely already hyperactivated, which strengthened our earlier findings wherein canagliflozin had a modest inhibitory effect on already-activated T cells. A further benefit of prescribing autoimmune patients canagliflozin is the protective effect against cardiovascular disease – a comorbidity causing significant morbidity and mortality in multiple autoimmune conditions (Schwartz et al., 2020). Collectively, the impaired effector function of T cells accompanied by systemic protective effects against cardiovascular disease highlights the exciting potential in repurposing canagliflozin for autoimmunity.

7.6 Further work and limitations

This work has outlined how canagliflozin impacts human T cell function, elucidating the mechanistic underpinnings that impair early TCR signalling events, downstream T cell activation and metabolism. In the setting of autoimmunity, we have demonstrated that canagliflozin impacts SLE and RA patient-derived T cell function *ex vivo*. Canagliflozin

treatment suppressed the effector function of both peripheral blood T cells and *ex vivo* SFMCs. To further evaluate the potential of canagliflozin in this setting, additional experiments involving autoimmune patient samples could be beneficial. For example, it would be interesting to treat whole tissue explants isolated from RA patients with canagliflozin *ex vivo* and measure the secretion of proinflammatory mediators characteristic of disease pathogenesis. Although understanding whether other immune cell populations respond to canagliflozin treatment in the same way as T cells is of great importance, this consideration is beyond the scope of this thesis. This would perhaps be best approached by employing single cell technologies that could harness the distinct changes that occur throughout the immune subsets analysed. Furthermore, the experiments needed to address these points require access to and the recruitment of RA patients undergoing procedures such as arthroscopy.

Another approach that could be employed to determine the impact of canagliflozin on T cell function in an autoimmune disease setting would be the use of an appropriate murine model. To this end, physiologically relevant doses of canagliflozin would be administered orally to mice in CD4⁺ T cell-driven models of autoimmunity such as antigen-induced arthritis or collagen-induced arthritis. Clinical indices of arthritis related to local and systemic infiltrating CD4⁺ T cell responses, as well as survival and effector characteristics, would be measured following oral administration of canagliflozin both prior to disease onset and in the effector phase of disease. The results of such analyses must also be approached with caution, given that the observed changes in the mouse model might not necessarily translate into the clinical setting in humans. As additional experiments to complement these data, Th cell-associated transcription factors (e.g., Tbet, GATA3 and ROR γ T) and proinflammatory effector cytokines (e.g., IFN γ , IL-4, IL-13, IL-17A, IL-17F, IL-21) could be tracked by various flow cytometry panels, whilst joint-infiltrating T cells could also be isolated for downstream analysis. Finally, assessment of joint histopathology in paraffin-embedded knee sections would be critical, particularly in the event of drug treatment showing an inhibitory effect on CD4⁺ T cell function. Whilst this strategy would provide an exciting, alternative angle to our findings, our work to date has focussed on the impact of canagliflozin on human T cell function, with the aim of improving the translational capacity of canagliflozin in humans. Autoimmune diseases are typically heterogeneous conditions, therefore further work is required to determine whether particular patient subgroups would respond more

favourably to canagliflozin therapy than others. Moreover, it is unknown whether physiologically relevant concentrations of canagliflozin are realised within the inflamed tissue – a consideration that requires further investigation. However, one such mechanism that canagliflozin could alternatively prosper from – as circulating levels of the drug are known from studies in T2D patients – is preventing the repopulation of inflammatory T cells at the site of inflammation. Moreover, canagliflozin is often prescribed in combination with metformin, therefore it would be pertinent to determine whether this would potentially enhance the immunosuppressive capabilities of this therapeutic strategy in autoimmunity, provided that there is a synergistic effect between both drugs. Given the protective nature of canagliflozin in published studies of other conditions with underlying inflammatory elements, such as chronic kidney disease (Perkovic et al., 2019) and cardiovascular disease (Spertus et al., 2022), we are optimistic that our *in vitro* and *ex vivo* data will complement these exciting manuscripts. Since canagliflozin is an FDA-approved medication, a future clinical trial is warranted to definitively determine whether canagliflozin would be of therapeutic benefit in patients with autoimmune disease.

7.7 The future for canagliflozin

Given the high rates of failure, significant financial costs and laborious procedures associated with the development of new drugs, repurposing already-approved drugs for use in alternative disease settings is an attractive prospect. A wealth of prior studies have reported that targeting T cell metabolism in autoimmunity can provide therapeutic benefit (see Chapter 1.6). This thesis has demonstrated that canagliflozin – a clinically available T2D medication that modulates metabolism – could have a protective effect in the setting of autoimmune disease through its ability to inhibit T cell function.

There has been a burgeoning interest in canagliflozin since its FDA approval in 2012, where studies have concentrated on two main areas of investigation. The first of these is understanding the impact that canagliflozin has on various cellular processes, particularly outside of its primary function to inhibit glucose uptake via sodium glucose-cotransporter 2 (SGLT2). For example, initial studies demonstrated the ‘off-target’ impact that canagliflozin has on complex I of the electron transport chain and mitochondrial GDH – inhibiting the function of both proteins (Secker et al., 2018; Villani et al., 2016). These observations have since been confirmed in other cell types, however, the impact that this had on cellular

metabolic pathways such as glycolysis is conflicting (Secker et al., 2018; Zugner et al., 2022). Most recently, investigations have demonstrated that canagliflozin is able to suppress multiple central metabolic pathways in several human kidney cell types via suppression of mTORC1 activity (Schaub et al., 2023). These findings lead to the second main area of investigation, which harnesses the described 'off-target' of canagliflozin for therapeutic benefit in other disease settings. Already, canagliflozin has been demonstrated to improve clinical outcomes in patients with chronic kidney disease (Perkovic et al., 2019) and cardiovascular disease (Spertus et al., 2022), whilst ongoing clinical trials are investigating the therapeutic effect of canagliflozin on liver inflammation in non-alcoholic fatty liver disease (National Library of Medicine [NLM], NCT05513729). Additionally, several proof-of-concept studies have investigated the anti-inflammatory properties of canagliflozin. To this end, canagliflozin has impaired proinflammatory cytokine production by monocyte / macrophage cell lines via metabolic suppression (Xu et al., 2018), whilst also demonstrating the ability to inhibit both Th1 and Th17 cell differentiation in murine models of myocarditis (Long et al., 2022). Unfortunately, these experiments do not employ the optimal models for these analyses, therefore this area warrants further investigation. Prior to the work of this thesis, the impact that canagliflozin has on human T cell function had yet to be elucidated.

Given these encouraging precedents, canagliflozin possesses exciting therapeutic potential in range of inflammatory conditions – particularly those underpinned by aberrant immune cell metabolism. Other SGLT2 inhibitors (empagliflozin) have already demonstrated the ability modulate human T cell metabolism and proinflammatory function *ex vivo* in an autoimmune patient cohort (Qin et al., 2022). Improving our understanding of how medications that target metabolism interact with immune cell populations is critical for our future success in repurposing other approved drugs for therapeutic benefit in inflammation. I anticipate that we will continue to see the repositioning of canagliflozin in other clinical settings in the near future.

Chapter Eight

Appendices

8 Appendices

8.1 Fructose reprogrammes glutamine-dependent oxidative metabolism to support LPS-induced inflammation



ARTICLE



OPEN

Fructose reprogrammes glutamine-dependent oxidative metabolism to support LPS-induced inflammation

Nicholas Jones^{1,7}, Julianna Blagih^{2,7}, Fabio Zani², April Rees¹, David G. Hill³, Benjamin J. Jenkins¹, Caroline J. Bull^{3,4}, Diana Moreira⁵, Azari I. M. Bantan¹, James G. Cronin¹, Daniele Avancini⁶, Gareth W. Jones³, David K. Finlay⁵, Karen H. Vousden², Emma E. Vincent^{3,4,8} & Catherine A. Thornton^{1,8}

Fructose intake has increased substantially throughout the developed world and is associated with obesity, type 2 diabetes and non-alcoholic fatty liver disease. Currently, our understanding of the metabolic and mechanistic implications for immune cells, such as monocytes and macrophages, exposed to elevated levels of dietary fructose is limited. Here, we show that fructose reprograms cellular metabolic pathways to favour glutaminolysis and oxidative metabolism, which are required to support increased inflammatory cytokine production in both LPS-treated human monocytes and mouse macrophages. A fructose-dependent increase in mTORC1 activity drives translation of pro-inflammatory cytokines in response to LPS. LPS-stimulated monocytes treated with fructose rely heavily on oxidative metabolism and have reduced flexibility in response to both glycolytic and mitochondrial inhibition, suggesting glycolysis and oxidative metabolism are inextricably coupled in these cells. The physiological implications of fructose exposure are demonstrated in a model of LPS-induced systemic inflammation, with mice exposed to fructose having increased levels of circulating IL-1 β after LPS challenge. Taken together, our work underpins a pro-inflammatory role for dietary fructose in LPS-stimulated mononuclear phagocytes which occurs at the expense of metabolic flexibility.

¹Institute of Life Science, Swansea University Medical School, Swansea University, Swansea, UK. ²The Francis Crick Institute, London, UK. ³Cellular and Molecular Medicine, University of Bristol, Bristol, UK. ⁴MRC Integrative Epidemiology Unit, University of Bristol, Bristol, UK. ⁵School of Biochemistry and Immunology, Trinity Biomedical Sciences Institute, Trinity College Dublin, Dublin, Ireland. ⁶San Raffaele Telethon Institute for Gene Therapy, San Raffaele Scientific Institute, Milan, Italy. ⁷These authors contributed equally: Nicholas Jones, Julianna Blagih. ⁸These authors jointly supervised this work: Emma E. Vincent, Catherine A. Thornton. [✉]email: emma.vincent@bristol.ac.uk; c.a.thornton@swansea.ac.uk

Typically, activation of the human innate immune system requires the rewiring of cellular metabolic pathways largely to favour glucose metabolism^{1–5}. However, in the various nutrient environments they inhabit, monocytes will be exposed to a range of different carbon sources, the availability of which will likely dictate their metabolism and phenotype. One such carbon source is fructose, the second most abundant dietary sugar found in humans. Fructose is metabolised by glycolysis either by ketohexokinase producing fructose-1-phosphate, a substrate for aldolase B⁶ (in the liver, kidneys and intestines for example) or converted to the glycolytic intermediate fructose-6-phosphate by hexokinase (HK), albeit at a lower rate than glucose^{7,8}.

Fructose intake has increased substantially throughout the Western world, largely attributed to elevated sucrose and high fructose corn syrup consumption⁹ and is thought to exacerbate various non-communicable conditions such as obesity, type 2 diabetes and non-alcoholic fatty liver disease⁹. Chronic fructose consumption in these conditions has recently been shown to drive hepatic fructolysis, where the expression of lipogenic genes is enhanced^{10–12}.

Typically, physiological levels of fructose in the circulation range from 0.04 to 0.2 mM¹³; however, there are several pathophysiological scenarios in which levels of fructose are elevated. For example, peripheral blood levels can exceed 1 mM in patients with haematological malignancies such as acute myeloid leukaemia and acute lymphoblastic leukaemia¹⁴. In addition, fructose concentrations in the bone marrow microenvironment of haematological cancer patients can reach up to 5 mM¹⁴. Alterations in the glucose to fructose ratio, particularly when glucose is scarce, enables acute myeloid leukaemia blasts to significantly enhance fructose uptake¹⁴. Localised mouse tissue microenvironments, such as the liver, kidneys and jejunum, also have elevated levels of fructose metabolism¹⁵. Therefore, there are various pathophysiological scenarios and tissue microenvironments where monocytes will be exposed to either equimolar concentrations of fructose and glucose or concentrations of fructose exceeding that of glucose.

The impact of elevated fructose exposure on the immune system has not been investigated extensively. Chronic fructose exposure in rats results in a more inflammatory phenotype of bone marrow mononuclear cells¹⁶. While there is some evidence that lipopolysaccharide (LPS)-stimulated human dendritic cells are able to produce enhanced levels of pro-inflammatory cytokines when cultured in fructose as opposed to glucose, the underlying metabolic rewiring that enables this pro-inflammatory phenotype has not been investigated¹⁷.

Here we characterise how human monocytes and mouse macrophages respond metabolically and functionally to fructose exposure. We show that activated mononuclear phagocytes demonstrate plasticity in engaging metabolism of this alternative carbon source, yet it leaves the cells metabolically inflexible and vulnerable to further metabolic challenge. Fructose exposure reprogrammes cellular pathways to favour glutaminolysis and oxidative metabolism, which support an inflammatory phenotype in both human and mouse mononuclear phagocytes. Finally, we demonstrate that a short-term high fructose diet promotes inflammation *in vivo*, suggesting that our findings have pathophysiological significance.

Results

Fructose exposure promotes an oxidative phenotype. We sought to investigate the metabolic response to fructose exposure in activated human monocytes in comparison to other monosaccharides (glucose and galactose) or complete sugar withdrawal. Galactose has been used previously to promote oxidative phosphorylation (OXPHOS) in T cells by reducing glycolysis¹⁸. Using

the Seahorse Bioanalyzer, we initially injected the monosaccharide (glucose, fructose or galactose) or media control containing no sugar. After 1 h, monocytes were stimulated with LPS and the corresponding extracellular acidification rate (ECAR) and oxygen consumption rate (OCR) were used to measure glycolysis and OXPHOS, respectively, for the duration.

Monocytes incubated with glucose demonstrated a robust increase in basal and LPS-induced ECAR (Fig. 1A). By contrast, monocytes treated with fructose or galactose had low baseline levels of glycolysis, only slightly greater than no sugar controls (Fig. 1A). In addition, monocytes treated with fructose, galactose or no sugar had only a modest increase in ECAR post-LPS exposure (Fig. 1A). Upon activation, glucose-treated cells reduced their OCR, consistent with the reported metabolic switch from OXPHOS to glycolysis upon activation³. Monocytes treated with fructose, galactose or no sugar had an initial burst of increased oxygen consumption and maintained higher OCR for the duration of the assay (Fig. 1B). This demonstrates metabolic flexibility of human monocytes, in this case towards OXPHOS when the cells are unable to engage in glycolysis.

After the introduction of 2-deoxy-D-glucose (2-DG), ECAR was reduced in all conditions (Fig. 1C). OCR was increased in glucose-treated monocytes, a compensatory response to glycolysis inhibition, whereas in fructose, galactose or no sugar treatment a decrease in OCR was observed (Fig. 1D). These data suggest that LPS-stimulated monocytes treated with fructose or galactose direct pyruvate towards the mitochondrial tricarboxylic acid (TCA) cycle for OXPHOS, whereas glucose treatment directs pyruvate towards lactate production. We confirmed extracellular levels of lactate are indeed reduced in fructose compared to glucose-treated monocytes (Supplementary Fig. 1A). This divergence appears to account for the differences in OXPHOS rates observed. Overall, LPS-stimulated human monocytes treated with fructose maintained an elevated oxidative phenotype with low ECAR, akin to galactose or no sugar treatment, whereas glucose availability preferentially maintained elevated levels of glycolysis at the expense of reduced oxygen consumption (Fig. 1E).

In agreement with a previous study, LPS-stimulated monocytes cultured for 24 h with galactose or no sugar had a significant reduction in viability in comparison to the glucose-treated control (Fig. 1F)¹⁹. However, we observed no difference in viability between glucose and fructose treatment (Fig. 1F).

To further elaborate fructose metabolism in LPS-stimulated monocytes, we incubated them with either uniformly labelled ¹³C₆-fructose or ¹³C₆-glucose and performed stable isotope tracer analysis (SITA). Activated monocytes were able to transport fructose into the cell (presumably via GLUT5 expression—Supplementary Fig. 1B) and incorporated comparable levels of carbon into intracellular lactate while increasing incorporation into TCA cycle intermediates and amino acids in comparison to glucose (Supplementary Fig. 1C–E). These results suggest that the cells have the ability to metabolise fructose carbon and use it in the TCA cycle.

Collectively, these data reveal that fructose treatment promotes a low glycolytic rate without compromising cell viability. This demonstrates the metabolic flexibility of human monocytes as well as their ability to utilise an alternative carbon source.

Glycolysis and OXPHOS are coupled in fructose-treated human monocytes. To confirm that the observed increase in OCR in fructose-treated monocytes was due to OXPHOS as opposed to an increase in other oxygen-consuming processes, we utilised the ATP synthase inhibitor, oligomycin. Here, monocytes were treated with either glucose or fructose and allowed to rest prior to LPS exposure. Oligomycin was later injected and the

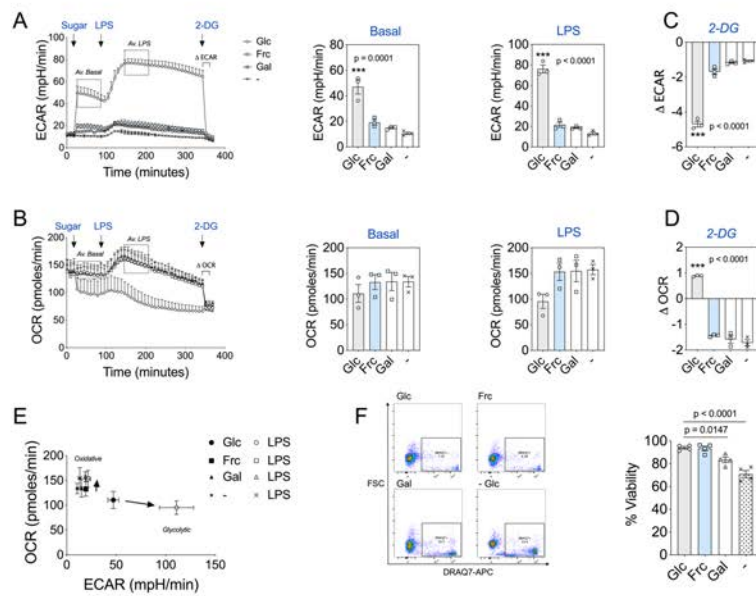


Fig. 1 Fructose mimics a metabolic profile akin to nutrient restriction. **A** Seahorse extracellular flux analysis of ECAR in monocytes before and following injections of glucose, fructose, galactose (11.1 mM) or no sugar, LPS (10 ng/mL) and 2-DG (100 μM) at the time points indicated with average basal (Av. basal) and LPS-stimulated (Av. LPS) ECAR values. **B** Analysis of OCR in monocytes with the same injections as in panel (A), including average basal (Av. basal) and LPS-stimulated (Av. LPS) OCR values. **C** Change in ECAR (Δ ECAR) post 2-DG treatment. **D** Change in OCR (Δ OCR) post 2-DG treatment. **E** OCR versus ECAR map of average basal and LPS-stimulated values for glucose, fructose, galactose and no sugar treatment groups. Arrows indicate the shift in metabolism from average basal to average LPS. **F** Representative flow cytometry plot and DRAQ7 viability measurements of glucose, fructose, galactose and no sugar monocytes cultured for 24 h with LPS (10 ng/mL). Statistical significance was assessed using a one-way ANOVA with Dunnett's (A–D) or Tukey's (F) multiple comparisons test. Data are either representative of either three (A–E) or four independent experiments (F). Data are expressed as mean \pm SEM; *** p \leq 0.001. Source data are provided as a Source Data file.

bioenergetic changes were monitored over time. While OCR of both glucose or fructose LPS-stimulated monocytes decreased to the same level upon oligomycin treatment (Fig. 2A), the drastic reduction of OCR in fructose-cultured monocytes reflects a greater reliance on OXPHOS. Cells reliant on OXPHOS may demonstrate metabolic flexibility upon oligomycin treatment by increasing glycolysis. However, surprisingly, ECAR in fructose-cultured monocytes decreased in response to oligomycin, suggesting the lack of metabolic adaptation in these cells (Fig. 2B, C).

Secondly, to establish whether the elevated ECAR levels post-LPS treatment reflected glycolytic activity as opposed to other acidifying processes, we used a lactate dehydrogenase inhibitor (GSK2837808A; LDHi). Here, the increased ECAR in response to LPS stimulation was reduced in glucose-treated monocytes upon LDHi treatment (Fig. 2D). By contrast, LDHi modestly impacted ECAR in fructose-treated cells, arguing that fructose-mediated glycolysis is coupled to OXPHOS. The low level of ECAR under this condition is most likely due to acidification of the media by an alternative source to lactate (Fig. 2D). We confirmed this was not due to changes in LDH phosphorylation in fructose- versus glucose-treated cells (Supplementary Fig. 1F).

The corresponding OCR levels increased in the glucose-treated monocytes upon LDHi treatment as pyruvate is directed towards

OXPHOS, again demonstrating the bioenergetic flexibility of human monocytes. By contrast, OCR in fructose-treated monocytes remained unchanged for the duration of the assay (Fig. 2E, F). These data further demonstrate that glycolysis and OXPHOS are tightly coupled in fructose-treated cells, revealing impaired metabolic flexibility in comparison to glucose-treated cells (Fig. 2C, F).

Fructose treatment enhances LPS-induced inflammation.

Given the distinct metabolic characteristics of human monocytes exposed to fructose (Fig. 1A), we were intrigued to investigate the impact on monocyte function. Fructose-treated monocytes produced elevated levels of a panel of secreted cytokines, namely interleukin-1 β (IL-1 β), IL-6, IL-8, IL-10 and tumour necrosis factor (TNF) (Fig. 3A–E), with IL-1 β , IL-8, IL-10 and TNF reaching statistical significance in comparison to glucose treatment. Despite elevated levels of cytokine secretion, there were no differences in various surface markers associated with monocyte activation (HLA-DR, CD80, CD86, CD62L, CCR5 and CCR2) between the glucose- or fructose-treated monocytes (Supplementary Fig. 2A).

To determine whether the increased production of cytokines was a consequence of increased transcription, we performed

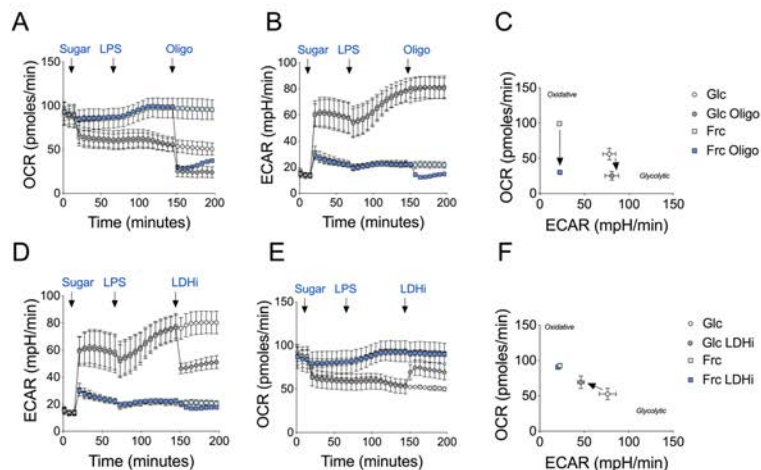


Fig. 2 Fructose treatment enhances oxidative metabolism. Seahorse extracellular flux analysis of **A** OCR and **B** ECAR in monocytes before and following injections of glucose or fructose (both 11.1 mM), LPS (10 ng/mL) and oligomycin (1 μ M) at the time points indicated. **C** OCR versus ECAR map of average of a single value pre- and post-oligomycin injection for glucose- and fructose-treated monocytes. Arrows indicate the shift in metabolism upon inhibitor exposure. Analysis of **D** ECAR and **E** OCR in monocytes as **A** with a final injection of a lactate dehydrogenase inhibitor (GSK2837808A, LDHi; 10 μ M). **F** OCR versus ECAR map as **C** with pre- and post-LDHi injection. Data are representative of three independent experiments and are expressed as mean \pm SEM. Source data are provided as a Source Data file.

RNA-sequencing (RNA-seq) analysis of LPS-stimulated monocytes treated with glucose or fructose. Surprisingly, we observed only five genes that were significantly changed between the two conditions, with no alteration to transcript levels for the cytokines of interest (Supplementary Fig. 2B). Consistent with this, the expression level of genes encoding cytokines was also comparable in monocytes treated with either glucose or fructose (Fig. 3F), suggesting that the increased cytokine production was not through transcriptional regulation. Fructose has recently been reported to activate mTORC1 via dihydroxyacetone phosphate sensing²⁰. Consistent with this, phosphorylation of the downstream mTORC1 target, S6 ribosomal protein, was elevated significantly in LPS-stimulated monocytes treated with fructose (Fig. 3G). Of note, we observed no differences in the induction of AMPK (AMP-activated protein kinase) signalling between the two groups (Supplementary Fig. 2C). Collectively, these observations demonstrate that LPS stimulation in the presence of fructose enhances inflammatory cytokine production, in part, through increased mTORC1-mediated translation.

Fructose treatment drives a sustained oxidative phenotype. LPS-stimulated monocytes in the presence of fructose clearly enhance oxygen consumption in the short term (Fig. 1C). Next, we wanted to determine whether heightened oxygen consumption was sustained long term in activated monocytes. Here, using the Seahorse Bioanalyzer, we performed a mitochondrial stress test with a final injection of the ionophore, monensin²¹, following a 24-h incubation period with either glucose or fructose. Elevated levels of oxygen consumption were indeed sustained long term in fructose-treated LPS-stimulated monocytes (Fig. 4A). This was characterised by increased levels of oxidative parameters such as basal respiration, ATP-linked respiration and a higher percentage

of coupling efficiency in comparison to glucose (Fig. 4B–D and Supplementary Fig. 3A–D). Corresponding ECAR levels were unsurprisingly higher in glucose-treated monocytes in comparison to fructose-treated cells (Fig. 4E, F and Supplementary Fig. 3E). Notably, fructose-treated monocytes had a significantly higher ratio of basal OCR/ECAR ratio in comparison to glucose, indicating their commitment to oxidative metabolism (Fig. 4G).

We next assessed the contributions of glycolysis derived- and OXPHOS-derived ATP production²¹. These analyses show glucose-treated monocytes as glycolytic cells functioning at their maximal glycolytic ATP production rate at baseline (Fig. 4H). At maximal bioenergetic capacity, they demonstrate flexibility towards ATP production from OXPHOS, but still derive the majority of their ATP from glycolysis and therefore remain classed as glycolytic cells (Fig. 4H and Supplementary Fig. 3F, G). By contrast, fructose-treated monocytes are oxidative (deriving the majority of their ATP from OXPHOS) at baseline and this phenotype is further exacerbated when cells are at maximal bioenergetic capacity (Fig. 4H and Supplementary Fig. 3F, G). They do, however, have some metabolic scope to increase ATP production from glycolysis (Fig. 4H).

We reasoned that differential mitochondrial properties might explain the heightened oxidative phenotype of fructose-treated monocytes. However, we observed no difference in mitochondrial content (MitoTracker Green), membrane potential (tetramethylrhodamine ethyl ester) or mitochondrial-derived reactive oxygen species (ROS) (Fig. 4I). Further to this, we also assessed levels of the individual respiratory complexes by immunoblot. Again, we observed no difference in the abundance of complexes I–IV between fructose- or glucose-treated monocytes (Fig. 4J). A high fructose diet has been shown to increase de novo lipogenesis in the liver¹⁰. This correlates with increased mitochondrial ATP production, which may support this energy-demanding process^{22,23}.

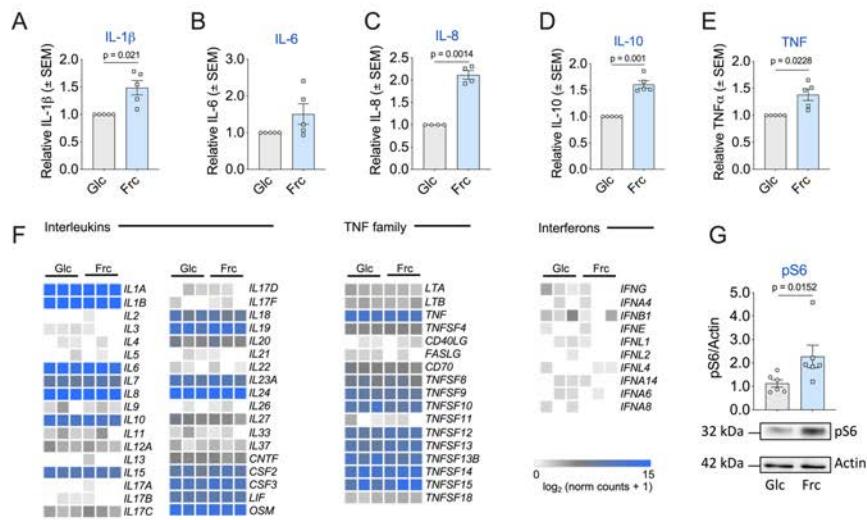


Fig. 3 Fructose promotes a more inflammatory phenotype. Extracellular cytokine release of **A** IL-1 β , **B** IL-6, **C** IL-8, **D** IL-10 and **E** TNF. **F** Heatmaps displaying the normalised read counts of selected cytokines from RNA-seq analysis of monocytes treated with glucose or fructose (both 11.1 mM) stimulated with LPS (10 ng/mL) for 24 h. **G** Representative immunoblot and pooled data of downstream mTOR target pS6 with housekeeping control, actin. Statistical significance was assessed using a one-sample t test (**A–E**) or an unpaired, two-tailed t test (**G**). Data are representative of five (**A, B, D, E**), four (**C**), three (**F**) and six independent experiments (**G**) and are expressed as mean \pm SEM. Source data are provided as a Source Data file.

Therefore, a potential explanation for the elevated ATP-linked respiration observed is that fructose-treated monocytes are supporting a higher level of lipogenesis. We observed no differences in phosphorylation of enzymes that catalyse the citrate-derived fatty acid synthesis steps; ATP citrate lyase (ACLY) or acetyl-CoA carboxylase (Supplementary Fig. 3H). However, fructose-cultured, LPS-stimulated monocytes have increased levels of the lipid mediator, prostaglandin E2 and greater sensitivity to the ACLY inhibitor, BMS303141, with regards to cytokine production (Supplementary Fig. 3I, J). Taken together, these data demonstrate that fructose treatment elevates ATP-linked oxygen consumption, independent of mitochondrial ROS and content.

Fructose increases TCA cycling and anaplerosis. To further characterise the metabolic activity of the mitochondria in glucose- and fructose-treated cells, we used SITA coupled with gas chromatography-mass spectrometry (GC-MS). Here, human monocytes were activated with LPS for 24 h and incubated with either $^{13}\text{C}_6$ -glucose or $^{13}\text{C}_6$ -fructose (Fig. 5A). Mass isotopologue distribution (MID) analysis of the TCA cycle intermediates—succinate, fumarate and malate—and amino acids—glutamate and aspartate—highlighted that there was increased cycling in the fructose-cultured monocytes compared to glucose. This was indicated by a reduced proportion of the unlabelled form of the metabolite ($m+0$) and an increased proportion of the labelled form (predominantly represented by $m+2$) (Fig. 5B, C and Supplementary Fig. 4A).

The TCA cycle relies on other metabolites to replenish it, a process termed anaplerosis. Glutamine-derived carbon enters the TCA cycle and also contributes to TCA-mediated amino acid biosynthesis, such as aspartate. To investigate whether fructose treatment increases

glutamine anaplerosis, we performed SITA with $^{13}\text{C}_5$ -glutamine. Here, monocytes were incubated with $^{13}\text{C}_5$ -glutamine in the presence of either glucose or fructose and activated with LPS (Fig. 5C). The mass isotopologue distribution analysis of the TCA cycle metabolites—succinate, fumarate and malate—demonstrated an increase in the percentage of ^{13}C into these intermediates in the presence of fructose (represented as $m+4$) (Fig. 5D and Supplementary Fig. 4B). Fructose-treated monocytes are able to incorporate elevated amounts of glutamine-derived carbon to the TCA cycle intermediates and amino acids in comparison to glucose-treated monocytes (Supplementary Fig. 4C–G). These data demonstrate that fructose treatment increases the proportion of both sugar and glutamine carbon into the TCA cycle to support the observed increased rates of OXPHOS.

Fructose-treated human monocytes are vulnerable to metabolic challenge. Thus far, we have demonstrated that fructose treatment promotes a reduced glycolytic rate and enhanced OXPHOS. Glucose and fructose are both metabolised by the enzyme HK, producing metabolites glucose 6-phosphate or fructose-6-phosphate respectively²⁴. Therefore, we sought to investigate the expression levels of the two predominant isoforms of HK: HKI and HKII. We observed no difference in expression levels of HKI; however, HKII levels were increased in fructose-treated, LPS-stimulated monocytes, in comparison to glucose (Fig. 6A, B). To further delineate the role of HK in monocyte function, we utilised the HK inhibitor, 2-DG. We treated activated monocytes in glucose or fructose for 24 h with 2-DG before measuring cytokine production. Following treatment with 2-DG, production of IL-1 β , IL-6 and TNF was largely unaffected in glucose-treated cells, with the exception of IL-10. By contrast, fructose-treated

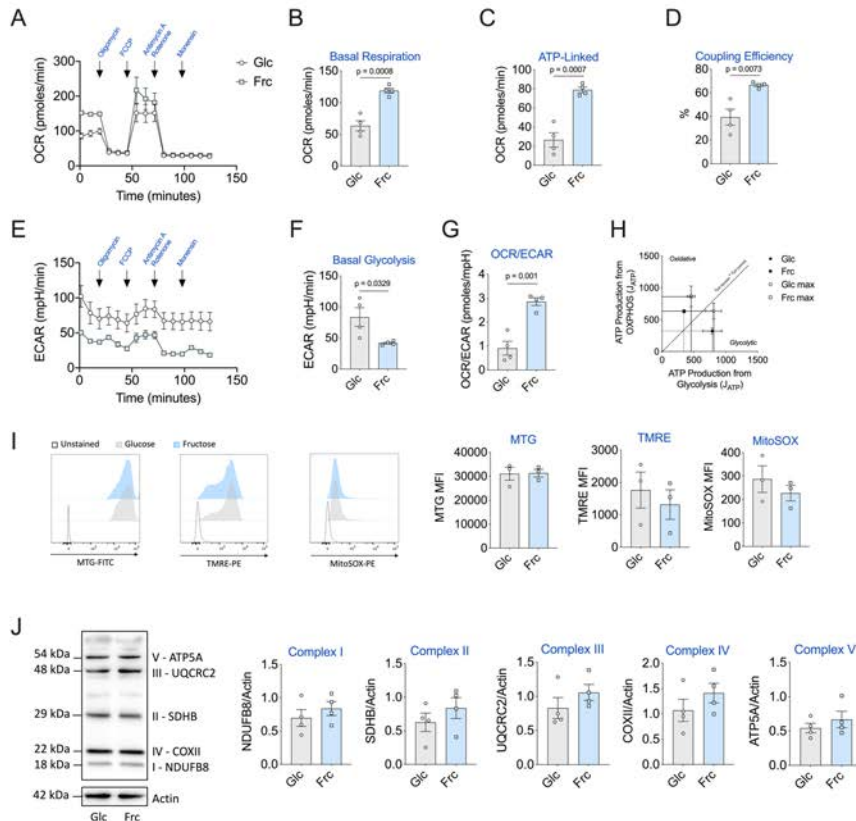


Fig. 4 Fructose-induced oxidative phenotype is maintained in LPS-stimulated monocytes. **A** Mitochondrial stress assay of monocytes cultured for 24 h in the presence of glucose or fructose (both 11.1 mM) and activated with LPS (10 ng/mL). Corresponding OCR measured with injections of oligomycin (1 μ M), FCCP (3 μ M), antimycin A (1 μ M) and rotenone (1 μ M) and monensin (20 μ M). Respective mitochondrial parameters **B** basal respiration, **C** ATP-linked respiration and **D** coupling efficiency calculated via ATP-linked respiration/basal respiration. **E** Equivalent ECAR rate measured with **F** basal glycolysis levels. **G** OCR/ECAR ratio calculated by basal respiration/basal glycolysis levels. **H** Bioenergetic scope examining the ATP production (J_{ATP}) of oxidative phosphorylation versus glycolysis of basal and maximal of glucose or fructose. Mitochondrial parameters **I** Content: MitoTracker Green (MTG), membrane potential: tetramethylrhodamine ethyl ester (TMRE) and mitochondrial-derived ROS: MitoSOX measured by flow cytometry. **J** Mitochondrial respiratory complex (I–V) assessment by western blot. Statistical significance was assessed using an unpaired, two-tailed *t* test (**B–D**, **F–H**). Data are representative of four (**A–H**, **J**) or three (**I**) independent experiments. Data are expressed as mean \pm SEM. Source data are provided as a Source Data file.

cells exhibited a dose-dependent decrease in all cytokines (Fig. 6C).

Having shown that 2-DG treatment reduced OXPHOS in fructose-treated cells (Fig. 1D), these results suggest the oxidative metabolic phenotype induced by fructose supports monocyte function. Given the enhanced reduction of cytokine expression, we next determined the level of cell viability for 2-DG-treated monocytes. Fructose-treated monocytes were acutely sensitive to 2-DG-mediated cell death in comparison to glucose-treated monocytes that were largely unaffected (Fig. 6D). We next wanted to assess whether the cells were similarly sensitive to inhibition of

oxidative metabolism. The viability of LPS-stimulated monocytes treated with glucose was minimally affected by inhibition of complex I (with rotenone), III (with antimycin A) and V (with oligomycin). However, monocytes treated with fructose were completely unable to tolerate incubation with these drugs, reflected by a striking reduction in viability (Fig. 6E). These data demonstrate that fructose treatment renders LPS-stimulated monocytes metabolically inflexible and dependent on oxidative metabolism. Sensitivity to both 2-DG and mitochondrial inhibitors suggest that glycolysis and oxidative metabolism become inextricably coupled upon exposure to fructose.

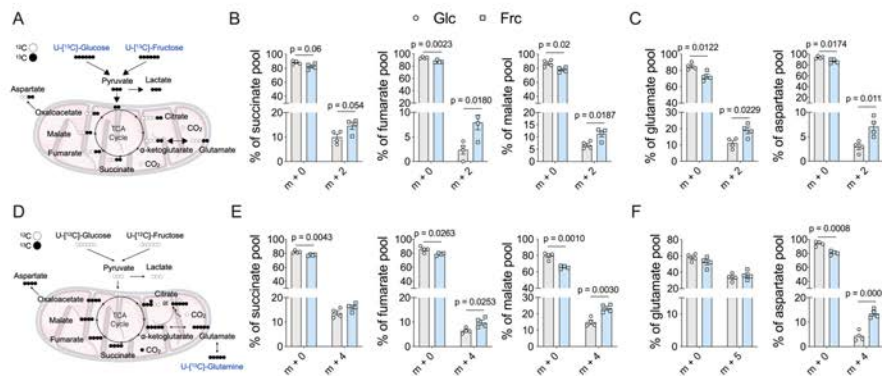


Fig. 5 Fructose treatment induces elevated metabolic cycling. **A** Stable isotope tracing of uniformly labelled ^{13}C -glucose or ^{13}C -fructose into the TCA cycle. **B** Mass isotopologue distribution (MID) represented as a % pool of TCA cycle metabolites: succinate, fumarate and malate or **C** amino acids: glutamate and aspartate of 24-h LPS-stimulated monocytes. Numbers on the x-axis represent the number of ^{13}C carbons incorporated. **D** Stable isotope tracing of uniformly labelled ^{13}C -glutamine in the presence of ^{12}C -glucose or ^{12}C -fructose of 24-h LPS-stimulated monocytes. **E** MID of succinate, fumarate and malate and **F** amino acids: glutamate and aspartate. Statistical significance of individual mass isotopomers was assessed using an unpaired, two-tailed t test (**B**, **C**, **E**, **F**). Data are representative of four independent experiments and are expressed as mean \pm SEM. Source data are provided as a Source Data file.

Dietary fructose increases inflammation in a mouse model.

Thus far, we have explored the metabolic and mechanistic implications of fructose exposure in human monocytes cultured *ex vivo*. In order to further investigate the impact of physiological fructose exposure on inflammation *in vivo*, we employed a mouse model. First, we determined whether mouse LPS-challenged bone marrow-derived macrophages (BMDMs) phenocopied human monocytes when exposed to fructose *in vitro*.

To better recapitulate the *in vivo* microenvironment, we incubated mouse macrophages with either glucose alone or a 1:1 ratio of glucose to fructose (maintaining the equivalent concentration of total monosaccharide). This strategy has been used previously in several studies to investigate the physiological impact of fructose exposure in an environment when glucose is also present^{10,15,25}. Consistent with human monocytes, LPS-stimulated mouse macrophages exposed to fructose produced elevated levels of cytokines TNF, IL-1 β , IL-6 and IL-12 at the protein level, but not the messenger RNA level in comparison to glucose alone (Fig. 7A and Supplementary Fig. 5A, B). Importantly, we demonstrated that this observation is not due to reduced glucose availability in the double monosaccharide condition (Supplementary Fig. 5C).

In order to confirm fructose uptake in the presence of glucose, we performed SITA analysis using mouse macrophages cultured in universally labelled $^{13}\text{C}_6$ -glucose alone or $^{13}\text{C}_6$ -glucose with $^{13}\text{C}_1$ -fructose (Fig. 7B). Indeed, fructose enters the cells in the presence of glucose as depicted by the presence of the $m+1$ isotopologue (Fig. 7C). Similar to human monocytes, BMDMs exposed to fructose significantly increased glutamine uptake and phosphorylation of the mTORC1 target, S6 ribosomal protein (Fig. 7D, E). Fructose treatment also led to an increase in Akt phosphorylation (Supplementary Fig. 5D).

Next, we investigated the role of glutamine metabolism in fructose-treated mouse macrophages and their response to LPS. The glutaminase inhibitor CB-839 did not alter levels of TNF; however, it significantly reduced IL-1 β and IL-12 in BMDMs cultured in the presence of both monosaccharides, whereas cytokine production was unchanged in cells cultured with glucose

alone (Fig. 7F). CB-839 also reduced phosphorylation of S6 in fructose-exposed cells (Supplementary Fig. 5E), suggesting that increased glutamine metabolism supports mTORC1 activity in the presence of fructose. Further exploring the role of mTORC1 in fructose-mediated inflammation, we treated BMDMs with the mTORC1 inhibitor, rapamycin. Here, rapamycin treatment significantly reduced cytokine production in both glucose-alone and glucose–fructose-treated macrophages (Fig. 7G). These data suggest that mouse macrophages require mTORC1 activity for cytokine production regardless of sugar exposure, yet those exposed to both monosaccharides (in contrast to those exposed to glucose alone) rely on glutaminolysis to support the increased cytokine production promoted by fructose exposure.

Finally, to determine if fructose supplementation can influence LPS-induced inflammation *in vivo*, we used a mouse LPS model of systemic inflammation. Here, mice were provided 10% glucose or 10% fructose/10% glucose solutions for 2 weeks (to preclude development of any metabolic disorders) prior to LPS challenge (Fig. 7H). Strikingly, serum IL-1 β levels were significantly increased in mice exposed to fructose, and an increasing trend of IL-6 and TNF was observed (Fig. 7I). This increase in serum IL-1 β was not due to fructose-enhancing baseline IL-1 β secretion, as seen at weeks 1 and 4 of sugar-water treatment in unchallenged mice (Supplementary Fig. 6A, B).

Interestingly, the presence of fructose does not result in a global increase in serum inflammatory markers, as while levels of CXCL5 were elevated in the presence of fructose, this did not reach statistical significance and there was no change in CXCL1 and CCL11 (Supplementary Fig. 6C–E). These data demonstrate that short-term fructose supplementation enhances LPS-induced systemic inflammation, suggesting physiological repercussions of high fructose exposure in mammals.

Fructose-supported inflammation does not occur in T cells.

Given our results of an effect of fructose on both human and mouse mononuclear phagocytes, we were intrigued as to whether fructose exposure might have an effect on other immune cell types. However, functional observations of heightened

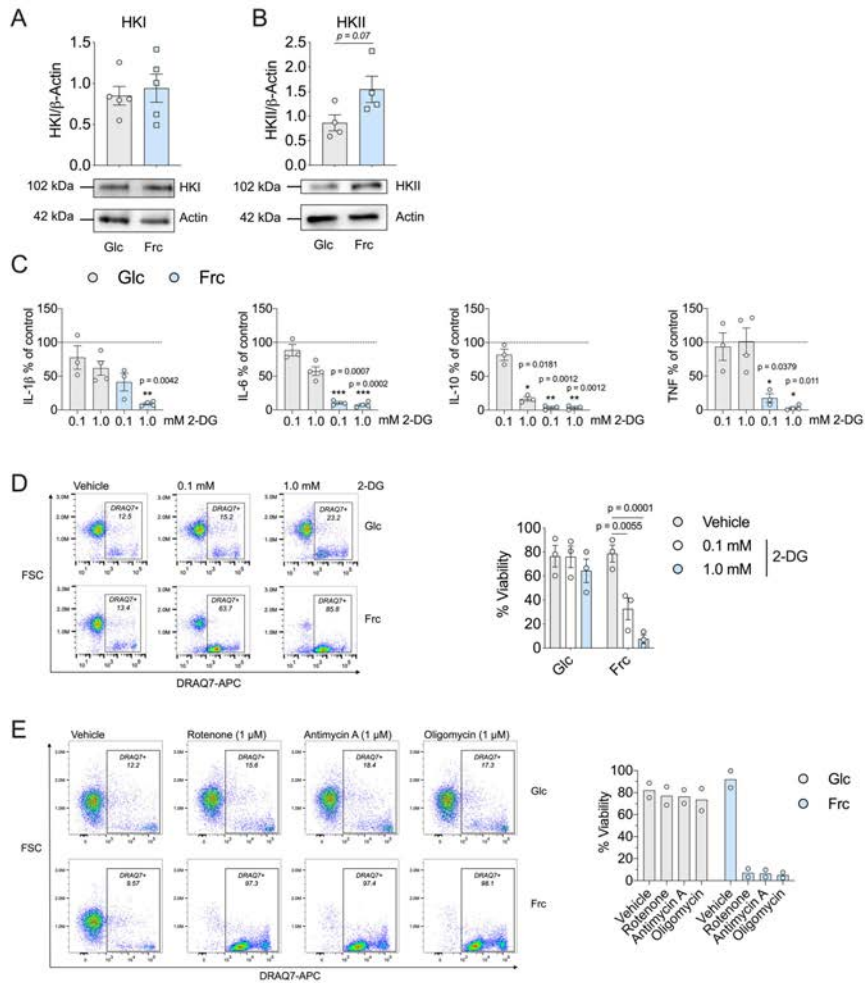
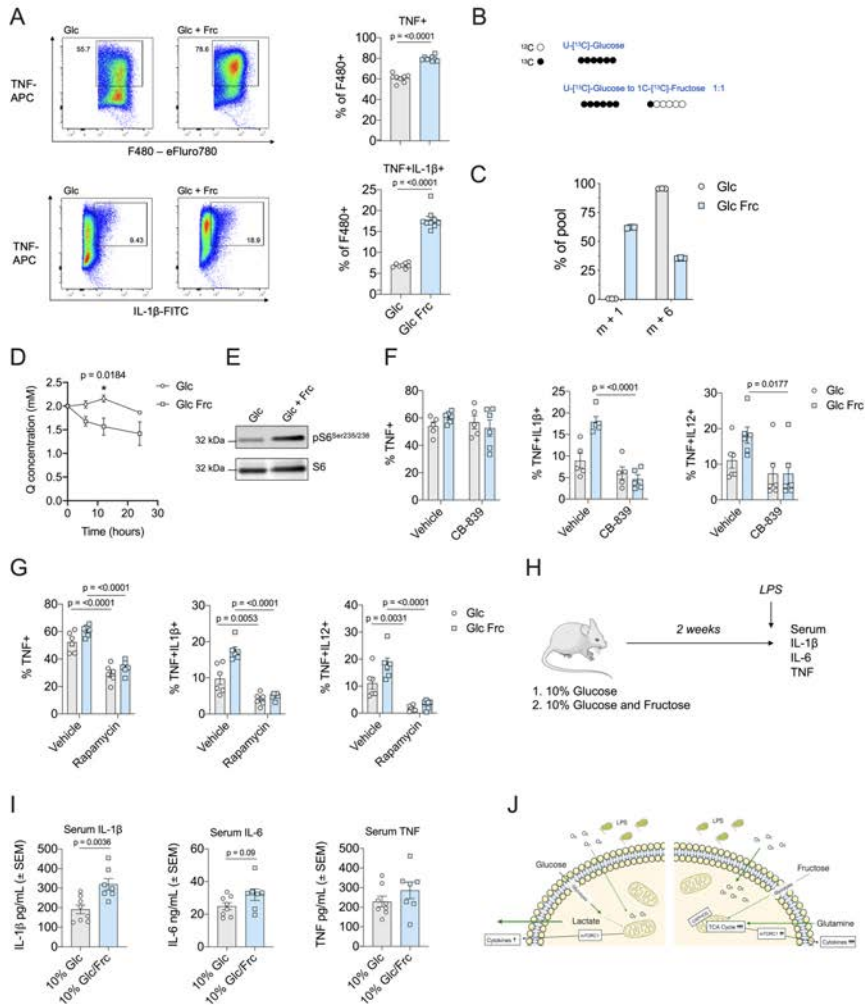


Fig. 6 Fructose-induced inflammatory monocytes are sensitive to metabolic inhibition. Immunoblot of LPS-stimulated monocytes in the presence of glucose or fructose with **A** hexokinase I or **B** hexokinase II analysed. **C** Cytokine release (% of control) of IL-1 β , IL-6, IL-10 and TNF (dotted line indicates control) and **D** representative flow cytometry plot including DRAQ7 viability of glucose or fructose LPS-stimulated monocytes in the presence or absence of glycolytic inhibitor, 2-DG (0.1 or 1.0 mM). **E** Representative flow cytometry plot including DRAQ7 viability of glucose or fructose LPS-stimulated monocytes in the presence or absence of complex I inhibitor, rotenone (1 μ M), complex III inhibitor antimycin A (1 μ M) or complex V inhibitor, oligomycin (1 μ M). Statistical significance was assessed using an unpaired, two-tailed t test (**A**, **B**) or a two-way ANOVA with Sidak's multiple comparison test (**C**, **D**). Data are representative of five (**A**), four (**B**), three-four (**C**), three (**D**) or two independent experiments (**E**) and are expressed as mean \pm SEM; * $p \leq 0.05$, ** $p \leq 0.01$ and *** $p \leq 0.001$. Source data are provided as a Source Data file.



inflammation were not reflected in the mouse T cell compartment. We did not observe any differences in CD4+ or CD8+ T cell proliferation (Supplementary Fig. 7A). CD4+ T cells can be programmed into inflammatory subsets, such as T-helper type 1 (Th1) or anti-inflammatory subsets such as inducible regulatory T cells. Fructose supplementation did not influence polarisation of either Th1 or inducible regulatory T cells (Supplementary Fig. 7B, C). This suggests that fructose has a specific effect on LPS-stimulated mononuclear phagocytes.

Discussion

Here, we investigate how activated human monocytes and mouse macrophages respond metabolically and functionally to fructose exposure. We demonstrate that mononuclear phagocytes from both species are metabolically plastic in engaging in the metabolism of an alternative carbon source and reprogramme cellular pathways to favour oxidative metabolism. Although able to rewire their metabolic pathways upon exposure to fructose, the cells are left metabolically inflexible and vulnerable to further metabolic

Fig. 7 Fructose enhances inflammation in the presence of glucose in macrophages. **A** Representative TNF and IL-1 β flow cytometry plots and bar graphs of glucose (24 mM) or glucose and fructose (both 12 mM) cultured mouse macrophages treated with LPS (1 ng/mL) for 5 h in the presence of GolgiStop™. **B** Schematic of ¹³C₆-glucose (10 mM) or ¹³C₆-glucose (5 mM) and ¹³C₅-fructose (5 mM) isotope tracing. **C** Hexose isotopologues, m + 1 or m + 6, in mouse macrophages stimulated with LPS (1 ng/mL) for 24 h. **D** Glutamine uptake in the media of BMDMs cultured with 24 mM glucose or 12 mM glucose and 12 mM fructose stimulated with LPS (1 ng/mL) for 0, 12 and 24 h. **E** Immunoblot analysis for pS6^{Ser235-236} in BMDMs stimulated with LPS overnight in the presence of glucose alone or glucose/fructose. Total S6 was used as a loading control. **F** Cytokine production assessed by flow cytometry and ICS for TNF, IL-1 β and IL-12 of macrophages treated for 18 h with CB-839 (1 μ M). **G** Cytokine production of TNF, IL-1 β and IL-12 produced by macrophages cultured as **A** with or without rapamycin (50 μ M). **H** Schematic of in vivo experiment. Mice fed a diet of 10% glucose (n = 8) or 10% glucose-fructose mixture (n = 7) for 2 weeks and stimulated with LPS (0.1 mg/kg) for 3 h (image of mouse obtained from Servier Medical Art). **I** Serum cytokine levels of IL-1 β , IL-6 and TNF. **J** Schematic outlining fructose metabolism promoting inflammation. mTORC1 mammalian target of rapamycin complex 1, OXPHOS oxidative phosphorylation, TCA tricarboxylic acid. Statistical significance was assessed using an unpaired, two-tailed t test (**A**, **I**) or a two-way ANOVA with Sidak's multiple comparison test (**D**, **F**, **G**). Data are representative of five (**A**), two (**B**, **C**), three (**D**–**G**) or seven–eight independent experiments (**I**) and are expressed as mean \pm SEM. Source data are provided as a Source Data file.

challenge. Importantly, we show that fructose exposure *ex vivo* promotes elevated cytokine production in both human and mouse mononuclear phagocytes and that a high fructose diet promotes an inflammatory phenotype *in vivo*, attributing pathophysiological relevance to our findings.

To date, most research has focused on the role of the disaccharide sucrose (glucose and fructose) in macrophage function. Sucrose stimulates pinocytosis in unstimulated macrophages and is broken down in the lysosome²⁶. The only link to date between fructose and macrophage-mediated inflammation is that supra-physiological concentrations of sucrose (300 mM) enhance IL-1 β secretion, most likely due to hypertonicity²⁷. There is some evidence that fructose enhances myeloid function, either by increasing cytokine production in human dendritic cells or phagocytosis in mouse alveolar macrophages; however, the metabolic mechanisms of fructose-mediated inflammation have not been explored^{17,28}. Coupled with this is a growing concern regarding high fructose corn syrup consumption globally—in some cases, accounting for 10% caloric intake in the USA²⁹—thus underscoring the need to understand the implications of fructose exposure on macrophage function and inflammation.

Here, for the first time, we show that LPS-stimulated human monocytes and mouse macrophages exposed to fructose have an enhanced inflammatory phenotype supported by oxidative metabolism and glutaminolysis. We suggest this supports cytokine production through increased supply of biosynthetic intermediates. Mechanistically, we demonstrate that fructose-exposed cells have increased mTORC1 activity, and while this is required to support cytokine production regardless of sugar exposure, those cells exposed to fructose rely specifically on glutaminolysis to support their inflammatory phenotype (Fig. 7). mTORC1 has previously been implicated in metabolic reprogramming in monocytes, with monocyte-specific deletion of Raptor (an mTORC1 scaffolding protein) leading to reduced oxidative metabolism during monocyte differentiation³⁰. mTORC1 has also been shown to be activated by glutaminolysis and α -ketoglutarate production³¹. This is consistent with our findings and further suggests that mTORC1 can act both upstream and downstream of metabolic reprogramming.

We demonstrate that fructose-dependent metabolic reprogramming is maintained long term, but this is independent of changes to mitochondrial dynamics. Instead, it appears due to increased metabolic intermediate supply. Our data show that fructose carbon can contribute to both glycolysis and the TCA cycle, and whether this is mediated by HK or ketohexokinase in both human and mouse mononuclear phagocytes requires further exploration. In comparison to glucose, fructose-derived pyruvate is not converted to lactate. This could be due to reduced activity or expression of LDH (although our data would suggest otherwise), increased activity of pyruvate dehydrogenase and

mitochondrial pyruvate carrier 1 or decreased activity of pyruvate dehydrogenase kinase^{132,33}. Fructose exposure has also been linked extensively to lipid biosynthesis, for example, fructose as a substrate is 30% more efficient at synthesising fatty acids than glucose, a phenomenon that has been implicated in the pathophysiology of non-alcoholic fatty liver disease^{34,35}. Consistent with this, cytokine production was more sensitive to ACLY inhibition and levels of prostaglandin E2 were elevated in our fructose-treated monocytes.

It is clear that fructose levels fluctuate throughout health and disease. With the increased prevalence of high fructose diets in the Western world, understanding the impact of fructose on human health is critical. Fructose contributes to numerous metabolic disorders such as obesity, cancer and non-alcoholic fatty liver disease; however, to date, our understanding of its impact on the immune system is lacking^{9,36,37}. A key strength of our study is the assessment of the impact of fructose on metabolism and inflammation across the two species. Akin to human monocytes, mouse macrophages increased consumption of glutamine, produced higher levels of cytokine production displayed and demonstrated elevated mTORC1 activity. A mouse model of LPS-induced inflammation allowed us to assess the physiological relevance of our findings. Previous *in vivo* studies of long-term high fructose exposure have been in the context of metabolic disorders such as steatosis and hyperglycaemia. Here, in order to circumvent any changes due to whole-body metabolism, we used a 2-week exposure strategy. This allowed us to demonstrate for the first time that fructose enhances inflammation independent of metabolic disease. Collectively, this provides direct evidence that fructose elevates inflammation under physiological conditions^{38,39}.

The increase in LPS-induced inflammation from dietary fructose was not due to an enhanced global inflammatory effect, with certain chemokines measured having no observable differences, in addition to no effect on the mouse T cell compartment. Whether this enhanced, fructose-mediated inflammation could contribute to downstream pathologies warrants further investigation. For instance, chronic fructose exposure and infection could heighten inflammation leading to non-alcoholic steatohepatitis or carcinogenesis¹². In addition, our work using metabolic inhibitors shows that fructose treatment leaves cells metabolically inflexible and acutely vulnerable to further metabolic challenge. This highlights a potential vulnerability of human monocytes exposed to fructose when facing metabolically challenging environments, such as during bacterial infection (including sepsis) or in the tumour microenvironment, particularly in those individuals with a high fructose diet.

Our results have highlighted the metabolic plasticity of human monocytes in response to fructose exposure and have elucidated the metabolic mechanisms supporting fructose-induced inflammation. These findings highlight the importance of the microenvironment

in shaping the innate immune response and could form the foundations of investigations for therapies in areas as diverse as cancer and infectious diseases.

Methods

Human monocyte isolation and culture. Peripheral blood was collected with informed written consent and ethical approval was obtained from Wales Research Ethics Committee 6 (13/WA/0190). Mononuclear cells were obtained by density gradient centrifugation (Histopaque-1077 (10771), Merck) Human CD14+ monocytes were isolated using CD14 microbeads (130-050-201; Miltenyi Biotec). The purity of monocytes was routinely monitored using anti-CD14 Pacific Blue (clone 63D3; 367122; BioLegend) via flow cytometry.

Monocytes (1.0×10^6 /mL) were activated with LPS (10 ng/mL; Ultrapure, tlr4:tlr4:tlr4:tlr4; Invivogen) and cultured in glucose (G7021) or fructose (F3510; 11.1 mM; Merck) containing glucose-free RPMI (11879020; Thermo Fisher) supplemented with 10% dialysed foetal bovine serum (FBS; A382001; Thermo Fisher Scientific), 2-DG (0.1–1 mM; D8375), oligomycin (1 μ M; 75351), antimycin A (1 μ M; A8674) and rotenone (1 μ M; R8875) were obtained from Merck. The ACLY inhibitor, BMS303141 (4609), was purchased from Tocris. LPS purchased from Invivogen (*Escherichia coli* K12; tlr4:tlr4) was used for the varying glucose concentration experiments.

Cells were harvested and analysed for flow cytometry (acquired with NovoExpress V1.4.1) and supernatants were stored at -20°C for cytokine analysis.

Mice. Animal experiments were subject to ethical review by the Francis Crick Animal Welfare and Ethical Review Body and regulation by the UK Home Office project licence P319AE968. All mice were housed under conditions in line with the Home Office guidelines (UK). Mice were housed 3–5 per cage and were kept in a 12-h day/night cycle 07:00–19:00. Food and water were available ad libitum and rooms were kept at 21°C at 55% humidity. All procedures were performed following the Animals (scientific procedures) Act 1986 and the EU Directive 2010.

C57/B6j mice were bred and housed at the Francis Crick Institute animal facility. All animals used were aged 6–15 weeks and littermates were randomly assigned to experimental groups.

Mouse BMDM differentiation and culture. Hind legs were collected from C57/B6j mice (aged 6–15 weeks) and cleaned using a scalpel, followed by flushing of the bone marrow with a 1 mL syringe, phosphate-buffered saline (PBS) and 25 G needle. Red blood cells were lysed using ACK lysis buffer following the manufacturer's instructions (10x red blood cell lysis buffer, 420301; BioLegend). Bone marrow cells were cultured on non-tissue culture-treated 10-cm Petri dishes in complete Iscove's modified Dulbecco's media (IMDM), 10% FBS, 50 μ M β -mercaptoethanol and supplemented with 25 ng/mL of macrophage colony-stimulating factor (315-02; Peprotech). BMDMs were supplemented with macrophage colony-stimulating factor every 3 days until day 7 of differentiation. BMDMs were activated with 1 ng/mL of LPS purchased from Sigma (*E. coli* O111:B4 LPS25) for either 5 or 18 h according to experiment type. Further experiments were performed with the glutaminase inhibitor CB-839 (Merck, AMB12D6FB23B) (1 μ M per well) or rapamycin (R8781; Sigma) (50 nM per well) with their respective vehicle controls.

Flow cytometry and intracellular cytokine staining

Human monocytes. Flow cytometry analysis was performed on monocytes after 24 h in culture. Cell death was monitored with DRAQ7 (1 μ M, DR71000; BioStatus) and DRAQ7-negative cells were analysed with anti-HLA-DR (clone AC122; 130-095-293), anti-CD80 (clone REA661; 130-110-270), anti-CD86 (clone FM95; 130-113-572), anti-CCR5 (clone REA245; 130-117-356) and anti-CCR2 (clone REA624; 130-109-595; all Miltenyi Biotec) and anti-CD62L (clone DREG-56; 304806; BioLegend).

For mitochondria staining, cells were incubated with 100 nM MitoTracker Green (M7514; Thermo Fisher) for 30 min at 37°C . For mitochondrial membrane potential and ROS, cells were incubated with tetramethylrhodamine ethyl ester 50 nM (ab113852; Abcam) and MitoSOX 5 μ M (M36008; Thermo Fisher), respectively, for 20 min at 37°C . Cells were acquired (Novocyte, ACEA) and downstream analysis was performed with FlowJo version 10 (TreeStar, USA).

Mouse macrophages. BMDMs were collected after 5 days of differentiation and switched into 24 mM glucose IMDM or 12 mM glucose/12 mM fructose IMDM for 2 days. BMDMs were plated in either in non-TC-treated 12- or 24-well plates (1×10^6 cells and 0.5×10^6 BMDM, respectively). Intracellular cytokine staining for IL-12, TNF, IL-6 and pro-IL-1 β (antibody details can be found below) was performed by adding 1 ng/mL of LPS and 0.8 μ L of BD GolgiStopTM per 1 mL followed by 5 h of incubation at 37°C .

BMDMs were scraped from the plastic and washed 1x in PBS. Surface staining was performed for F4/80 and viability dye (Viability Dye eFluorTM 780) was used to exclude dead cells. Cells were permeabilized, fixed, and stained with fluorescence-conjugated anti-IL-12, TNF, IL-6 or pro-IL-1 β using the eBioscienceTM Foxp3 Transcription Factor Staining Buffer Set.

Antibodies. Fluorescence-conjugated PerCP-Cy5.5 F4/80 (clone BMR; 123128), PE IL-6 (clone MP5-20F3; 504504) and PeCy7 IL-12/23 (clone XM5.6; 505210) antibodies were purchased from BioLegend. FITC-IFN γ (clone XMG1.2; 35-7311), PE-FOXp3 (clone 3G3; 50-5773) and Violet Fluor450-CD4 (clone RM4-5; 750042) were purchased from Tonbo Biosciences. FITC-IL-1 β -pro was purchased from Invitrogen (clone NITEN3; 11-7114-82). TNF conjugated to APC (clone MP6-XT22; 506308) was purchased from eBioscience Life Technologies. All antibodies were used at a dilution of 1/300 for surface and intracellular staining.

Carboxyfluorescein succinimidyl ester stock at 5 mM was purchased from BioLegend (423801) and used at a final concentration of 85 nM. Viable cells were detected using the Fixable Viability dye eFluor780 (65-0865-14; eBioscience) at a dilution of 1/1000. Samples were acquired using BD FACSDiva V8.0.1 on the BD FACSymphonyTM Flow Cytometer and data were analysed using FlowJo V10.3 (BD). An example gating strategy can be found in the Supplementary information (Supplementary Fig. 8).

Metabolic analysis. Metabolic analysis of monocytes was carried out using the Seahorse Extracellular Flux Analyzer (Agilent Technologies). Monocytes (0.25×10^6 cells) were seeded onto a Cell-Tak (354240; Corning)-coated microplate allowing for immediate adhesion. To observe the glycolytic switch, cells were seeded in Seahorse XF assay media supplemented with 1% foetal calf serum (HyClone, 10703464; Fisher Scientific, USA) and 2 mM glutamine (G7515; Merck). Monocytes were given an initial injection of glucose, fructose, galactose (G5388; 11.1 mM; Merck) or media and allowed to equilibrate. LPS (10 ng/mL; Ultrapure, Invivogen) was injected after 1 h. To arrest glycolysis, a final injection of 2-DG (100 mM; Merck) was added. Corresponding OCR/ECAR (oxygen consumption rate/extracellular acidification rate) changes were monitored for the duration of the experiment. Alternatively, monocytes were given a third injection of oligomycin (1 μ M) or GSK2837808A (LDH1, 10 μ M; 5189; Tocris).

For the mitochondrial stress assay, monocytes were resuspended in Seahorse XF assay media supplemented with 11.1 mM glucose or fructose and 1 mM sodium pyruvate (103578-100; Agilent Technologies). Injections were of oligomycin (1 μ M), FCCP (3 μ M), antimycin A (1 μ M), rotenone (1 μ M) and monensin (20 μ M; M5273; Sigma). Data were acquired using the Seahorse Wave software v2.6 (Agilent).

Enzyme-linked immunosorbent assay. IL-1 β (DY201), IL-6 (DY206), IL-8 (DY208-05), IL-10 (DY217B), TNF (DY210) and prostaglandin E2 (KGE004B) were analysed using ELISA (DuoSets; R&D Systems).

Mouse serum samples were analysed using ELISA for IL-1 β (Sigma, RAB0274), TNF (Mouse Uncoated ELISA Kit; Invitrogen, 88-7324-22), IL-6 (Mouse Uncoated ELISA Kit; Invitrogen, 88-7064-22), CXCL1 (Raybiotech, ELM-KC-1), CXCL5 (Raybiotech, ELM-LIX-1) and CCL11 (LEGEND MAXTM, BioLegend, 443907).

ELISA plates were coated with the capture antibody and left overnight at 4°C . Samples were appropriately diluted and incubated for 2 h at room temperature with gentle agitation, 2 h with the kit-specific secondary antibody and 20 min with streptavidin-horse radish peroxidase. The plate was then incubated at room temperature with a 1:1 mixture of hydrogen peroxide and tetramethylbenzidine (555214; BD Biosciences). Absorbance was measured at 450 nm after the addition of sulfuric acid (Merck) to each well and values were corrected to the blank.

Extracellular lactate measurement. Extracellular lactate was measured using the L-Lactate Assay Kit I (120001100A; Eton Bioscience). Samples and standards were appropriately diluted and mixed with the L-lactate assay solution and incubated at 37°C for 30 min. Absorbance was then measured at 490 nm and concentrations calculated from the linear regression of the standard curve.

RNA extraction and quantitative PCR of BMDMs. Total RNA was extracted using RNeasy[®] columns (Qiagen) from three separate wells per condition according to the manufacturer's instructions. Genomic DNA was removed using On-Column DNA digestion (Qiagen). Complementary DNA (cDNA) was generated using the High-Capacity cDNA Reverse Transcription Kit (4368814; Thermo Fisher) according to the manufacturer's instructions. Power upTM SYBR[®] Green Master Mix (Applied Biosystem) was used to perform quantitative PCR. Primer sequences can be found in Supplementary Table 1. Gene expression values are calculated according to Pfaffl method⁴⁰ and are expressed as relative units compared to the control group. Quantitative PCR data were collected using QuantStudio Design & Analysis software v1.3.

RNA-seq sample preparation and sequencing. Total RNA quality and quantity were assessed using Agilent 2100 Bioanalyser and an RNA Nano 6000 Kit (Agilent Technologies). Sequencing libraries were prepared with 100–900 ng of total RNA with an RNA integrity number value >8 using the Illumina[®] TruSeq[®] Stranded Total RNA with Ribo-Zero GoldTM Kit (Illumina Inc.). The steps included ribosomal RNA depletion and cleanup, RNA fragmentation, first-strand cDNA synthesis, second-strand cDNA synthesis, adenylation of 3' ends, adapter ligation and PCR amplification (12 cycles). The manufacturer's instructions were followed except for the cleanup after the ribozero depletion step where Ampure[®] XP beads (Beckman Coulter) and 80% ethanol were used. Libraries were validated using the Agilent 2100 Bioanalyser

and a High-Sensitivity Kit (Agilent Technologies) to ascertain the insert size, and the Qubit® (Life Technologies) was used to perform the fluorometric quantitation. Following validation, the libraries were normalised to 4 nM, pooled together and clustered on the cBot 2 following the manufacturer's recommendations. The pool was then sequenced using a 75-base paired-end (2 × 75 bp PE) dual index read format on the Illumina® HiSeq4000 according to the manufacturer's instructions.

RNA-seq analysis and differential gene expression. Raw sequencing files were trimmed to remove adapter sequences and poor quality reads using Trimm-Galore. Trimmed reads were aligned with the STAR aligner (v2.5.1b) to the GRCh38 assembly of the human genome⁴¹. Raw counts were then calculated using Subread featureCounts (v1.5.1)⁴², and a differential expression analysis comparing glucose- and fructose-treated monocytes was performed using DESeq2 (Bioconductor)⁴³. The resultant *p* values were corrected for multiple testing using the Benjamini and Hochberg method⁴⁴. Differentially regulated genes were defined as those with a log₂FC > ±1 and an adjusted *p* value < 0.05. Heatmaps were generated using Morpheus (Broad Institute).

Immunoblot

Human monocytes. Monocyte lysate proteins were quantified, denatured and separated using sodium dodecyl sulfate-polyacrylamide gel electrophoresis. Polyvinylidene difluoride membranes were probed with antibodies targeting HK1 (2024), HKII (2867), phospho-S6 ribosomal protein (pS6; Ser235-236; 4858), phospho-AMPKα (2535), phospho-ACLY (4331), phospho-acetyl-CoA carboxylase 1 (3661), phospho-LDH (8176), pan-Akt (2920), phospho-AktSer473 (4060) and phospho-AktThr308 (4056). All antibodies were purchased from Cell Signaling (Danvers, MA) and used at a 1:1000 dilution. The total OXPHOS human cocktail (ab110411) and GLUT5 (ab41533) were purchased from Abcam and used at a dilution of 1:200 and 1:700, respectively. Protein loading was evaluated and normalised using β-actin (ab8226; Abcam). Densitometry on non-saturated immunoblots was measured using ImageJ software (Fiji)⁴⁵.

Mouse BMDM. Macrophages were lysed using RIPA buffer supplemented with 1% sodium dodecyl sulfate and phosphatase inhibitors (La Roche Ltd), denatured at 95 °C, and resolved on NuPAGE polyacrylamide pre-cast gels (Thermo Fisher Scientific) before the transfer of gels onto nitrocellulose membranes using the iBlot2 (Invitrogen). Lysates were probed for phospho-S6 Ser235/236 (4858) ribosomal protein, total pS6 (clone 54D2; 2317), phospho-AktThr308 (clone 244F9; 4056), phospho-AktSer473 (clone D9E; 4060) and pan-Akt (clone 40D4; 2920). All antibodies were purchased from Cell Signaling Technologies. Secondary antibodies were purchased from LI-COR IRDye 800CW (donkey anti-mouse; 926-32212) and 680LT (donkey anti-rabbit; 926-68023). Fluorescence analysis was collected using the LI-COR Image Studio software v5.2. All original uncropped blots can be found in the Supplementary information (Supplementary Fig. 9).

Gas chromatography-mass spectrometry. Isolated monocytes were incubated with heavily labelled ¹³C₆-glutamine (2 mM; CLM-1822; Cambridge Isotopes) in RPMI phenol red-free media (Agilent Technologies) supplemented with 11.1 mM glucose or fructose and 10% dialysed FBS (Thermo Fisher Scientific). Alternatively, monocytes were cultured with ¹³C₆-glucose (CLM-1396) or ¹³C₆-fructose (CLM-1553; 11.1 mM; Cambridge Isotopes) in glucose-free RPMI (Thermo Fisher Scientific) supplemented with 10% dialysed FBS (Thermo Fisher Scientific). Monocytes were activated with LPS (10 ng/mL) for 24 h, washed twice with ice-cold saline and lysed in 80% methanol. Cell extracts were then dried down at 4 °C using a speed-vacuum concentrator.

Cellular metabolites were extracted and analysed by GC-MS using protocols described previously^{46,47}. Metabolite extracts were derived using MTBSTFA (N-(tert-butylidimethylsilyl)-N-methyltrifluoroacetamide), D₂-Myristic acid (750 ng/sample) was added as an internal standard to metabolite extracts, and metabolite abundance was expressed relative to the internal standard. GC/MS analysis was performed using an Agilent 5975C GC/MS equipped with a DB-5MS + DG (30 m × 250 μm × 0.25 μm) capillary column (Agilent J&W, Santa Clara, CA, USA). Data were acquired using ChemStation E.02.02.1431. For SITA experiments, mass isotopomer distribution was determined using a custom algorithm developed at the McGill University⁴⁶.

Liquid chromatography-mass spectrometry. ¹³C₆-glucose was purchased from Cambridge Isotope Laboratories and D-fructose-¹³C₆ (587621) was purchased from Sigma-Aldrich. SITA with ¹³C₆-glucose and ¹³C₆-fructose allowed for the identification of isotopomer distribution of metabolites. Both ¹³C₆ fructose and glucose were added in glucose-free Dulbecco's modified Eagle's medium supplemented with 10% dialysed FBS and 50 μM β-mercaptoethanol in the presence of LPS (10 ng/mL). Metabolites were extracted after 24 h of LPS activation and analysed by liquid chromatography-mass spectrometry (LC-MS) using methods previously described⁴⁸. In brief, 1 × 10⁶ BMDMs were washed with cold PBS and metabolites were extracted with 200 μL of ice-cold extraction buffer (methanol, acetonitrile and water (50:30:20)). Samples were centrifuged at 21.1 × g for 10 min at 4 °C and the supernatant was collected for LC-MS analysis. Extracellular metabolites were extracted using 10 μL of culture media added to 490 μL of ice-cold extraction buffer

and centrifuged at the aforementioned speed. Supernatants were collected and run through LC-MS analysis. LC-MS machine information and operation is further described in Labuschagne et al.⁴⁹. Spectra analysis was performed using the Thermo TraceFinder software.

LPS-induced systemic inflammation model. Female C57/B6J mice aged 8–10 weeks were randomly assigned either to 10% glucose water or 10% glucose/fructose (stock solution at 60% fructose and 40% glucose) water for 2 weeks prior to LPS challenge. Mice were injected intraperitoneally with LPS from *E. coli* (0111:54; Sigma L4391) at a dose of 0.1 mg/kg. Mice were sacrificed 3 h post challenge and blood collected by cardiac puncture into EDTA-coated collection tubes. Blood was spun at 2000 × g for 15 min at 4 °C and serum was collected and stored at –80 °C.

Data analysis. Statistical analysis was performed using GraphPad Prism version 9 (USA). Data are represented as the mean ± standard error of the mean with significance taken as **p* ≤ 0.05, ***p* ≤ 0.01 and ****p* ≤ 0.001.

Reporting summary. Further information on research design is available in the Nature Research Reporting Summary linked to this article.

Data availability

RNA-seq data have been deposited in GEO under the accession code GSE164058. All other data are available upon request or can be found within the manuscript and Supplementary information files. Source data are provided with this manuscript.

Received: 29 April 2020; Accepted: 14 January 2021;

Published online: 22 February 2021

References

1. Diskin, C. & Pålsson-McDermott, E. M. Metabolic modulation in macrophage effector function. *Front. Immunol.* **9**, 270 (2018).
2. Izquierdo, E. et al. Reshaping of human macrophage polarization through modulation of glucose catabolic pathways. *J. Immunol.* **195**, 2442–2451 (2015).
3. Raulien, N. et al. Fatty acid oxidation compensates for lipopolysaccharide-induced Warburg effect in glucose-deprived monocytes. *Front. Immunol.* **8**, 609 (2017).
4. Lee, M. K. S. et al. Glycolysis is required for LPS-induced activation and adhesion of human CD14+ CD16– monocytes. *Front. Immunol.* **10**, 2054 (2019).
5. Dominguez-Andrés, J. et al. Rewiring monocyte glucose metabolism via C-type lectin signaling protects against disseminated candidiasis. *PLoS Pathog.* **13**, e1006632 (2017).
6. Lanasa, M. A. et al. Ketohexokinase C blockade ameliorates fructose-induced metabolic dysfunction in fructose-sensitive mice. *J. Clin. Invest.* **128**, 2226–2238 (2018).
7. Legerza, B. et al. Fructose, glucocorticoids and adipose tissue: Implications for the metabolic syndrome. *Nutrients* **9**, 426 (2017).
8. SLEIN, M. W., CORI, G. T. & CORI, C. F. A comparative study of hexokinase from yeast and animal tissues. *J. Biol. Chem.* **186**, 763–780 (1950).
9. Herman, M. A. & Samuel, V. T. The sweet path to metabolic demise: fructose and lipid synthesis. *Trends Endocrinol. Metab.* **27**, 719–730 (2016).
10. Zhao, S. et al. Dietary fructose feeds hepatic lipogenesis via microbiota-derived acetate. *Nature* **579**, 586–591 (2020).
11. Samuel, V. T. Fructose induced lipogenesis: from sugar to fat to insulin resistance. *Trends Endocrinol. Metab.* **22**, 60–65 (2011).
12. Todoric, J. et al. Fructose stimulated de novo lipogenesis is promoted by inflammation. *Nat. Metab.* **2**, 1034–1045 (2020).
13. Hannou, S. A., Haslam, D. E., McKeown, N. M. & Herman, M. A. Fructose metabolism and metabolic disease. *J. Clin. Invest.* **128**, 545–555 (2018).
14. Chen, W. L. et al. Enhanced fructose utilization mediated by SLC2A5 is a unique metabolic feature of acute myeloid leukemia with therapeutic potential. *Cancer Cell* **30**, 779–791 (2016).
15. Jang, C. et al. The small intestine converts dietary fructose into glucose and organic acids. *Cell Metab.* **27**, 351–361.e3 (2018).
16. Porto, M. L. et al. Increased oxidative stress and apoptosis in peripheral blood mononuclear cells of fructose-fed rats. *Toxicol. Vit.* **29**, 1977–1981 (2015).
17. Jaiswal, N., Agrawal, S. & Agrawal, A. High fructose-induced metabolic changes enhance inflammation in human dendritic cells. *Clin. Exp. Immunol.* **197**, 237–249 (2019).
18. Chang, C. H. et al. XPosttranscriptional control of T cell effector function by aerobic glycolysis. *Cell* **153**, 1239 (2013).

19. Venter, G. et al. Glucose controls morphodynamics of LPS-stimulated macrophages. *PLoS ONE* **9**, e96786 (2014).
20. Orozco, J. M. et al. Dihydroxyacetone phosphate signals glucose availability to mTORC1. *Nat. Metab.* **2**, 893–901 (2020).
21. Mookerjee, S. A., Gerencser, A. A., Nicholls, D. G. & Brand, M. D. Quantifying intracellular rates of glycolytic and oxidative ATP production and consumption using extracellular flux measurements. *J. Biol. Chem.* **292**, 7189–7207 (2017).
22. Crescenzo, R. et al. Increased hepatic de novo lipogenesis and mitochondrial efficiency in a model of obesity induced by diets rich in fructose. *Eur. J. Nutr.* **52**, 537–545 (2013).
23. Fussell, J. et al. A lipogenic-switch shifts metabolism from glycolysis to mitochondrial respiration during aging. *Free Radic. Biol. Med.* **100**, S83 (2016).
24. Johnson, R. J. et al. Hypothesis: could excessive fructose intake and uric acid cause type 2 diabetes? *Endocr. Rev.* **30**, 96–116 (2009).
25. Jang, C. et al. The small intestine shields the liver from fructose-induced steatosis. *Nat. Metab.* **2**, 586–593 (2020).
26. Knapp, P. E. & Swanson, J. A. Plasticity of the tubular lysosomal compartment in macrophages. *J. Cell Sci.* **95**, 433–439 (1990).
27. Ferrari, D. et al. Extracellular ATP triggers IL-1 beta release by activating the purinergic P2Z receptor of human macrophages. *J. Immunol.* **159**, 1451–1458 (1997).
28. Everett, K. D. E., Barghouthi, S. & Speert, D. P. In vitro culture of murine peritoneal and alveolar macrophages modulates phagocytosis of *Pseudomonas aeruginosa* and glucose transport. *J. Leukoc. Biol.* **59**, 539–544 (1996).
29. Vos, M. B. & McClain, C. J. Fructose takes a toll. *Hepatology* **50**, 1004–1006 (2009).
30. Karmaus, P. W. F. et al. Critical roles of mTORC1 signaling and metabolic reprogramming for M-CSF-mediated myelopoiesis. *J. Exp. Med.* **214**, 2629–2647 (2017).
31. Durán, R. V. et al. Glutaminolysis activates Rag-mTORC1 signaling. *Mol. Cell* **47**, 349–358 (2012).
32. Menk, A. V. et al. Early TCR signaling induces rapid aerobic glycolysis enabling distinct acute T cell effector functions. *Cell Rep.* **22**, 1509–1521 (2018).
33. Lam, W. Y. et al. Mitochondrial pyruvate import promotes long-term survival of antibody-secreting plasma cells. *Immunity* **45**, 60–73 (2016).
34. Liu, L. et al. Triose kinase controls the lipogenic potential of fructose and dietary tolerance. *Cell Metab.* **32**, 605–618.e7 (2020).
35. Basaranoglu, M., Basaranoglu, G. & Buglani, E. Carbohydrate intake and nonalcoholic fatty liver disease: fructose as a weapon of mass destruction. *Hepatobiliary Surg. Nutr.* **4**, 109–116 (2015).
36. Nakagawa, T. et al. Fructose contributes to the Warburg effect for cancer growth. *Cancer Metab.* **8**, 16 (2020).
37. Santhekadur, P. K. The dark face of fructose as a tumor promoter. *Genes Dis.* **7**, 163–165 (2020).
38. Spruss, A. et al. Toll-like receptor 4 is involved in the development of fructose-induced hepatic steatosis in mice. *Hepatology* **50**, 1094–1104 (2009).
39. Harris, H. W., Rockey, D. C., Young, D. M. & Welch, W. J. Diet-induced protection against lipopolysaccharide includes increased hepatic NO production. *J. Surg. Res.* **82**, 339–345 (1999).
40. Pfaffl, M. W. A new mathematical model for relative quantification in real-time RT-PCR. *Nucleic Acids Res.* **29**, e45 (2001).
41. Dobin, A. et al. Mapping RNA-seq with STAR. *Curr. Protoc. Bioinform.* **51**, 11.14.1–11.14.19 (2015).
42. Liao, Y., Smyth, G. K. & Shi, W. FeatureCounts: an efficient general purpose program for assigning sequence reads to genomic features. *Bioinformatics* **30**, 923–930 (2014).
43. Love, M. I., Huber, W. & Anders, S. Moderated estimation of fold change and dispersion for RNA-seq data with DESeq2. *Genome Biol.* **15**, 500 (2014).
44. Benjamini, Y. & Hochberg, Y. Controlling the false discovery rate: a practical and powerful approach to multiple test. *J. R. Stat. Soc. Ser. B* **57**, 289–300 (1995).
45. Schindelin, J. et al. Fiji: An open-source platform for biological-image analysis. *Nat. Methods* **9**, 676–682 (2012).
46. McGuirk, S. et al. PGC-1 α supports glutamine metabolism in breast cancer. *Cancer Metab.* **1**, 22 (2013).
47. Vincent, E. E. et al. Mitochondrial phosphoenolpyruvate carboxykinase regulates metabolic adaptation and enables glucose-independent tumor growth. *Mol. Cell* **60**, 195–207 (2015).
48. Labuschagne, C. F., van den Broek, N. J. F., Mackay, G. M., Vousden, K. H. & Maddocks, O. D. K. Serine, but not glycine, supports one-carbon metabolism and proliferation of cancer cells. *Cell Rep.* **7**, 1248–1258 (2014).
49. Labuschagne, C. F., Cheung, E. C., Blagih, J., Domart, M. C. & Vousden, K. H. Cell clustering promotes a metabolic switch that supports metastatic colonization. *Cell Metab.* **30**, 720–734.e5 (2019).

Acknowledgements

We thank E. Ma, D. Elder and D. Skibiński for useful discussion, D. Avizonis and L. Chomiere from McGill University Metabolomics Core Facility, the staff in the Joint Clinical Research Facility for phlebotomy and all blood donors. We also thank the Metabolomics Facility at the Francis Crick Institute for their support. We acknowledge the Wales Gene Park for their insight, expertise and technical support in generating the NGS data that assisted this research. Wales Gene Park is a Health and Care Research Wales funded infrastructure support group. This work was supported with grants awarded by Life Sciences Research Network Wales (NRN). G.W.J. is funded by a Versus Arthritis Career Development Fellowship (20305); J.B. was funded by a Canadian Institute for Health Research Postdoctoral Fellowship and the Kuok Family Postdoctoral Fellowship. E.E.V. is supported by a Diabetes UK RD Lawrence Fellowship (17/0005587) and by Cancer Research UK (C18281/A29019). This work was funded by Cancer Research UK Grants C596/A10419 and C596/A26855, and supported by the Francis Crick Institute, which receives its core funding from Cancer Research UK (FC001557), the UK Medical Research Council (FC001557) and the Wellcome Trust (FC001557).

Author contributions

N.J., J.B., F.Z., A.R., B.J.J. and A.I.M.B. performed experiments. N.J., J.B., F.Z., C.J.B., D. M., J.G.C., D.K.F., K.H.V., E.E.V. and C.A.T. designed the experiments and provided intellectual discussion. N.J., J.B., F.Z., D.G.H., C.J.B., D.A., G.W.J. and E.E.V. analysed the data. N.J., J.B., D.K.F., E.E.V. and C.A.T. wrote the manuscript. All authors critically revised and approved the manuscript.

Competing interests

K.H.V. is on the board of directors and shareholder of Bristol Myers Squibb, a shareholder of GRAIL, and on the science advisory board of PMV Pharma, RAZE Therapeutics, Volstra Pharmaceuticals and Ludwig Cancer. K.H.V. is a co-founder and consultant of Faeth Therapeutics, funded by Khosla Ventures. All other authors declare no competing interests.

Additional information


Supplementary information The online version contains supplementary material available at <https://doi.org/10.1038/s41467-021-21461-4>.

Correspondence and requests for materials should be addressed to E.E.V. or C.A.T.

Peer review information *Nature Communications* thanks Claudio Mauro and the other, anonymous reviewer(s) for their contribution to the peer review of this work. Peer review reports are available.

Reprints and permission information is available at <http://www.nature.com/reprints>

Publisher's note Springer Nature remains neutral with regard to jurisdictional claims in published maps and institutional affiliations.

 **Open Access** This article is licensed under a Creative Commons Attribution 4.0 International License, which permits use, sharing, adaptation, distribution and reproduction in any medium or format, as long as you give appropriate credit to the original author(s) and the source, provide a link to the Creative Commons license, and indicate if changes were made. The images or other third party material in this article are included in the article's Creative Commons license, unless indicated otherwise in a credit line to the material. If material is not included in the article's Creative Commons license and your intended use is not permitted by statutory regulation or exceeds the permitted use, you will need to obtain permission directly from the copyright holder. To view a copy of this license, visit <http://creativecommons.org/licenses/by/4.0/>.

© The Author(s) 2021

8.2 A role for metabolism in determining neonatal immune function



Received: 16 July 2020 | Revised: 19 May 2021 | Accepted: 3 June 2021
DOI: 10.1111/pai.13583

REVIEW ARTICLE

WILEY

A role for metabolism in determining neonatal immune function

Sean R. Holm | Ben J. Jenkins | James G. Cronin | Nicholas Jones |
Catherine A. Thornton

Institute of Life Science, Swansea
University Medical School, Swansea
University, Swansea, UK

Correspondence
Catherine A. Thornton, Rm 226 Institute
of Life Science, Singleton Campus,
Swansea University, Swansea, UK SA2
8PP.
Email: c.a.thornton@swansea.ac.uk

Funding information
Work in the group is supported by Ser
Cymru Welsh Government, Swansea
University, Diabetes UK and MRC.

Editor: Ömer Kalaycı

Abstract

Immune responses of neonates differ markedly to those of adults, with skewed cytokine phenotypes, reduced inflammatory properties and drastically diminished memory function. Recent research efforts have started to unravel the role of cellular metabolism in determining immune cell fate and function. For studies in humans, much of the work on metabolic mechanisms underpinning innate and adaptive immune responses by different haematopoietic cell types is in adults. Studies investigating the contribution of metabolic adaptation in the unique setting of early life are just emerging, and much more work is needed to elucidate the contribution of metabolism to neonatal immune responses. Here, we discuss our current understanding of neonatal immune responses, examine some of the latest developments in neonatal immunometabolism and consider the possible role of altered metabolism to the distinctive immune phenotype of the neonate. Understanding the role of metabolism in regulating immune function at this critical stage in life has direct benefit for the child by affording opportunities to maximize immediate and long-term health. Additionally, gaining insight into the diversity of human immune function and naturally evolved immunometabolic strategies that modulate immune function could be harnessed for a wide range of opportunities including new therapeutic approaches.

KEYWORDS

immunometabolism, metabolic adaptation, neonatal immunity, T cells, umbilical cord blood

1 | INTRODUCTION

Birth represents a relatively dramatic transition from an environment with a low microbial burden to one abundant in commensal and potentially pathogenic challenges that the neonatal immune system must be able to respond to. Immune responses in preterm and term neonates differ from those of adults, generally being characterized as diminished, tolerant or Th skewed although we must be mindful

that these are highly evolved, stage of life appropriate responses. Efforts to clarify the phenotypes and mechanisms prevalent at this time are ongoing so that we can better understand the significance of differences at this stage of development for long-term health. The need to understand how the neonatal immune response differs to that of adults is driven by the mortality and morbidity associated with infection and sepsis in newborns and infants and the need for protective vaccine responses that can mitigate these.

This is an open access article under the terms of the Creative Commons Attribution License, which permits use, distribution and reproduction in any medium, provided the original work is properly cited.

© 2021 The Authors. *Pediatric Allergy and Immunology* published by European Academy of Allergy and Clinical Immunology and John Wiley & Sons Ltd.

1616 | wileyonlinelibrary.com/journal/pai

Pediatr Allergy Immunol. 2021;32:1616–1628.

10990008, 2021, K, Downloaded from https://onlinelibrary.wiley.com/doi/10.1111/pai.13583 by Swansea University, Wiley Online Library on [06/01/2021]. See the Terms and Conditions (https://onlinelibrary.wiley.com/terms-and-conditions) on Wiley Online Library for rules of use; OA articles are governed by the applicable Creative Commons License

Recent decades have also seen growing appreciation that neonatal immune phenotypes, shaped predominantly by environmental factors during pregnancy, are linked to the later development of non-communicable immunoinflammatory diseases.¹⁻³ Finally, while the therapeutic capacity of umbilical cord blood is already being harnessed through transplantation, there is growing appreciation of the wider regenerative capacity of neonatal immune cells, for example in the regeneration of heart tissue.⁴ Given this diversity, there is a real need to elucidate the mechanisms that uniquely programme neonatal immune cell phenotype.

The development and maturation of lymphoid progenitors during foetal and early post-natal life are influenced by a multitude of factors including cytokine profiles, transcription factors, expression of surface proteins, prostaglandins produced by the placenta and altered levels of metabolites, such as adenosine, in neonatal plasma.⁵⁻⁷ Maternal immune status during pregnancy also appears to affect neonatal and infant immune development. For example, infants of mothers who suffer from allergic disease have reduced interleukin (IL)-6 production and p38 mitogen-activated protein kinase (MAPK) phosphorylation compared with age-matched healthy controls.⁸ It also has been long recognized that maternal and neonatal nutrition have lasting effects on immune development, contributing to the development of allergic disease, metabolic syndrome and chronic inflammatory conditions.⁹ Energy demands in early life are extremely high with little to no energy, especially fatty acids and proteins, reserves. The metabolic and energetic demands required for growth in early life severely limit nutrient availability for highly energetically demanding immune responses.¹⁰ Disease tolerance, wherein the goal is to limit disease immunopathology versus the pathogen per se, is suggested as an evolved method of host defence in early life to limit harm to the host in the face of these reduced energy reserves. Energy demands of neonates and the disease tolerance hypothesis have been reviewed extensively elsewhere.¹⁰⁻¹⁴

Immunometabolism is a relatively recently emerged field of research that seeks to elucidate the crucial role metabolic pathways have in shaping immune cell fate and function. The activation and function of most immune cells is dependent on metabolic reprogramming to a state of aerobic glycolysis to enable effector function. In this setting, the primary fuel is glucose which is metabolized through the central metabolism pathways of glycolysis to pyruvate (Figure 1). Aerobic glycolysis rapidly generates adenosine triphosphate (ATP) via substrate-level phosphorylation as well as reducing nicotinamide adenine dinucleotide (NAD)⁺ to NADH. Many cells also convert pyruvate to lactate to recycle NADH, thus maintaining glycolytic flux. Glucose metabolism also supports activation of immune cells by generating anabolic intermediates required for cell growth, division and function.¹⁵ Pyruvate enters the Krebs cycle via conversion to acetyl-CoA. NADH and flavin adenine dinucleotide (FAD)H₂ are the major products of the Krebs cycle, which support oxidative phosphorylation (OXPHOS) by transfer of electrons to the electron transport chain. Catabolism in the Krebs cycle also supports cell growth, producing the anabolic building blocks for amino acids and lipids. To support catabolism, the Krebs cycle must be

Key Message

Despite great advances in our understanding of immunometabolism, few advances have been made in applying these insights to human neonatal immune responses. Emerging evidence suggests a central role for metabolism in defining the immune responses of neonates and these could underpin functional differences implicated in the development of atopic disease for example. Here, we summarize the latest findings on immunometabolism and highlight gaps in the literature with specific regard to neonates, exploring connections between metabolism and neonatal immune phenotype. A better understanding of immunometabolism in neonates could have impacts ranging from improved health to new regenerative treatments.

replenished, in a process called anaplerosis, converting various substrates such as the amino acid glutamine into Krebs cycle intermediates (Figure 1). Fatty acid oxidation (FAO) also feeds into the Krebs cycle via acetyl-CoA as well as supporting OXPHOS through NADH and FADH₂ (Figure 1).

The differential utilization of fuels, including in competition with other cells in the tissue microenvironment, can impact on cell fate and function.¹⁶ We suggest that immunometabolism provides a framework for understanding phenotypic and functional differences in the neonatal and adult immune systems and also between neonates linked to individual disease susceptibility. While data supporting this are emerging, these studies are still very much in their early days and there are many unanswered questions. In this review, we will discuss the current understanding of differences between neonate and adult immune responses; how metabolism may influence these changes and the further work that is required.

2 | INNATE IMMUNE RESPONSES

The innate immune system provides front-line cellular and humoral defence through the release of cytokines and other mediators that amplify the immune response, recruitment of first responders and education of the adaptive immune response to help counter the threat and develop immunological memory. These processes demand energy and biosynthetic intermediates that are generated via cellular metabolic pathways.

2.1 | Neutrophils

Neutrophils comprise 70% of the leukocytes in blood. They extravasate from the blood and quickly travel to the site of insult along a chemokine gradient typically released by tissue-resident macrophages. Once in the tissues, neutrophils engulf and kill pathogens

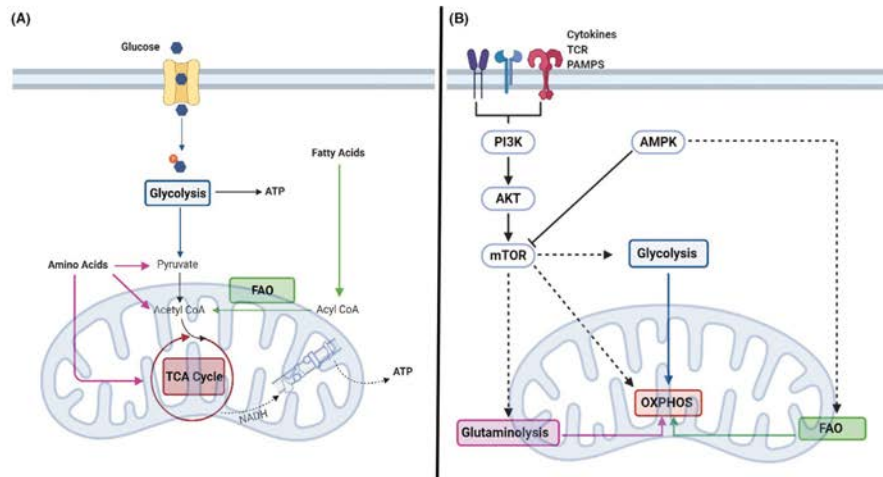


FIGURE 1 Basic metabolism and metabolic signalling pathways. A) Glucose, amino acids and fatty acids are the major metabolites utilized by cells of the immune system. These metabolites feed into the TCA cycle, through glycolysis, fatty acid oxidation or other metabolic pathways. Oxidation of these metabolites, through these metabolic pathways, generates ATP via substrate-level phosphorylation or through the electron transport chain. B) Metabolic pathways are influenced by a number of external stimuli including cytokines, specialized receptors, such as the T-cell receptor, and PAMPs. Resultant signalling cascades via PI3K/AKT increase mTOR signalling, in turn enhancing metabolic pathways typically associated with pro-inflammatory responses. AMPK, on the other hand, inhibits mTOR signalling and upregulates metabolic pathways associated with anti-inflammatory responses. Created using biorender.com

before undergoing controlled apoptosis. In neonates, there is a transient rise in neutrophil frequency shortly before birth, as measured by neutrophil-derived soluble FcR3 (CD16) levels in plasma of preterm and term infants. However, neutrophil frequency reduces again shortly after birth to levels below that of adults, contributing to diminished first responder function.^{17,18} Neonatal neutrophils also have reduced functional capacity; their chemotaxis response is reduced through slower velocities and lower expression of the surface adhesion molecules L-selectin and Mac1, contributing to a near 50% reduction in neutrophil transmigration to the site of infection.^{19,20} Lower expression of TLR4 and defective downstream signalling by myeloid differentiation primary response 88 (MyD88) and p38 MAPK from TLR4 and TLR2 impair neutrophil response.²¹ High levels of adenosine in neonatal blood increase cyclic adenosine monophosphate (cAMP) leading to protein kinase A (PKA)-dependent/TLR-independent inhibition of tumour necrosis factor (TNF).⁷ For neonatal neutrophils, some reports also show reduced capacity, or entire loss, of their primary effector functions of phagocytosis, neutrophilic oxidative burst and formation of neutrophil extracellular traps.^{17,22} All of these are energetically demanding requiring high levels of glycolysis, the main metabolic pathway in neutrophils and, to a lesser extent, glutaminolysis to support them.^{23,24} Inhibition of these metabolic pathways can

entirely prevent effector functions of adult neutrophils.^{23,24} For instance, NETosis is dependent on lactate derived from glycolysis in both NOX-dependent and independent pathways.²⁵ Whether changes in neonatal neutrophil metabolism are responsible for their decreased effector functions has not been elucidated but clearly warrants investigation. Ketone metabolism may be a key pathway to consider as ketone bodies provide an important fuel for neonates²⁶ and may be required for effector functions like NET formation.²⁷

2.2 | Eosinophils

Elevated eosinophil counts in newborns have been reported with infection in preterm infants and have been linked to later atopy.²⁸ Little is known about the metabolic functions of eosinophils in general though experiments in adults show that eosinophils do use glycolytic metabolism.²⁹ However, eosinophil metabolic plasticity was demonstrated recently with both increased glucose-derived lactate production, when reactive oxygen species are inhibited, and generation of TCA intermediates from both glucose and glutamine, on cytokine stimulation.³⁰ Further work is needed to explore the role of metabolism in determining eosinophil function and to evaluate

whether there is any role for altered metabolism in eosinophilia in neonates.

2.3 | Type 2 innate lymphoid cells

Type 2 innate lymphoid cells (ILC2) are found at epithelial barriers such as in the lung and are a major source of IL-5 that can induce eosinophilia. ILC2 numbers rapidly increase in the lungs after birth, peaking at three times that of adults by day 10 but quickly decreasing to adult levels.³¹ Among the ILC subsets, ILC2 is the most functionally mature compared with ILC1 and ILC3.³² The alarmin IL-33, produced by epithelial cells, recruits eosinophils and ILC2 to the lungs and acts as a potent activator of ILC2.³¹ Despite higher IL-33 levels in neonates, ILC2 activation is not as potent as in adults. The high levels of endogenous IL-33 in the neonatal lung are suggested to train the ILC2 response for a more efficient response to challenges in later life.³³ It is also worth noting that IL-33 signalling via ST2 under neonatal hypoxia is important for the expression of asthma-related genes.³⁴ Given that hypoxia-inducible factor- α strongly stimulates glycolysis, this suggests that a highly glycolytic programme of ILC2s in early life might have harmful effects.

In adults, ILC2 demonstrates the capacity to augment mitochondrial respiration above basal conditions when activated with IL-33. Arg1 is suggested as key to the function of ILC2 as inhibition leads to decreased production of effector cytokines such as IL-5 and IL-13 accompanied by significantly reduced glycolytic capacity.³⁵ Evidence indicating a glycolytic programme in ILC2 comes from experiments inhibiting glycolysis via PD1 which resulted in decreased expression of effector cytokines and reduced proliferation and cell survival.³⁶ Conflicting evidence using helminth infection in mouse models suggests fatty acid oxidation, rather than glycolysis, is necessary for expansion and cytokine production by ILC2.³⁷ Differing methods of ILC2 activation as well as differences between mouse and human responses may account for the conflicting results with further experiments needed to clarify this. Furthermore, given that neonates exhibit less potent responses than adults, despite increased IL-33 signalling and the emerging role of metabolism in ILC2 effector cytokine production, an investigation into the metabolic function of neonatal ILC2 is warranted.

2.4 | Monocytes/macrophages

Monocytes and macrophages perform key innate roles in clearing threats through phagocytosis and oxidative killing and contribute to adaptive responses through antigen presentation to T cells. Monocytes are better studied in neonates compared with macrophages as they can be isolated from blood. Studies of pattern recognition receptors are essentially restricted to TLRs, and neonates have similar expression levels compared with adults. However, neonatal monocytes have impaired TLR-mediated production of TNF α and other pro-inflammatory cytokines.³⁸ Reduced expression of

TNF α has been associated with high levels of adenosine, a metabolite with immunomodulatory properties. Adenosine acts via the A3 adenosine receptor inducing production of the secondary messenger cAMP which inhibits TLR-mediated TNF α production.⁷ Reduced MyD88 expression has also been implicated in failure to produce pro-inflammatory cytokines such as TNF α and IL-12p70. While limiting innate immune responses, this reduced capacity to produce key cytokines along with reduced expression of human leukocyte antigen (HLA)-DR and co-stimulatory molecules such as CD40 at the basal state also affect the ability to activate T cells.^{39,40} However, after LPS treatment, expression of co-stimulatory molecules, MHC-II and CD80, does not differ significantly from adults.⁴¹ Altered cellular metabolism is now emerging as a critical regulator of neonatal monocyte function, especially cytokine production. Whole-blood transcriptomic data suggest significantly increased activity in glucose and cholesterol metabolic pathways. Three glycolytic regulatory nodes—glucose transporter GLUT3 and glycolytic enzymes 6-phosphofructo-2-kinase and hexokinase 3—were upregulated in response to infection, but the cellular provenance of these was not identified.⁴² Monocytes isolated from term and preterm umbilical cord blood have reduced glycolysis compared with adults. Glycolysis was required for cytokine production but not for phagocytosis which was unaffected by inhibition of glycolysis using 2-deoxy-D-glucose (2DG).⁵ More recently, umbilical cord blood monocyte-derived macrophages were also shown to be broadly defective in glycolysis and to exhibit reduced oxidative phosphorylation compared with adult peripheral blood monocyte-derived macrophages.⁴³ IL-10-polarized umbilical cord blood-derived macrophages had adult-like levels of OXPHOS but reduced glycolysis. As for adenosine, circulating factors in umbilical cord blood seem to mediate this effect as treating adult peripheral blood-derived macrophages with cord blood plasma dramatically inhibited glycolysis. This was attributed to high expression of the S100 proteins S100A8/A9 in neonates.⁴³ Furthermore, cord blood monocyte-derived macrophages have reduced expression of co-stimulatory CD80 and CD86 and reduced capacity to stimulate T cells.⁴⁴

Mammalian target of rapamycin (mTOR) and its downstream targets are essential for metabolic reprogramming of macrophages, with signalling through this pathway required for glycolytic reprogramming (Figure 1).⁴⁵ Surprisingly, mTOR transcripts are elevated in cord blood compared with adult blood-derived macrophages but total mTOR protein expression and mTOR phosphorylation are both reduced compared with adults. This disparity suggests post-transcriptional regulation of mTOR expression in neonates. Downstream targets of mTORC1, ribosomal protein s6 and eukaryotic translation initiation factor 4E-binding protein 1 also showed reduced expression and phosphorylation respectively compared with adults.⁴³

The findings summarized above highlight that monocyte metabolism is critical to regulating the neonatal immune response. As variation in TLR-mediated cytokine production at birth has been linked to maternal health status and later development of allergic disease by the child,^{46–48} identifying possible metabolic determinants of this

might provide insight into why this occurs and how it might be prevented or rectified. Therefore, links between metabolic control of innate cell function in neonates and immediate and long-term health outcomes deserve further investigation.

2.5 | Natural killer cells

Natural killer (NK) cells are crucial to the resolution of acute respiratory viral infections such as those caused by influenza or respiratory syncytial virus. Mature NK cells can be subdivided into two main subsets, a CD56bright CD16dim subset, which produces high amounts of inflammatory cytokines, and CD56dim CD16bright, which are a highly cytotoxic subset.⁴⁹ NK cell function is regulated by the balance of inhibitory and activating receptors expressed on the cell surface especially HLA-E binding members of the CD94/NKG2 family such as inhibitory NKG2A and stimulatory NKG2C and NKG2D.⁵⁰ Neonatal NK cells have been shown consistently to have reduced degranulation and cytotoxicity as well as reduced interferon (IFN) γ production.^{51,52} This seems to be despite high degrees of similarity in phenotypic markers in comparison with adults, though upregulated expression of inhibitory NKG2A on cord blood CD56dim NK cells has been suggested to contribute to these reduced responses although this might be counterbalanced by upregulated NKG2D.^{50,53}

Emerging data about the role of metabolism in NK cell function identify key pathways that should be investigated in the neonate. Murine NK cells rely on OXPHOS for homeostatic function and acute responses such as cytokine production, following short-term activation.⁵⁴ In human NK cells, early cytokine responses can occur independent of glucose.⁵⁵ Long-term activation of NK cells upregulates both OXPHOS and glycolysis to meet the metabolic demands of effector function⁵⁶ supported by increased expression of nutrient transporters such as GLUT1, CD98 and CD71 following stimulation.^{56,57} Inhibition of OXPHOS limits NK cell IFN γ production and degranulation, whereas glycolytic inhibition impairs cytotoxic functions such as target cell killing and degranulation.^{56,58} Regulatory factor mTORC1 is required for successful NK cell function—inhibition of its activity in murine NK cells prevents the upregulation of glycolysis needed for granzyme B and IFN γ production.⁵⁹ mTORC1 activity is also needed for NKG2D-mediated IFN γ production in human NK cell subsets.⁵⁷ Given the importance of metabolic reprogramming for the function of NK cells as summarized here, metabolic differences may be a key determinant of altered function of neonatal NK cells.

Given the possibility that metabolism may underpin changes seen in neonatal NK cell function, this leads to the question of what local environmental factors might regulate NK cell metabolism in early life. Various factors abundant in the neonatal circulation like adenosine and S100A8/A9 as discussed above might contribute to this along with TGF β which is a candidate for regulating NK cell metabolism. TGF β is abundant in utero and during early life^{60–62} and is known to affect NK cell function including inhibition of cytotoxicity^{63,64} and of

CD16-induced IFN γ production through SMAD3 repression of transcription.⁶³ These inhibitory effects of TGF β have been attributed to its role in inhibiting cellular metabolism. In short-term activation assays, IL-15-stimulated mouse and human NK cells treated with TGF β had reduced mTOR signalling (primarily mTORC1), impaired cellular metabolism and reduced cytokine production.⁶⁵ While this also might be mTORC1 independent,⁶⁶ it seems that TGF β inhibits metabolic pathways, such as glycolysis and OXPHOS, in human NK cells. As efforts are made to understand neonatal NK cell metabolism, parallel efforts should consider the role of TGF β and similar immunomodulatory cytokines.

2.6 | Dendritic cells

Dendritic cells (DCs) have a critical role in educating and priming the adaptive immune response through integrating signals from the local microenvironment to modulate MHC, co-stimulatory molecules and cytokine expression, thereby orchestrating T-cell activation and effector function. The two major groups of DCs in humans are classical (cDCs) and plasmacytoid (pDCs). These are typically found in a ratio of around 3:1 in adult peripheral blood but occur at a ratio of 1:3 (cDCs to pDCs) in umbilical cord blood.⁶⁷ Neonatal monocyte-derived DCs have been described to favour the Th2-biased cytokine effector function of neonates (Figure 2).⁶⁸ This might reflect that, despite similar expression of TLRs to adult DCs, neonatal DCs have altered cytokine responses after TLR stimulation. Reduced secretion of the Th1-inducing cytokine IL-12p70 (Figure 2), along with decreased IFN γ secretion,⁶⁸ might underpin this. Upon stimulation with LPS, neonatal DCs also have attenuated expression of HLA-DR, CD86, CD80 and CD40 that might contribute to their reduced capacity to activate naïve cord blood T cells.⁶⁹ Similarly, in murine neonatal models, DCs have been shown to efficiently migrate and be capable of antigen presentation but fail to upregulate co-stimulatory molecules in response to IFN γ .⁷⁰

In human adults, metabolic rewiring supports DC activation. During differentiation from monocytes and from bone marrow progenitor cells, DCs use OXPHOS as the primary means of energy production.⁷¹ On activation, DCs switch to a glycolytic metabolism and inhibition of glycolysis decreases surface expression of IL-12p70, MHC class I and class II as well as co-stimulatory CD40 and CD86.⁷² When looking at specific subsets of DCs, pDCs use both glycolysis and glutaminolysis fuelled OXPHOS to support activation with inhibition of these pathways resulting in decreased expression of HLA-DR, CD80, CD86 and IFN α .^{73,74} However, cDCs rely more exclusively on glycolysis which is crucial for CD40 and IL-12 expression. In contrast to pDCs, TLR stimulation reduces OXPHOS in cDCs.⁷⁴ Given the known down regulation of co-stimulatory molecules and reduced cytokine production in neonatal DCs and their established link with metabolic reprogramming, investigation of underlying metabolic differences in neonates is warranted including comparison to other subsets, especially monocytes, to look for common denominators.

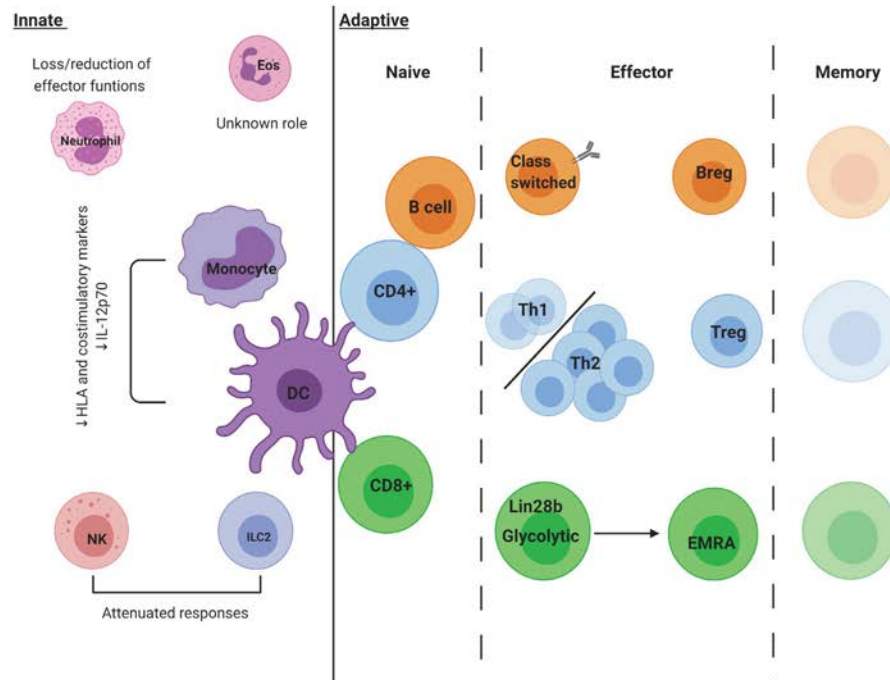


FIGURE 2 Immune responses of neonates. Innate responses of neonates are characterized by attenuated responses and reduced pro-inflammatory phenotype with loss of some effector functions entirely. Adaptive responses are dominated by naive cell subsets and generally less inflammatory responses, preferring the generation of regulatory cells. Created using biorender.com

2.7 | Myeloid-derived suppressor cells

Myeloid-derived suppressor cells (MDSC) are a heterogeneous population of early myeloid-derived progenitor cells which share an immature state and the ability to suppress T-cell activation. While dichotomized into monocytic MDSC (M-MDSC) and granulocytic MDSC (G-MDSC) subsets, in humans these phenotypes are poorly established. However, general consensus defines these subsets as CD11b+ CD14+ HLA-DR-/low CD15- and CD11b+ CD14- CD15+, respectively.⁷⁵ In adults, MDSC are typically associated with the pro-inflammatory environment of tumours and other chronic inflammatory conditions. As such, MDSC have been studied primarily for their immune suppressive role in the tumour microenvironment where they potently suppress T-cell expansion and effector functions.

Recently in humans, the suppressive capacity of M-MDSC has been linked to specific metabolic adaptations. Compared with monocytes, the dicarbonyl metabolite methylglyoxal is 30-fold higher in M-MDSC inhibiting glycolysis in these cells.⁷⁶ M-MDSC also transfer

cytoplasmic methylglyoxal to T cells in a contact-dependent manner and inhibit T-cell metabolic reprogramming to suppress their expansion and effector functions.⁷⁶ Methylglyoxal also selectively depletes L-arginine and L-glutamine,⁷⁶ which are both amino acids required for T-cell function and might explain reports of depletion of L-arginine by MDSC.⁷⁷ Other studies have demonstrated that fatty acid uptake and FAO mediated by STAT3/STAT5 and lipid uptake by CD36 are required for generation of highly suppressive MDSC in the tumour microenvironment.^{78,79}

Compared with healthy adults, MDSC are transiently increased at birth with cord blood levels equivalent to those of cancer patients.⁸⁰ MDSC frequency in neonates positively correlates with birth weight.⁸¹ MDSC from healthy weight neonates have greater suppressive capacity than those from very low weight neonates, potentially indicating a link between nutrient availability and MDSC function. Interestingly, breastmilk lactoferrin is key to generating M-MDSC and G-MDSC able to suppress neonatal T cells; however, the same effect is not observed in adult MDSC.^{80,82} Additionally,

lactoferrin treatment induced potent bacterial killing function in neonatal MDSC⁸⁰ demonstrating potential roles beyond immune suppression. In mouse models of neonatal necrotizing enterocolitis, lactoferrin-treated MDSC are currently being investigated as a potential therapeutic due to their ability to suppress T-cell activation and inflammation.^{80,81}

3 | ADAPTIVE IMMUNE RESPONSES

The adaptive immune system of neonates is commonly described as immature. While memory T-cell populations can be identified within the foetus, possibly arising from the foetal intestine,^{83,84} nearly all neonatal T and B lymphocytes display markers of antigen inexperienced naive cells.^{77,83,84} Recent studies have also revealed the failure of human and mouse neonatal lymphocytes to differentiate into long-lived memory cells and their reduced secondary responses upon antigen re-exposure.^{85–87}

3.1 | B cells

Neonatal B lymphocytes are almost exclusively antigen inexperienced naive B cells. Neonates have reduced class-switched antibody production, with almost no IgG or IgA antibody production on activation compared with adults which have been suggested to contribute to greater susceptibility to infection of neonates.⁸⁸ Depending on the method of activation used, neonatal B cells exhibit both enhanced and reduced proliferation, leading researchers to conclude that while reduction in B-cell proliferation may be observed in some settings; neonatal B cells do not have a general defect in proliferation.⁸⁸ However, survival of neonatal B cells across various subsets is decreased with most methods of activation. While much less is known about the immunometabolic features of B cells compared with other immune cells, we do know that unlike most other immune cells the upregulation of glycolysis does not appear to be crucial for their activation, proliferation or differentiation, despite increased import of glucose after activation.⁸⁹ Rather, B cells appear to rely on OXPHOS to meet the demands of activation and proliferation, likely supported by glutaminolysis rather than glucose metabolism.⁸⁹ However, glucose does seem to be required for class switch recombination which is known to be impaired in neonates.^{88,89} When assessing B-cell subsets for enzymes related to glycolytic and oxidative metabolic pathways, naive B cells were found to have the lowest expression across all enzymes examined. Memory subsets had higher expression of metabolic enzymes while plasma cells had the highest expression of all enzymes.⁹⁰ A recently identified subset of B cells, now termed regulatory B cells (Bregs), characterized as CD25hi CD38hi performs important regulatory functions, promoting tolerance during pregnancy.⁹¹ Bregs suppress the immune system through direct cell-to-cell signalling via CD80/CD86, IL-10 and adenosine generation by the purine ecto-enzyme CD73. Bregs preferentially downregulate IFN γ production along with the differentiation

of Th1 and Th17 cells but not regulatory T cells (Tregs).^{92,93} Increased frequency of Bregs in cord blood has been suggested to play a role in the altered immune response of neonates, with their suppressive role postulated to be primarily through production of IL-10 and costimulatory CD80/CD86 signalling to T cells.^{94,95} Adenosine production is unlikely to be a mechanism used by neonatal Bregs for immune suppression as CD73 is markedly and selectively downregulated.⁹⁶

Along with the observations summarized for other cell types above, impaired glycolysis might be a common mechanism of altered neonatal immune cell function although the upstream determinants of this might differ by cell type.

3.2 | T cells

T cells are highly diverse and perform a multitude of specialized functions contributing to and orchestrating the immune response. Here, we will focus primarily on CD4+ (T helper), CD8+ (cytotoxic T cells) and CD4+FoxP3+ regulatory T cells.

3.2.1 | CD4+ T helper cells

While the neonate is not devoid of memory CD4+ T cells, as already noted, neonatal CD4+ T cells are predominantly naive (CD45RA+CCR7+) and overwhelmingly display characteristics of recent thymic emigrants (RTEs) (Figure 2).⁹⁷ Neonatal CD4+ T cells that do not receive signals from IL-7 or other common γ chain cytokines are more susceptible to apoptosis leading to a high cell turnover rate.^{97,98} IL-7 promotes the survival and maturation of CD4+ RTEs without inducing differentiation,⁹⁹ and this is supported by higher telomerase expression in neonates, which prevents shortening of the telomeres in this early stage of development.¹⁰⁰ This high IL-7-induced proliferative capacity is suggested to help maintain diversity in the T-cell repertoire¹⁰¹ and, at least in mice, IL-7-induced neonatal T-cell proliferation is linked to higher STAT5 activation, a signalling pathway shared with humans.¹⁰² The metabolic requirements to support rapid T-cell proliferation in neonates are unknown however, in adults aerobic glycolysis and OXPHOS drive proliferation and differentiation of CD4+ T cells.¹⁰³ We have shown a requirement for STAT5 signalling in very early adult naive T-cell activation. Inhibiting STAT5 in naive but not effector or central memory CD4+ T cells resulted in reduced glutamine-dependent anaplerosis and loss of IL-2 production,¹⁰⁴ highlighting the critical role of metabolic reprogramming and the use of glutamine in the very earliest stages of T-cell activation in the periphery.

As mentioned earlier, CD4+ T-cell cytokine responses are considered to be Th2 skewed in neonates (Figure 2), in part due to altered functions of cells such as DCs. Additional to antigen-presenting cells influencing neonate T-cell phenotype through diminished IL-12-p70 (as discussed previously), monocyte-derived pro-inflammatory cytokines have been shown to suppress IL-2 production inducing non-classic Th2 cells.⁴⁶ However, characteristic

interleukin production of naïve CD4+ T cells also has been linked to epigenetic modification. Hypermethylation at CpG and non-CpG sites occurs within and adjacent to the IFN γ promoter region in neonatal naïve CD4+ T cells and is accompanied by markedly reduced IFN γ production by neonates upon T-cell activation.¹⁰⁵ Although reduced IFN γ production is widely reported in neonatal $\alpha\beta$ T cells, it is, however, worth noting that neonatal $\gamma\delta$ T cells do not exhibit the same defect.¹⁰⁶

In mice, neonates are poised for a Th2 type response. They exhibit pre-existing CpG hypomethylation at the CNS-1 locus when resting and CpG methylation at the CNS-1 locus remains lower than in adult mice after 5 days, under Th2-polarizing conditions.¹⁰⁷ In human neonates, the Th2 locus is extensively remodelled, with hypomethylation and permissive histone modifications selectively in Th2 cells cultured under Th2-polarizing conditions.¹⁰⁸ A novel subset of neonatal naïve CD31+ CD4+ T cells storing an unglycosylated isoform of IL-4, not present in adults, has also been described, however, any unique function of these cells has not yet been identified.¹⁰⁹ The relative balance of cytokines has implications in early life programming of later immune function and allergic disease risk in particular.³ Greater expression of IL-13 at birth, along with other epigenetic variations in metabolic genes such as *RPTOR*, *PIK3D* and *MAPK1*, has been linked with subsequent susceptibility to atopic disease in childhood.^{108,110} Reduced IFN γ at this time is a long-recognized hallmark of allergic disease risk.¹¹¹ Therefore, there is much value in elucidating the immunometabolic regulation of T-cell effector cytokine production at this stage of development to provide mechanistic insight and therapeutic targets for mitigating non-communicable disease risk.

T-cell effector function has been linked closely with metabolism in various studies¹⁶ and may have a role to play in skewed T-cell responses of neonates. Glycolysis is a specific requirement for IFN γ production in humans and in mice through post-transcriptional regulation by the glycolysis enzyme glyceraldehyde phosphate dehydrogenase (GAPDH).^{112–114} In vitro and in vivo blockade of glycolysis is also known to reduce expression of the Th2 cytokines IL-4 and IL-13 and whether GAPDH has a role to play here too is still unknown.¹¹⁵ Furthermore, TGF β signalling significantly inhibits mitochondrial complex V resulting in decreased ATP production and impaired IFN γ production in human CD4+ T cells.¹¹⁶ Some work has begun to explore how altered mitochondrial respiration in neonates might contribute to altered T-cell activity. So far, mitochondrial mass of neonatal CD4+ T cells has been shown to be lower than adults and accompanied by reduced levels of ATP.^{117,118} However, on activation of T cells from preterm infants, higher calcium flux into the mitochondria than adults is observed along with increased ERK phosphorylation suggesting enhanced signalling for metabolic reprogramming.¹¹⁹ Finally, nutritional regulation of T-cell development has been shown in mice where oligosaccharide diets were found to have a role in regulating neonatal Th1 type responses in respiratory syncytial virus infection models.¹²⁰ Such approaches might offer therapeutic strategies should immunometabolic signatures be found associated with disease outcomes.

3.2.2 | CD8+ cytotoxic T cells

A number of features of neonatal CD8+ T cells have been associated with increased susceptibility of neonates to infection. CD8+ T-cell responses in neonates are described as innate-like, with reduced cytotoxic capability and increased expression of anti-microbial protein transcripts.¹²¹ Exploration of the epigenomic landscape has revealed changes associated with lower TCR signalling and cytotoxicity but higher expression of genes involved in cell cycle.¹²¹ In line with these findings, it is widely reported that neonatal CD8+ T cells are highly proliferative through homeostatic proliferation.^{100,122,123} This highly proliferative programme extends into activation.¹²⁴ Neonatal CD8+ T cells divide more than their adult counterparts over the first three days of activation with the cells entering division sooner after initial activation and each division then happening faster in neonates. Differentiation, measured by CD62L and Ly6C expression, also occurs faster in neonates (Figure 2) yet they become terminally differentiated, shown by CD127 downregulation and KLRG1 upregulation, and fail to differentiate into long-lived memory cells (Figure 2), producing weak CD8+ T-cell expansion on secondary challenge.^{124,125} Rapid proliferation and differentiation in neonates are suggested to impair the development of memory CD8+ T cells.¹²⁴ Studies in mice suggest a role for the inhibitor of let-7 microRNA, *lin28b*, in maintaining a neonate-like phenotype by CD8+ T cells (Figure 2).¹²⁶

To support their highly proliferative phenotype, murine neonatal CD8+ T cells preferentially rely on glycolysis.⁸⁵ Indeed, neonatal mice exhibit higher glycolytic metabolism than adults, a response attributable to functional programming by *lin28b* (Figure 2). High glycolytic metabolism was also linked directly to the inability of neonates to form memory populations with pharmacological inhibition of glycolysis with 2DG able to restore formation of memory cells.⁸⁵ In comparison with mice, our understanding of human neonatal CD8+ T-cell metabolism is not as well developed and what little evidence there is contrasts. For example, human umbilical cord blood CD8+ T cells have a propensity to differentiate into non-classical T cytotoxic (Tc)2 cells, when activated and this was associated with a decrease in glycolysis and an increase in fatty acid metabolism of Tc2 cells.¹²⁷ Much more work is needed to properly understand the role metabolism has to play in the fate of human neonatal CD8+ T cells.

3.2.3 | Regulatory T cells

Regulatory T cells (Tregs) are crucial in preventing immune dysregulation and promoting peripheral tolerance. The subset defined by expression of the transcription factor forkhead box (FOX)p3 will be the focus here. Tregs have emerged as critical to the success of pregnancy playing a vital role in maternal tolerance of the foetus and immunoregulation more generally at the foetal-maternal interface.¹²⁸ Furthermore, maternal factors such as allergy have been suggested to reduce Treg suppressive function in the offspring.¹²⁹ IL-2R-STAT5 and TGF β -SMAD signalling promote Treg differentiation through recruitment to CNS2 and CNS1 of the FOXP3 locus, respectively.^{130,131}

Tregs have high mitochondrial mass, relying on OXPHOS via mitochondrial oxidation of pyruvate and lipids upon activation, unlike conventional T cells that primarily rely on aerobic glycolysis.^{132,133} While proliferation of Tregs is fuelled primarily through OXPHOS, glycolysis appears to be crucial to the suppressor function of Tregs. Enolase-1, a glycolytic enzyme, functions as a regulator of conserved non-coding sequence (CNS)2, preventing the transcription of a FOXP3 splice isoform containing exon-2 (FOXP3-E2).¹³⁴ Exogenous metabolites might also affect the stability of Tregs. Tregs have increased cell surface expression of ecto-nucleotidases CD39 and CD73, which convert ATP into immunosuppressive adenosine.¹³⁵ In neonatal T cells, CD39 expression is highest in activated Tregs, demonstrating the importance of their immunomodulatory function; the frequency of this population of Tregs correlates inversely with clinical severity of sepsis in neonates.¹³⁶ Intriguingly, neonatal CD4+FOXP3- T cells display a natural propensity to differentiate into Tregs⁹⁸ (Figure 2) likely reflecting suboptimal stimulation via TCR.¹³⁷ Given the role metabolism has in determining T-cell fate, an intrinsic metabolic programme in naive neonatal CD4+ cells linked to early post-TCR activation events might favour the preferential generation of Tregs contributing to the development of immune tolerance at this time.

3.3 | Outlook

Immunometabolism is now a well-established field enabling significant advances in our understanding of human immune cell fate and function. However, to date, little progress has been made in applying this to the understanding of human neonatal immune responses. Some initial work is revealing fundamental differences in cellular metabolism likely underpinning well-described phenotypic and functional differences across the life course. However, caution must be taken when the focus remains on umbilical cord blood collected at the transition from intrauterine to extrauterine life and the changes in fuel demand and provision that occur around this time. We also must be mindful that neonates do not simply lack in comparison with adults and alternative fuel substrates (e.g. ketone bodies as above) and higher levels of exogenous metabolites (e.g. adenosine as above) might drive unique phenotypes at this stage of development. Much more work is needed especially extending observations beyond umbilical cord blood to samples collected in the days, weeks and months after birth. Such work is limited by sample volumes and will need to focus on single-cell functional genomic approaches linking transcriptional and translational regulation of the mechanisms at play accompanying these with emerging flow cytometry-based approaches to the study of immunometabolism such as SCENITH.¹³⁸ Future work should establish the metabolic underpinnings of neonatal immune cell function and explore how the unique energy demands, immune requirements and rapid development of neonates have led to this highly evolved, age-appropriate phenotype. Understanding immunometabolism in neonates is an exciting field of research potentially

harbouring new ways of combatting many diseases by providing untapped insight into diverse functional roles of the immune system.

IRB STATEMENT

All of our work involving samples from human participants is reviewed and approved by a Health Research Authority or University research ethics committee with samples and data collected with informed consent of the donor.

ACKNOWLEDGEMENTS

The authors would like to thank Swansea Bay University Health Board for their long-standing and ongoing support of our research endeavours.

CONFLICT OF INTEREST

None to declare.

AUTHOR CONTRIBUTION

Sean R Holm: Writing-original draft (lead). **Benjamin James Jenkins:** Writing-original draft (supporting); Writing-review & editing (supporting). **April Rees:** Writing-review & editing (supporting). **James G Cronin:** Supervision (supporting); Writing-review & editing (supporting). **Nicholas Jones:** Supervision (supporting); Writing-review & editing (supporting). **Catherine A Thornton:** Supervision (lead); Writing-original draft (supporting); Writing-review & editing (lead).

PEER REVIEW

The peer review history for this article is available at <https://pubsonline.informaworld.com/pubon/10.1111/pai.13583>.

ORCID

Catherine A. Thornton  <https://orcid.org/0000-0002-5153-573X>

REFERENCES

- Herberth G, Hinz D, Bauer M, et al. Environmental exposure during pregnancy modulates fetal Treg development with consequences for the allergy risk of the child. *J Reprod Immunol*. 2012;94(1):54. <https://doi.org/10.1016/j.jri.2012.03.336>
- Grieger JA, Clifton VL, Tuck AR, Wooldridge AL, Robertson SA, Gatford KL. In utero programming of allergic susceptibility. *Int Arch Allergy Imm*. 2016;169(2):80-92. <https://doi.org/10.1159/000443961>
- Campbell DE, Boyle RJ, Thornton CA, Prescott SL. Mechanisms of allergic disease—environmental and genetic determinants for the development of allergy. *Clin Exp Allergy*. 2015;45(5):844-858. <https://doi.org/10.1111/cea.12531>
- Sattler S, Rosenthal N. The neonate versus adult mammalian immune system in cardiac repair and regeneration. *BBA-Mol Cell Res*. 2016;1863(7):1813-1821. <https://doi.org/10.1016/j.bbamcr.2016.01.011>
- Kan B, Michalski C, Fu H, et al. Cellular metabolism constrains innate immune responses in early human ontogeny. *Nat Commun*. 2018;9(1):94822. <https://doi.org/10.1038/s41467-018-07215-9>

6. Saito S. Cytokine network at the feto-maternal interface. *J Reprod Immunol*. 2000;47(2):87-103. [https://doi.org/10.1016/s0165-0378\(00\)0060-7](https://doi.org/10.1016/s0165-0378(00)0060-7)
7. Levy O, Coughlin M, Cronstein BN, Roy RM, Desai A, Wessels MR. The adenosine system selectively inhibits TLR-mediated TNF-alpha production in the human newborn. *J Immunol*. 2006;177(3):1956-1966. <https://doi.org/10.4049/jimmunol.177.3.1956>
8. Saghafiyan-Hedengren S, Holmlund U, Amoudruz P, Nilsson C, Sverremark-Ekstrom E. Maternal allergy influences p38-mitogen-activated protein kinase activity upon microbial challenge in CD14(+) monocytes from 2-year-old children. *Clin Exp Allergy*. 2008;38(3):449-457. <https://doi.org/10.1111/j.1365-2222.2007.02917.x>
9. Palmer AC. Nutritionally mediated programming of the developing immune system. *Adv Nutr*. 2011;2(5):377-395. <https://doi.org/10.3945/an.111.000570>
10. Shew SB, Jakscic T. The metabolic needs of critically ill children and neonates. *Semin Pediatr Surg*. 1999;8(3):131-139.
11. Butte NF. Energy requirements of infants. *Public Health Nutr*. 2005;8(7A):953-967. <https://doi.org/10.1079/phn2005790>
12. Brook B, Harbeson D, Ben-Othman R, Viemann D, Kollmann TR. Newborn susceptibility to infection vs. disease depends on complex in vivo interactions of host and pathogen. *Semin Immunopathol*. 2017;39(6):615-625. <https://doi.org/10.1007/s00281-017-0651-z>
13. Harbeson D, Francis F, Bao W, Amenogbe NA, Kollmann TR. Energy demands of early life drive a disease tolerant phenotype and dictate outcome in neonatal bacterial sepsis. *Front Immunol*. 2018;9:1918. <https://doi.org/10.3389/fimmu.2018.01918>
14. Harbeson D, Ben-Othman R, Amenogbe N, Kollmann TR. Outgrowing the immaturity myth: the cost of defending from neonatal infectious disease. *Front Immunol*. 2018;9:1077. <https://doi.org/10.3389/fimmu.2018.01077>
15. O'Neill LAJ, Kishton RJ, Rathmell J. A guide to immunometabolism for immunologists. *Nat Rev Immunol*. 2016;16(9):553-565. <https://doi.org/10.1038/nri.2016.70>
16. Geltink RIK, Kyle RL, Pearce EL. Unraveling the complex interplay between T cell metabolism and function. *Annu Rev Immunol*. 2018;36(36):461-488. <https://doi.org/10.1146/annurev-immunol-042617-053019>
17. Basha S, Surendran N, Pichichero M. Immune responses in neonates. *Expert Rev Clin Immunol*. 2014;10(9):1171-1184. <https://doi.org/10.1586/1744666x.2014.942288>
18. Carr R, Huizinga TWJ, Kleijer M, Davies JM. Changes in plasma FcRIII demonstrate increasing receptor production during late pregnancy and after preterm birth. *Pediatr Res*. 1992;32(5):505-508. <https://doi.org/10.1203/00006450-199211000-00001>
19. Kim SK, Keeney SE, Alpard SK, Schmalstieg FC. Comparison of L-selectin and CD11b on neutrophils of adults and neonates during the first month of life. *Pediatr Res*. 2003;53(1):132-136. <https://doi.org/10.1203/01.pdr.0000041515.78650.11>
20. Raymond SL, Hawkins RB, Murphy TJ, et al. Impact of toll-like receptor 4 stimulation on human neonatal neutrophil spontaneous migration, transcriptomics, and cytokine production. *J Mol Med*. 2018;96(7):673-684. <https://doi.org/10.1007/s00109-018-1646-5>
21. Al-Hertani W, Yan SR, Byers DM, Bortolussi R. Human newborn polymorphonuclear neutrophils exhibit decreased levels of MyD88 and attenuated p38 phosphorylation in response to lipopolysaccharide. *Clin Invest Med*. 2007;30(2):E44-E53.
22. Yost CC, Cody MJ, Harris ES, et al. Impaired neutrophil extracellular trap (NET) formation: a novel innate immune deficiency of human neonates. *Blood*. 2009;113(25):6419-6427. <https://doi.org/10.1182/blood-2008-07-171629>
23. Rodriguez-Espinosa O, Rojas-Espinosa O, Moreno-Altamirano MMB, Lopez-Villegas EO, Sanchez-Garcia FJ. Metabolic requirements for neutrophil extracellular traps formation. *Immunology*. 2015;145(2):213-224. <https://doi.org/10.1111/imm.12437>
24. Borregaard N, Herlin T. Energy-metabolism of human-neutrophils during phagocytosis. *J Clin Invest*. 1982;70(3):550-557. <https://doi.org/10.1172/jci110647>
25. Awasthi D, Nagarkoti S, Sadaf S, Chandra T, Kumar S, Dikshit M. Glycolysis dependent lactate formation in neutrophils: a metabolic link between NOX-dependent and independent NETosis. *BBA-Mol Basis Dis*. 2019;1865(12):165542. <https://doi.org/10.1016/j.bbadis.2019.165542>
26. Bougneres PF, Lemmel C, Ferre P, Bier DM. Ketone-body transport in the human neonate and infant. *J Clin Invest*. 1986;77(1):42-48. <https://doi.org/10.1172/jci112299>
27. Grinberg N, Elazar S, Rosenshine I, Shpigel NY. Beta-hydroxybutyrate abrogates formation of bovine neutrophil extracellular traps and bactericidal activity against mammary pathogenic *Escherichia coli*. *Infect Immun*. 2008;76(6):2802-2807. <https://doi.org/10.1128/iai.00051-08>
28. Juul SE, Haynes JW, McPherson RJ. Evaluation of eosinophilia in hospitalized preterm infants. *J Perinatol*. 2005;25(3):182-188. <https://doi.org/10.1038/sj.jp.7211226>
29. Porter L, Toepfner N, Bashant KR, et al. Metabolic profiling of human eosinophils. *Front Immunol*. 2018;9:1404. <https://doi.org/10.3389/fimmu.2018.01404>
30. Jones N, Vincent EE, Felix LC, et al. Interleukin-5 drives glycolysis and reactive oxygen species-dependent citric acid cycling by eosinophils. *Allergy*. 2020;75(6):1361-1370. <https://doi.org/10.1111/all.14158>
31. Steer CA, Martinez-Gonzalez I, Ghaedi M, Allinger P, Matha L, Takei F. Group 2 innate lymphoid cell activation in the neonatal lung drives type 2 immunity and allergen sensitization. *J Allergy Clin Immunol*. 2017;140(2):593-595.e3. <https://doi.org/10.1016/j.jaci.2016.12.984>
32. Bennisstein SB, Scherenschlich N, Weinhold S, et al. Transcriptional and functional characterization of neonatal circulating ILCs. *Stem Cells Transl Med*. 2021;10(6):867-882. <https://doi.org/10.1002/sctm.20-0300>
33. Steer CA, Matha L, Shim H, Takei F. Lung group 2 innate lymphoid cells are trained by endogenous IL-33 in the neonatal period. *JCI Insight*. 2020;5(14):e135961. <https://doi.org/10.1172/jci.insight.135961>
34. Cheon IS, Son YM, Jiang LL, et al. Neonatal hyperoxia promotes asthma-like features through IL-33-dependent ILC2 responses. *J Allergy Clin Immunol*. 2018;142(4):1100-1112. <https://doi.org/10.1016/j.jaci.2017.11.025>
35. Monticelli LA, Buck MD, Flamar AL, et al. Arginase 1 is an innate lymphoid-cell-intrinsic metabolic checkpoint controlling type 2 inflammation. *Nat Immunol*. 2016;17(6):656-665. <https://doi.org/10.1038/ni.3421>
36. Helou DG, Shafiei-Jahani P, Lo R, et al. PD-1 pathway regulates ILC2 metabolism and PD-1 agonist treatment ameliorates airway hyperreactivity. *Nat Commun*. 2020;11(1):3398. <https://doi.org/10.1038/s41467-020-17813-1>
37. Wilhelm C, Harrison OJ, Schmitt V, et al. Critical role of fatty acid metabolism in ILC2-mediated barrier protection during malnutrition and helminth infection. *J Exp Med*. 2016;213(8):1409-1418. <https://doi.org/10.1084/jem.20151448>
38. Levy O, Zarembek KA, Roy RM, Cywes C, Godowski PJ, Wessels MR. Selective impairment of TLR-mediated innate immunity in human newborns: neonatal blood plasma reduces monocyte TNF-alpha induction by bacterial lipopeptides, lipopolysaccharide, and imiquimod, but preserves the response to R-848. *J Immunol*. 2004;173(7):4627-4634. <https://doi.org/10.4049/jimmunol.173.7.4627>
39. Han P, McDonald T, Hodge G. Potential immaturity of the T-cell and antigen-presenting cell interaction in cord blood with particular emphasis on the CD40-CD40 ligand costimulatory pathway. *Immunology*. 2004;113(1):26-34. <https://doi.org/10.1111/j.1365-2567.2004.01933.x>
40. Hegge I, Niepel F, Lange A, Vogelgesang A, Heckmann M, Ruhnau J. Functional analysis of granulocyte and monocyte subpopulations

- in neonates. *Mol Cell Pediatr*. 2019;6(1):5. <https://doi.org/10.1186/s40348-019-0092-y>
41. Hikita N, Cho Y, Tachibana D, Hamazaki T, Koyama M, Tokuhara D. Cell surface antigens of neonatal monocytes are selectively impaired in basal expression, but hyperresponsive to lipopolysaccharide and zymosan. *J Reprod Immunol*. 2019;136:102614. <https://doi.org/10.1016/j.jri.2019.102614>
 42. Smith CL, Dickinson P, Forster T, et al. Identification of a human neonatal immune-metabolic network associated with bacterial infection. *Nat Commun*. 2014;5(1):5649. <https://doi.org/10.1038/ncomms5649>
 43. Dreschers S, Ohl K, Lehrke M, et al. Impaired cellular energy metabolism in cord blood macrophages contributes to abortive response toward inflammatory threats. *Nat Commun*. 2019;10:1685. <https://doi.org/10.1038/s41467-019-09359-8>
 44. Dreschers S, Ohl K, Schulte N, Tenbrock K, Orlikowsky TW. Impaired functional capacity of polarised neonatal macrophages. *Sci Rep*. 2020;10(1):624. <https://doi.org/10.1038/s41598-019-56928-4>
 45. Covarubias AJ, Aksoylar HI, Horng T. Control of macrophage metabolism and activation by mTOR and Akt signaling. *Semin Immunol*. 2015;27(4):286-296. <https://doi.org/10.1016/j.smim.2015.08.001>
 46. Zhang YX, Collier F, Naselli G, et al. Cord blood monocyte-derived inflammatory cytokines suppress IL-2 and induce nonclassical "T(H)2-type" immunity associated with development of food allergy. *Sci Transl Med*. 2016;8(321):321ra8. <https://doi.org/10.1126/scitranslmed.aad4322>
 47. Prescott SL, Noakes P, Chow BWY, et al. Presymptomatic differences in toll-like receptor function in infants who have allergy. *J Allergy Clin Immunol*. 2008;122(2):391-399. <https://doi.org/10.1016/j.jaci.2008.04.042>
 48. Tulic MK, Hodder M, Forsberg A, et al. Differences in innate immune function between allergic and nonallergic children: New insights into immune ontogeny. *J Allergy Clin Immunol*. 2011;127(2):470-478.e1. <https://doi.org/10.1016/j.jaci.2010.09.020>
 49. Vivier E, Tomasello E, Baratin M, Walzer T, Ugolini S. Functions of natural killer cells. *Nature Immunol*. 2008;9(5):503-510. <https://doi.org/10.1038/ni1582>
 50. Shereck E, Day NS, Awasthi A, et al. Immunophenotypic, cytotoxic, proteomic and genomic characterization of human cord blood vs. peripheral blood CD56(Dim) NK cells. *Innate Immunity*. 2019;25(5):294-304. <https://doi.org/10.1177/1753425919846584>
 51. Strauss-Albee DM, Liang EC, Ranganath T, Aziz N, Blish CA. The newborn human NK cell repertoire is phenotypically formed but functionally reduced. *Cytometry Part B*. 2017;92(1):33-41. <https://doi.org/10.1002/cyto.b.21485>
 52. Luevano M, Daryouzeh M, Alnabhan R, et al. The unique profile of cord blood natural killer cells balances incomplete maturation and effective killing function upon activation. *Hum Immunol*. 2012;73(3):248-257. <https://doi.org/10.1016/j.humimm.2011.12.015>
 53. Sundstrom Y, Nilsson C, Lilja G, Karre K, Troye-Blomberg M, Berg L. The expression of human natural killer cell receptors in early life. *Scand J Immunol*. 2007;66(2-3):335-344. <https://doi.org/10.1111/j.1365-3083.2007.01980.x>
 54. Keppel MP, Saucier N, Mah AY, Vogel TP, Cooper MA. Activation-specific metabolic requirements for NK cell IFN-gamma production. *J Immunol*. 2015;194(4):1954-1962. <https://doi.org/10.4049/jimmunol.1402099>
 55. Velasquez SY, Himmelhan BS, Kassner N, et al. Innate cytokine induced early release of IFN gamma and CC chemokines from hypoxic human NK cells is independent of glucose. *Cells*. 2020;9(3):734. <https://doi.org/10.3390/cells9030734>
 56. Keating SE, Zaiatz-Bittencourt V, Loftus RM, et al. Metabolic reprogramming supports IFN-gamma production by CD56(bright) NK cells. *J Immunol*. 2016;196(6):2552-2560. <https://doi.org/10.4049/jimmunol.1501783>
 57. Jensen H, Potempa M, Gotthardt D, Lanier LL. Cutting edge: IL-2-induced expression of the amino acid transporters SLC1A5 and CD98 is a prerequisite for NKG2D-mediated activation of human NK cells. *J Immunol*. 2017;199(6):1967-1972. <https://doi.org/10.4049/jimmunol.1700497>
 58. Wang ZX, Guan D, Wang S, Chai LYA, Xu SL, Lam KP. Glycolysis and oxidative phosphorylation play critical roles in natural killer cell receptor-mediated natural killer cell functions. *Front Immunol*. 2020;11:202. <https://doi.org/10.3389/fimmu.2020.00202>
 59. Donnelly RP, Loftus RM, Keating SE, et al. mTORC1-Dependent metabolic reprogramming is a prerequisite for NK cell effector function. *J Immunol*. 2014;193(9):4477-4484. <https://doi.org/10.4049/jimmunol.1401558>
 60. Singh M, Orazulike NC, Ashmore J, Konje JC. Changes in maternal serum transforming growth factor beta-1 during pregnancy: a cross-sectional study. *Biomed Res Int*. 2013;2013:1-5. <https://doi.org/10.1155/2013/318464>
 61. Frost BL, Jilling T, Lapin B, Maheshwari A, Caplan MS. Maternal breast milk transforming growth factor-beta and feeding intolerance in preterm infants. *Pediatr Res*. 2014;76(4):386-393. <https://doi.org/10.1038/pr.2014.96>
 62. Power LL, Poppellwell EJ, Holloway JA, Diaper ND, Warner JO, Jones CA. Immunoregulatory molecules during pregnancy and at birth. *J Reprod Immunol*. 2002;56(1-2):19-28. [https://doi.org/10.1016/S0165-0378\(01\)00146-2](https://doi.org/10.1016/S0165-0378(01)00146-2)
 63. Trotta R, Dal Col J, Yu JH, et al. TGF-beta utilizes SMAD3 to inhibit CD16-mediated IFN-gamma production and antibody-dependent cellular cytotoxicity in human NK cells. *J Immunol*. 2008;181(6):3784-3792. <https://doi.org/10.4049/jimmunol.181.6.3784>
 64. Wilson EB, El-Jawhari JJ, Neilson AL, et al. Human tumour immune evasion via TGF-beta blocks NK cell activation but not survival allowing therapeutic restoration of anti-tumour activity. *PLoS ONE*. 2011;6(9):e22842. <https://doi.org/10.1371/journal.pone.0022842>
 65. Viel S, Marçais A, Guimaraes FSF, et al. TGF-beta inhibits the activation and functions of NK cells by repressing the mTOR pathway. *Sci Signal*. 2016;9(415):ra19. <https://doi.org/10.1126/scisignal.aad1884>
 66. Zaiatz-Bittencourt V, Finlay DK, Gardiner CM. Canonical TGF-beta signaling pathway represses human NK cell metabolism. *J Immunol*. 2018;200(12):3934-3941. <https://doi.org/10.4049/jimmunol.1701461>
 67. Borrás FE, Matthews NC, Lowdell MW, Navarrete CV. Identification of both myeloid CD11c(+) and lymphoid CD11c(-) dendritic cell subsets in cord blood. *Br J Haematol*. 2001;113(4):925-931. <https://doi.org/10.1046/j.1365-2141.2001.02840.x>
 68. Langrish CL, Buddle JC, Thrasher AJ, Goldblatt D. Neonatal dendritic cells are intrinsically biased against Th-1 immune responses. *Clin Exp Immunol*. 2002;128(1):118-123. <https://doi.org/10.1046/j.1365-2249.2002.01817.x>
 69. De Wit D, Toton S, Orlislagers V, et al. Impaired responses to toll-like receptor 4 and toll-like receptor 3 ligands in human cord blood. *J Autoimmun*. 2003;21(3):277-281. <https://doi.org/10.1016/j.jaut.2003.08.003>
 70. Lau-Kilby AW, Turfkruyer M, Kehl M, et al. Type I IFN ineffectively activates neonatal dendritic cells limiting respiratory antiviral T-cell responses. *Mucosal Immunol*. 2020;13(2):371-380. <https://doi.org/10.1038/s41385-019-0234-5>
 71. Wculek SK, Khoulili SC, Priego E, Heras-Murillo I, Sancho D. Metabolic control of dendritic cell functions: digesting information. *Front Immunol*. 2019;10:10775. <https://doi.org/10.3389/fimmu.2019.00775>
 72. Everts B, Amiel E, Huang SCC, et al. TLR-driven early glycolytic reprogramming via the kinases TBK1-IRK epsilon supports the anabolic demands of dendritic cell activation. *Nature Immunol*. 2014;15(4):323. <https://doi.org/10.1038/ni.2833>
 73. Bajwa G, DeBerardinis RJ, Shao B, Hall B, Farrar JD, Gill MA. Cutting edge: critical role of glycolysis in human plasmacytoid

- dendritic cell antiviral responses. *J Immunol*. 2016;196(5):2004-2009. <https://doi.org/10.4049/jimmunol.1501557>
74. Basit F, Mathan T, Sancho D, de Vries IJM. Human dendritic cell subsets undergo distinct metabolic reprogramming for immune response. *Front Immunol*. 2018;9:92489. <https://doi.org/10.3389/fimmu.2018.02489>
 75. Sica A, Strauss L. Energy metabolism drives myeloid-derived suppressor cell differentiation and functions in pathology. *J Leuk Biol*. 2017;102(2):325-334. <https://doi.org/10.1189/jlb.4MR1116-476R>
 76. Baumann T, Dunkel A, Schmid C, et al. Regulatory myeloid cells paralyze T cells through cell-cell transfer of the metabolite methylglyoxal. *Nat Immunol*. 2020;21(5):555-566. <https://doi.org/10.1038/s41590-020-0666-9>
 77. Rodriguez PC, Ochoa AC. Arginine regulation by myeloid derived suppressor cells and tolerance in cancer: mechanisms and therapeutic perspectives. *Immunol Rev*. 2008;222:180-191. <https://doi.org/10.1111/j.1600-065X.2008.00608.x>
 78. Hossain F, Al-Khami AA, Wyczzechowska D, et al. Inhibition of fatty acid oxidation modulates immunosuppressive functions of myeloid-derived suppressor cells and enhances cancer therapies. *Cancer Immunol Res*. 2015;3(11):1236-1247. <https://doi.org/10.1158/2326-6066.cir-15-0036>
 79. Al-Khami AA, Zheng L, Del Valle L, et al. Exogenous lipid uptake induces metabolic and functional reprogramming of tumor-associated myeloid-derived suppressor cells. *Oncoimmunology*. 2017;6(10):e1344804. <https://doi.org/10.1080/2162402x.2017.1344804>
 80. Gervassi A, Lejarcegui N, Dross S, et al. Myeloid derived suppressor cells are present at high frequency in neonates and suppress in vitro T cell responses. *PLoS ONE*. 2014;9(9):e107816. <https://doi.org/10.1371/journal.pone.0107816>
 81. Liu Y, Perego M, Xiao Q, et al. Lactoferrin-induced myeloid-derived suppressor cell therapy attenuates pathologic inflammatory conditions in newborn mice. *J Clin Invest*. 2019;129(10):4261-4275. <https://doi.org/10.1172/jci128164>
 82. He YM, Li X, Perego M, et al. Transitory presence of myeloid-derived suppressor cells in neonates is critical for control of inflammation. *Nat Med*. 2018;24(2):224-231. <https://doi.org/10.1038/nm.4467>
 83. Zhang X, Mozeski B, Lemoine S, et al. CD4 T cells with effector memory phenotype and function develop in the sterile environment of the fetus. *Sci Transl Med*. 2014;6(238):238ra72. <https://doi.org/10.1126/scitranslmed.3008748>
 84. Li NA, van Unen V, Abdelaal T, et al. Memory CD4(+) T cells are generated in the human fetal intestine. *Nat Immunol*. 2019;20(3):301-312. <https://doi.org/10.1038/s41590-018-0294-9>
 85. Tabillas C, Wang J, Liu XJ, Locasale JW, Smith NL, Rudd BD. Cutting edge: elevated glycolytic metabolism limits the formation of memory CD8(+) T cells in early life. *J Immunol*. 2019;203(10):2571-2576. <https://doi.org/10.4049/jimmunol.1900426>
 86. Cossarizza A, Ortolani C, Paganelli R, et al. CD45 isoforms expression on CD4(+) and CD8(+) T cells throughout life, from newborns to centenarians: implications for T cell memory. *Mech Ageing Dev*. 1996;86(3):173-195. [https://doi.org/10.1016/0047-6374\(95\)01691-0](https://doi.org/10.1016/0047-6374(95)01691-0)
 87. Morbach H, Eichhorn EM, Liese JG, Girschick HJ. Reference values for B cell subpopulations from infancy to adulthood. *Clin Exp Immunol*. 2010;162(2):271-279. <https://doi.org/10.1111/j.1365-2249.2010.04206.x>
 88. Glaesener S, Jaenke C, Habener A, et al. Decreased production of class-switched antibodies in neonatal B cells is associated with increased expression of miR-181b. *PLoS ONE*. 2018;13(2):e0192230. <https://doi.org/10.1371/journal.pone.0192230>
 89. Waters LR, Ahsan FM, Wolf DM, Shirihai O, Teitell MA. Initial B cell activation induces metabolic reprogramming and mitochondrial remodeling. *iScience*. 2018;5:99-109. <https://doi.org/10.1016/j.isci.2018.07.005>
 90. Glass DR, Tsai AG, Oliveria JP, et al. An integrated multi-omic single-cell atlas of human B cell identity. *Immunity*. 2020;53(1):217-232.e5. <https://doi.org/10.1016/j.immuni.2020.06.013>
 91. Lima J, Martins C, Leandro MJ, et al. Characterization of B cells in healthy pregnant women from late pregnancy to post-partum: a prospective observational study. *BMC Pregnancy Childbirth*. 2016;16(1):16139. <https://doi.org/10.1186/s12884-016-0927-7>
 92. Blair PA, Noreña LY, Flores-Borja F, et al. CD19(+)/CD24(hi) CD38(hi) B cells exhibit regulatory capacity in healthy individuals but are functionally impaired in systemic lupus erythematosus patients. *Immunity*. 2010;32(1):129-140. <https://doi.org/10.1016/j.immuni.2009.11.009>
 93. Flores-Borja F, Bosma A, Ng D, et al. CD19(+)/CD24(hi)/CD38(hi) B cells maintain regulatory T cells while limiting T(H)1 and T(H)17 differentiation. *Sci Transl Med*. 2013;5(173):173ra23. <https://doi.org/10.1126/scitranslmed.3005407>
 94. Esteve-Solé A, Teixidó I, Deyà-Martínez A, et al. Characterization of the highly prevalent regulatory CD24(hi)CD38(hi) B-cell population in human cord blood. *Front Immunol*. 2017;8:201. <https://doi.org/10.3389/fimmu.2017.00201>
 95. Sarvaria A, Basar R, Mehta RS, et al. IL-10(+) regulatory B cells are enriched in cord blood and may protect against cGVHD after cord blood transplantation. *Blood*. 2016;128(10):1346-1361. <https://doi.org/10.1182/blood-2016-01-695122>
 96. Pettengill MA, Levy O. Circulating human neonatal naive B cells are deficient in CD73 impairing purine salvage. *Front Immunol*. 2016;7:121. <https://doi.org/10.3389/fimmu.2016.00121>
 97. Hassan J, Reen DJ. Human recent thymic emigrants-identification, expansion, and survival characteristics. *J Immunol*. 2001;167(4):1970-1976. <https://doi.org/10.4049/jimmunol.167.4.1970>
 98. Thornton CA, Upham JW, Wikstrom ME, et al. Functional maturation of CD4(+)CD25(+)CTLA4(+)CD45RA(+) T regulatory cells in human neonatal T cell responses to environmental antigens/allergens. *J Immunol*. 2004;173(5):3084-3092. <https://doi.org/10.4049/jimmunol.173.5.3084>
 99. Soares MVD, Borthwick NJ, Maini MK, Janosy G, Salmon M, Akbar AN. IL-7-dependent extrathymic expansion of CD45RA(+) T cells enables preservation of a naive repertoire. *J Immunol*. 1998;161(11):5909-5917.
 100. Schönland SO, Zimmer JK, Lopez-Benitez CM, et al. Homeostatic control of T-cell generation in neonates. *Blood*. 2003;102(4):1428-1434. <https://doi.org/10.1182/blood-2002-11-3591>
 101. Hassan J, Reen DJ. IL-7 promotes the survival and maturation but not differentiation of human post-thymic CD4(+) T cells. *Eur J Immunol*. 1998;28(10):3057-3065.
 102. Opiela SJ, Koru-Sengul T, Adkins B. Murine neonatal recent thymic emigrants are phenotypically and functionally distinct from adult recent thymic emigrants. *Blood*. 2009;113(22):5635-5643. <https://doi.org/10.1182/blood-2008-08-173658>
 103. Macintyre AN, Gerriets VA, Nichols AG, et al. The glucose transporter Glut1 is selectively essential for CD4 T cell activation and effector function. *Cell Metab*. 2014;20(1):61-72. <https://doi.org/10.1016/j.cmet.2014.05.004>
 104. Jones N, Vincent EE, Cronin JG, et al. Akt and STAT5 mediate naive human CD4+T-cell early metabolic response to TCR stimulation. *Nat Commun*. 2019;10:2042. <https://doi.org/10.1038/s41467-019-10023-4>
 105. White GP, Watt PM, Holt BJ, Holt PG. Differential patterns of methylation of the IFN-gamma promoter at CpG and Non-CpG sites underlie differences in IFN-gamma gene expression between human neonatal and adult CD45RO(-) T cells. *J Immunol*. 2002;168(6):2820-2827. <https://doi.org/10.4049/jimmunol.168.6.2820>
 106. Gibbons DL, Haque SFY, Silberzahn T, et al. Neonates harbour highly active gamma delta T cells with selective impairments in

- preterm infants. *Eur J Immunol*. 2009;39(7):1794-1806. <https://doi.org/10.1002/eji.200939222>
107. Rose S, Lichtenheld M, Foote MR, Adkins B. Murine neonatal CD4(+) cells are poised for rapid Th2 effector-like function. *J Immunol*. 2007;178(5):2667-2678. <https://doi.org/10.4049/jimmuol.178.5.2667>
 108. Webster RB, Rodriguez Y, Klimecki WT, Vercelli D. The human IL-13 locus in neonatal CD4(+) T cells is refractory to the acquisition of a repressive chromatin architecture. *J Biol Chem*. 2007;282(1):700-709. <https://doi.org/10.1074/jbc.M609501200>
 109. Hebel K, Weinert S, Kuroopka B, et al. CD4(+) T cells from human neonates and infants are poised spontaneously to run a nonclassical IL-4 program. *J Immunol*. 2014;192(11):5160-5170. <https://doi.org/10.4049/jimmunol.1302539>
 110. Martino D, Neeland M, Dang T, et al. Epigenetic dysregulation of naive CD4+T-cell activation genes in childhood food allergy. *Nat Commun*. 2018;9:3308. <https://doi.org/10.1038/s41467-018-05608-4>
 111. Tang MLK, Kemp AS, Thorburn J, Hill DJ. Reduced interferon-gamma secretion in neonates and subsequent atopy. *Lancet*. 1994;344(8928):983-985. [https://doi.org/10.1016/s0140-6736\(94\)91641-1](https://doi.org/10.1016/s0140-6736(94)91641-1)
 112. Jones N, Cronin JG, Dolton G, et al. Metabolic adaptation of human CD4(+) and CD8(+) T-cells to T-cell receptor-mediated stimulation. *Front Immunol*. 2017;8:1516. <https://doi.org/10.3389/fimmu.2017.01516>
 113. Chang C-H, Curtis J, Maggi L, et al. Posttranscriptional control of T cell effector function by aerobic glycolysis. *Cell*. 2013;153(6):1239-1251. <https://doi.org/10.1016/j.cell.2013.05.016>
 114. Gubser PM, Bantug GR, Razik L, et al. Rapid effector function of memory CD8(+) T cells requires an immediate-early glycolytic switch. *Nat Immunol*. 2013;14(10):1064-1072. <https://doi.org/10.1038/ni.2687>
 115. Tibbitt CA, Stark JM, Martens L, et al. Single-Cell RNA sequencing of the T helper cell response to house dust mites defines a distinct gene expression signature in airway Th2 cells. *Immunity*. 2019;51(1):169-184. <https://doi.org/10.1016/j.immuni.2019.05.014>
 116. Dimeloe S, Gubser P, Loeliger J, et al. Tumor-derived TGF-beta inhibits mitochondrial respiration to suppress IFN-gamma production by human CD4(+) T cells. *Sci Signal*. 2019;12(599):eaav3334. <https://doi.org/10.1126/scisignal.aav3334>
 117. Mészáros G, Orbán CS, Kaposi A, et al. Altered mitochondrial response to activation of T-cells in neonate. *Acta Physiol Hung*. 2015;102(2):216-227. <https://doi.org/10.1556/036.102.2015.2.12>
 118. Aquilano G, Capretti MG, Nanni F, et al. Altered intracellular ATP production by activated CD4+T-Cells in very preterm infants. *J Immunol Res*. 2016;8374328. <https://doi.org/10.1155/2016/8374328>
 119. Pallin AC, Ramachandran V, Acharya S, Lewis DB. Human neonatal naive CD4(+) T cells have enhanced activation-dependent signaling regulated by the microRNA miR-181a. *J Immunol*. 2013;190(6):2682-2691. <https://doi.org/10.4049/jimmunol.1202534>
 120. Schijff MA, Kruijsen D, Bastiaans J, et al. Specific dietary oligosaccharides increase Th1 responses in a mouse respiratory syncytial virus infection model. *J Virol*. 2012;86(21):11472-11482. <https://doi.org/10.1128/jvi.06708-11>
 121. Galindo-Albarrán A, López-Portales O, Gutiérrez-Reyna D, et al. CD8(+) T cells from human neonates are biased toward an innate immune response. *Cell Rep*. 2016;17(8):2151-2160. <https://doi.org/10.1016/j.celrep.2016.10.056>
 122. Le Campion A, Bourgeois C, Lambalez F, et al. Naive T cells proliferate strongly in neonatal mice in response to self-peptide/self-MHC complexes. *P Natl Acad Sci USA*. 2002;99(7):4538-4543. <https://doi.org/10.1073/pnas.062621699>
 123. Schuler T, Hammerling GJ, Arnold B. Cutting edge: IL-7-dependent homeostatic proliferation of CD8(+) T cells in neonatal mice allows the generation of long-lived natural memory T cells. *J Immunol*. 2004;172(1):15-19. <https://doi.org/10.4049/jimmunol.172.1.15>
 124. Smith NL, Wissink E, Wang J, et al. Rapid proliferation and differentiation impairs the development of memory CD8(+) T cells in early life. *J Immunol*. 2014;193(1):177-184. <https://doi.org/10.4049/jimmunol.1400553>
 125. Reynaldi A, Smith NL, Schlub TE, Venturi V, Rudd BD, Davenport MP. Modeling the dynamics of neonatal CD8(+) T-cell responses. *Immunol Cell Biol*. 2016;94(9):838-848. <https://doi.org/10.1038/icb.2016.47>
 126. Wang J, Wissink EM, Watson NB, Smith NL, Grimson A, Rudd BD. Fetal and adult progenitors give rise to unique populations of CD8(+) T cells. *Blood*. 2016;128(26):3073-3082. <https://doi.org/10.1182/blood-2016-06-725366>
 127. Zhang YX, Maksimovic J, Huang B, et al. Cord blood CD8(+) T cells have a natural propensity to express IL-4 in a fatty acid metabolism and caspase activation-dependent manner. *Front Immunol*. 2018;9:879. <https://doi.org/10.3389/fimmu.2018.00879>
 128. Jorgensen N, Persson G, Hviid TVF. The tolerogenic function of regulatory T cells in pregnancy and cancer. *Front Immunol*. 2019;10:911. <https://doi.org/10.3389/fimmu.2019.00911>
 129. Cerny V, Hrdy J, Novotna O, et al. Distinct characteristics of Tregs of newborns of healthy and allergic mothers. *PLoS ONE*. 2018;13(11):e0207998. <https://doi.org/10.1371/journal.pone.0207998>
 130. Xu LL, Kitani A, Stuelten C, McGrady G, Fuss I, Strober W. Positive and negative transcriptional regulation of the Foxp3 Gene is mediated by access and binding of the Smad3 protein to enhancer 1. *Immunity*. 2010;33(3):313-325. <https://doi.org/10.1016/j.immuni.2010.09.001>
 131. Feng YQ, Arvey A, Chinen T, Van der Veeken JD, Gasteiger G, Rudensky AY. Control of the inheritance of regulatory T cell identity by a cis element in the Foxp3 locus. *Cell*. 2014;158(4):749-763. <https://doi.org/10.1016/j.cell.2014.07.031>
 132. Beier UH, Angelin A, Akimova T, et al. Essential role of mitochondrial energy metabolism in Foxp3(+) T-regulatory cell function and allograft survival. *Faseb J*. 2015;29(6):2315-2326. <https://doi.org/10.1096/fj.14-268409>
 133. Michalek RD, Gerriets VA, Jacobs SR, et al. Cutting edge: distinct glycolytic and lipid oxidative metabolic programs are essential for effector and regulatory CD4(+) T cell subsets. *J Immunol*. 2011;186(6):3299-3303. <https://doi.org/10.4049/jimmunol.1003613>
 134. De Rosa V, Galgani M, Porcellini A, et al. Glycolysis controls the induction of human regulatory T cells by modulating the expression of FOXP3 exon 2 splicing variants. *Nat Immunol*. 2015;16(11):1174-1184. <https://doi.org/10.1038/ni.3269>
 135. Borsellino G, Kleinewietfeld M, Di Mitri D, et al. Expression of ectonucleotidase CD39 by Foxp3(+) Treg cells: hydrolysis of extracellular ATP and immune suppression. *Blood*. 2007;110(4):1225-1232. <https://doi.org/10.1182/blood-2006-12-064527>
 136. Timperi E, Folgori L, Amodio D, et al. Expansion of activated regulatory T cells inversely correlates with clinical severity in septic neonates. *J Allergy Clin Immunol*. 2016;137(5):1617. <https://doi.org/10.1016/j.jaci.2015.10.048>
 137. Wang GH, Miyahara Y, Guo ZY, Khattar M, Stepkowski SM, Chen WH. "Default" generation of neonatal regulatory T cells. *J Immunol*. 2010;185(1):71-78. <https://doi.org/10.4049/jimmunol.0903806>
 138. Arguello RJ, Combes AJ, Char R, et al. SCENITH: A flow cytometry-based method to functionally profile energy metabolism with single-cell resolution. *Cell Metab*. 2020;32(6):1063-1075.e7. <https://doi.org/10.1016/j.cmet.2020.11.007>

How to cite this article: Holm SR, Jenkins BJ, Cronin JG, Jones N, Thornton CA. A role for metabolism in determining neonatal immune function. *Pediatr Allergy Immunol*. 2021;32:1616-1628. <https://doi.org/10.1111/pai.13583>

8.3 Does Altered Cellular Metabolism Underpin the Normal Changes to the Maternal Immune System during Pregnancy?

Review

Does Altered Cellular Metabolism Underpin the Normal Changes to the Maternal Immune System during Pregnancy?

Benjamin J. Jenkins, April Rees, Nicholas Jones, Catherine A. Thornton *

Institute of Life Science, Swansea University Medical School, Swansea, Wales SA2 8PP, UK

* Correspondence: Catherine A. Thornton,
Email: c.a.thornton@swansea.ac.uk.

ABSTRACT

Pregnancy is characterised by metabolic changes that occur to support the growth and development of the fetus over the course of gestation. These metabolic changes can be classified into two distinct phases: an initial anabolic phase to prepare an adequate store of substrates and energy which are then broken down and used during a catabolic phase to meet the energetic demands of the mother, placenta and fetus. Dynamic readjustment of immune homeostasis is also a feature of pregnancy and is likely linked to the changes in energy substrate utilisation at this time. As cellular metabolism is increasingly recognised as a key determinant of immune cell phenotype and function, we consider how changes in maternal metabolism might contribute to T cell plasticity during pregnancy.

KEYWORDS: immunometabolism; maternal metabolism; pregnancy; Treg; Th2

INTRODUCTION

Successful pregnancy involves various maternal adaptations that support the fetus [1]. Metabolic changes allow the preferential passage of nutrients across the materno-fetal interface for optimal fetal growth and development; immune changes ensure tolerance of the fetus [1,2].

Maternal metabolic changes during pregnancy are well described in tissues such as adipose, liver and skeletal muscle (summarised in Table 1 and Figure 1). Early pregnancy is characterised by the accretion of metabolic substrates in tissues, which is supported by increases in maternal energy intake [3,4]. In this anabolic phase, insulin promotes the uptake of glucose into tissues where it is either stored [5–7], or in the case of adipose tissue, used for lipogenesis [8,9]. In addition to enhanced lipogenesis, circulating fatty acids (FA) are taken up by and accumulate in maternal adipose tissue [10,11]. Disappearance of amino acids from maternal circulation is also characteristic of pregnancy where nitrogen is either accreted in maternal tissues or the developing fetus [12–14]. However, decreasing insulin sensitivity as pregnancy progresses results in

Open Access

Received: 28 June 2021

Accepted: 15 September 2021

Published: 04 October 2021

Copyright © 2021 by the author(s). Licensee Hapres, London, United Kingdom. This is an open access article distributed under the terms and conditions of [Creative Commons Attribution 4.0 International License](#).

Immunometabolism. 2021;3(4):e210031. <https://doi.org/10.20900/immunometab20210031>

a state of insulin resistance in late pregnancy [15,16]. This promotes a catabolic phase of metabolism wherein glucose preferentially passes to the developing fetus [7] and lipids are hydrolysed to bring about maternal hyperlipidemia [17,18]. Despite gestational changes in glucose utilisation, plasma glucose levels are relatively stable throughout pregnancy [5]. Failure to establish these metabolic changes is associated with numerous gestational complications, such as gestational diabetes mellitus (GDM), pre-eclampsia and cholestasis [19–21].

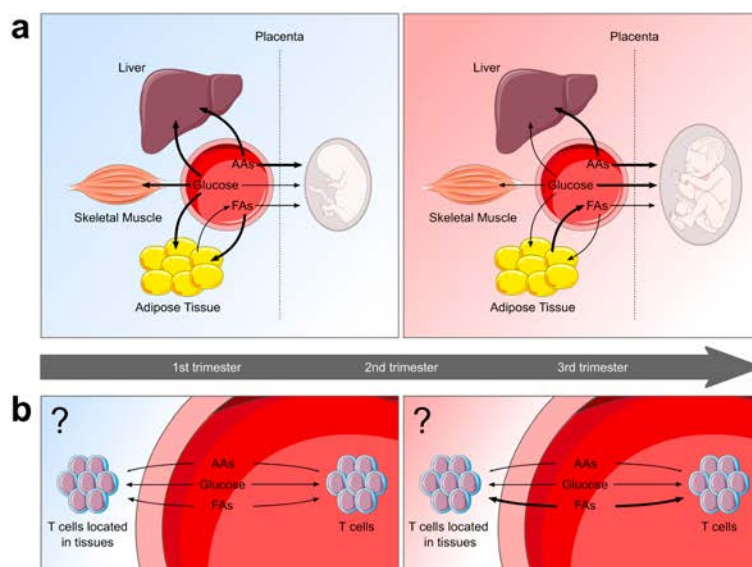


Figure 1. Overview of maternal substrate utilisation across gestation. (a) During early pregnancy, there is increased glucose uptake into surrounding tissues. In adipose tissue, glucose is used for the synthesis of triglycerides. Increased breakdown of lipoprotein-triglycerides by lipoprotein lipase results in increased uptake of hydrolytic products into adipose tissue, where they are used in lipogenesis. Lipolytic activity of adipose tissue is also reduced to promote lipid storage. Amino acids also accumulate in tissues, causing hypoaminoacidemia. Transfer of metabolites to the fetus is limited, with amino acids the main contributor. During late pregnancy, glucose uptake into maternal tissues is reduced, and preferentially passes across the placenta to the fetus. In adipose tissue, there is a switch from lipogenesis to lipolysis. Glycerol and free fatty acids (FFA) produced are transferred to lipoproteins, increasing plasma levels of lipoprotein-triglycerides. The fate of amino acid metabolism remains largely unchanged from early pregnancy. **(b)** During early pregnancy there is limited availability of circulating amino acids for uptake by immune cells such as T cells. In the third trimester, the maternal circulation provides T cells with a fatty-acid rich, amino-acid depleted microenvironment. These metabolic conditions could favour Treg and Th2 cell survival and function, as is seen during pregnancy. These changes might not be limited to circulating T cells and could underly the functions of tissue-resident T cells involved in driving pregnancy-related improvements in rheumatoid arthritis and multiple sclerosis. AA, amino acids; FA, fatty acids; TCA, tricarboxylic acid.

Table 1. Overview of known metabolic changes that occur during pregnancy.

Metabolite	Change during pregnancy	Species	Reference
Glucose	Plasma glucose concentrations remain at pre-gravid levels throughout pregnancy	Human	[5]
	Glucose uptake into maternal tissues decreases in the 3rd trimester	Human	[7]
	Glucose oxidation is reduced during the 3 rd trimester	Human	[7]
	Increased utilisation of glucose for lipid synthesis, which declines rapidly towards the end of pregnancy	Rat	[22]
Fatty acids (FA)	Increased accumulation of FAs in adipose tissue in the first and second trimester	Human	[11]
	Elevated lipogenesis in maternal tissues during the first and second trimester	Rat	[8]
	Increased lipoprotein lipase (LPL) activity during the first and second trimester drives FA uptake by surrounding tissues	Human	[10]
	Decreased LPL and hepatic lipase activity during the third trimester reduces lipid uptake into tissues	Human	[10]
	Increased lipolysis occurs within adipose tissue at the end of pregnancy and results in hyperlipidemia	Rat	[18]
	Circulating lipoprotein levels increase throughout pregnancy	Human	[10]
Amino acids	Hypoaminoacidemia occurs early in pregnancy and remains throughout	Human	[12,23,24]
	Relative urea production and excretion is reduced throughout pregnancy	Human	[13]
	Protein oxidation is reduced at the end of pregnancy	Human	[25]

The influence of cellular metabolism on leukocyte phenotype and function is an increasingly exciting area of immunology. Mechanisms underpinning immune plasticity in pregnancy such as enhanced activity of suppressive or regulatory immune cells and increasing susceptibility of pregnant women to severe responses to some viral infections such as influenza are unknown. Immunometabolism might provide a framework for understanding these dynamic adaptations from pre-conception, through pregnancy and into the postpartum. Although maternal metabolic changes are established in many tissues, it is unknown what effect if any there is on immune cells [26]. This review aims to focus on changes to T cells, especially the regulatory T (Treg) cell and T helper (Th)2 cell biased responses that characterise pregnancy and how changes in maternal energy substrate utilisation might link to changes in the activity of these cells during pregnancy.

METABOLISM AND THE IMMUNE SYSTEM

In addition to the metabolic adaptations that are known to occur predominantly in adipose tissue, skeletal muscle and liver, such adaptation in the immune system might underpin the immune plasticity

that occurs with pregnancy. Altered energy substrate utilisation is increasingly understood to dictate immune cell fate and function and maternal immunological adaptation might be secondary to the long recognised wider metabolic changes that characterise pregnancy. Expression and activity of pyruvate kinase is reported to be decreased within T cells and neutrophils during normal pregnancy and this will decrease the availability of pyruvate within immune cells [27]. This might suggest that maternal immune cells downregulate their use of glucose for energy substrate production which would alter their function during pregnancy. Indeed, cellular metabolic analysis showed reduced glycolysis in peripheral blood mononuclear cells (PBMCs) of late pregnant women versus non-pregnant women [28]. While this early evidence is suggestive of immunometabolic adaptation in pregnancy, we are a long way from understanding these processes or elaborating their contribution to pregnancy outcome. However, our existing understanding of the immunometabolic characteristics of some immune cell types can provide insight into mechanisms of plasticity during pregnancy with CD4⁺/FoxP3⁺ regulatory T (Treg) cells and Th2 cells perhaps the best examples of this.

CD4⁺/FOXP3⁺ REGULATORY T CELLS

Treg cells are important in the control of self-reactive immune cells to maintain immunological self-tolerance [29] and are increased in both the decidua and maternal peripheral blood with pregnancy [30,31]. The majority of the maternal Treg population consists of effector Treg cells not resulting from clonal expansion [32,33]. Reduced numbers of peripheral Treg cells have been associated with several adverse pregnancy outcomes including recurrent miscarriage and preeclampsia [34,35]. Mouse models of pregnancy have demonstrated that Treg cells are required to mediate maternal tolerance to the fetus [36]. Their absence is characterised by significant lymphocyte infiltration and haemorrhage at the materno-fetal interface, which ultimately results in abnormal fetal development and gestational failure [36]. Additionally, aberrant Treg function also results in abortion and the transfer of Treg cells from healthy pregnancies to these abortion-prone mice improves pregnancy outcome [37]. This highlights the important role for Treg cell biased responses in ensuring successful pregnancy.

Maternal Treg cells are likely to play an important role in facilitating peripheral immune tolerance as evidenced by improved outcome of some autoimmune diseases during pregnancy. For example, decreased disease severity and complete remission have been seen in pregnant women with rheumatoid arthritis (RA) [38,39]. RA disease severity is inversely correlated with maternal Treg cell numbers in humans and Treg cells from pregnant mice alleviated disease when transferred into non-pregnant RA mice [40,41]. Pregnancy-induced amelioration of multiple sclerosis is associated with the expansion and enhanced function of maternal Treg cells [42–44]. In contrast maternal Treg cells can confer increased susceptibility to infection through their immunosuppressive function [45].

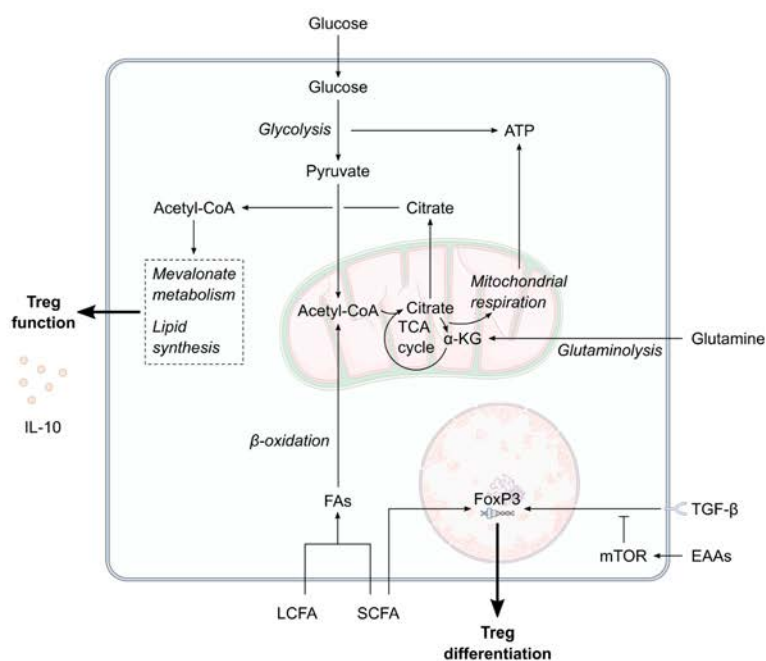


Figure 2. The potential effect of maternal metabolism on Treg differentiation and function. Decreased extracellular amino acid concentrations combined with increased transforming growth factor- β concentrations during pregnancy would enhance the FoxP3-mediated regulatory T cell (Treg) differentiation. Short-chain fatty acids amongst the increased maternal extracellular fatty acid pool would also enhance Treg differentiation. Increased circulating fatty acid concentrations could increase the availability of cellular acetyl-coA. Flux of acetyl-coA through mevalonate metabolism and lipid synthesis is vital for Treg function, such as interleukin-10 (IL-10) production, and Treg survival. α -KG, α -ketoglutarate; EAAs, essential amino acids; FA, fatty acid; IL-10, interleukin-10; LCFA, long-chain fatty acid, mTOR, mechanistic target of rapamycin; SCFA, short-chain fatty acid; TCA, tricarboxylic acid; TGF- β , transforming growth factor- β ; Treg, regulatory T cell.

Together, this provides evidence that changes to maternal Treg cell function are not limited to the fetal-placental interface but also occur systemically during pregnancy and are best exemplified by measures in maternal peripheral blood although in humans these observations relate predominantly to relative changes in abundance rather than functional readouts. However, it remains unknown what the underlying mechanisms are that drive increased Treg cell function during pregnancy. Given our understanding of the role of metabolism in Treg cell development and function more generally, it is likely that the altered metabolism that occurs

in normal pregnancy as described above contributes to changes in Treg cell function (Figure 2). Metabolism likely interacts with hormone-dependent and fetal antigen-driven changes to Treg responses in pregnancy; indeed placental hormones are key drivers of the metabolic adaptations summarised above and in Table 1. Increased Treg numbers are common in both allogeneic and syngeneic pregnancies highlighting the role of pregnancy hormones [36], with a greater increase in allogeneic pregnancies [46], suggesting that fetal alloantigens make a telling contribution. While the impact that the local metabolic environment might have on Treg fate and function has yet to be elucidated in pregnancy, the following subsections will highlight areas of the literature that suggest it could contribute to gestational changes in Treg responses.

Amino Acids and Treg Differentiation

There are numerous features of the maternal metabolic environment that might favour enhanced Treg function. Maternal hypoaminoacidemia presents early in pregnancy and persists throughout gestation [12,23,24]. Amino acid deprivation can influence Treg differentiation and has been highlighted by the induction of a Treg phenotype during tryptophan starvation [47]. Tryptophan depletion and the immunoregulatory tryptophan catabolite kynurenine modulate FoxP3 expression through general control nonderepressible (GCN)-2 kinase activation and TGF- β signalling to induce a regulatory phenotype [47]. Plasma tryptophan levels are decreased during the 2nd and 3rd trimesters, decreasing as pregnancy progresses [48], which might suggest that the maternal circulation provides a favourable microenvironment for differentiation towards Treg cells. Although kynurenine levels in maternal plasma remain stable during pregnancy, the increase in kynurenine to tryptophan ratio with each trimester [48] could further promote the induction of CD4⁺/FoxP3⁺ T cells. Notably, this scenario very much reflects our focus on the changes that occur peripherally in pregnant women especially as pregnancy progresses. Local metabolic changes within the early pregnant uterus that might underpin pregnancy-favouring behaviours of Treg cells and other key effectors of implantation and placentation success such as decidual NK cells remain to be established. Similarly, perturbations in these that might then link to adverse pregnancy outcomes such as miscarriage remain to be elucidated.

The availability of other essential amino acids can also influence FoxP3⁺ Treg cell differentiation from CD4⁺ T cells and the concentration of TGF- β required for differentiation is lower in conditions of essential amino acid deprivation [49]. Of the essential and conditionally-essential amino acids that drive FoxP3 induction at limited concentrations in synergy with TGF- β , four have reduced plasma concentrations during pregnancy—valine, arginine, phenylalanine and tryptophan [50]. Under conditions of amino acid deprivation, mechanistic target of rapamycin (mTOR) regulates differentiation of CD4⁺ T cells to FoxP3⁺ induced Treg (iTreg) cells [49,51]. Inhibition of mTOR favours Treg cell differentiation, as mTOR

activity limits FoxP3 induction by key transcription factors SMAD and FOXO. TGF- β -induced SMAD3 and SMAD4 function and nuclear localisation of FOXO1 and FOXO3 are inhibited by mTORC1 and mTORC2 respectively [52]. The activation of both mTORC1 and mTORC2 is controlled directly by extracellular amino acids [53,54]. Indeed, essential amino acid deprivation reduces S6 phosphorylation in CD4⁺ T cells which then increases Treg cell differentiation [49]. Increased TGF- β concentrations in maternal serum during pregnancy [55] could also play a significant contribution towards Treg induction, especially when coupled with hypoaminoacidemia.

Additionally, reduced levels of glutamine can also promote Treg differentiation from CD4⁺ T cells through inhibition of mTOR [56,57]. The effects of glutamine deprivation on mTOR activity can be rescued by the addition of α -ketoglutarate (α -KG), the product of glutaminolysis, therefore it is possible that this pathway underpins the modulation of mTOR by glutamine [56]. Given that the same restorative effect of α -KG was not observed in human iTreg cells [57], glutamine deprivation might also influence differentiation via alternative mechanisms. α -KG can further regulate Treg differentiation from CD4⁺ T cells through epigenetic modification of FoxP3 [58]. Hypermethylation within the Treg-specific demethylated region of the FoxP3 gene by 2-hydroxyglutarate, derived from α -KG, inhibits the expression of the FoxP3⁺ Treg phenotype [58]. Therefore, glutamine-deprived conditions would limit the availability of α -KG for conversion to 2-hydroxyglutarate and would maintain the demethylated status of the FoxP3 Treg-specific region, allowing its transcription and the consequent differentiation to Treg cells. Glutamine could also affect Treg differentiation from CD4⁺ T cells independent of glutaminolysis as inhibition of glutaminase, responsible for the conversion of glutamine to glutamate, does not induce the differentiation of Treg cells [59]. Plasma glutamine levels are reduced during the third trimester, whilst there is also a trimester-by-trimester decrease in the availability of branched chain amino acids (BCAA) that can act as a nitrogen pool for glutamine synthesis [50,60]. Glutamine uptake in CD4⁺ T cells is also required for leucine uptake via SLC7A5-CD98 amino acid transporter [61]. Leucine import results in activation of mTORC1, favouring differentiation towards other non-Treg subsets [61]. Decreased extracellular glutamine availability, as seen in pregnancy, could therefore limit leucine-mediated mTOR activity to skew towards a regulatory phenotype. Trimestral decreases in plasma leucine [50] could further hamper T cell mTOR activation and favour induction of Tregs. Thus, the amino acid-depleted environment of the maternal circulation during pregnancy potentially favours Treg cell differentiation.

Fatty Acids and Treg Differentiation

Fatty acid (FA) metabolism also plays an important role in controlling the fate of Treg cells and the enhanced efflux of lipid breakdown products

from maternal adipose tissue during the third trimester could support Treg cell expansion. Exogenous FA uptake by iTreg cells allows sustained proliferation and favours a regulatory phenotype [62]. iTreg cells are less dependent on acetyl-CoA carboxylase (ACC)1 for their development and can instead convert exogenous FAs into palmitate for phospholipid synthesis [62]. ACC1 inhibition and its effect on de novo FA synthesis does not affect iTreg development and promotes differentiation towards a regulatory lineage [62]. In particular, the oxidation of FAs taken up by CD4⁺ T cells is important for their development as iTreg cells—addition of FAs alone enhances differentiation towards the regulatory lineage whilst addition together with TGF- β further skews differentiation [63]. Underlying this process are the actions of both mTOR and AMP-activated protein kinase (AMPK)—reduced mTOR activity and heightened AMPK activity enhancing lipid metabolism which in turn increases the generation of CD4⁺/FoxP3⁺ T cells [63]. Consequently, pharmacological activators of AMPK such as metformin and 5-aminoimidazole-4-carboxamide ribonucleotide (AICAR) are capable of enhancing Treg differentiation [63,64]. Inhibiting carnitine palmitoyltransferase 1a (CPT1a), the rate controlling enzyme of long-chain FA oxidation, with etomoxir blocks Treg differentiation from CD4⁺ T cells and outlines the importance of lipid oxidation [63]. Indeed, direct activation of AMPK by AICAR promotes Treg differentiation from CD4⁺ T cells through increased mitochondrial biogenesis and FA uptake and depends on the latter to exert its effect on differentiation [64]. However, emerging understanding of the off-target effects of etomoxir need to be taken into account when interpreting these data [65]. The metabolic sensor LKB1, upstream of AMPK, has also been identified as an important regulator of T cell metabolism and survival [66,67]. Compromised OXPHOS and ATP production upon *LKB1* deletion ultimately resulted in reduced Treg numbers [66,67]. However, it is understood that LKB1 function in Treg cells occurs independently of conventional AMPK pathways and instead mediates MAPK signalling [66].

Short-chain FAs (SCFAs) also promote Treg differentiation [68]. SCFAs polarise CD4⁺ T cells towards a regulatory phenotype through inhibition of the JNK1 and the p38 pathway [68]. Increasing levels of the SCFA β -hydroxybutyrate have been reported across pregnancy [50]. The sodium salt of butyrate can regulate the Th17/Treg balance to favour CD4⁺/FoxP3⁺ Treg cells [69]. Nuclear translocation and activation of the Nrf-2/HO-1 pathway is critical in sodium butyrate-mediated modulation of Th17 differentiation and the reciprocal increase of CD4⁺/FoxP3⁺ T cells [69]. Additionally, butyrate can act directly on peripheral and splenic naive CD4⁺ T cells to enhance their differentiation to FoxP3⁺ Treg cells by stabilising the acetylation of the critical transcription factor FoxP3 [70,71]. The SCFA propionate can act on CD4⁺ T cells in the same manner as butyrate and presents an alternative method through which SCFAs can regulate Treg differentiation [70]. As maternal plasma is enriched with SCFAs [50], it is plausible that this could contribute

to the expanded Treg population observed during pregnancy. The contribution of the maternal gut microbiome to these SCFAs is beyond the scope of this review but there is immense interest in the relationship between the maternal microbiota and immune programming of the offspring [72]. Together, our current understanding of both maternal metabolism during pregnancy and the role of metabolism underlying Treg differentiation would suggest that the maternal circulation provides a highly favourable environment for Treg cells—especially during the third trimester. Given that this population of T cells is increased during pregnancy, it is possible that this occurs due to the amino acid-depleted landscape of maternal peripheral blood, and is further supplemented by the increased appearance of FAs during the third trimester.

Hormonal Regulation of Treg Function

Further to the aforementioned effect that pregnancy hormones have on Treg cells, metabolic hormones such as leptin can also influence Treg responses. Treg cells express higher amounts of the leptin receptor (ObR) than other T cell subsets, which suggests that leptin might have a greater influence in shaping their functional output [73]. Indeed, leptin negatively regulates Treg proliferation, but does not have a significant effect on the suppressive capacity of these cells [73]. The absence of leptin, or chronic blockade of its receptor, increases Treg cell numbers which has led to resistance in models of autoimmune diseases [73,74]. Leptin also plays some important roles during pregnancy—recombinant leptin improved conception in infertile mice, whilst regulatory roles in immunomodulation, angiogenesis and nutrient transport have been described in the placenta [75,76]. Usually produced in adipose tissue, placenta-derived leptin emerges as a novel pregnancy hormone and during the second and third trimester plasma leptin levels become elevated including a contribution of the placenta as a pregnancy-specific source of leptin [77,78]. Leptin resistance develops during the second trimester and has a role in supporting the growth of the fetus [79,80], whilst maternal obesity has been associated with further leptin resistance in the placenta [81]. While the leptin-rich environment that presents during the second and third trimester might be expected to contradict the known effects of leptin on Treg number, the accompanying leptin resistance would favour increased Tregs [73,74], although we do not know if this leptin resistance extends to the immune system and more specifically Treg cells.

Fatty Acids and Treg Function

Metabolism not only dictates Treg differentiation but also controls Treg cell effector function. Thymic Treg (tTreg) cells engage glycolysis upon activation through TNF receptor 2 co-stimulation, which is required for their expression of key transcription factors such as FoxP3, as well as their suppressive function [82]. As maternal plasma glucose levels are limited

during pregnancy [5], our focus has shifted to other elements of metabolism, such as fatty acids and amino acids, whose changes are more profound during pregnancy and are key contributors to cellular metabolic pathways. Treg cells with significantly reduced lipid synthesis have reduced survival and attenuated immunosuppressive function [66,67,83]. Upon stimulation through PD-1 and CTLA-4 and induction of FoxP3 expression, iTreg cells prepare for effector function by lowering the rate of glycolysis whilst concomitantly increasing oxidative metabolism and FA oxidation [84]. iTreg cells fail to upregulate Myc upon stimulation which results in restrained glycolysis [85]. Inhibition of either OXPHOS or FA oxidation diminishes the suppressive function of iTreg cells and thus underlines the importance of metabolism in directing a Treg response [85,86]. In a mixed population of iTreg and tTreg cells, uptake and oxidation of exogenous FA contributed to OXPHOS and favoured Treg stability [87]. Inhibition of the mevalonate pathway through deletion of HMG-CoA reductase also causes defective Treg cell function in both iTreg and tTreg cells and culminates in an autoimmune disease phenotype [83,88,89]. LKB-1 deficient iTreg cells produce less IL-10 and have decreased surface expression of effector molecules such as CTLA-4, PD-1, CD39 and CD73, instead enhancing their production of inflammatory cytokines which ultimately results in failure to inhibit autoimmunity [83]. The mevalonate pathway is impaired in LKB-1 deficient iTreg cells and inhibition of HMG-CoA reductase induces a similar inflammatory phenotype to that of LKB1 deletion [83]. Suppressive iTreg function is restored upon treatment with mevalonate and geranylgeranyl pyrophosphate (GGPP) [83]. Increased plasma lipid concentrations, as seen during late pregnancy, would enhance substrate availability to these pathways and might explain enhanced gestational Treg cell function as pregnancy progresses.

Recently, fatty acids have emerged as key regulators of Treg cell mitochondrial health [90,91]. Expression of CD36, a fatty acid translocase, is required for the immunosuppressive function and survival of intratumoural Treg cells [90]. CD36 also modulates the mitochondrial fitness of both intratumoural Treg cells and iTreg cells and supports their metabolic adaptation within the microenvironment [90]. Lipid chaperones responsible for the uptake and intracellular transport of lipids, such as fatty acid binding protein 5 (FABP5) are also implicated in maintaining mitochondrial health in iTreg cells [91]. Inhibition results in impaired oxidative respiration, loss of cristae structure and ablated lipid metabolism [91]. Under these circumstances there was a reduction in iTreg cell number, however, suppressive function was augmented through the release of mitochondrial DNA caused by mitochondrial dysfunction [91]. The resulting cGAS-STING signalling and subsequent type I IFN signalling promote IL-10 expression and drive suppressive Treg function [91].

Amino Acids and Treg Function

Amino acids play a more reserved role in orchestrating suppressive Treg function. Glutamine depletion produces iTreg cells with suppressive function such as IL-4 production, however, these cells also express pro-inflammatory cytokines IL-17 and IFN γ [57]. This might suggest that balanced amino acid levels are required for successful regulatory function. Collectively, these data support the hypothesis that maternal immunological adaptation is secondary to changes in metabolism and energy substrate utilisation. It is important to note that the majority of the studies discussed in this manuscript analyse the fate and function of iTreg cells, with those concerning tTreg cells highlighted. Whether the concepts addressed throughout this section apply to both iTreg and tTreg cells is not known, but would be an important factor to consider in any future research. It is also important to acknowledge that other Treg populations, such as those localised at the decidua, might be differentially affected compared to the peripheral blood Treg cells discussed. For example, little is known about that the metabolic environment at the materno-fetal interface, therefore understanding the effect that this local metabolic environment might impose on Treg cells could be fundamental to elucidating reduced Treg numbers in women with recurrent pregnancy loss and other adverse pregnancy outcomes. As yet there are no experimental data to support this hypothesis other than the coalignment of what we know about changing Treg cell number in pregnancy and the changes to substrate availability. Detailed investigation of the metabolic changes to Treg cells that accompany pregnancy normally and in adverse pregnancy outcomes such as miscarriage and preeclampsia are certainly warranted.

TH2 CELLS

In addition to Treg cells, there is an increase in the activity of Th2 cells during pregnancy. T helper (Th) cells have been long characterised by their cytokine profile and this allows their classification into different subsets [92]. Th2 responses are characterised by the release of IL-4, IL-5, IL-9 and IL-13. Naïve CD4⁺ T cells differentiate to a Th2 phenotype through activation of signal transducer and activator of transcription (STAT)6 and GATA3. Increased Th2 cell activity occurs at both the fetal-placental interface and in peripheral blood and is measured as a ratio of the activity of Th2 cells compared to Th1 cells. During pregnancy, there is an increase in the secretion of type 2 immune cytokines—so origins possibly other than T cells such as IL-4, with a relative increase compared to cytokines such as IFN γ and IL-2 [93,94]. This likely occurs due to changes at the protein level that reflect increased IL-4 mRNA expression in T cells whilst IFN γ mRNA expression is decreased [95]. This ratio remains throughout gestation and reverts to non-pregnant levels postpartum [96,97]. Some studies suggest that Th2 activity declines as early as the latter stages of labour [98]. Although enhanced Th2 activity has been demonstrated throughout human

pregnancy, the complete absence of a Th2 response does not affect allogenic mouse pregnancy, which suggests that Th2 cells are not essential in maintaining the materno-fetal tolerance—at least in mice [99].

Amino Acids and Th2 Responses

Global changes in maternal metabolism also could underpin the Th2 biased responses that are observed during pregnancy as metabolic pathways are key regulators of both Th2 differentiation and function. Characteristic reductions in plasma amino acid concentrations during pregnancy, particularly reduced glutamine [12,50], potentially tips the Th1/Th2 ratio in favour of Th2 cells. Treatment of PBMCs with high concentrations of glutamine *in vitro* impairs Th2-like responses through suppression of IL-10 production and augmenting IFN γ production [100]. These changes are realised physiologically as dietary glutamine shapes the Th1/Th2 balance towards Th1 cells over Th2 cells, reflected by increased IL-2 production and decreased IL-4 production [101]. In fact, Th2 cells are not dependent on glutamine and rather have improved function in its absence [61]. Deletion of ASCT2 enhanced the generation of Th2 cells, increasing the expression of both GATA3 and IL-4 [61]. A possible mechanism of action for glutamine-mediated T cell regulation is its inhibition of cytosolic phospholipase A₂ activity [102]. Th2 cytokine production is reduced in the presence of glutamine which culminates in failure to recruit neutrophils and eosinophils to inflamed airways [102]. Cytosolic phospholipase A₂ is important in facilitating the release of arachidonic acid from glycerophospholipids for their incorporation into Th2-related inflammatory mediators.

The contribution of tryptophan metabolism to Th2 function has already been demonstrated in the setting of murine pregnancy [103]. Decreased tryptophan metabolism in the uterus balances the Th1/Th2 ratio in the favour of Th1 cells which increases the likelihood of pregnancy failure [103]. In human pregnancy, low levels of tryptophan but maintained levels of its metabolites such as kynurenine suggest increased tryptophan metabolism and utilisation of the metabolites [48] and would present a Th2 favouring milieu. The absence of tryptophan catabolising enzymes in the lung impaired Th2-mediated inflammatory airway responses with reductions in IL-5, IL-13 and IL-4 production [104]. The activity of the tryptophan-catabolising enzyme indoleamine-2,3-dioxygenase (IDO) is thought to be increased during pregnancy, playing an important role in immune activation [105]. Additionally, tryptophan catabolism deficiency had less of an impact on Th1 responses [104]. Interestingly, metabolites of the kynurenine pathway cause apoptosis of Th1 but do not impact Th2 survival [47]. Together, these data suggest that increased flux through tryptophan catabolism pathways supports Th2 responses in the Th1/Th2 balance. Thus, the amino acid landscape of pregnancy could support the Th2-skewed Th1/Th2 ratio that is observed.

Fatty Acids and Th2 Responses

Lipid metabolism is also implicated in Th2 cell expansion and function. Inhibition of ACC1 impairs Th2 induction and underlines the importance of lipid synthesis in mediating Th2 responses [62,106]. Lipid pathways also play an important role in Th2 development. Upon stimulation and subsequent activation of CD4⁺ T cells, FA uptake is increased and is essential for successful proliferation [106]. Lipid synthesis through ACC1 was also important for proliferation and made a significant contribution to glycolysis [106].

Peroxisome proliferator-activated receptor (PPAR) γ —the master regulator of lipid metabolism and storage—entwines cellular metabolism with Th2 effector function. PPAR γ inhibition inflicted the same metabolic and functional effects on CD4⁺ T cells as ACC1 inhibition, suggesting that PPAR γ -mediated metabolic reprogramming directs the activation of Th2 cells [106]. Gene expression analysis has revealed that activated Treg cells are enriched in genes associated with lipid metabolism [107]. There are more PPAR γ binding sites on open chromatin at loci that facilitate enhanced expression of the lipid-associated target genes needed for glucose metabolism and promoting Th2 functions such as recruitment of eosinophils to inflamed airways [107]. Included in the target genes for PPAR γ binding are IL-5 and IL-13, and key Th2 transcription factor GATA3 [108]. Th2 cells lacking PPAR γ failed to mount a Th2 response to allergic challenge in the airways of mice [109]. PPAR γ deletion reduced the production of IL-5 and IL-13 by Th2 cells and reduced the presence of eosinophils and mucus-secreting goblet cells, culminating in an impaired pathogenic response [109]. Similar responses were also seen in other mouse models of allergic airway inflammation and *H. polygyrus* infection [109,110], emphasising the importance of PPAR γ in protective immunity. IL-33 plays a critical role in PPAR γ signalling in Th2 cells. IL-33R ligation upregulates the expression of PPAR γ , which itself can upregulate the expression of IL-33R subunit ST2, creating a positive feedback loop [109,110].

The role of PPAR γ activity in IL-4 production remains unclear, with reports that it can enhance [110], suppress [111] or have no effect [109] on IL-4 expression. It has also been proposed that PPAR γ can influence Th2 response indirectly via the actions of dendritic cells [110]. Expression of PPAR γ by dendritic cells is controlled by IL-4 and IL-33 and drives polarisation of T cells towards a Th2 phenotype [110]. Production of IL-9 also has been associated with PPAR γ , giving rise to a subset of T cells that also produce increased amounts of IL-5 and IL-13 [112]. However, activation by TGF- β and IL-4, which enhance the expression of PPAR γ , promotes a Th9 phenotype where Th2 cytokines are downregulated [112]. The ability of PPAR γ to influence metabolic pathways likely underpins its role in controlling Th2 functions. In the absence of PPAR γ , FA uptake was attenuated with mediators such as FABP5 downregulated [106], whilst carbohydrate synthesis, metabolite transport, lipid storage and lipolysis were also all affected [109].

The influence of SCFAs on Th2 function remains unclear. Early work suggests that SCFAs have a negative effect on Th2 responses, with long-term defects on IL-5 and IL-13 production upon propionate treatment [113]. However, recently various C2–4 SCFAs have been shown to increase the expression of IL-5 following FFAR3-mediated signalling [114]. In vivo, SCFA treatment materialises as enhanced Th2 cytokine production and a consequent increase in eosinophil recruitment [114]. The hyperlipidemic maternal phenotype appears tailored for enhanced Th2 cell function (Figure 3). Increased lipid availability would provide the substrates necessary for enhanced type 2 cytokine production, as is seen in normal pregnancy, and perhaps explains the mechanisms underpinning the Th2 biased responses seen during pregnancy. However, as for Tregs above there are no direct data to support this postulated, but such studies warrant investigation.

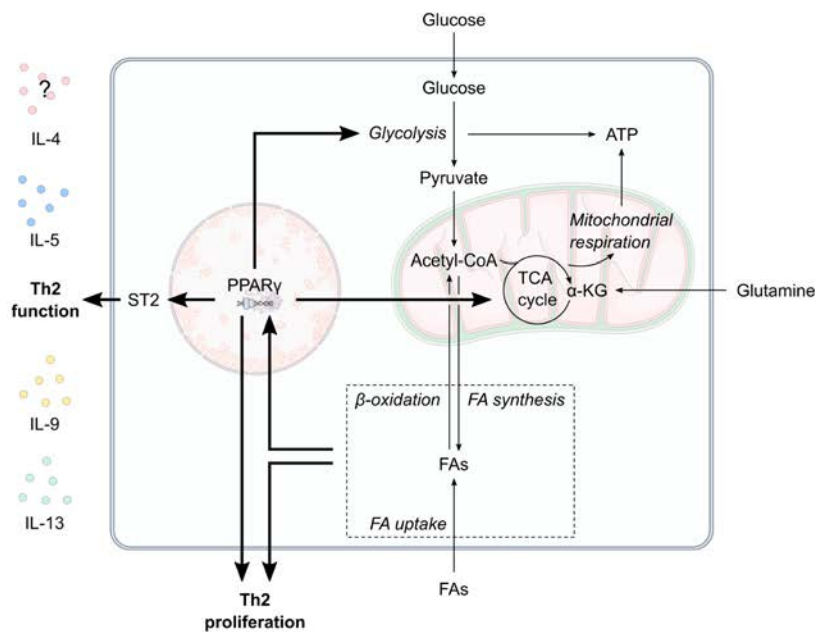


Figure 3. The potential effect of maternal metabolism on Th2 proliferation and function. Peroxisome proliferator-activated receptor (PPAR)- γ is central to T helper 2 (Th2) cell glycolytic and oxidative metabolism, function and proliferation. Pregnancy is associated with increased circulating fatty acid (FA) levels. Enhanced lipid metabolism, such as increased fatty acid uptake, oxidation and synthesis, likely influences PPAR γ activity to increase Th2 proliferation. PPAR γ also promotes ST2 expression to increase the expression of Th2-related cytokines such as IL-9, IL-13, IL-15 and possibly IL-4. α -KG, α -ketoglutarate; FA, fatty acid; IL, interleukin; TCA, tricarboxylic acid; TH2, T helper 2 cell.

CONCLUDING REMARKS

Metabolic adaptation during pregnancy is essential for successful fetal growth and development. This is achieved through many tightly regulated processes occurring as a result of the overarching increase in insulin resistance as gestation progresses. The effect of these processes on tissues such as the liver, adipose and skeletal muscle are well described, however it is unknown how these processes might affect the immune system. Immune plasticity is required during pregnancy, both to ensure tolerance of the semi-allogenic fetus and to protect mother and fetus from infection. Metabolism has emerged as a central regulator of immune cell phenotype and function, therefore it is increasingly likely that maternal immunological adaptation is governed by wider metabolic changes characteristic of gestation. Understanding the pathways underlying changes in immunometabolism and immune cell fate and function could reveal potential therapeutic targets to alleviate disease severity during pregnancy, benefitting the long-term health of both the mother and newborn. This will also reveal the spectrum of normal immunometabolic programming and plasticity in humans that could be harnessed for therapeutic benefit in disease settings outside of pregnancy.

CONFLICTS OF INTEREST

The authors declare that they have no conflicts of interest.

ACKNOWLEDGEMENTS

BJJ is supported by a Swansea University Research Excellence Scholarship and CAT is supported by Ser Cymru II, Welsh Government and MRC (MR/V037013).

REFERENCES

1. Mor G, Cardenas I. The Immune System in Pregnancy: A Unique Complexity. *Am J Reprod Immunol.* 2010;63(6):425-33.
2. Di Cianni G, Miccoli R, Volpe L, Lencioni C, Del Prato S. Intermediate metabolism in normal pregnancy and in gestational diabetes. *Diabetes Metab Res Rev.* 2003;19(4):259-70.
3. Murphy SP, Abrams BF. Changes in energy intakes during pregnancy and lactation in a national sample of United-States women. *Am J Public Health.* 1993;83(8):1161-3.
4. Piers LS, Diggavi SN, Thangam S, Vanraaij JMA, Shetty PS, Hautvast J. Changes in energy-expenditure, anthropometry, and energy-intake during the course of pregnancy and lactation in well-nourished Indian women. *Am J Clin Nutr.* 1995;61(3):501-13.
5. Catalano PM, Tyzbir ED, Wolfe RR, Roman NM, Amini SB, Sims EAH. Longitudinal changes in basal hepatic glucose-production and suppression during insulin infusion in normal pregnant-women. *Am J Obstet Gynecol.* 1992;167(4):913-9.

6. Catalano PM, Tyzbir ED, Wolfe RR, Calles J, Roman NM, Amini SB, et al. Carbohydrate-metabolism during pregnancy in control subjects and women with gestational diabetes. *Am J Physiol.* 1993;264(1):E60-7.
7. Sivan E, Chen XH, Homko CJ, Reece EA, Boden G. Longitudinal study of carbohydrate metabolism in healthy obese pregnant women. *Diabetes Care.* 1997;20(9):1470-5.
8. Ramos MP, Crespo-Solans MD, del Campo S, Cacho J, Herrera E. Fat accumulation in the rat during early pregnancy is modulated by enhanced insulin responsiveness. *Am J Physiol Endocrinol Metab.* 2003;285(2):E318-28.
9. Herrera E, del Campo S, Marciniak J, Sevillano J, Ramos MP. Enhanced utilization of glycerol for glyceride synthesis in isolated adipocytes from early pregnant rats. *J Physiol Biochem.* 2010;66(3):245-53.
10. Alvarez JJ, Montelongo A, Iglesias A, Lasuncion MA, Herrera E. Longitudinal study on lipoprotein profile, high density lipoprotein subclass, and postheparin lipases during gestation in women. *J Lipid Res.* 1996;37(2):299-308.
11. Villar J, Cogswell M, Kestler E, Castillo P, Menendez R, Repke JT. Effect of fat and fat-free mass deposition during pregnancy on birth-weight. *Am J Obstet Gynecol.* 1992;167(5):1344-52.
12. Felig P, Kim YJ, Lynch V, Hendler R. Amino-acid metabolism during starvation in human pregnancy. *J Clin Invest.* 1972;51(5):1195-1202.
13. Forrester T, Badaloo AV, Persaud C, Jackson AA. Urea production and salvage during pregnancy in normal Jamaican women. *Am J Clin Nutr.* 1994;60(3):341-6.
14. Kalhan SC, Parimi PS. Transamination of leucine and nitrogen accretion in human pregnancy and the newborn infant. *J Nutr.* 2006;136(1):281S-7.
15. Ryan EA, Osullivan MJ, Skyler JS. Insulin action during pregnancy - studies with the euglycemic clamp technique. *Diabetes.* 1985;34(4):380-9.
16. Catalano PM, Tyzbir ED, Roman NM, Amini SB, Sims EAH. Longitudinal changes in insulin release and insulin resistance in nonobese pregnant-women. *Am J Obstet Gynecol.* 1991;165(6):1667-72.
17. Herrera E, Lasuncion MA, Gomezcoronado D, Aranda P, Lopezluna P, Maier I. Role of lipoprotein-lipase activity on lipoprotein metabolism and the fate of circulating triglycerides in pregnancy. *Am J Obstet Gynecol.* 1988;158(6):1575-83.
18. Knopp RH. Carbohydrate metabolism in pregnancy .8. metabolism of adipose tissue isolated from fed and fasted pregnant rats during late gestation. *J Clin Invest.* 1970;49(7):1438-46.
19. Alberti K, Zimmet PZ, Consultation WHO. Definition, diagnosis and classification of diabetes mellitus and its complications part 1: Diagnosis and classification of diabetes mellitus - Provisional report of a WHO consultation. *Diabetic Med.* 1998;15(7):539-53.
20. Mol BJ, Roberts CT, Thangaratnam S, Magee LA, de Groot CJM, Hofmeyr GJ. Pre-eclampsia. *Lancet.* 2016;387(10022):999-1011.
21. Williamson C, Geenes V. Intrahepatic cholestasis of pregnancy. *Obstet Gynecol.* 2014;124(1):120-33.

22. Palacin M, Lasuncion MA, Asuncion M, Herrera E. Circulating metabolite utilization by peruterine adipose-tissue insitu in the pregnant rat. *Metabolism*. 1991;40(5):534-9.
23. Metzger BE, Unger RH, Freinkel N. Carbohydrate metabolism in pregnancy. XIV. Relationships between circulating glucagon, insulin, glucose and amino acids in response to a "mixed meal" in late pregnancy. *Metabolism*. 1977 Feb;26(2):151-6.
24. Schoengold DM, Defiore RH, Parlett RC. Free amino-acids in plasma throughout pregnancy. *Am J Obstet Gynecol*. 1978;131(5):490-9.
25. Butte NF, Hopkinson JM, Mehta N, Moon JK, Smith EO. Adjustments in energy expenditure and substrate utilization during late pregnancy and lactation. *Am J Clin Nutr*. 1999;69(2):299-307.
26. Thiele K, Diao LH, Arck PC. Immunometabolism, pregnancy, and nutrition. *Semin Immunopathol*. 2018;40(2):157-74.
27. Xu Y, Madsen-Bouterse SA, Romero R, Hassan S, Mittal P, Elfline M, et al. Leukocyte Pyruvate Kinase Expression is Reduced in Normal Human Pregnancy but not in Pre-eclampsia. *Am J Reprod Immunol*. 2010;64(2):137-51.
28. Jones N, Piasecka J, Bryant AH, Jones RH, Skibinski DOF, Francis NJ, et al. Bioenergetic analysis of human peripheral blood mononuclear cells. *Clin Exp Immunol*. 2015;182(1):69-80.
29. Sakaguchi S. Naturally arising CD4(+) regulatory T cells for immunologic self-tolerance and negative control of immune responses. *Annu Rev Immunol*. 2004;22:531-62.
30. Sasaki Y, Sakai M, Miyazaki S, Higuma S, Shiozaki A, Saito S. Decidual and peripheral blood CD4(+)CD25(+) regulatory T cells in early pregnancy subjects and spontaneous abortion cases. *Mol Hum Reprod*. 2004;10(5):347-53.
31. Somerset DA, Zheng Y, Kilby MD, Sansom DM, Drayson MT. Normal human pregnancy is associated with an elevation in the immune suppressive CD25(+) CD4(+) regulatory T-cell subset. *Immunology*. 2004;112(1):38-43.
32. Loewendorf AI, Nguyen TA, Yesayan MN, Kahn DA. Normal Human Pregnancy Results in Maternal Immune Activation in the Periphery and at the Uteroplacental Interface. *PLoS One*. 2014;9(5):e96723.
33. Tsuda S, Zhang XX, Hamana H, Shima T, Ushijima A, Tsuda K, et al. Clonally Expanded Decidual Effector Regulatory T Cells Increase in Late Gestation of Normal Pregnancy, but Not in Preeclampsia, in Humans. *Front Immunol*. 2018;9:1934.
34. Jin LP, Chen QY, Zhang T, Guo PF, Li DJ. The CD4(+)CD25(bright) regulatory T cells and CTLA-4 expression in peripheral and decidual lymphocytes are down-regulated in human miscarriage. *Clin Immunol*. 2009;133(3):402-10.
35. Hsu P, Santner-Nanan B, Joung S, Peek MJ, Nanan R. Expansion of CD4(+)JHLA-G(+) T Cell in Human Pregnancy is Impaired in Pre-eclampsia. *Am J Reprod Immunol*. 2014;71(3):217-28.
36. Aluvihare VR, Kallikourdis M, Betz AG. Regulatory T cells mediate maternal tolerance to the fetus. *Nat Immunol*. 2004;5(3):266-71.

37. Zenclussen AC, Gerlof K, Zenclussen ML, Sollwedel A, Bertoja AZ, Ritter T, et al. Abnormal T-cell reactivity against paternal antigens in spontaneous abortion: Adoptive transfer of pregnancy-induced CD4⁺CD25⁺ T regulatory cells prevents fetal rejection in a murine abortion model. *Am J Pathol.* 2005;166(3):811-22.
38. Da Silva JAP, Spector TD. The role of pregnancy in the course and aetiology of rheumatoid arthritis. *Clin Rheumatol.* 1992;11(2):189-94.
39. Barrett JH, Brennan P, Fiddler M, Silman AJ. Does rheumatoid arthritis remit during pregnancy and relapse postpartum? Results from a nationwide study in the United Kingdom performed prospectively from late pregnancy. *Arthritis Rheum.* 1999;42(6):1219-27.
40. Forger F, Marcoli N, Gadola S, Moller B, Villiger PM, Ostensen M. Pregnancy induces numerical and functional changes of CD4⁺CD25^{high} regulatory T cells in patients with rheumatoid arthritis. *Ann Rheum Dis.* 2008;67(7):984-90.
41. Munoz-Suano A, Kallikourdis M, Sarris M, Betz AG. Regulatory T cells protect from autoimmune arthritis during pregnancy. *J Autoimmun.* 2012;38(2-3):J103-8.
42. Confavreux C, Hutchinson M, Hours MM, Cortinovis-Tourniaire P, Moreau T. Rate of pregnancy-related relapse in multiple sclerosis. *New Engl J Med.* 1998;339(5):285-91.
43. Sanchez-Ramon S, Navarro J, Aristimuno C, Rodriguez-Mahou M, Bellon JM, Fernandez-Cruz E, et al. Pregnancy-induced expansion of regulatory T-lymphocytes may mediate protection to multiple sclerosis activity. *Immunol Lett.* 2005;96(2):195-201.
44. Iorio R, Frisullo G, Nociti V, Patanella KA, Bianco A, Marti A, et al. T-bet, pSTAT1 and pSTAT3 expression in peripheral blood mononuclear cells during pregnancy correlates with post-partum activation of multiple sclerosis. *Clin Immunol.* 2009;131(1):70-83.
45. Rowe JH, Ertelt JM, Aguilera MN, Farrar MA, Way SS. Foxp3⁺ Regulatory T Cell Expansion Required for Sustaining Pregnancy Compromises Host Defense against Prenatal Bacterial Pathogens. *Cell Host Microbe.* 2011;10(1):54-64.
46. Zhao JX, Zeng YY, Liu Y. Fetal alloantigen is responsible for the expansion of the CD4⁺CD25⁺ regulatory T cell pool during pregnancy. *J Reprod Immunol.* 2007;75(2):71-81.
47. Fallarino F, Grohmann U, You S, McGrath BC, Cavener DR, Vacca C, et al. The combined effects of tryptophan starvation and tryptophan catabolites down-regulate T cell receptor zeta-chain and induce a regulatory phenotype in naive T cells. *J Immunol.* 2006;176(11):6752-61.
48. Schrocksnadel H, BaierBitterlich G, Dapunt O, Wachter H, Fuchs D. Decreased plasma tryptophan in pregnancy. *Obstet Gynecol.* 1996;88(1):47-50.
49. Cobbold SP, Adams E, Farquhar CA, Nolan KF, Howie D, Lui KO, et al. Infectious tolerance via the consumption of essential amino acids and mTOR signaling. *Proc Natl Acad Sci U S A.* 2009 Jul 21;106(29):12055-60.

50. Lindsay KL, Hellmuth C, Uhl O, Buss C, Wadhwa PD, Koletzko B, et al. Longitudinal Metabolomic Profiling of Amino Acids and Lipids across Healthy Pregnancy. *PLoS One*. 2015;10(12):e0145794.
51. Sinclair LV, Rolf J, Emslie E, Shi YB, Taylor PM, Cantrell DA. Control of amino-acid transport by antigen receptors coordinates the metabolic reprogramming essential for T cell differentiation. *Nat Immunol*. 2013;14(5):500-8.
52. Chi H. Regulation and function of mTOR signalling in T cell fate decisions. *Nat Rev Immunol*. 2012;12(5):325-38.
53. Jewell JL, Russell RC, Guan KL. Amino acid signalling upstream of mTOR. *Nat Rev Mol Cell Biol*. 2013;14(3):133-9.
54. Saxton RA, Knockenhauer KE, Wolfson RL, Chantranupong L, Pacold ME, Wang T, et al. METABOLISM Structural basis for leucine sensing by the Sestrin2-mTORC1 pathway. *Science*. 2016;351(6268):53-8.
55. Power LL, Popplewell EJ, Holloway JA, Diaper ND, Warner JO, Jones CA. Immunoregulatory molecules during pregnancy and at birth. *J Reprod Immunol*. 2002;56(1-2):19-28.
56. Klysz D, Tai XG, Robert PA, Craveiro M, Cretenet G, Oburoglu L, et al. Glutamine-dependent alpha-ketoglutarate production regulates the balance between T helper 1 cell and regulatory T cell generation. *Sci Signal*. 2015;8(396):ra97.
57. Metzler B, Gfeller P, Guinet E. Restricting Glutamine or Glutamine-Dependent Purine and Pyrimidine Syntheses Promotes Human T Cells with High FOXP3 Expression and Regulatory Properties. *J Immunol*. 2016;196(9):3618-30.
58. Xu T, Stewart KM, Wang XH, Liu K, Xie M, Ryu JK, et al. Metabolic control of T(H)17 and induced T-reg cell balance by an epigenetic mechanism. *Nature*. 2017;548(7666):228-33.
59. Johnson MO, Wolf MM, Madden MZ, Andrejeva G, Sugiura A, Contreras DC, et al. Distinct Regulation of Th17 and Th1 Cell Differentiation by Glutaminase-Dependent Metabolism. *Cell*. 2018;175(7):1780-95.e19.
60. Darmaun D, Dechelotte P. Role of leucine as a precursor of glutamine alpha-amino nitrogen in vivo in humans. *Am J Physiol*. 1991;260(2):E326-9.
61. Nakaya M, Xiao YC, Zhou XF, Chang JH, Chang M, Cheng XH, et al. Inflammatory T Cell Responses Rely on Amino Acid Transporter ASCT2 Facilitation of Glutamine Uptake and mTORC1 Kinase Activation. *Immunity*. 2014;40(5):692-705.
62. Berod L, Friedrich C, Nandan A, Freitag J, Hagemann S, Harmrolfs K, et al. De novo fatty acid synthesis controls the fate between regulatory T and T helper 17 cells. *Nat Med*. 2014;20(11):1327-33.
63. Michalek RD, Gerriets VA, Jacobs SR, Macintyre AN, MacIver NJ, Mason EF, et al. Cutting Edge: Distinct Glycolytic and Lipid Oxidative Metabolic Programs Are Essential for Effector and Regulatory CD4(+) T Cell Subsets. *J Immunol*. 2011;186(6):3299-303.
64. Gualdoni GA, Mayer KA, Goschl L, Boucheron N, Ellmeier W, Zlabinger GJ. The AMP analog AICAR modulates the T-reg/T(h)17 axis through enhancement of fatty acid oxidation. *FASEB J*. 2016;30(11):3800-9.

65. Raud B, Roy DG, Divakaruni AS, Tarasenko TN, Franke R, Ma EH, et al. Etomoxir Actions on Regulatory and Memory T Cells Are Independent of Cpt1a-Mediated Fatty Acid Oxidation. *Cell Metab.* 2018;28(3):504-15.e7.
66. Yang K, Blanco DB, Neale G, Vogel P, Avila J, Clish CB, et al. Homeostatic control of metabolic and functional fitness of Treg cells by LKB1 signalling. *Nature.* 2017;548(7669):602-6.
67. He NH, Fan WW, Henriquez B, Yu RT, Atkins AR, Liddle C, et al. Metabolic control of regulatory T cell (Treg) survival and function by Lkb1. *Proc Natl Acad Sci U S A.* 2017;114(47):12542-7.
68. Haghikia A, Jorg S, Duscha A, Berg J, Manzel A, Waschbisch A, et al. Dietary Fatty Acids Directly Impact Central Nervous System Autoimmunity via the Small Intestine. *Immunity.* 2015;43(4):817-29.
69. Chen XQ, Su WR, Wan TS, Yu JF, Zhu WJ, Tang F, et al. Sodium butyrate regulates Th17/Treg cell balance to ameliorate uveitis via the Nrf2/F10-1 pathway. *Biochem Pharmacol.* 2017;142:111-9.
70. Arpaia N, Campbell C, Fan XY, Dikly S, van der Veeken J, deRoos P, et al. Metabolites produced by commensal bacteria promote peripheral regulatory T-cell generation. *Nature.* 2013;504(7480):451-5.
71. Furusawa Y, Obata Y, Fukuda S, Endo TA, Nakato G, Takahashi D, et al. Commensal microbe-derived butyrate induces the differentiation of colonic regulatory T cells. *Nature.* 2013;504(7480):446-50.
72. de Agüero MG, Ganai-Vonarburg SC, Fuhner T, Rupp S, Uchimura Y, Li H, et al. The maternal microbiota drives early postnatal innate immune development. *Science.* 2016;351(6279):1296-301.
73. De Rosa V, Procaccini C, Cali G, Pirozzi G, Fontana S, Zappacosta S, et al. A key role of leptin in the control of regulatory T cell proliferation. *Immunity.* 2007;26(2):241-55.
74. Matarese G, Di Giacomo A, Sanna V, Lord GM, Howard JK, Di Tuoro A, et al. Requirement for leptin in the induction and progression of autoimmune encephalomyelitis. *J Immunol.* 2001;166(10):5909-16.
75. Chehab FE, Lim ME, Lu RH. Correction of the sterility defect in homozygous obese female mice by treatment with the human recombinant leptin. *Nat Genet.* 1996;12(3):318-20.
76. Jansson N, Greenwood SL, Johansson BR, Powell TL, Jansson T. Leptin stimulates the activity of the system A amino acid transporter in human placental villous fragments. *J Clin Endocrinol Metab.* 2003;88(3):1205-11.
77. Masuzaki H, Ogawa Y, Sagawa N, Hosoda K, Matsumoto T, Mise H, et al. Nonadipose tissue production of leptin: Leptin as a novel placenta-derived hormone in humans. *Nat Med.* 1997;3(9):1029-33.
78. Senaris R, GarciaCaballero T, Casabiell X, Gallego R, Castro R, Considine RV, et al. Synthesis of leptin in human placenta. *Endocrinology.* 1997;138(10):4501-4.
79. Trujillo-Guiza ML, Senaris R. Leptin resistance during pregnancy is also exerted at the periphery. *Biol Reprod.* 2018;98(5):654-63.
80. Tessier DR, Ferraro ZM, Gruslin A. Role of leptin in pregnancy: Consequences of maternal obesity. *Placenta.* 2013;34(3):205-11.

81. Farley DM, Choi J, Dudley DJ, Li C, Jenkins SL, Myatt L, et al. Placental Amino Acid Transport and Placental Leptin Resistance in Pregnancies Complicated by Maternal Obesity. *Placenta*. 2010;31(8):718-24.
82. de Kivit S, Mensink M, Hoekstra AT, Berlin I, Derks RJE, Both D, et al. Stable human regulatory T cells switch to glycolysis following TNF receptor 2 costimulation. *Nat Metab*. 2020 Oct;2(10):1046-61.
83. Timilshina M, You ZW, Lacher SM, Acharya S, Jiang LY, Kang YR, et al. Activation of Mevalonate Pathway via LKB1 Is Essential for Stability of T-reg Cells. *Cell Rep*. 2019;27(10):2948-61.e7.
84. Gerriets VA, Kishton RJ, Johnson M, Cohen S, Siska PJ, Nichols AG, et al. Foxp3 and Toll-like receptor signaling balance T-reg cell anabolic metabolism for suppression. *Nat Immunol*. 2016;17(12):1459-66.
85. Angelin A, Gil-de-Gomez L, Dahiya S, Jiao J, Guo LL, Levine MH, et al. Foxp3 Reprograms T Cell Metabolism to Function in Low-Glucose, High-Lactate Environments. *Cell Metabol*. 2017;25(6):1282-93.e7.
86. Beier UH, Angelin A, Akimova T, Wang LQ, Liu YJ, Xiao HY, et al. Essential role of mitochondrial energy metabolism in Foxp3(+) T-regulatory cell function and allograft survival. *FASEB J*. 2015;29(6):2315-26.
87. Cluxton D, Petrasca A, Moran B, Fletcher JM. Differential Regulation of Human Treg and Th17 Cells by Fatty Acid Synthesis and Glycolysis. *Front Immunol*. 2019 Feb 4;10:115.
88. Zeng H, Yang K, Cloer C, Neale G, Vogel P, Chi HB. mTORC1 couples immune signals and metabolic programming to establish T-reg-cell function. *Nature*. 2013;499(7459):485-90.
89. Lacher SM, Bruttger J, Kalt B, Berthelet J, Rajalingam K, Wortge S, et al. HMG-CoA reductase promotes protein prenylation and therefore is indispensable for T-cell survival. *Cell Death Dis*. 2017 May 25;8(5):e2824.
90. Wang HP, Franco F, Tsui YC, Xie X, Trefny MP, Zappasodi R, et al. CD36-mediated metabolic adaptation supports regulatory T cell survival and function in tumors. *Nat Immunol*. 2020 Mar;21(3):298-308.
91. Field CS, Baixauli F, Kyle RL, Puleston DJ, Cameron AM, Sanin DE, et al. Mitochondrial Integrity Regulated by Lipid Metabolism Is a Cell-Intrinsic Checkpoint for Treg Suppressive Function. *Cell Metab*. 2020;31(2):422-37.e5.
92. Raphael I, Nalawade S, Eagar TN, Forsthuber TG. T cell subsets and their signature cytokines in autoimmune and inflammatory diseases. *Cytokine*. 2015;74(1):5-17.
93. Marzi M, Vigano A, Trabattoni D, Villa ML, Salvaggio A, Clerici E, et al. Characterization of type 1 and type 2 cytokine production profile in physiologic and pathologic human pregnancy. *Clin Exp Immunol*. 1996;106(1):127-33.
94. Reinhard G, Noll A, Schlebusch H, Mallmann P, Ruecker AV. Shifts in the TH1/TH2 balance during human pregnancy correlate with apoptotic changes. *Biochem Biophys Res Commun*. 1998;245(3):933-8.
95. Tranchot-Diallo J, Gras G, ParnetMathieu F, Benveniste O, Marce D, Roques P, et al. Modulations of cytokine expression in pregnant women. *Am J Reprod Immunol*. 1997;37(3):215-26.

96. Saito S, Sakai M, Sasaki Y, Tanebe K, Tsuda H, Michimata T. Quantitative analysis of peripheral blood Th0, Th1, Th2 and the Th1: Th2 cell ratio during normal human pregnancy and preeclampsia. *Clin Exp Immunol*. 1999;117(3):550-5.
97. Kuwajima T, Suzuki S, Sawa R, Yoneyama Y, Takeshita T, Araki T. Changes in maternal peripheral T helper 1-type and T helper 2-type immunity during labor. *Tohoku J Exp Med*. 2001;194(2):137-40.
98. Omu AE, Al-Qattan F, Diejomaoh ME, Al-Yatama M. Differential levels of T helper cytokines in preeclampsia: pregnancy, labor and puerperium. *Acta Obstet Gynecol Scand*. 1999;78(8):675-80.
99. Fallon PG, Jolin HE, Smith P, Emson CL, Townsend MJ, Fallon R, et al. IL-4 induces characteristic Th2 responses even in the combined absence of IL-5, IL-9, and IL-13. *Immunity*. 2002;17(1):7-17.
100. Chang WK, Yang KD, Shaio MF. Effect of glutamine on Th1 and Th2 cytokine responses of human peripheral blood mononuclear cells. *Clin Immunol*. 1999;93(3):294-301.
101. Caris AV, Lira FS, de Mello MT, Oyama LM, dos Santos RVT. Carbohydrate and glutamine supplementation modulates the Th1/Th2 balance after exercise performed at a simulated altitude of 4500 m. *Nutrition*. 2014;30(11-12):1331-6.
102. Ko HM, Kang NI, Kim YS, Lee YM, Jin ZW, Jung YJ, et al. Glutamine preferentially inhibits T-helper type 2 cell-mediated airway inflammation and late airway hyperresponsiveness through the inhibition of cytosolic phospholipase A(2) activity in a murine asthma model. *Clin Exp Allergy*. 2008;38(2):357-64.
103. Clark DA, Blois S, Kandil J, Handjiski B, Manuel J, Arck PC. Reduced uterine indoleamine 2,3-dioxygenase versus increased Th1/Th2 cytokine ratios as a basis for occult and clinical pregnancy failure in mice and humans. *Am J Reprod Immunol*. 2005;54(4):203-16.
104. Xu H, Oriss TB, Fei MJ, Henry AC, Melgert BN, Chen L, et al. Indoleamine 2,3-dioxygenase in lung dendritic cells promotes Th2 responses and allergic inflammation. *Proc Natl Acad Sci U S A*. 2008;105(18):6690-5.
105. Schrocksnadel K, Widner B, Bergant A, Neutrauer G, Schennach H, Schrocksnadel H, et al. Longitudinal study of tryptophan degradation during and after pregnancy. *Life Sci*. 2003;72(7):785-93.
106. Angela M, Endo Y, Asou HK, Yamamoto T, Tumes DJ, Tokuyama H, et al. Fatty acid metabolic reprogramming via mTOR-mediated inductions of PPAR gamma directs early activation of T cells. *Nat Commun*. 2016;7:13683.
107. Tibbitt CA, Stark JM, Martens L, Ma JJ, Mold JE, Deswarte K, et al. Single-Cell RNA Sequencing of the T Helper Cell Response to House Dust Mites Defines a Distinct Gene Expression Signature in Airway Th2 Cells. *Immunity*. 2019;51(1):169-84.
108. Henriksson J, Chen X, Gomes T, Ullah U, Meyer KB, Miragaia R, et al. Genome-wide CRISPR Screens in T Helper Cells Reveal Pervasive Crosstalk between Activation and Differentiation. *Cell*. 2019;176(4):882-96.e18.

109. Chen T, Tibbitt CA, Feng XG, Stark JM, Rohrbeck L, Rausch L, et al. PPAR-gamma promotes type 2 immune responses in allergy and nematode infection. *Sci Immunol*. 2017 Mar 10;2(9):eaal5196.
110. Nobs SP, Natali S, Pohlmeier L, Okreglicka K, Schneider C, Kurrer M, et al. PPAR gamma in dendritic cells and T cells drives pathogenic type-2 effector responses in lung inflammation. *J Exp Med*. 2017;214(10):3015-35.
111. Park HJ, Kim DH, Choi JY, Kim WJ, Kim JY, Senejani AG, et al. PPAR gamma Negatively Regulates T Cell Activation to Prevent Follicular Helper T Cells and Germinal Center Formation. *PLoS One*. 2014 Jun 12;9(6):e99127.
112. Micosse C, von Meyenn L, Steck O, Kipfer E, Adam C, Simillion C, et al. Human "T(H)9" cells are a subpopulation of PPAR-gamma(+) T(H)2 cells. *Sci Immunol*. 2019 Jan 18;4(31):eaat5943.
113. Trompette A, Gollwitzer ES, Yadava K, Sichelstiel AK, Sprenger N, Ngom-Bru C, et al. Gut microbiota metabolism of dietary fiber influences allergic airway disease and hematopoiesis. *Nat Med*. 2014;20(2):159-66.
114. Wen T, Aronow BJ, Rochman Y, Rochman M, Kiran KC, Dexheimer PJ, et al. Single-cell RNA sequencing identifies inflammatory tissue T cells in eosinophilic esophagitis. *J Clin Invest*. 2019;129(5):2014-28.

How to cite this article:

Jenkins BJ, Rees A, Jones N, Thornton CA. Does Altered Cellular Metabolism Underpin the Normal Changes to the Maternal Immune System during Pregnancy? *Immunometabolism*. 2021;3(4):e210031. <https://doi.org/10.20900/immunometab20210031>

8.4 Immunometabolic adaptation and immune plasticity in pregnancy and the bi-directional effects of obesity

Clinical and Experimental Immunology, 2022, **208**, 133–148
<https://doi.org/10.1093/cxi/uxac003>
Advance access publication 24 February 2022
Review



OXFORD

Review

Immunometabolic adaptation and immune plasticity in pregnancy and the bi-directional effects of obesity

April Rees, Oliver Richards, Megan Chambers, Benjamin J. Jenkins, James G. Cronin, Catherine A. Thornton*

Institute of Life Science, Swansea University Medical School, Swansea, Wales SA2 8PP, UK

*Corresponding author: Cathy Thornton, IL51, Swansea University Medical School, Singleton Campus, Swansea University, Swansea, Wales SA2 8PP, UK.
Email: c.a.thornton@swansea.ac.uk

Summary

Mandatory maternal metabolic and immunological changes are essential to pregnancy success. Parallel changes in metabolism and immune function make immunometabolism an attractive mechanism to enable dynamic immune adaptation during pregnancy. Immunometabolism is a burgeoning field with the underlying principle being that cellular metabolism underpins immune cell function. With whole body changes to the metabolism of carbohydrates, protein and lipids well recognised to occur in pregnancy and our growing understanding of immunometabolism as a determinant of immunoinflammatory effector responses, it would seem reasonable to expect immune plasticity during pregnancy to be linked to changes in the availability and handling of multiple nutrient energy sources by immune cells. While studies of immunometabolism in pregnancy are only just beginning, the recognised bi-directional interaction between metabolism and immune function in the metabolic disorder obesity might provide some of the earliest insights into the role of immunometabolism in immune plasticity in pregnancy. Characterised by chronic low-grade inflammation including in pregnant women, obesity is associated with numerous adverse outcomes during pregnancy and beyond for both mother and child. Concurrent changes in metabolism and immunoinflammation are consistently described but any causative link is not well established. Here we provide an overview of the metabolic and immunological changes that occur in pregnancy and how these might contribute to healthy versus adverse pregnancy outcomes with special consideration of possible interactions with obesity.

Keywords: obesity, pregnancy, immunometabolism, plasticity

Abbreviations: AT, adipose tissue; ATP, adenosine triphosphate; BMI, body mass index; FAO, fatty acid oxidation; FAT, fatty acid translocase; FFA, free fatty acids; GDM, gestational diabetes mellitus; GLUT, glucose transporters; HDL, high-density lipoprotein; LDL, low-density lipoprotein; LPS, lipopolysaccharide; mTOR, mammalian target of rapamycin; OXPHOS, oxidative phosphorylation; P3C, Pam3CysSK₂; ROS, reactive oxygen species; sCD38, soluble CD38; T2DM, type 2 diabetes mellitus; VLDL, very low density lipoprotein

Introduction

To meet the high-energy demands of pregnancy, mandatory maternal physiological changes are required to provide a suitable and continuous metabolic supply from the mother to the foetus [1]. Some metabolic adaptations include the switch from accumulating lipids [2–4] to lipolysis [5] accompanied by the development of insulin resistance [6] through gestation (Fig. 1). In addition to metabolic changes, immunological changes are required to prevent maternal rejection of the foetus, which expresses paternal antigens and is referred to as a semi-allograft [7]. It is now well recognised that the immunoinflammatory processes initiated in response to the blastocyst, embryo then foetus are essential to every stage of pregnancy ensuring successful implantation, gestation, and finally parturition [8–13]. Cellular metabolism has emerged as a key determinant of immune cell function; the pivotal contribution of this is recognised through the term immunometabolism and the associated burgeoning literature [14–17]. Immunometabolic adaptations are well recognised

to alter cytokine production, phagocytosis, proliferation, reactive oxygen species (ROS) production, cell death and other effector function of all immune cell types, and there are plenty of reviews that explore this generally [18, 19] or in disease specific settings especially cancer and cardiovascular disease [20, 21].

Exquisite temporal and spatial control of immunoinflammatory and metabolic pathways ensure a successful pregnancy that delivers a healthy baby at full term. Disrupted immunoinflammatory and metabolic homeostasis consequently underpin a host of adverse obstetric outcomes from miscarriage [22] to preeclampsia [23–25], gestational diabetes [26–28], and preterm birth [11]. Understanding this interplay in adverse and healthy pregnancy serves two key purposes. With regards to adverse pregnancy, elucidating underpinning mechanisms will clearly have positive impacts on prognosis, diagnosis, intervention, and treatment for better pregnancy outcomes. In parallel, illuminating the normal immunometabolic adaptations that occur in healthy

Received 15 September 2021; Revised 16 December 2021; Accepted for publication 24 January 2022

© The Author(s) 2022. Published by Oxford University Press on behalf of the British Society for Immunology. All rights reserved. For permissions, please e-mail: journals.permissions@oup.com

The above article has now been published Open Access.

© The Author(s) 2022. Published by Oxford University Press on behalf of the British Society for Immunology. Distributed under the terms of a Creative Commons Attribution 4.0 International License (CC BY 4.0).

Library Research Support/Open Access Team 21/12/2023.



Figure 1: The key whole body metabolic changes that occur as pregnancy progresses. The accumulation of lipids decreases with pregnancy while lipolysis increases. The mother becomes less tolerant to glucose and insulin resistance is induced.

pregnancy will increase our knowledge of the breadth of immune plasticity possible in humans and enable us to harness this therapeutically for multiple diseases, including those outside of the setting of pregnancy. For example, clinical improvements in rheumatoid arthritis and multiple sclerosis are common in pregnant women, especially in the third trimester [29–32], so understanding why this occurs could reveal shared mechanistic processes in these diseases as well as targets for disease improvement in all people with these autoimmune diseases.

Abnormal and/or excessive fat accumulation with systemic low-grade inflammation to create a health risk characterises obesity [33]. A body mass index (BMI = weight (kg)/height (m)²) above 30.0 is classed as obese in accordance with World Health Organisation (WHO) criteria, with those with a BMI \geq 40.0 classed as morbidly obese. Obesity is a global epidemic, with prevalence rates increasing worldwide in both developing and developed countries. In England 2019, 29% of adults and 18% of children were classed as obese [34]. Obesity leads to serious comorbidities such as type 2 diabetes mellitus (T2DM), reproductive dysfunction, and cardiovascular disease. In England 2019, 10,660 and 711,000 hospital admissions were directly caused by obesity or where obesity was a factor, respectively [34]. The majority of these hospital admissions were female (74% and 66%, respectively) [34]. In women of reproductive age the prevalence of obesity is between 20% and 28% [34]. Obesity is considered a chronic inflammatory disorder with reciprocal effects on adipose tissue (AT) and immune cells that extend beyond AT into the peripheral circulation and other tissues such as the liver [35]. The interplay between immune and metabolic pathways regulates inflammatory cascades typically initiated by pathogen- and danger-associated molecular patterns (PAMPs and DAMPs) and obesity is now well recognised to perturb a diverse range of inflammatory cascades through effects on these pathways. This is best evidenced by infection complications and increased risk of vaccine failure [36, 37]. Examples include a higher risk for viral and bacterial infections along with secondary infections such as sepsis (women only) and

community-acquired pneumonia [38, 39]. Immunometabolic derangement of key immune cells such as AT macrophages is well described in animal models of obesity and our understanding of similar processes in humans is growing [40]. Given the apparent importance of immunometabolism in immune plasticity in pregnancy, the epidemic of obesity recognised for the bi-directional interaction between the immune system and metabolism [40] poses a particular risk to the maternal-foetal dyad. Here we will review the metabolic changes that occur in pregnancy, explore how they link to immune function at this time and consider the effects of obesity on these. Our focus is inflammation and the contribution of monocytes and macrophages given that obesity is a low-grade chronic systemic inflammatory and balancing pro- and anti-inflammatory processes is critical to pregnancy success.

Pregnancy and immune plasticity

The maternal immune system undergoes dynamic adaptation to pregnancy. This is now well recognised to occur at the materno-foetal interface which is composed of foetal-derived trophoblast cells of the placenta and chorionic membrane juxtaposed to the maternal decidual cell populations in intimate contact with the placenta proper and the foetal-placental membranes but also maternal blood-borne cells within the intervillous space of the placenta as it develops. Systemic changes in maternal immune function also occur with extracellular vesicles of various size from the placenta present in the maternal circulation offering a further site of materno-foetal interaction [41]. Together, this ensures immunoregulatory processes that prevent rejection of the foetus yet maintain protection against pathogens, with the underpinning immune plasticity described as an immune clock [42]. Additional to changes in immune cell subsets both within the uterus and systemically that are extensively reviewed elsewhere [7, 43], both pro- and anti-inflammatory pregnancy stage-specific changes occur as a healthy pregnancy progresses [44]. Contrary to past perceived detrimental effects of these responses, provoking inflammatory cascades

within the uterus and systemically facilitates pregnancy. At the maternal-foetal interface, pro-inflammatory M1 macrophages are dominant in the first stage of pregnancy supporting implantation and contributing to the high levels of tumour necrosis factor- α (TNF α), interleukin (IL)-6, and IL-1 β observed [8, 9]. With the emergence of the developing placenta, an anti-inflammatory M2 milieu becomes dominant supporting trophoblast invasion and vascular remodelling, and includes secretion of mediators such as IL-10 and TGF β [10]. A recent study has further highlighted the critical homeostatic regulatory role of macrophages in a successful pregnancy, with murine models exhibiting insufficient maternal CD11b+ myeloid cells resulting in neonatal death and preterm birth [45]. The expansion of paternal antigen-specific Treg cells and a switch to a Th2 profile with the secretion of IL-4 and IL-10 assists in the prevention of allograft rejection [46, 47]. During the last two trimesters of pregnancy, maternal systemic immunity favours an anti-inflammatory innate phenotype [48]. A number of studies demonstrate that plasma levels of many pro-inflammatory cytokines (e.g. IL-18, TNF α , CCL2, CXCL10, IL-6) are decreased in pregnancy, whereas mediators with immunomodulatory and anti-inflammatory properties (e.g. IL-1 receptor agonist (RA), soluble (s) TNF-receptor II, and sTNF-RII) are elevated [48, 49]. Consequently, perturbed levels of pro-inflammatory cytokines are associated with adverse obstetric outcomes. For example, systemic elevation of IL-6 is associated with preeclampsia [24]. The induction of labour is then associated with a pro-inflammatory state, with pro-inflammatory macrophages infiltrating the decidua to promote uterine contractions [11]. Prior to this, in preparation for delivery, elevated levels of predominantly pro-inflammatory cytokines are observed (e.g. IL-1 β , IL-1 α , IL-6, and IL-8) [12, 13].

As key contributors to inflammatory processes in both pregnancy and obesity, monocytes and macrophages will be the focus of our considerations hereon. Monocytes are key innate effector cells and precursors of macrophages so have a central role in inflammation. They can be characterised as classical CD14⁺CD16⁻ monocytes that account typically for 90–95% of total monocytes, intermediate CD14⁺CD16⁺ monocytes that account for < 1%, and non-classical CD14⁺CD16⁺ that account for 5–10%. While classical monocytes are more prevalent, non-classical monocytes are more pro-inflammatory [50] and are elevated in inflammatory states such as Gram-negative sepsis and rheumatoid arthritis [51–53] and are increased with pregnancy [54]. Monocytes are also typically more activated during pregnancy when compared with non-pregnant women evidence by increased expression of the activation markers CD14, CD64, and CD11b [55, 56]. Monocytes in pregnancy also produce more oxygen-free radicals [55], with elevated oxidative burst [56], but their ability to produce cytokines in comparison to those from non-pregnant women seems to depend on the cell stimulation used [57–61]. Monocytes in pregnancy also appear primed to express IL-12, a type 1 cytokine [60], further implicating monocytes as being in a state of heightened activation in pregnancy.

Despite advances in our understanding of macrophage heterogeneity, they are typically classified into two subsets: M1, typically IFN γ or lipopolysaccharide (LPS) conditioned, that are classically activated and pro-inflammatory; and M2, typically IL-4 conditioned, that are alternatively activated and anti-inflammatory. Macrophages are critical to the

development of the placenta and we have recently reviewed their plasticity in reproduction [62]. They are abundant in the decidua where they contribute to the local tissue micro-environment and in the cycling endometrium in not pregnant women where, due to their fluctuating numbers during the menstrual cycle, they are thought to be regulated by hormonal signalling [63]. Decidual macrophages, which are maternal in origin, have a vital role in implantation producing factors to promote angiogenesis and tissue remodelling and the clearing of apoptotic cells to prevent release of pro-inflammatory products in preparation for trophoblast invasion [64, 65]. The balance of decidual M1/M2 macrophages is critical to successful pregnancy with imbalances linked to complications such as preeclampsia and miscarriage [22, 23, 25, 62], with M1-like polarisation linked to spontaneous preterm labour [66]. Decidual M1 macrophages are associated with the onset of labour as during the third trimester they infiltrate the decidua which can occur prematurely in preterm delivery [11]. Studies have shown, however, that mapping the conventional M1/M2 paradigm to decidual macrophages is challenging, due to their divergent phenotype in the first and second trimester [10, 67]. It is the accumulation of the M1 subset of macrophages in AT which is associated with obesity and confers local inflammation and insulin resistance [68]. AT macrophages are activated via TLR4 by LPS which is elevated in obesity, potentially due to alterations in the gut microbiota, dubbed metabolic endotoxemia [69]. These activated macrophages recruit monocytes and other leukocytes into the AT via expression of chemokine receptors such as CCR2 and CCR5, as well as secretion of chemokines and cytokines. Due to the difficulty in reconciling macrophage phenotypes in humans *in vivo*, future studies should consider unsupervised or high-dimensional approaches such as flow or mass cytometry or single-cell genomics. Advances in multiplex immunohistochemistry and digital spatial profiling that can be conducted on tissue sections likely to revolutionise our understanding of human reproduction biology.

Pregnancy and metabolism

Pregnancy has been described as a diabetogenic state due to increased maternal glucose production, glucose intolerance, and insulin resistance [70]. This is to ensure a continuous supply of glucose to the foetus for growth and development. To fuel her own energy demands over the term of her pregnancy, the mother transitions from an anabolic state in which she stores lipids, to a catabolic state of breaking them down via lipolysis [71]. This is evidenced by a decrease in maternal adipose tissue deposits and an increase in levels of postprandial-free fatty acids (FFAs) in late pregnancy [72]. To meet these energy demands, appetite and therefore food intake is increased, and activity is reduced. Over the course of pregnancy, approximately 30 000 kcal of energy reserves are established, ~3.5 kg of fat is accumulated and the mother, foetus, and placenta synthesise 900 g of new protein. The net energy cost of reproduction has been estimated to be between 75 000 and 85 000 kcal [73] which is equivalent roughly to running 850 miles. During early pregnancy, glycogen and protein synthesis in muscle is increased, whereas in the liver glycogenolysis is increased and glycolysis is decreased. Insulin levels are increased at the start of pregnancy but insulin resistance starts as early as 12–14 weeks of gestation [2]. During the third trimester, there is an increase in maternal ketone

production, intestinal dietary fat absorption is increased, and, in the liver, gluconeogenesis is decreased [74]. Maternal protein storage is also increased during the first half of pregnancy, with these utilised more economically than in the non-pregnant setting in the second half of pregnancy [75, 76].

In the first two trimesters, heightened lipogenesis allows for the accumulation of maternal adipose tissue deposits which are catabolised in the last trimester [4]. The synthesis of triglycerides increases by 40% by 18 weeks of gestation, and by 250% by term [4, 77]. High-density lipoprotein (HDL), very-low density lipoprotein (VLDL), and low-density lipoprotein (LDL) are part of a family termed lipoproteins which are a combination of various types of fats and proteins. They are necessary for the transport of cholesterol and triglycerides through the blood. In the first 24 weeks of gestation, HDL levels increase progressively before decreasing until 32 weeks where they plateau [4]. LDL levels undergo a small decrease during the initial stages of pregnancy before rising steadily [4]. During the second and third trimester, VLDL levels increase threefold. These net increases of lipoprotein levels are due to cholesterol levels being 50% higher in late pregnancy in comparison to pre-pregnancy [4, 77].

Metabolic processes during pregnancy are influenced by hormones such as oestrogen, human placental lactogen, progesterone, and potentially the satiety hormone leptin. These hormones can alter the action of insulin and the utilisation of glucose, leading to the observed diabetic state which pregnancy has been likened to. This can also induce changes in the metabolism of proteins and lipids, as well as increase amino acid and glucose availability for the foetus, whilst meeting the maternal needs by providing FFAs as an alternative energy substrate to maintain homeostasis. The importance of metabolic adaptation in pregnancy is evidenced by the ability to use measures of circulating metabolites to predict gestational age and time to labour onset [78].

Leptin

Leptin signalling plays an important role during pregnancy and obesity independently and with known effects on leukocyte function needs to be considered as a mediator of any interaction between obesity and pregnancy. Leptin is increased with both obesity and pregnancy, but in pregnancies with obesity maternal leptin is actually decreased in comparison to lean pregnant women [79]. Leptin classically controls food intake by interacting with leptin receptor (OB-R; CD295) in the brain [80] and leptin resistance leads to over-indulgence and further fat storage [81]. Leptin is also responsive to other hormones, such as insulin and cortisol which induce upregulation [82] while catecholamines downregulate leptin [83]. Leptin expression is regulated by a multitude of other factors such as TNF α which increases leptin secretion [84] and by glucose and fatty acids [85]. Leukocytes also express OB-R so leptin can have effects on both innate and adaptive immune features. It can activate innate immune cells (e.g. monocytes, NK cells, neutrophils), improve their survival by downregulating apoptosis and upregulating cell proliferation and chemotaxis [86], and enhance their functions such as cytotoxicity (NK cells), phagocytosis (macrophages) and cytokine release [87]. Leptin also favours pro-inflammatory CD16⁺ non-classical monocytes [88] and induces the proliferation of most adaptive immune cell types, except Tregs, and improves their responsiveness to chemotactic signals, while promoting a switch towards

pro-inflammatory Th1 [87]. Overall, leptin promotes a pro-inflammatory phenotype.

Leptin is essential for some reproductive functions, with leptin injections improving the likelihood of conception in infertile mice [89] and leptin initiating the onset of puberty in human females [90]. In normal pregnancy, elevated levels of leptin occur due to not only AT accumulation but also placental production [91]. Leptin has been described as having various gestational regulatory roles including placental angiogenesis, nutrient transport, and immunomodulation [92]. Central leptin resistance develops as a normal part of pregnancy during the second trimester [93] with maternal obesity linked to the development of placental leptin resistance [94]. Foetal growth is supported through central leptin resistance mechanisms in healthy women, but placental leptin resistance in women with obesity adversely affects foeto-placental growth and development [95]. It also seems that central leptin resistance mechanisms might differ in healthy versus pregnant women with obesity and this has been reviewed elsewhere [95]. Very little is known about the immunomodulatory effects of leptin in pregnancies with maternal obesity, although it has been suggested that pre-gravid high circulating leptin levels in women with obesity prime the placental inflammation observed in these pregnancies [96].

Pregnancy and immunometabolism

Immunometabolism is a burgeoning field with the main tenet being that the metabolism of immune cells impacts function (Fig. 2) [14] and we have summarised elsewhere how changes in metabolism with pregnancy might impact T-cell function [97]. Upon activation, many leukocytes appear to prefer glycolysis over oxidative phosphorylation: while less adenosine triphosphate (ATP) is produced per molecule of glucose, glycolysis provides more rapid ATP production along with key biosynthetic intermediates, supporting a rapid effector response [14]. This is evidenced by the elevated appetite for glucose of activated macrophages and CD4⁺ T cells [15, 16] and the inhibition of macrophage activation *in vitro* and suppression of inflammation that occurs *in vivo* after inhibition of glycolysis [98, 99]. Glycolysis is initiated more rapidly via upregulation of enzymes involved in the pathway, whilst increasing oxidative phosphorylation (OXPHOS) is a much slower process requiring mitochondrial biogenesis. Glycolysis at higher rates also enables production of biosynthetic intermediates to support cell growth and proliferation. However, other ATP and metabolite generating pathways do have a role in immune function. For example, the differentiation of macrophages and the production and maintenance of memory CD8⁺ T cells require fatty acid oxidation (FAO) [14].

Our focus in this review is monocytes and macrophages so immunometabolism of these will be a critical determinant of their function in both pregnancy and obesity. Monocyte metabolism has been described mostly in tandem with macrophages which has been well reviewed elsewhere [100, 101]. From the little information about monocytes that we have already the key message seems to be that the metabolic programmes which govern their function are unique to individual stimuli and there is not a "one size fits all" switch to glycolysis [102]. There is a rapid increase in glycolysis in response to the TLR4 ligand LPS but this is not seen with the TLR2 ligand P3C (Pam₂CysSK₄) or alternative bacterial

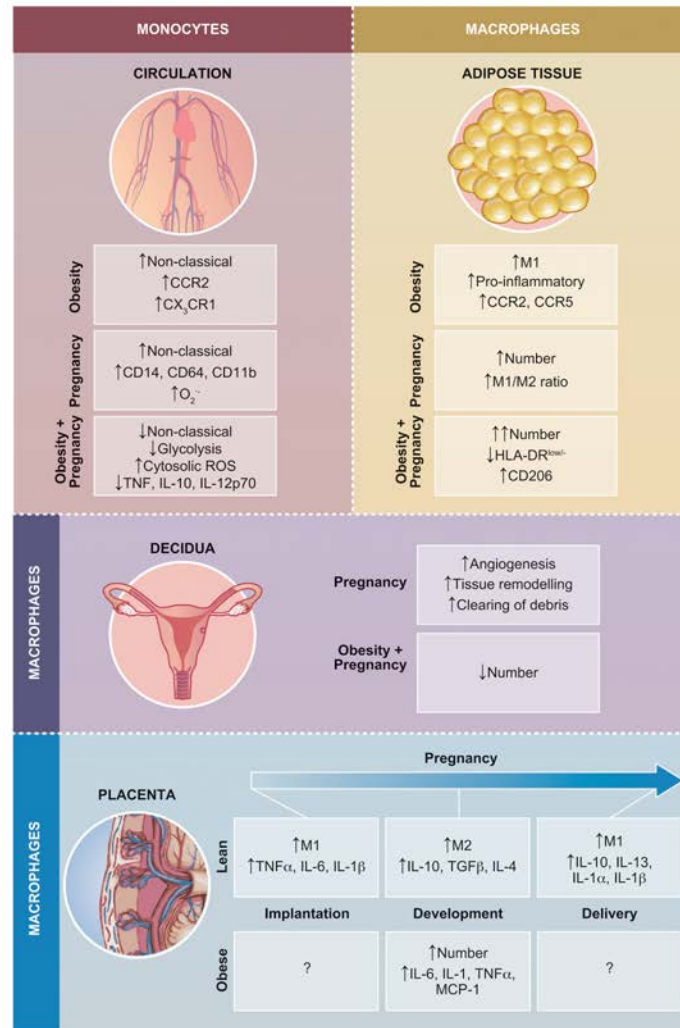


Figure 2: A summary of the effects obesity has on monocytes in the blood and macrophages in adipose tissue and in the placenta. Monocytes: in comparison to lean, obesity is associated with an increase in non-classical (CD14^{high}CD16^{low}) monocytes [212], which are thought to be more pro-inflammatory, as well as an increase in the expression of CCR2 and CX₃CR1 [50, 51]. Pregnancy is also accompanied by an increase in non-classical monocytes. Monocytes in pregnancy also have increased expression of CD14, CD11b and CD64, as well as increased superoxide production [53]. Adipose tissue: obesity is associated with an increase in M1 macrophages, inducing a more pro-inflammatory environment [213]. These macrophages also have elevated expression of chemokine receptors CCR2 and CCR5. During a healthy pregnancy, the number of total macrophages increases in adipose tissue and there is an increase in the M1/M2 ratio. The effect obesity has on pregnancy shows that the number of macrophages is further exacerbated, and also increases the induction of apoptosis. Surface markers on these macrophage changes: lower HLA-DR^{low} and elevated CD206 [22]. Decidua: during a healthy gestation, decidual macrophages promote angiogenesis, tissue remodelling and the clearance of apoptotic cells [68, 214]. Very little is currently understood about decidual macrophages in an obese environment, but their overall numbers are reduced [23]. Placenta:

lysates [102]. To retain their phagocytic and cytokine activity in response to P3C, increased OXPHOS by monocytes is necessary [102]. Mitochondrial morphology might contribute to these differences, as larger mitochondria were observed in the monocytes stimulated with LPS in comparison with P3C after 24-hr stimulation [102].

Early evidence of immunometabolic changes with pregnancy is emerging and includes observations such as reduced pyruvate kinase expression in neutrophils and lymphocytes in pregnancy [103], and reduced glycolytic capacity and basal glycolysis but elevated bioenergetics health index in peripheral blood mononuclear cells of pregnant women [104]. Cyclic ADP ribose hydrolase (CD38), a glycoprotein found on the surface of many leukocytes, provides the best example so far of the potentially diverse effects of immunometabolism on pregnancy. CD38 is a multi-functional ectoenzyme which catalyses reactions that produce cyclic ADP-ribose and nicotinic acid adenine dinucleotide phosphate (NAADP) from NAD⁺ and NADP⁺, respectively, and has been postulated to have critical roles in pregnancy. Soluble CD38 (sCD38) from seminal fluid has a vital role in the establishment of maternal immune tolerance in mice [105]. sCD38 promotes the development of forkhead box P3⁺ (Foxp3⁺) Treg cells and uterine tolerogenic DCs to prevent rejection of the allogeneic foetus, with knockout models showing that pregnancy loss occurs [105]. CD38 is also more highly expressed on NK cells during pregnancy where it is postulated to have role in enhancing their ability to combat-infected cells [106]. This clearly needs elaborating given the contradictory effects on mitochondrial function attributed to CD38 outside of pregnancy. For example, in malignant myeloma cells, CD38 is required for oxidative phosphorylation and intercellular mitochondrial transfer [107], yet studies in aging have found that CD38 levels are inversely proportional to mitochondrial function [108]. Elevated expression of CD38 on NK cells could suggest reduced reliance on mitochondrial respiration, and therefore further investigation into the link between cellular metabolism and function is warranted. The normal immunological adaptations that accompany pregnancy are vital to ensuring pregnancy success so compromise of these could underpin adverse pregnancy outcomes associated with maternal obesity. CD38 expression on monocytes and macrophages is induced in inflammatory conditions [109] and a decrease in the expression of CD38 correlates with suppression of adipogenesis and lipogenesis in adipose tissue in mouse models [110]. Inhibitors of CD38, such as the flavonoid apigenin from foods such as parsley, have shown beneficial effects in tackling obesity in animal models [111]. In these models, elevated cellular levels of NAD⁺ are beneficial, and CD38 knockout increases the NAD⁺ levels and protects against obesity [111].

Pregnancy and obesity

Obesity has been implicated in impaired reproductive function and, in pregnancy, is associated with increased risk of miscarriage and other adverse outcomes such as gestational diabetes mellitus (GDM) and preeclampsia [112–114].

Maternal obesity also increases the risk of foetal mortality, childhood obesity stemming from macrosomia, and metabolic syndromes for both the mother and the foetus [115–117]. Adverse perinatal outcomes linked to obesity have been associated with increased placental and systemic inflammation, oxidative stress, pre-pregnancy maternal insulin levels and hyperinsulinemia [96, 118–120]. Much of the current research on obesity and pregnancy focuses primarily on the effects on the offspring rather than on the pregnant woman herself beyond the immediate obstetric challenges. Studies of the maternal contribution to the obesity-related milieu in pregnancy also tend to focus on the placenta and to a lesser extent AT, and seldom consider the role of or effect on the peripheral, circulating immune system herein represented by monocytes (see Fig. 3 for summary of all three). This is important because obesity has serious effects on the immune system outside of pregnancy with down-regulated immune responsiveness best evidenced by infection complications and increased risk of vaccine failure [36, 37]. Specific examples include a higher risk for viral and bacterial infections along with secondary infections such as sepsis (women only) and community-acquired pneumonia [38, 39]. Obesity is also an indicator for severity of COVID-19 symptoms, with high levels of C reactive protein (CRP) indicating strong critical illness risk [121].

Obesity commonly induces insulin resistance by chronic activation of inflammatory pathways and heightened infiltration of immune cells into metabolic tissue. This leads to impairment of glucose and lipid homeostasis altering nutrient availability and cellular metabolism. TLR signalling has a role in controlling immunometabolism with saturated and polyunsaturated fatty acids acting via TLR4 to induce immunomodulatory effects. In high saturated fat fed mice, TLR4 deficiency protects the mice from obesity [122, 123]. Palmitate, present in high concentrations in the circulation of similarly fed mice, activates the inflammasome and induces macrophage secretion of IL-1 β and IL-18 [124]. Palmitate levels are elevated in obese compared with lean pregnant women [125] and palmitate activates the nucleotide-binding oligomerisation domain-like receptor family pyrin domain containing 3 inflammasome in the placenta for elevated IL-1 β secretion [126]. Increased foetal growth is often correlated with maternal obesity; rat models have shown that placental insulin, IGF-1, mammalian target of rapamycin (mTOR) and leptin signalling pathways are more highly activated in maternal obesity, stimulating increased amino acid transport across the placenta and contributing to elevated foetal growth [127]. AMPK and mTORC1 are nutrient sensing pathways which highly influence macrophage polarisation, suggesting that obesity-associated alterations in metabolite signals induce the accompanying altered immune function described but this has not been studied in pregnancy. Mitochondrial dysfunction and deficiencies have been linked with obesity [128]. Adipocytes in obese AT have reduced mitochondrial oxidative capabilities, lowered mitochondrial biogenesis, and downregulated OXPHOS proteins [129–131].

throughout a healthy pregnancy placental macrophage undergo many changes. At implantation, M1 macrophages are dominant and contribute to the high levels of TNF α , IL-6 and IL-1 β observed [215, 216]. As pregnancy develops, a switch occurs so that M2 are the dominant macrophage phenotype, along with the increased production of IL-10, TGF- β , and IL-4 [217]. At delivery, the macrophages switch back to an M1 phenotype which coincides with elevated production of IL-10, IL-13, IL-1 α , and IL-1 β [8–10]. Little is known about the effect obesity has on macrophages in the placenta but it has been shown that there are more placental macrophages in obesity, and an increase in pro-inflammatory cytokines IL-6, IL-1, TNF α , and MCP-1 [96].

Insight into the possible effect of obesity on immunoinflammatory processes in pregnant women can be provided by the many studies of the general adult population. Excessive leukocyte infiltration in adipose tissue occurs with obesity and contributes to the superfluous production of cytokines, adipokines, and other mediators that drive the characteristic low-grade systemic inflammation [132–134]. Macrophages are postulated to be the primary initiator of this, in turn recruiting other cell types such as monocytes, T cells and B cells, leading to further inflammation. Eosinophils in particular have garnered attention in recent times for their homeostatic roles in AT [135] but consideration of these is beyond the scope of this review. The products of this inflammatory environment are measurable in the circulation such as increased levels of IL-6 and leptin [136, 137]. Obesity has been linked repeatedly to altered peripheral blood leukocyte function at least in the not pregnant population with PBMCs from obese individuals contributing to the systemic chronic low-grade inflammation with their heightened pro-inflammatory phenotype [138]. Inflammation-related adipokines such as osteopontin, lipocalin-2, chitinase-3-like protein 1, and chemerin gene expression are also all upregulated in PBMCs from obese individuals [139].

While the focus of this review is the effects of maternal obesity on monocytes and macrophages obesity in the general population is also recognised to negatively affect the function of multiple lymphocyte populations. This ranges from suppression of T- and NK-cell function – including reductions in cytotoxicity, IFN γ production, and expression of perforin and granzymes [140] – and altered B-cell activity that manifests as reduced class-switching and immunoglobulin activity [141]. Maternal obesity diminishes the numbers of uterine resident NK cells and alters their contribution to extracellular matrix remodelling and growth factor signalling to compromise trophoblast survival and spiral artery remodelling [142]. A reduced CD8+ T-cell count in peripheral blood with obesity in both the general population [143] and pregnant women [144] has been described and possibly links to their accumulation in adipose tissue which, from mouse models, precedes that of macrophages [143]. The cytokine producing capacity of T cells also changes with obesity in the general population and obesity-associated inflammation is in part driven by a shift to Th1 and Th17 which is thought to be mediated by leptin [145]. Th1 and Th17 cytokines such as TNF and IFN γ are detrimental to pregnancy [146]. Conversely, a Th2 and regulatory T-cell (Treg) dominated environment is considered essential to pregnancy success [146]. We do not yet know how maternal obesity impacts this critical cytokine balance but maladaptation of adaptive immune processes could very much underpin obesity-associated adverse obstetric outcomes with upregulation of Th1 described in GDM [147].

The non-classical subpopulation of monocytes is increased with obesity [148] and this is accompanied by functional differences in monocytes. As for heterogenous PBMCs, the response by monocytes also favours a pro-inflammatory phenotype through heightened provision of cytokines such as IL-1 β and RANTES upon LPS stimulation [149]. Non-classical and classical monocytes can also be identified by chemokine receptor expression as being CX $_3$ CR1^{high}/CCR2^{low} or CX $_3$ CR1^{low}/CCR2^{high}, respectively. CCR2 is elevated on total monocytes in obese individuals, and more specifically on classical and intermediate monocytes [149, 150], along with increased intrinsic migratory capacity, potentially due to

this elevated CCR2 expression [150]. Higher expression of CX $_3$ CR1 by all three subsets suggests an inclination to recruitment by CX $_3$ CL1-secreting AT [149]. If these chemokine receptors are found to be exacerbated further during pregnancy with maternal obesity, this might suggest that CCR2-mediated recruitment of maternal monocytes is responsible for the accumulation of pro-inflammatory placental macrophages.

Like pregnancy, there appears to be very little research surrounding specific immune cell bioenergetics in obesity although the spare respiratory capacity of monocytes has been negatively correlated with percentage body fat [151]. A study investigating the effect of the bioenergetic function of peripheral monocytes in obese and lean women with HIV illustrated that the monocytes in obese infected women had impaired bioenergetic health (reduced basal and maximal oxygen consumption rate as well as decreased bioenergetic health index) in comparison to lean infected women [152].

Pregnancy, immunometabolism, and obesity

Inflammatory alterations which occur normally in a healthy pregnancy may be exacerbated with maternal obesity. Further elevated circulating maternal IL-6 and CRP levels have been reported in pregnant women with obesity [96]. This has consequences for the foetus with increased leptin and IL-6 in umbilical cord plasma and acquisition of insulin resistance in utero of new borns of obese mothers [153]. FFA and AT deposits are in excess with maternal obesity and elevated foetal exposure to FFA correlates with neonatal adiposity and potential future obesity of the child [154]. However, the impact of obesity on maternal immunometabolism is largely unknown with also little known about the effects of maternal obesity on monocytes and macrophages. Given the dramatic effects on monocytes of either obesity or pregnancy alone further consideration of the combined effect is certainly warranted. A recent study has shown that at 37 weeks of pregnancy, monocytes from pregnant women with obesity have reduced extracellular acidification rate (glycolysis indicator) at baseline and following LPS and glucose injections [155]. This supports maladapted immunometabolism with maternal obesity and is accompanied by fewer monocytes performing phagocytosis and reduced cytokine response to LPS. The consequences of this effect on monocytes with maternal obesity, however, cannot be concluded without data on how the monocytes adapt metabolically in a healthy pregnancy, and the effect on the monocytes at different trimesters.

Maternal obesity has been associated with changes to macrophages in the placenta and decidua and these have been reviewed elsewhere [156]. Briefly, increased inflammation including heightened gene expression of IL-6, IL-1, TNF α , and MCP-1 linked to increased number of macrophages have been described to occur in the placentas of obese versus lean pregnant women [96] although there are some conflicting findings regarding changes to the number of placental macrophages with maternal obesity [157]. In contrast, decidual macrophage levels are reduced in obese compared with lean women [158]. These changes have been postulated to be linked to placental dysfunction and foetal programming of later child health [96]. AT macrophages in pregnant women are not well studied due to the difficulty obtaining AT from pregnant women. One study using visceral adipose tissue collected from the omentum during caesarean section

found that pregnant women who were overweight or obese had adipocyte hypertrophy and changes to specific populations of macrophages in AT (e.g. lower number of resident HLA-DR^{low} macrophages, higher expression of CD206 on resident and recruited macrophages, and elevated CD11c expression on resident HLA-DR⁺ macrophages) [159].

The fatty acid translocase (FAT) CD36 has been implicated in various obesity-related complications. For example, CD36 is normally highly expressed in AT and is up-regulated further in obesity and T2DM [160]. Animal studies support a role for CD36 in impaired glucose tolerance and insulin signalling in obesity as well as macrophage infiltration into AT and overproduction of inflammatory cytokines and chemokines [161]. While much less studied in humans, monocytes of obese non-pregnant women aged 25–45 years showed significantly decreased expression of CD36 compared with lean individuals [162] but such studies have not been extended to pregnant women. If this phenotype does extend to monocytes from pregnant women, it suggests that the monocytes would be less capable of combating PAMPs or DAMPs, with decreased ability to take up fatty acids, and reduced capability to partake in non-opsonic phagocytosis (which is another role of the scavenger receptor [163, 164]). While little is known about changes in expression of nutrient transporters systemically in pregnant women either with or without obesity the contribution to placental function in health and disease is recognised increasingly and there are also some studies in AT of pregnant women [165]. CD36 is expressed by the placenta supporting responsiveness to lipoproteins in maternal plasma [166]. Upregulation of other transporters in the placenta such as long chain neutral amino acid transporter (LAT1; CD98) and sodium-coupled neutral amino acid transporter (SNAT) 2 has been linked with foetal macrosomia secondary to maternal obesity in murine models [127]. Glucose is transported across the cell plasma membrane via glucose transporters (GLUT). Different GLUTs have different distributions and functions. GLUT1 is expressed on all cells but is expressed most highly in erythrocytes [167] and barrier tissue endothelial cells [168]; GLUT3 is expressed predominantly in neurons [169] and the placenta [170] and GLUT4 in AT [171] and striated muscle [172]. Glucose intolerance is observed commonly in both pregnancy and obesity independently of each other, and in rat models impaired glucose tolerance is further exacerbated in obese pregnancy [173]. GLUT1 is naturally overexpressed in macrophages in obesity, and this induces a pro-inflammatory response dependent on glycolysis and ROS [174]. How these pathways support the immune functions of placental macrophages and trophoblast cells remains to be determined although metabolic disarray of trophoblast cells linked to GDM is a common finding [175, 176].

Obesity is a risk factor for adverse pregnancy outcomes

Gestational diabetes mellitus

Indeed, perhaps the greatest evidence of a link between metabolism and immunoinflammation in pregnancy and a bi-directional interaction with obesity is provided by adverse pregnancy outcomes such as GDM. GDM is characterised by varying severity of glucose intolerance, with onset or recognition during pregnancy and while it usually resolves postpartum [177] it is a risk factor for later development of T2DM [178]. In the not pregnant setting, obesity

induces insulin resistance and T2DM through the release of cytokines such as TNF α and IL-6 [179, 180]. GDM can lead to adverse obstetric outcomes including preeclampsia, birth trauma, and neonatal hypoglycaemia; the offspring have increased risk of developing metabolic and cardiovascular disorders [181, 182]. Obesity, ethnicity, age, and family history of diabetes are strong risk factors for GDM. Acceleration of the insulin resistance that emerges naturally as normal pregnancy progresses (Fig. 1), driven by lifestyle and genetic factors, is potentially what happens in GDM [183, 184]. This could have profound effects on immunoinflammatory phenotypes and thereby disease development and progression if immunometabolism is indeed a key driver of changing immune-cell function in pregnancy. While not extensively studied there are changes in maternal systemic immunity with GDM including upregulation of the Th1 phenotype which alters the Th1/Th2 ratio in comparison to a normal pregnancy [147]. A recent review [185] has described the current understanding of the effect of GDM on maternal peripheral leukocytes highlighting pro-inflammatory effects mostly evidenced by increases in NK cells [186] and activated T cells [187]. However, few studies investigate changes in immune function prior to or in the early stages of GDM and there is a real shortcoming of functional studies assessing the effects of GDM on maternal immunometabolism and the immune response. The placenta has tended to be the focus of GDM investigations and placental changes with GDM include elevated oxidative stress and foetal thrombosis [188, 189]; a recent review aptly describes the pathophysiology of GDM [190]. With regards to immune-cell populations, an increase in NK cells in the placenta of GDM mothers has been reported [186]. Reports of effects of GDM on placental macrophage numbers and function are conflicting. Several studies have reported a more pro-inflammatory phenotype [27, 28, 191], whilst others show that the M2 phenotype is maintained [192] but the contribution of alterations to immunometabolic process remains unknown.

Preeclampsia

Preeclampsia is a hypertensive disorder of pregnancy accompanied by proteinuria which can cause severe effects for mother and foetus. In developed countries, 16% of maternal deaths are caused by hypertensive disorders [193]. The overall risk of preeclampsia is increased by obesity, with the risk increasing as BMI increases and weight loss reducing this risk [194, 195]. It has been hypothesised that obesity is a contributing factor to hypertension via a myriad of mechanisms including: oxidative stress caused by reducing nitric oxide, increased release of free fatty acids from adipocytes, and elevated angiotensinogen [196]. CRP, IL-6, TNF α , and leptin, as discussed above, are found to be elevated in individuals with obesity and are also strongly associated with the development of preeclampsia [197–199]. Abnormalities in placental growth and function drive the pathophysiology of preeclampsia, with changes such as reduced perfusion and oxidative stress inducing a hypertensive environment [200]. As in obesity, both circulating and decidual neutrophils [201, 202] and monocytes [203, 204] have been described to be excessively activated in preeclampsia, with the more pro-inflammatory monocyte subsets (non-classical and intermediate) being elevated even further than they are in a healthy pregnancy [54]. T cells, NK cells and DCs have also been shown to have an altered response in preeclampsia, with

a tendency towards being pro-inflammatory rather than supporting the immune tolerance [205–207].

Conclusion and future outlooks

Much of the effort to understand the contribution of cellular metabolism to immunoinflammatory phenotype and function in pregnancy lies in recent reviews that have covered topics such as the potential role of lactic acid in the uterine micro-environment especially during early pregnancy [208], the potential wider roles of immunometabolism at the maternal-foetal interface [209, 210], the possible contribution of immunometabolism of macrophage fate and function in the pregnant and not pregnant uterus [62], maternal T-cell plasticity in pregnancy [97] and the related area of neonatal immune function [211]. It seems we are on the cusp of greater than ever before understanding of the mechanisms that drive dynamic immune adaption in pregnancy by considering this from the perspective of immunometabolism especially how this links with pregnancy hormone and foetal antigen-driven reactivity. Deep immune phenotyping, other single-cell analysis strategies and spatial profiling of placenta (and adipose tissue) are well placed to support such an analysis.

Acknowledgements

The authors acknowledge the support from Alison Schroeder Medical Illustrator for producing the illustrations in this review.

Funding

C.T. and O.R. receive funding from Diabetes UK. C.T. also receives funding from the Welsh Government – Sêr Cymru scheme, and UKRI (MRC and NERC).

Conflict of interests

None declared.

Author contributions

A.R. and C.T. envisaged and designed the review. A.R. wrote the first draft of the manuscript. O.R., M.C., B.J.J., J.C.G., and C.T. wrote sections of the manuscript. J.C.G. provided oversight of immunometabolism. All authors contributed to the article and approved the final submitted version.

Data availability

Not applicable.

References

- Mouzon SH-d, Lassance L. *Endocrine and metabolic adaptations to pregnancy; impact of obesity*. *Horm Mol Biol Clin Invest* 2015, 24, 65–72. doi:10.1515/hmbci-2015-0042.
- Catalano PM, Tyzbir ED, Wolfe RR, et al Carbohydrate metabolism during pregnancy in control subjects and women with gestational diabetes. *Am J Physiol Endocrinol Metab* 1993, 264, E60.
- Catalano PM, Tyzbir ED, Wolfe RR, Roman NM, Amini SB, Sims EAH. Longitudinal changes in basal hepatic glucose production and suppression during insulin infusion in normal pregnant women. *Am J Obstet Gynecol* 1992, 167, 913–9.
- Alvarez JJ, Montelongo A, Iglesias A, Lasunción MA, Herrera E. Longitudinal study on lipoprotein profile, high density lipoprotein subclass, and postheparin lipases during gestation in women. *J Lipid Res* 1996, 37, 299–308.
- Herrera E, Lasunción MA, Gomez-Coronado D, Aranda P, López-Luna P, Maier I. Role of lipoprotein lipase activity on lipoprotein metabolism and the fate of circulating triglycerides in pregnancy. *Am J Obstet Gynecol* 1988, 158, 1575–83. doi:10.1016/0002-9378(88)90193-7.
- Catalano PM, Tyzbir ED, Roman NM, Amini SB, Sims EAH. Longitudinal changes in insulin release and insulin resistance in nonobese pregnant women. *Am J Obstet Gynecol* 1991, 165, 1667–72. doi:10.1016/0002-9378(91)90012-g.
- Mor G, Aldo P, Alvero AB. The unique immunological and microbial aspects of pregnancy. *Nat Rev Immunol* 2017, 17, 469–82. doi:10.1038/nri.2017.64.
- Rieger L, Honig A, Sutterlin M, et al Antigen-presenting cells in human endometrium during the menstrual cycle compared to early pregnancy. *J Soc Gynecologic Investig* 2004, 11, 488–93.
- Ramhorst R, Grasso E, Paparini D, et al. Decoding the chemokine network that links leukocytes with decidual cells and the trophoblast during early implantation. *Cell Adb Migr* 2016, 10, 197–207. doi:10.1080/19336918.2015.1135285.
- Svensson J, Jenmalm MC, Matussek A, Geffers R, Berg G, Ernerudh J. Macrophages at the fetal-maternal interface express markers of alternative activation and are induced by M-CSF and IL-10. *J Immunol* 2011, 187, 3671–82. doi:10.4049/jimmunol.1100130.
- Hamilton S, Oomomian Y, Stephen G, et al. Macrophages infiltrate the human and rat decidua during term and preterm labor: evidence that decidual inflammation precedes labor. *Biol Reprod* 2012, 86, 1–9.
- Dubicke A, Fransson E, Centini G, et al. Pro-inflammatory and anti-inflammatory cytokines in human preterm and term cervical ripening. *J Reprod Immunol* 2010, 84, 176–85. doi:10.1016/j.jri.2009.12.004.
- Osman I, Young A, Ledingham MA, et al. Leukocyte density and pro-inflammatory cytokine expression in human fetal membranes, decidua, cervix and myometrium before and during labour at term. *Mol Hum Reprod* 2003, 9, 41–5. doi:10.1093/molehr/gag001.
- O'Neill LAJ, Kishton RJ, Rathmell J. A guide to immunometabolism for immunologists. *Nat Rev Immunol* 2016, 16, 553–65. doi:10.1038/nri.2016.70.
- Newsholme P, Curi R, Gordon S, Newsholme EA. Metabolism of glucose, glutamine, long-chain fatty acids and ketone bodies by murine macrophages. *Biochem J* 1986, 239, 121–5. doi:10.1042/bj2390121.
- Alonso D, Nungester W. Comparative study of host resistance of guinea pigs and rats. V. The effect of pneumococcal products on glycolysis and oxygen uptake by polymorphonuclear leukocytes. *J Infect Dis* 1956, 99, 174–81.
- Jones N, Blagih J, Zani F, et al Fructose reprograms glutamine-dependent oxidative metabolism to support LPS-induced inflammation. *Nat Commun* 2021, 12, 1209. doi:10.1038/s41467-021-21461-4
- Loftus RM, Finlay DK. Immunometabolism: cellular metabolism turns immune regulator. *J Biol Chem* 2016, 291, 1–10. doi:10.1074/jbc.R115.693903.
- Norata Giuseppe D, Caligiuri G, Chavakis T, et al. The cellular and molecular basis of translational immunometabolism. *Immunity* 2015, 43, 421–34.
- Zhao S, Peralta RM, Avina-Ochoa N, Delgoffe GM, Kaech SM. Metabolic regulation of T cells in the tumor microenvironment by nutrient availability and diet. *Semin Immunol* 2021, 101485. doi:10.1016/j.smim.2021.101485.
- Ketelhuth DFJ, Lutgens E, Bäck M, et al. Immunometabolism and atherosclerosis: perspectives and clinical significance: a position paper from the Working Group on Atherosclerosis and Vascular Biology of the European Society of Cardiology. *Cardiovasc Res* 2019, 115, 1385–92. doi:10.1093/cvr/cvz166.

22. Tsao F-Y, Wu M-Y, Chang Y-L, Wu C-T, Ho H-N. M1 macrophages decrease in the deciduae from normal pregnancies but not from spontaneous abortions or unexplained recurrent spontaneous abortions. *J Formos Med Assoc* 2018, 117, 204–11. doi:10.1016/j.jfma.2017.03.011.
23. Xu J, Gu Y, Sun J, Zhu H, Lewis DF, Wang Y. Reduced CD200 expression is associated with altered Th1/Th2 cytokine production in placental trophoblasts from preeclampsia. *Am J Reprod Immunol* 2018, 79, 10.1111/aji.12763.
24. Freeman Dilys J, McManus F, Brown Elizabeth A, et al. Short- and long-term changes in plasma inflammatory markers associated with preeclampsia. *Hypertension* 2004, 44, 708–14.
25. Li Z-H, Wang L-L, Liu H, et al. Galectin-9 alleviates LPS-induced preeclampsia-like impairment in rats via switching decidual macrophage polarization to M2 subtype. *Front Immunol* 2019, 9, 3142–3142.
26. Futerman AH. Lipid analysis: a practical approach edited by R. J. Hamilton and S. Hamilton. *J Neurochem* 2016, 64, 1424–5.
27. Mrizak I, Grissa O, Henault B, et al. Placental infiltration of inflammatory markers in gestational diabetic women. *Gen Physiol Biophys* 2014, 33, 169–76. doi:10.4149/gpb_2013075.
28. Pantham P, Aye ILMH, Powell TL. Inflammation in maternal obesity and gestational diabetes mellitus. *Placenta* 2015, 36, 709–15. doi:10.1016/j.placenta.2015.04.006.
29. Confavreux C, Hutchinson M, Hours MM, Cortinovis-Tourniaire P, Moreau T. Rate of pregnancy-related relapse in multiple sclerosis. *N Engl J Med* 1998, 339, 285–91. doi:10.1056/nejm199807303390501.
30. Neuteboom RF, Verbraak E, Wierenga-Wolf AF, et al. Pregnancy-induced fluctuations in functional T-cell subsets in multiple sclerosis patients. *Multiple Sclerosis Journal* 2010, 16, 1073–8. doi:10.1177/1352458510373939.
31. Iannello A, Rolla S, Maghione A, et al. Pregnancy epigenetic signature in T helper 17 and T regulatory cells in multiple sclerosis. *Front Immunol* 2019, 9, 3075. doi:10.3389/fimmu.2018.03075.
32. Pannu N, Singh R, Sharma S, Chopra S, Bhatnagar A. Altered Tregs and oxidative stress in pregnancy associated lupus. *Adv Rheumatol* 2019, 59, 38.
33. Lee H, Lee IS, Choue R. Obesity, inflammation and diet. *Pediatric Gastroenterol Hepatol Nutr* 2013, 16, 143–52. doi:10.5223/pghn.2013.16.3.143.
34. NHS Digital LT. *Statistics on Obesity, Physical Activity and Diet, England, 2019. Statistics on Obesity, Physical Activity and Diet, England: NHS Digital*; 2019.
35. Fabbri E, Sullivan S, Klein S. Obesity and nonalcoholic fatty liver disease: biochemical, metabolic, and clinical implications. *Hepatology (Baltimore, MD)* 2010, 51, 679–89. doi:10.1002/hep.23280.
36. Bochicchio GV, Joshi M, Bochicchio K, Nehman S, Tracy JK, Scalea TM. Impact of obesity in the critically ill trauma patient: a prospective study. *J Am Coll Surg* 2006, 203, 533–8. doi:10.1016/j.jamcollsurg.2006.07.001.
37. Sheridan PA, Paich HA, Handy J, et al. Obesity is associated with impaired immune response to influenza vaccination in humans. *Int J Obes (Lond)* 2012, 36, 1072–7. doi:10.1038/ijo.2011.208.
38. Ghilotti F, Bellocco R, Ye W, Adami H-O, Trolle Lagerros Y. Obesity and risk of infections: results from men and women in the Swedish National March Cohort. *Int J Epidemiol* 2019, 48, 1783–94. doi:10.1093/ije/dyz129.
39. Baik I, Curhan GC, Rimm EB, Bendich A, Willett WC, Fawzi WW. A Prospective study of age and lifestyle factors in relation to community-acquired pneumonia in US men and women. *Arch Intern Med* 2000, 160: 3082–8. doi: 10.1001/archinte.160.20.3082.
40. Ray I, Mahata SK, De RK. Obesity: an immunometabolic perspective. *Front Endocrinol* 2016, 7, 157. doi:10.3389/fendo.2016.00157.
41. Bai K, Li X, Zhong J, et al. Placenta-derived exosomes as a modulator in maternal immune tolerance during pregnancy. *Front Immunol* 2021, 12, 671093–671093. doi:10.3389/fimmu.2021.671093.
42. Aghaeepour N, Ganio EA, McIlwain D, et al. An immune clock of human pregnancy. *Sci Immunol* 2017, 2, ean2946.
43. PrabhuDas M, Bonney E, Caron K, et al. Immune mechanisms at the maternal-fetal interface: perspectives and challenges. *Nat Immunol* 2015, 16, 328–34. doi:10.1038/ni.3131.
44. Murrieta-Coxa JM, Rodríguez-Martínez S, Cancino-Díaz ME, Markert UR, Favaro RR, Morales-Prieto DM. IL-36 cytokines: regulators of inflammatory responses and their emerging role in immunology of reproduction. *Int J Mol Sci* 2019, 20, 1649. doi:10.3390/ijms20071649.
45. Gomez-Lopez N, Garcia-Flores V, Chin PY, et al. Macrophages exert homeostatic actions in pregnancy to protect against preterm birth and fetal inflammatory injury. *JCI insight* 2021, 6, e146089.
46. Svensson-Arvelund J, Mehta RB, Lindau R, et al. The human fetal placenta promotes tolerance against the semiallogeneic fetus by inducing regulatory T cells and homeostatic m2 macrophages. *J Immunol* 2015, 194, 1534–44. doi:10.4049/jimmunol.1401536.
47. Tsuda S, Nakashima A, Shima T, Saito S. New paradigm in the role of regulatory T cells during pregnancy. *Front Immunol* 2019, 10, 573. doi:10.3389/fimmu.2019.00573.
48. Graham C, Chooniedass R, Stefura WP, et al. In vivo immune signatures of healthy human pregnancy: inherently inflammatory or anti-inflammatory?. *PLoS One* 2017, 12, e0177813. doi:10.1371/journal.pone.0177813.
49. Bränn E, Edvinsson A, Rostedt Punga A, Sundström-Paromaa I, Skalkidou A. Inflammatory and anti-inflammatory markers in plasma: from late pregnancy to early postpartum. *Sci Rep* 2019, 9, 1863. doi:10.1038/s41598-018-38304-w.
50. Ziegler-Heitbrock L. The CD14+ CD16+ blood monocytes: their role in infection and inflammation. *J Leukoc Biol* 2007, 81, 584–92. doi:10.1189/jlb.0806510.
51. Gainaru G, Papadopoulos A, Tsangaris I, Lada M, Giamarellos-Bourboulis EJ, Pisticaki A. Increases in inflammatory and CD14(dim)/CD16(pos)/CD45(pos) patrolling monocytes in sepsis: correlation with final outcome. *Crit Care* 2018, 22, 56–56. doi:10.1186/s13054-018-1977-1.
52. Fingerle G, Pforste A, Passlick B, Blumenstein M, Ströbel M, Ziegler-Heitbrock HW. The novel subset of CD14+CD16+ blood monocytes is expanded in sepsis patients. *Blood* 1993, 82, 3170–6.
53. Lacerte P, Brunet A, Egarnes B, Duchêne B, Brown JP, Gosse J. Overexpression of TLR2 and TLR9 on monocyte subsets of active rheumatoid arthritis patients contributes to enhance responsiveness to TLR agonists. *Arthritis Res Therapy* 2016, 18, 10–10. doi:10.1186/s13075-015-0901-1.
54. Melgert BN, Spaans F, Borghuis T, et al. Pregnancy and preeclampsia affect monocyte subsets in humans and rats. *PLoS One* 2012, 7, e45229–e45229. doi:10.1371/journal.pone.0045229.
55. Sacks GP, Studena K, Sargent IL, Redman CWG. Normal pregnancy and preeclampsia both produce inflammatory changes in peripheral blood leukocytes akin to those of sepsis. *Am J Obstet Gynecol* 1998, 179, 80–6.
56. Naccasha N, Gervasi M-T, Chaiworapongsa T, et al. Phenotypic and metabolic characteristics of monocytes and granulocytes in normal pregnancy and maternal infection. *Am J Obstet Gynecol* 2001, 185, 1118–23. doi:10.1067/mob.2001.117682.
57. Luppi P, Haluszczak C, Betteres D, Richard CAH, Trucco M, DeLoia JA. Monocytes are progressively activated in the circulation of pregnant women. *J Leukoc Biol* 2002, 72, 874–84.
58. Veenstra van Nieuwenhoven AL, Bouman A, Moes H, et al. Endotoxin-induced cytokine production of monocytes of third-trimester pregnant women compared with women in the follicular phase of the menstrual cycle. *Am J Obstet Gynecol* 2003, 188, 1073–7.
59. Faas MM, Kunnen A, Dekker DC, et al. Porphyromonas gingivalis and E-coli induce different cytokine production patterns in pregnant women. *PLoS One* 2014, 9, e86355. doi:10.1371/journal.pone.0086355.

60. Sacks GP, Redman CWG, Sargent IL. Monocytes are primed to produce the Th1 type cytokine IL-12 in normal human pregnancy: an intracellular flow cytometric analysis of peripheral blood mononuclear cells. *Clin Exp Immunol* 2003, 131, 490–7.
61. Faas MM, Spaans F, De Vos P. Monocytes and macrophages in pregnancy and pre-eclampsia. *Front Immunol* 2014, 5, 298–298. doi:10.3389/fimmu.2014.00298.
62. Chambers M, Rees A, Cronin JG, Nair M, Jones N, Thornton CA. Macrophage plasticity in reproduction and environmental influences on their function. *Front Immunol* 2021, 11, 3491. doi:10.3389/fimmu.2020.607328.
63. Hunt JS, Miller L, Platt JS. Hormonal regulation of uterine macrophages. *Dev Immunol* 1998, 6, 105–10. doi:10.1155/1998/87527.
64. Gustafsson C, Mjösberg J, Matussek A, et al. Gene expression profiling of human decidual macrophages: evidence for immunosuppressive phenotype. *PLoS One* 2008, 3, e2078–e2078. doi:10.1371/journal.pone.0002078.
65. Abrahams VM, Kim YM, Straszewski SL, Romero R, Mor G. Macrophages and apoptotic cell clearance during pregnancy. *Am J Reprod Immunol* 2004, 51, 275–82. doi:10.1111/j.1600-0897.2004.00156.x.
66. Xu Y, Romero R, Miller D, et al. An M1-like macrophage polarization in decidual tissue during spontaneous preterm labor that is attenuated by rosiglitazone treatment. *J Immunol* 2016, 196, 2476–91. doi:10.4049/jimmunol.1502055.
67. Hunt JS, Manning LS, Wood GW. Macrophages in murine uterus are immunosuppressive. *Cell Immunol* 1984, 85, 499–510. doi:10.1016/0008-8749(84)90262-4.
68. Lumeng CN, Bodzin JL, Saltiel AR. Obesity induces a phenotypic switch in adipose tissue macrophage polarization. *J Clin Invest* 2007, 117, 175–84. doi:10.1172/JCI29881.
69. Cani PD, Amar J, Iglesias MA, et al. Metabolic endotoxemia initiates obesity and insulin resistance. *Diabetes* 2007, 56, 1761–72. doi:10.2337/db06-1491.
70. Hodson K, Dalla Man C, Smith FE, et al. Mechanism of insulin resistance in normal pregnancy. *Horm Metab Res* 2013, 45, 567–71.
71. Diderholm B, Stridsberg M, Ewald U, Lindeberg-Nordén S, Gustafsson J. Increased lipolysis in non-obese pregnant women studied in the third trimester. *BJOG* 2005, 112, 713–8.
72. Barbour LA, McCurdy CE, Hernandez TL, Kirwan JP, Catalano PM, Friedman JE. Cellular mechanisms for insulin resistance in normal pregnancy and gestational diabetes. *Diab Care* 2007, 30, S112–9. doi:10.2337/dc07-s202.
73. Hytten F. Nutritional requirements in pregnancy: what happens if they are not met?. *Midwifery* 1990, 6, 140–5. doi:10.1016/s0266-6138(05)80171-8.
74. Herrera E. Lipid metabolism in pregnancy and its consequences in the fetus and newborn. *Endocrine* 2002, 19, 43–55. doi:10.1385/ENDO:19:1:43.
75. Butte NE, Hopkinson JM, Mehta N, Moon JK, Smith EOB. Adjustments in energy expenditure and substrate utilization during late pregnancy and lactation. *Am J Clin Nutr* 1999, 69, 299–307. doi:10.1093/ajcn/69.2.299.
76. Felig P, Kim YJ, Lynch V, Hendlar R. Amino acid metabolism during starvation in human pregnancy. *J Clin Invest* 1972, 51, 1195–202. doi:10.1172/JCI106913.
77. Sattar N, Greer IA, Loudon J, et al. Lipoprotein subfraction changes in normal pregnancy: threshold effect of plasma triglyceride on appearance of small, dense low density lipoprotein. *J Clin Endocrinol Metabolism* 1997, 82, 2483–91.
78. Liang L, Rasmussen M-LH, Piening B, et al. Metabolic dynamics and prediction of gestational age and time to delivery in pregnant women. *Cell* 2020, 181, 1680–1692.e15. doi:10.1016/j.cell.2020.05.002.
79. Misra VK, Straughen JK, Trudeau S. Maternal serum leptin during pregnancy and infant birth weight: the influence of maternal overweight and obesity. *Obesity (Silver Spring, MD)* 2013, 21, 1064–9. doi:10.1002/oby.20128.
80. Couce ME, Burguera B, Parisi JE, Jensen MD, Lloyd RV. Localization of leptin receptor in the human brain. *Neuroendocrinology* 1997, 66, 145–50. doi:10.1159/000127232.
81. Frederich RC, Hamann A, Anderson S, Löllmann B, Lowell BB, Flier JS. Leptin levels reflect body lipid content in mice: evidence for diet-induced resistance to leptin action. *Nat Med* 1995, 1, 1311–4. doi:10.1038/nm1295-1311.
82. Wabitsch M, Bo Jensen P, Blum WF, et al. Insulin and cortisol promote leptin production in cultured human fat cells. *Diabetes* 1996, 45, 1435–8. doi:10.2337/diab.45.10.1435.
83. Ricci MR, Fried SK. Isoproterenol decreases leptin expression in adipose tissue of obese humans. *Obesity Res* 1999, 7, 233–40. doi:10.1002/j.1550-8528.1999.tb00401.x.
84. Trujillo ME, Lee M-J, Sullivan S, et al. Tumor necrosis factor α and glucocorticoid synergistically increase leptin production in human adipose tissue: role for p38 mitogen-activated protein kinase. *J Clin Endocrinol Metabolism* 2006, 91, 1484–90. doi:10.1210/jc.2005-1901.
85. Minokoshi Y, Toda C, Okamoto S. Regulatory role of leptin in glucose and lipid metabolism in skeletal muscle. *Indian J Endocrinol Metab* 2012, 16, S562–8. doi:10.4103/2230-8210.105573.
86. Bruno A, Conus S, Schmid I, Simon H-U. Apoptotic pathways are inhibited by leptin receptor activation in neutrophils. *J Immunol* 2005, 174, 8090–6. doi:10.4049/jimmunol.174.12.8090.
87. Francisco V, Pino J, Campos-Cabaleiro V, et al. Obesity, fat mass and immune system: role for leptin. *Front Physiol* 2018, 9, 640–640. doi:10.3389/fphys.2018.00640.
88. Cannon JG, Sharma G, Sloan G, et al. Leptin regulates CD16 expression on human monocytes in a sex-specific manner. *Physiol Rep* 2014, 2, e12177. doi:10.14814/phy2.12177.
89. Chehab FF, Lim ME, Lu R. Correction of the sterility defect in homozygous obese female mice by treatment with the human recombinant leptin. *Nat Genet* 1996, 12, 318–20. doi:10.1038/ng0396-318.
90. Matkovic V, Ilich JZ, Skugor M, et al. Leptin is inversely related to age at menarche in human females. *J Clin Endocrinol Metab* 1997, 82, 3239–45.
91. Señaris R, Garcia-Caballero T, Casabiell X, et al. Synthesis of leptin in human placenta. *Endocrinology* 1997, 138, 4501–4.
92. Jansson N, Greenwood SL, Johansson BR, Powell TL, Jansson T. Leptin stimulates the activity of the system a amino acid transporter in human placental villous fragments. *J Clin Endocrinol Metab* 2003, 88, 1205–11. doi:10.1210/jc.2002-021332.
93. Trujillo-Güiza ML, Señaris R. Leptin resistance during pregnancy is also exerted at the periphery†. *Biol Reprod* 2018, 98, 654–63. doi:10.1093/biolre/iy024.
94. Farley DM, Choi J, Dudley DJ, et al. Placental amino acid transport and placental leptin resistance in pregnancies complicated by maternal obesity. *Placenta* 2010, 31, 718–24. doi:10.1016/j.placenta.2010.06.006.
95. Tessier DR, Ferraro ZM, Gruslin A. Role of leptin in pregnancy: consequences of maternal obesity. *Placenta* 2013, 34, 205–11. doi:10.1016/j.placenta.2012.11.035.
96. Challier JC, Basu S, Bintein T, et al. Obesity in pregnancy stimulates macrophage accumulation and inflammation in the placenta. *Placenta* 2008, 29, 274–81. doi:10.1016/j.placenta.2007.12.010.
97. Jenkins BJ, Rees A, Jones N, Thornton CA. Does altered cellular metabolism underpin the normal changes to the maternal immune system during pregnancy?. *Immunometabolism* 2021; 3: e210031 (Abstract e210031). doi: 10.20900/immunometab20210031
98. Michl J, Ohlbaum D, Silverstein S. 2-Deoxyglucose selectively inhibits Fc and complement receptor-mediated phagocytosis in mouse peritoneal macrophages. I. Description of the inhibitory effect. *J Exp Med* 1976, 144, 1465–83.
99. Hamilton JA, Vairo G, Lingelbach SR. CSF-1 stimulates glucose uptake in murine bone marrow-derived macrophages. *Biochem Biophys Res Commun* 1986, 138, 445–54. doi:10.1016/0006-291x(86)90301-3.

100. O'Neill LAJ, Pearce EJ. Immunometabolism governs dendritic cell and macrophage function. *J Exp Med* 2016, 213, 15–23. doi:10.1084/jem.20151570.
101. Mouton AJ, Li X, Hall ME, Hall JE. Obesity, hypertension, and cardiac dysfunction: novel roles of immunometabolism in macrophage activation and inflammation. *Circ Res* 2020, 126, 789–806. doi:10.1161/CIRCRESAHA.119.312321.
102. Lachmandas E, Boutens L, Ratter JM, et al. Microbial stimulation of different Toll-like receptor signalling pathways induces diverse metabolic programmes in human monocytes. *Nat Microbiol* 2016, 2, 16246. doi:10.1038/nmicrobiol.2016.246.
103. Xu Y, Madsen-Bouterse SA, Romero R, et al. Leukocyte pyruvate kinase expression is reduced in normal human pregnancy but not in pre-eclampsia. *Am J Reprod Immunol* 2010, 64, 137–51.
104. Jones N, Piascecka J, Bryant AH, et al. Bioenergetic analysis of human peripheral blood mononuclear cells. *Clin Exp Immunol* 2015, 182, 69–80. doi:10.1111/cei.12662.
105. Kim B-J, Choi Y-M, Rah S-Y, et al. Seminal CD38 is a pivotal regulator for fetomaternal tolerance. *Proc Natl Acad Sci USA* 2015, 112, 1559–64. doi:10.1073/pnas.1413493112.
106. Le Gars M, Seiler C, Kay AW, et al. Pregnancy-induced alterations in NK cell phenotype and function. *Front Immunol* 2019, 10, 2469. doi:10.3389/fimmu.2019.02469.
107. Marlein CR, Piddock RE, Mistry JJ, et al. CD38-driven mitochondrial trafficking promotes bioenergetic plasticity in multiple myeloma. *Cancer Res* 2019, 79, 2285–97. doi:10.1158/0008-5472.CAN-18-0773.
108. Camacho-Pereira J, Tarrago MG, Chini CCS, et al. CD38 dictates age-related NAD decline and mitochondrial dysfunction through an SIRT3-dependent mechanism. *Cell Metab* 2016, 23, 1127–39. doi:10.1016/j.cmet.2016.05.006.
109. Amici SA, Young NA, Narvaez-Miranda J, et al. CD38 is robustly induced in human macrophages and monocytes in inflammatory conditions. *Front Immunol* 2018, 9, 1593. doi:10.3389/fimmu.2018.01593.
110. Wang L-F, Miao L-J, Wang X-N, et al. CD38 deficiency suppresses adipogenesis and lipogenesis in adipose tissues through activating Sirt1/PPAR γ signalling pathway. *J Cell Mol Med* 2018, 22, 101–10. doi:10.1111/jcmm.13297.
111. Escande C, Nin V, Price NL, et al. Flavonoid apigenin is an inhibitor of the NADase CD38. *Diabetes* 2013, 62, 1084–93. doi:10.2337/db12-1139.
112. Lashen H, Fear K, Sturdee DW. Obesity is associated with increased risk of first trimester and recurrent miscarriage: matched case-control study. *Human Reproduction* 2004, 19, 1644–6.
113. Roberts JM, Bodnar LM, Patrick TE, Powers RW. The role of obesity in preeclampsia. *Pregnancy Hyperten* 2011, 1, 6–16. doi:10.1016/j.preghy.2010.10.013.
114. Chu SY, Callaghan WM, Kim SY, et al. Maternal obesity and risk of gestational diabetes mellitus. *Diabetes Care* 2007, 30, 2070–6. doi:10.2337/dc06-2559a.
115. Catalano PM. Management of obesity in pregnancy. *Obstet Gynecol* 2007, 109, 419–33. doi:10.1097/01.aog.0000253311.44696.85.
116. Aune D, Saugstad OD, Henriksen T, Tonstad S. Maternal body mass index and the risk of fetal death, stillbirth, and infant death: a systematic review and meta-analysis. *JAMA* 2014, 311, 1536–46. doi:10.1001/jama.2014.2269.
117. Boney CM, Verma A, Tucker R, Vohr BR. Metabolic syndrome in childhood: association with birth weight, maternal obesity, and gestational diabetes mellitus. *Pediatrics* 2005, 115, e290–6. doi:10.1542/peds.2004-1808.
118. Madan JC, Davis JM, Craig WY, et al. Maternal obesity and markers of inflammation in pregnancy. *Cytokine* 2009, 47, 61–4. doi:10.1016/j.cyto.2009.05.004.
119. Ramsay JE, Ferrell WR, Crawford L, Wallace AM, Greer IA, Sattar N. Maternal obesity is associated with dysregulation of metabolic, vascular, and inflammatory pathways. *J Clin Endocrinol Metab* 2002, 87, 4231–7. doi:10.1210/jc.2002-020311.
120. Catalano PM. The impact of gestational diabetes and maternal obesity on the mother and her offspring. *J Dev Origins Health Dis* 2010, 1, 208–15. doi:10.1017/S2040174410000115.
121. Petrilli CM, Jones SA, Yang J, et al. Factors associated with hospital admission and critical illness among 5279 people with coronavirus disease 2019 in New York City: prospective cohort study. *BMJ* 2020, 369, m1966. doi:10.1136/bmj.m1966.
122. Lee JY, Ye J, Gao Z, et al. Reciprocal modulation of toll-like receptor-4 signaling pathways involving MyD88 and phosphatidylinositol 3-kinase/AKT by saturated and polyunsaturated fatty acids. *J Biol Chem* 2003, 278, 37041–51. doi:10.1074/jbc.m305213200.
123. Davis JE, Gabler NK, Walker-Daniels J, Spurlock ME. Tlr-1255 deficiency selectively protects against obesity induced by diets high in saturated fat. *Obesity* 2008; 16: 1248–1255. doi:10.1038/oby.2008.210.
124. Wen H, Gris D, Lei Y, et al. Fatty acid-induced NLRP3-ASC inflammasome activation interferes with insulin signaling. *Nat Immunol* 2011, 12, 408–15. doi:10.1038/ni.2022.
125. Chen X, Scholl TO, Leskiw M, Savaile J, Stein TP. Differences in maternal circulating fatty acid composition and dietary fat intake in women with gestational diabetes mellitus or mild gestational hyperglycemia. *Diabetes Care* 2010, 33, 2049–54. doi:10.2337/dc10-0693.
126. Rogers LM, Serevani CH, Eastman AJ, et al. Palmitate induces apoptotic cell death and inflammasome activation in human placental macrophages. *Placenta* 2020, 90, 45–51. doi:10.1016/j.placenta.2019.12.009.
127. Rosario FJ, Kanai Y, Powell TL, Jansson T. Increased placental nutrient transport in a novel mouse model of maternal obesity with fetal overgrowth. *Obesity (Silver Spring, Md)* 2015, 23, 1663–70. doi:10.1002/oby.21165.
128. Bourmat JC, Brown CW. Mitochondrial dysfunction in obesity. *Curr Opin Endocrinol Diabetes Obes* 2010, 17, 446–52. doi:10.1097/MED.0b013e32833c3026.
129. Yin X, Lanza IR, Swain JM, Sarr MG, Nair KS, Jensen MD. Adipocyte mitochondrial function is reduced in human obesity independent of fat cell size. *J Clin Endocrinol Metab* 2014, 99, E209–16. doi:10.1210/jc.2013-3042.
130. Semple RK, Crowley VC, Sewter CP, et al. Expression of the thermogenic nuclear hormone receptor coactivator PGC-1 α is reduced in the adipose tissue of morbidly obese subjects. *Int J Obes* 2004, 28, 176–9.
131. Heinonen S, Buzkova J, Muniandy M, et al. Impaired mitochondrial biogenesis in adipose tissue in acquired obesity. *Diabetes* 2015, 64, 3135–45. doi:10.2337/db14-1937.
132. Weinstock A, Moura Silva H, Moore Kathryn J, Schmidt Ann M, Fisher Edward A. Leukocyte heterogeneity in adipose tissue, including in obesity. *Circ Res* 2012, 112, 1590.
133. Anderson EK, Gutierrez DA, Hasty AH. Adipose tissue recruitment of leukocytes. *Curr Opin Lipidol* 2010, 21, 172–7. doi:10.1097/MOL.0b013e3283393867.
134. Apostolopoulos V, de Courten MPJ, Stojanovska L, Blatch GL, Tangalakis K, de Courten B. The complex immunological and inflammatory network of adipose tissue in obesity. *Mol Nutr Food Res* 2016, 60, 43–57. doi:10.1002/mnfr.201500272.
135. Davoine F, Lacy P. Eosinophil cytokines, chemokines, and growth factors: emerging roles in immunity. *Front Immunol* 2014, 5, 570–570. doi:10.3389/fimmu.2014.00570.
136. Park HS, Park JY, Yu R. Relationship of obesity and visceral adiposity with serum concentrations of CRP, TNF- α and IL-6. *Diabetes Res Clin Pract* 2005, 69, 29–35. doi:10.1016/j.diabetes.2004.11.007.
137. Bulló M, García-Lorda P, Megias I, Salas-Salvado J. Systemic inflammation, adipose tissue tumor necrosis factor, and leptin expression. *Obesity Res* 2003, 11, 525–31. doi:10.1038/oby.2003.74.
138. Dicker D, Salook MA, Marcovicu D, Djaldetti M, Bessler H. Role of peripheral blood mononuclear cells in the predisposition of

- obese individuals to inflammation and infection. *Obesity Facts* 2013, 6, 146–51. doi:10.1159/000350775.
139. Catalán V, Gómez-Ambrosi J, Rodríguez A, et al. Peripheral mononuclear blood cells contribute to the obesity-associated inflammatory state independently of glycemic status: involvement of the novel proinflammatory adipokines chemerin, chitinase-3-like protein 1, lipocalin-2 and osteopontin. *Genes Nutr* 2015, 10, 460–460. doi:10.1007/s12263-015-0460-8.
 140. Michelet X, Dyck L, Hogan A, et al. Metabolic reprogramming of natural killer cells in obesity limits antitumor responses. *Nat Immunol* 2018, 19, 1330–40. doi:10.1038/s41590-018-0251-7.
 141. Frasca D, Ferracci F, Diaz A, Romero M, Lechner S, Blomberg BB. Obesity decreases B cell responses in young and elderly individuals. *Obesity* 2016, 24, 615–25. doi:10.1002/oby.21383.
 142. Perdu S, Castellana B, Kim Y, Chan K, DeLuca L, Beristain AG. Maternal obesity drives functional alterations in uterine NK cells. *JCI Insight* 2016, 1, e85560–e85560. doi:10.1172/jci.insight.85560.
 143. Nishimura S, Manabe I, Nagasaki M, et al. CD8+ effector T cells contribute to macrophage recruitment and adipose tissue inflammation in obesity. *Nat Med* 2009, 15, 914–20. doi:10.1038/nm.1964.
 144. Sen S, Iyer C, Klebenov D, Histed A, Aviles JA, Meydani SN. Obesity impairs cell-mediated immunity during the second trimester of pregnancy. *Am J Obstet Gynecol* 2013, 208, 139.e131–8.
 145. Reis BS, Lee K, Fanok MH, et al. Leptin receptor signaling in T cells is required for Th17 differentiation. *J Immunol* 2015, 194, 5253–60.
 146. Hadfield KA, McCracken SA, Ashton AW, Nguyen TG, Morris JM. Regulated suppression of NF- κ B throughout pregnancy maintains a favourable cytokine environment necessary for pregnancy success. *J Reprod Immunol* 2011, 89, 1–9. doi:10.1016/j.jri.2010.11.008.
 147. Seck A, Hichami A, Doucouré S, et al. Th1/Th2 dichotomy in obese women with gestational diabetes and their macrosomic babies. *J Diab Res* 2018, 2018, 8474617. doi:10.1155/2018/8474617.
 148. Rogacev KS, Ulrich C, Blömer L, et al. Monocyte heterogeneity in obesity and subclinical atherosclerosis. *Eur Heart J* 2009, 31, 369–76. doi:10.1093/eurheartj/ehp308.
 149. Devèvre EF, Renovato-Martins M, Clément K, Sautès-Fridman C, Cremer I, Poirou C. Profiling of the three circulating monocyte subpopulations in human obesity. *J Immunol* 2015, 194, 3917–23. doi:10.4049/jimmunol.1402655.
 150. Kriminger P, Ensenauer R, Ehlers K, et al. Peripheral monocytes of obese women display increased chemokine receptor expression and migration capacity. *J Clin Endocrinol Metab* 2014, 99, 2500–9. doi:10.1210/jc.2013-2611.
 151. Bellissimo M, Fleischer C, Tran P, et al. Mitochondrial bioenergetic metabolism is associated with total body composition and influenced by normal weight obesity (P21-039-19). *Curr Dev Nutr* 2019, 3, 21–39. doi:10.1093/cdn/nzz041.P21-039-19.
 152. Willig AL, Kramer PA, Chacko BK, Darley-Usmar VM, Heath SL, Overton ET. Monocyte bioenergetic function is associated with body composition in virologically suppressed HIV-infected women. *Redox Biol* 2017, 12, 648–56. doi:10.1016/j.redox.2017.04.005.
 153. Catalano PM, Presley L, Minium J, Hauguel-de Mouzon S. Fetuses of obese mothers develop insulin resistance in utero. *Diabetes Care* 2009, 32, 1076–80. doi:10.2337/dc08-2077.
 154. Baker PR, II, Patinkin Z, Shapiro AL, et al. Maternal obesity and increased neonatal adiposity correspond with altered infant mesenchymal stem cell metabolism. *JCI insight* 2017; 2: e94200.
 155. Sureshchandra S, Marshall NE, Mendoza N, Jankeel A, Zulu MZ, Messaoudi I. Functional and genomic adaptations of blood monocytes to pregravid obesity during pregnancy. *iScience* 2021, 24, 102690–102690. doi:10.1016/j.isci.2021.102690.
 156. Kelly Amy C, Powell Theresa L, Jansson T. Placental function in maternal obesity. *Clin Sci* 2020, 134, 961–84.
 157. Roberts KA, Riley SC, Reynolds RM, et al. Placental structure and inflammation in pregnancies associated with obesity. *Placenta* 2011, 32, 247–54. doi:10.1016/j.placenta.2010.12.023.
 158. Laskewitz A, van Benthem KL, Kieffer TEC, et al. The influence of maternal obesity on macrophage subsets in the human decidua. *Cell Immunol* 2019, 336, 75–82. doi:10.1016/j.cellimm.2019.01.002.
 159. Bravo-Flores E, Mancilla-Herrera I, Espino Y, Sosa S, et al. Macrophage populations in visceral adipose tissue from pregnant women: potential role of obesity in maternal inflammation. *Int J Mol Sci* 2018; 19: 1074.
 160. Bonen A, Tandon NN, Glatz JFC, Luiken JJFF, Heigenhauser GJF. The fatty acid transporter FAT/CD36 is upregulated in subcutaneous and visceral adipose tissues in human obesity and type 2 diabetes. *Int J Obes* 2006, 30, 877–83. doi:10.1038/sj.ijo.0803212.
 161. Kennedy DJ, Kuchibhotla S, Westfall KM, Silverstein RL, Morton RE, Febbraio MA. CD36-dependent pathway enhances macrophage and adipose tissue inflammation and impairs insulin signalling. *Cardiovasc Res* 2011, 89, 604–13.
 162. Kuliczowska-Plaksej J, Bednarek-Tupikowska G, Filus A. Receptor CD36 expression on peripheral blood monocytes in women with visceral obesity. *Endokrynol Pol* 2008, 59, 483–9.
 163. Dehn S, Thorp EB. Myeloid receptor CD36 is required for early phagocytosis of myocardial infarcts and induction of Nr4a1-dependent mechanisms of cardiac repair. *FASEB J* 2018, 32, 254–64.
 164. Fadok VA, Warner ML, Bratton DL, Henson PM. cd36 is required for phagocytosis of apoptotic cells by human macrophages that use either a phosphatidyserine receptor or the vitronectin receptor ($\alpha_v\beta_3$). *J Immunol* 1998, 161, 6250.
 165. Michelle C, Michael P, Martha L. Diabetes and obesity during pregnancy alter insulin signalling and glucose transporter expression in maternal skeletal muscle and subcutaneous adipose tissue. *J Mol Endocrinol* 2010, 44, 213–23.
 166. Diaz P, Harris J, Rosario FJ, Powell TL, Jansson T. Increased placental fatty acid transporter 6 and binding protein 3 expression and fetal liver lipid accumulation in a mouse model of obesity in pregnancy. *Am J Physiol Regul Integr Comp Physiol* 2015, 309, R1569–77. doi:10.1152/ajpregu.00385.2015.
 167. Zhang J-Z, Ismail-Beigi F. Activation of Glut1 glucose transporter in human erythrocytes. *Arch Biochem Biophys* 1998, 356, 86–92. doi:10.1006/abbi.1998.0760.
 168. Morgello S, Usón RR, Schwartz EJ, Haber RS. The human blood-brain barrier glucose transporter (GLUT1) is a glucose transporter of gray matter astrocytes. *Glia* 1995, 14, 43–54. doi:10.1002/glia.440140107.
 169. Maher F, Davies-Hill TM, Lysko PG, Henneberry RC, Simpson IA. Expression of two glucose transporters, GLUT1 and GLUT3, in cultured cerebellar neurons: Evidence for neuron-specific expression of GLUT3. *Mol Cell Neurosci* 1991, 2, 351–60. doi:10.1016/1044-7431(91)90066-w.
 170. Brown K, Heller DS, Zamudio S, Illsley NP. Glucose transporter 3 (GLUT3) protein expression in human placenta across gestation. *Placenta* 2011, 32, 1041–9. doi:10.1016/j.placenta.2011.09.014.
 171. Flores-Opazo M, Boland E, Garnham A, Murphy RM, McGee SL, Hargreaves M. Exercise and GLUT4 in human subcutaneous adipose tissue. *Physiol Rep* 2018, 6, e13918–e13918. doi:10.1481/phy2.13918.
 172. Richter EA, Hargreaves M. Exercise, GLUT4, and skeletal muscle glucose uptake. *Physiol Rev* 2013, 93, 993–1017. doi:10.1152/physrev.00038.2012.
 173. Song L, Sun B, Boersma GJ, et al. Prenatal high-fat diet alters placental morphology, nutrient transporter expression, and mtorc1 signaling in rat. *Obesity* 2017, 25, 909–19. doi:10.1002/oby.21821.
 174. Freereman AJ, Johnson AR, Sacks GN, et al. Metabolic reprogramming of macrophages: glucose transporter 1 (GLUT1)-mediated glucose metabolism drives a proinflammatory

- phenotype. *J Biol Chem* 2014, 289, 7884–96. doi:10.1074/jbc.M113.522037.
175. Valent AM, Choi H, Kolahi KS, Thornburg KL. Hyperglycemia and gestational diabetes suppress placental glycolysis and mitochondrial function and alter lipid processing. *FASEB J* 2021; 35: e21423. doi:10.1096/fj.202000326RR
176. Fisher JJ, Vanderpeet CL, Bartho LA, et al Mitochondrial dysfunction in placental trophoblast cells experiencing gestational diabetes mellitus. *J Physiol* 2021, 599, 1291–305. doi:10.1111/JP280593.
177. American Diabetes Association. Diagnosis and classification of diabetes mellitus. *Diabetes Care* 2010; 33(Suppl 1): S62–S69.
178. Wei W, He Y, Wang X, et al. Gestational diabetes mellitus: the genetic susceptibility behind the disease. *Horm Metab Res* 2021, 53, 489–98. doi:10.1055/a-1546-1652.
179. Kern PA, Ranganathan S, Li C, Wood L, Ranganathan G. Adipose tissue tumor necrosis factor and interleukin-6 expression in human obesity and insulin resistance. *Am J Physiol Endocrinol Metab* 2001, 280, E745–51. doi:10.1152/ajpendo.2001.280.5.e745.
180. Pradhan AD, Manson JE, Rifai N, Buring JE, Ridker PM. C-reactive protein, interleukin 6, and risk of developing type 2 diabetes mellitus. *JAMA* 2001, 286, 327–34. doi:10.1001/jama.286.3.327.
181. Pettitt DJ, Lawrence JM, Beyer J, et al. Association between maternal diabetes in utero and age at offspring's diagnosis of type 2 diabetes. *Diabetes Care* 2008, 31, 2126–30. doi:10.2337/dc08-0769.
182. Yu Y, Arah OA, Liew Z, et al. Maternal diabetes during pregnancy and early onset of cardiovascular disease in offspring: population based cohort study with 40 years of follow-up. *BMJ* 2019, 367, l6398. doi:10.1136/bmj.l6398.
183. Bowers K, Tobias DK, Yeung E, Hu FB, Zhang CA. Prospective study of prepregnancy dietary fat intake and risk of gestational diabetes. *Am J Clin Nutr* 2012, 95, 446–53.
184. Anghelhem-Oliveira MI, Martins BR, Alberton D, Ramos EAS, Picheth G, Rego FGM. Type 2 diabetes-associated genetic variants of FTO, LEPR, PPAR α , and TCF7L2 in gestational diabetes in a Brazilian population. *Arch Endocrinol Metab* 2017, 61, 238–48. doi:10.1590/2359-3997000000258.
185. De Luccia TPB, Pendelowski KPT, Ono E, et al. Unveiling the pathophysiology of gestational diabetes: studies on local and peripheral immune cells. *Scand J Immunol* 2020, 91, e12860. doi:10.1111/sji.12860.
186. Hara CdCP, França EL, Fagundes DLG, et al. Characterization of natural killer cells and cytokines in maternal placenta and fetus of diabetic mothers. *J Immunol Res* 2016; 2016: 7154524.
187. Schober L, Radnai D, Spratte J, et al. The role of regulatory T cell (Treg) subsets in gestational diabetes mellitus. *Clin Exp Immunol* 2014, 177, 76–85.
188. Taricco E, Radaelli T, Rossi G, et al. Effects of gestational diabetes on fetal oxygen and glucose levels in vivo. *BJOG* 2009, 116, 1729–35. doi:10.1111/j.1471-0528.2009.02341.x.
189. Gorar S, Alioglu B, Ademoglu E, et al. Is there a tendency for thrombosis in gestational diabetes mellitus?. *J Lab Physicians* 2016, 8, 101–5. doi:10.4103/0974-2727.180790.
190. Plows JF, Stanley JL, Baker PN, Reynolds CM, Vickers MH. The pathophysiology of gestational diabetes mellitus. *Int J Mol Sci* 2018, 19, 3342.
191. Sisino G, Bouckenooghe T, Auriens S, Fontaine P, Storme L, Vambergue A. Diabetes during pregnancy influences Hofbauer cells, a subtype of placental macrophages, to acquire a pro-inflammatory phenotype. *Biochim Biophys Acta* 2013, 1832, 1959–68. doi:10.1016/j.bbdis.2013.07.009.
192. Schlieffsteiner C, Peinhaupt M, Kopp S, et al. Human placental hofbauer cells maintain an anti-inflammatory M2 phenotype despite the presence of gestational diabetes mellitus. *Front Immunol* 2017, 8, 888–888. doi:10.3389/fimmu.2017.00888.
193. Khan KS, Wojdyla D, Say L, Gülmezoglu AM, Van Look PFA. WHO analysis of causes of maternal death: a systematic review. *The Lancet* 2006, 367, 1066–74.
194. Motedayen M, Rafiei M, Rezaei Tavirani M, Sayehmiri K, Dousti M. The relationship between body mass index and preeclampsia: a systematic review and meta-analysis. *Int J Reproduct Biomed* 2019, 17, 463–72. doi:10.18502/ijrm.v17i7.4857.
195. Mostello D, Jen Chang J, Allen J, Luehr L, Shyken J, Leet T. recurrent preeclampsia: the effect of weight change between pregnancies. *Obstet Gynecol* 2010, 116, 667–72. doi:10.1097/aog.0b013e3181ed74ea.
196. Dandona P, Ajada A, Chaudhuri A, Mohanty P, Garg R. Metabolic syndrome. *Circulation* 2005, 111, 1448–54. doi:10.1161/01.CIR.0000158483.13093.9D.
197. Bodnar LM, Ness RB, Harger GF, Roberts JM. Inflammation and triglycerides partially mediate the effect of prepregnancy body mass index on the risk of preeclampsia. *Am J Epidemiol* 2005, 162, 1198–206. doi:10.1093/aje/kwi334.
198. Conrad KP, Miles TM, Benyo DF. Circulating levels of immunoreactive cytokines in women with preeclampsia. *Am J Reprod Immunol* 1998, 40, 102–11. doi:10.1111/j.1600-0897.1998.tb00398.x.
199. Teppa RJ, Ness RB, Crombleholme WR, Roberts JM. Free leptin is increased in normal pregnancy and further increased in preeclampsia. *Metab Clin Exp* 2000, 49, 1043–8.
200. Roberts JM, Escudero C. The placenta in preeclampsia. *Pregnancy Hypertens* 2012, 2, 72–83. doi:10.1016/j.preghy.2012.01.001.
201. Butterworth BH, Greer IA, Liston WA, Haddad NG, Johnston TA. Immunocytochemical localization of neutrophil elastase in term placenta decidua and myometrium in pregnancy-induced hypertension. *BJOG* 1991, 98, 929–33.
202. Greer IA, Dawes J, Johnston TA, Calder AA. Neutrophil activation is confined to the maternal circulation in pregnancy-induced hypertension. *Obstet Gynecol* 1991, 78, 28–32.
203. Germain SJ, Sacks GP, Soorana SR, Sargent IL, Redman CW. Systemic inflammatory priming in normal pregnancy and preeclampsia: the role of circulating syncytiotrophoblast microparticles. *J Immunol* 2007, 178, 5949–56. doi:10.4049/jimmunol.178.9.5949.
204. Luppi P, DeLoia JA. Monocytes of preeclamptic women spontaneously synthesize pro-inflammatory cytokines. *Clin Immunol* 2006, 118, 268–75. doi:10.1016/j.clim.2005.11.001.
205. Santner-Nanan B, Peek MJ, Khanam R, et al Systemic increase in the ratio between Foxp3⁺ and IL-17-producing CD4⁺ T cells in healthy pregnancy but not in preeclampsia. *J Immunol* 2009, 183, 7023–30. doi:10.4049/jimmunol.0901154.
206. Hsu P, Santner-Nanan B, Dahlstrom JE, et al. Altered decidual DC-SIGN⁺ antigen-presenting cells and impaired regulatory T-cell induction in preeclampsia. *Am J Pathol* 2012, 181, 2149–60. doi:10.1016/j.ajpath.2012.08.032.
207. Molvarec A, Ito M, Shima T, et al Decreased proportion of peripheral blood vascular endothelial growth factor-expressing T and natural killer cells in preeclampsia. *Am J Obstet Gynecol* 2010, 203, 567.e561–567.e568.
208. Ma L-N, Huang X-B, Muyayalo KP, Mor G, Liao A-H. Lactic acid: a novel signaling molecule in early pregnancy?. *Front Immunol* 2020, 11, 279–279. doi:10.3389/fimmu.2020.00279.
209. Thiele K, Diao L, Arck PC. Immunometabolism, pregnancy, and nutrition. *Semin Immunopathol* 2018, 40, 157–74. doi:10.1007/s00281-017-0660-y.
210. Wei Y, Ding J, Li J, et al Metabolic reprogramming of immune cells at the maternal-fetal interface and the development of techniques for immunometabolism. *Front Immunol* 2021, 12, 3685. doi:10.3389/fimmu.2021.717014.
211. Holm SR, Jenkins BJ, Cronin JG, Jones N, Thornton CA. A role for metabolism in determining neonatal immune function. *Pediatr Allergy Immunol* 2021, 32, 1616–28. doi:10.1111/pai.13583.
212. Bytautiene E, Romero R, Vedernikov YP, El-Zeky F, Saade GR, Garfield RE. Induction of premature labor and delivery by allergic reaction and prevention by histamine H₁ receptor antagonist. *Am J Obstet Gynecol* 2004, 191, 1356–61.

213. Sureshchandra S, Wilson RM, Rais M, et al Maternal pregravid obesity remodels the DNA methylation landscape of cord blood monocytes disrupting their inflammatory program. *J Immunol* 2017, 199, 2729–44. doi:10.4049/jimmunol.1700434.
214. Bachy V, Williams DJ, Ibrahim MAA. Altered dendritic cell function in normal pregnancy. *J Reprod Immunol* 2008, 78, 11–21. doi:10.1016/j.jri.2007.09.004.
215. Aarli A, Kristoffersen EK, Jensen TS, Ulvestad E, Matre R. Suppressive effect on lymphoproliferation in vitro by soluble annexin II released from isolated placental membranes. *Am J Reprod Immunol* 1997, 38, 313–9. doi:10.1111/j.1600-0897.1997.tb00306.x.
216. Blackburn S, Loper D. The hematologic and hemostatic systems. *Maternal Fetal/Neonatal Physiolo A Clin Perspect* 1992, 5, 159–200.
217. Bulmer JN, Williams PJ, Lash GE. Immune cells in the placental bed. *Int J Dev Biol* 2010, 54, 281–94. doi:10.1387/ijdb.082763jb.

Chapter Nine

Bibliography

9 Bibliography

- Abdollahi, E., Keyhanfar, F., Delbandi, A. A., Falak, R., Hajimiresmaiel, S. J., & Shafiei, M. (2022). Dapagliflozin exerts anti-inflammatory effects via inhibition of LPS-induced TLR-4 overexpression and NFκB activation in human endothelial cells and differentiated macrophages. *European Journal of Pharmacology*, 918, Article 174715. <https://doi.org/10.1016/j.ejphar.2021.174715>
- Acuto, O., & Michel, F. (2003). CD28-mediated co-stimulation: A quantitative support for TCR signalling. *Nature Reviews Immunology*, 3(12), 939-951. <https://doi.org/10.1038/nri1248>
- Adamo, L., Rocha-Resende, C., Prabhu, S. D., & Mann, D. L. (2020). Reappraising the role of inflammation in heart failure. *Nature Reviews Cardiology*, 17(5), 269-285. <https://doi.org/10.1038/s41569-019-0315-x>
- Afkarian, M., Sedy, J. R., Yang, J., Jacobson, N. G., Cereb, N., Yang, S. Y., . . . Murphy, K. M. (2002). T-bet is a STAT1-induced regulator of IL-12R expression in naive CD4⁺ T cells. *Nature Immunology*, 3(6), 549-557. <https://doi.org/10.1038/ni794>
- Akchurin, O. M., & Kaskel, F. (2015). Update on Inflammation in Chronic Kidney Disease. *Blood Purification*, 39(1-3), 84-92. <https://doi.org/10.1159/000368940>
- Alamanos, Y., & Drosos, A. A. (2005). Epidemiology of adult rheumatoid arthritis. *Autoimmunity Reviews*, 4(3), 130-136. <https://doi.org/10.1016/j.autrev.2004.09.002>
- Alvarado-Sanchez, B., Hernandez-Castro, B., Portales-Perez, D., Baranda, L., Layseca-Espinosa, E., Abud-Mendoza, C., . . . Gonzalez-Amaro, R. (2006). Regulatory T cells in patients with systemic lupus erythematosus. *Journal of Autoimmunity*, 27(2), 110-118. <https://doi.org/10.1016/j.jaut.2006.06.005>
- Angela, M., Endo, Y., Asou, H. K., Yamamoto, T., Tumes, D. J., Tokuyama, H., . . . Nakayama, T. (2016). Fatty acid metabolic reprogramming via mTOR-mediated inductions of PPARγ directs early activation of T cells. *Nature Communications*, 7, Article 13683. <https://doi.org/10.1038/ncomms13683>
- Angiari, S., Runtsch, M. C., Sutton, C. E., Palsson-McDermott, E. M., Kelly, B., Rana, N., . . . O'Neill, L. A. J. (2020). Pharmacological Activation of Pyruvate Kinase M2 Inhibits CD4⁺ T Cell Pathogenicity and Suppresses Autoimmunity. *Cell Metabolism*, 31(2), 391-+. <https://doi.org/10.1016/j.cmet.2019.10.015>
- Arnorini, A. M., Nociti, V., Petzold, A., Gasperini, C., Quartuccio, E., Lazzarino, G., . . . Tavazzi, B. (2014). Serum lactate as a novel potential biomarker in multiple sclerosis. *Biochimica Et Biophysica Acta-Molecular Basis of Disease*, 1842(7), 1137-1143. <https://doi.org/10.1016/j.bbadis.2014.04.005>
- Avouac, J., Gossec, L., & Dougados, M. (2006). Diagnostic and predictive value of anti-cyclic citrullinated protein antibodies in rheumatoid arthritis: a systematic literature review. *Annals of the Rheumatic Diseases*, 65(7), 845-851. <https://doi.org/10.1136/ard.2006.051391>
- Azzouz, D., Omarbekova, A., Heguy, A., Schwudke, D., Gisch, N., Rovin, B. H., . . . Silverman, G. J. (2019). Lupus nephritis is linked to disease-activity associated expansions and immunity to a gut commensal. *Annals of the Rheumatic Diseases*, 78(7), 947-956. <https://doi.org/10.1136/annrheumdis-2018-214856>
- Bailis, W., Shyer, J. A., Zhao, J., Canaveras, J. C. G., Al Khazal, F. J., Qu, R. H., . . . Flavell, R. A. (2019). Distinct modes of mitochondrial metabolism uncouple T cell differentiation and function. *Nature*, 571(7765), 403-+. <https://doi.org/10.1038/s41586-019-1311-3>
- Balmer, M. L., Ma, E. H., Bantug, G. R., Grahlert, J., Pfister, S., Glatter, T., . . . Hess, C. (2016). Memory CD8⁺ T Cells Require Increased Concentrations of Acetate Induced by Stress for Optimal Function. *Immunity*, 44(6), 1312-1324. <https://doi.org/10.1016/j.immuni.2016.03.016>
- Banica, L. M., Besliu, A. N., Pistol, G. C., Stavaru, C., Vlad, V., Predeteanu, D., . . . Matache, C. (2016). Dysregulation of anergy-related factors involved in regulatory T cells defects in Systemic Lupus Erythematosus patients: Rapamycin and Vitamin D efficacy in restoring regulatory T

- cells. *International Journal of Rheumatic Diseases*, 19(12), 1294-1303.
<https://doi.org/10.1111/1756-185x.12509>
- Bapat, S. P., Whitty, C., Mowery, C. T., Liang, Y. Q., Yoo, A., Jiang, Z. W., . . . Marson, A. (2022). Obesity alters pathology and treatment response in inflammatory disease. *Nature*, 604(7905), 337-+. <https://doi.org/10.1038/s41586-022-04536-0>
- Barber, E. K., Dasgupta, J. D., Schlossman, S. F., Trevillyan, J. M., & Rudd, C. E. (1989). The CD4 and CD8 antigens are coupled to a protein-tyrosine kinase (p56Lck) that phosphorylates the CD3 complex. *Proceedings of the National Academy of Sciences of the United States of America*, 86(9), 3277-3281. <https://doi.org/10.1073/pnas.86.9.3277>
- Basdeo, S. A., Moran, B., Cluxton, D., Canavan, M., McCormick, J., Connolly, M., . . . Fletcher, J. M. (2015). Polyfunctional, Pathogenic CD161⁺ Th17 Lineage Cells Are Resistant to Regulatory T Cell-Mediated Suppression in the Context of Autoimmunity. *Journal of Immunology*, 195(2), 528-540. <https://doi.org/10.4049/jimmunol.1402990>
- Bazzazi, H., Aghaei, M., Memarian, A., Asgarian-Omran, H., Behnampour, N., & Yazdani, Y. (2018). Th1-Th17 Ratio as a New Insight in Rheumatoid Arthritis Disease. *Iranian Journal of Allergy Asthma and Immunology*, 17(1), 68-77.
- Behnammanesh, G., Durante, Z. E., Peyton, K. J., Martinez-Lemus, L. A., Brown, S. M., Bender, S. B., & Durante, W. (2019). Canagliflozin Inhibits Human Endothelial Cell Proliferation and Tube Formation. *Frontiers in Pharmacology*, 10, Article 362.
<https://doi.org/10.3389/fphar.2019.00362>
- Berod, L., Friedrich, C., Nandan, A., Freitag, J., Hagemann, S., Harmrolfs, K., . . . Sparwasser, T. (2014). De novo fatty acid synthesis controls the fate between regulatory T and T helper 17 cells. *Nature Medicine*, 20(11), 1327-1333. <https://doi.org/10.1038/nm.3704>
- Bharath, L. P., Agrawal, M., McCambridge, G., Nicholas, D. A., Hasturk, H., Liu, J., . . . Nikolajczyk, B. S. (2020). Metformin Enhances Autophagy and Normalizes Mitochondrial Function to Alleviate Aging-Associated Inflammation. *Cell Metabolism*, 32(1), 44-+.
<https://doi.org/10.1016/j.cmet.2020.04.015>
- Blagih, J., Coulombe, F., Vincent, E. E., Dupuy, F., Galicia-Vazquez, G., Yurchenko, E., . . . Jones, R. G. (2015). The Energy Sensor AMPK Regulates T Cell Metabolic Adaptation and Effector Responses In Vivo. *Immunity*, 42(1), 41-54. <https://doi.org/10.1016/j.immuni.2014.12.030>
- Blanchet, F., Cardona, A., Letimier, F. A., Hershfield, M. S., & Acuto, O. (2005). CD28 costimulatory signal induces protein arginine methylation in T cells. *Journal of Experimental Medicine*, 202(3), 371-377. <https://doi.org/10.1084/jem.20050176>
- Bonelli, M., Savitskaya, A., von Dalwigk, K., Steiner, C. W., Aletaha, D., Smolen, J. S., & Scheinecker, C. (2008). Quantitative and qualitative deficiencies of regulatory T cells in patients with systemic lupus erythematosus (SLE). *International Immunology*, 20(7), 861-868.
<https://doi.org/10.1093/intimm/dxn044>
- Boyman, O., & Sprent, J. (2012). The role of interleukin-2 during homeostasis and activation of the immune system. *Nature Reviews Immunology*, 12(3), 180-190.
<https://doi.org/10.1038/nri3156>
- Brown, G. J., Canete, P. F., Wang, H., Medhavy, A., Bones, J., Roco, J. A., . . . Vinuesa, C. G. (2022). TLR7 gain-of-function genetic variation causes human lupus. *Nature*, 605(7909), 349-+.
<https://doi.org/10.1038/s41586-022-04642-z>
- Brown, J., Abboud, G., Ma, L., Choi, S. C., Kanda, N., Zeumer-Spataro, L., . . . Morel, L. (2022). Microbiota-mediated skewing of tryptophan catabolism modulates CD4⁺ T cells in lupus-prone mice. *iScience*, 25(5), 104241.
- Buck, M. D., O'Sullivan, D., Geltink, R. I. K., Curtis, J. D., Chang, C. H., Sanin, D. E., . . . Pearce, E. L. (2016). Mitochondrial Dynamics Controls T Cell Fate through Metabolic Programming. *Cell*, 166(1), 63-76. <https://doi.org/10.1016/j.cell.2016.05.035>
- Buck, M. D., O'Sullivan, D., & Pearce, E. L. (2015). T cell metabolism drives immunity. *Journal of Experimental Medicine*, 212(9), 1345-1360. <https://doi.org/10.1084/jem.20151159>

- Burr, J. S., Savage, N. D. L., Messah, G. E., Kimzey, S. L., Shaw, A. S., Arch, R. H., & Green, J. M. (2001). Cutting edge: Distinct motifs within CD28 regulate T cell proliferation and induction of Bcl-X-L. *Journal of Immunology*, *166*(9), 5331-5335. <https://doi.org/10.4049/jimmunol.166.9.5331>
- Cammarata, I., Martire, C., Citro, A., Raimondo, D., Fruci, D., Melaiu, O., . . . Barnaba, V. (2019). Counter-regulation of regulatory T cells by autoreactive CD8⁺ T cells in rheumatoid arthritis. *Journal of Autoimmunity*, *99*, 81-97. <https://doi.org/10.1016/j.jaut.2019.02.001>
- Cano-Gamez, E., Soskic, B., Roumeliotis, T. I., So, E., Smyth, D. J., Baldrighi, M., . . . Trynka, G. (2020). Single-cell transcriptomics identifies an effectorness gradient shaping the response of CD4⁺ T cells to cytokines. *Nature Communications*, *11*(1), Article 1801. <https://doi.org/10.1038/s41467-020-15543-y>
- Cantor, J. R., Abu-Remaileh, M., Kanarek, N., Freinkman, E., Gao, X., Louissaint, A., . . . Sabatini, D. M. (2017). Physiologic Medium Rewires Cellular Metabolism and Reveals Uric Acid as an Endogenous Inhibitor of UMP Synthase. *Cell*, *169*(2), 258-272. <https://doi.org/10.1016/j.cell.2017.03.023>
- Cao, D., Malmstrom, V., Baecher-Allan, C., Hafler, D., Klareskog, L., & Trollmo, C. (2003). Isolation and functional characterization of regulatory CD25^{bright}CD4⁺ T cells from the target organ of patients with rheumatoid arthritis. *European Journal of Immunology*, *33*(1), 215-223. <https://doi.org/10.1002/immu.200390024>
- Cao, Y., Rathmell, J. C., & Macintyre, A. N. (2014). Metabolic Reprogramming towards Aerobic Glycolysis Correlates with Greater Proliferative Ability and Resistance to Metabolic Inhibition in CD8 versus CD4 T Cells. *Plos One*, *9*(8), Article e104104. <https://doi.org/10.1371/journal.pone.0104104>
- Caris, A. V., Lira, F. S., de Mello, M. T., Oyama, L. M., & dos Santos, R. V. T. (2014). Carbohydrate and glutamine supplementation modulates the Th1/Th2 balance after exercise performed at a simulated altitude of 4500 m. *Nutrition*, *30*(11-12), 1331-1336. <https://doi.org/10.1016/j.nut.2014.03.019>
- Carr, E. L., Kelman, A., Wu, G. S., Gopaul, R., Senkevitch, E., Aghvanyan, A., . . . Frauwirth, K. A. (2010). Glutamine Uptake and Metabolism Are Coordinately Regulated by ERK/MAPK during T Lymphocyte Activation. *Journal of Immunology*, *185*(2), 1037-1044. <https://doi.org/10.4049/jimmunol.0903586>
- Carrasco, S., & Merida, I. (2004). Diacylglycerol-dependent binding recruits PKC θ and RasGRP1 C1 domains to specific subcellular localizations in living T lymphocytes. *Molecular Biology of the Cell*, *15*(6), 2932-2942. <https://doi.org/10.1091/mbc.E03-11-0844>
- Cascao, R., Moura, R. A., Perpetuo, I., Canhao, H., Vieira-Sousa, E., Mourao, A. F., . . . Fonseca, J. E. (2010). Identification of a cytokine network sustaining neutrophil and Th17 activation in untreated early rheumatoid arthritis. *Arthritis Research & Therapy*, *12*(5), Article R196. <https://doi.org/10.1186/ar3168>
- Chabaud, M., Fossiez, F., Taupin, J. L., & Miossec, P. (1998). Enhancing effect of IL-17 on IL-1-induced IL-6 and leukemia inhibitory factor production by rheumatoid arthritis synoviocytes and its regulation by Th2 cytokines. *Journal of Immunology*, *161*(1), 409-414.
- Chan, A. C., Iwashima, M., Turck, C. W., & Weiss, A. (1992). ZAP-70 - a 70 kDa protein-tyrosine kinase that associates with the TCR ζ chain. *Cell*, *71*(4), 649-662. [https://doi.org/10.1016/0092-8674\(92\)90598-7](https://doi.org/10.1016/0092-8674(92)90598-7)
- Chang, W. K., Yang, K. D., & Shaio, M. F. (1999). Effect of glutamine on Th1 and Th2 cytokine responses of human peripheral blood mononuclear cells. *Clinical Immunology*, *93*(3), 294-301. <https://doi.org/10.1006/clim.1999.4788>
- Chauhan, A. K., Moore, T. L., Bi, Y., & Chen, C. (2016). Fc γ RIIIa-Syk Co-signal Modulates CD4⁺ T-cell Response and Up-regulates Toll-like Receptor (TLR) Expression. *Journal of Biological Chemistry*, *291*(3), 1368-1386. <https://doi.org/10.1074/jbc.M115.684795>
- Chemin, K., Pollastro, S., James, E., Ge, C. R., Albrecht, I., Herrath, J., . . . Malmstrom, V. (2016). A Novel HLA-DRB1*10:01-Restricted T Cell Epitope From Citrullinated Type II Collagen Relevant

- to Rheumatoid Arthritis. *Arthritis & Rheumatology*, 68(5), 1124-1135. <https://doi.org/10.1002/art.39553>
- Chen, F., Liu, Z. G., Wu, W. H., Rozo, C., Bowdridge, S., Millman, A., . . . Gause, W. C. (2012). An essential role for T_H2-type responses in limiting acute tissue damage during experimental helminth infection. *Nature Medicine*, 18(2), 260-266. <https://doi.org/10.1038/nm.2628>
- Chen, J., Williams, S., Ho, S., Loraine, H., Hagan, D., Whaley, J. M., & Feder, J. N. (2010). Quantitative PCR tissue expression profiling of the human SGLT2 gene and related family members. *Diabetes Ther*, 1(2), 57-92.
- Chen, T., Tibbitt, C. A., Feng, X. G., Stark, J. M., Rohrbeck, L., Rausch, L., . . . Coquet, J. M. (2017). PPAR γ promotes type 2 immune responses in allergy and nematode infection. *Science Immunology*, 2(9), Article eaal5196. <https://doi.org/10.1126/sciimmunol.aal5196>
- Chen, W. J., Jin, W. W., Hardegen, N., Lei, K. J., Li, L., Marinos, N., . . . Wahl, S. M. (2003). Conversion of peripheral CD4⁺CD25⁻ naive T cells to CD4⁺CD25⁺ regulatory T cells by TGF- β induction of transcription factor Foxp3. *Journal of Experimental Medicine*, 198(12), 1875-1886. <https://doi.org/10.1084/jem.20030152>
- Chen, X. Q., Su, W. R., Wan, T. S., Yu, J. F., Zhu, W. J., Tang, F., . . . Zheng, S. G. (2017). Sodium butyrate regulates Th17/Treg cell balance to ameliorate uveitis via the Nrf2/F10-1 pathway. *Biochemical Pharmacology*, 142, 111-119. <https://doi.org/10.1016/j.bcp.2017.06.136>
- Choi, J. Y., Ho, J. H. E., Pasoto, S. G., Bunin, V., Kim, S. T., Carrasco, S., . . . Craft, J. (2015). Circulating Follicular Helper-Like T Cells in Systemic Lupus Erythematosus. *Arthritis & Rheumatology*, 67(4), 988-999. <https://doi.org/10.1002/art.39020>
- Choi, S. C., Brown, J., Gong, M., Ge, Y., Zadeh, M., Li, W., . . . Morel, L. (2020). Gut microbiota dysbiosis and altered tryptophan catabolism contribute to autoimmunity in lupus-susceptible mice. *Sci Transl Med*, 12(551).
- Choi, S. C., Titov, A. A., Abboud, G., Seay, H. R., Brusko, T. M., Roopenian, D. C., . . . Morel, L. (2018). Inhibition of glucose metabolism selectively targets autoreactive follicular helper T cells. *Nature Communications*, 9, Article 4369. <https://doi.org/10.1038/s41467-018-06686-0>
- Chu, Y., Wang, F. M., Zhou, M., Chen, L. J., & Lu, Y. H. (2014). A preliminary study on the characterization of follicular helper T (T_{fh}) cells in rheumatoid arthritis synovium. *Acta Histochemica*, 116(3), 539-543. <https://doi.org/10.1016/j.acthis.2013.10.009>
- Clark, D. A., Blois, S., Kandil, J., Handjiski, B., Manuel, J., & Arck, P. C. (2005). Reduced uterine indoleamine 2,3-dioxygenase versus increased Th1/Th2 cytokine ratios as a basis for occult and clinical pregnancy failure in mice and humans. *American Journal of Reproductive Immunology*, 54(4), 203-216. <https://doi.org/10.1111/j.1600-0897.2005.00299.x>
- Cluxton, D., Petrasca, A., Moran, B., & Fletcher, J. M. (2019). Differential Regulation of Human Treg and Th17 Cells by Fatty Acid Synthesis and Glycolysis. *Frontiers in Immunology*, 10, Article 115. <https://doi.org/10.3389/fimmu.2019.00115>
- Cobbold, S. P., Adams, E., Farquhar, C. A., Nolan, K. F., Howie, D., Lui, K. O., . . . Waldmann, H. (2009). Infectious tolerance via the consumption of essential amino acids and mTOR signaling. *Proceedings of the National Academy of Sciences of the United States of America*, 106(29), 12055-12060. <https://doi.org/10.1073/pnas.0903919106>
- Coffman, R. L., Seymour, B. W. P., Hudak, S., Jackson, J., & Rennick, D. (1989). Antibody to interleukin-5 inhibits helminth-induced eosinophilia in mice. *Science*, 245(4915), 308-310. <https://doi.org/10.1126/science.2787531>
- Constantin, A., Loubet-Lescoulie, P., Lambert, N., Yassine-Diab, B., Abbal, M., Mazieres, B., . . . Cantagrel, A. (1998). Antiinflammatory and immunoregulatory action of methotrexate in the treatment of rheumatoid arthritis - Evidence of increased interleukin-4 and interleukin-10 gene expression demonstrated in vitro by competitive reverse transcriptase polymerase chain reaction. *Arthritis and Rheumatism*, 41(1), 48-57. [https://doi.org/10.1002/1529-0131\(199801\)41:1<48::aid-art7>3.3.co;2-b](https://doi.org/10.1002/1529-0131(199801)41:1<48::aid-art7>3.3.co;2-b)

- Contreras, G., Mattiazzi, A., Guerra, G., Ortega, L. M., Tozman, E. C., Li, H., . . . Roth, D. (2010). Recurrence of Lupus Nephritis after Kidney Transplantation. *Journal of the American Society of Nephrology*, 21(7), 1200-1207. <https://doi.org/10.1681/asn.2009101093>
- Costantino, C. M., Baecher-Allan, C., & Hafler, D. A. (2008). Multiple Sclerosis and Regulatory T Cells. *Journal of Clinical Immunology*, 28(6), 697-706. <https://doi.org/10.1007/s10875-008-9236-x>
- Coyle, A. J., Lehar, S., Lloyd, C., Tian, J., Delaney, T., Manning, S., . . . Gutierrez-Ramos, J. C. (2000). The CD28-related molecule ICOS is required for effective T cell-dependent immune responses. *Immunity*, 13(1), 95-105. [https://doi.org/10.1016/s1074-7613\(00\)00011-x](https://doi.org/10.1016/s1074-7613(00)00011-x)
- D'Ambrosio, D., Cantrell, D. A., Frati, L., Santoni, A., & Testi, R. (1994). Involvement of p21(RAS) activation in T-cell CD69 expression. *European Journal of Immunology*, 24(3), 616-620. <https://doi.org/10.1002/eji.1830240319>
- D'Souza, L. J., Wright, S. H., & Bhattacharya, D. (2022). Genetic evidence that uptake of the fluorescent analog 2NBDG occurs independently of known glucose transporters. *Plos One*, 17(8), Article e0261801. <https://doi.org/10.1371/journal.pone.0261801>
- Dajani, E. Z., & Islam, K. (2008). Cardiovascular and gastrointestinal toxicity of selective cyclooxygenase-2 inhibitors in man. *Journal of Physiology and Pharmacology*, 59, 117-133.
- Damasio, M. P., Marchingo, J. M., Spinelli, L., Hukelmann, J. L., Cantrell, D. A., & Howden, A. J. M. (2021). Extracellular signal-regulated kinase (ERK) pathway control of CD8⁺ T cell differentiation. *Biochemical Journal*, 478(1), 79-98. <https://doi.org/10.1042/bcj20200661>
- Danchenko, N., Satia, J., & Anthony, M. (2006). Epidemiology of systemic lupus erythematosus: a comparison of worldwide disease burden. *Lupus*, 15(5), 308-318. <https://doi.org/10.1191/0961203306lu2305xx>
- Darrah, P. A., Patel, D. T., De Luca, P. M., Lindsay, R. W., Davey, D. F., Flynn, B. J., . . . Seder, R. A. (2007). Multifunctional TH1 cells define a correlate of vaccine-mediated protection against *Leishmania major*. In *Nat Med* (Vol. 13, pp. 843-850). <https://doi.org/10.1038/nm1592>
- Davis, M. M., & Bjorkman, P. J. (1988). T-cell antigen receptor genes and T-cell recognition. *Nature*, 334(6181), 395-402. <https://doi.org/10.1038/334395a0>
- Delgoffe, G. M., Kole, T. P., Zheng, Y., Zarek, P. E., Matthews, K. L., Xiao, B., . . . Powell, J. D. (2009). The mTOR Kinase Differentially Regulates Effector and Regulatory T Cell Lineage Commitment. *Immunity*, 30(6), 832-844. <https://doi.org/10.1016/j.immuni.2009.04.014>
- Delgoffe, G. M., Pollizzi, K. N., Waickman, A. T., Heikamp, E., Meyers, D. J., Horton, M. R., . . . Powell, J. D. (2011). The kinase mTOR regulates the differentiation of helper T cells through the selective activation of signaling by mTORC1 and mTORC2. *Nature Immunology*, 12(4), 295-U117. <https://doi.org/10.1038/ni.2005>
- Deng, Q. C., Luo, Y. Y., Chang, C., Wu, H. J., Ding, Y., & Xiao, R. (2019). The Emerging Epigenetic Role of CD8⁺T Cells in Autoimmune Diseases: A Systematic Review. *Frontiers in Immunology*, 10, Article 856. <https://doi.org/10.3389/fimmu.2019.00856>
- Devineni, D., Curtin, C. R., Polidori, D., Gutierrez, M. J., Murphy, J., Rusch, S., & Rothenberg, P. L. (2013). Pharmacokinetics and Pharmacodynamics of Canagliflozin, a Sodium Glucose Co-Transporter 2 Inhibitor, in Subjects With Type 2 Diabetes Mellitus. *Journal of Clinical Pharmacology*, 53(6), 601-610. <https://doi.org/10.1002/jcph.88>
- Dimeloe, S., Gubser, P., Loeliger, J., Frick, C., Develioglu, L., Fischer, M., . . . Hess, C. (2019). Tumor-derived TGF- β inhibits mitochondrial respiration to suppress IFN- γ production by human CD4⁺ T cells. *Science Signaling*, 12(599), Article eaav3334. <https://doi.org/10.1126/scisignal.aav3334>
- Ding, L., Chen, X., Zhang, W., Dai, X., Guo, H., Pan, X., . . . Yang, B. (2023). Canagliflozin primes antitumor immunity by triggering PD-L1 degradation in endocytic recycling. *J Clin Invest*, 133(1).
- Doherty, E., Oaks, Z., & Perl, A. (2014). Increased Mitochondrial Electron Transport Chain Activity at Complex I Is Regulated by N-Acetylcysteine in Lymphocytes of Patients with Systemic Lupus

- Erythematosus. *Antioxidants & Redox Signaling*, 21(1), 56-65.
<https://doi.org/10.1089/ars.2013.5702>
- Dolhain, R. J., van der Heiden, A. N., ter Haar, N. T., Breedveld, F. C., & Miltenburg, A. M. (1996). Shift toward T lymphocytes with a T helper 1 cytokine-secretion profile in the joints of patients with rheumatoid arthritis. *Arthritis Rheum*, 39(12), 1961-1969.
<https://doi.org/10.1002/art.1780391204>
- Dugan, L. L., You, Y. H., Ali, S. S., Diamond-Stanic, M., Miyamoto, S., DeClevés, A. E., . . . Sharma, K. (2013). AMPK dysregulation promotes diabetes-related reduction of superoxide and mitochondrial function. *Journal of Clinical Investigation*, 123(11), 4888-4899.
<https://doi.org/10.1172/jci66218>
- Duhen, T., Geiger, R., Jarrossay, D., Lanzavecchia, A., & Sallusto, F. (2009). Production of interleukin 22 but not interleukin 17 by a subset of human skin-homing memory T cells. In *Nat Immunol* (Vol. 10, pp. 857-863). <https://doi.org/10.1038/ni.1767>
- DuPage, M., & Bluestone, J. A. (2016). Harnessing the plasticity of CD4⁺ T cells to treat immune-mediated disease. *Nature Reviews Immunology*, 16(3), 149-163.
<https://doi.org/10.1038/nri.2015.18>
- Durak, A., Olgar, Y., Degirmenci, S., Akkus, E., Tuncay, E., & Turan, B. (2018). A SGLT2 inhibitor dapagliflozin suppresses prolonged ventricular-repolarization through augmentation of mitochondrial function in insulin-resistant metabolic syndrome rats. *Cardiovascular Diabetology*, 17, Article 144. <https://doi.org/10.1186/s12933-018-0790-0>
- Ehrenstein, M. R., Evans, J. G., Singh, A., Moore, S., Warnes, G., Isenberg, D. A., & Mauri, C. (2004). Compromised function of regulatory T cells in rheumatoid arthritis and reversal by anti-TNF α therapy. *Journal of Experimental Medicine*, 200(3), 277-285.
<https://doi.org/10.1084/jem.20040165>
- Ellis, C. N., Varani, J., Fisher, G. J., Zeigler, M. E., Pershadsingh, H. A., Benson, S. C., . . . Kurtz, T. W. (2000). Troglitazone improves psoriasis and normalizes models of proliferative skin disease - Ligands for peroxisome proliferator-activated receptor- γ inhibit keratinocyte proliferation. *Archives of Dermatology*, 136(5), 609-616. <https://doi.org/10.1001/archderm.136.5.609>
- Enyedy, E. J., Nambiar, M. P., Liou, S. N. C., Dennis, G., Kammer, G. M., & Tsokos, G. C. (2001). Fc ϵ receptor type I γ chain replaces the deficient T cell receptor ζ chain in T cells of patients with systemic lupus erythematosus. *Arthritis and Rheumatism*, 44(5), 1114-1121.
[https://doi.org/10.1002/1529-0131\(200105\)44:5<1114::aid-ar192>3.3.co;2-2](https://doi.org/10.1002/1529-0131(200105)44:5<1114::aid-ar192>3.3.co;2-2)
- Ethgen, O., Esteves, F. D., Bruyere, O., & Reginster, J. Y. (2013). What do we know about the safety of corticosteroids in rheumatoid arthritis? *Current Medical Research and Opinion*, 29(9), 1147-1160. <https://doi.org/10.1185/03007995.2013.818531>
- Evans, H. G., Roostalu, U., Walter, G. J., Gullick, N. J., Frederiksen, K. S., Roberts, C. A., . . . Taams, L. S. (2014). TNF- α blockade induces IL-10 expression in human CD4⁺T cells. *Nature Communications*, 5, Article 1038. <https://doi.org/10.1038/ncomms4199>
- Fava, R., Olsen, N., Kesioja, J., Moses, H., & Pincus, T. (1989). Active and latent forms of transforming growth factor- β activity in synovial effusions. *Journal of Experimental Medicine*, 169(1), 291-296. <https://doi.org/10.1084/jem.169.1.291>
- Feinstein, D. L., Galea, E., Gavrilyuk, V., Brosnan, C. F., Whitacre, C. C., Dumitrescu-Ozimek, L., . . . Heneka, M. T. (2002). Peroxisome proliferator-activated receptor- γ agonists prevent experimental autoimmune encephalomyelitis. *Annals of Neurology*, 51(6), 694-702.
<https://doi.org/10.1002/ana.10206>
- Fernandez, D., Bonilla, E., Mirza, N., Niland, B., & Perl, A. (2006). Rapamycin reduces disease activity and normalizes T cell activation-induced calcium fluxing in patients with systemic lupus erythematosus. *Arthritis and Rheumatism*, 54(9), 2983-2988.
<https://doi.org/10.1002/art.22085>
- Fernandez, D. R., Telarico, T., Bonilla, E., Li, Q., Banerjee, S., Middleton, F. A., . . . Perl, A. (2009). Activation of Mammalian Target of Rapamycin Controls the Loss of TCR ζ in Lupus T Cells

- through HRES-1/Rab4-Regulated Lysosomal Degradation. *Journal of Immunology*, 182(4), 2063-2073. <https://doi.org/10.4049/jimmunol.0803600>
- Fernandez-Garcia, J., Franco, F., Parik, S., Altea-Manzano, P., Pane, A. A., Broekaert, D., . . . Fendt, S. M. (2022). CD8⁺ T cell metabolic rewiring defined by scRNA-seq identifies a critical role of ASNS expression dynamics in T cell differentiation. *Cell Reports*, 41(7), Article 111639. <https://doi.org/10.1016/j.celrep.2022.111639>
- Field, C. S., Baixauli, F., Kyle, R. L., Puleston, D. J., Cameron, A. M., Sanin, D. E., . . . Pearce, E. L. (2020). Mitochondrial Integrity Regulated by Lipid Metabolism Is a Cell-Intrinsic Checkpoint for Treg Suppressive Function. *Cell Metabolism*, 31(2), 422-+. <https://doi.org/10.1016/j.cmet.2019.11.021>
- Finlay, D. K., Rosenzweig, E., Sinclair, L. V., Feijoo-Carnero, C., Hukelmann, J. L., Rolf, J., . . . Cantrell, D. A. (2012). PDK1 regulation of mTOR and hypoxia-inducible factor 1 integrate metabolism and migration of CD8⁺ T cells. *Journal of Experimental Medicine*, 209(13), 2441-2453. <https://doi.org/10.1084/jem.20112607>
- Floudas, A., Canavan, M., McGarry, T., Mullan, R., Nagpal, S., Veale, D. J., & Fearon, U. (2021). ACPA Status Correlates with Differential Immune Profile in Patients with Rheumatoid Arthritis. *Cells*, 10(3), Article 647. <https://doi.org/10.3390/cells10030647>
- Floudas, A., Neto, N., Orr, C., Canavan, M., Gallagher, P., Hurson, C., . . . Fearon, U. (2022). Loss of balance between protective and pro-inflammatory synovial tissue T-cell polyfunctionality predates clinical onset of rheumatoid arthritis. *Annals of the Rheumatic Diseases*, 81(2), 193-205. <https://doi.org/10.1136/annrheumdis-2021-220458>
- Fossiez, F., Banchereau, J., Murray, R., Van Kooten, C., Garrone, P., & Lebecque, S. (1998). Interleukin-17. *Int Rev Immunol*, 16(5-6), 541-551. <https://doi.org/10.3109/08830189809043008>
- Frauwirth, K. A., Riley, J. L., Harris, M. H., Parry, R. V., Rathmell, J. C., Plas, D. R., . . . Thompson, C. B. (2002). The CD28 signaling pathway regulates glucose metabolism. *Immunity*, 16(6), 769-777. [https://doi.org/10.1016/s1074-7613\(02\)00323-0](https://doi.org/10.1016/s1074-7613(02)00323-0)
- Fujita, T., Kutsumi, H., Sanuki, T., Hayakumo, T., & Azuma, T. (2013). Adherence to the preventive strategies for nonsteroidal anti-inflammatory drug- or low-dose aspirin-induced gastrointestinal injuries. *Journal of Gastroenterology*, 48(5), 559-573. <https://doi.org/10.1007/s00535-013-0771-8>
- Gabriel, S. E., Coyle, D., & Moreland, L. W. (2001). A clinical and economic review of disease-modifying antirheumatic drugs. *Pharmacoeconomics*, 19(7), 715-728. <https://doi.org/10.2165/00019053-200119070-00002>
- Gaide, O., Favier, B., Legler, D. F., Bonnet, D., Brissoni, B., Valitutti, S., . . . Thome, M. (2002). CARMA1 is a critical lipid raft-associated regulator of TCR-induced NF-κB activation. *Nature Immunology*, 3(9), 836-843. <https://doi.org/10.1038/ni830>
- Gaud, G., Lesourne, R., & Love, P. E. (2018). Regulatory mechanisms in T cell receptor signalling. *Nature Reviews Immunology*, 18(8), 485-497. <https://doi.org/10.1038/s41577-018-0020-8>
- Gergely, P., Grossman, C., Niland, B., Puskas, F., Neupane, H., Allam, F., . . . Perl, A. (2002). Mitochondrial hyperpolarization and ATP depletion in patients with systemic lupus erythematosus. *Arthritis and Rheumatism*, 46(1), 175-190. [https://doi.org/10.1002/1529-0131\(200201\)46:1<175::aid-art10015>3.0.co;2-h](https://doi.org/10.1002/1529-0131(200201)46:1<175::aid-art10015>3.0.co;2-h)
- Germain, R. N. (2002). T-cell development and the CD4-CD8 lineage decision. *Nature Reviews Immunology*, 2(5), 309-322. <https://doi.org/10.1038/nri798>
- Gerriets, V. A., Kishton, R. J., Nichols, A. G., Macintyre, A. N., Inoue, M., Ilkayeva, O., . . . Rathmell, J. C. (2015). Metabolic programming and PDHK1 control CD4⁺ T cell subsets and inflammation. *Journal of Clinical Investigation*, 125(1), 194-207. <https://doi.org/10.1172/jci76012>
- Gerstner, C., Dubnovitsky, A., Sandin, C., Kozhukh, G., Uchtenhagen, H., James, E. A., . . . Malmstrom, V. (2016). Functional and Structural Characterization of a Novel HLA-DRB1*04:01-Restricted

- alpha-Enolase T Cell Epitope in Rheumatoid Arthritis. *Frontiers in Immunology*, 7, Article 494. <https://doi.org/10.3389/fimmu.2016.00494>
- Gharib, M., Elbaz, W., Darweesh, E., Sabri, N. A., & Shawki, M. A. (2021). Efficacy and Safety of Metformin Use in Rheumatoid Arthritis: A Randomized Controlled Study. *Frontiers in Pharmacology*, 12, Article 726490. <https://doi.org/10.3389/fphar.2021.726490>
- Glatz, J. F. C., Luiken, J., & Bonen, A. (2010). Membrane Fatty Acid Transporters as Regulators of Lipid Metabolism: Implications for Metabolic Disease. *Physiological Reviews*, 90(1), 367-417. <https://doi.org/10.1152/physrev.00003.2009>
- Godfrey, D. I., Kennedy, J., Suda, T., & Zlotnik, A. (1993). A developmental pathway involving four phenotypically and functionally distinct subsets of CD3-CD4-CD8- triple-negative adult mouse thymocytes defined by CD44 and CD25 expression. *J Immunol*, 150(10), 4244-4252.
- Gracie, J. A., Forsey, R. J., Chan, W. L., Gilmour, A., Leung, B. P., Greer, M. R., . . . McInnes, I. B. (1999). A proinflammatory role for IL-18 in rheumatoid arthritis. *Journal of Clinical Investigation*, 104(10), 1393-1401. <https://doi.org/10.1172/jci7317>
- Greene, J. A. L., Leytze, G. M., Emswiler, J., Peach, R., Bajorath, J., Cosand, W., & Linsley, P. S. (1996). Covalent dimerization of CD28/CTLA-4 and oligomerization of CD80/CD86 regulate T cell costimulatory interactions. *Journal of Biological Chemistry*, 271(43), 26762-26771. <https://doi.org/10.1074/jbc.271.43.26762>
- Griffin, G. K., Newton, G., Tarrío, M. L., Bu, D. X., Maganto-Garcia, E., Azcutia, V., . . . Lichtman, A. H. (2012). IL-17 and TNF- α Sustain Neutrophil Recruitment during Inflammation through Synergistic Effects on Endothelial Activation. *Journal of Immunology*, 188(12), 6287-6299. <https://doi.org/10.4049/jimmunol.1200385>
- Gualdoni, G. A., Mayer, K. A., Goschl, L., Boucheron, N., Ellmeier, W., & Zlabinger, G. J. (2016). The AMP analog AICAR modulates the T_{reg}/T_h17 axis through enhancement of fatty acid oxidation. *Faseb Journal*, 30(11), 3800-3809. <https://doi.org/10.1096/fj.201600522R>
- Gubser, P. M., Bantug, G. R., Razik, L., Fischer, M., Dimeloe, S., Hoenger, G., . . . Hess, C. (2013). Rapid effector function of memory CD8⁺ T cells requires an immediate-early glycolytic switch. *Nature Immunology*, 14(10), 1064-+. <https://doi.org/10.1038/ni.2687>
- Gudgeon, N., Munford, H., Bishop, E. L., Hill, J., Fulton-Ward, T., Bending, D., . . . Dimeloe, S. (2022). Succinate uptake by T cells suppresses their effector function via inhibition of mitochondrial glucose oxidation. *Cell Reports*, 40(7), Article 111193. <https://doi.org/10.1016/j.celrep.2022.111193>
- Gustafsson, K., Herrmann, T., & Dieli, F. (2020). Editorial: Understanding $\gamma\delta$ T Cell Multifunctionality-Towards Immunotherapeutic Applications. *Frontiers in Immunology*, 11, Article 921. <https://doi.org/10.3389/fimmu.2020.00921>
- Haas, R., Smith, J., Rocher-Ros, V., Nadkarni, S., Montero-Melendez, T., D'Acquisto, F., . . . Mauro, C. (2015). Lactate Regulates Metabolic and Proinflammatory Circuits in Control of T Cell Migration and Effector Functions. *Plos Biology*, 13(7), Article e1002202. <https://doi.org/10.1371/journal.pbio.1002202>
- Harada, H., Salama, A. D., Sho, M., Izawa, A., Sandner, S. E., Ito, T., . . . Sayegh, M. H. (2003). The role of the ICOS-B7h T cell costimulatory pathway in transplantation immunity. *Journal of Clinical Investigation*, 112(2), 234-243. <https://doi.org/10.1172/jci200317008>
- Hawley, S. A., Ford, R. J., Smith, B. K., Gowans, G. J., Mancini, S. J., Pitt, R. D., . . . Hardie, D. G. (2016). The Na⁺/Glucose Cotransporter Inhibitor Canagliflozin Activates AMPK by Inhibiting Mitochondrial Function and Increasing Cellular AMP Levels. *Diabetes*, 65(9), 2784-2794. <https://doi.org/10.2337/db16-0058>
- He, H. T., Lellouch, A., & Marguet, D. (2005). Lipid rafts and the initiation of T cell receptor signaling. *Seminars in Immunology*, 17(1), 23-33. <https://doi.org/10.1016/j.smim.2004.09.001>
- He, J., Zhang, X., Wei, Y. B., Sun, X. L., Chen, Y. P., Deng, J., . . . Li, Z. G. (2016). Low-dose interleukin-2 treatment selectively modulates CD4⁺ T cell subsets in patients with systemic lupus erythematosus. *Nature Medicine*, 22(9), 991-+. <https://doi.org/10.1038/nm.4148>

- He, N. H., Fan, W. W., Henriquez, B., Yu, R. T., Atkins, A. R., Liddle, C., . . . Evans, R. M. (2017). Metabolic control of regulatory T cell (Treg) survival and function by Lkb1. *Proceedings of the National Academy of Sciences of the United States of America*, *114*(47), 12542-12547. <https://doi.org/10.1073/pnas.1715363114>
- Henriksson, J., Chen, X., Gomes, T., Ullah, U., Meyer, K. B., Miragaia, R., . . . Teichmann, S. A. (2019). Genome-wide CRISPR Screens in T Helper Cells Reveal Pervasive Crosstalk between Activation and Differentiation. *Cell*, *176*(4), 882-+. <https://doi.org/10.1016/j.cell.2018.11.044>
- Hermann, M., & Ruschitzka, F. (2006). Coxibs, non-steroidal anti-inflammatory drugs and cardiovascular risk. *Internal Medicine Journal*, *36*(5), 308-U305. <https://doi.org/10.1111/j.1445-5994.2006.01056.x>
- Herrath, J., Chemin, K., Albrecht, I., Catrina, A. I., & Malmström, V. (2014). Surface expression of CD39 identifies an enriched Treg-cell subset in the rheumatic joint, which does not suppress IL-17A secretion. *Eur J Immunol*, *44*(10), 2979-2989. <https://doi.org/10.1002/eji.201344140>
- Herrath, J., Muller, M., Amoudruz, P., Janson, P., Michaelsson, J., Larsson, P. T., . . . Malmstrom, V. (2011). The inflammatory milieu in the rheumatic joint reduces regulatory T-cell function. *European Journal of Immunology*, *41*(8), 2279-2290. <https://doi.org/10.1002/eji.201041004>
- Hesterberg, R. S., Liu, M., Elmarsafawi, A. G., Koomen, J. M., Welsh, E. A., Hesterberg, S. G., . . . Cleveland, J. L. (2022). TCR-Independent Metabolic Reprogramming Precedes Lymphoma-Driven Changes in T-cell Fate. *Cancer Immunology Research*, *10*(10), 1263-1279. <https://doi.org/10.1158/2326-6066.cir-21-0813>
- Hinz, M., & Scheidereit, C. (2014). The IκB kinase complex in NFκB regulation and beyond. *Embo Reports*, *15*(1), 46-61. <https://doi.org/10.1002/embr.201337983>
- Hoffmann, P., Eder, R., Boeld, T. J., Doser, K., Piseshka, B., Andreesen, R., & Edinger, M. (2006). Only the CD45RA⁺ subpopulation of CD4⁺CD25^{high} T cells gives rise to homogeneous regulatory T-cell lines upon in vitro expansion. *Blood*, *108*(13), 4260-4267. <https://doi.org/10.1182/blood-2006-06-027409>
- Horejsi, V., Zhang, W. G., & Schraven, B. (2004). Transmembrane adaptor proteins: Organizers of immunoreceptor signalling. *Nature Reviews Immunology*, *4*(8), 603-616. <https://doi.org/10.1038/nri1414>
- Hosios, A. M., Hecht, V. C., Danai, L. V., Johnson, M. O., Rathmell, J. C., Steinhauser, M. L., . . . Vander Heiden, M. G. (2016). Amino Acids Rather than Glucose Account for the Majority of Cell Mass in Proliferating Mammalian Cells. *Developmental Cell*, *36*(5), 540-549. <https://doi.org/10.1016/j.devcel.2016.02.012>
- Howden, A. J. M., Hukelmann, J. L., Brenes, A., Spinelli, L., Sinclair, L. V., Lamond, A. I., & Cantrell, D. A. (2019). Quantitative analysis of T cell proteomes and environmental sensors during T cell differentiation. *Nature Immunology*, *20*(11), 1542-+. <https://doi.org/10.1038/s41590-019-0495-x>
- Hu, X. L., Kim, H., Raj, T., Brennan, P. J., Trynka, G., Teslovich, N., . . . Raychaudhuri, S. (2014). Regulation of Gene Expression in Autoimmune Disease Loci and the Genetic Basis of Proliferation in CD4⁺ Effector Memory T Cells. *Plos Genetics*, *10*(6), Article e1004404. <https://doi.org/10.1371/journal.pgen.1004404>
- Huang, H., Vandekeere, S., Kalucka, J., Bierhansl, L., Zecchin, A., Bruning, U., . . . Carmeliet, P. (2017). Role of glutamine and interlinked asparagine metabolism in vessel formation. *Embo Journal*, *36*(16), 2334-2352. <https://doi.org/10.15252/emboj.201695518>
- Hubo, M., Trinschek, B., Kryczanowsky, F., Tuettenberg, A., Steinbrink, K., & Jonuleit, H. (2013). Costimulatory molecules on immunogenic versus tolerogenic human dendritic cells. *Frontiers in Immunology*, *4*, Article 82. <https://doi.org/10.3389/fimmu.2013.00082>
- Human Protein Atlas. (2019, December 20). SLC5A2 – immune cell. <https://www.proteinatlas.org/ENSG00000140675-SLC5A2/immune+cell>
- Human Protein Atlas. (2019, December 20). SLC22A1 – immune cell. <https://www.proteinatlas.org/ENSG00000175003-SLC22A1/immune+cell>

- Humrich, J. Y., von Spee-Mayer, C., Siegert, E., Alexander, T., Hiepe, F., Radbruch, A., . . . Riemekasten, G. (2015). Rapid induction of clinical remission by low-dose interleukin-2 in a patient with refractory SLE. *Annals of the Rheumatic Diseases*, *74*(4), 791-U196. <https://doi.org/10.1136/annrheumdis-2014-206506>
- Hutloff, A., Dittrich, A. M., Beier, K. C., Eljaschewitsch, B., Kraft, R., Anagnostopoulos, I., & Kroczeck, R. A. (1999). ICOS is an inducible T-cell co-stimulator structurally and functionally related to CD28. *Nature*, *397*(6716), 263-266. <https://doi.org/10.1038/16717>
- Hymowitz, S. G., Filvaroff, E. H., Yin, J. P., Lee, J., Cai, L. P., Risser, P., . . . Starovasnik, M. A. (2001). IL-17s adopt a cystine knot fold: structure and activity of a novel cytokine, IL-17F, and implications for receptor binding. *Embo Journal*, *20*(19), 5332-5341. <https://doi.org/10.1093/emboj/20.19.5332>
- Isgro, J., Gupta, S., Jacek, E., Pavri, T., Duculan, R., Kim, M., . . . Pernis, A. B. (2013). Enhanced Rho-Associated Protein Kinase Activation in Patients With Systemic Lupus Erythematosus. *Arthritis and Rheumatism*, *65*(6), 1592-1602. <https://doi.org/10.1002/art.37934>
- Ivanov, I. I., McKenzie, B. S., Zhou, L., Tadokoro, C. E., Lepelley, A., LaFaille, J. J., . . . Littman, D. R. (2006). The orphan nuclear receptor ROR γ t directs the differentiation program of proinflammatory IL-17⁺ T helper cells. *Cell*, *126*(6), 1121-1133. <https://doi.org/10.1016/j.cell.2006.07.035>
- Jacquemin, C., Schmitt, N., Contin-Bordes, C., Liu, Y., Narayanan, P., Seneschal, J., . . . Blanco, P. (2015). OX40 Ligand Contributes to Human Lupus Pathogenesis by Promoting T Follicular Helper Response. *Immunity*, *42*(6), 1159-1170. <https://doi.org/10.1016/j.immuni.2015.05.012>
- James, E. A., Rieck, M., Pieper, J., Gebe, J. A., Yue, B. B., Tatum, M., . . . Buckner, J. H. (2014). Citrulline-Specific Th1 Cells Are Increased in Rheumatoid Arthritis and Their Frequency Is Influenced by Disease Duration and Therapy. *Arthritis & Rheumatology*, *66*(7), 1712-1722. <https://doi.org/10.1002/art.38637>
- Jiang, S. P., & Dong, C. (2013). A complex issue on CD4⁺ T-cell subsets. *Immunological Reviews*, *252*, 5-11. <https://doi.org/10.1111/imr.12041>
- Johnson, M. O., Wolf, M. M., Madden, M. Z., Andrejeva, G., Sugiura, A., Contreras, D. C., . . . Rathmell, J. C. (2018). Distinct Regulation of Th17 and Th1 Cell Differentiation by Glutaminase-Dependent Metabolism. *Cell*, *175*(7), 1780-+. <https://doi.org/10.1016/j.cell.2018.10.001>
- Jones, N., Cronin, J. G., Dolton, G., Panetti, S., Schauenburg, A. J., Galloway, S. A. E., . . . Francis, N. J. (2017). Metabolic Adaptation of Human CD4⁺ and CD8⁺ T-cells to T-cell Receptor-Mediated Stimulation. *Frontiers in Immunology*, *8*, Article 1516. <https://doi.org/10.3389/fimmu.2017.01516>
- Jones, N., Vincent, E. E., Cronin, J. G., Panetti, S., Chambers, M., Holm, S. R., . . . Thornton, C. A. (2019). Akt and STAT5 mediate naive human CD4⁺ T-cell early metabolic response to TCR stimulation. *Nature Communications*, *10*, Article 2042. <https://doi.org/10.1038/s41467-019-10023-4>
- Jovanovic, D. V., Di Battista, J. A., Martel-Pelletier, J., Jolicoeur, F. C., He, Y., Zhang, M., . . . Pelletier, J. P. (1998). IL-17 stimulates the production and expression of proinflammatory cytokines, IL- β and TNF- α , by human macrophages. *Journal of Immunology*, *160*(7), 3513-3521.
- Jury, E. C., Isenberg, D. A., Mauri, C., & Ehrenstein, M. R. (2006). Atorvastatin restores Lck expression and lipid raft-associated signaling in T cells from patients with systemic lupus erythematosus. *Journal of Immunology*, *177*(10), 7416-7422. <https://doi.org/10.4049/jimmunol.177.10.7416>
- Jury, E. C., Kabouridis, P. S., Flores-Borja, F., Mageed, R. A., & Isenberg, D. A. (2004). Altered lipid raft-associated signaling and ganglioside expression in T lymphocytes from patients with systemic lupus erythematosus. *Journal of Clinical Investigation*, *113*(8), 1176-1187. <https://doi.org/10.1172/jci200420345>

- Kaiser, C. C., Shukla, D. K., Stebbins, G. T., Skias, D. D., Jeffery, D. R., Stefoski, D., . . . Feinstein, D. L. (2009). A pilot test of pioglitazone as an add-on in patients with relapsing remitting multiple sclerosis. *Journal of Neuroimmunology*, *211*(1-2), 124-130.
<https://doi.org/10.1016/j.jneuroim.2009.04.011>
- Kang, B. Y., Chung, S. W., Im, S. Y., Choe, Y. K., & Kim, T. S. (1999). Sulfasalazine prevents T-helper 1 immune response by suppressing interleukin-12 production in macrophages. *Immunology*, *98*(1), 98-103.
- Kang, K. Y., Kim, Y. K., Yi, H., Kim, J., Jung, H. R., Kim, I. J., . . . Ju, J. H. (2013). Metformin downregulates Th17 cells differentiation and attenuates murine autoimmune arthritis. *International Immunopharmacology*, *16*(1), 85-92.
<https://doi.org/10.1016/j.intimp.2013.03.020>
- Kasichayanula, S., Liu, X. N., LaCreta, F., Griffen, S. C., & Boulton, D. W. (2014). Clinical Pharmacokinetics and Pharmacodynamics of Dapagliflozin, a Selective Inhibitor of Sodium-Glucose Co-transporter Type 2. *Clinical Pharmacokinetics*, *53*(1), 17-27.
<https://doi.org/10.1007/s40262-013-0104-3>
- Kato, H., & Perl, A. (2014). Mechanistic Target of Rapamycin Complex 1 Expands Th17 and IL-4⁺ CD4-CD8-Double-Negative T Cells and Contracts Regulatory T Cells in Systemic Lupus Erythematosus. *Journal of Immunology*, *192*(9), 4134-4144.
<https://doi.org/10.4049/jimmunol.1301859>
- Kaufmann, U., Kahlfuss, S., Yang, J., Ivanova, E., Koralov, S. B., & Feske, S. (2019). Calcium Signaling Controls Pathogenic Th17 Cell-Mediated Inflammation by Regulating Mitochondrial Function. *Cell Metabolism*, *29*(5), 1104-+. <https://doi.org/10.1016/j.cmet.2019.01.019>
- Kaymak, I., Luda, K. M., Duimstra, L. R., Ma, E. H., Longo, J., Dahabieh, M. S., . . . Jones, R. G. (2022). Carbon source availability drives nutrient utilization in CD8⁺ T cells. *Cell Metabolism*, *34*(9), 1298-+. <https://doi.org/10.1016/j.cmet.2022.07.012>
- Keir, M. E., Butte, M. J., Freeman, G. J., & Sharpe, A. H. (2008). PD-1 and its ligands in tolerance and immunity. *Annual Review of Immunology*, *26*, 677-704.
<https://doi.org/10.1146/annurev.immunol.26.021607.090331>
- Kim, B., Li, J., Jang, C., & Arany, Z. (2017). Glutamine fuels proliferation but not migration of endothelial cells. *EMBO J*, *36*(16), 2321-2333.
- Kim, H. J., Krenn, V., Steinhäuser, G., & Berek, C. (1999). Plasma cell development in synovial germinal centers in patients with rheumatoid and reactive arthritis. *Journal of Immunology*, *162*(5), 3053-3062.
- Kim, W. U., Cho, M. L., Kim, S. I., Yoo, W. H., Lee, S. S., Joo, Y. S., . . . Kim, H. Y. (2000). Divergent effect of cyclosporine on Th1/Th2 type cytokines in patients with severe, refractory rheumatoid arthritis. *Journal of Rheumatology*, *27*(2), 324-331.
- Klarenbeek, P. L., de Hair, M. J. H., Doorenspleet, M. E., van Schaik, B. D. C., Esveldt, R. E. E., van de Sande, M. G. H., . . . de Vries, N. (2012). Inflamed target tissue provides a specific niche for highly expanded T-cell clones in early human autoimmune disease. *Annals of the Rheumatic Diseases*, *71*(6), 1088-1093. <https://doi.org/10.1136/annrheumdis-2011-200612>
- Klysz, D., Tai, X. G., Robert, P. A., Craveiro, M., Cretenet, G., Oburoglu, L., . . . Taylor, N. (2015). Glutamine-dependent α -ketoglutarate production regulates the balance between T helper 1 cell and regulatory T cell generation. *Science Signaling*, *8*(396), Article ra97.
<https://doi.org/10.1126/scisignal.aab2610>
- Ko, H. M., Kang, N. I., Kim, Y. S., Lee, Y. M., Jin, Z. W., Jung, Y. J., . . . Lee, H. K. (2008). Glutamine preferentially inhibits T-helper type 2 cell-mediated airway inflammation and late airway hyperresponsiveness through the inhibition of cytosolic phospholipase A₂ activity in a murine asthma model. In *Clin Exp Allergy* (Vol. 38, pp. 357-364).
<https://doi.org/10.1111/j.1365-2222.2007.02900.x>
- Koga, T., Hedrich, C. M., Mizui, M., Yoshida, N., Otomo, K., Lieberman, L. A., . . . Tsokos, G. C. (2014). CaMK4-dependent activation of AKT/mTOR and CREM- α underlies autoimmunity-associated

- Th17 imbalance. *Journal of Clinical Investigation*, 124(5), 2234-2245.
<https://doi.org/10.1172/jci73411>
- Koga, T., Ichinose, K., Mizui, M., Crispin, J. C., & Tsokos, G. C. (2012). Calcium/Calmodulin-Dependent Protein Kinase IV Suppresses IL-2 Production and Regulatory T Cell Activity in Lupus. *Journal of Immunology*, 189(7), 3490-3496. <https://doi.org/10.4049/jimmunol.1201785>
- Koga, T., Otomo, K., Mizui, M., Yoshida, N., Umeda, M., Ichinose, K., . . . Tsokos, G. C. (2016). Calcium/Calmodulin-Dependent Kinase IV Facilitates the Recruitment of Interleukin-17-Producing Cells to Target Organs Through the CCR6/CCL20 Axis in Th17 Cell-Driven Inflammatory Diseases. *Arthritis & Rheumatology*, 68(8), 1981-1988.
<https://doi.org/10.1002/art.39665>
- Kolev, M., Dimeloe, S., Le Fric, G., Navarini, A., Arbore, G., Povoleri, G. A., . . . Kemper, C. (2015). Complement Regulates Nutrient Influx and Metabolic Reprogramming during Th1 Cell Responses. *Immunity*, 42(6), 1033-1047. <https://doi.org/10.1016/j.immuni.2015.05.024>
- Kominsky, D. J., Campbell, E. L., & Colgan, S. P. (2010). Metabolic Shifts in Immunity and Inflammation. *Journal of Immunology*, 184(8), 4062-4068.
<https://doi.org/10.4049/jimmunol.0903002>
- Kono, M., Yoshida, N., Maeda, K., Skinner, N. E., Pan, W. L., Kyttaris, V. C., . . . Tsokos, G. C. (2018). Pyruvate dehydrogenase phosphatase catalytic subunit 2 limits Th17 differentiation. *Proceedings of the National Academy of Sciences of the United States of America*, 115(37), 9288-9293. <https://doi.org/10.1073/pnas.1805717115>
- Kopf, M., Legros, G., Bachmann, M., Lamers, M. C., Bluethmann, H., & Kohler, G. (1993). Disruption of the murine IL-4 gene blocks Th2 cytokine responses. *Nature*, 362(6417), 245-248.
<https://doi.org/10.1038/362245a0>
- Kremer, J. M., Westhovens, R., Leon, M., Di Giorgio, E., Alten, R., Steinfeld, S., . . . Moreland, L. W. (2003). Treatment of rheumatoid arthritis by selective inhibition of T-cell activation with fusion protein CTLA4Ig. *New England Journal of Medicine*, 349(20), 1907-1915.
<https://doi.org/10.1056/NEJMoa035075>
- Krishnan, S., Juang, Y. T., Chowdhury, B., Magilavy, A., Fisher, C. U., Nguyen, H., . . . Tsokos, G. C. (2008). Differential Expression and Molecular Associations of Syk in Systemic Lupus Erythematosus T Cells. *Journal of Immunology*, 181(11), 8145-8152.
<https://doi.org/10.4049/jimmunol.181.11.8145>
- Krishnan, S., Nambiar, M. P., Warke, V. G., Fisher, C. U., Mitchell, J., Delaney, N., & Tsokos, G. C. (2004). Alterations in lipid raft composition and dynamics contribute to abnormal T cell responses in systemic lupus erythematosus. *Journal of Immunology*, 172(12), 7821-7831.
<https://doi.org/10.4049/jimmunol.172.12.7821>
- Lai, Z. W., Hanczko, R., Bonilla, E., Caza, T. N., Clair, B., Bartos, A., . . . Perl, A. (2012). N-Acetylcysteine Reduces Disease Activity by Blocking Mammalian Target of Rapamycin in T Cells From Systemic Lupus Erythematosus Patients A Randomized, Double-Blind, Placebo-Controlled Trial. *Arthritis and Rheumatism*, 64(9), 2937-2946. <https://doi.org/10.1002/art.34502>
- Lai, Z. W., Kelly, R., Winans, T., Marchena, I., Shadakshari, A., Yu, J., . . . Perl, A. (2018). Sirolimus in patients with clinically active systemic lupus erythematosus resistant to, or intolerant of, conventional medications: a single-arm, open-label, phase 1/2 trial. *Lancet*, 391(10126), 1186-1196. [https://doi.org/10.1016/s0140-6736\(18\)30485-9](https://doi.org/10.1016/s0140-6736(18)30485-9)
- Langrish, C. L., Chen, Y., Blumenschein, W. M., Mattson, J., Basham, B., Sedgwick, J. D., . . . Cua, D. J. (2005). IL-23 drives a pathogenic T cell population that induces autoimmune inflammation. *Journal of Experimental Medicine*, 201(2), 233-240. <https://doi.org/10.1084/jem.20041257>
- Lee, J., Park, M. K., Lim, M. A., Park, E. M., Kim, E. K., Yang, E. J., . . . Cho, M. L. (2013). Interferon Gamma Suppresses Collagen-Induced Arthritis by Regulation of Th17 through the Induction of Indoleamine-2,3-Deoxygenase. *Plos One*, 8(4), Article e60900.
<https://doi.org/10.1371/journal.pone.0060900>

- Lee, K. M., Chuang, E., Griffin, M., Khattri, R., Hong, D. K., Zhang, W. G., . . . Bluestone, J. A. (1998). Molecular basis of T cell inactivation by CTLA-4. *Science*, *282*(5397), 2263-2266. <https://doi.org/10.1126/science.282.5397.2263>
- Lee, S. Y., Lee, S. H., Yang, E. J., Kim, E. K., Kim, J. K., Shin, D. Y., & Cho, M. L. (2015). Metformin Ameliorates Inflammatory Bowel Disease by Suppression of the STAT3 Signaling Pathway and Regulation of the between Th17/Treg Balance. *Plos One*, *10*(9), Article e0135858. <https://doi.org/10.1371/journal.pone.0135858>
- Lee, S. Y., Moon, S. J., Kim, E. K., Seo, H. B., Yang, E. J., Son, H. J., . . . Cho, M. L. (2017). Metformin Suppresses Systemic Autoimmunity in Roquin^{san/san} Mice through Inhibiting B Cell Differentiation into Plasma Cells via Regulation of AMPK/mTOR/STAT3. *Journal of Immunology*, *198*(7), 2661-2670. <https://doi.org/10.4049/jimmunol.1403088>
- Leney-Greene, M. A., Boddapati, A. K., Su, H. C., Cantor, J. R., & Lenardo, M. J. (2020). Human Plasma-like Medium Improves T Lymphocyte Activation. *Iscience*, *23*(1), Article 100759. <https://doi.org/10.1016/j.isci.2019.100759>
- Lenschow, D. J., Walunas, T. L., & Bluestone, J. A. (1996). CD28/B7 system of T cell costimulation. *Annual Review of Immunology*, *14*, 233-258. <https://doi.org/10.1146/annurev.immunol.14.1.233>
- Lewis, J. D., Lichtenstein, G. R., Stein, R. B., Deren, J. J., Judge, T. A., Fogt, F., . . . Wu, G. D. (2001). An open-label trial of the PPAR gamma ligand rosiglitazone for active ulcerative colitis. *American Journal of Gastroenterology*, *96*(12), 3323-3328.
- Li, N. Y., Ragheb, K., Lawler, G., Sturgist, J., Rajwa, B., Melendez, J. A., & Robinson, J. P. (2003). Mitochondrial complex I inhibitor rotenone induces apoptosis through enhancing mitochondrial reactive oxygen species production. *Journal of Biological Chemistry*, *278*(10), 8516-8525. <https://doi.org/10.1074/jbc.M210432200>
- Li, P., Zheng, Y., & Chen, X. (2017). Drugs for Autoimmune Inflammatory Diseases: From Small Molecule Compounds to Anti-TNF Biologics. *Frontiers in Pharmacology*, *8*, Article 460. <https://doi.org/10.3389/fphar.2017.00460>
- Li, Y. Y., Shen, Y., Hohensinner, P., Ju, J. H., Wen, Z. K., Goodman, S. B., . . . Weyand, C. M. (2016). Deficient Activity of the Nuclease MRE11A Induces T Cell Aging and Promotes Arthritogenic Effector Functions in Patients with Rheumatoid Arthritis. *Immunity*, *45*(4), 903-916. <https://doi.org/10.1016/j.immuni.2016.09.013>
- Li, Y. Y., Shen, Y., Jin, K., Wen, Z. K., Cao, W. Q., Wu, B. W., . . . Weyand, C. M. (2019). The DNA Repair Nuclease MRE11A Functions as a Mitochondrial Protector and Prevents T Cell Pyroptosis and Tissue Inflammation. *Cell Metabolism*, *30*(3), 477-+. <https://doi.org/10.1016/j.cmet.2019.06.016>
- Lin, S. C., Chen, K. H., Lin, C. H., Kuo, C. C., Ling, Q. D., & Chan, C. H. (2007). The quantitative analysis of peripheral blood FOXP3-expressing T cells in systemic lupus erythematosus and rheumatoid arthritis patients. *European Journal of Clinical Investigation*, *37*(12), 987-996. <https://doi.org/10.1111/j.1365-2362.2007.01882.x>
- Liossis, S. N. C., Ding, X. Z., Dennis, G. J., & Tsokos, G. C. (1998). Altered pattern of TCR/CD3-mediated protein-tyrosyl phosphorylation in T cells from patients with systemic lupus erythematosus - Deficient expression of the T cell receptor ζ chain. *Journal of Clinical Investigation*, *101*(7), 1448-1457. <https://doi.org/10.1172/jci1457>
- Liu, X. L., Zhang, Y., Li, W., & Zhou, X. (2022). Lactylation, an emerging hallmark of metabolic reprogramming: Current progress and open challenges. *Frontiers in Cell and Developmental Biology*, *10*, Article 972020. <https://doi.org/10.3389/fcell.2022.972020>
- Liu, Y., Liao, J. Y., Zhao, M., Wu, H. J., Yung, S. S., Chan, T. M., . . . Lu, Q. J. (2015). Increased expression of TLR2 in CD4⁺ T cells from SLE patients enhances immune reactivity and promotes IL-17 expression through histone modifications. *European Journal of Immunology*, *45*(9), 2683-2693. <https://doi.org/10.1002/eji.201445219>

- Loftus, R. M., Assmann, N., Kedia-Mehta, N., O'Brien, K. L., Garcia, A., Gillespie, C., . . . Finlay, D. K. (2018). Amino acid-dependent cMyc expression is essential for NK cell metabolic and functional responses in mice. *Nat Commun*, *9*, Article 2341. <https://doi.org/10.1038/s41467-018-04719-2>
- Lohoff, M., & Mak, T. W. (2005). Roles of interferon-regulatory factors in T-helper-cell differentiation. *Nature Reviews Immunology*, *5*(2), 125-135. <https://doi.org/10.1038/nri1552>
- Long, Q., Li, L. X., Yang, H. M., Lu, Y., Yang, H., Zhu, Y. X., . . . Yuan, J. (2022). SGLT2 inhibitor, canagliflozin, ameliorates cardiac inflammation in experimental autoimmune myocarditis. *International Immunopharmacology*, *110*, Article 109024. <https://doi.org/10.1016/j.intimp.2022.109024>
- Longo, J., Watson, M. J., Vos, M. J., Williams, K. S., & Jones, R. G. (2022). PYGBacking on glycogen metabolism to fuel early memory T cell recall responses. *Molecular Cell*, *82*(16), 2918-2921. <https://doi.org/10.1016/j.molcel.2022.07.016>
- Lyssuk, E. Y., Torgashina, A. V., Soloviev, S. K., Nasonov, E. L., & Bykovskaia, S. N. (2007). Reduced number and function of CD4⁺CD25^{high} FoxP3⁺ regulatory T cells in patients with systemic lupus erythematosus. *Immune-Mediated Diseases: from Theory to Therapy*, *601*, 113-119.
- Ma, D. X., Zhu, X. J., Zhao, P., Zhao, C. H., Li, X. F., Zhu, Y. Y., . . . Hou, M. (2008). Profile of Th17 cytokines (IL-17, TGF- β , IL-6) and Th1 cytokine (IFN- γ) in patients with immune thrombocytopenic purpura. *Annals of Hematology*, *87*(11), 899-904. <https://doi.org/10.1007/s00277-008-0535-3>
- Ma, J., Zhu, C. L., Ma, B., Tian, J., Baidoo, S. E., Mao, C. M., . . . Wang, S. J. (2012). Increased Frequency of Circulating Follicular Helper T Cells in Patients with Rheumatoid Arthritis. *Clinical & Developmental Immunology*, Article 827480. <https://doi.org/10.1155/2012/827480>
- Macintyre, A. N., Gerriets, V. A., Nichols, A. G., Michalek, R. D., Rudolph, M. C., Deoliveira, D., . . . Rathmell, J. C. (2014). The Glucose Transporter Glut1 Is Selectively Essential for CD4 T Cell Activation and Effector Function. *Cell Metabolism*, *20*(1), 61-72. <https://doi.org/10.1016/j.cmet.2014.05.004>
- Macintyre, A. N., & Rathmell, J. C. (2013). Activated lymphocytes as a metabolic model for carcinogenesis. *Cancer Metab*, *1*(1), 5.
- Mahnke, Y. D., Beddall, M. H., & Roederer, M. (2013). OMIP-017: Human CD4⁺ helper T-cell subsets including follicular helper cells. *Cytometry Part A*, *83A*(5), 439-440. <https://doi.org/10.1002/cyto.a.22269>
- Mahnke, Y. D., Brodie, T. M., Sallusto, F., Roederer, M., & Lugli, E. (2013). The who's who of T-cell differentiation: Human memory T-cell subsets. *European Journal of Immunology*, *43*(11), 2797-2809. <https://doi.org/10.1002/eji.201343751>
- Mak, T. W., Grusdat, M., Duncan, G. S., Dostert, C., Nonnenmacher, Y., Cox, M., . . . Brenner, D. (2017). Glutathione Primes T Cell Metabolism for Inflammation. *Immunity*, *46*(4), 675-689. <https://doi.org/10.1016/j.immuni.2017.03.019>
- Mancini, S. J., Boyd, D., Katwan, O. J., Strembitska, A., Almabrouk, T. A., Kennedy, S., . . . Salt, I. P. (2018). Canagliflozin inhibits interleukin-1 β -stimulated cytokine and chemokine secretion in vascular endothelial cells by AMP-activated protein kinase-dependent and -independent mechanisms. *Scientific Reports*, *8*, Article 5276. <https://doi.org/10.1038/s41598-018-23420-4>
- Marchingo, J. M., Sinclair, L. V., Howden, A. J. M., & Cantrell, D. A. (2020). Quantitative analysis of how Myc controls T cell proteomes and metabolic pathways during T cell activation. *Elife*, *9*, Article e53725. <https://doi.org/10.7554/eLife.53725>
- Maruotti, N., Cantatore, P., Crivellato, E., Vacca, A., & Ribatti, D. (2007). Macrophages in rheumatoid arthritis. *Histology and Histopathology*, *22*(5), 581-586.

- McDonald, G., Deepak, S., Miguel, L., Hall, C. J., Isenberg, D. A., Magee, A. I., . . . Jury, E. C. (2014). Normalizing glycosphingolipids restores function in CD4⁺ T cells from lupus patients. *Journal of Clinical Investigation*, *124*(2), 712-724. <https://doi.org/10.1172/jci69571>
- Metzler, B., Gfeller, P., & Guinet, E. (2016). Restricting Glutamine or Glutamine-Dependent Purine and Pyrimidine Syntheses Promotes Human T Cells with High FOXP3 Expression and Regulatory Properties. *Journal of Immunology*, *196*(9), 3618-3630. <https://doi.org/10.4049/jimmunol.1501756>
- Michalek, R. D., Gerriets, V. A., Jacobs, S. R., Macintyre, A. N., MacIver, N. J., Mason, E. F., . . . Rathmell, J. C. (2011). Cutting Edge: Distinct Glycolytic and Lipid Oxidative Metabolic Programs Are Essential for Effector and Regulatory CD4⁺ T Cell Subsets. *Journal of Immunology*, *186*(6), 3299-3303. <https://doi.org/10.4049/jimmunol.1003613>
- Miller, D. H., MacMannus, D., Miszkiel, K., Gionvannoni, G., Young, C., Hawkins, C. P., . . . Avandia Multiple Sclerosis Study, G. (2005). Efficacy of six months' therapy with oral rosiglitazone maleate in relapsing-remitting multiple sclerosis. *Multiple Sclerosis*, *11*, S164-S164.
- Miller, M. J., Safrina, O., Parker, I., & Cahalan, M. D. (2004). Imaging the single cell dynamics of CD4⁺ T cell activation by dendritic cells in lymph nodes. *Journal of Experimental Medicine*, *200*(7), 847-856. <https://doi.org/10.1084/jem.20041236>
- Miller, R. A., Harrison, D. E., Allison, D. B., Bogue, M., Debarba, L., Diaz, V., . . . Strong, R. (2020). Canagliflozin extends life span in genetically heterogeneous male but not female mice. *JCI Insight*, *5*(21).
- Miltenburg, A. M. M., Vanlaar, J. M., Dekuiper, R., Daha, M. R., & Breedveld, F. C. (1992). T-cells cloned from human rheumatoid synovial-membrane functionally represent the Th1 subset. *Scandinavian Journal of Immunology*, *35*(5), 603-610. <https://doi.org/10.1111/j.1365-3083.1992.tb03260.x>
- Miyara, M., Amoura, Z., Parizot, C., Badoual, C., Dorgham, K., Trad, S., . . . Gorochov, G. (2005). Global natural regulatory T cell depletion in active systemic lupus erythematosus. *Journal of Immunology*, *175*(12), 8392-8400. <https://doi.org/10.4049/jimmunol.175.12.8392>
- Mizuno, M., Kuno, A., Yano, T., Miki, T., Oshima, H., Sato, T., . . . Miura, T. (2018). Empagliflozin normalizes the size and number of mitochondria and prevents reduction in mitochondrial size after myocardial infarction in diabetic hearts. *Physiological Reports*, *6*(12), Article e13741. <https://doi.org/10.14814/phy2.13741>
- Mombaerts, P., Iacomini, J., Johnson, R. S., Herrup, K., Tonegawa, S., & Papaioannou, V. E. (1992). RAG-1-deficient mice have no mature B and T lymphocytes. *Cell*, *68*(5), 869-877. [https://doi.org/10.1016/0092-8674\(92\)90030-g](https://doi.org/10.1016/0092-8674(92)90030-g)
- Mookerjee, S. A., Gerencser, A. A., Nicholls, D. G., & Brand, M. D. (2017). Quantifying intracellular rates of glycolytic and oxidative ATP production and consumption using extracellular flux measurements. *Journal of Biological Chemistry*, *292*(17), 7189-7207. <https://doi.org/10.1074/jbc.M116.774471>
- Morinobu, A., Wang, Z. Y., & Kumagai, S. (2000). Bucillamine suppresses human Th1 cell development by a hydrogen peroxide-independent mechanism. *Journal of Rheumatology*, *27*(4), 851-858.
- Morita, Y., Yamamura, M., Nishida, K., Harada, S., Okamoto, H., Inoue, H., . . . Makino, H. (1998). Expression of interleukin-12 in synovial tissue from patients with rheumatoid arthritis. *Arthritis and Rheumatism*, *41*(2), 306-314. [https://doi.org/10.1002/1529-0131\(199802\)41:2<306::aid-art15>3.3.co;2-w](https://doi.org/10.1002/1529-0131(199802)41:2<306::aid-art15>3.3.co;2-w)
- Mosley, J. F., 2nd, Smith, L., Everton, E., & Fellner, C. (2015). Sodium-Glucose Linked Transporter 2 (SGLT2) Inhibitors in the Management Of Type-2 Diabetes: A Drug Class Overview. *P T*, *40*(7), 451-462.
- Mosmann, T. R., & Coffman, R. L. (1989). TH1-cell and TH2-cell - different patterns of lymphokine secretion lead to different functional properties. *Annual Review of Immunology*, *7*, 145-173. <https://doi.org/10.1146/annurev.immunol.7.1.145>

- Murphy, M. P., Bayir, H., Belousov, V., Chang, C. J., Davies, K. J. A., Davies, M. J., . . . Halliwell, B. (2022). Guidelines for measuring reactive oxygen species and oxidative damage in cells and in vivo. *Nature Metabolism*, 4(6), 651-662. <https://doi.org/10.1038/s42255-022-00591-z>
- Murray, M. D., & Brater, D. C. (1993). Renal toxicity of the non-steroidal anti-inflammatory drugs. *Annual Review of Pharmacology and Toxicology*, 33, 434-465.
- Nagy, G., Barcza, M., Gonchoroff, N., Phillips, P. E., & Perl, A. (2004). Nitric oxide-dependent mitochondrial biogenesis generates Ca²⁺ signaling profile of lupus T cells. *Journal of Immunology*, 173(6), 3676-3683. <https://doi.org/10.4049/jimmunol.173.6.3676>
- Nakano, D., Kawaguchi, T., Iwamoto, H., Hayakawa, M., Koga, H., & Torimura, T. (2020). Effects of canagliflozin on growth and metabolic reprogramming in hepatocellular carcinoma cells: Multi-omics analysis of metabolomics and absolute quantification proteomics (iMPAQT). *Plos One*, 15(4), Article e0232283. <https://doi.org/10.1371/journal.pone.0232283>
- Nakaya, M., Xiao, Y. C., Zhou, X. F., Chang, J. H., Chang, M., Cheng, X. H., . . . Sun, S. C. (2014). Inflammatory T Cell Responses Rely on Amino Acid Transporter ASCT2 Facilitation of Glutamine Uptake and mTORC1 Kinase Activation. *Immunity*, 40(5), 692-705. <https://doi.org/10.1016/j.immuni.2014.04.007>
- Nambiar, M. P., Fisher, C. U., Warke, V. G., Krishnan, S., Mitchell, J. P., Delaney, N., & Tsokos, G. C. (2003). Reconstitution of deficient T cell receptor ζ chain restores T cell signaling and augments T cell Receptor/CD3-induced interleukin-2 production in patients with systemic lupus erythematosus. *Arthritis and Rheumatism*, 48(7), 1948-1955. <https://doi.org/10.1002/art.11072>
- Nath, N., Khan, M., Paintlia, M. K., Hoda, M. N., & Giri, S. (2009). Metformin Attenuated the Autoimmune Disease of the Central Nervous System in Animal Models of Multiple Sclerosis. *Journal of Immunology*, 182(12), 8005-8014. <https://doi.org/10.4049/jimmunol.0803563>
- National Library of Medicine (U.S.). (2015, December – 2016, December). A Phase 2 Study to Evaluate the Safety, Tolerability, and Activity of Fontolizumab in Subjects With Active Rheumatoid Arthritis. Identifier NCT00281294. <https://clinicaltrials.gov/ct2/show/NCT00281294>
- National Library of Medicine (U.S.). (2022, August –). Effect of Canagliflozin on Liver Inflammation Damage in Type 2 Diabetes Patients With Nonalcoholic Fatty Liver Disease. Identifier NCT05513729. <https://clinicaltrials.gov/ct2/show/NCT05513729>
- Negrotto, L., Farez, M. F., & Correale, J. (2016). Immunologic Effects of Metformin and Pioglitazone Treatment on Metabolic Syndrome and Multiple Sclerosis. *Jama Neurology*, 73(5), 520-528. <https://doi.org/10.1001/jamaneurol.2015.4807>
- Nobs, S. P., Natali, S., Pohlmeier, L., Okreglicka, K., Schneider, C., Kurrer, M., . . . Kopf, M. (2017). PPAR γ in dendritic cells and T cells drives pathogenic type-2 effector responses in lung inflammation. *Journal of Experimental Medicine*, 214(10), 3015-3035. <https://doi.org/10.1084/jem.20162069>
- O'Gorman, W. E., Hsieh, E. W. Y., Savig, E. S., Gherardini, P. F., Hernandez, J. D., Hansmann, L., . . . Davis, M. M. (2015). Single-cell systems-level analysis of human Toll-like receptor activation defines a chemokine signature in patients with systemic lupus erythematosus. *Journal of Allergy and Clinical Immunology*, 136(5), 1326-1336. <https://doi.org/10.1016/j.jaci.2015.04.008>
- O'Neill, L. A. J., Kishton, R. J., & Rathmell, J. (2016). A guide to immunometabolism for immunologists. *Nature Reviews Immunology*, 16(9), 553-565. <https://doi.org/10.1038/nri.2016.70>
- O'Sullivan, D., van der Windt, G. J. W., Huang, S. C. C., Curtis, J. D., Chang, C. H., Buck, M. D., . . . Pearce, E. L. (2014). Memory CD8⁺ T Cells Use Cell-Intrinsic Lipolysis to Support the Metabolic Programming Necessary for Development. *Immunity*, 41(1), 75-88. <https://doi.org/10.1016/j.immuni.2014.06.005>

- Ohl, K., & Tenbrock, K. (2011). Inflammatory Cytokines in Systemic Lupus Erythematosus. *Journal of Biomedicine and Biotechnology*, Article 432595. <https://doi.org/10.1155/2011/432595>
- Ohl, K., & Tenbrock, K. (2015). Regulatory T cells in systemic lupus erythematosus. *European Journal of Immunology*, 45(2), 344-355. <https://doi.org/10.1002/eji.201344280>
- Okkenhaug, K., Wu, L., Garza, K. M., La Rose, J., Khoo, W., Odermatt, B., . . . Rottapel, R. (2001). A point mutation in CD28 distinguishes proliferative signals from survival signals. *Nature Immunology*, 2(4), 325-332. <https://doi.org/10.1038/86327>
- Okunuki, Y., Usui, Y., Nakagawa, H., Tajima, K., Matsuda, R., Ueda, S., . . . Goto, H. (2013). Peroxisome proliferator-activated receptor- γ agonist pioglitazone suppresses experimental autoimmune uveitis. *Experimental Eye Research*, 116, 291-297. <https://doi.org/10.1016/j.exer.2013.09.017>
- Or, R., Renz, H., Terada, N., & Gelfand, E. W. (1992). IL-4 and IL-2 promote human T-cell proliferation through symmetrical but independent pathways. *Clinical Immunology and Immunopathology*, 64(3), 210-217. [https://doi.org/10.1016/0090-1229\(92\)90202-y](https://doi.org/10.1016/0090-1229(92)90202-y)
- Ospelt, C. (2017). Synovial fibroblasts in 2017. *Rmd Open*, 3(2), Article UNSP e000471. <https://doi.org/10.1136/rmdopen-2017-000471>
- Paintlia, A. S., Mohan, S., & Singh, I. (2013). Combinatorial Effect of Metformin and Lovastatin Impedes T-cell Autoimmunity and Neurodegeneration in Experimental Autoimmune Encephalomyelitis. *J Clin Cell Immunol*, 4.
- Papadopoli, D., Uchenunu, O., Palia, R., Chekkal, N., Hulea, L., Topisirovic, I., . . . St-Pierre, J. (2021). Perturbations of cancer cell metabolism by the antidiabetic drug canagliflozin. *Neoplasia*, 23(4), 391-399. <https://doi.org/10.1016/j.neo.2021.02.003>
- Park, H. J., Kim, D. H., Choi, J. Y., Kim, W. J., Kim, J. Y., Senejani, A. G., . . . Choi, J. M. (2014). PPAR γ Negatively Regulates T Cell Activation to Prevent Follicular Helper T Cells and Germinal Center Formation. *Plos One*, 9(6), Article e99127. <https://doi.org/10.1371/journal.pone.0099127>
- Park, J., Kim, M., Kang, S. G., Jannasch, A. H., Cooper, B., Patterson, J., & Kim, C. H. (2015). Short-chain fatty acids induce both effector and regulatory T cells by suppression of histone deacetylases and regulation of the mTOR-S6K pathway. *Mucosal Immunology*, 8(1), 80-93. <https://doi.org/10.1038/mi.2014.44>
- Park, M. J., Lee, S. Y., Moon, S. J., Son, H. J., Lee, S. H., Kim, E. K., . . . Cho, M. L. (2016). Metformin attenuates graft-versus-host disease via restricting mammalian target of rapamycin/signal transducer and activator of transcription 3 and promoting adenosine monophosphate-activated protein kinase-autophagy for the balance between T helper 17 and Tregs. *Translational Research*, 173, 115-130. <https://doi.org/10.1016/j.trsl.2016.03.006>
- Park, S. J., Gavrilova, O., Brown, A. L., Soto, J. E., Bremner, S., Kim, J., . . . Chung, J. H. (2017). DNA-PK Promotes the Mitochondrial, Metabolic, and Physical Decline that Occurs During Aging. *Cell Metabolism*, 25(5), 1135-+. <https://doi.org/10.1016/j.cmet.2017.04.008>
- Parker, S. J., Encarnacion-Rosado, J., Hollinshead, K. E. R., Hollinshead, D. M., Ash, L. J., Rossi, J. A. K., . . . Kimmelman, A. C. (2021). Spontaneous hydrolysis and spurious metabolic properties of α -ketoglutarate esters. *Nature Communications*, 12(1), Article 4905. <https://doi.org/10.1038/s41467-021-25228-9>
- Parnes, J. R., Vonhoegen, P., Miceli, M. C., & Zamoyska, R. (1989). Role of CD4 and CD8 in enhancing T-cell responses to antigen. *Cold Spring Harbor Symposia on Quantitative Biology*, 54, 649-655.
- Patsoukis, N., Bardhan, K., Chatterjee, P., Sari, D., Liu, B. L., Bell, L. N., . . . Boussiotis, V. A. (2015). PD-1 alters T-cell metabolic reprogramming by inhibiting glycolysis and promoting lipolysis and fatty acid oxidation. *Nature Communications*, 6, Article 6692. <https://doi.org/10.1038/ncomms7692>
- Paz, P. E., Wang, S. J., Clarke, H., Lu, X. B., Stokoe, D., & Abo, A. (2001). Mapping the Zap-70 phosphorylation sites on LAT (linker for activation of T cells) required for recruitment and

- activation of signalling proteins in T cells. *Biochemical Journal*, 356, 461-471.
<https://doi.org/10.1042/0264-6021:3560461>
- Pearce, E. L., Walsh, M. C., Cejas, P. J., Harms, G. M., Shen, H., Wang, L. S., . . . Choi, Y. W. (2009). Enhancing CD8 T-cell memory by modulating fatty acid metabolism. *Nature*, 460(7251), 103-118. <https://doi.org/10.1038/nature08097>
- Pene, J., Chevalier, S., Preisser, L., Venereau, E., Guilleux, M. H., Ghannam, S., . . . Gascan, H. (2008). Chronically inflamed human tissues are infiltrated by highly differentiated Th17 lymphocytes. *Journal of Immunology*, 180(11), 7423-7430.
<https://doi.org/10.4049/jimmunol.180.11.7423>
- Peng, M., Yin, N., Chhangawala, S., Xu, K., Leslie, C. S., & Li, M. O. (2016). Aerobic glycolysis promotes T helper 1 cell differentiation through an epigenetic mechanism. *Science*, 354(6311), 481-484. <https://doi.org/10.1126/science.aaf6284>
- Perkovic, V., Jardine, M. J., Neal, B., Bompoint, S., Heerspink, H. J. L., Charytan, D. M., . . . Investigators, C. T. (2019). Canagliflozin and Renal Outcomes in Type 2 Diabetes and Nephropathy. *New England Journal of Medicine*, 380(24), 2295-2306.
<https://doi.org/10.1056/NEJMoa1811744>
- Perl, A., Hanczko, R., Lai, Z. W., Oaks, Z., Kelly, R., Borsuk, R., . . . Phillips, P. (2015). Comprehensive metabolome analyses reveal N-acetylcysteine-responsive accumulation of kynurenine in systemic lupus erythematosus: implications for activation of the mechanistic target of rapamycin. *Metabolomics*, 11(5), 1157-1174. <https://doi.org/10.1007/s11306-015-0772-0>
- Perry, D. J., Titov, A. A., Sobel, E. S., Brusko, T. M., & Morel, L. (2020). Immunophenotyping reveals distinct subgroups of lupus patients based on their activated T cell subsets. *Clinical Immunology*, 221, Article 108602. <https://doi.org/10.1016/j.clim.2020.108602>
- Pershadsingh, H. A., Heneka, M. T., Saini, R., Amin, N. M., Broeske, D. J., & Feinstein, D. L. (2004). Effect of pioglitazone treatment in a patient with secondary multiple sclerosis. *Journal of Neuroinflammation*, 1, Article 3. <https://doi.org/10.1186/1742-2094-1-3>
- Pollizzi, K. N., Sun, I. H., Patel, C. H., Lo, Y. C., Oh, M. H., Waickman, A. T., . . . Powell, J. D. (2016). Asymmetric inheritance of mTORC1 kinase activity during division dictates CD8⁺ T cell differentiation. *Nature Immunology*, 17(6), 704+. <https://doi.org/10.1038/ni.3438>
- Preston, G. C., Sinclair, L. V., Kaskar, A., Hukelmann, J. L., Navarro, M. N., Ferrero, I., . . . Cantrell, D. A. (2015). Single cell tuning of Myc expression by antigen receptor signal strength and interleukin-2 in T lymphocytes. *Embo Journal*, 34(15), 2008-2024.
<https://doi.org/10.15252/emj.201490252>
- Pucino, V., Bombardieri, M., Pitzalis, C., & Mauro, C. (2017). Lactate at the crossroads of metabolism, inflammation, and autoimmunity. *European Journal of Immunology*, 47(1), 14-21.
<https://doi.org/10.1002/eji.201646477>
- Pucino, V., Certo, M., Bulusu, V., Cucchi, D., Goldmann, K., Pontarini, E., . . . Mauro, C. (2019). Lactate Buildup at the Site of Chronic Inflammation Promotes Disease by Inducing CD4⁺ T Cell Metabolic Rewiring. *Cell Metabolism*, 30(6), 1055-+.
<https://doi.org/10.1016/j.cmet.2019.10.004>
- Pugliatti, M., Rosati, G., Carton, H., Riise, T., Drulovic, J., Vecsei, L., & Milanov, I. (2006). The epidemiology of multiple sclerosis in Europe. *European Journal of Neurology*, 13(7), 700-722.
<https://doi.org/10.1111/j.1468-1331.2006.01342.x>
- Putney, J. W. (1987). Formation and actions of calcium-mobilizing messenger, inositol 1,4,5-triphosphate. *American Journal of Physiology*, 252(2), G149-G157.
<https://doi.org/10.1152/ajpgi.1987.252.2.G149>
- Qin, J., Liu, Q., Liu, A. L., Leng, S. Q., Wang, S. W., Li, C. Y., . . . Xu, M. (2022). Empagliflozin modulates CD4⁺ T-cell differentiation via metabolic reprogramming in immune thrombocytopenia. *British Journal of Haematology*, 198(4), 765-775. <https://doi.org/10.1111/bjh.18293>

- Qureshi, O. S., Zheng, Y., Nakamura, K., Attridge, K., Manzotti, C., Schmidt, E. M., . . . Sansom, D. M. (2011). Trans-Endocytosis of CD80 and CD86: A Molecular Basis for the Cell-Extrinsic Function of CTLA-4. *Science*, *332*(6029), 600-603. <https://doi.org/10.1126/science.1202947>
- Ramesh, R., Kozhaya, L., McKeivitt, K., Djuretic, I. M., Carlson, T. J., Quintero, M. A., . . . Sundrud, M. S. (2014). Pro-inflammatory human Th17 cells selectively express P-glycoprotein and are refractory to glucocorticoids. *Journal of Experimental Medicine*, *211*(1), 89-104. <https://doi.org/10.1084/jem.20130301>
- Rao, D. A., Gurish, M. F., Marshall, J. L., Slowikowski, K., Fonseka, C. Y., Liu, Y. Y., . . . Renner, M. B. B. (2017). Pathologically expanded peripheral T helper cell subset drives B cells in rheumatoid arthritis. *Nature*, *542*(7639), 110-+. <https://doi.org/10.1038/nature20810>
- Raphael, I., Nalawade, S., Eagar, T. N., & Forsthuber, T. G. (2015). T cell subsets and their signature cytokines in autoimmune and inflammatory diseases. *Cytokine*, *74*(1), 5-17. <https://doi.org/10.1016/j.cyto.2014.09.011>
- Raud, B., Roy, D. G., Divakaruni, A. S., Tarasenko, T. N., Franke, R., Ma, E. H., . . . Berod, L. (2018). Etomoxir Actions on Regulatory and Memory T Cells Are Independent of Cpt1a-Mediated Fatty Acid Oxidation. *Cell Metabolism*, *28*(3), 504-+. <https://doi.org/10.1016/j.cmet.2018.06.002>
- Ray, W. A., Stein, C. M., Daugherty, J. R., Hall, K., Arbogast, P. G., & Griffin, M. R. (2002). COX-2 selective non-steroidal anti-inflammatory drugs and risk of serious coronary heart disease. *Lancet*, *360*(9339), 1071-1073. [https://doi.org/10.1016/s0140-6736\(02\)11131-7](https://doi.org/10.1016/s0140-6736(02)11131-7)
- Ribot, J. C., Lopes, N., & Silva-Santos, B. (2021). $\gamma\delta$ T cells in tissue physiology and surveillance. *Nature Reviews Immunology*, *21*(4), 221-232. <https://doi.org/10.1038/s41577-020-00452-4>
- Robey, E., & Fowlkes, B. J. (1994). Selective events in T-cell development. *Annual Review of Immunology*, *12*, 675-705. <https://doi.org/10.1146/annurev.iy.12.040194.003331>
- Roda, G., Jharap, B., Neeraj, N., & Colombel, J. F. (2016). Loss of Response to Anti-TNFs: Definition, Epidemiology, and Management. *Clinical and Translational Gastroenterology*, *7*, Article e135. <https://doi.org/10.1038/ctg.2015.63>
- Roose, J. P., Mollenauer, M., Gupta, V. A., Stone, J., & Weiss, A. (2005). A diacylglycerol-protein kinase C-RasGRP1 pathway directs Ras activation upon antigen receptor stimulation of T cells. *Molecular and Cellular Biology*, *25*(11), 4426-4441. <https://doi.org/10.1128/mcb.25.11.4426-4441.2005>
- Rosenzweig, M., Lorenzon, R., Cacoub, P., Pham, H. P., Pitoiset, F., El Soufi, K., . . . Klatzmann, D. (2019). Immunological and clinical effects of low-dose interleukin-2 across 11 autoimmune diseases in a single, open clinical trial. *Annals of the Rheumatic Diseases*, *78*(2), 209-217. <https://doi.org/10.1136/annrheumdis-2018-214229>
- Rossetti, R. G., Seiler, C. M., DeLuca, P., Laposata, M., & Zurier, R. B. (1997). Oral administration of unsaturated fatty acids: effects on human peripheral blood T lymphocyte proliferation. *Journal of Leukocyte Biology*, *62*(4), 438-443. <https://doi.org/10.1002/jlb.62.4.438>
- Sakaguchi, S. (2004). Naturally arising CD4⁺ regulatory T cells for immunologic self-tolerance and negative control of immune responses. *Annual Review of Immunology*, *22*, 531-562. <https://doi.org/10.1146/annurev.immunol.21.120601.141122>
- Samelson, L. E., Patel, M. D., Weissman, A. M., Harford, J. B., & Klausner, R. D. (1986). Antigen activation of murine T-cells induces tyrosine phosphorylation of a polypeptide associated with the T-cell antigen receptor. *Cell*, *46*(7), 1083-1090. [https://doi.org/10.1016/0092-8674\(86\)90708-7](https://doi.org/10.1016/0092-8674(86)90708-7)
- Samson, M., Audia, S., Janikashvili, N., Ciudad, M., Trad, M., Fraszczak, J., . . . Bonnotte, B. (2012). Brief Report: Inhibition of interleukin-6 function corrects Th17/Treg cell imbalance in patients with rheumatoid arthritis. *Arthritis and Rheumatism*, *64*(8), 2499-2503. <https://doi.org/10.1002/art.34477>

- Satoh, Y., Nakano, K., Yoshinari, H., Nakayamada, S., Iwata, S., Kubo, S., . . . Tanaka, Y. (2018). A case of refractory lupus nephritis complicated by psoriasis vulgaris that was controlled with secukinumab. *Lupus*, *27*(7), 1202-1206. <https://doi.org/10.1177/0961203318762598>
- Schaub, J. A., AlAkwa, F. M., McCown, P. J., Naik, A. S., Nair, V., Eddy, S., . . . Bjornstad, P. (2023). SGLT2 inhibitors mitigate kidney tubular metabolic and mTORC1 perturbations in youth-onset type 2 diabetes. *J Clin Invest*, *133*(5).
- Schmidt, S., Moric, E., Schmidt, M., Sastre, M., Feinstein, D. L., & Heneka, M. T. (2004). Anti-inflammatory and antiproliferative actions of PPAR- γ agonists on T lymphocytes derived from MS patients. *Journal of Leukocyte Biology*, *75*(3), 478-485. <https://doi.org/10.1189/jlb.0803402>
- Schroder, A. E., Greiner, A., Seyfert, C., & Berek, C. (1996). Differentiation of B cells in the nonlymphoid tissue of the synovial membrane of patients with rheumatoid arthritis. *Proceedings of the National Academy of Sciences of the United States of America*, *93*(1), 221-225. <https://doi.org/10.1073/pnas.93.1.221>
- Schroder, K., Hertzog, P. J., Ravasi, T., & Hume, D. A. (2004). Interferon- γ : an overview of signals, mechanisms and functions. *Journal of Leukocyte Biology*, *75*(2), 163-189. <https://doi.org/10.1189/jlb.0603252>
- Schulze-Koops, H., & Kalden, J. K. (2001). The balance of Th1/Th2 cytokines in rheumatoid arthritis. *Best Practice & Research in Clinical Rheumatology*, *15*(5), 677-691. <https://doi.org/10.1053/berh.2001.0187>
- Schwartz, D. M., Burma, A. M., Kitakule, M. M., Luo, Y. M., & Mehta, N. N. (2020). T Cells in Autoimmunity-Associated Cardiovascular Diseases. *Frontiers in Immunology*, *11*, Article 588776. <https://doi.org/10.3389/fimmu.2020.588776>
- Sebestyen, Z., Prinz, I., Dechanet-Merville, J., Silva-Santos, B., & Kuball, J. (2020). Translating gammadelta ($\gamma\delta$) T cells and their receptors into cancer cell therapies. *Nature Reviews Drug Discovery*, *19*(3), 169-184. <https://doi.org/10.1038/s41573-019-0038-z>
- Secker, P. F., Beneke, S., Schlichenmaier, N., Delp, J., Gutbier, S., Leist, M., & Dietrich, D. R. (2018). Canagliflozin mediated dual inhibition of mitochondrial glutamate dehydrogenase and complex I: an off-target adverse effect. *Cell Death & Disease*, *9*, Article 226. <https://doi.org/10.1038/s41419-018-0273-y>
- Selmaj, K., Raine, C. S., Cannella, B., & Brosnan, C. F. (1991). Identification of lymphotoxin and tumor necrosis factor in multiple sclerosis lesions. *Journal of Clinical Investigation*, *87*(3), 949-954. <https://doi.org/10.1172/jci115102>
- Shah, K., Al-Haidari, A., Sun, J. M., & Kazi, J. U. (2021). T cell receptor (TCR) signaling in health and disease. *Signal Transduction and Targeted Therapy*, *6*(1), Article 412. <https://doi.org/10.1038/s41392-021-00823-w>
- Shao, L., Fujii, H., Colmegna, I., Oishi, H., Goronzy, J. J., & Weyand, C. M. (2009). Deficiency of the DNA repair enzyme ATM in rheumatoid arthritis. *Journal of Experimental Medicine*, *206*(6), 1435-1449. <https://doi.org/10.1084/jem.20082251>
- Shao, L., Goronzy, J. J., & Weyand, C. M. (2010). DNA-dependent protein kinase catalytic subunit mediates T-cell loss in rheumatoid arthritis. *Embo Molecular Medicine*, *2*(10), 415-427. <https://doi.org/10.1002/emmm.201000096>
- Shaw, J. P., Utz, P. J., Durand, D. B., Toole, J. J., Emmel, E. A., & Crabtree, G. R. (1988). Identification of a putative regulator of early T-cell activation genes. *Science*, *241*(4862), 202-205. <https://doi.org/10.1126/science.3260404>
- Shen, Y., Wen, Z. K., Li, Y. Y., Matteson, E. L., Hong, J. S., Goronzy, J. J., & Weyand, C. M. (2017). Metabolic control of the scaffold protein TKS5 in tissue-invasive, proinflammatory T cells. *Nature Immunology*, *18*(9), 1025-+. <https://doi.org/10.1038/ni.3808>
- Shi, L. Z., Wang, R., Huang, G., Vogel, P., Neale, G., Green, D. R., & Chi, H. (2011). HIF1 α -dependent glycolytic pathway orchestrates a metabolic checkpoint for the differentiation of TH17 and Treg cells. *J Exp Med*, *208*(7), 1367-1376.

- Shin, B. Y., Benavides, G. A., Geng, J. L., Korolov, S. B., Hu, H., Darley-Usmar, V. M., & Harrington, L. E. (2020). Mitochondrial Oxidative Phosphorylation Regulates the Fate Decision between Pathogenic Th17 and Regulatory T Cells. *Cell Reports*, *30*(6), 1898-+. <https://doi.org/10.1016/j.celrep.2020.01.022>
- Shinkai, Y., Koyasu, S., Nakayama, K., Murphy, K. M., Loh, D. Y., Reinherz, E. L., & Alt, F. W. (1993). Restoration of T-cell development in RAG-2 deficient mice by functional TCR transgenes. *Science*, *259*(5096), 822-825. <https://doi.org/10.1126/science.8430336>
- Shukla, D. K., Kaiser, C. C., Stebbins, G. T., & Feinstein, D. L. (2010). Effects of pioglitazone on diffusion tensor imaging indices in multiple sclerosis patients. *Neuroscience Letters*, *472*(3), 153-156. <https://doi.org/10.1016/j.neulet.2010.01.046>
- Silva-Santos, B., Mensurado, S., & Coffelt, S. B. (2019). $\gamma\delta$ T cells: pleiotropic immune effectors with therapeutic potential in cancer. *Nature Reviews Cancer*, *19*(7), 392-404. <https://doi.org/10.1038/s41568-019-0153-5>
- Sinclair, L. V., Barthelemy, C., & Cantrell, D. A. (2020). Single Cell Glucose Uptake Assays: A Cautionary Tale. *Immunometabolism*, *2*(4), e200029.
- Sinclair, L. V., Neyens, D., Ramsay, G., Taylor, P. M., & Cantrell, D. A. (2018). Single cell analysis of kynurenine and System L amino acid transport in T cells. *Nature Communications*, *9*, Article 1981. <https://doi.org/10.1038/s41467-018-04366-7>
- Sinclair, L. V., Rolf, J., Emslie, E., Shi, Y. B., Taylor, P. M., & Cantrell, D. A. (2013). Control of amino acid transport by antigen receptors coordinates the metabolic reprogramming essential for T cell differentiation. *Nature Immunology*, *14*(5), 500-+. <https://doi.org/10.1038/ni.2556>
- Skosey, J. L. (1988). Comparison of responses to and adverse effects of graded doses of sulfasalazine in the treatment of rheumatoid arthritis. *Journal of Rheumatology*, *15*, 5-8.
- Smith-Garvin, J. E., Koretzky, G. A., & Jordan, M. S. (2009). T Cell Activation. *Annual Review of Immunology*, *27*, 591-619. <https://doi.org/10.1146/annurev.immunol.021908.132706>
- Son, H. J., Lee, J., Lee, S. Y., Kim, E. K., Park, M. J., Kim, K. W., . . . Cho, M. L. (2014). Metformin Attenuates Experimental Autoimmune Arthritis through Reciprocal Regulation of Th17/Treg Balance and Osteoclastogenesis. *Mediators of Inflammation*, *2014*, Article 973986. <https://doi.org/10.1155/2014/973986>
- Spertus, J. A., Birmingham, M. C., Nassif, M., Damaraju, C. V., Abbate, A., Butler, J., . . . Januzzi, J. L. (2022). The SGLT2 inhibitor canagliflozin in heart failure: the CHIEF-HF remote, patient-centered randomized trial. *Nature Medicine*, *28*(4), 809-+. <https://doi.org/10.1038/s41591-022-01703-8>
- Sprent, J., & Surh, C. D. (2011). Normal T cell homeostasis: the conversion of naive cells into memory-phenotype cells. *Nature Immunology*, *12*(6), 478-484. <https://doi.org/10.1038/ni.2018>
- Srikanth, S., & Gwack, Y. (2013). Orai1-NFAT signalling pathway triggered by T cell receptor stimulation. *Molecules and Cells*, *35*(3), 182-194. <https://doi.org/10.1007/s10059-013-0073-2>
- Suarez-Fueyo, A., Barber, D. F., Martinez-Ara, J., Zea-Mendoza, A. C., & Carrera, A. C. (2011). Enhanced Phosphoinositide 3-Kinase δ Activity Is a Frequent Event in Systemic Lupus Erythematosus That Confers Resistance to Activation-Induced T Cell Death. *Journal of Immunology*, *187*(5), 2376-2385. <https://doi.org/10.4049/jimmunol.1101602>
- Suen, W. E., Bergman, C. M., Hjelmstrom, P., & Ruddle, N. H. (1997). A critical role for lymphotoxin in experimental allergic encephalomyelitis. *Journal of Experimental Medicine*, *186*(8), 1233-1240. <https://doi.org/10.1084/jem.186.8.1233>
- Sukumar, M., Liu, J., Ji, Y., Subramanian, M., Crompton, J. G., Yu, Z. Y., . . . Gattinoni, L. (2013). Inhibiting glycolytic metabolism enhances CD8⁺ T cell memory and antitumor function. *Journal of Clinical Investigation*, *123*(10), 4479-4488. <https://doi.org/10.1172/jci69589>
- Sun, F. F., Geng, S. K., Wang, H. T., Wang, H. J., Liu, Z., Wang, X. D., . . . Ye, S. (2020). Effects of metformin on disease flares in patients with systemic lupus erythematosus: post hoc

- analyses from two randomised trials. *Lupus Science & Medicine*, 7(1), Article e000429. <https://doi.org/10.1136/lupus-2020-000429>
- Sun, F. F., Wang, H. J., Liu, Z., Geng, S. K., Wang, H. T., Wang, X. D., . . . Ye, S. (2020). Safety and efficacy of metformin in systemic lupus erythematosus: a multicentre, randomised, double-blind, placebo-controlled trial. *Lancet Rheumatology*, 2(4), E210-E216. [https://doi.org/10.1016/s2665-9913\(20\)30004-7](https://doi.org/10.1016/s2665-9913(20)30004-7)
- Sun, L. J., Deng, L., Ea, C. K., Xia, Z. P., & Chen, Z. J. J. (2004). The TRAF6 ubiquitin ligase and TAK1 kinase mediate IKK activation by BCL10 and MALT1 in T lymphocytes. *Molecular Cell*, 14(3), 289-301. [https://doi.org/10.1016/s1097-2765\(04\)00236-9](https://doi.org/10.1016/s1097-2765(04)00236-9)
- Sun, Y. F., Tian, T., Gao, J., Liu, X. Q., Hou, H. Q., Cao, R. J., . . . Guo, L. (2016). Metformin ameliorates the development of experimental autoimmune encephalomyelitis by regulating T helper 17 and regulatory T cells in mice. *Journal of Neuroimmunology*, 292, 58-67. <https://doi.org/10.1016/j.jneuroim.2016.01.014>
- Sunahori, K., Nagpal, K., Hedrich, C. M., Mizui, M., Fitzgerald, L. M., & Tsokos, G. C. (2013). The Catalytic Subunit of Protein Phosphatase 2A (PP2Ac) Promotes DNA Hypomethylation by Suppressing the Phosphorylated Mitogen-activated Protein Kinase/Extracellular Signal-regulated Kinase (ERK) Kinase (MEK)/Phosphorylated ERK/DNMT1 Protein Pathway in T-cells from Controls and Systemic Lupus Erythematosus Patients. *Journal of Biological Chemistry*, 288(30), Article 21936. <https://doi.org/10.1074/jbc.M113.467266>
- Suwannaroj, S., Lagoo, A., Keisler, D., & McMurray, R. W. (2001). Antioxidants suppress mortality in the female NZB x NZW F1 mouse model of systemic lupus erythematosus (SLE). *Lupus*, 10(4), 258-265. <https://doi.org/10.1191/096120301680416940>
- Suzuki, Y., Orellana, M. A., Schreiber, R. D., & Remington, J. S. (1988). Interferon- γ - the major mediator of resistance against *Toxoplasma gondii*. *Science*, 240(4851), 516-518. <https://doi.org/10.1126/science.3128869>
- Szabo, S. J., Dighe, A. S., Gubler, U., & Murphy, K. M. (1997). Regulation of the interleukin (IL)-12R beta 2 subunit expression in developing T helper 1 (Th1) and Th2 cells. *Journal of Experimental Medicine*, 185(5), 817-824. <https://doi.org/10.1084/jem.185.5.817>
- Szamel, M., Rehermann, B., Krebs, B., Kurrle, R., & Resch, K. (1989). Activation signals in human lymphocytes. Incorporation of polyunsaturated fatty acids into plasma membrane phospholipids regulates IL-2 synthesis via sustained activation of protein kinase C. *J Immunol*, 143(9), 2806-2813.
- Talaat, R. M., Mohamed, S. F., Bassyouni, I. H., & Raouf, A. A. (2015). Th1/Th2/Th17/Treg cytokine imbalance in systemic lupus erythematosus (SLE) patients: Correlation with disease activity. *Cytokine*, 72(2), 146-153. <https://doi.org/10.1016/j.cyto.2014.12.027>
- Tan, C., & Gery, I. (2012). The Unique Features of Th9 Cells and their Products. *Critical Reviews in Immunology*, 32(1), 1-10.
- Tan, Y. K., Yu, K., Liang, L., Liu, Y. S., Song, F. Q., Ge, Q. L., . . . Wang, P. (2021). Sodium-Glucose Co-Transporter 2 Inhibition With Empagliflozin Improves Cardiac Function After Cardiac Arrest in Rats by Enhancing Mitochondrial Energy Metabolism. *Frontiers in Pharmacology*, 12, Article 758080. <https://doi.org/10.3389/fphar.2021.758080>
- Tanimine, N., Germana, S. K., Fan, M., Hippen, K., Blazar, B. R., Markmann, J. F., . . . Priyadharshini, B. (2019). Differential effects of 2-deoxy-D-glucose on in vitro expanded human regulatory T cell subsets. *Plos One*, 14(6), Article e0217761. <https://doi.org/10.1371/journal.pone.0217761>
- Thomas, R., McIlraith, M., Davis, L. S., & Lipsky, P. E. (1992). Rheumatoid synovium is enriched in CD45RBdim mature memory T-cells that are potent helpers for B-cell differentiation. *Arthritis and Rheumatism*, 35(12), 1455-1465. <https://doi.org/10.1002/art.1780351209>
- Tian, T., Yu, S., & Ma, D. X. (2013). Th22 and related cytokines in inflammatory and autoimmune diseases. *Expert Opinion on Therapeutic Targets*, 17(2), 113-125. <https://doi.org/10.1517/14728222.2013.736497>

- Tibbitt, C. A., Stark, J. M., Martens, L., Ma, J. J., Mold, J. E., Deswarte, K., . . . Coquet, J. M. (2019). Single-Cell RNA Sequencing of the T Helper Cell Response to House Dust Mites Defines a Distinct Gene Expression Signature in Airway Th2 Cells. *Immunity*, *51*(1), 169-184. <https://doi.org/10.1016/j.immuni.2019.05.014>
- Timilshina, M., You, Z. W., Lacher, S. M., Acharya, S., Jiang, L. Y., Kang, Y. R., . . . Chang, J. H. (2019). Activation of Mevalonate Pathway via LKB1 Is Essential for Stability of T-reg Cells. *Cell Reports*, *27*(10), 2948+. <https://doi.org/10.1016/j.celrep.2019.05.020>
- Tsokos, G. C. (2011). Systemic Lupus Erythematosus. *New England Journal of Medicine*, *365*(22), 2110-2121. <https://doi.org/10.1056/NEJMra1100359>
- Uhlen, M., Karlsson, M. J., Zhong, W., Tebani, A., Pou, C., Mikes, J., . . . Brodin, P. (2019). A genome-wide transcriptomic analysis of protein-coding genes in human blood cells. *Science*, *366*(6472), 1471+, Article eaax9198. <https://doi.org/10.1126/science.aax9198>
- Urban, J. F., Noben-Trauth, N., Donaldson, D. D., Madden, K. B., Morris, S. C., Collins, M., & Finkelman, F. D. (1998). IL-13, IL-4R alpha, and Stat6 are required for the expulsion of the gastrointestinal nematode parasite *Nippostrongylus brasiliensis*. *Immunity*, *8*(2), 255-264. [https://doi.org/10.1016/s1074-7613\(00\)80477-x](https://doi.org/10.1016/s1074-7613(00)80477-x)
- Valencia, X., Yarboro, C., Illei, G., & Lipsky, P. E. (2007). Deficient CD4⁺CD25^{high} T regulatory cell function in patients with active systemic lupus erythematosus. *Journal of Immunology*, *178*(4), 2579-2588. <https://doi.org/10.4049/jimmunol.178.4.2579>
- van Amelsfort, J. M. R., Jacobs, K. M. G., Bijlsma, J. W. J., Lafeber, F., & Taams, L. S. (2004). CD4+CD25+ regulatory T cells in rheumatoid arthritis - Differences in the presence, phenotype, and function between peripheral blood and synovial fluid. *Arthritis and Rheumatism*, *50*(9), 2775-2785. <https://doi.org/10.1002/art.20499>
- van der Windt, G. J. W., Everts, B., Chang, C. H., Curtis, J. D., Freitas, T. C., Amiel, E., . . . Pearce, E. L. (2012). Mitochondrial Respiratory Capacity Is a Critical Regulator of CD8⁺ T Cell Memory Development. *Immunity*, *36*(1), 68-78. <https://doi.org/10.1016/j.immuni.2011.12.007>
- van der Windt, G. J. W., O'Sullivan, D., Everts, B., Huang, S. C. C., Buck, M. D., Curtis, J. D., . . . Pearce, E. L. (2013). CD8 memory T cells have a bioenergetic advantage that underlies their rapid recall ability. *Proceedings of the National Academy of Sciences of the United States of America*, *110*(35), 14336-14341. <https://doi.org/10.1073/pnas.1221740110>
- van Hamburg, J. P., Asmawidjaja, P. S., Davelaar, N., Mus, A. M., Colin, E. M., Hazes, J. M., . . . Lubberts, E. (2011). Th17 cells, but not Th1 cells, from patients with early rheumatoid arthritis are potent inducers of matrix metalloproteinases and proinflammatory cytokines upon synovial fibroblast interaction, including autocrine interleukin-17A production. *Arthritis Rheum*, *63*(1), 73-83. <https://doi.org/10.1002/art.30093>
- Vargas-Rojas, M. I., Crispín, J. C., Richaud-Patin, Y., & Alcocer-Varela, J. (2008). Quantitative and qualitative normal regulatory T cells are not capable of inducing suppression in SLE patients due to T-cell resistance. In *Lupus* (Vol. 17, pp. 289-294). <https://doi.org/10.1177/0961203307088307>
- Veldhoen, M., Hocking, R. J., Atkins, C. J., Locksley, R. M., & Stockinger, B. (2006). TGFβ in the context of an inflammatory cytokine milieu supports de novo differentiation of IL-17-producing T cells. *Immunity*, *24*(2), 179-189. <https://doi.org/10.1016/j.immuni.2006.01.001>
- Venigalla, R. K., Tretter, T., Krienke, S., Max, R., Eckstein, V., Blank, N., . . . Lorenz, H. M. (2008). Reduced CD4+,CD25- T cell sensitivity to the suppressive function of CD4+,CD25high,CD127 - /low regulatory T cells in patients with active systemic lupus erythematosus. *Arthritis Rheum*, *58*(7), 2120-2130. <https://doi.org/10.1002/art.23556>
- Veras, F. P., Peres, R. S., Saraiva, A. L. L., Pinto, L. G., Louzada, P., Cunha, T. M., . . . Alves, J. C. (2015). Fructose 1,6-bisphosphate, a high-energy intermediate of glycolysis, attenuates experimental arthritis by activating anti-inflammatory adenosinergic pathway. *Scientific Reports*, *5*, Article 15171. <https://doi.org/10.1038/srep15171>

- Verbist, K. C., Guy, C. S., Milasta, S., Liedmann, S., Kaminski, M. M., Wang, R. N., & Green, D. R. (2016). Metabolic maintenance of cell asymmetry following division in activated T lymphocytes. *Nature*, *532*(7599), 389-+. <https://doi.org/10.1038/nature17442>
- Vermeire, K., Heremans, H., Vandeputte, M., Huang, S., & Matthys, P. (1997). Accelerated collagen-induced arthritis in IFN- γ receptor-deficient mice. *Journal of Immunology*, *158*(11), 5507-5513.
- Versini, M., Jeandel, P. Y., Rosenthal, E., & Shoenfeld, Y. (2014). Obesity in autoimmune diseases: not a passive bystander. In *Autoimmun Rev* (Vol. 13, pp. 981-1000). © 2014 Elsevier B.V. <https://doi.org/10.1016/j.autrev.2014.07.001>
- Verweij, C. L., Geerts, M., & Aarden, L. A. (1991). Activation of interleukin-2 gene transcription via the T-cell surface molecule CD28 is mediated through an NF- κ B-like response element. *Journal of Biological Chemistry*, *266*(22), 14179-14182.
- Viatte, S., Plant, D., Han, B., Fu, B., Yarwood, A., Thomson, W., . . . Barton, A. (2015). Association of HLA-DRB1 Haplotypes With Rheumatoid Arthritis Severity, Mortality, and Treatment Response. *Jama-Journal of the American Medical Association*, *313*(16), 1645-1656. <https://doi.org/10.1001/jama.2015.3435>
- Villani, L. A., Smith, B. K., Marcinko, K., Ford, R. J., Broadfield, L. A., Green, A. E., . . . Steinberg, G. R. (2016). The diabetes medication Canagliflozin reduces cancer cell proliferation by inhibiting mitochondrial complex-I supported respiration. *Molecular Metabolism*, *5*(10), 1048-1056. <https://doi.org/10.1016/j.molmet.2016.08.014>
- Vincent, F. B., Northcott, M., Hoi, A., Mackay, F., & Morand, E. F. (2013). Clinical associations of serum interleukin-17 in systemic lupus erythematosus. *Arthritis Research & Therapy*, *15*(4), Article R97. <https://doi.org/10.1186/ar4277>
- von Boehmer, H., Teh, H. S., & Kisielow, P. (1989). The thymus selects the useful, neglects the useless and destroys the harmful. *Immunology Today*, *10*(2), 57-61. [https://doi.org/10.1016/0167-5699\(89\)90307-1](https://doi.org/10.1016/0167-5699(89)90307-1)
- von Spee-Mayer, C., Siegert, E., Abdirama, D., Rose, A., Klaus, A., Alexander, T., . . . Humrich, J. Y. (2016). Low-dose interleukin-2 selectively corrects regulatory T cell defects in patients with systemic lupus erythematosus. *Annals of the Rheumatic Diseases*, *75*(7), 1407-1415. <https://doi.org/10.1136/annrheumdis-2015-207776>
- Vrhovac, I., Eror, D. B., Klessen, D., Burger, C., Breljak, D., Kraus, O., . . . Koepsell, H. (2015). Localizations of Na⁺-D-glucose cotransporters SGLT1 and SGLT2 in human kidney and of SGLT1 in human small intestine, liver, lung, and heart. *Pflugers Archiv-European Journal of Physiology*, *467*(9), 1881-1898. <https://doi.org/10.1007/s00424-014-1619-7>
- Vyse, T. J., & Todd, J. A. (1996). Genetic analysis of autoimmune disease. *Cell*, *85*(3), 311-318. [https://doi.org/10.1016/s0092-8674\(00\)81110-1](https://doi.org/10.1016/s0092-8674(00)81110-1)
- Waddington, K. E., Robinson, G. A., Rubio-Cuesta, B., Chrifi-Alaoui, E., Andreone, S., Poon, K. S., . . . Pineda-Torra, I. (2021). LXR directly regulates glycosphingolipid synthesis and affects human CD4⁺T cell function. *Proceedings of the National Academy of Sciences of the United States of America*, *118*(21), Article e2017394118. <https://doi.org/10.1073/pnas.2017394118>
- Wagner, A., Wang, C., Fessler, J., DeTomaso, D., Avila-Pacheco, J., Kaminski, J., . . . Yosef, N. (2021). Metabolic modeling of single Th17 cells reveals regulators of autoimmunity. *Cell*, *184*(16), 4168-+. <https://doi.org/10.1016/j.cell.2021.05.045>
- Wahl, D. R., Petersen, B., Warner, R., Richardson, B. C., Glick, G. D., & Opipari, A. W. (2010). Characterization of the metabolic phenotype of chronically activated lymphocytes. *Lupus*, *19*(13), 1492-1501. <https://doi.org/10.1177/0961203310373109>
- Waickman, A. T., & Powell, J. D. (2012). mTOR, metabolism, and the regulation of T-cell differentiation and function. *Immunological Reviews*, *249*, 43-58. <https://doi.org/10.1111/j.1600-065X.2012.01152.x>
- Wang, D. H., Matsumoto, R., You, Y., Che, T. J., Lin, X. Y., Gaffen, S. L., & Lin, X. (2004). CD3/CD28 costimulation-induced NF- κ B activation is mediated by recruitment of protein kinase C- θ ,

- Bcl10, and I κ B kinase β to the immunological synapse through CARMA1. *Molecular and Cellular Biology*, 24(1), 164-171. <https://doi.org/10.1128/mcb.24.1.164-171.2003>
- Wang, H. P., Franco, F., Tsui, Y. C., Xie, X., Trefny, M. P., Zappasodi, R., . . . Ho, P. C. (2020). CD36-mediated metabolic adaptation supports regulatory T cell survival and function in tumors. *Nature Immunology*, 21(3), 298-+. <https://doi.org/10.1038/s41590-019-0589-5>
- Wang, H. T., Li, T., Chen, S., Gu, Y. Y., & Ye, S. (2015). Neutrophil Extracellular Trap Mitochondrial DNA and Its Autoantibody in Systemic Lupus Erythematosus and a Proof-of-Concept Trial of Metformin. *Arthritis & Rheumatology*, 67(12), 3190-3200. <https://doi.org/10.1002/art.39296>
- Wang, J., Shan, Y., Jiang, Z., Feng, J., Li, C., Ma, L., & Jiang, Y. (2013). High frequencies of activated B cells and T follicular helper cells are correlated with disease activity in patients with new-onset rheumatoid arthritis. *Clinical and Experimental Immunology*, 174(2), 212-220. <https://doi.org/10.1111/cei.12162>
- Wang, J. W., Huang, X. Y., Liu, H. J., Chen, Y. H., Li, P. P., Liu, L. L., . . . Dai, X. Z. (2022). Empagliflozin Ameliorates Diabetic Cardiomyopathy via Attenuating Oxidative Stress and Improving Mitochondrial Function. *Oxidative Medicine and Cellular Longevity*, 2022, Article 1122494. <https://doi.org/10.1155/2022/1122494>
- Wang, L., Zhao, P. W., Ma, L., Shan, Y. X., Jiang, Z. Y., Wang, J., & Jiang, Y. F. (2014). Increased Interleukin 21 and Follicular Helper T-like Cells and Reduced Interleukin 10+B cells in Patients with New-onset Systemic Lupus Erythematosus. *Journal of Rheumatology*, 41(9), 1781-1792. <https://doi.org/10.3899/jrheum.131025>
- Wang, R. N., Dillon, C. P., Shi, L. Z., Milasta, S., Carter, R., Finkelstein, D., . . . Green, D. R. (2011). The Transcription Factor Myc Controls Metabolic Reprogramming upon T Lymphocyte Activation. *Immunity*, 35(6), 871-882. <https://doi.org/10.1016/j.immuni.2011.09.021>
- Wang, Y. H., Viscarra, J., Kim, S. J., & Sul, H. S. (2015). Transcriptional regulation of hepatic lipogenesis. *Nature Reviews Molecular Cell Biology*, 16(11), 678-689. <https://doi.org/10.1038/nrm4074>
- Watts, T. H. (2005). TNF/TNFR family members in costimulation of T cell responses. *Annual Review of Immunology*, 23, 23-68. <https://doi.org/10.1146/annurev.immunol.23.021704.115839>
- Wen, Z. K., Jin, K., Shen, Y., Yang, Z., Li, Y. Y., Wu, B. W., . . . Weyand, C. M. (2019). N-myristoyltransferase deficiency impairs activation of kinase AMPK and promotes synovial tissue inflammation. *Nature Immunology*, 20(3), 313-+. <https://doi.org/10.1038/s41590-018-0296-7>
- Weyand, C. M., & Goronzy, J. J. (2021). The immunology of rheumatoid arthritis. *Nature Immunology*, 22(1), 10-18. <https://doi.org/10.1038/s41590-020-00816-x>
- Williams, M. A., Tyznik, A. J., & Bevan, M. J. (2006). Interleukin-2 signals during priming are required for secondary expansion of CD8⁺ memory T cells. *Nature*, 441(7095), 890-893. <https://doi.org/10.1038/nature04790>
- Wilson, C. S., Stocks, B. T., Hoopes, E. M., Rhoads, J. P., McNew, K. L., Major, A. S., & Moore, D. J. (2021). Metabolic preconditioning in CD4⁺ T cells restores inducible immune tolerance in lupus-prone mice. *Jci Insight*, 6(19), Article e143245. <https://doi.org/10.1172/jci.insight.143245>
- Wisniewski, J. R., Hein, M. Y., Cox, J., & Mann, M. (2014). A "Proteomic Ruler" for Protein Copy Number and Concentration Estimation without Spike-in Standards. *Molecular & Cellular Proteomics*, 13(12), 3497-3506. <https://doi.org/10.1074/mcp.M113.037309>
- Wong, C. K., Ho, C. Y., Li, E. K., & Lam, C. W. K. (2000). Elevation of proinflammatory cytokine (IL-18, IL-17, IL-12) and Th2 cytokine (IL-4) concentrations in patients with systemic lupus erythematosus. *Lupus*, 9(8), 589-593. <https://doi.org/10.1191/096120300678828703>
- Wong, C. K., Lit, L. C. W., Tam, L. S., Li, E. K. M., Wong, P. T. Y., & Lam, C. W. K. (2008). Hyperproduction of IL-23 and IL-17 in patients with systemic lupus erythematosus: Implications for Th17-mediated inflammation in auto-immunity. *Clinical Immunology*, 127(3), 385-393. <https://doi.org/10.1016/j.clim.2008.01.019>

- Wong, R. H. F., Chang, I., Hudak, C. S. S., Hyun, S., Kwan, H. Y., & Sul, H. S. (2009). A Role of DNA-PK for the Metabolic Gene Regulation in Response to Insulin. *Cell*, *136*(6), 1056-1072. <https://doi.org/10.1016/j.cell.2008.12.040>
- Wu, B., Goronzy, J. J., & Weyand, C. M. (2020). Metabolic Fitness of T Cells in Autoimmune Disease. *Immunometabolism*, *2*(2).
- Wu, B. W., Qiu, J. T., Zhao, T. T. V., Wang, Y. N., Maeda, T., Goronzy, J. J., . . . Weyand, C. M. (2020). Succinyl-CoA Ligase Deficiency in Pro-inflammatory and Tissue-Invasive T Cells. *Cell Metabolism*, *32*(6). <https://doi.org/10.1016/j.cmet.2020.10.025>
- Wu, B. W., Zhao, T. V., Jin, K., Hu, Z. L., Abdel, M. P., Warrington, K. J., . . . Weyand, C. M. (2021). Mitochondrial aspartate regulates TNF biogenesis and autoimmune tissue inflammation. *Nature Immunology*, *22*(12), 1551-+. <https://doi.org/10.1038/s41590-021-01065-2>
- Xu, C. K., Wang, W., Zhong, J., Lei, F., Xu, N. H., Zhang, Y. O., & Xie, W. D. (2018). Canagliflozin exerts anti-inflammatory effects by inhibiting intracellular glucose metabolism and promoting autophagy in immune cells. *Biochemical Pharmacology*, *152*, 45-59. <https://doi.org/10.1016/j.bcp.2018.03.013>
- Xu, H., Oriss, T. B., Fei, M. J., Henry, A. C., Melgert, B. N., Chen, L., . . . Ray, A. (2008). Indoleamine 2,3-dioxygenase in lung dendritic cells promotes Th2 responses and allergic inflammation. *Proceedings of the National Academy of Sciences of the United States of America*, *105*(18), 6690-6695. <https://doi.org/10.1073/pnas.0708809105>
- Xu, H. H., Liu, J., Cui, X., Zuo, Y. H., Zhang, Z. F., Li, Y. X., . . . Pang, J. (2015). Increased frequency of circulating follicular helper T cells in lupus patients is associated with autoantibody production in a CD40L-dependent manner. *Cellular Immunology*, *295*(1), 46-51. <https://doi.org/10.1016/j.cellimm.2015.01.014>
- Xu, T., Stewart, K. M., Wang, X. H., Liu, K., Xie, M., Ryu, J. K., . . . Ding, S. (2017). Metabolic control of T_H17 and induced T-reg cell balance by an epigenetic mechanism. *Nature*, *548*(7666), 228-+. <https://doi.org/10.1038/nature23475>
- Xu, W., Patel, C. H., Zhao, L., Sun, I. H., Oh, M. H., Sun, I. M., . . . Powell, J. D. (2023). GOT1 regulates CD8⁺ effector and memory T cell generation. *Cell Rep*, *42*(1), 111987.
- Yang, K., Blanco, D. B., Neale, G., Vogel, P., Avila, J., Clish, C. B., . . . Chi, H. B. (2017). Homeostatic control of metabolic and functional fitness of Treg cells by LKB1 signalling. *Nature*, *548*(7669), 602-+. <https://doi.org/10.1038/nature23665>
- Yang, X. Y., Wang, L. H., Chen, T. S., Hodge, D. R., Resau, J. H., DaSilva, L., & Farrar, W. L. (2000). Activation of human T lymphocytes is inhibited by peroxisome proliferator-activated receptor γ (PPAR γ) agonists - PPAR γ co-association with transcription factor NFAT. *Journal of Biological Chemistry*, *275*(7), 4541-4544. <https://doi.org/10.1074/jbc.275.7.4541>
- Yang, Z., Fujii, H., Mohan, S. V., Goronzy, J. J., & Weyand, C. M. (2013). Phosphofructokinase deficiency impairs ATP generation, autophagy, and redox balance in rheumatoid arthritis T cells. *Journal of Experimental Medicine*, *210*(10), 2119-2134. <https://doi.org/10.1084/jem.20130252>
- Yang, Z., Shen, Y., Oishi, H., Matteson, E. L., Tian, L., Goronzy, J. J., & Weyand, C. M. (2016). Restoring oxidant signaling suppresses proarthritogenic T cell effector functions in rheumatoid arthritis. *Science Translational Medicine*, *8*(331), Article 331ra38. <https://doi.org/10.1126/scitranslmed.aad7151>
- Yap, T. A., Daver, N., Mahendra, M., Zhang, J., Kamiya-Matsuoka, C., Meric-Bernstam, F., . . . Konopleva, M. (2023). Complex I inhibitor of oxidative phosphorylation in advanced solid tumors and acute myeloid leukemia: phase I trials. In *Nat Med* (Vol. 29, pp. 115-126). © 2022. The Author(s), under exclusive licence to Springer Nature America, Inc. <https://doi.org/10.1038/s41591-022-02103-8>
- Yin, Y. M., Choi, S. C., Xu, Z. W., Perry, D. J., Seay, H., Croker, B. P., . . . Morel, L. (2015). Normalization of CD4⁺ T cell metabolism reverses lupus. *Science Translational Medicine*, *7*(274), Article 274ra18. <https://doi.org/10.1126/scitranslmed.aaa0835>

- Yin, Y. M., Choi, S. C., Xu, Z. W., Zeumer, L., Kanda, N., Croker, B. P., & Morel, L. (2016). Glucose Oxidation Is Critical for CD4⁺ T Cell Activation in a Mouse Model of Systemic Lupus Erythematosus. *Journal of Immunology*, *196*(1), 80-90. <https://doi.org/10.4049/jimmunol.1501537>
- Yoshida, N., Comte, D., Mizui, M., Otomo, K., Rosetti, F., Mayadas, T. N., . . . Tsokos, G. C. (2016). ICER is requisite for Th17 differentiation. *Nature Communications*, *7*, Article 12993. <https://doi.org/10.1038/ncomms12993>
- Yoshinaga, S. K., Whoriskey, J. S., Khare, S. D., Sarmiento, U., Guo, J., Horan, T., . . . Senaldi, G. (1999). T-cell co-stimulation through B7RP-1 and ICOS. *Nature*, *402*(6763), 827-832. <https://doi.org/10.1038/45582>
- Yu, J., Heck, S., Patel, V., Levan, J., Yu, Y., Bussel, J. B., & Yazdanbakhsh, K. (2008). Defective circulating CD25 regulatory T cells in patients with chronic immune thrombocytopenic purpura. *Blood*, *112*(4), 1325-1328. <https://doi.org/10.1182/blood-2008-01-135335>
- Yuan, J., Cao, A. L., Yu, M., Lin, Q. W., Yu, X., Zhang, J. H., . . . Liao, Y. H. (2010). Th17 Cells Facilitate the Humoral Immune Response in Patients with Acute Viral Myocarditis. *Journal of Clinical Immunology*, *30*(2), 226-234. <https://doi.org/10.1007/s10875-009-9355-z>
- Zhang, F., Wei, K., Slowikowski, K., Fonseka, C. Y., Rao, D. A., Kelly, S., . . . Accelerating Medicines, P. (2019). Defining inflammatory cell states in rheumatoid arthritis joint synovial tissues by integrating single-cell transcriptomics and mass cytometry. *Nature Immunology*, *20*(7), 928+. <https://doi.org/10.1038/s41590-019-0378-1>
- Zhang, W. G., Sloan-Lancaster, J., Kitchen, J., Tribble, R. P., & Samelson, L. E. (1998). LAT: The ZAP-70 tyrosine kinase substrate that links T cell receptor to cellular activation. *Cell*, *92*(1), 83-92. [https://doi.org/10.1016/s0092-8674\(00\)80901-0](https://doi.org/10.1016/s0092-8674(00)80901-0)
- Zhang, X., Tao, Y. Z., Troiani, L., & Markovic-Plese, S. (2011). Simvastatin Inhibits IFN Regulatory Factor 4 Expression and Th17 Cell Differentiation in CD4⁺ T Cells Derived from Patients with Multiple Sclerosis. *Journal of Immunology*, *187*(6), 3431-3437. <https://doi.org/10.4049/jimmunol.1100580>
- Zhao, C. M., Gu, Y. B., Zeng, X. Y., & Wang, J. (2018). NLRP3 inflammasome regulates Th17 differentiation in rheumatoid arthritis. *Clinical Immunology*, *197*, 154-160. <https://doi.org/10.1016/j.clim.2018.09.007>
- Zhong, X., Tumang, J. R., Gao, W., Bai, C., & Rothstein, T. L. (2007). PD-L2 expression extends beyond dendritic cells/macrophages to B1 cells enriched for V_H11/V_H12 and phosphatidylcholine binding. *Eur J Immunol*, *37*(9), 2405-2410. <https://doi.org/10.1002/eji.200737461>
- Zhou, H., Wang, S. Y., Zhu, P. J., Hu, S. Y., Chen, Y. D., & Ren, J. (2018). Empagliflozin rescues diabetic myocardial microvascular injury via AMPK-mediated inhibition of mitochondrial fission. *Redox Biology*, *15*, 335-346. <https://doi.org/10.1016/j.redox.2017.12.019>
- Zhu, J. F., & Paul, W. E. (2008). CD4 T cells: fates, functions, and faults. *Blood*, *112*(5), 1557-1569. <https://doi.org/10.1182/blood-2008-05-078154>
- Zhu, M. X., Yang, H., Lu, Y., Yang, H. M., Tang, Y. H., Li, L. X., . . . Yuan, J. (2021). Cardiac ectopic lymphoid follicle formation in viral myocarditis involving the regulation of podoplanin in Th17 cell differentiation. *Faseb Journal*, *35*(11), Article e21975. <https://doi.org/10.1096/fj.202101050RR>
- Ziolkowska, N., Koc, A., Luszczkiewicz, G., Ksiezopolska-Pietrzak, K., Klimczak, E., Chwalinska-Sadowska, H., & Maslinski, W. (2000). High levels of IL-17 in rheumatoid arthritis patients: IL-15 triggers in vitro IL-17 production via cyclosporin A-sensitive mechanism. *Journal of Immunology*, *164*(5), 2832-2838. <https://doi.org/10.4049/jimmunol.164.5.2832>
- Zou, R. J., Shi, W. T., Qiu, J. X., Zhou, N., Du, N., Zhou, H., . . . Ma, L. (2022). Empagliflozin attenuates cardiac microvascular ischemia/reperfusion injury through improving mitochondrial homeostasis. *Cardiovascular Diabetology*, *21*(1), Article 106. <https://doi.org/10.1186/s12933-022-01532-6>

Zugner, E., Yang, H. C., Kotzbeck, P., Boulgaropoulos, B., Sourij, H., Hagvall, S., . . . Magnes, C. (2022). Differential In Vitro Effects of SGLT2 Inhibitors on Mitochondrial Oxidative Phosphorylation, Glucose Uptake and Cell Metabolism. *International Journal of Molecular Sciences*, 23(14), Article 7966. <https://doi.org/10.3390/ijms23147966>